

**New Peptide-Mimicking Scaffolds:
Influence of Stereochemistry, Connectivity, and Topology**

D i s s e r t a t i o n

zur Erlangung des akademischen Grades

d o c t o r r e r u m n a t u r a l i u m

(Dr. rer. nat.)

im Fach Chemie

eingereicht an der

Mathematisch-Naturwissenschaftlichen Fakultät I

der Humboldt Universität zu Berlin

von

Dipl.-Chem. Sebastian Hartwig

geboren am 10.02.1979 in Kassel

Präsident der Humboldt Universität zu Berlin

Prof. Dr. Dr. h.c. Christoph Marksches

Dekan der Mathematisch-Naturwissenschaftlichen Fakultät I

Prof. Dr. Lutz-Helmut Schön

Gutachter: 1. Prof. Stefan Hecht, PhD
 2. Prof. Dr. Christoph Arenz

Tag der mündlichen Prüfung: 05.06.2009

Die vorliegende Arbeit wurde in der Zeit von September 2004 bis Dezember 2004 am Institut für Chemie/Organische Chemie der Freien Universität Berlin, von Januar 2005 bis September 2006 am Max-Planck-Institut für Kohlenforschung in Mülheim an der Ruhr und von Oktober 2006 bis April 2009 am Institut für Chemie der Humboldt Universität zu Berlin unter Anleitung von Herrn Prof. Stefan Hecht PhD durchgeführt.

Hiermit versichere ich, Sebastian Hartwig, geboren am 10.02.1979 in Kassel, die vorliegende Arbeit selbständig und nur mit Hilfe der zulässigen und angegebenen Mittel verfasst zu haben.

Sebastian Hartwig

Danksagung

Prof. Dr. Stefan Hecht danke ich für die Möglichkeit, ein interessantes und herausforderndes Thema unter stets optimalen Bedingungen zu bearbeiten. Die hervorragenden Arbeitsbedingungen und die engagierte fachliche Betreuung haben wesentlich zum Gelingen dieser Arbeit beigetragen.

Ich möchte mich bei allen Service-Mitarbeitern am MPI Mülheim bedanken, deren zügige und qualitativ hochwertige Arbeit mich schwer beeindruckt hat. Ich möchte mich persönlich bei Alfred Deege und Heike Hinrichs, bei denen ich mich – auch mit unliebsamen Proben – jederzeit herzlich willkommen gefühlt habe. Die fachlichen und persönlichen Gespräche habe ich stets sehr genossen. Des weiteren möchte ich mich bei den Service-Abteilungen der HU Berlin, speziell bei Frau Thiesies für die stets unkomplizierte Zusammenarbeit bedanken.

Ich möchte mich bei all meinen Kollegen aus dem Arbeitskreis bedanken, die mich während der Promotion an den verschiedenen Instituten unterstützt haben. Besonderer Dank geht dabei an die Mülheim-Connection, die das Ruhrgebiet und alle damit verbundenen Entbehrungen zu einem unvergesslichen Event gemacht haben. Maike Peters, Marco Balbo-Block, Robert Meudtner und Ragnar Stoll, ohne Euch wäre es einfach nicht dasselbe gewesen. Vielen Dank auch an die nachwachsende Generation der Hecht-Gruppe: Ihr wart super! Besonderer Dank geht dabei an Denise für das angenehme Laborklima und an Jan, Volker, Susanne, Marie und Maria für die wohl besten Kaffeepausen der Welt. Jutta Schwarz danke ich für die Unterstützung bei der Synthese der Pseudopeptide.

Dem AK Seitz, speziell Franziska Mende danke ich für die großartige Unterstützung bei der Peptid-Synthese.

Weiterhin möchte ich mich beim Fonds der chemischen Industrie für die großzügige finanzielle Unterstützung im Rahmen des Kekulé-Stipendiums bedanken. Besonderer Dank geht an Woldemar Juschko, der die Anfangszeit in Berlin unvergesslich gemacht hat.

Ich möchte mich ganz besonders bei Joana Kraege bedanken. Ohne sie wäre einfach alles anders.

Zum Schluss möchte ich mich bei meiner Familie bedanken, ohne deren Unterstützung ich nicht bis hierher gekommen wäre.

Abstract

Inspired by the naturally occurring antibiotics of the Gramicidin family and their D-(*alt*)-L amino acid sequence, enabling these oligopeptides to adopt a β -helical secondary structure, the work presented in this thesis targeted the synthesis and characterization of peptides and diverse pseudopeptides with regular *all*-L and D-(*alt*)-L sequences and the influence of this stereochemical variation on the compounds' structures and properties. Further diversification of the structures as obtained by replacing amide bonds in the peptide backbone with different isosteres, affording unique pseudopeptide structures. In addition spherical molecules were generated by introducing branching into the linear peptide scaffold. Throughout all projects, the aim was the design and synthesis of discrete oligomers for structural investigations and the incorporation of the respective structural elements into polymers via the polymerization of suitable monomers, in order to generate nanoscale macromolecular and supramolecular objects.

The divergent/convergent synthesis of a series of oligo-D-(*alt*)-L-lysines targeted the generation of hydrophilic, pH-sensitive nanotubular structures. The design and attempted synthesis of a macrocyclic *N*-carboxy anhydride (NCA) monomer aimed at the incorporation of an alternating stereochemistry into linear narrow disperse polymers.

The stepwise replacement of peptide backbone amide bonds with ester-(*alt*)-urea moieties afforded *all*-L and D-(*alt*)-L oligopseudoleucines with 50% and 0% amide content. The influence of stereochemistry and changed hydrogen bonding pattern on aggregation was investigated by proton shift NMR experiments. The incorporation of these structural elements into polymers was targeted by design and attempted synthesis of a corresponding macrocyclic monomer.

The design, synthesis, and polymerization of an AB-“Click”-monomer, based on *all*-L and L-(*alt*)-D lysine dipeptides afforded high molecular weight, triazole containing polypseudopeptides. Quantitative coupling to pyrene butyric acid afforded the respective side chain labeled polymers.

The introduction of branching into glutamate peptides afforded fully chiral dendrimers with addressable focal and peripheral functionalities and variable charge density. The straightforward and high yielding synthesis was based on a divergent/convergent synthesis approach. The design, synthesis, and polymerization of a glutamate based AB₂-“Click”-monomer led to related chiral hyperbranched polypseudopeptides.

Kurzzusammenfassung

Inspiziert von den natürlich vorkommenden Antibiotika der Gramicidin Familie und ihrer D-(*alt*)-L Aminosäuresequenz, die es diesen Oligopeptiden ermöglicht, eine β -helikale Sekundärstruktur einzunehmen, war das Hauptziel dieser Arbeit die Synthese und Charakterisierung von Peptiden und diversen Pseudopeptiden mit regulärer *all*-L und D-(*alt*)-L Sequenz und die Untersuchung des Einflusses dieser stereochemischen Variation auf die Strukturen und Eigenschaften dieser Verbindungen. Zusätzlich ergab der Austausch von Amid-Bindungen im Peptid-Rückgrat durch verschiedene Isostere diverse, teils einzigartige Pseudopeptid-Strukturen, wohingegen Verzweigung des linearen Peptid-Rückgrates zu sphärischen Molekülen führte. Alle Projekte zielten auf die Entwicklung und Synthese diskreter Oligomere für Strukturuntersuchungen, sowie auf die Einbindung der jeweiligen Strukturelemente in Polymere. Die Polymerization geeigneter Monomere zu Polymeren soll zu makro- und supramolekularen Nano-Objekten führen.

Die divergent/konvergente Synthese einer Serie von Oligo-D-(*alt*)-L-lysinen zielte auf die Generierung hydrophiler, pH-sensitiver nanotubularer Strukturen. Design und versuchte Synthese makrocyclischer *N*-carboxy Anhydride (NCA) zielten auf die Einbindung dieser alternierenden Stereochemie in Polymere.

Schrittweiser Austausch von Amid-Bindungen des Peptid-Rückgrates durch Ester-(*alt*)-Urea-Einheiten führte zu *all*-L und D-(*alt*)-L Oligopseudoleucinen mit 50% und 0% Amid-Bindungs-Anteil. Der Einfluss von Stereochemie und verändertem H-Brücken Muster auf die Aggregation wurde mit NMR-Experimenten untersucht. Design und versuchte Synthese geeigneter makrocyclischer Monomere zielten auf die Einbindung dieser Strukturelemente in Polymere.

Design, Synthese und Polymerisation von AB-“Click“-Monomeren, basierend auf *all*-L and L-(*alt*)-D lysin Dipeptiden, ergaben hochmolekulare, Triazol-enthaltende Polypseudopeptide, deren Seitenketten mit Pyrenbuttersäure quantitativ post-funktionalisiert werden konnten.

Die Einführung von Verzweigung in Glutamat-Peptide ergab chirale Dendrimere mit adressierbaren fokalen und periphären Funktionalitäten, sowie variabler Ladungsdichte. Die divergent/konvergente Synthese erlaubte ein schnelles Dendrimer-Wachstum in hohen Ausbeuten. Design, Synthese und Polymerisation eines Glutamat basierenden AB₂-“Click“-Monomers lieferte verwandte chirale hypervverzweigte Polypseudopeptide.

Table of Contents

1	Introduction.....	1
1.1	Literature.....	5
2	General Part.....	7
2.1	Introduction	7
2.2	Linear D,L-Alternating Peptides	10
2.2.1	Gramicidin	11
2.2.2	Synthetic Gramicidin-mimicking Peptides	13
2.2.3	D,L-Alternating Polypeptides	15
2.3	Peptide Synthesis	16
2.3.1	Coupling Reagents	16
2.3.1.1	Carbodiimides.....	17
2.3.1.2	Uronium Salts.....	19
2.3.1.3	Phosphonium Salts	21
2.3.2	Racemization.....	21
2.3.3	Protecting Groups	23
2.3.4	Synthesis In Solution.....	25
2.3.5	Synthesis On Solid Support	27
2.3.6	Synthesis On Soluble Support.....	30
2.4	Polypeptide Synthesis	31
2.4.1	Synthesis Of Homo-L-polypeptides.....	31
2.4.1.1	NCA Synthesis	33
2.4.2	Synthesis Of Homo-D-(<i>alt</i>)-L-polypeptides	35
2.5	Depsipeptides (Ester-isosteres)	36
2.6	Triazole Isosteres	38
2.7	Peptide Dendrimers	40
2.8	Literature.....	44

Table of Contents

3	Linear D-(<i>alt</i>)-L-peptides	49
3.1	Linear Oligo-D-(<i>alt</i>)-L-peptides	49
3.1.1	General Considerations	49
3.1.2	Synthetic Considerations	49
3.1.3	Synthesis On Soluble Support	50
3.1.4	Synthesis In Solution	51
3.1.4.1	Divergent/Convergent Synthesis	52
3.1.4.2	Stepwise Convergent Synthesis	58
3.1.5	Attempted Side Chain Deprotection Of 2Cl-Z Group	59
3.1.6	Changed Protecting Group Strategy	62
3.1.7	Side Chain Deprotection Of The 2Cl-Z Group	67
3.1.8	Investigation Of Conformation In Solution	69
3.2	Linear Poly-D-(<i>alt</i>)-L-peptides	73
3.2.1	General Considerations	73
3.2.2	Synthetic Considerations	74
3.2.3	Attempted Monomer Synthesis	75
3.2.4	Alternative NCA-synthesis	76
3.3	Experimental Part	79
3.3.1	General	79
3.3.2	General Procedures	81
3.3.3	Synthetic Procedures	82
3.4	Literature	145
4	Linear (Ester-[<i>alt</i>]-urea)s	147
4.1	Linear Poly(ester-[<i>alt</i>]-urea)s With Variable Stereochemistry	147
4.1.1	General Considerations	147
4.1.2	Synthetic Considerations	149
4.1.3	Monomer Synthesis: Pathway One	151

4.1.4	Monomer Synthesis: Pathway Two	155
4.1.5	Polymerization Of Linear Monomer	161
4.2	Linear Oligo(ester-[<i>a/t</i>]-urea)s With Variable Stereochemistry And Isostere Incorporation	164
4.2.1	General Considerations	164
4.2.2	Synthetic Considerations	166
4.2.3	Synthesis Of 0% Amide Containing Pseudopeptide	166
4.2.4	Synthesis Of 50% Amide Containing Pseudopeptides	171
4.2.5	Synthesis Of The Peptide	178
4.2.6	Aggregation Studies	181
4.2.6.1	NMR Studies	181
4.2.7	Tentative Structural Proposal	195
4.3	Experimental Part	200
4.3.1	General	200
4.3.2	General Procedures	201
4.3.3	Synthetic Procedures	202
4.4	Literature	264
5	Linear Triazole Containing Polypseudopeptides	267
5.1	Linear Triazole Containing Polypseudopeptides With Variable Stereochemistry	267
5.1.1	General Considerations	267
5.1.2	Synthetic Considerations I	267
5.1.3	Monomer Synthesis I	271
5.1.3.1	Synthesis Of Part A	271
5.1.3.2	Synthesis Of Part B	273
5.1.3.3	Coupling Of Part A And Part B	273
5.1.4	Polymerization I	274

Table of Contents

5.1.5	Synthetic Considerations II	276
5.1.6	Monomer Synthesis II.....	277
5.1.6.1	Synthesis Of Part A.....	277
5.1.6.2	Synthesis Of Part B.....	278
5.1.6.3	Coupling Of Parts A And B And Conversion To The AB-“Click”-monomer	279
5.1.7	Polymerization II	280
5.1.8	Boc Deprotection Of Polymers.....	283
5.2	Model Compounds	285
5.2.1	General And Synthetic Considerations	285
5.2.2	Synthesis Of The Modelcompounds.....	287
5.2.3	Circular Dichroism Studies	290
5.3	Side Chain Labeling	298
5.3.1	General Considerations	298
5.3.2	Synthesis.....	300
5.3.3	Spectroscopic Studies.....	303
5.3.3.1	UV	304
5.3.3.2	Fluorescence	306
5.3.3.3	Circular Dichroism	309
5.4	Experimental Part.....	312
5.4.1	General	312
5.4.2	General Procedures	314
5.4.3	Synthetic Procedures.....	315
5.5	Literature	342
6	Glutamate Dendrimers	343
6.1	Discrete Glutamate Dendrimers With Variable Stereochemistry	343
6.1.1	General Considerations	343

6.1.2	Synthetic Considerations.....	343
6.1.3	Dendrimer Synthesis	344
6.1.4	Circular Dichroism Studies	355
6.1.5	Dendrimer Complexation Experiments	357
6.1.6	Core Functionalization With Dyes	359
6.1.6.1	Bifunctional Core	365
6.2	Hyperbranched Polyglutamate Based Polymers	368
6.2.1	Monomer Synthesis.....	368
6.2.2	Polymerizations	369
6.3	Experimental Part.....	376
6.3.1	General	376
6.3.2	General Procedures	378
6.3.3	Synthetic Procedures.....	379
6.4	Literature	403
7	Summary and Outlook.....	405
7.1	Linear Oligo- and Poly-D-(<i>alt</i>)-L-peptides.....	405
7.2	Linear Oligo- and Poly(ester-[<i>alt</i>]-urea)s With Variable Stereochemistry	405
7.3	Linear Triazole Containing Polypseudopeptides With Variable Stereochemistry	406
7.4	Glutamate Dendrimers With Variable Stereochemistry	407
8	Appendix.....	409
8.1	Abbreviations	409

1 Introduction

In recent years, the word *nano* has become very popular and has been implemented into peoples' standard vocabulary, rendering even non-scientists to use it for all kinds of purposes. This household word is widely applied as synonym for *very small*, oftentimes paired with certain technological finesses. A *Google*-search, entering the word *nano* leads to approximately 80 million hits in a tenth of a second. But there is significantly more to this word than just its exploitation in the *en vogue* descriptions of portable music player devices or small and tiny cars. It is not by chance that a screen of the scientific literature reveals more than 45.000 publications dealing with the word *nano*, indicating a pronounced increase within the last decade. The ability to create size and shape defined objects in the range of a few nanometers has tremendous impact on modern semiconductor industries or drug development and applied medicine.^[1-5] The achievements in lithographic techniques for the generation of nanoscale objects and patterns can not be underestimated, regarding for example the ongoing miniaturization of computing devices.^[6-12] The down-scaling *via* this top-down approach (Figure 1) is intrinsically limited in size, due to the physical constraints of the techniques applied.^[13] These limitations can be overcome by a bottom-up creation of nanoscale objects (Figure 1), assembling smaller building blocks (i.e. atoms or molecules) to defined larger architectures of nanosize dimensions.^[12, 14-18]

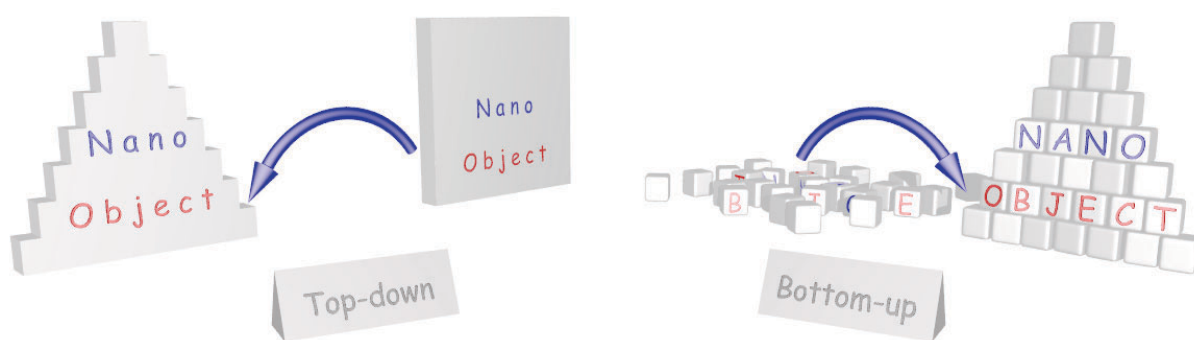


Figure 1: Cartoon illustrating the general difference between top-down and bottom-up approaches. Carving larger objects to nanoscale features characterizes the top-down approach (left), whereas the bottom-up approach (right) is based on the assembly and manipulation of smaller building blocks (i.e. atoms or molecules) to larger nanosized objects.

1 Introduction

The principal requirement for this approach is the precise control over the assembly process to accurate structures, necessitating a profound understanding of aggregation and folding processes of appropriately designed building blocks. Considering precision, efficiency, versatility, and functionality, artificial bottom-up processes aim to reach for the quality benchmark set by Nature. Utilizing a very basic pool of different building blocks (i.e. amino acids, ribonucleic acids, sugars or fatty acids), Nature manages to tackle complex tasks on the molecular level, such as data and energy storage as well as transfer, generation of compartments and transport of chemical entities. A permanently present actor in this context is the substance class of proteins, which are nanoscale macromolecules, involved in an impressingly large number of biological processes. Their synthesis by connecting amino acids to polypeptide strands, which subsequently fold and aggregate to well defined secondary, tertiary and - if necessary - quaternary structures represent arguably one of the most important bottom-up nanofabrication processes.

The undeniable beauty and overwhelming accuracy of these biological structures and processes inspired generations of scientists in different domains and led to extensive research in this field. A crucial step in mimicking natural protein architectures and adapting these evolutionary optimized processes to artificial bottom-up syntheses is the elucidation and detailed understanding of structure-property relationships. The successful application of NMR spectroscopy to complex protein structures and the development of matrix assisted laser desorption ionization (MALDI) and electrospray ionization (ESI) mass spectrometry can be considered as a milestone in protein structure analysis, which was honored with the Nobel price in 2002.^[19-21] Even more important for mimicking the natural bottom-up process than the structure elucidation of existing proteins is the synthesis and variation of protein subunits and small peptides, leading to a direct correlation of primary and secondary structure. The achievements of Merrifield in peptide synthesis (also honored with the Nobel price in 1984) enabled researchers to synthesize libraries of diverse peptides and investigate their structures.^[22,23] The number of possible primary structure mutations of a peptide is immense using the 22 proteinogenic amino acids and becomes even more colossal, when non-proteinogenic or D-configured amino

acids are taken into account. Besides the variation of the side chains and their orientation, extensive research has been carried out, modifying the peptide backbone by the implementation of for example β -, γ - or *N*-methylated amino acids or various amide isosteres.^[24] The flexibility of this approach seems to be almost unlimited, possibly leading to manifold structural motifs and unique properties and thereby enabling a deeper insight into the rules that govern translation of monomer sequence into the 3D macromolecular structure.

Ongoing research in this field will generate detailed knowledge about the fundamentals of biological structure formation and help to unravel and exploit Nature's smart design concepts by applying them to artificial systems. With regard to medicine and biochemistry, these efforts continue to affect drug design and delivery, tissue engineering, or DNA transfection, leading to compounds with improved properties (such as higher selectivity, lower toxicity or tunable biodegradability).

Aim of this work:

The aim of this work presented in this thesis is the synthesis and characterization of peptides and pseudopeptides and their structural investigation. Inspired by the naturally occurring antibiotics of the Gramicidin family, the main focus throughout all projects was set on the stereochemical variation from regular *all*-L sequences to alternating, i.e. D-(*alt*)-L, sequences and its influence on compounds' structures and properties. Additionally, the peptide backbone was modified by replacing amide bonds with different isosteres, affording unique pseudopeptide structures and by introducing branching into the linear peptide scaffold, affording spherical molecules. Every project targeted the design and synthesis of discrete oligomers for structural investigations and incorporation of the respective structural elements into polymers by the polymerization of suitable monomers to generate nanoscale macromolecular and supramolecular objects.

1 Introduction

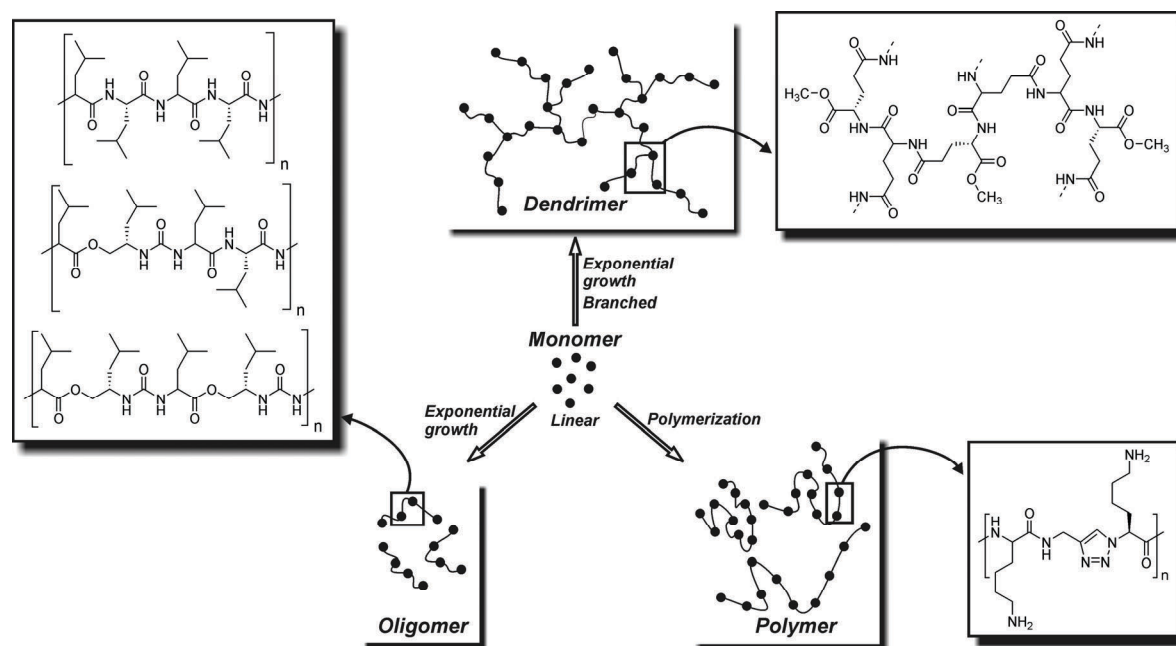


Figure 2: Approach to manifold peptide and pseudopeptide architectures arising from a pool of few amino acid building blocks achieved by versatile syntheses. Varying connectivity and stereochemistry of the monomers readily enables the generation of unique peptides and pseudopeptides with novel architectures and properties.

The synthesis of discrete lysine oligomers with D,L-alternating stereochemistry and the design of a macrocyclic NCA monomer aimed for the generation of a pH-sensitive nanotube (Chapter 3). The influence of stereochemistry and hydrogen bonding pattern on aggregation behavior was studied by the synthesis of leucine peptides and the stepwise replacement of amide bonds by ester-(*alt*)-urea moieties (Figure 2, left). The generation of polymers with these unique structural motifs was targeted with the design and attempted synthesis of suitable cyclic monomers (Chapter 4). The straightforward synthesis of AB-“Click”-monomers and their polymerization to triazole containing polypseudopeptides (Figure 2, bottom right) targeted the generation of nanosize pH-sensitive polycations (Chapter 5). The introduction of branching into glutamate peptides afforded fully chiral dendrimers with addressable focal and peripheral functionalities and variable charge density via an exponential growth approach (Figure 2, top right). The high yielding and straightforward synthesis of a glutamate based AB₂-“Click”-monomer and its polymerization led to related chiral hyperbranched polypseudopeptides (Chapter 6).

1.1 Literature

- [1] S. Heck, D. Pinner, McKinsey & Company, **2007**.
- [2] A. S. Hoffman, P. S. Stayton, M. E. H. Ei-Sayed, N. Murthy, V. Bulmus, C. Lackey, C. Cheung, *J. Biomed. Nanotechnol.* **2007**, 3, 213.
- [3] P. X. Ma, *Adv. Drug Deliv. Rev.* **2008**, 60, 184.
- [4] H. Klefenz, *Eng. Life Sci.* **2004**, 4, 211.
- [5] G. B. Wei, P. X. Ma, *Adv. Funct. Mater.* **2008**, 18, 3568.
- [6] G. M. Wallraff, W. D. Hinsberg, *Chem. Rev.* **1999**, 99, 1801.
- [7] Y. N. Xia, J. A. Rogers, K. E. Paul, G. M. Whitesides, *Chem. Rev.* **1999**, 99, 1823.
- [8] Y. N. Xia, G. M. Whitesides, *Angew. Chem., Int. Ed.* **1998**, 37, 551.
- [9] B. D. Gates, Q. B. Xu, M. Stewart, D. Ryan, C. G. Willson, G. M. Whitesides, *Chem. Rev.* **2005**, 105, 1171.
- [10] M. Geissler, Y. N. Xia, *Adv. Mater.* **2004**, 16, 1249.
- [11] D. S. Ginger, H. Zhang, C. A. Mirkin, *Angew. Chem., Int. Ed.* **2004**, 43, 30.
- [12] *Special Issue of Scientific American 2001*, 285, Issue: 3.
- [13] T. Ito, S. Okazaki, *Nature* **2000**, 406, 1027.
- [14] J.-M. Lehn, *Angew. Chem., Int. Ed.* **1988**, 27, 89.
- [15] J. M. Lehn, *Angew. Chem., Int. Ed.* **1990**, 29, 1304.
- [16] G. A. Ozin, *Adv. Mater.* **1992**, 4, 612.
- [17] V. Balzani, A. Credi, F. M. Raymo, J. F. Stoddart, *Angew. Chem., Int. Ed.* **2000**, 39, 3349.
- [18] E. R. Kay, D. A. Leigh, F. Zerbetto, *Angew. Chem., Int. Ed.* **2007**, 46, 72.
- [19] K. Tanaka, *Angew. Chem., Int. Ed.* **2003**, 42, 3860.
- [20] J. B. Fenn, *Angew. Chem., Int. Ed.* **2003**, 42, 3871.
- [21] K. Wuthrich, *Angew. Chem., Int. Ed.* **2003**, 42, 3340.

- [22] R. B. Merrifield, *Angew. Chem., Int. Ed.* **1985**, 24, 799.
- [23] R. B. Merrifield, *J. Am. Chem. Soc.* **1963**, 85, 2149.
- [24] N. Sewald, H.-D. Jakubke, *Peptides: Chemistry and Biology*, Wiley-VCH, Weinheim, **2003**.

2 General Part

2.1 Introduction

The elucidation of biochemical processes is of major importance for the comprehension of physiology and medicine. Diseases for example are oftentimes the result of a malfunction on molecular level. Since peptides are involved in most biological processes, the understanding of their structures and properties is crucial for most biomolecular investigations.

Peptides are short polymers consisting of amino acids, which are linked via an amide bond. The sequence and number of the amino acids in the peptide chain is the so called primary structure. Due to several intramolecular forces, such as hydrogen bonding or steric repulsion, the peptide is able to organize itself in three dimensions and form a secondary structure. The best understood secondary structures are the α -helix, the parallel and antiparallel β -sheet, and turn structures, such as the γ -turn. In longer peptides and proteins, these secondary structure units can organize themselves in space to give a defined tertiary structure, which is also held together by additional intramolecular forces. The next possible step is the organization of tertiary structures (protein sub units) to a quaternary structure, which is stabilized by intermolecular hydrogen bonds, salt bridges or coordination to metal ions (see Figure 1). It is important to note that secondary, tertiary and – if existing – quaternary structure are a direct result of the primary structure. This means that very complex structural motifs such as helices can be obtained by controlling the primary structure of the peptide.

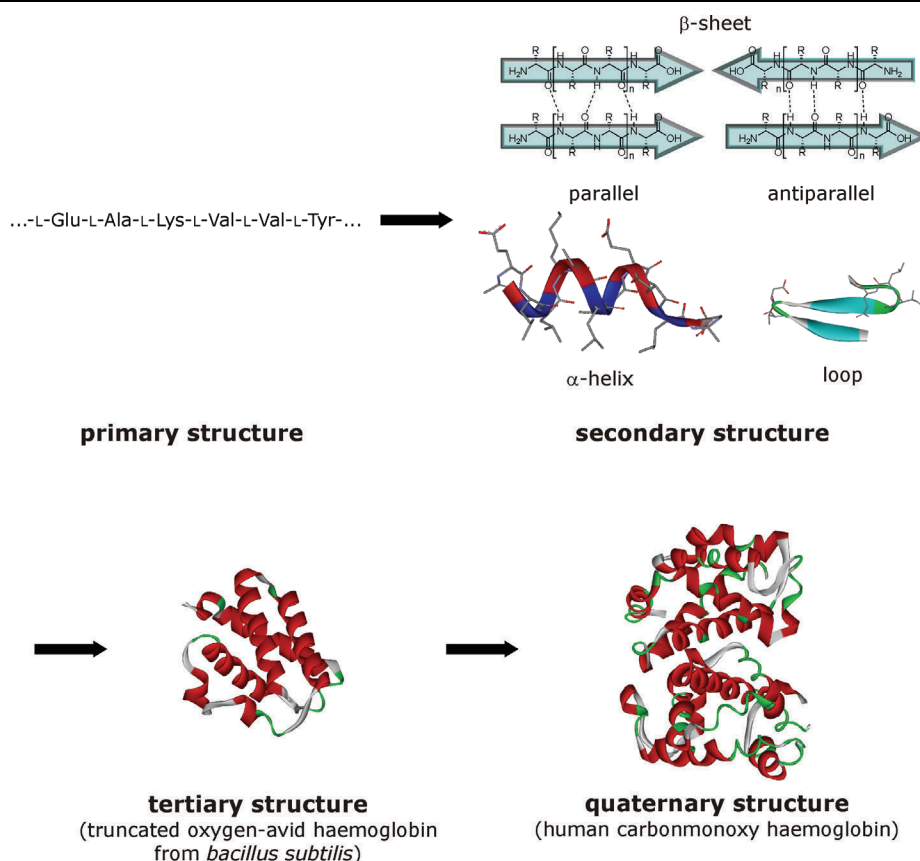


Figure 1: Levels of structure formation in peptides from primary to quaternary structure. (Structures derived from protein data bank (PDB). PDB codes: 1ux8 (tertiary structure), 1hco (quaternary structure)).

Amino acids are chiral substances and can occur in D- and L-configuration. Nature generally uses L-configured amino acid to build up peptides and proteins. There are 22 proteinogenic amino acids, of which 20 occur in the human body. It can easily be realized that the possibilities to create new structures and properties are immense, especially, when also D-configured amino acids are taken into consideration.

Very simplified, the amino acids can be categorized into hydrophilic and hydrophobic amino acids, depending on the nature of their side chain. This is very interesting for the generation of peptides with helical secondary structures, since the resulting helices can be hydrophobic, hydrophilic or also amphiphilic, depending on the amino acid sequence. Peptides, which consist of amino acids with basic or acidic side chains (i.e. polylysine or polyglutamate) can form secondary structures depending on the pH of the surrounding solvent. Polylysine

for example adopts an α -helical secondary structure in basic pH. When the pH is lowered, the free amines in the side chain are protonated, resulting in a Coulomb repulsion and a (reversible) unfolding of the helix to a coil structure. This effect can be monitored by CD spectroscopy (Figure 2).

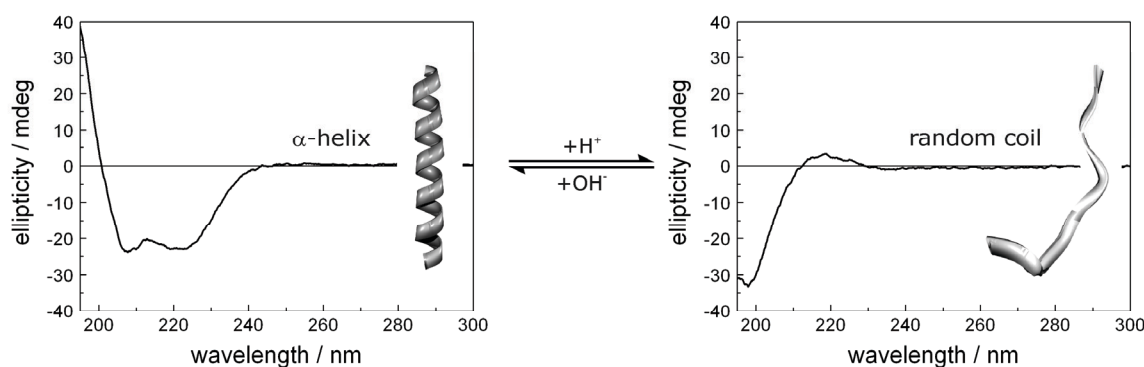


Figure 2: pH-switchable helix-coil-transition of polylysine with the corresponding characteristic CD signatures.

Structural analysis of peptides is very complex and demanding. In a synthetic peptide, its primary structure is known due to the synthesis and can be confirmed by degradation experiments and subsequent fragment analysis. The determination of three dimensional structures is much more complex. In the rare case that crystals of the peptide can be grown, its structure can be determined by X-ray analysis. It should always be kept in mind that the resulting structures are solid state structures and represent not necessarily the preferred conformations in solution. In the rather likely case that the peptide cannot be crystallized, electron diffraction and IR can provide interesting information. Oftentimes, the structure of the peptide in solution is very interesting for the understanding of biological processes. For the determination of solution structures, NMR, IR, and CD are useful, but also very demanding methods. NMR of peptides for example is very complex and requires significant heterogeneity since the signals in the spectrum have to be resolved for proper assignment. For homo-peptides, which consist of one type of amino acid, repeat unit structure analysis via NMR is hardly possible since all signals are overlapping and cannot be assigned. IR can give information on hydrogen bonding patterns in the peptide and by this hints on the secondary structure. By

CD, the presence or absence of a characteristic secondary structure can be determined. Structural motifs can be determined in comparison to CD signals, which have already been assigned. The α -helical motif for example has a very characteristic CD signature. However, please note that the analysis of CD signals, which result from new structural motifs, is by far not trivial.

As described above, the three dimensional structure of a peptide is strictly determined by its primary structure and can be varied by the use of different amino acids. In order to vary the structure and properties of a peptide, one can also alter the stereochemistry in the peptide backbone from an *all*-L- to for example an D-(*a/t*)-L-configuration while maintaining the original sequence. Another interesting possibility to vary the structure is the change of the peptide backbone by replacing amide bonds with isosteres. Possible isosteres are for example esters yielding depsipeptides or triazoles. These replacements can also lead to fundamental changes in the three dimensional structure of the peptide (or peptidomimetic). Finally, structural changes can be achieved, when deviating from linearity. The introduction of branching obviously changes the overall structure of a peptide. All these variations are also important for biomedical applications since native peptides suffer some major disadvantages in their use as pharmacologically active compounds (i.e. rapid degradation by proteases). These chemical modifications can therefore greatly improve the bioavailability and metabolic stability of such peptide-mimics.

2.2 Linear D,L-Alternating Peptides

Linear D,L-alternating peptides are a fascinating class of peptides with interesting and unique structures and properties. In contrast to conventional peptides, which consist of natural amino acids with L-configuration, the stereochemistry of the amino acids in the sequence of those peptides is strictly alternating. This difference in the primary structure enables D,L-alternating peptides to adopt unique secondary structures such as the β -helix (Figure 3). In this β -helix, the amino acid residues have conformations located in their respective β -regions and the hydrogen bonding is made as in β -structures (parallel or antiparallel, depending on the helix). One of the most popular D,L-alternating peptides is the naturally occurring antibiotic Gramicidin.

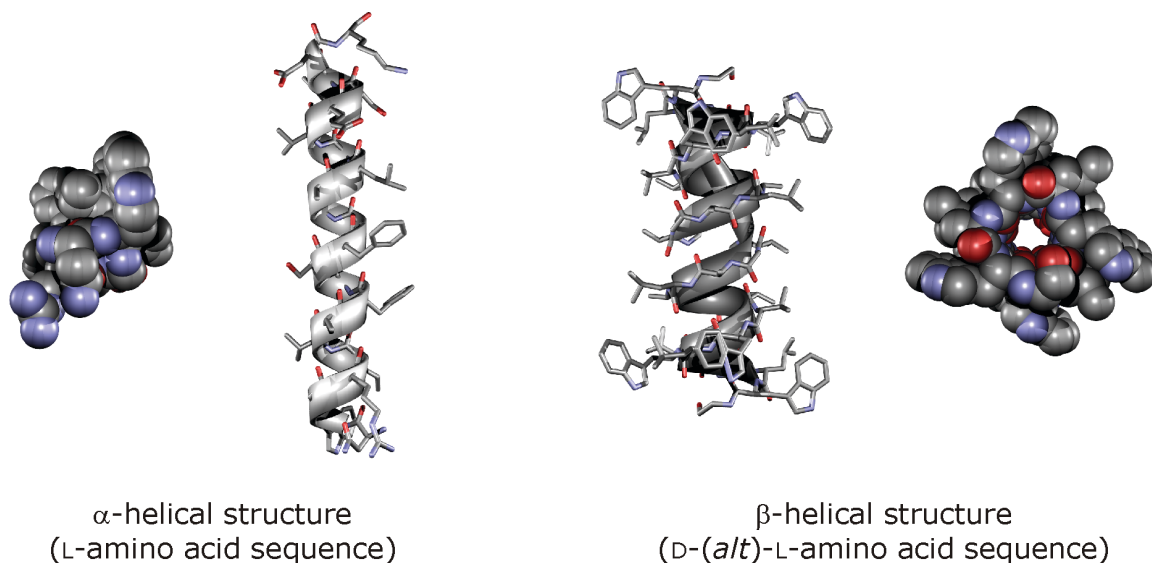


Figure 3: α -helical Structure of a L-amino acid sequence (left) in comparison to the β -helical structure of a D,L-alternating peptide. (Structures derived from protein data bank (PDB). PDB codes: 1ux8 (α -helix), 1mag (β -helix)).

2.2.1 Gramicidin

The antibiotic Gramicidin is produced by *bacillus brevis* as a mixture of Gramicidin A, B, C and S. Gramicidin S is a cyclic decapeptide. The Gramicidins A, B and C are D,L-alternating pentadecapeptides with hydrophobic sidechains, which were found to have antibiotic properties. They kill the bacterium by interrupting the synthesis of Adenosin-triphosphate (ATP) from ADP. They are doing so by simply drilling a hole into the cell membrane and allowing the exchange of charge carriers. In this case they are allowing monocations such as K^+ or Na^+ to pass through the membrane and thereby undoing the charge gradient, which is established in the processes of the respiratory chain and necessary for the formation of ATP. By this mechanism, they are toxic for procaryotic as well as for eucaryotic cells. This limits its therapeutic use to topological applications, since internal administration also leads to hemolysis. The three Gramicidins differ in the amino acid in position 11 of the primary structure (Figure 4). Gramicidin A carries a tryptophane in this position, Gramicidin B a phenylalanine and Gramicidin C a tyrosine. Since Gramicidin A is the major product in this mixture, most of the investigations were focused on it. First interests in the structure of Gramicidin can be traced back to 1941.^[1]

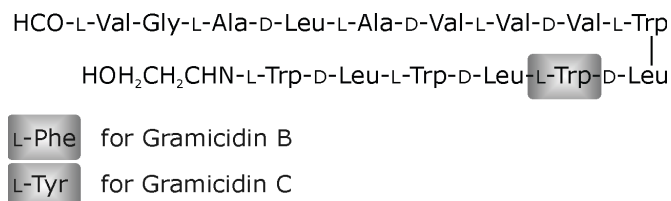


Figure 4: Primary structure of Gramicidin.

In ion-conductance measurements through membranes, Hladky and Haydon experienced that the ion conductance through the membrane in the presence of Gramicidin was discrete, in accordance with the theory of a channel formation and not with the presence of a carrier molecule.^[2] It was also postulated that the conducting species had to be a dimeric structure. The observed steps in the conduction, i.e. its commencement and termination, were attributed to the formation and dissociation of a dimer. The elucidation of the structure of this dimer was the main subject of an extensive research, which started in the 1970's and still continues. The structure of Gramicidin was investigated in the solid state, in solution, and in membrane-resembling environments.

Gramicidin in the solid state is polymorph and its crystal structure strongly depends on the solvent, from which it is crystallized and on the presence of ions or lipids. Pioneering work in the determination of the Gramicidin crystal structures has been done by Wallace and Langs.^[3-8] They found out that the two main species are a channel and a pore structure (Figure 5).

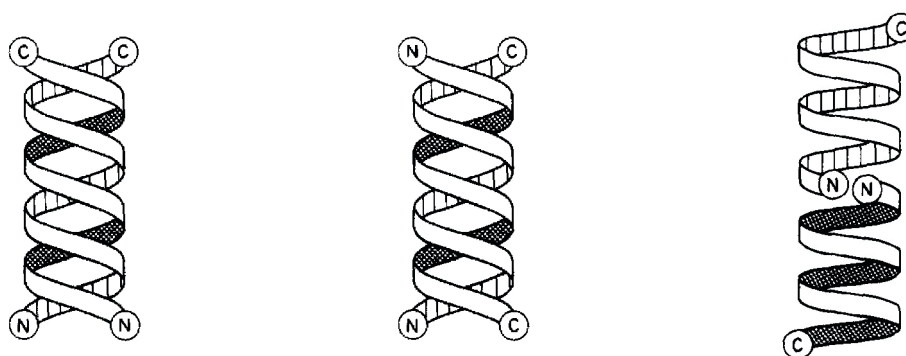


Figure 5: Schematic representation of the parallel and antiparallel double helical pore structures (left and middle) and the end-to-end dimerized channel structure (right) of Gramicidin (taken from^[4])

In the crystal, the pore structure is a left handed antiparallel double helix with varying size and inner diameter, depending on the presence or absence of

incorporated ions. The channel structure is an end-to-end helical dimer, which is only obtained in a lipid complex of Gramicidin.^[9] In both cases, the structures are β -helical and hollow and would meet the requirements for an ion-conducting molecule.

In solution, several interconverting structures are present, making the structure elucidation far more complex. Intensive work on this subject has been done by Urry and Veatch and Blout. Urry was the first one who suggested the existence of a new type of helix after CD- and NMR-experiments with Gramicidin A.^[10,11] The existence of the two double helical pore structures has been derived by Veatch and Blout by means of CD-, NMR- and IR-measurements.^[12,13] Antiparallel and parallel double-helices are interconverting via a monomeric helix.

In membrane-resembling environment, extensive work had been carried out by Urry. He observed ion-conducting activity after a covalent head-to-head dimerization of deformyl-Gramicidin with malonic acid and therefore could prove that the dimeric channel structure was an active form of Gramicidin A.^[14] Several other conformations depending on the experiment conditions were also observed.^[15-17]

In summary, Gramicidin can adopt a variety of different structures, depending on its environment. In the solid state, the antiparallel double-helix occurs, in solution, antiparallel and parallel double-helices are interconverting, whereas in membrane-resembling environment, the head-to-head dimer of the single-stranded β -helix is one active structure.

2.2.2 Synthetic Gramicidin-mimicking Peptides

The fascinating structural variety of Gramicidin gave rise to the synthesis of model compounds for a deeper understanding of the structural behavior of D,L-alternating peptides. Extensive research on the synthesis and structures of hydrophobic homo-D,L-alternating oligopeptides has been carried out by Lorenzi and coworkers.^[18-30] In some of their works, they describe the racemization-free synthesis and structure elucidation of oligo-D-(*alt*)-L-valines and oligo-D-(*alt*)-L-phenylalanines with variable lengths. The most detailed studied model peptide was the oligo-D-(*alt*)-L-valine-system. Di Blasio and Lorenzi were able to solve

the crystal structure of Boc-(L-Val-D-Val)₄-OMe and provided detailed conformational parameters of an antiparallel double-stranded β -helix.^[26] NMR- and CD studies in solution were carried out with members of the series Boc-(D-Val)_m-(L-Val-D-Val)_{(n-m)/2}-OMe, with $m = 0$ or 1 and $n = 7, 8, 9, 12, 15, 16$.^[19] It could be demonstrated that in CHCl₃ (in some cases, solvent mixtures with CH₂Cl₂ or cyclohexane were used), the oligovalines occurred as β -helix. In dependence on the chain length and on the stereochemistry of the last residue in the chain, different types of β -helix could be observed. The four occurring helix-species were the right- and left-handed monomeric $\beta^{4.4}$ -helices (P) $\beta^{4.4}$ and (M) $\beta^{4.4}$ with 4.4 residues per turn and the left-handed antiparallel and parallel double helices $\beta^{5.6}$ with 5.6 residues per turn. In the monomeric $\beta^{4.4}$ -helix, the number of possible hydrogen bonds is smaller than in the $\beta^{5.6}$ -helix ($n-4$ for (P) $\beta^{4.4}$, $n-3$ for (M) $\beta^{4.4}$ and $n-1$ for both $\beta^{5.6}$), rendering the double helix generally more favorable. On the other hand, the steric repulsion of the residues in the tighter $\beta^{4.4}$ -helix is smaller than in the $\beta^{5.6}$ -helix. Since the steric conflicts among the side chains augment on increasing chain length, whereas the differences in the number of hydrogen bonds that can be established in both helices remain constant, the tendency to form $\beta^{4.4}$ -helices should increase with increasing chain length. So only with shorter oligovalines with even n the double helix conformation occurred in an observable degree, whereas oligovalines with odd n and longer ones had the tendency to form exclusively the single stranded $\beta^{4.4}$ -helix (Figure 6).

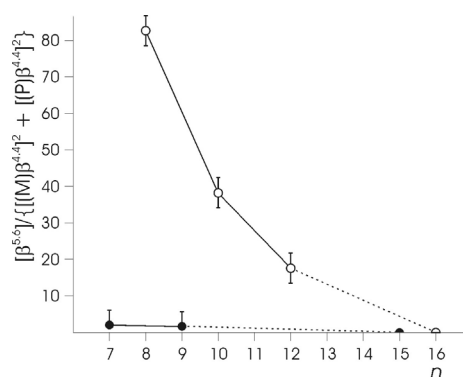


Figure 6: Helix conformation of oligo-D-(*alt*)-L-valines in dependence on chain length. (x-axis: number of residues, y-axis: amount of double β -helix ($\beta^{5.6}$) divided by the amount of monomeric left- and right-handed β -helix ($\beta^{4.4}$)). (taken from ^[19])

The helix twist sense of the $\beta^{4.4}$ -helix was reported to be overwhelmingly left-handed for odd n and prevailingly right-handed when n was even, but this preference was leveling off with increasing chain length. For the left-handed double stranded $\beta^{5.6}$ -helix, the population of the antiparallel $\beta^{5.6}$ -helix was about three times higher than that of the parallel $\beta^{5.6}$ -helix.

Later 2D-NMR-studies treating the solution structure of a D,L-alternating oligonorleucines were carried out by Celda and Navarro.^[31-33] In combination with molecular dynamics calculations, they identified the antiparallel double stranded $\beta^{5.6}$ -helix to be the major conformation of these peptides, which is in equilibrium with the single stranded $\beta^{4.4}$ -helix.

These unique structural properties of D,L-alternating oligopeptides make the D-(*alt*)-L-motif very attractive for polypeptides as well, opening the door to a new class of polymers with new properties and application fields.

2.2.3 D,L-Alternating Polypeptides

Inspired by the Gramicidin motif of a strictly D,L-alternating amino acid sequence, D-(*alt*)-L-polypeptides had been synthesized and investigated, expecting a new class of polymers with just as remarkable structures. The most famous representative of this polymer class is poly(γ -benzyl-D-L-glutamate). Most of the work has been done by Lotz, Heitz, and Spach.^[34-37] They investigated poly(γ -benzyl-D-L-glutamate) in the solid state by IR, X-ray, and electron diffraction and found a family of double-helices for poly(γ -benzyl-D-L-glutamate), strongly depending on the conditions they applied to the polymer (Figure 7).

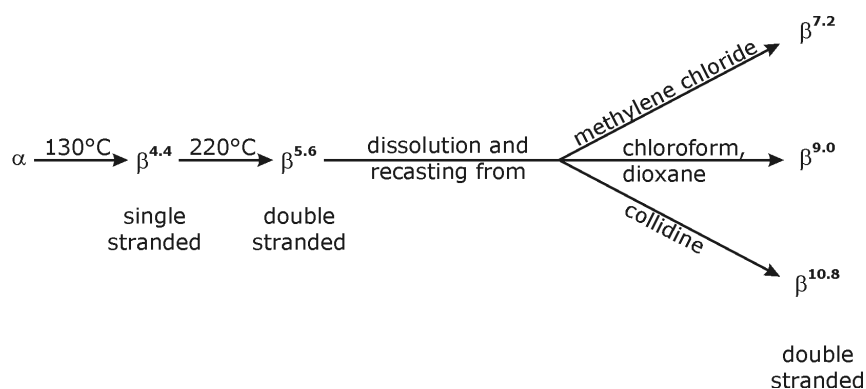
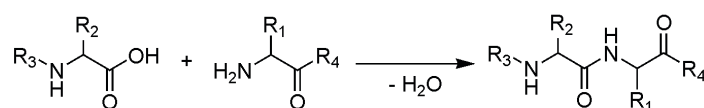


Figure 7: Helix transitions of poly(γ -benzyl-D-L-glutamate) (taken from ^[34]).

A fresh sample of poly(γ -benzyl-D-L-glutamate), dissolved and recast from chloroform at room temperature was in the α -helical conformation. When the same sample was heated to 130 °C, and cooled to room temperature, it was found to exist in a monomeric, single stranded $\beta^{4.4}$ -conformation. After further heating to 220 °C to 230 °C and cooling to room temperature again, the dimeric, double stranded $\beta^{5.6}$ -conformation was obtained, which was only stable in the absence of solvent. When the same sample was dissolved and recast from methylene chloride, the double stranded $\beta^{7.2}$ -conformation was obtained. When dissolved and recast from chloroform or dioxane, the double stranded $\beta^{9.0}$ -conformation and when dissolved and recast from collidine, the double stranded $\beta^{10.8}$ -conformation was obtained. It appears that the size and shape of the $\beta^{7.2}$ -, the $\beta^{9.0}$ -, and the $\beta^{10.8}$ -helix was determined by the solvent, which was included in the hollow core of the helix.

2.3 Peptide Synthesis

Very simplified, the synthesis of peptides is the story of making amide bonds between amino acids (Scheme 1). In reality, peptide synthesis is much more complex.^[38,39] Several factors have to be considered including a proper protecting group strategy, the choice of coupling reagents, secondary structure formation during the synthesis (influencing solubility and reactivity), and purification issues. Since some of these factors are not readily predictable, peptide synthesis needs a certain kind of anticipation for the procedures that is not clearly stated in protocols.



Scheme 1: Net reaction of an amide coupling

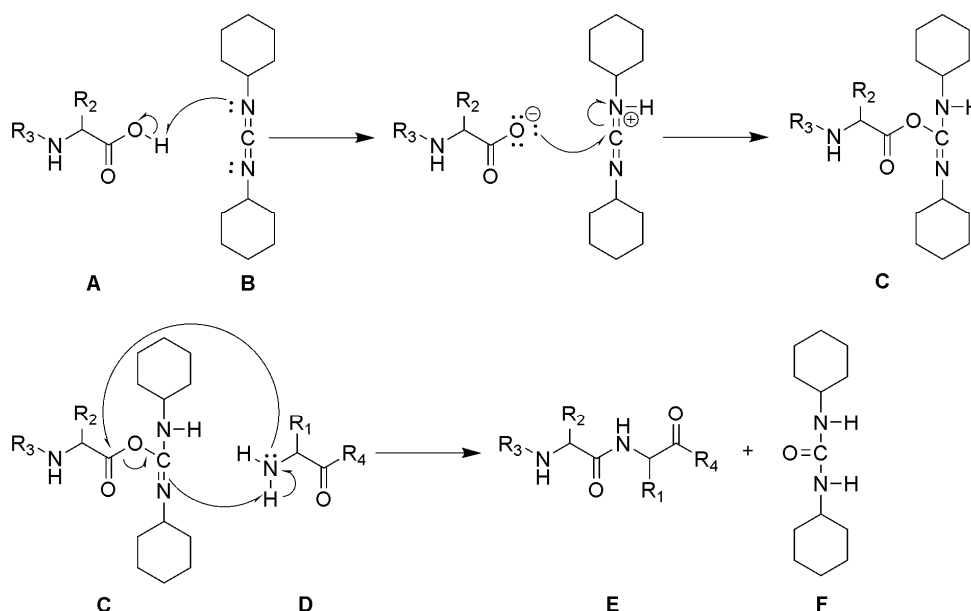
2.3.1 Coupling Reagents

The reaction of a carboxylic acid with a primary amine to the resulting amide as depicted in Scheme 1 would not take place without coupling reagents since the carboxyl group of the acid function is not electrophilic enough to react with the amine. Instead, an acid-base reaction would give the resulting ammonium salt of the carboxylic acid. A coupling reagent transforms the carboxylic acid into a

more reactive species, which is then able to react with the nucleophile (in this case an amine). Additionally it should bind or remove the water, which is liberated within the reaction. The acid activation via the formation of an acid chloride (i.e. with thionylchloride) is very efficient because of its high reactivity towards nucleophiles. Nevertheless it is not a convenient method in peptide chemistry due to the high degree of racemization during the reaction. State of the art coupling reagents can in general be divided in three classes: Carbodiimides, uronium salts, and phosphonium salts.

Carbodiimides

The reaction mechanism of a carbodiimide mediated coupling is depicted in Scheme 2 with DCC as example.



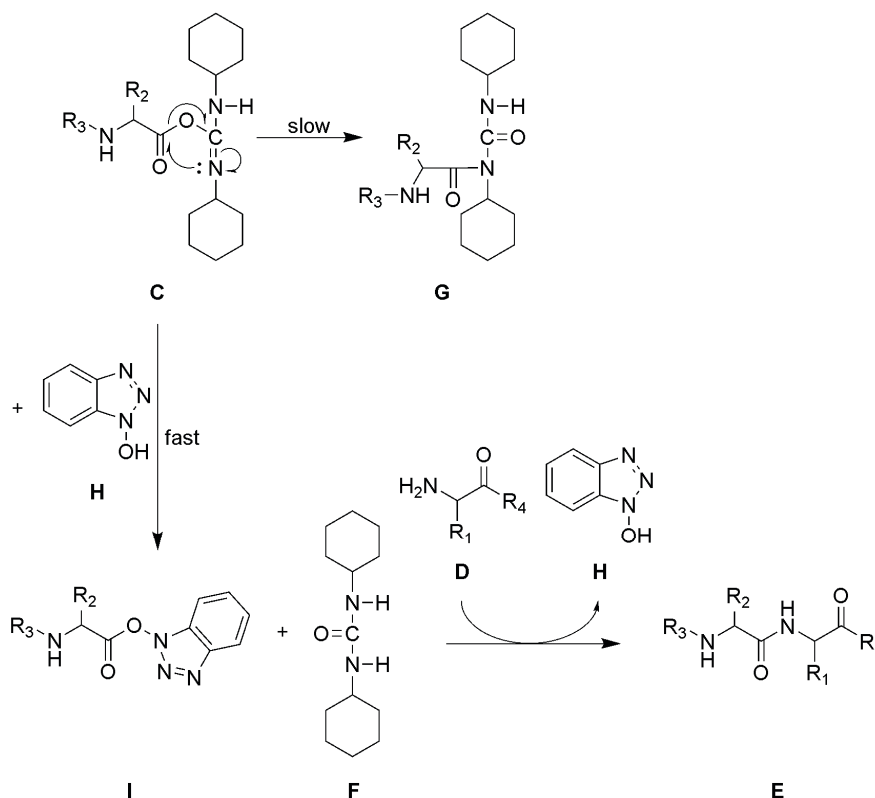
Scheme 2: Reaction mechanism of a DCC mediated peptide coupling

In the first step of the reaction, the carboxylic acid **A** is deprotonated by the lone pair on the carbodiimide nitrogen atom. In the next step, the oxygen atom of the carboxylate attacks the electrophilic carbon atom of the protonated carbodiimide to give the O-acylisourea **C**. In the presence of a potent nucleophile, such as the amino acid **D**, the reaction proceeds as shown. The lone pair on the nitrogen atom in **D** attacks the electrophilic carbonyl group in **C** to form the future amide bond. The resulting tetrahedral transition state, which the molecule passes through is not shown in this scheme. After a

2 General Part

deprotonation/protonation step, the desired peptide **E** and the dicyclohexyl urea is obtained.

A major drawback of this method is the side reaction, which slowly takes place, in case that no potent nucleophile is able to react with **C**. Then, the molecule is proceeding an intramolecular self-acylation (Scheme 3).



Scheme 3: Reaction pathways of the *O*-acylisourea **C** in presence and absence of a potent nucleophile.

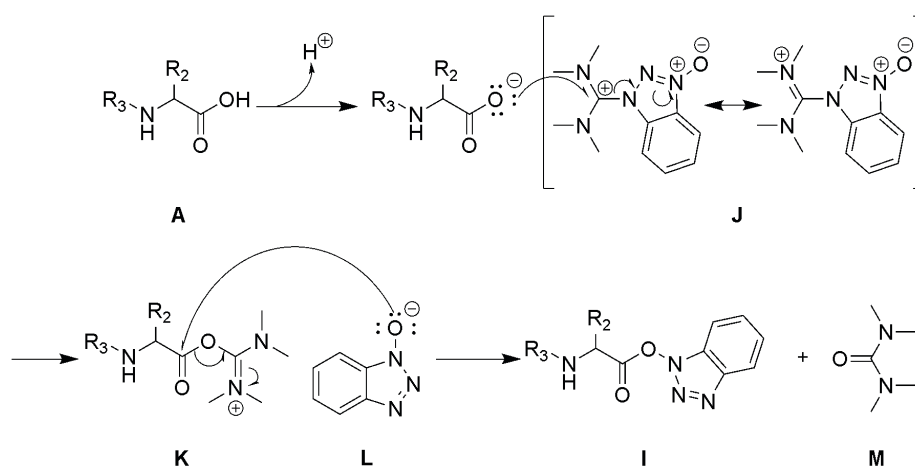
In this self-acylation, the lone pair on the nitrogen atom attacks the carbonyl group. The molecule then passes through a 4-membered, cyclic, tetrahedral intermediate (not shown) to finally give the *N*-acylurea **G**, which is a formal amide derivative and no acylation reagent anymore. In order to avoid this undesired side reaction, a potent nucleophile such as 1-hydroxybenzotriazole (**H**) is added, which reacts fast with **C** to give the active ester **I** and the dicyclohexyl urea **F**. This active ester is still an acylating reagent and conserves a major part of the reactivity of the *O*-acylisourea **C**. In contrast to **C**, the active ester **I** does not decompose. The last step of the sequence follows the same mechanism as shown in Scheme 2 to give the desired peptide **E**. 1-

hydroxybenzotriazole **H** is liberated in this last step, can reenter the reaction, and could in theory be used in catalytical amounts. The most commonly used additives in peptide synthesis are 4-*N,N*-Dimethylaminopyridine (DMAP), Pentafluorophenol and 1-hydroxybenzotriazole (HOBt). It should be noted that the use of DMAP can lead to a certain amount of racemization during the reaction. The use of HOBt is also not undisputable due to the fact that it is explosive.

The mechanism shown in Scheme 2 and Scheme 3 is basic for peptide coupling reactions using a carbodiimide/additive mixture, although the use of DCC is not state of the art anymore. The poor solubility of DCC in the reaction media lowers its reactivity and the resulting dicyclohexylurea can hardly be removed from the resulting peptide, what makes it quite unattractive for peptide couplings. Diisopropylcarbodiimide (DIC) is a carbodiimide with improved solubility, but its resulting diisopropylurea can also be hardly removed from the desired peptide. To circumvent this issue, 1-(3-dimethylaminopropyl)-3-ethylcarbodiimide hydrochloride (EDC) is used. EDC is easily soluble in most organic solvents and after the reaction, excess of EDC and the resulting urea can easily be removed from the peptide by simple aqueous work-up or a short silica filtration.

2.3.1.1 Uronium Salts

Uronium salts are among the most used coupling reagents. The additive (i.e. HOBt) is already included in the molecule and is liberated within the reaction. In theory, the additive can be bound to the activating unit via the oxygen or via the nitrogen atom. The resulting structures are then uronium or guanidinium structures, respectively. Against earlier assumptions Carpino found that the guanidinium structure is the favored one, what makes the name *uronium salts* misleading.^[40] Uronium salts have a higher reactivity than carbodiimides and circumvent the problem of self-acylation. The general reaction mechanism of an uronium salt mediated peptide coupling is shown in Scheme 4.



Scheme 4: Reaction mechanism of an uronium salt mediated peptide coupling.

The sequence starts with the deprotonation of the amino acid **A** and the subsequent nucleophilic attack of the carboxylate on the electrophilic uronium salt carbon atom in **J** to give **K** and deprotonated HOBT **L**. The lone pair of the oxygen atom in **L** attacks the carbonyl group of **K** to give the active ester **I** and tetramethylurea **M**. In analogy to the carbodiimide coupling mechanism (see Scheme 3), **I** reacts to the desired peptide.

In uronium mediated peptide couplings, the addition of a base (DIPEA or collidine) is mandatory in order to dissolve the coupling reagent and initiate the coupling. To suppress racemization processes during the coupling, the addition of HOBT to the mixture is recommended. The most commonly used uronium salts in peptide synthesis are depicted in Figure 8.

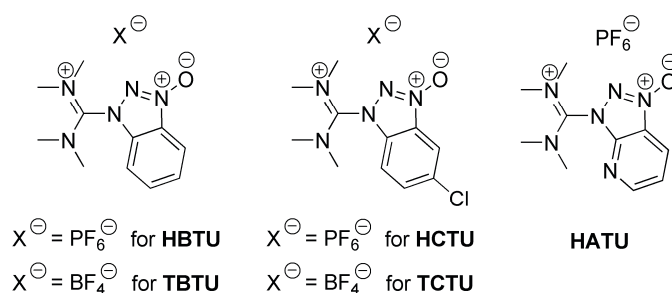


Figure 8: Most used uronium salts in peptide synthesis.

A drawback of uronium salts is their potential reactivity towards amines, what could become an issue in special sequences or in ring closing reactions. This issue can be circumvented with phosphonium salts.

2.3.1.2 Phosphonium Salts

Phosphonium salts are also much more reactive than carbodiimides and together with the uronium salts the most used coupling reagents. The coupling mechanism is comparable to that of uronium salts (see Scheme 4). The structure of the most popular phosphonium salt PyBOP is shown in Figure 9.

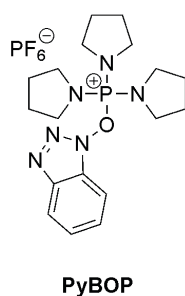


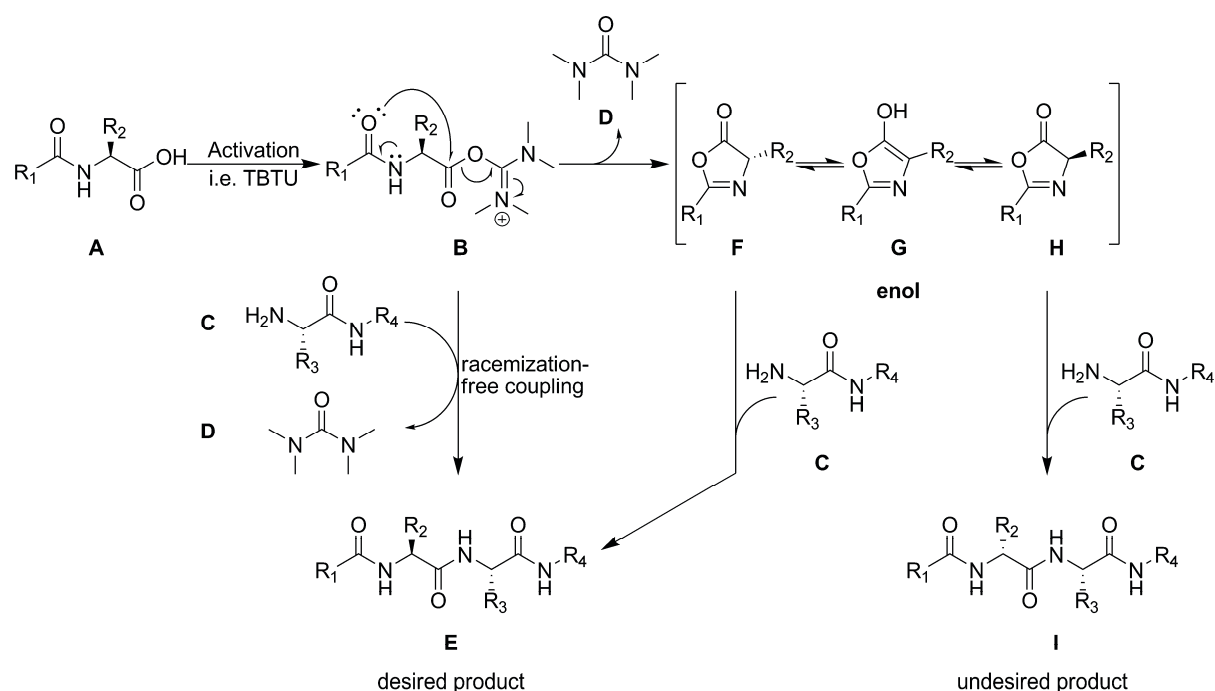
Figure 9: Structure of the most popular phosphonium salt PyBOP.

Due to the high oxophilicity of the phosphor center, HOBT is bound to the activation reagent via the oxygen atom (in contrast to the favored guanidinium structure of uronium salts). An advantage of this oxophilicity is the high chemoselectivity towards *O*-nucleophiles, even in the presence of free amines. This makes it a potent coupling reagent, even for difficult sequences and cyclizations.

These days a variety of different coupling reagents and additives is commercially available, so that the coupling conditions can be adapted very precisely to the reaction. Hence if a reaction does not proceed satisfyingly, a change in the coupling reagents may solve this issue.

2.3.2 Racemization

One of the major problems in peptide synthesis is racemization during the coupling reaction. Since several coupling steps are necessary to build up a peptide sequence, even a very small degree of racemization in each coupling step has fatal consequences. Besides the lowered yield, separation and identification of the product and its epimers is oftentimes impossible. The general oxazolone mechanism for racemization is depicted in Scheme 5.



Scheme 5: Oxazolone mechanism for racemization in peptide couplings.

Amino acid **A** is activated (in this example with an uronium salt) to give activated species **B**, which has in this case two potential reaction pathways. In the presence of a potent nucleophile such as amino acid **C**, the racemization-free coupling to the peptide with the desired stereochemistry **E** can take place. In the absence of a potent nucleophile, **B** can undergo an intramolecular ring closing to the oxazolone **F**, which can tautomerize to the achiral enol form **G**. In this step, the stereochemical information of the molecule gets lost, since **G** can tautomerize back to **F** or with a comparable probability to the oxazolone **H**, which has the opposite stereochemistry than the starting material. The further coupling of **F** with a nucleophile such as the amino acid **C** still gives the desired peptide **E**, but the same coupling of **H** results in peptide **I**, which has the undesired stereochemistry.

The probability of racemization strongly depends on the acidity of the proton on the chiral center C_α , which is also influenced by the electron withdrawing effect of residue R_1 . In the case that amino acid **A** carries a carbamate protecting group (i.e. Boc or Fmoc), no racemization takes place under appropriate conditions. In the case that amino acid **A** is the terminus of a peptide chain, the probability of racemization increases notably. This is also one of the reasons

why peptides are synthesized from *C*- to *N*-terminus. Approaches of inverse peptide synthesis (the peptide chain grows from *N*- to *C*-terminus), as well as fragment condensations oftentimes suffer from racemization.

2.3.3 Protecting Groups

The examples shown so far were very simplified since the reactants were monofunctional so that the carboxylic acid of one amino acid can only react with the amine of another. In reality, amino acids are at least bifunctional, necessitating the use of protecting groups. Protecting groups are blocking reactive centers of the amino acid in order to avoid their undesired reaction during the coupling step. Protecting groups have to be easily removable. The deprotection has to proceed in high yields and ideally without the necessity of a subsequent purification step. In the synthesis of a peptide, at least two different protecting groups have to be used. It is necessary that those two protecting groups are orthogonal to each other. This means that each protecting group can be cleaved in the presence of the other one, without (partial) deprotection of the latter. The more functional groups are incorporated in the peptide (side chain functionality), the more complex the protecting group strategy. The protecting group strategy also depends on the synthesis as such. Peptide chemistry in solution needs one protecting group more than peptide synthesis of the same peptide on polymeric support, since in the latter the *C*-terminus is bound to the support and cannot undergo undesired side reactions. In a linear peptide synthesis, protecting groups of the backbone functional groups are so called temporary protecting groups, since they are cleaved after each coupling step, whereas protecting groups of side chain functionalities are so called permanent protecting groups, since they are cleaved at the end of the synthesis. Therefore, permanent protecting groups have to be stable enough to undergo several coupling/deprotection-cycles.

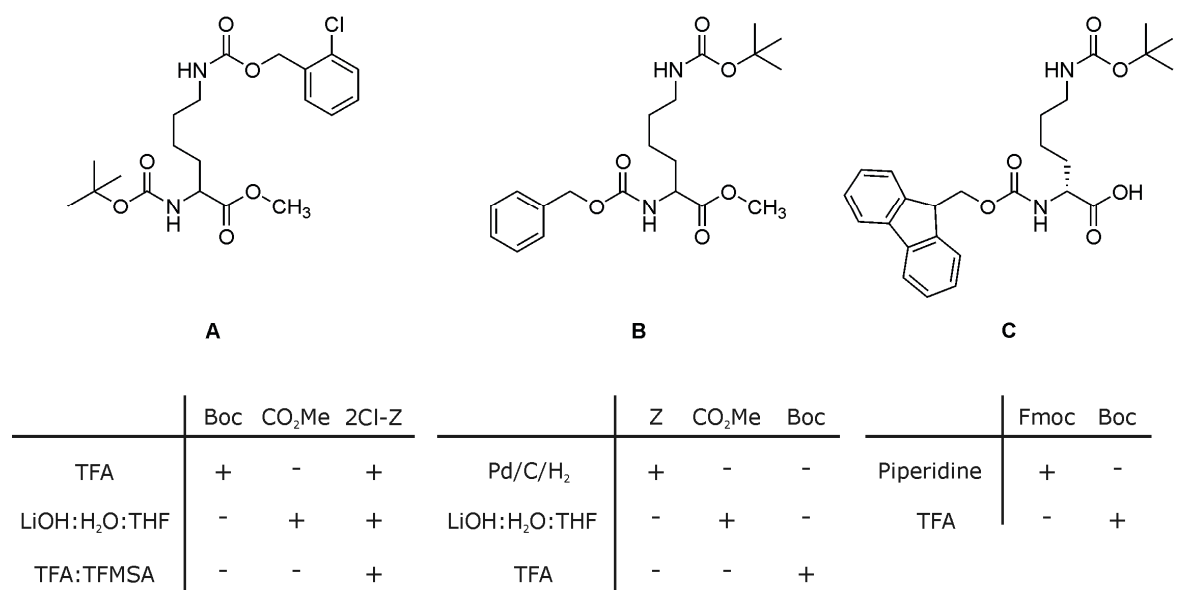


Figure 10: Examples for protecting group strategies.

Some of the most commonly used protecting groups are depicted in Figure 10. The protected amino acid **A** carries a Boc group at the *N*-terminus (temporary protecting group), a methyl ester at the *C*-terminus (temporary protecting group) and a 2Cl-Z group at the amine functionality of the side chain (permanent protecting group). The Boc group can be cleaved with dilute or concentrated TFA in CH₂Cl₂. Under these cleaving conditions, the other two protecting groups are stable. All formed byproducts and excess TFA can easily be removed by washing (synthesis on support) or under vacuum (synthesis in solution). The methyl ester is cleaved under very mild basic conditions with LiOH in water:THF-mixtures. Under these conditions, the other two protecting groups are stable. All byproducts can easily be removed by aqueous work-up (synthesis in solution). The 2Cl-Z group is cleaved under super-acidic conditions with TFA:TFMSA. These conditions are very harsh and cleave the Boc group quantitatively and the methyl ester partially, but since the cleavage of the permanent protecting groups is usually the last step of the synthesis, this is no real drawback. The purification of the resulting peptide proceeds via precipitation procedures (and preparative HPLC). Boc and methyl ester are so called orthogonal protecting groups, whereas the 2Cl-Z group is in this strategy quasi-orthogonal to them. In peptide synthesis on support, no *C*-terminal

protecting group is needed and the resulting strategy is the so called Boc/Bzl-strategy.

Amino acid **B** (Figure 10) carries Z group at the *N*-terminus (temporary protecting group), a methyl ester at the *C*-terminus (temporary protecting group) and a Boc group at the amine functionality of the side chain (permanent protecting group). The Z group can i.e. be cleaved under hydrogenation with Pd/C/H₂ in organic solvents like ethyl acetate or alcohols. Under these conditions, the other two protecting groups are stable. Boc group and methyl ester can be cleaved as described above. In this case, all three protecting groups are orthogonal.

Amino acid **C** (Figure 10) carries a Fmoc group at the *N*-terminus (temporary protecting group) and a Boc group at the amine functionality of the side chain (permanent protecting group). The Fmoc group can easily be removed with dilute piperidine solutions in organic solvents. Under these mild conditions, the Boc group is stable. A byproduct in this reaction is a fluorene derivative, which has to be removed in a purification step. In synthesis on support, this purification is easily done by washing procedures, but since this washing is no option for the synthesis in solution (especially of small peptides), Fmoc develops his high potential only in synthesis on support. The Boc group can be cleaved as described above. The amino acid shown here finds its application in solid phase peptide synthesis. The protecting group strategy is the so called Fmoc/*t*Bu-strategy.

2.3.4 Synthesis In Solution

Until the years 1960, peptide synthesis was done in solution. In a standard protocol (see Figure 11), the two amino acids with appropriate protecting groups are dissolved in a non-nucleophilic organic solvent, such as CH₂Cl₂, DMF or NMP and coupling reagents are added (coupling). After the reaction is complete, aqueous work-up follows. The impure peptide is then purified via column chromatography or recrystallization (work-up / purification) to give the desired, pure peptide, which reenters the cycle. In the next step, the peptide is deprotected (at the *N*-terminus). Most deprotection steps require a subsequent work-up procedure and if necessary also purification. The *N*-deprotected peptide

is then coupled again with an *N*-protected amino acid. Work-up and purification are as described. This procedure has some major drawbacks. The purification of the peptide has to follow after each coupling and is very time consuming. The purification as such is different for every peptide. Recrystallization works only for small peptides and column chromatography also has its limits in peptide size. The solubility of the peptide is another issue, since with increasing length, the solubility of the protected peptides usually decreases. This makes the use of solvents such as DMF or NMP obligate. These solvents and the solubility as such make a purification via the classical means of organic chemistry (column chromatography, recrystallization) impossible. With increasing length of the peptide, the differences between unreacted peptide and product vanish, rendering a purification without preparative HPLC impossible. Peptide synthesis in solution limits the maximum size of the peptide to typically less than 10, in rare cases up to 20 residues.

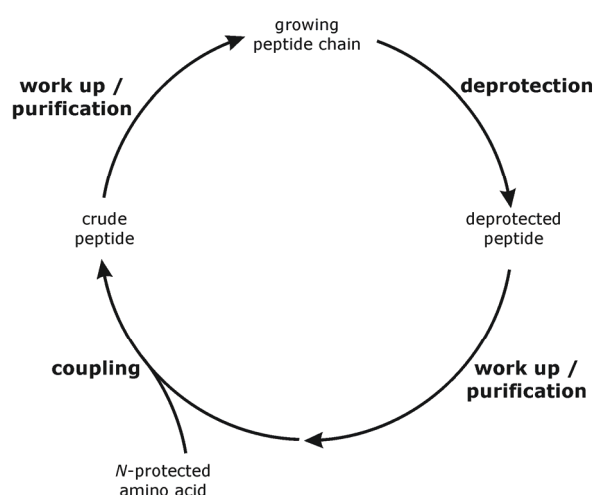


Figure 11: Schematic representation of a linear peptide synthesis in solution.

The only advantages of synthesis in solution are the accessibility to every organic chemist without material effort, the possibility of producing gram scale amounts of peptides and the high quality and purity of the resulting peptides.

In summary, synthesis in solution can make sense for very small peptides (up to a maximum of eight amino acids), if needed on a gram scale. For example, all peptides of the Lorenzi group (see section 2.2.2) were synthesized in solution. Nevertheless, one should always keep in mind that each peptide is unique and

every sequence has its own properties. This makes peptides so fascinating, but also every synthesis unique and demanding.

2.3.5 Synthesis On Solid Support

The two major disadvantages of peptide synthesis in solution are its length limitation and the tedious and time consuming purification steps after each coupling. In 1963, Merrifield published the development of peptide synthesis on solid support (solid phase synthesis), which circumvented these issues and revolutionized peptide chemistry and had a large impact on organic chemistry in general.^[41] For this outstanding development, Merrifield was honored with the Nobel prize in 1984.

In solid phase synthesis the growing peptide chain is anchored to a polymeric support, which is insoluble in the reaction media. The peptide as such is pseudo solvated in the solvent and can undergo chemical reactions as if in solution. Since the peptide remains attached to the insoluble polymeric support, its purification is achieved by simple washing procedures of the polymer. At the end of the synthesis, the peptide is cleaved from the resin and purified. The advantage of this strategy is the fact that it can easily be automatized. These days, solid phase synthesis is done by peptide synthesizers, which are capable to synthesize long peptide sequences in few days. The length limitation of the resulting peptide is about 50 residues.

A schematic representation of a typical solid phase peptide synthesis is depicted in Figure 12. The initial step of the synthesis is the anchoring of an *N*-protected amino acid to the resin (loading). This loading also includes capping of unreacted polymeric chain ends with acetic anhydride. The next step of the protocol is the deprotection of the *N*-terminus of the resin-bound amino acid (deprotection), followed by a washing step to remove impurities (washing). The next step in the synthesis is the coupling of the next *N*-protected amino acid to give the crude, resin-bound peptide (coupling). All impurities are removed by washing the resin (washing). Unreacted peptide chain ends have to be terminated with acetic anhydride in order to avoid further reactions in the next coupling cycles, since this would lead to errors in the sequence (capping). Removing of impurities is achieved by a further washing step (washing). This

cycle is run until the desired peptide sequence is synthesized. The peptide is in the end cleaved from the polymeric support to give the crude peptide (cleavage), which is purified i.e. via preparative HPLC (purification). Main impurities are break-off sequences.

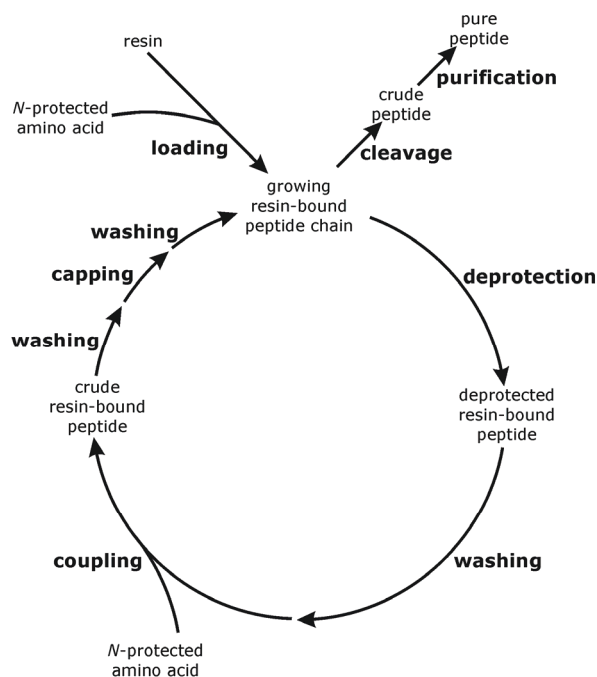


Figure 12: Schematic representation of a linear solid phase peptide synthesis.

Over the years, two protecting group strategies for solid phase synthesis turned out to be very efficient. On the one hand the Fmoc/*t*Bu-strategy and on the other hand the Boc/Bzl-strategy. In Europe, the Fmoc/*t*Bu-strategy is very popular. Fmoc is the temporary protecting group, which is cleaved after every coupling, *t*Bu protecting groups (i.e. Boc) are used as permanent protecting groups. The Boc/Bzl-strategy is leading in the american region. The Boc group is the temporary protecting group and benzyl protecting groups (i.e. 2Cl-Z) are permanent. The Boc/Bzl-strategy works under very harsh reaction conditions, what corrodes the peptide synthesizers very quickly.

A very important aspect in the solid phase peptide synthesis plays the choice of the polymeric support. In general, the support consists of a polymer and a linker, which connects the peptide with the polymer. Important features of the polymer are its swelling properties in the reaction solvent, its loading capacity and its inert chemical behavior. In general, the polymer is polystyrol, which is

crosslinked with 1% *m*-divinylbenzene. The linker can be understood as a sort of permanent, polymer bound C-terminal protecting group, which is cleaved after the synthesis. To improve swelling properties of the resin, spacing units, such as polyethyleneglycol can be placed between the polymer and the linker. These days, a variety of different resins with different linkers is commercially available. The choice of the resin depends on the protecting group strategy and the desired C-terminus.

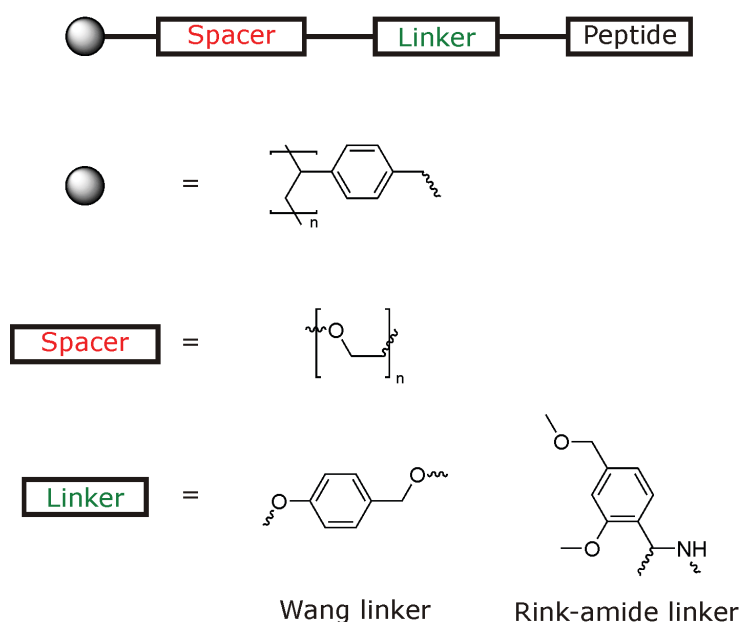


Figure 13: Schematic representation of a peptide synthesis resin.

The schematic representation of a peptide synthesis resin is shown in Figure 14. The spacer unit is optional. The linkers shown are two representative examples for peptide synthesis with Fmoc/*t*Bu-strategy. The Wang linker gives the resulting peptide after cleavage with free COOH-terminus, whereas the Rink-amide linker terminates the peptide as an amide. Not shown are linkers using the Boc/Bzl-strategy. Here, the Merrifield resin and the PAM resin are popular. The former one gives the COOH-terminated peptide after cleavage, the latter one gives the resulting amide.

In summary, solid phase peptide synthesis is the state of the art approach to peptide synthesis. It can be automatized and can produce the resulting peptide much faster as compared to synthesis in solution. With this approach, peptides to a maximum length of 50 residues are realizable, what is approximately five

times the length of a peptide accessible in solution. Its major disadvantage compared to synthesis in solution is the scale limitation to much less than a gram.

2.3.6 Synthesis On Soluble Support

Another approach to peptide synthesis is the synthesis on soluble support.^[42] Here the growing peptide chain is anchored to a polymeric support, which is in contrast to solid phase peptide synthesis soluble in the reaction media. This solubility increases the solvation of the peptide and thereby its reactivity, what makes the coupling steps more efficient.

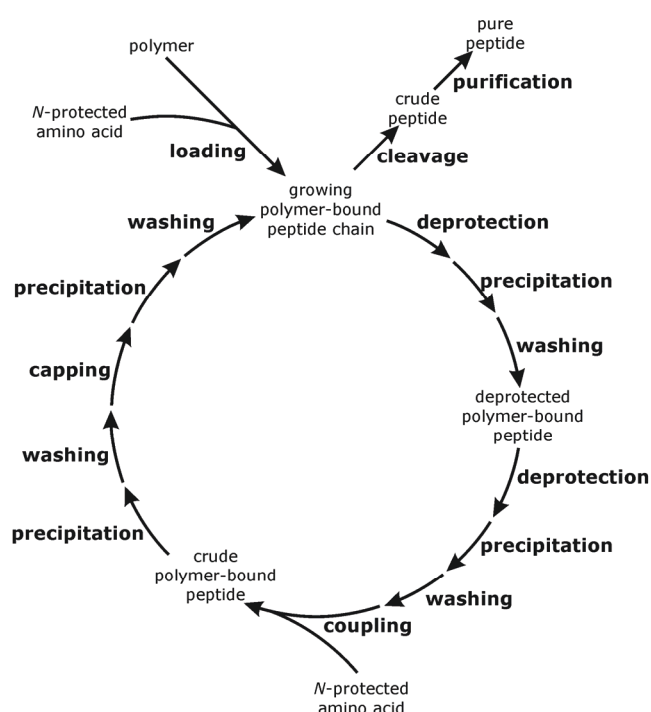


Figure 14: Schematic representation of a linear peptide synthesis on soluble support.

The polymeric support is for example monomethylethyleneglycol with average molecular weights around 5000 g/mol (MPEG 5000). This polymer easily dissolves in all coupling reagents and precipitates quantitatively in cold diethylether. After the reaction, the polymer anchored peptide is precipitated and soluble impurities are removed by washing procedures, so that tedious purifications as in synthesis in solution are unnecessary. The schematic representation of a solution phase synthesis is shown in Figure 14. Every

reaction step requires a subsequent precipitation and washing procedure. One disadvantage of this protocol is the fact that it cannot be automatized, another, that most impurities, which occur in the synthesis are not soluble in diethylether, rendering a purification by washing very inefficient. In summary, solution phase chemistry is no state of the art approach to peptide synthesis.

2.4 Polypeptide Synthesis

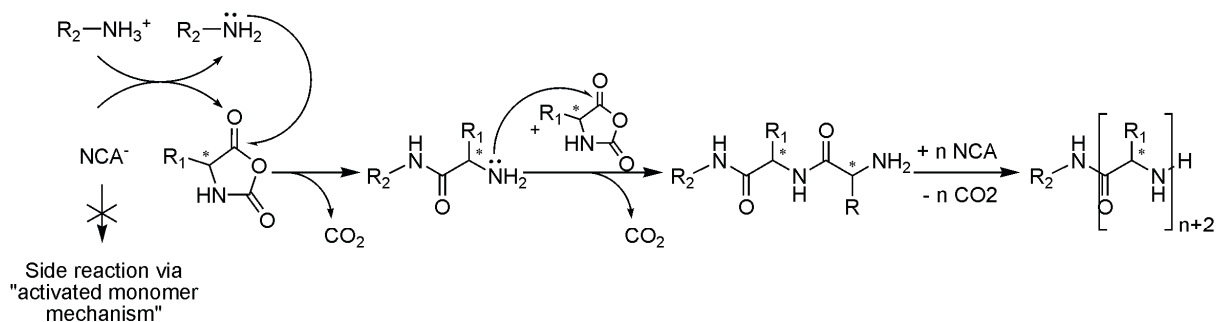
Polypeptides with their interesting structure-property relations and their potential biocompatibility are very important for biomedical applications such as drug delivery or DNA-complexation and -transfection. Polypeptides cannot be synthesized by the conventional means of peptide synthesis described in paragraph 2.3, due to length limitation and small scale, but have to be synthesized via polymerization reactions. The resulting peptides should be optical pure and with a narrow polydispersity.

2.4.1 Synthesis Of Homo-L-polypeptides

The state of the art polypeptide synthesis, which meets the requirements of optical pure products with a small polydispersity index is the ring opening polymerization of α -amino acid *N*-carboxyanhydrides (NCA). The two major approaches to this are shown in Scheme 6.

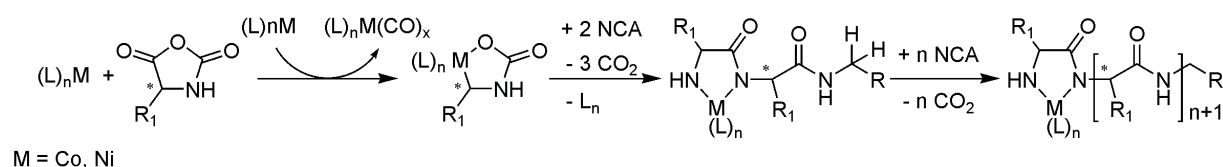
The ring opening polymerizations of NCAs can be initiated by a nucleophile such as a primary amine. A problematic side reaction can be the deprotonation of the NCA by the basic amine initiator. The deprotonated NCA itself can now act as an initiator, leading to an undesired broader polydispersity of the product. Schlaad circumvented this issue by using the ammonium salt of the initiator, which protonated the NCA first and thereby suppressed the side reaction via the so called "activated monomer mechanism" (see Scheme 6, top).^[43] Deming used cobalt and nickel complexes for the polymerization (see Scheme 6, bottom).^[44-47] Both polymerization approaches gave the polypeptides in high optical purity with very narrow polydispersities. With the ring opening polymerization, only homo-polypeptides or co-block-polypeptides can be synthesized.

2 General Part



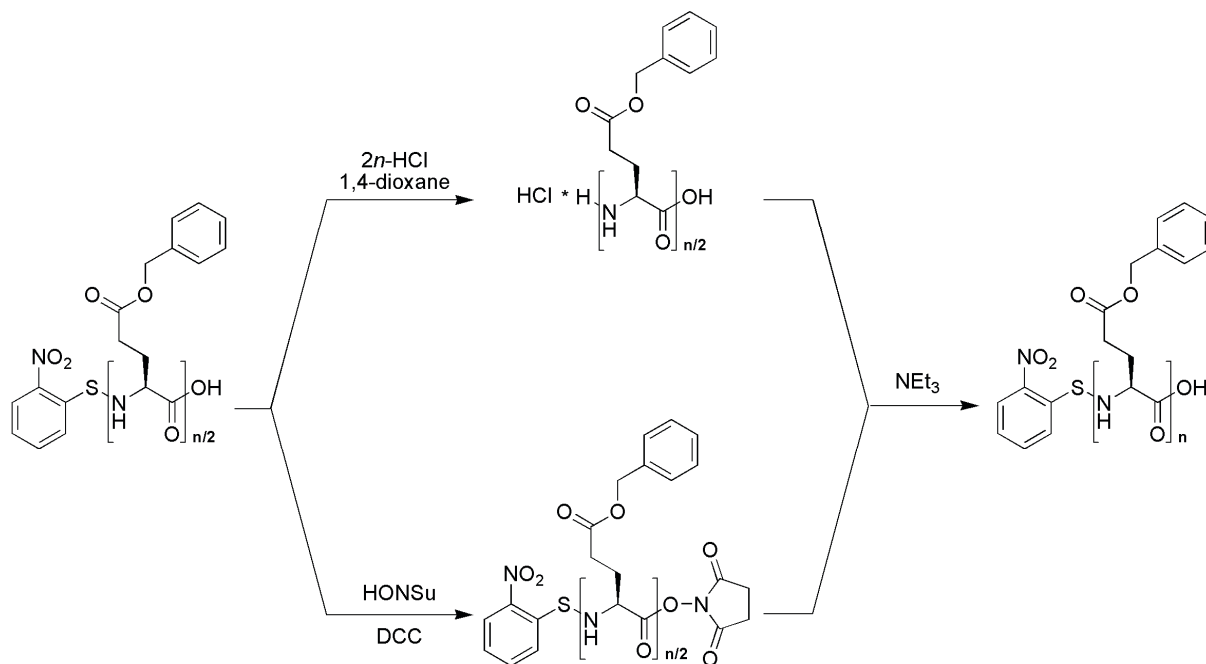
Schlaad

Deming



Scheme 6: Schematic representation of two efficient NCA polymerization approaches.

Shoji realized the synthesis of monodisperse poly(γ -benzyl-L-glutamate) by a divergent/convergent synthesis approach.^[48] He was able to synthesize Nps-[L-Glu(Obzl)]₁₂₈-OH via stepwise synthesis in solution (Scheme 7).

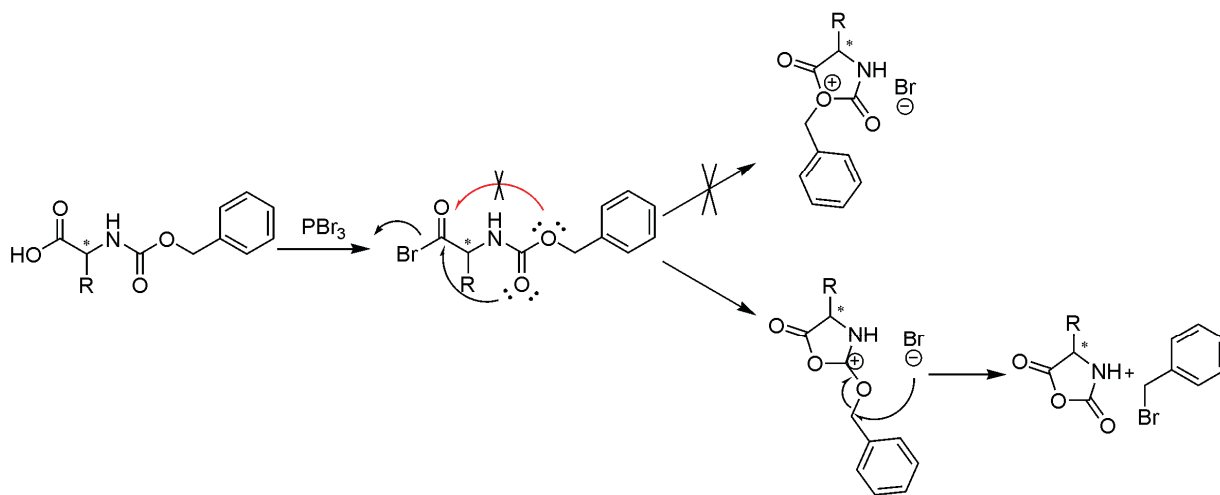


Scheme 7: Divergent/convergent synthesis approach to polypeptides.

With the divergent/convergent (or split/pool) synthesis approach, peptides with high molecular weights can be synthesized very fast, since the peptide chain grows with 2^n , with n equals the number of coupling steps. By this, it is possible to synthesize discrete polymers with well defined length in quite short time. The major drawback of this method compared to NCA polymerizations is the much higher synthetic effort and since it is a repetitive fragment condensation it also suffers from racemization. The longer polymers were only obtained in very low yields, probably resulting of secondary structure formation during the coupling. The poor solubility of most longer protected oligopeptides also limits this synthetic approach to few amino acids.

2.4.1.1 NCA Synthesis

α -amino acid *N*-carboxyanhydrides are the anhydrides of carbamic acids and display very high reactivity. The driving force of their ring opening is the loss of carbondioxide, which is released within the reaction. This makes the NCA a very reactive monomer. Two approaches for the synthesis of NCAs turned out to be very efficient over the past decades.^[49]

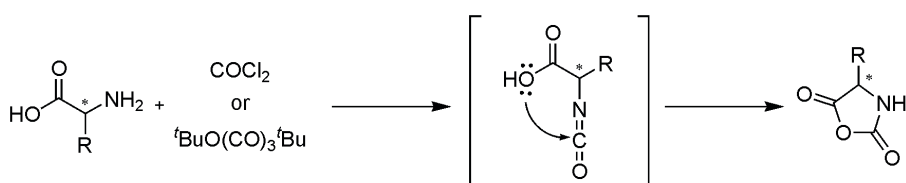


Scheme 8: NCA synthesis after Leuchs method.

The original Leuchs method uses *N*-ethoxycarbonyl and *N*-methoxycarbonyl amino acid chlorides for cyclization.^[50-52] This procedure has the main shortcoming of relatively high reaction temperatures (close to the decomposition temperatures of NCAs). The further development of the Leuchs method is shown in Scheme 8. The improved synthesis uses *N*-

benzyloxycarbonyl amino acid bromides, lowering the reaction temperature to around room temperature. The cyclization proceeds via a nucleophilic attack of the carbonyl oxygen of the Z group (black arrow) on the acid bromide to give the five membered ring. Bromide substitutes oxygen at the benzyl position via a nucleophilic displacement to give the NCA and benzyl bromide. The cyclization does not proceed via a nucleophilic attack of the ester oxygen atom of the Z group (red arrow).

Another approach to the synthesis of NCAs is the Fuchs-Farthing method, which is shown in Scheme 9.^[53-56]



Scheme 9: NCA synthesis after Fuchs-Farthing.

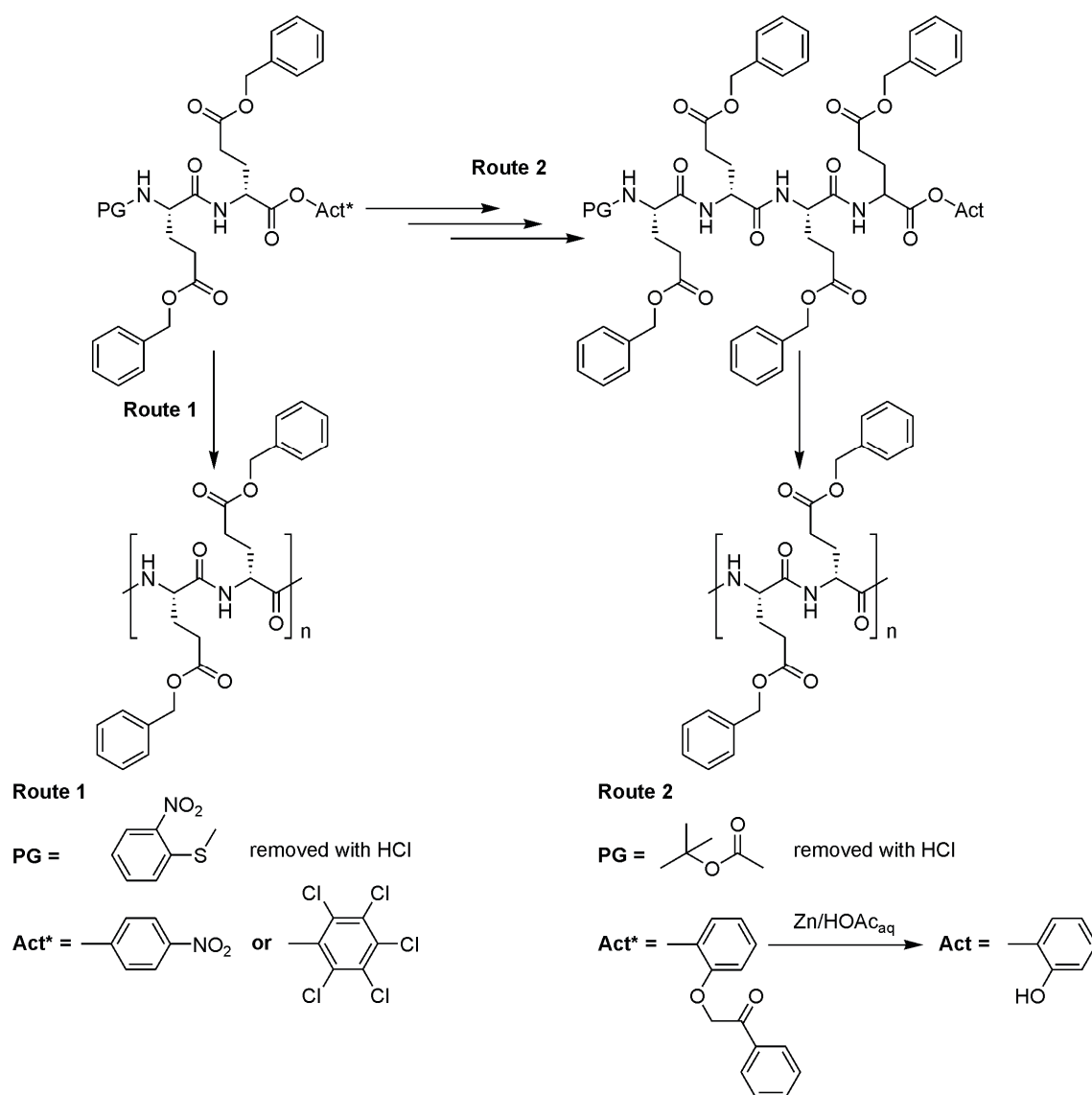
In the Fuchs-Farthing method, an unprotected amino acid is treated with phosgene to give the amino acid isocyanate. In the next step, a nucleophilic attack of the carboxyl oxygen on the isocyanate closes the ring to the desired NCA. The major drawback of this synthesis is the use of gaseous, highly toxic phosgene, of which the exact amount can not be dosed. Endo improved the synthesis by using the solid triphosgene instead.^[57] This is also highly toxic, but much easier to handle.

A very crucial step in the synthesis of NCAs is their isolation and purification after the reaction, since they are very reactive molecules. It is possible to do a very quick aqueous work-up with ice cold water and dilute NaHCO₃-solution to remove HCl and to quench excess phosgene. After this work-up, the product is obtained by crystallization. The NCAs used in polymerizations have to be very pure in order to react properly to high molecular weight polymers with narrow polydispersity. The purification of the isolated NCAs is achieved by several recrystallization steps.

2.4.2 Synthesis Of Homo-D-(*alt*)-L-polypeptides

The synthesis of homo-peptides by ring opening polymerization of NCAs is well established and yields optical pure material in the desired length scale with small polydispersity index, but for more diverse polypeptides with defined amino acid sequences, no such sophisticated procedure is known so far.

The polypeptides investigated by Lotz, Heitz, and Spach (see 2.2.3) were synthesized by polycondensation reactions, yielding the resulting polypeptides within a very broad polydispersity.^[58,59] The synthesis of these polymers is shown in Scheme 10.



Scheme 10: Synthetic approach to homo-D-(*alt*)-L-polypeptides by Heitz and Spach.

In order to obtain a polypeptide with strictly alternating stereochemistry, the D-(*alt*)-L information has to be incorporated into the monomer. A copolymerization of D- and L-configured NCAs would lead to statistical polymers with no determined sequence, i.e. stereocontrol. In a first attempt, Heitz and Spach were using the γ -benzyl protected D-(*alt*)-L-glutamate dimer to synthesize the polypeptide. The *N*-terminus was protected with the *N*-*o*-nitrophenylsulphenyl group, which was cleaved with HCl in diethylether. The carboxylic acid was activated by transferring it into the 4-nitrophenyl ester (ONp) or the pentachlorophenyl ester (OPcp). This synthesis suffers from racemization and the formation of diketopiperazine. The use of OPcp gives the polypeptide in higher yields, but with a higher degree of racemization. To overcome the issue of diketopiperazine formation, they used the γ -benzyl protected D-(*alt*)-L-glutamate tetramer as monomer. For the tetramer synthesis, the *N*-terminus was Boc protected, and the *C*-terminus was protected with a phenacyloxyphenyl ester. After successful tetramer synthesis, the Boc group was removed under acidic conditions and the phenacyloxyphenyl ester was transferred into the activating *o*-hydroxyphenyl ester with Zn/acetic acid. This tetrapeptide was now directly used in polymerization reactions to give high molecular weight polypeptides with no racemization observed.

2.5 Depsipeptides (Ester-isosteres)

The variations of the peptides mentioned so far were always maintaining the backbone integrity, only changing the residues in the sequence or their stereochemistry. Another option is the change of the chemical nature of the peptide chain by replacing amide bonds by amide analogues such as esters, ketomethylene, vinyl, amine or cyclopropene. The approach of replacing amide bonds in peptides by esters is also done by nature.^[60] Therefore, α -amino acids in the chain are replaced by the corresponding α -hydroxy acids (Figure 15 a). The resulting compounds are so called depsipeptides.

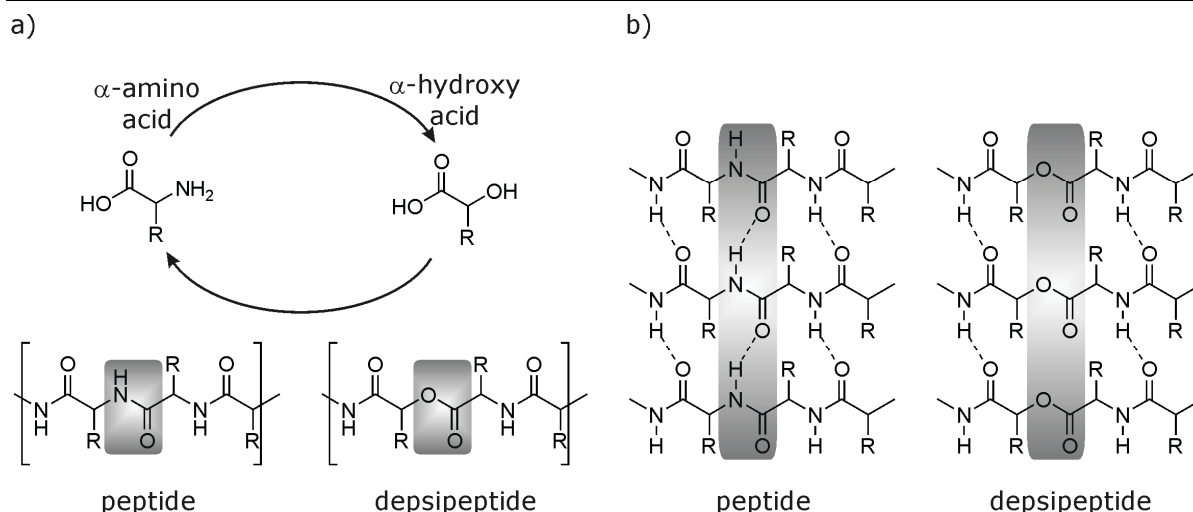


Figure 15: a) Peptide backbone variation by replacing an amino acid by the corresponding hydroxy carboxylic acid, b) hydrogen bonding patterns for peptides and depsipeptides.

Secondary amide linkages and esters have some key structural features in common. They are both planar, have electronic resonance structures and the alkyl substituent on the nitrogen or the oxygen atom prefers to be syn to the carbonyl oxygen. This replacement of amides by esters keeps the number of atoms in the backbone constant, so that the intramolecular distances remain comparable, but has extreme influences on the hydrogen bonding. The formal exchange of one nitrogen by one oxygen atom eliminates one hydrogen bond donor from the molecule, and hence can have drastic consequences for the hydrogen bonding pattern (Figure 15 b). In numerous works, the influence of amide-ester exchange on peptide structures has been investigated.^[61-65] For helical structures, Katakai found by X-ray analysis that the ester group (even the carbonyl) was not involved into intramolecular H-bonding.^[66-69] The depsipeptide solved the issue of a missing hydrogen bond by helix deformation. This deformation was depending on the number of incorporated esters and their location in the backbone. Andersen and Koeppe were investigating the influence of amide-ester exchange in Gramicidin A on ion conductance and found a drastic change in channel formation of the depsi-Gramicidin A.^[70] They replaced the Val-Gly-amide bond of the first two residues in the sequence by a Val-O-Gly ester to give the depsipeptide. The ester bond in this location of the sequence influences intramolecular and intermolecular hydrogen bonding, of which the

latter one is essential for the head-to-head channel formation of Gramicidin. The investigations showed that the channel events were very short and could not be analyzed quantitatively. Experiments with the depsi-Gramicidin/Gramicidin-heterodimer showed a measurable ion conductance providing that the β -helical conformation was possible for depsi-Gramicidin. So in the case of Gramicidin, an amide-ester exchange between the first two amino acids led to a remarkable destabilization of the β -helical conformation and also decreased the head-to-head dimerization ability to afford the channel structure.

2.6 Triazole Isosteres

The use of triazoles as amide mimics in peptides and proteins has become very popular within the last years. This has two main reasons: First, the triazole unit meets the structural and electronical requirements for amide replacement quite well and second, it is synthetically easy accessible. The replacement of an amide by a triazole is structurally more drastic than the replacement by an ester, since it usually elongates the peptide backbone by one atom (Figure 16).

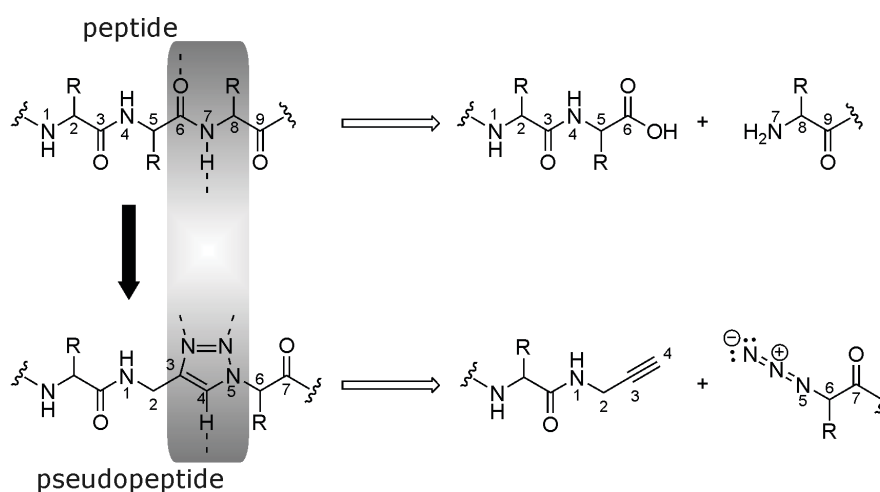


Figure 16: Elongation of the peptide chain by amide-triazole exchange and retrosynthetic approach (hydrogen bonding pattern is indicated with dotted lines).

The rise of triazole as amide mimics was also driven by its easy and high yielding synthesis and the compatibility of the reaction conditions with peptides and proteins. Triazoles can be obtained by the copper-catalyzed Huisgen 1,3-dipolar cycloaddition of azides and alkynes.^[71] This reaction is atom-efficient, regioselective and proceeds in high yields at room temperature in water. The regioselectivity of the reaction yields only 1,4- and no 1,5-triazoles. The

reaction is copper-catalyzed, involving copper center(s) in the catalytic cycle. Yet, the exact mechanism of this reaction has not been elucidated.^[72] The easy accessibility of the azide- and alkyne-derivatives of amino acids makes the so called "Click"-reaction a versatile tool for triazole incorporation into peptides and proteins.^[73] As depicted in Figure 16, azido amino acids and amino acid propargylamides can react to the desired triazoles.

Ghadiri was investigating the synthesis and structure of cyclic peptides with D-L-alternating stereochemistry and their self-assembly to tubular structures.^[74,75] In his work, he also incorporated triazole units into the backbone by synthesizing heterocycles consisting of four amino acids and two triazole units.^[76, 77] In the solid state, these heterocycles self-assembled to solvent-filled nanotubes, which were held together by an extended network of intermolecular amide backbone hydrogen bonds.

Arora replaced every peptide bond by 1,4-triazoles and by this synthesized nonpeptidic foldamers from amino acids (Figure 17 a).^[78] The triazole dimer unit could adopt two *anti* and two *syn* conformations, which are defined based on the relative direction of the dipoles in adjacent rings (Figure 17 b).

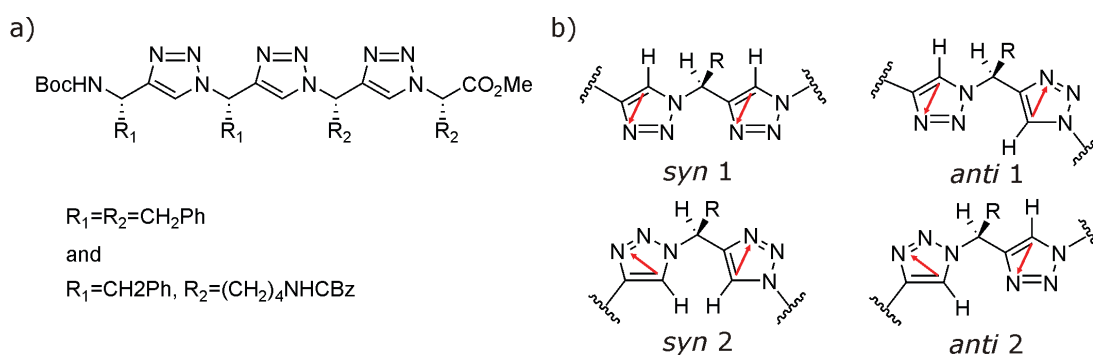


Figure 17: a) Structure of synthesized nonpeptidic foldamers, b) different orientations of the triazoles (qualitative representation of dipole moments with red arrows).

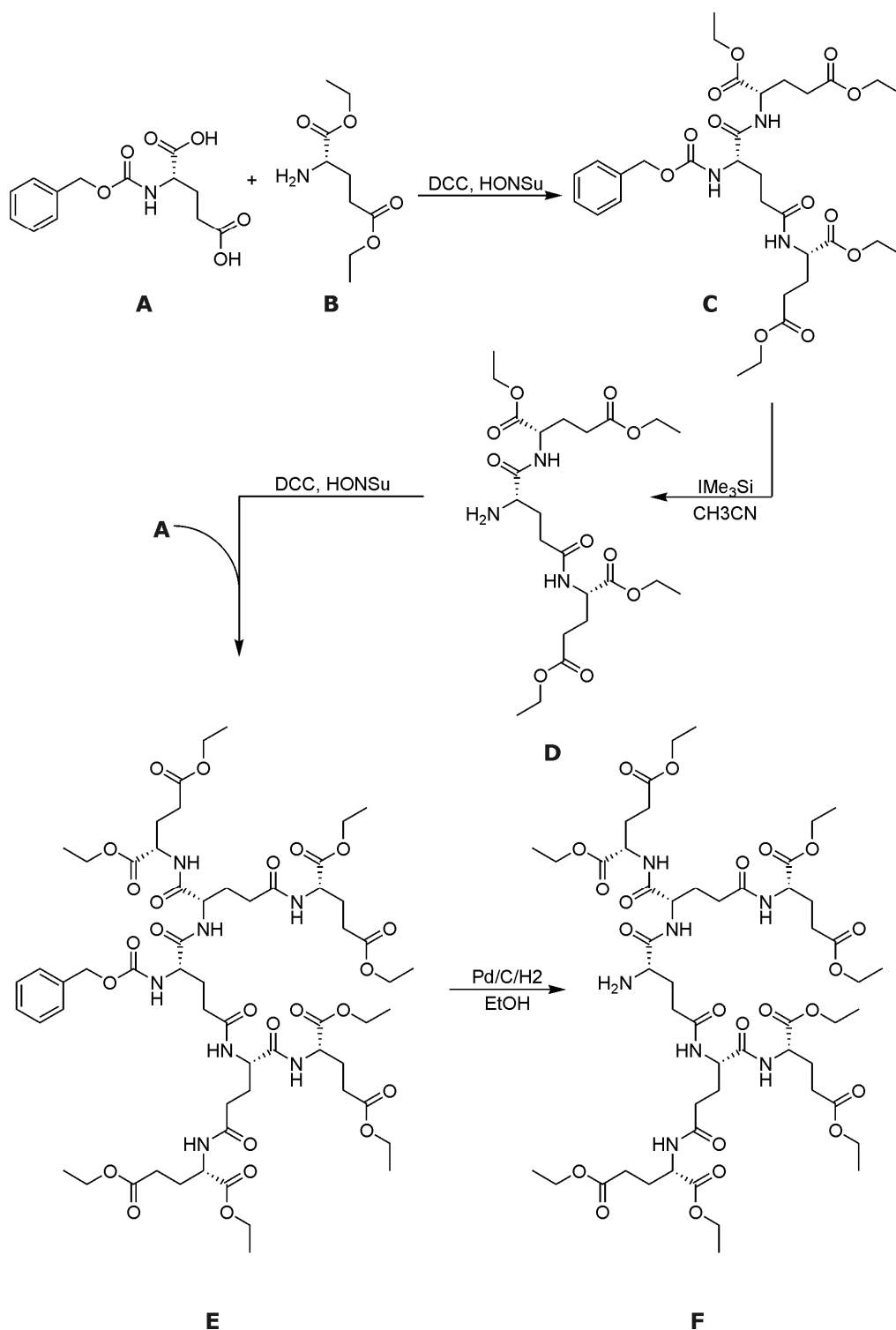
Molecular mechanics and *ab initio* calculations predicted the *anti* conformation to be more stable due to the large triazole dipole (~5 D). Solution NMR analysis suggested that the tetramers shown in Figure 17a adopt a zigzag conformation, which closely mimics the β -strand structure.

The results of these works and the ease of the synthesis show that triazole units can be an interesting mimic for amide bonds and thereby lead to backbone motifs with interesting (structural) properties.

2.7 Peptide Dendrimers

All peptide modifications mentioned so far were focused on side chains and their stereochemistry and on backbone modifications by amide replacement. Branching of peptides differs from these variations since it does not maintain a linear backbone in the molecule, but introduces branching points where the main chain is splitting. This leads to a drastic change in secondary structure formation since the molecules become spherical and cannot adopt the classical peptide secondary structures such as helix, sheet or loop anymore. Branching of peptides requires a functional group in the side chain of the amino acid, that can be addressed. Consequent branching of a peptide leads to a dendritic growth of the molecule, generation for generation.

Peptide dendrimers are totally chiral, rendering them interesting for biomedical applications and recognition processes. Denkewalter reported the first synthesis of a chiral polylysine dendritic macromolecule in 1983, however little attention has been paid to these molecules and their full characterization has never been reported.^[79] Mitchell published the synthesis of a fully chiral glutamate dendrimer.^[80,81] He used the bifunctional glutamic acid as branching unit and could synthesize the glutamate dendrimer up to the third generation (Scheme 11 and Scheme 12).

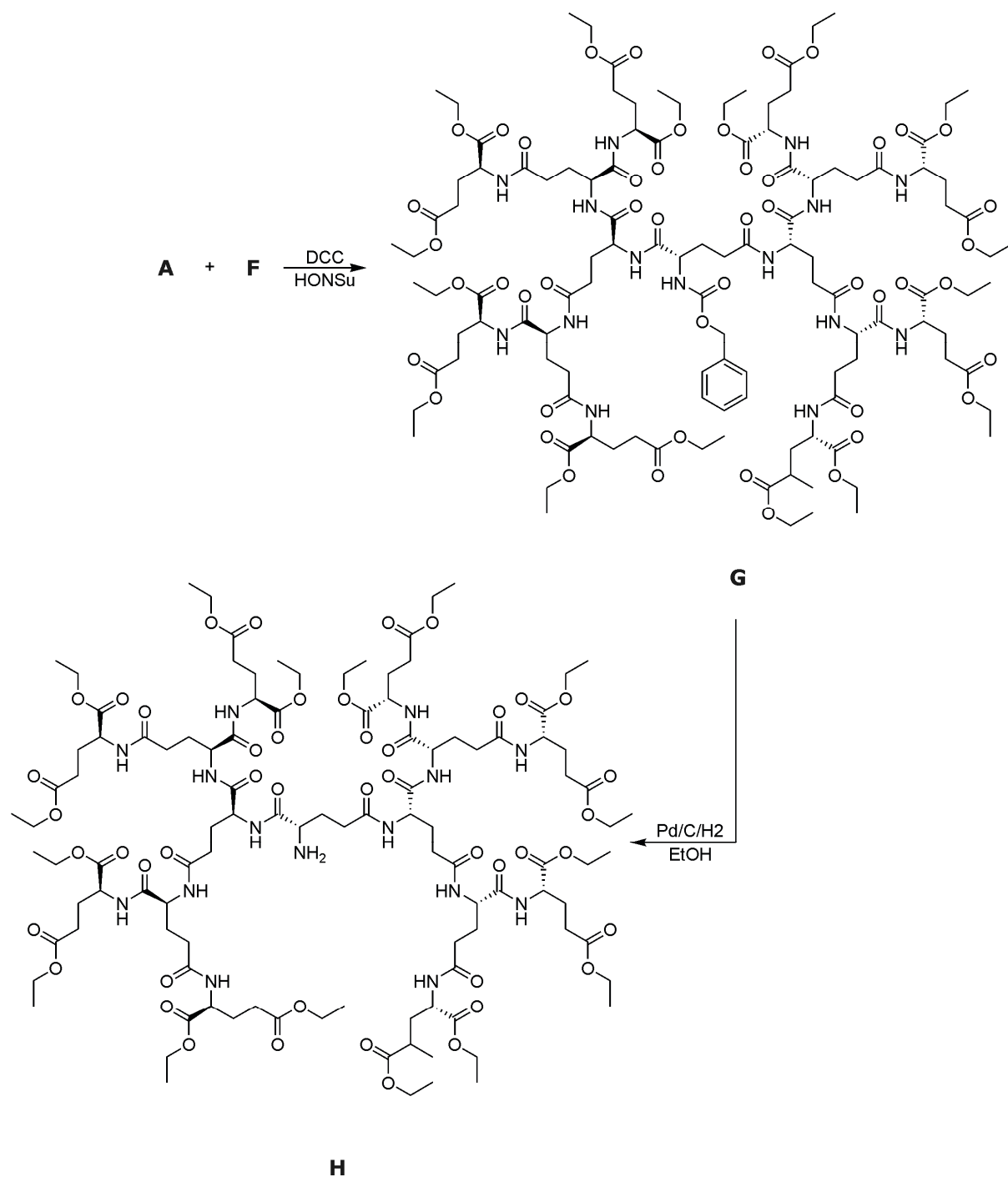


Scheme 11: Synthesis of the fully chiral *N*-deprotected Glu-G2-dendrimer.

The synthesis started from *N*-Z-protected L-glutamic acid **A**, which was coupled with L-glutamic acid diethylester **B** at both acid functionalities to give the *N*-Z-protected first generation dendron **C** in 84% yield. The Z group was removed

2 General Part

with iodotrimethylsilane in acetonitrile to give the *N*-deprotected G1 dendron **D** in 94% yield. In the next step, **D** was coupled with **A** to the fully protected G2 dendron **E** as a single diastereomer in 84%. Subsequent cleavage of the Z group with Pd/C/H₂ gave the *N*-deprotected G2 dendron in 73% yield.



Scheme 12: Synthesis to the fully chiral *N*-deprotected Glu-G3-dendrimer.

Coupling of **A** with **F** gave the fully protected G3 dendron **G** as a single diastereomer in 51% yield. The G3 dendron was obtained by catalytic hydrogenation using Pd/C/H₂ in 53% yield. Further couplings to G4 dendrons were not possible, probably due to shielding of the reactive center in the core of the molecule by the bulky substituents. Further attempts to synthesize dendrimers from aspartic acid or lysine were not as successful.

Other interesting works on the synthesis of amino acid based dendrimers have been reported since then.^[82-90]

2.8 Literature

- [1] R. D. Hotchkiss, Dubos, R. J., *J. Biol. Chem.* **1941**, 141, 171.
- [2] S. B. Hladky, D. A. Haydon, *Nature* **1970**, 5231, 451.
- [3] B. A. Wallace, K. Ravikumar, *Science* **1988**, 241, 182.
- [4] B. A. Wallace, *Prog. Biophys. Mol. Biol.* **1992**, 57, 59.
- [5] D. A. Doyle, B. A. Wallace, *J. Mol. Biol.* **1997**, 266, 963.
- [6] D. A. Langs, *Science* **1988**, 241, 188.
- [7] D. A. Langs, G. D. Smith, C. Courseille, G. Precigoux, M. Hospital, *Proc. Natl. Acad. Sci. U. S. A.* **1991**, 88, 5345.
- [8] D. A. Langs, *Biopolymers* **1989**, 28, 259.
- [9] B. A. Wallace, R. W. Janes, *J. Mol. Biol.* **1991**, 217, 625.
- [10] D. W. Urry, J. D. Glickson, D. F. Mayers, J. Haider, *Biochemistry* **1972**, 11, 487.
- [11] D. W. Urry, *Proc. Natl. Acad. Sci. U. S. A.* **1971**, 68, 672.
- [12] W. R. Veatch, E. R. Blout, *Biochemistry* **1974**, 13, 5257.
- [13] W. R. Veatch, E. T. Fossel, E. R. Blout, *Biochemistry* **1974**, 13, 5249.
- [14] D. W. Urry, M. C. Goodall, J. D. Glickson, D. F. Mayers, *Proc. Natl. Acad. Sci. U. S. A.* **1971**, 68, 1907.
- [15] B. A. Wallace, W. R. Veatch, E. R. Blout, *Biochemistry* **1981**, 20, 5754.
- [16] D. W. Urry, A. Spisni, A. Khaled, *Biochem. Biophys. Res. Commun.* **1979**, 88, 940.
- [17] J. A. Killian, K. U. Prasad, D. Hains, D. W. Urry, *Biochemistry* **1988**, 27, 4848.
- [18] G. P. Lorenzi, C. Gerber, H. Jaeckle, *Biopolymers* **1984**, 23, 1905.
- [19] G. P. Lorenzi, L. Tomasic, *Makromol. Chem.* **1988**, 189, 207.
- [20] G. P. Lorenzi, L. Tomasic, *J. Am. Chem. Soc.* **1977**, 99, 8322.
- [21] G. P. Lorenzi, L. Tomasic, F. Bangerter, P. Neuenschwander, B. Di Blasio, *Helv. Chim. Acta* **1983**, 66, 2129.

-
- [22] G. P. Lorenzi, L. Tomasic, H. Jaeckle, *Makromol. Chem. Rapid Commun.* **1980**, *1*, 729.
- [23] G. P. Lorenzi, H. Jaeckle, L. Tomasic, V. Rizzo, C. Pedone, *J. Am. Chem. Soc.* **1982**, *104*, 1728.
- [24] G. P. Lorenzi, H. Jaeckle, L. Tomasic, C. Pedone, B. Di Blasio, *Helv. Chim. Acta* **1983**, *66*, 158.
- [25] L. Tomasic, A. Stefani, G. P. Lorenzi, *Helv. Chim. Acta* **1980**, *63*, 2000.
- [26] E. Benedetti, B. Di Blasio, C. Pedone, G. P. Lorenzi, L. Tomasic, V. Gramlich, *Nature* **1979**, 282, 630.
- [27] B. Di Blasio, E. Benedetti, V. Pavone, C. Pedone, O. Spiniello, G. P. Lorenzi, *Biopolymers* **1989**, *28*, 193.
- [28] G. P. Lorenzi, V. Muri-Valle, F. Bangerter, *Helv. Chim. Acta* **1984**, *67*, 1588.
- [29] G. P. Lorenzi, T. Paganetti, *J. Am. Chem. Soc.* **1977**, *99*, 1282.
- [30] G. P. Lorenzi, C. Gerber, H. Jaeckle, *Macromolecules* **1985**, *18*, 154.
- [31] E. Navarro, R. Tejero, E. Fenude, B. Celda, *Biopolymers* **2001**, *59*, 110.
- [32] E. Navarro, E. Fenude, B. Celda, *Biopolymers* **2002**, *64*, 198.
- [33] E. Navarro, E. Fenude, B. Celda, *Biopolymers* **2004**, *73*, 229.
- [34] B. Lotz, F. Colonna-Cesari, F. Heitz, G. Spach, *J. Mol. Biol.* **1976**, *106*, 915.
- [35] F. Heitz, G. Spach, *Macromolecules* **1975**, *8*, 740.
- [36] F. Heitz, G. Spach, *Macromolecules* **1977**, *10*, 520.
- [37] F. Heitz, B. Lotz, G. Spach, *J. Mol. Biol.* **1975**, *92*, 1.
- [38] S. Y. Han, Y. A. Kim, *Tetrahedron* **2004**, *60*, 2447.
- [39] F. Albericio, *Curr. Opin. Chem. Biol.* **2004**, *8*, 211.
- [40] L. A. Carpino, H. Imazumi, A. El-Faham, F. J. Ferrer, C. Zhang, Y. Lee, B. M. Foxman, P. Henklein, C. Hanay, C. Mugge, H. Wenschuh, J. Klose, M. Beyermann, M. Bienert, *Angew. Chem., Int. Ed.* **2002**, *41*, 441.

- [41] R. B. Merrifield, *J. Am. Chem. Soc.* **1963**, 85, 2149.
- [42] D. J. Gravert, K. D. Janda, *Chem. Rev.* **1997**, 97, 489.
- [43] I. Dimitrov, H. Schlaad, *Chem. Commun.* **2003**, 2944.
- [44] T. J. Deming, S. A. Curtin, *J. Am. Chem. Soc.* **2000**, 122, 5710.
- [45] T. J. Deming, *J. Polym. Sci. Part A: Polym. Chem.* **2000**, 38, 3011.
- [46] T. J. Deming, *J. Am. Chem. Soc.* **1998**, 120, 4240.
- [47] T. J. Deming, *J. Am. Chem. Soc.* **1997**, 119, 2759.
- [48] T. Ozaki, A. Shoji, *Makromol. Chem. Rapid Commun.* **1982**, 3, 157.
- [49] H. R. Kricheldorf, *α -Amino acid N-carboxy anhydrides and related heterocycles: Syntheses, properties, peptide synthesis, polymerization*, **1987**.
- [50] H. Leuchs, *Berichte Der Deutschen Chemischen Gesellschaft* **1905**, 38, 1937.
- [51] H. Leuchs, W. Geiger, *Ber. Dtsch. Chem. Ges.* **1908**, 41, 1721.
- [52] H. Leuchs, W. Manasse, *Ber. Dtsch. Chem. Ges.* **1907**, 40, 3235.
- [53] A. C. Farthing, *J. Chem. Soc.* **1950**, 3213.
- [54] A. C. Farthing, R. J. W. Reynolds, *Nature* **1950**, 165, 647.
- [55] F. Fuchs, *Ber. Dtsch. Chem. Ges.* **1922**, 55, 2943.
- [56] C. J. Brown, D. Coleman, A. C. Farthing, *Nature* **1949**, 163, 834.
- [57] A. Nagai, D. Sato, J. Ishikawa, B. Ochiai, H. Kudo, T. Endo, *Macromolecules* **2004**, 37, 2332.
- [58] B. Lotz, F. Heitz, G. Spach, *C. R. Acad. Sci., C, Sci. Chim.* **1973**, 276, 1715.
- [59] A. Caille, F. Heitz, G. Spach, *J. Chem. Soc., Perkin Trans. 1* **1974**, 1621.
- [60] Shemyaki.Mm, Shchukin.La, Vinograd.Ei, G. A. Ravdel, Ovchinni.Ya, *Experientia* **1966**, 22, 535.
- [61] M. Goodman, *Biopolymers* **1985**, 24, 137.
- [62] O. Arad, M. Goodman, *Biopolymers* **1990**, 29, 1633.

-
- [63] O. Arad, M. Goodman, *Biopolymers* **1990**, 29, 1651.
- [64] I. L. Karle, C. Das, P. Balaram, *Biopolymers* **2001**, 59, 276.
- [65] E. A. Gallo, S. H. Gellman, *J. Am. Chem. Soc.* **1993**, 115, 9774.
- [66] R. Katakai, K. Kobayashi, N. Yonezawa, M. Yoshida, *Biopolymers* **1996**, 38, 285.
- [67] H. Oku, K. Yamada, R. Katakai, *Biopolymers* **2008**, 89, 270.
- [68] T. Ohyama, H. Oku, A. Hiroki, Y. Maekawa, M. Yoshida, R. Katakai, *Biopolymers* **2000**, 54, 375.
- [69] T. Ohyama, H. Oku, M. Yoshida, R. Katakai, *Biopolymers* **2001**, 58, 636.
- [70] A. R. Jude, L. L. Providence, S. E. Schmutzer, S. Shobana, D. V. Greathouse, O. S. Andersen, R. E. Koeppe, *Biochemistry* **2001**, 40, 1460.
- [71] H. C. Kolb, M. G. Finn, K. B. Sharpless, *Angew. Chem., Int. Ed.* **2001**, 40, 2004.
- [72] V. O. Rodionov, V. V. Fokin, M. G. Finn, *Angew. Chem., Int. Ed.* **2005**, 44, 2210.
- [73] Y. L. Angell, K. Burgess, *Chem. Soc. Rev.* **2007**, 36, 1674.
- [74] D. T. Bong, T. D. Clark, J. R. Granja, M. R. Ghadiri, *Angew. Chem., Int. Ed.* **2001**, 40, 988.
- [75] J. D. Hartgerink, T. D. Clark, M. R. Ghadiri, *Chem.-Eur. J.* **1998**, 4, 1367.
- [76] J. H. van Maarseveen, W. S. Horne, M. R. Ghadiri, *Org. Lett.* **2005**, 7, 4503.
- [77] W. S. Horne, C. D. Stout, M. R. Ghadiri, *J. Am. Chem. Soc.* **2003**, 125, 9372.
- [78] N. G. Angelo, P. S. Arora, *J. Am. Chem. Soc.* **2005**, 127, 17134.
- [79] R. G. Denkwalter, J. F. Kolc, W. J. Lukasavage, (Allied Corp., USA). *Us*, **1983**, pp. 9 pp. Cont.
- [80] L. Twyman, A. E. Beezer, J. C. Mitchell, *Tetrahedron Lett.* **1994**, 35, 4423.

- [81] L. J. Twyman, A. E. Beezer, R. Esfand, B. T. Mathews, J. C. Mitchell, *J. Chem. Res.-S* **1998**, 758.
- [82] F. E. Appoh, D. S. Thomas, H. B. Kraatz, *Macromolecules* **2005**, 38, 7562.
- [83] F. E. Appoh, D. S. Thomas, H. B. Kraatz, *Macromolecules* **2006**, 39, 5629.
- [84] H. Xu, G. R. Kinsel, J. Zhang, M. L. Li, D. A. Rudkevich, *Tetrahedron* **2003**, 59, 5837.
- [85] Y. Kim, F. W. Zeng, S. C. Zimmerman, *Chem.-Eur. J.* **1999**, 5, 2133.
- [86] G. M. Dykes, L. J. Brierley, D. K. Smith, P. T. McGrail, G. J. Seeley, *Chem.-Eur. J.* **2001**, 7, 4730.
- [87] A. J. Brouwer, S. J. E. Mulders, R. M. J. Liskamp, *Eur. J. Org. Chem.* **2001**, 1903.
- [88] D. Ranganathan, S. Kurur, K. P. Madhusudanan, R. Roy, I. L. Karle, *J. Pept. Res.* **1998**, 51, 297.
- [89] D. Ranganathan, S. Kurur, R. Gilardi, I. L. Karle, *Biopolymers* **2000**, 54, 289.
- [90] S. A. Vinogradov, L. W. Lo, D. F. Wilson, *Chem.-Eur. J.* **1999**, 5, 1338.

3 Linear D-(*alt*)-L-peptides

3.1 Linear Oligo-D-(*alt*)-L-peptides

3.1.1 General Considerations

With the elucidation of the Gramicidins' secondary structure and the synthesis of and structural investigations on oligo- and poly-D-(*alt*)-L-peptides, it was shown that peptides with D,L-alternating stereochemistry are able to adopt β -helical conformations.^[1-7] In these conformations, the hydrogen bonding pattern is comparable to that in a β -sheet and the amino acid side chain conformations are located in their respective β -regions. This enables the peptide to adopt a helical structure, where the amino acid residues are on the outside of the helix, revealing a hydrophilic hollow core. In the case of Gramicidin, this hollow core can host ions, which can be transported through the helix, in the case of poly-D-(*alt*)-L-peptides, solvent molecules can be located inside the helix. Thermodynamically, the β -helix represents a local energy minimum for these peptide chains. As the process of folding into the helix is reversible, the peptide chain can adopt a defect-free minimum structure.

With its key features, the β -helix can be considered as a defect-free organic nanotube.^[8,9] Since the secondary structure information is encoded in the primary structure of the peptide, it is possible to create a defect-free organic nanotube just by linking amino acids to a linear peptide, which by itself folds into the tubular structure. All work on D,L-alternating peptides so far has focused on hydrophobic peptides with a low degree of functional groups on the periphery of the helix.^[10-25] In analogy to the pH-dependent α -helical folding and unfolding of polylysine, it is very interesting to create a hydrophilic D,L-alternating peptide, which folds into a β -helix dependent on the pH of the medium. This peptide structure can be considered as a pH-sensitive switchable organic nanotube. Therefore, the aim of this work was the synthesis of oligo-D-(*alt*)-L-lysine in order to create a pH-sensitive switchable β -helices.

3.1.2 Synthetic Considerations

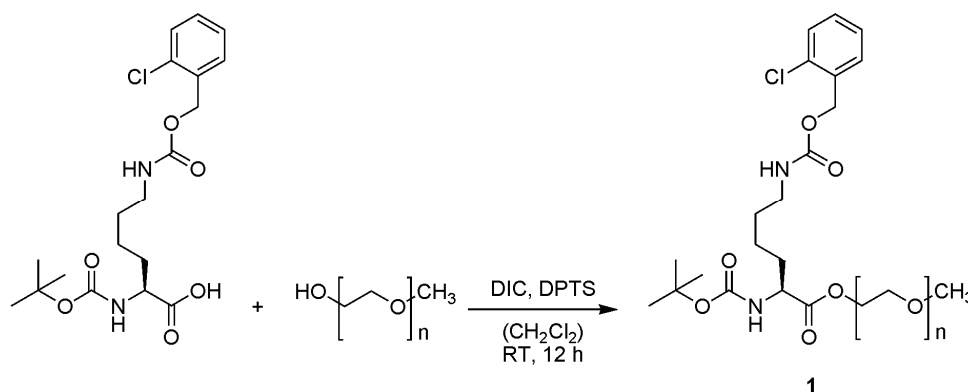
The first important points to be considered regarding the synthesis of the desired peptide are: How long is the targeted peptide sequence? What is the desired amount of peptide? In close analogy to Gramicidin and the work of

3 Linear D-(*alt*)-L-peptides

Lorenzi, the interesting peptide length is within the range of 8 to 20 amino acids. The amount of target peptide ideally should be within the one gram scale. These two limiting factors and the non-existing technical expertise in solid phase peptide synthesis in the Hecht research group eliminated this methodology. The synthesis was carried out in solution as well as on soluble support.

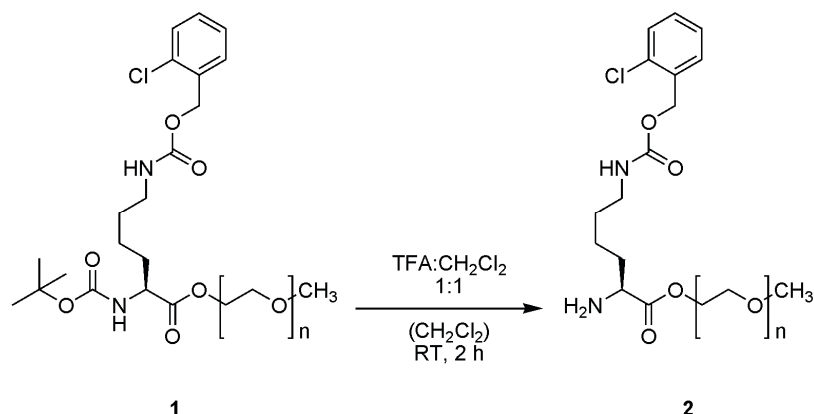
3.1.3 Synthesis On Soluble Support

For the synthesis on soluble support, polyethyleneglycolmonomethylether (MPEG) with an average molecular weight of 5000 g/mol was chosen as the polymeric support. The Boc/Bzl-protecting group strategy was followed, so that Boc-Lys(2Cl-Z) was chosen as amino acid building block. Hence, the deprotection of the growing peptide chain could easily be achieved with diluted TFA-solutions in methylene chloride. Purification was achieved via precipitation in ice-cold diethylether and subsequent washing.



Scheme 1: Anchoring of Boc-L-Lys(2Cl-Z) to MPEG 5000.

The first step in the synthesis is the anchoring of protected Boc-L-Lys(2Cl-Z) to the polymeric support MPEG 5000 (Scheme 1). The coupling was accomplished with DIC/DPTS in methylene chloride. After 12 hours, the reaction was stopped and the product **1** purified via precipitation and washing procedures. The subsequent capping step was done with acetic anhydride and DMAP in methylene chloride. To ensure quantitative coupling of the polymer chain ends, the coupling and capping steps were repeated once.



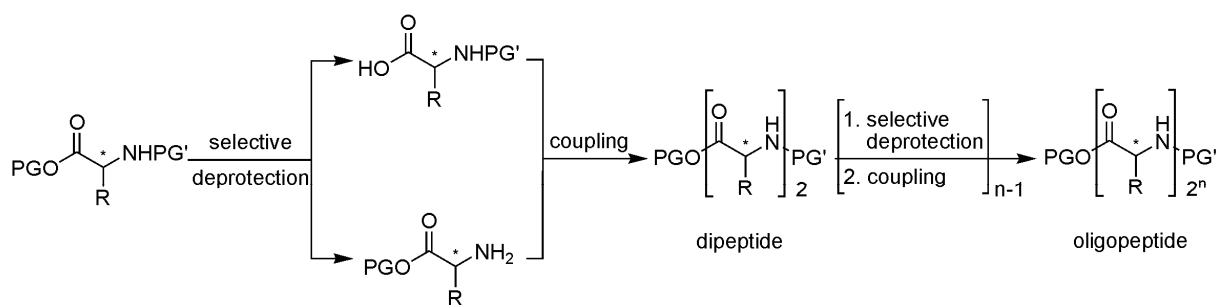
Scheme 2: Cleavage of the Boc protecting group with TFA.

The Boc cleavage of **1** was achieved with TFA in methylene chloride to give Lys(2Cl-Z)-MPEG **2** after precipitation and purification (Scheme 2). After this step, the synthesis on soluble support was stopped, as it turned out to be very unpractical for several reasons. The online monitoring of the reaction by TLC was not possible. The product analysis by NMR was not precise, since the polymer signals were dominating the spectrum, rendering the integration of the amino acid signals and hence the calculation of the degree of polymer loading at NMR concentrations very difficult. Most importantly, the purification of the product by precipitation and subsequent washing suffered from the fact that almost all impurities were also precipitating in diethylether and could not be removed by this rather time consuming procedure. Finally, the mass proportion of amino acid to polymer of approximately 1:15 led to a huge amount of substance that was impractical to handle. Although solution phase synthesis has been advocated as an alternative to solid phase synthesis, we came to the conclusion that for the reasons detailed above, it is not practical and hence subsequent work focused on synthesis in solution.

3.1.4 Synthesis In Solution

The synthesis in solution followed the divergent/convergent synthesis of Shoji,^[26] because it was expected to be very fast and efficient (Scheme 3). The peptide chain grows exponentially i.e. with 2^n , with n equals the number of coupling steps in the synthesis.

3 Linear D-(*alt*)-L-peptides

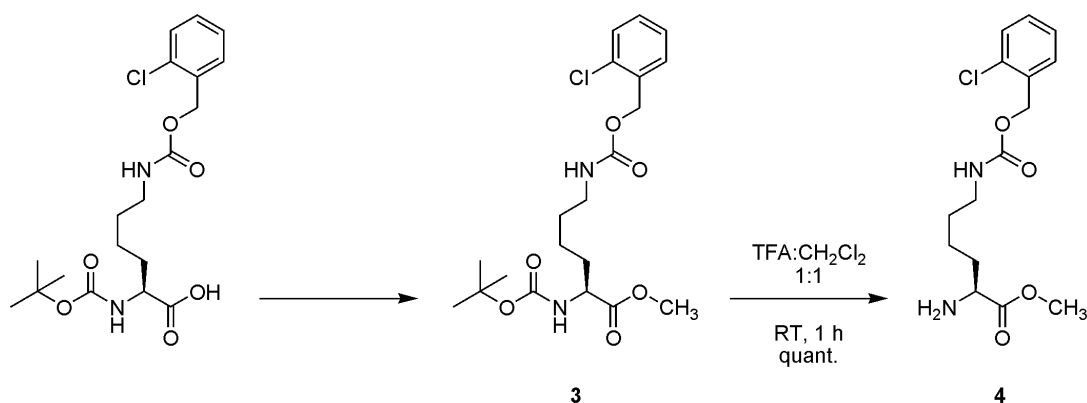


PG orthogonal to PG'

Scheme 3: Divergent/convergent linear growth approach in peptide synthesis.

3.1.4.1 Divergent/Convergent Synthesis

This protocol required two orthogonal temporary protecting groups and another (quasi-)orthogonal permanent protecting group at the side chain. The Boc group is a potent temporary protecting group for the *N*-terminus, which can easily be cleaved using TFA. The permanent side chain protecting group has to be stable under the cleaving conditions of the temporary protecting groups. The 2Cl-Z group is most commonly used in combination with Boc, rendering Boc-Lys(2Cl-Z) the commercially available starting material of the synthesis. Boc-Lys(2Cl-Z) was transformed into the methyl ester to fulfill the protecting group requirements for the targeted synthesis (Scheme 4). In a first attempt, methyl iodide was used to methylate the acid under basic conditions with Cs_2CO_3 . This reaction to the methyl ester **3** proceeded in quantitative yields, but with a loss of ee of 5 to 20%, determined by chiral HPLC. Racemization probably occurred during the work-up procedure, where DMF was evaporated at elevated temperature. Obviously, the temperature of approximately 50 °C in the presence of Cs_2CO_3 as a base enables partial racemization. In order to avoid this racemization, the acid was instead esterified, using DIC and HOBT as coupling reagents. This reaction proceeded much faster, in 98% yield and without any loss of chirality. The product was purified via column chromatography on silica.



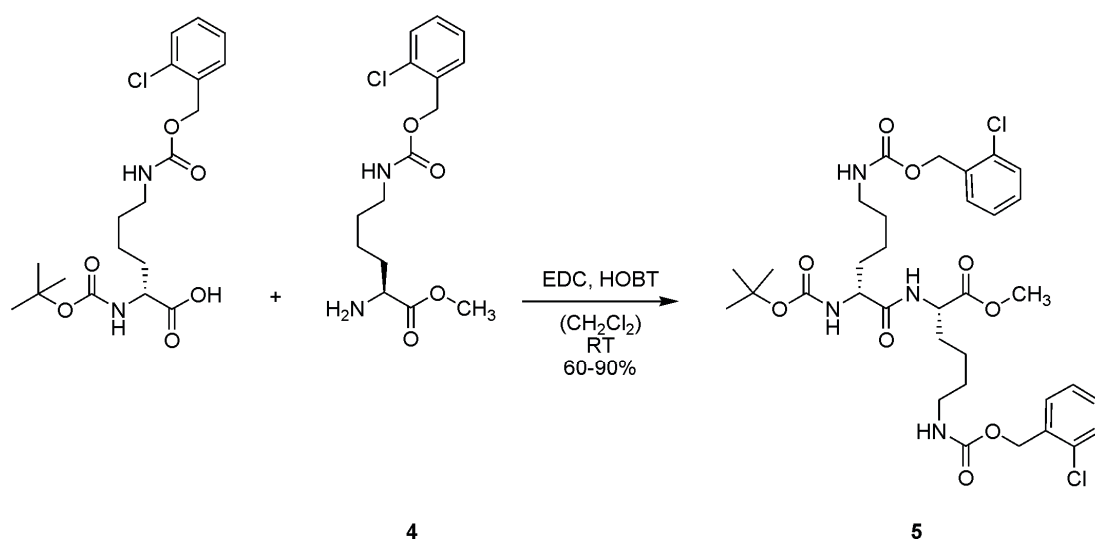
Reaction conditions	Yield	ee
Cs_2CO_3 , CH_3I , DMF, RT, 16 h	quantitative	80% to 96%
DIC, HOBT, $\text{MeOH}:\text{CH}_2\text{Cl}_2$ 1:1 RT, 2 h	96%	>99.9%

Scheme 4: Synthesis to L-Lys(2Cl-Z)-Me starting from Boc-L-Lys(2Cl-Z).

The Boc protecting group was cleaved with TFA in a 1:1 mixture with methylene chloride. This reaction proceeded very fast and gave **4** in quantitative yields without loss of chiral information and in high purity. Lower yields around 90% were most likely caused by loss of the hydrophilic product during aqueous work-up. Further purification of the product was generally not necessary, but could be achieved by column chromatography on silica.

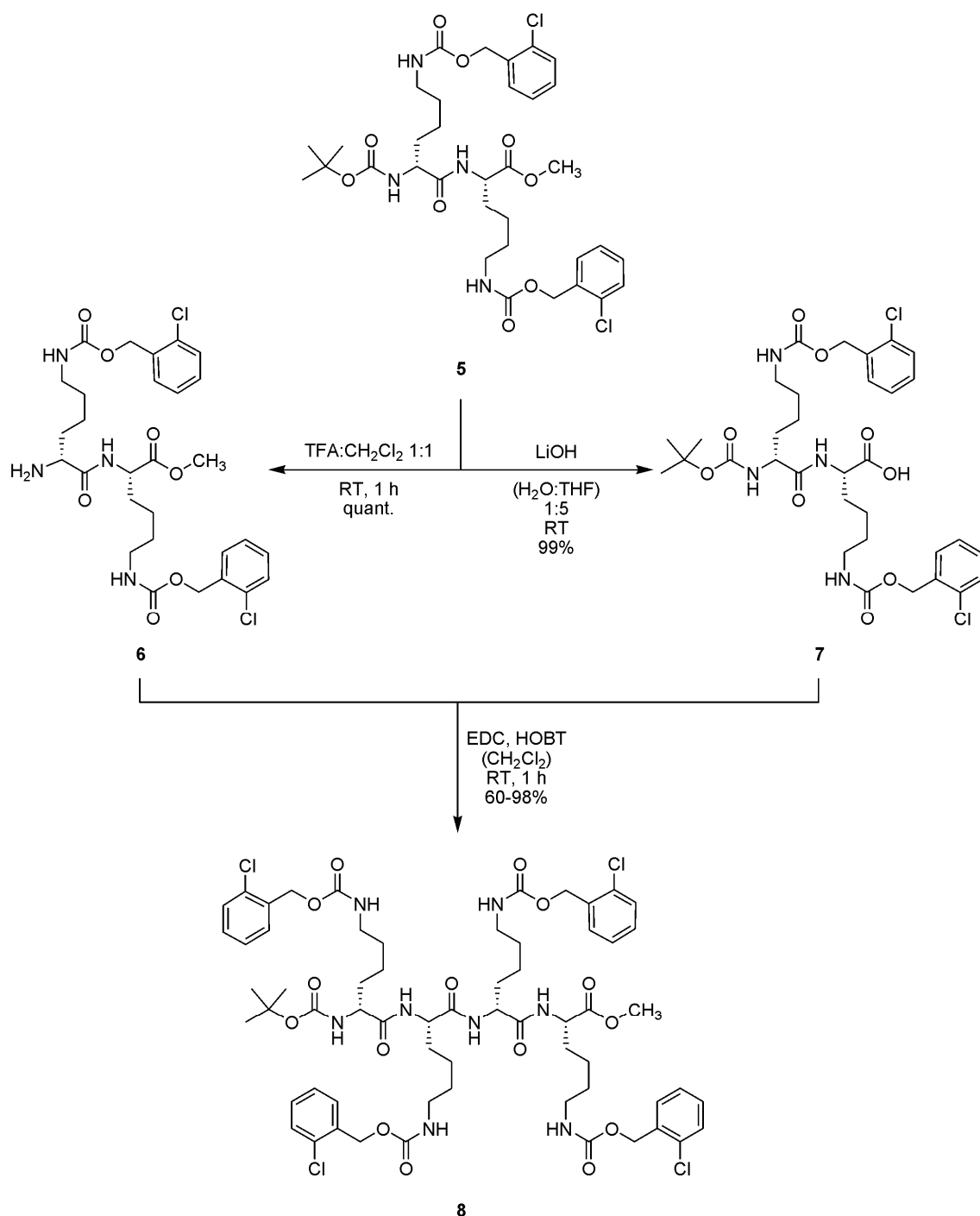
In the next step, **4** was coupled with Boc-D-Lys(2Cl-Z) to Boc-D-Lys(2Cl-Z)-L-Lys(2Cl-Z)-Me (**5**) with DIC and HOBT as coupling reagents (Scheme 5). The high yields (90%) obtained on small scales of this racemization-free coupling dropped notably on bigger scales to 60-80%. Within oligomer synthesis, DIC was replaced by EDC because EDC has several advantages compared to DIC. It is a solid, which is easy to handle and dissolves very well in methylene chloride, it is less toxic and as the most important feature, EDC and its resulting urea are water soluble, hence it can be removed easily by aqueous work-up or by a quick silica plug. Another important point is the reactivity of the reagent, which is comparable with DIC and coupling reactions with EDC gave approximately the same yields.

3 Linear D-(*alt*)-L-peptides



Scheme 5: Coupling to afford key dimer building block **5**.

One half of dipeptide **5** was then deprotected at the *N*-terminus, the other half at the *C*-terminus (Scheme 6). The Boc deprotection proceeded in high yields and without racemization. The saponification of the methyl ester was achieved with LiOH in a water:THF mixture and proceeded without any loss of chirality as well. Earlier attempts, using KOH instead of LiOH led to a noticeable degree of racemization. To ensure racemization-free synthesis, every reaction to the deprotected dipeptides was checked via chiral HPLC. For this purpose, the Boc-D-Lys(2Cl-Z)-D-Lys(2Cl-Z)-Me diastereomer of **5** was also synthesized and deprotected, in order to have a reference for chiral HPLC analysis.



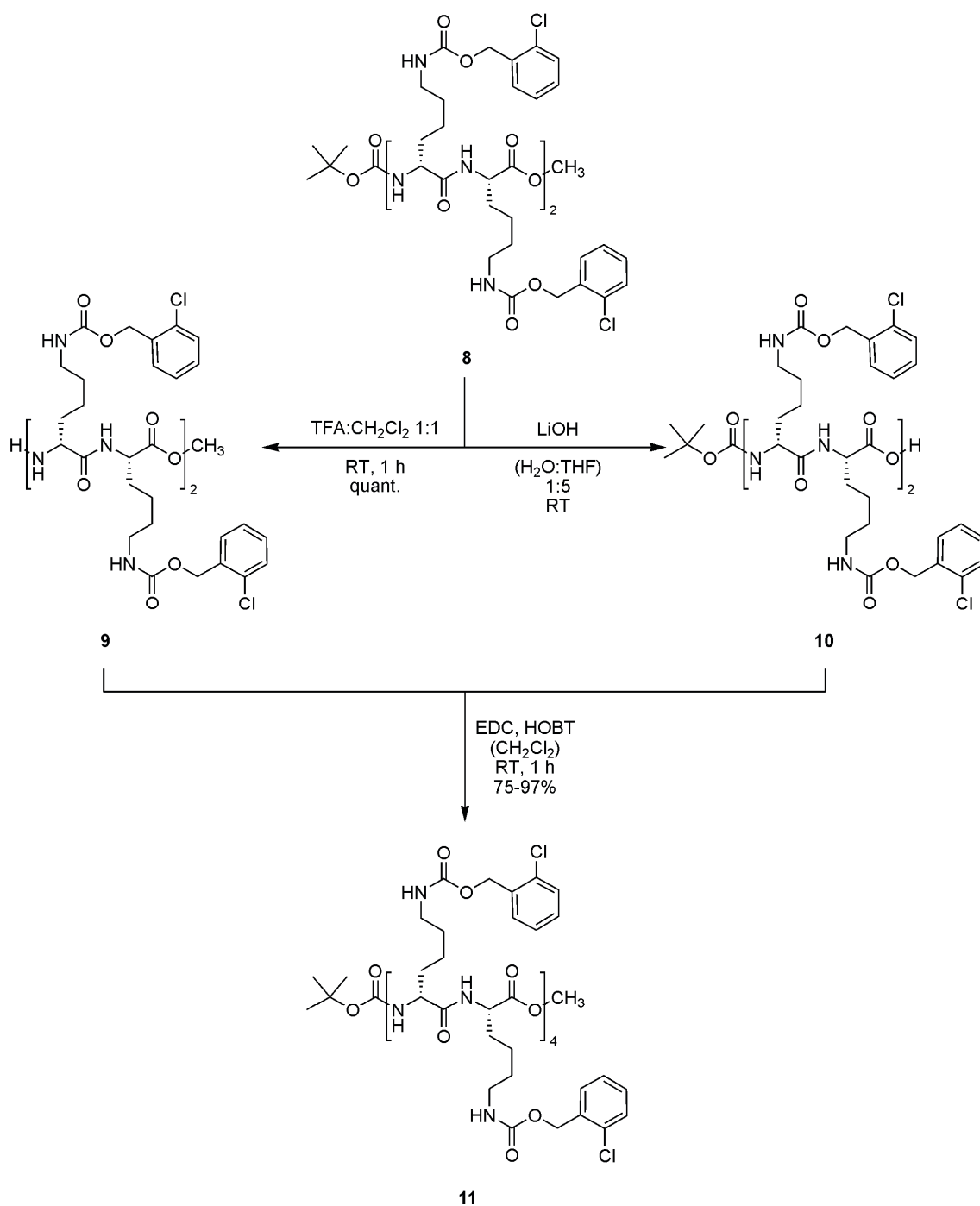
Scheme 6: Divergent/convergent synthesis of tetrapeptide **8** by divergent deprotection reactions of dipeptide **5** to the free amine **6** and the free acid **7** and subsequent convergent coupling.

In the next step of the divergent/convergent protocol, the two dipeptide fragments were coupled to the tetrapeptide **8**. This coupling proceeded in moderate to high yields, depending on the scale of the reaction. Larger scales

3 Linear D-(*alt*)-L-peptides

led to lower yields. Important to notice is the improved purification of the tetrapeptide. After aqueous work-up, the resulting solid was suspended in ethyl acetate and filtered. This procedure was repeated several times to give the product as a white solid in high purity. The purification via this procedure was much faster than column chromatography and it was possible to remove impurities with similar R_F -values.

After improvements of the synthetic protocol, the tetrapeptide **8** could easily be synthesized on a 20 gram scale within 10 days. The next step of the synthesis was the selective deprotection of the tetrapeptide **8** and the subsequent coupling to the octapeptide **11** (Scheme 7). Both deprotection reactions proceeded in high yields and without the necessity of purification of the products. The coupling of the two deprotected tetrapeptide fragments **9** and **10** proceeded in good yields (75-97%) and gave the desired product in high purity after purification (95% according to HPLC). For solubility reasons, the coupling required the addition of DMF, since the deprotected tetrapeptides were not soluble in neat methylene chloride. The reaction to the octapeptide was also feasible on the gram scale, since the purification could easily be carried out as described for the tetrapeptide.



Scheme 7: Divergent/convergent synthesis of octapeptide **11** by divergent deprotection reactions of tetrapeptide **8** to the free amine **9** and the free acid **10** and subsequent convergent coupling.

The deprotection reactions of the octapeptide were done in analogy to the tetrapeptide deprotection and gave the resulting deprotected octapeptides in quantitative yields and high purity. Unfortunately, it turned out that the subsequent coupling of these octapeptide fragments to the hexadecapeptide

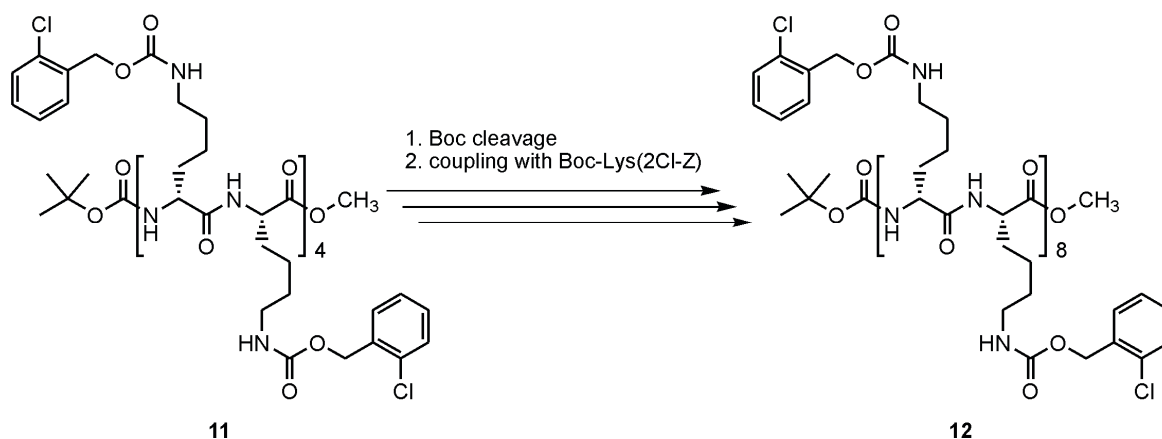
3 Linear D-(*alt*)-L-peptides

was not possible. The reaction resulted in a product mixture, which could not be analyzed by HPLC. Solubility issues and probably secondary structure formation rendered the HPLC analysis impossible.

The next approach to the synthesis of the hexadecapeptide was the coupling of the C- or N-deprotected octapeptide with smaller fragments (i.e: tetrapeptide or dipeptide), but these routes also failed. HPLC-MS analysis of the resulting dodeca- and decapeptides showed two overlapping peaks with identical mass, probably the result of epimerization during the coupling. Several attempts including variation of the coupling conditions and reagents for coupling the N- or the C-deprotected octapeptide all led to similar disappointing results. For this reason, the synthesis to oligomers longer than octapeptide via a divergent/convergent route was abandoned. Hence, for longer oligomers, a more conventional stepwise convergent synthesis starting from octapeptide **10** was used.

3.1.4.2 Stepwise Convergent Synthesis

Starting from the octapeptide **11**, repetitive Boc cleavage of the peptide chain and subsequent coupling with monomer building blocks Boc-L-Lys(2Cl-Z) and Boc-D-Lys(2Cl-Z), respectively yielded the resulting peptide series (Scheme 8).



Scheme 8: Stepwise convergent synthesis of the hexadecapeptide **12** starting from octapeptide **11**.

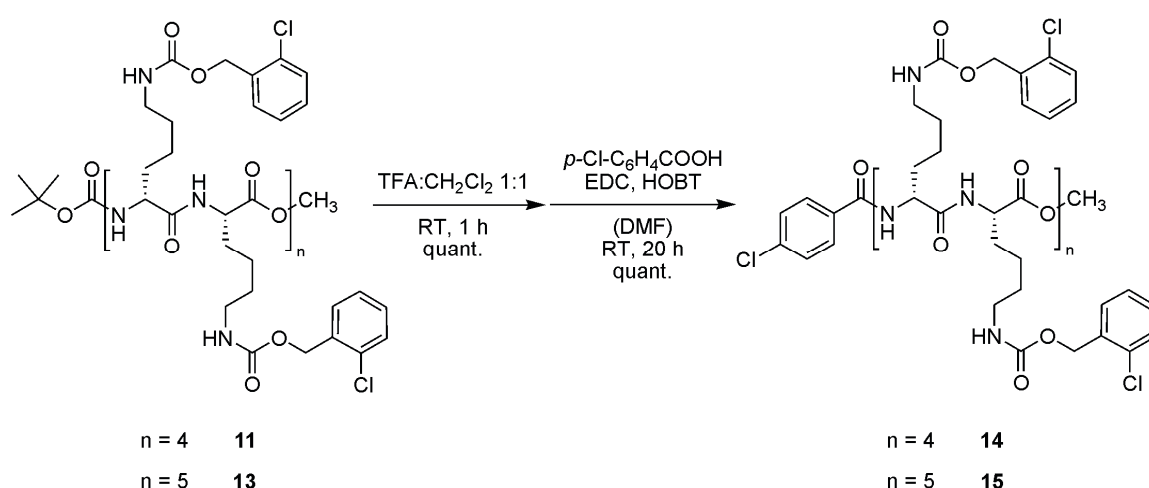
As the peptide chain was growing, the synthesis became more and more tedious. As expected, the solubility of the peptides decreased, further complicating the handling and purification of the substances. Product and

starting material had similar solubilities, rendering the purification of the peptides via suspension and filtration (in analogy to the tetra- and octapeptides) impossible. Column chromatography was hardly possible, since the poor solubility prevented an adjustment of the eluent polarity to the separation problem. From tetradecapeptide on, HPLC traces showed a remarkable tailing, which avoided quantitative analysis of the product and increased with increasing chain length, most likely due to aggregation processes.

In summary, in solution the divergent/convergent synthesis was a very efficient tool to synthesize grams of octapeptide in several days. For longer oligopeptides, in solution stepwise convergent synthesis turned out to be the only option. Although the synthesis was time-consuming, it was possible to synthesize a series of D,L-alternating oligolysines up to a total length of 16 residues in a scale of several hundred milligrams.

3.1.5 Attempted Side Chain Deprotection Of 2Cl-Z Group

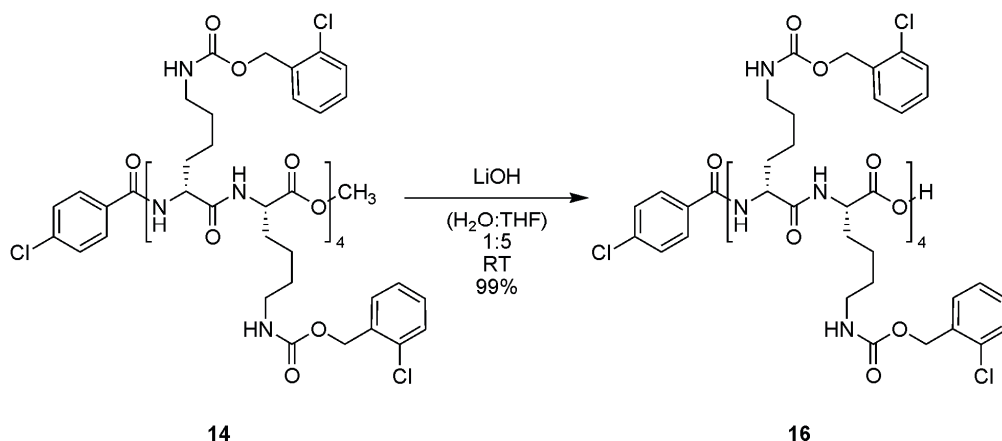
The deprotection of the 2Cl-Z-*N* ϵ -protecting group was the next step in the synthesis. In order to be able to detect the deprotected peptide more easily, octa- and decapeptide were deprotected at the *N*-terminus and coupled with a UV active *p*-Cl-benzoic acid lable (Scheme 9). The Boc deprotection and the subsequent coupling with *p*-Cl-benzoic acid proceeded in quantitative yields and gave the resulting peptide in high purity after column chromatography.



Scheme 9: Labeling of octa- and decapeptide with *p*-Cl-benzoic acid.

3 Linear D-(*alt*)-L-peptides

Since one possible side reaction in the cleavage of the 2Cl-Z group could be the cleavage of the methyl ester, octapeptide **14** was additionally saponified to minimize the number of possible byproducts (Scheme 10). The saponification affords the free acid in very high yields and in high purity.



Scheme 10: Saponification of labeled octapeptide **14**.

With this set of different peptides, the reductive cleavage of the 2Cl-Z protecting group was attempted. The different conditions and results are shown in Table 1. The factors that were varied were the palladium catalyst, the hydrogen source, the temperature, the hydrogen pressure, and the solvent. Two different types of palladium catalysts have been used. Palladium on charcoal and palladium hydroxide on charcoal. The hydrogen source was varied from gaseous H₂ to formic acid, ammonium formate and 1,4-cyclohexadiene. The temperature was varied within the range of 25-75 °C, the hydrogen pressure was raised up to 30 bar. Methanol, ethyl acetate, DMF or 1 M HCl were used as solvents. The reactions were monitored by TLC. When TLC monitoring showed conversion of the starting material to more polar substances, the reaction mixture was worked up and analyzed by ¹H NMR, Capillary Electro-Chromatography (CEC) or ESI-MS. By ¹H NMR, the vanishing protecting group signals were monitored, ESI-MS was used to detect the desired product mass while CEC was indicating how many substances were present in the reaction mixture.

Table 1: Summary of different 2Cl-Z cleavage attempts.

Peptide	Reaction conditions	Result
8	Pd/C/H ₂ ca.2 bar, RT, 4 h	Mixture ¹
8	Pd/C formic acid (20%), RT, 6 d	No reaction ²
8	Pd/C ammonium formate, RT, 24 h	Mixture ¹
8	Pd/C/H ₂ 30 bar, RT, 20 h	Mixture ¹
8	Pd/C 1,4-cyclohexadiene, RT, 6 d	No reaction ²
11	Pd/C/H ₂ ca.2 bar, 14 h, then Pd(OH) ₂ ca 2 bar, 24 h	Mixture ¹
11	Pd/C/H ₂ 10 bar, (<i>i</i> Pr) ₂ NEt, 20 h, then Pd(OH) ₂ and 14 bar, 2 weeks	Mixture ¹
14	Pd/C ammonium formate, 50 °C, 24 h	No reaction ²
14	Pd/C formic acid (10%), 50 °C, 2 h, 60 °C, 2 h	Mixture ¹
14	Pd/C formic acid (>10%), 60 °C, 4 h	Mixture ¹
15	Pd/C formic acid (>10%), 75 °C, 60 h	Mixture ¹
15	Pd/C/H ₂ 8 bar, 60 °C, 4 h, 75 °C, 2 h	Mixture ¹
16	Pd/C/H ₂ 8 bar, 75 °C, 20 h	Mixture ¹
16	Pd/C formic acid, 75 °C, 20 h, then Pd(OH) ₂ formic acid 75 °C, 18 h	Mixture ¹
16	Pd/C/H ₂ 8-30 bar, 75 °C, 2 d	Mixture ¹
16	Pd/C 1,4-cyclohexadiene, 70 °C, 6 h	No reaction ²
16	Pd/C formic acid (>10%), 60 °C, 20 h	Mixture ¹
16	Pd/C/H ₂ 30 bar, 70 °C, 6 h	Mixture ¹
16	Pd/C/H ₂ 1 M HCl _{aq} , 30 bar, 50 °C, 24 h	Mixture ¹
16	Pd/C/H ₂ 1 M HCl _{aq} , 30 bar, 60 °C, 3 h	Mixture ¹
16	Pd/C formic acid, 70 °C, 50 h	Mixture ¹

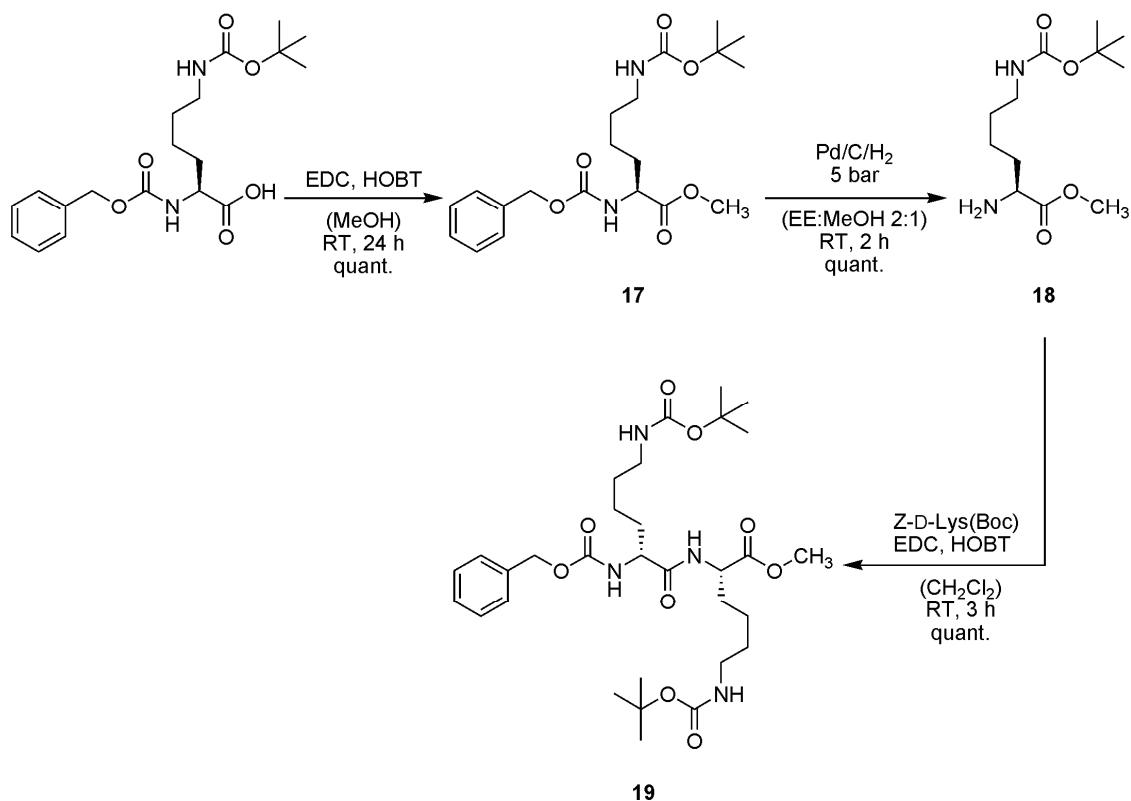
¹ Mixture of partially deprotected peptides, product, starting material and undefined substances. Analysis via ¹H NMR, ESI-MS, CEC; ² As determined via TLC.

In most reactions, the mixtures consisted of starting material, partially deprotected peptides, product and indefinable decomposition products. Clearly, the electron withdrawing effect of the chlorine in *ortho*-position seemed to deactivate the aromatic system, and hence the 2Cl-Z group was too electron deficient to be cleaved under reductive hydrogenation conditions. This is surprising, since the 2Cl-Z group is widely used and despite its robustness expected to be easily cleavable. Summarizing all results, it was not possible to deprotect the peptides quantitatively and isolate the desired products by means of reductive cleavage.

3.1.6 Changed Protecting Group Strategy

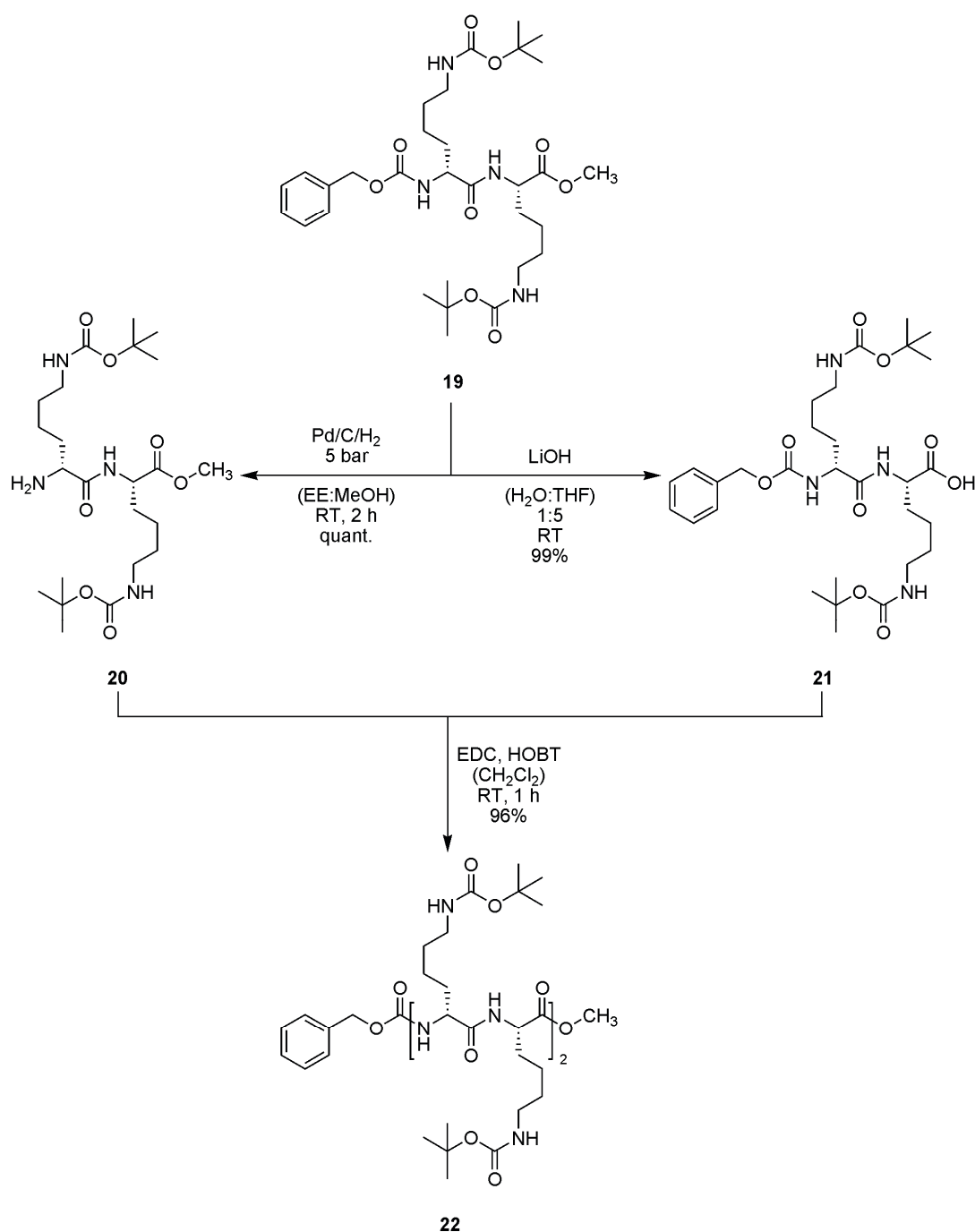
Due to the fact that it was not possible to remove all 2Cl-Z groups quantitatively by palladium catalyzed reductive hydrogenolysis, the synthesis was modified following another protection strategy, involving the easily cleavable Boc group to protect the side chains. The terminal Boc group was exchanged by the Z group, which can easily be cleaved by hydrogenolysis. The methyl ester was kept to give altogether 3 orthogonal protecting groups. The synthesis was planned to follow the divergent/convergent growth approach to the stage of octapeptide.

The synthesis to the dimer (Scheme 11) involved the C-protection of Z-L-Lys(Boc) using EDC/HOBT and methanol. This reaction was high yielding (99%) and gave the pure product **17** according to TLC and NMR even without purification via column chromatography on silica. The Z-deprotection via hydrogenolysis at 5 bar hydrogen pressure proceeded smoothly and gave pure product **18**, which was in the next step coupled with Z-D-Lys(Boc) to the dipeptide **19**. The coupling proceeded in high yields (>95%) and one purification via column chromatography using a solvent gradient gave the product in very high purity (99%) according to HPLC.



Scheme 11: Coupling to afford key dimer building block **19**.

The following deprotection reactions proceeded smoothly and were high yielding (Scheme 12). The Z-deprotection with H₂ on Pd/C under 5 bar pressure proceeded without any problems and gave product **20** in high yield. The saponification also proceeded in quantitative yield and gave product **21**. The two selectively deprotected dimers were coupled to the tetrapeptide **22** using EDC/HOBT. This coupling proceeded in yields >95% after one purification step via column chromatography on silica and gave the tetrapeptide **22** in high purity according to HPLC.

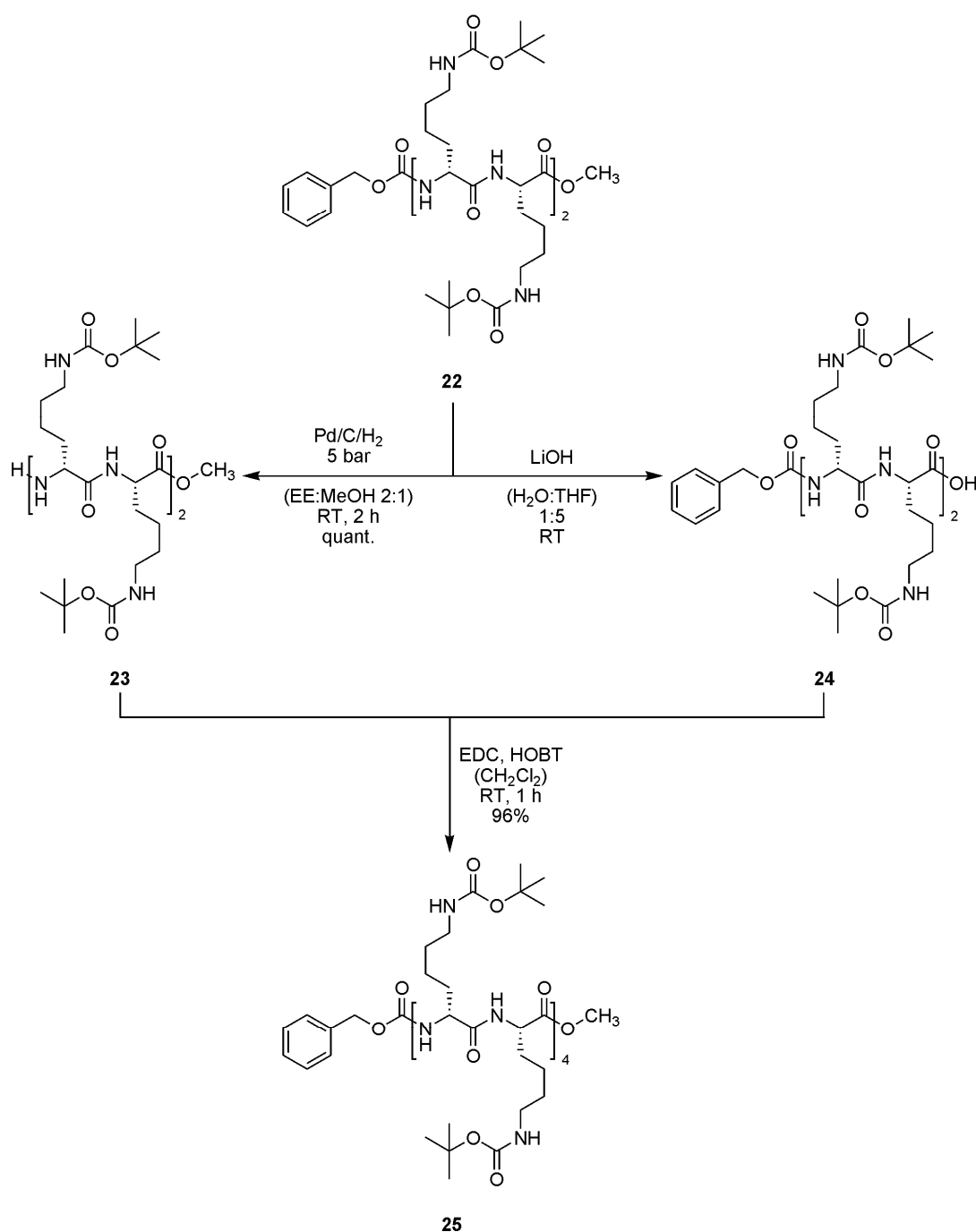


Scheme 12: Divergent/convergent synthesis of tetrapeptide **22** by divergent deprotection reactions of dipeptide **19** to the free amine **20** and the free acid **21** and subsequent convergent coupling.

According to the divergent/convergent synthesis, the tetrapeptide **22** was selectively deprotected at the *N*- and at the *C*-terminus (Scheme 13). The cleavage of the Z group proceeded satisfyingly to **23**, when longer reaction times were chosen and when the reaction was monitored by TLC. The

saponification of the methyl ester was not successful. TLC analysis of the isolated product after work-up showed three spots, of which the most polar was expected to be the desired product **24**. ESI-MS of the mixture showed only the mass of the desired product. TLC monitoring of the reaction showed that product and side products were formed simultaneously. At 0 °C TLC monitoring showed exactly the same phenomenon, only proceeding more slowly.

3 Linear D-(*alt*)-L-peptides



Scheme 13: Attempted synthesis of octapeptide **25** via divergent/convergent synthesis.

Separation of the pure product via column chromatography on silica was possible but very time and solvent consuming and therefore not practical. When the reaction was run for 20 h, HPLC-ESI-MS did not show any evidence for neither product, nor starting material. The elucidation of the outcome of this reaction seemed to be important since the resulting octapeptide could not be

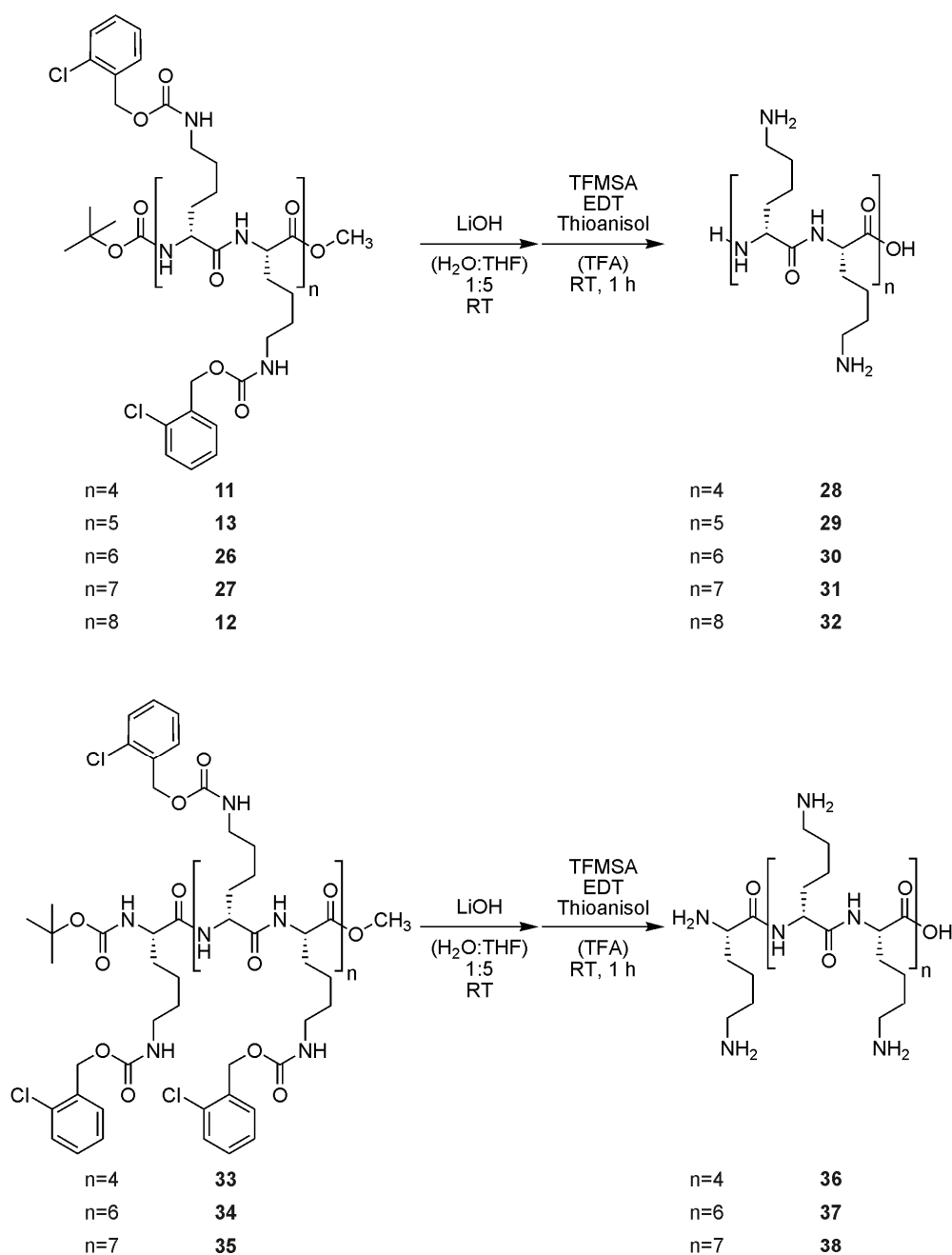
isolated by means of standard laboratory purification via column chromatography and even not via preparative HPLC.

In summary, the divergent/convergent synthesis in solution using Z-Lys(Boc) as building block was only feasible to the stage of tetrapeptide. Further growth could not be accomplished since the saponification of the tetrapeptide led to decomposition. Instead of putting more effort into this synthesis, a new approach for the cleavage of the 2Cl-Z group was tried.

3.1.7 Side Chain Deprotection Of The 2Cl-Z Group

Since the alternative route to side chain deprotected oligolysine failed, another protocol to cleave the 2Cl-Z group was tried. In this approach, the 2Cl-Z group was cleaved under super acidic conditions, using TFMSA in TFA. This procedure removed the Boc group quantitatively but also partially cleaved the methyl ester. To avoid a product mixture of C-protected and C-deprotected peptides, the oligolysines were saponified prior to the deprotection (Scheme 14).

3 Linear D-(*alt*)-L-peptides



Scheme 14: Saponification and subsequent super acidic cleavage of the 2Cl-Z and the Boc group to afford target peptide series **28-32**, **36-38**.

The saponification proceeded smoothly in a THF:water mixture using LiOH and gave the resulting peptides in quantitative yields. For the super acidic cleavage, the peptides were stirred in a thioanisol/ethanedithiol-mixture, cooled to 0 °C and then dissolved by the addition of TFA. TFMSA was slowly added and the mixture stirred for one hour at room temperature. The peptide was isolated by precipitation in diethylether and purified by preparative HPLC. Following the

super acidic cleavage protocol, it was possible to deprotect the series of octa-, nona-, deca-, dodeca-, trideca-, tetradeca-, pentadeca-, and hexadeca-D-(*alt*)-L-Lys(2Cl-Z)-Me. The HPLC-traces of all purified peptides are shown in Figure 1 in an overlay. HPLC was run on C18 with an acetonitrile:water gradient (0-10 vol-% acetonitrile in 30 minutes). The saw tooth shape of the peaks seems to be characteristic for these peptides and may be attributed to strong interaction of the peptide with the stationary phase.

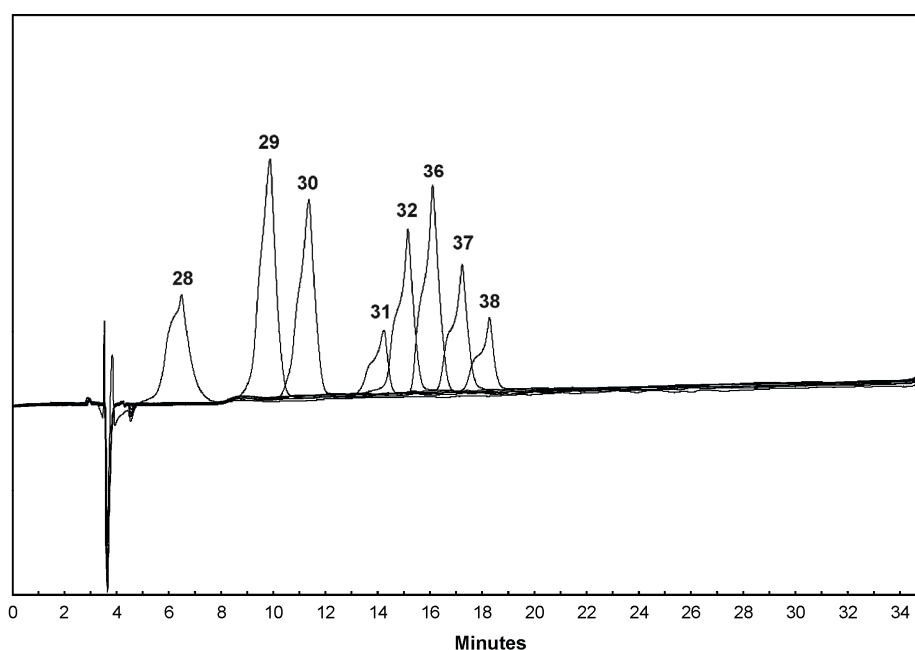


Figure 1: Overlay of HPLC-traces of all deprotected peptides. (HPLC was run on C18 with acetonitrile:water gradient: 0-10 vol-% acetonitrile in 30 minutes).

3.1.8 Investigation Of Conformation In Solution

For the determination of solution structures, NMR, IR, and CD are useful, but also very demanding methods. NMR requires a significant heterogeneity since the signals in the spectrum have to be resolved for proper assignment, necessary for proton shift analysis and NOESY experiments. IR in solution can give useful hints on hydrogen bonding patterns, but is restricted to peptide analysis in non-aqueous media, since measurement cells are water sensible. By CD, the presence or absence of a characteristic secondary structure can be determined. Structural motifs can be determined in comparison to CD signals, which have already been assigned. The oligo-D-(*alt*)-L-lysines are homopeptides and their pH-dependent folding and unfolding is to be investigated in aqueous

3 Linear D-(*alt*)-L-peptides

solutions. These restrictions eliminate NMR and IR, rendering CD the method of choice.

The longest deprotected oligopeptides **32** and **38** were subjected to circular dichroism studies in water. The oligolysines with chargeable side chain functionalities were expected to display a pH-dependent secondary structure switching behavior, which should result in a detectable change in CD-signature (Figure 2).

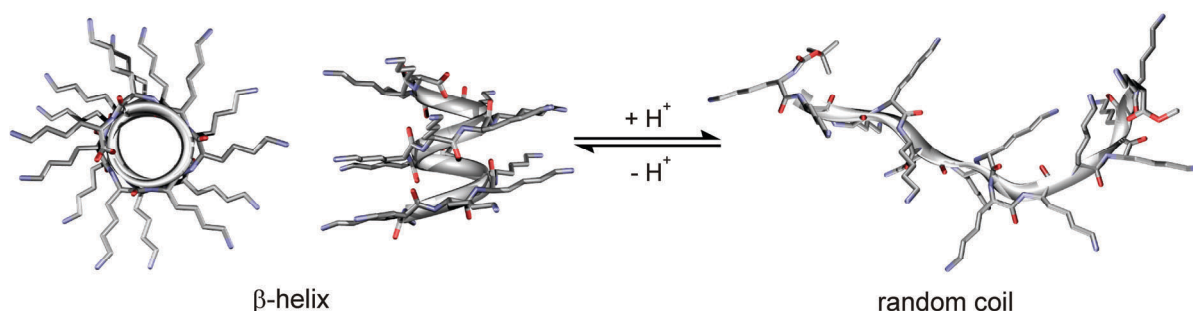


Figure 2: pH-induced helix-coil-transition of oligo-D-(*alt*)-L-Lys.

CD spectra were recorded in water in a 1 mm cuvette at 25 °C in a wavelength region between 180 to 250 nm. Due to the absence of other chromophores than the amide bonds, no signals were expected at higher wavelengths. The measurement at lower wavelengths than 180 nm was impossible due to the low transmission of the solvent. The peptides were measured at concentrations in the range of 1×10^{-5} mol/L, where sufficient UV-absorbance was detectable. Peptide **32** was also measured at higher concentration (5×10^{-4} mol/L), at basic pH (pH=10.7), and in a water:TFE (1:1) mixture. Untreated peptide solutions were at slightly acidic pH (pH=5). Results of the CD-experiments are shown in Figure 3.

The oligopeptides **32** and **38** displayed no CD-signal in aqueous solutions at slightly acidic and basic pH. The tenfold higher concentrated solution of **32** did not display a CD signal either and the addition of the folding promoter TFE yields no detectable signal. The small deviation from zero at wavelengths below 190 nm were attributed to the low transmission and the resulting high photomultiplier voltages and hence considered as noise. Unordered peptides usually display a detectable random coil CD-signal, which results from the

superposition of the CD-signals of the chiral, separated amino acid units. This random coil signal is weak in comparison to i.e. the signal of an α -helix and more diffuse. The absence of the random coil signal in the CD-experiments with **32** and **38** could be explained by the presence of equal amounts of D- and L-configured amino acids in the peptide. In *all*-L-peptides, every amide chromophore is connected to two adjacent L-configured amino acid $C\alpha$. The addition of the signals of the separated amide chromophores in the peptide yields the random coil signal. In the case of D-(*alt*)-L-peptides, the amide chromophores are flanked by L- and D-amino acids $C\alpha$'s. The superposition of all opposed signals could result in an annihilation of the CD-signal, yielding the zero line in Figure 3.

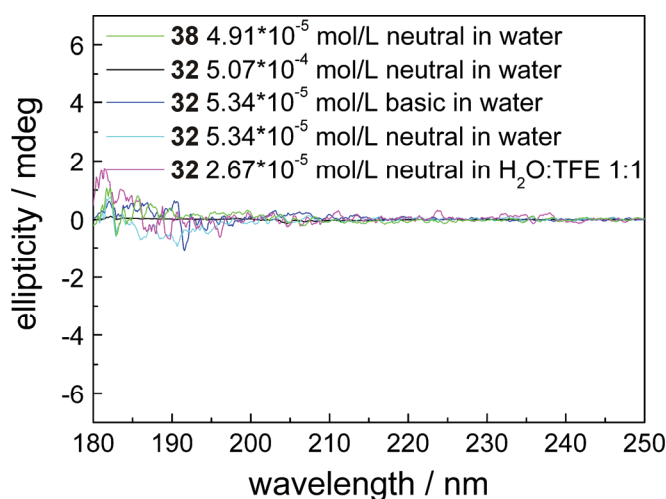


Figure 3: Results of CD-experiments with oligopeptides **32** and **38**. Spectra are normalized to a concentration of $1 \cdot 10^{-5}$ mol/L. Concentrations are given. Spectra were collected in a 1 mm cuvette in water at pH=5 (neutral) and pH=10.6 (basic) and in a water:TFE (1:1) mixture.

The absence of a CD-signal in the studies of peptides **32** and **38** could be explained by a random coil structure, which was expected for acidic pH. The measurements in basic aqueous solutions and in water:TFE mixtures were expected to display a CD-signal, indicating an ordered structure. Since this was not the case, peptides **32** and **38** were supposed to be present in the random coil structure under all applied conditions.

3 Linear D-(*alt*)-L-peptides

The peptides investigated by Lorenzi and coworkers and Gramicidin carry hydrophobic side chains. The peptide backbone as such has hydrophilic properties and avoids contact to apolar solvents. In such solvents, these peptides expose the hydrophobic side chains to the solvent thereby minimizing the backbone-solvent-contact. This hydrophobic effect is one of the driving forces for secondary structure formation of these peptides. The alternating stereochemistry enables the molecules to adopt a β -helical structure. In contrast to these peptides, the deprotected peptides **32** and **38** have hydrophilic side chains. In aqueous solutions, side chains and backbone are well soluble. This vanishing hydrophobicity-difference reduces the hydrophobic effect notably and thereby the driving force for the peptide to adopt an ordered structure. Despite all efforts, no secondary structure formation of the oligo-D-(*alt*)-L-peptides could be detected by CD.

Besides these aspects folding into helical structures is also a function of (peptide) length. Helical folding is a cooperative process, which requires a certain chain length (Figure 4). The beginning of the folding process is energetically up-hill (red line) until at a certain length (associated with n_{nuc} repeating units) the chain is folded to the first nucleating loop. When the peptide has passed this activation barrier associated with nucleation, the folding process becomes more and more facile until above a critical length associated with n_{crit} the helical conformation is thermodynamically more stable. Therefore, the longer the peptide chain, the more energy can be gained by the folding process and the more stable the resulting helix. Oligopeptides **32** and **38** may still be shorter than the critical length n_{crit} and hence not adopt a helical conformation. For this reason, the synthesis and investigation of longer peptides, i.e. polypeptides was targeted.

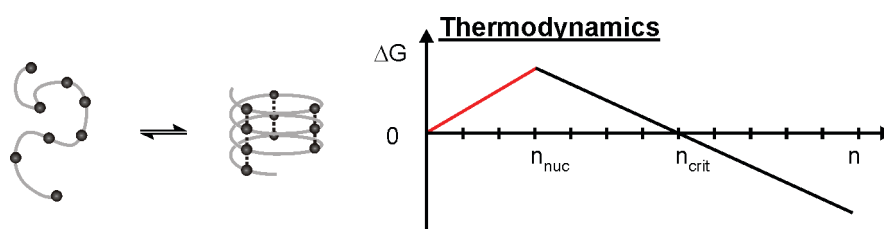


Figure 4: Thermodynamics of the helical folding process.

3.2 Linear Poly-D-(*alt*)-L-peptides

3.2.1 General Considerations

Linear poly-D-(*alt*)-L-peptides have interesting structural features and the potential to form nanotubular structures on the polymeric level. Unfortunately, no synthesis to poly-D-(*alt*)-L-peptides with appropriate length and narrow polydispersity has been reported so far. One attractive approach to the synthesis of such poly-D-(*alt*)-L-peptides would be based on the ring opening polymerization of α -amino acid *N*-carboxy-anhydrides (NCAs). This reaction is well known for NCAs resulting from the ring closure of one single α -amino acid and leads to polypeptides with very narrow polydispersities and acceptable lengths. But these polypeptides have no alternating stereochemistry.

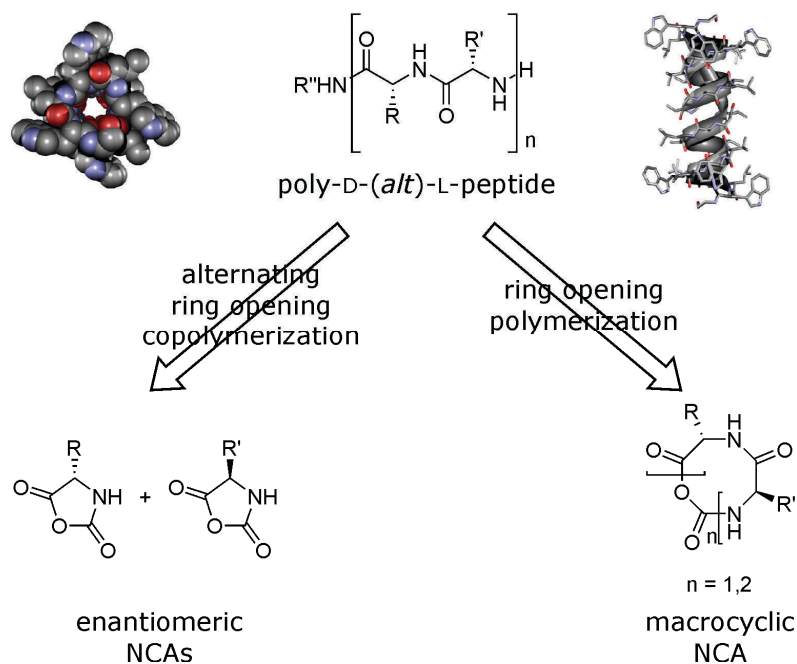


Figure 5: Possible approaches to the synthesis of poly-D-(*alt*)-L-peptides.

Following the NCA approach, alternating stereochemistry within a polypeptide could be realized following two pathways (Figure 5). One possibility is the alternating copolymerization of a pair of NCA enantiomers. This approach requires a potent catalyst system, which is able to alternate its preference for the ring opening of one and the opposite enantiomer. The development of such a catalyst system would be a daunting task. On the other hand the creation and ring opening polymerization of a macrocyclic NCA, which already contains the

3 Linear D-(*alt*)-L-peptides

alternating stereochemistry appears to be much more convenient. This could be achieved by ring closing a D-(*alt*)-L-dipeptide to the corresponding NCA. Results of initial calculations at the PM3-level concerning the stability of macrocyclic NCAs are summarized in Table 2.

Table 2: Stability of macrocyclic NCAs as predicted by semiempirical calculations (PM3).

Peptide	L-Ala NCA	L-Ala-D-Ala NCA	L-Ala-D-Ala-L-Ala NCA	(L-Ala-D-Ala) ₂ NCA
$\Delta\Delta H_f /$ [kcal/mol] ¹	25.4	-20.6	14.1	22.6

¹ $\Delta H_f(\text{open chain}) - \Delta H_f(\text{NCA})$.

For each peptide, the heat of formation was calculated. Given is the difference of heat of formation of the open chain and ring closed NCA. These relative values could be compared in order to obtain a first approximation of the stability of macrocyclic NCAs. The calculations were done with alanine, for simplicity and to reduce computing time. The value of L-Ala NCA could be considered as reference. $\Delta\Delta H_f$ for the NCA resulting from the ring closing of a D-(*alt*)-L-alanine dimer was negative, meaning that the NCA is expected to be less stable than the reference NCA due to significant ring strain in the 8-membered ring. Although the NCA resulting from the tripeptide had a positive $\Delta\Delta H_f$ -value indicating a much reduced ring strain. However, it does not provide an alternating stereochemistry in the polymer. The NCA resulting from the tetrapeptide also displays a positive $\Delta\Delta H_f$ -value comparable to that of the reference NCA. As this macrocyclic NCA seemed to be synthetically feasible and would give rise to the desired alternating stereochemistry in the polymer, its synthesis was targeted.

3.2.2 Synthetic Considerations

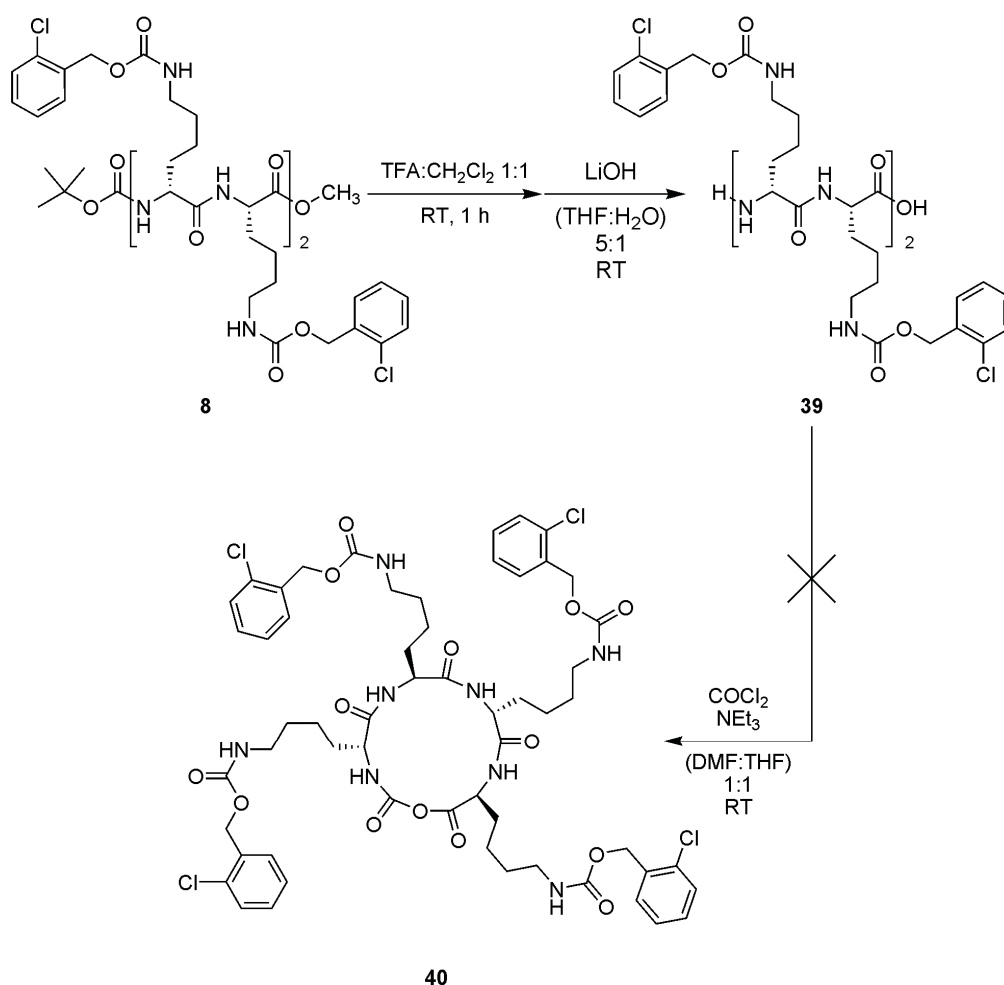
There are four key steps in the synthesis to poly-D-(*alt*)-L-peptides, following the approach of a ring opening polymerization of macrocyclic NCAs. First, the synthesis of the tetrapeptide. Second, the ring closing to the macrocyclic NCA. Third, the purification of the NCA and fourth, the optimization of the polymerization reaction. The synthesis of the tetrapeptide was already achieved

(3.1.4.1), so that the next crucial step was the synthesis of the macrocyclic NCA.

3.2.3 Attempted Monomer Synthesis

The ring closure was attempted following the Fuchs-Farthing method. Therefore, the tetrapeptide **8** was deprotected at the *N*- and the *C*-terminus (Scheme 15). These reactions proceeded smoothly and gave the desired deprotected tetrapeptide **39** in high yield. The ring closing reaction was tried using phosgene in a highly diluted DMF:THF mixture. Usually, Fuchs-Farthing reactions are done in THF or ethyl acetate, but since **39** was insoluble in both solvents, DMF had to be used instead. Phosgene (in toluene) was dissolved in THF and slowly added to the peptide. One issue in the synthesis of these tetrapeptide NCAs was the analysis of the reaction mixture, since the product itself (if it was being formed) was supposed to be highly reactive – a property desired at the polymerization stage but rather problematic for monomer synthesis. The only possible detection methods were IR and ESI-MS.

3 Linear D-(*alt*)-L-peptides



Scheme 15: Attempted monomer synthesis following the Fuchs-Farthing method.

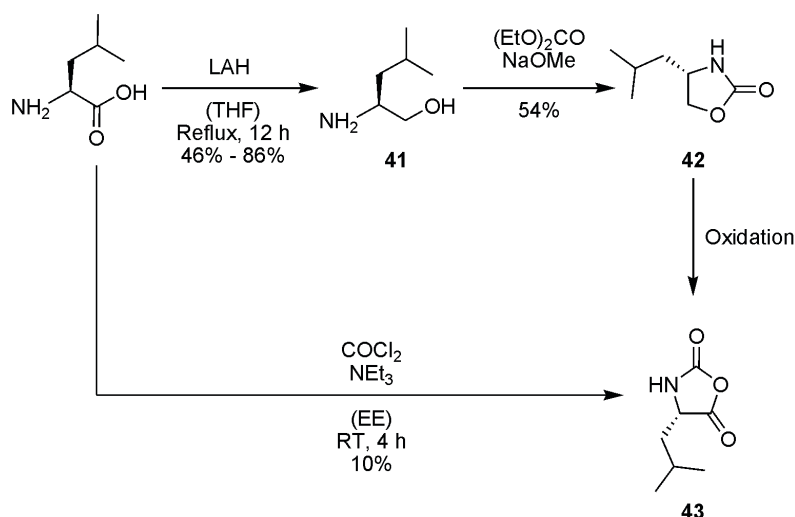
Unfortunately, the reaction did not afford the desired NCA (as indicated by ESI-MS). Other experiments in the group with tetra-D-(*alt*)-L-leucine led to the result that the tetrapeptide NCA had been formed in detectable amounts, but that its isolation was not possible.^[27] The probability for the formation of the 14-membered ring seemed to be too low and the small amount of formed NCA was too reactive and decomposed during isolation attempts.

3.2.4 Alternative NCA-synthesis

The main issue in the synthesis of a macrocyclic NCA was the isolation and purification of the highly reactive monomer. To overcome this issue, one could synthesize a stable cyclic precursor, which could be purified and characterized and then transferred into the highly reactive NCA monomer. It should be possible to synthesize the tripeptide and couple it with the amino alcohol of the

fourth amino acid, so that the ring closure of the tetramer gives the stable carbamate instead of the NCA. This molecule could be purified and subsequently oxidized to the NCA. The remaining carbamate should not interfere in the polymerization reaction and could be tolerated.

Oxidations of cyclic ethers (such as THF) to lactones are well established. Several such examples have been reported, using ruthenium tetra oxide,^[28] ruthenium(II),^[29] or cobalt catalysts,^[30] chromium salts,^[31] zinc permanganate^[32] and lewis acid assisted permanganate oxidation,^[33] hydrogen peroxide,^[34] aqueous bromine,^[35] sodium bromate,^[36] or peroxyphosphoric acid.^[37] Oxidations of oxazolidin-2-ones to the corresponding NCAs have not been reported so far. Applying the oxidation conditions of the ether oxidations to the oxazolidin-2-one could in principle yield the desired NCA. Some of the oxidations use very sophisticated catalyst systems and hence are not feasible. Others are reported to proceed via a ring-opening-oxidation-lactonization-mechanism. Since the ring closure was expected to be the critical step in the NCA synthesis, these oxidations also have to be excluded. The most promising protocols for this type of oxidation use $\text{KMnO}_4/\text{FeCl}_3$ ^[33] or trimethylsilylnitrate-chromium trioxide ($\text{TMSONO}_2\text{-CrO}_3$).^[31] The approach of oxazolidin-2-one oxidation is shown in Scheme 16 with the example of a conventional L-leucine NCA.



Scheme 16: Oxazolidinone oxidation approach to the NCA synthesis.

3 Linear D-(*a/t*)-L-peptides

In this approach, L-leucine was first reduced to L-leucinol (**41**) and subsequently cyclized to (*S*)-4-isobutyloxazolidin-2-one (**42**). In the last step, the oxidation of the oxazolidinone to the desired NCA **43** was attempted. In order to have comparable analytical data, such as NMR, IR or MS, the L-leucine NCA **43** was also synthesized, following the Fuchs-Farthing method. The direct ring closure of L-leucine to the corresponding NCA **43** proceeded in very low yield (10%) after recrystallization. The other pathway started with the reduction of L-leucine to L-leucinol (**41**) using lithium aluminum hydride. The reaction mixture was quenched by the addition of Baekstrom salt,^[38] which was extensively washed with solvent after the filtration. The low yield of 46% in the first attempt could be explained by the purification process. Since the freshly distilled, colorless amino alcohol rapidly started to be oxidized, it was used directly after distillation. The reaction to the oxazolidinone **42** with diethyl carbonate and sodium methoxide proceeded smoothly. Purification of the crude product by column chromatography and subsequent crystallization from hexane gave the desired product in 54% yield and very high purity (>99% according to GC) with an ee of 98.4% probably reflecting the ee of the starting material. Oxidation of oxazolidinone **42** was attempted with KMnO₄/FeCl₃ in acetone or methylene chloride but failed. Another attempt using TMSOONO₂-CrO₃ showed no conversion of the starting material at room temperature and also at 60 °C and at 80 °C.

In summary, the most promising approaches to the oxidation of oxazolidin-2-ones to the corresponding NCAs failed. Since this attempt to synthesize the NCA also failed, no further effort was invested in the synthesis of mixed NCA monomers for the preparation of poly-D-(*a/t*)-L-peptides.

3.3 Experimental Part

3.3.1 General

General Methods: Starting materials were commercial and used as received. All solvents used at FU Berlin and HU Berlin were distilled once prior to usage, all solvents used at MPI were used without further purification. THF was in all cases stored over KOH and freshly distilled prior to usage. Dry solvents were kindly provided by the respective facility of the MPI. Dry DMF was purchased from Acros. If mentioned, solvents were degassed by freeze drying or by purging with argon. Column chromatography was carried out with 130 – 140 mesh silica gel. Dialysis of the compounds was achieved using regenerated cellulose dialysis tubes Spectra/Por Dialysis Membrane MWCO:1000 or MWCO:25000. Slow compound addition was achieved using a Harvard Apparatus 11Plus syringe pump. Compound lyophilization was performed using Christ Alpha 2-4 LDC-1m apparatus. Microwave assisted reactions were performed in a CEM-Discover monomode microwave reactor having a continuous microwave power delivery system from 0 to 300 W. The reactions were carried out in 10 mL sealed glass vials. The temperature was monitored by an IR sensor on the outer surface of the reaction vessel. All the reactions were performed with max. power and super-cooling.

Analytic Methods:

NMR (^1H and ^{13}C , respectively) were recorded on Bruker DPX 300 (300.1 and 75 MHz for ^1H and ^{13}C , respectively), Bruker AV400 (400.1 and 100.6 MHz for ^1H and ^{13}C , respectively) spectrometers at 23 \pm 2 $^\circ\text{C}$ using residual protonated solvent signals as internal standard (^1H : $\delta(\text{CHCl}_3)$ = 7.26 ppm, $\delta(\text{DMSO})$ = 2.50 ppm, $\delta(\text{CH}_3\text{OH})$ = 3.31 ppm, $\delta(\text{H}_2\text{O})$ = 4.79 ppm, $\delta(\text{CH}_3\text{CN})$ = 4.79 ppm, $\delta(\text{CH}_2\text{Cl}_2)$ = 5.32 ppm, and ^{13}C : $\delta(\text{CHCl}_3)$ = 77.16 ppm, $\delta(\text{DMSO})$ = 39.52 ppm, $\delta(\text{CH}_3\text{OH})$ = 49.00 ppm, $\delta(\text{CH}_3\text{CN})$ = 1.32 ppm and 118.26 ppm, $\delta(\text{CH}_2\text{Cl}_2)$ = 53.80 ppm).

Mass spectrometry was performed on a Bruker APEX III Fourier Transform Ion Cyclotron Resonance Mass Spectrometer (FTICR-MS) or on a Waters LCT Premier XE.

3 Linear D-(*alt*)-L-peptides

TLC was performed on Merck Silica Gel 60 F254 TLC plates with a fluorescent indicator with a 254 nm excitation wavelength. Compounds were visualized under UV light at 254 nm and developed with ninhydrin solution.

HPLC/UPLC was performed with a Waters UPLC Acquity equipped with a Waters LCT Premier XE Mass detector for UPLC-HR-MS, with Waters Alliance systems (consisting of a Waters Separations Module 2695, a Waters Diode Array detector 996 and a Waters Mass Detector ZQ 2000) equipped with the columns described with the corresponding substances, with Shimadzu LC-10A systems equipped with a photodiode array detector (PAD or DAD).

GPC measurements in DMF as the mobile phase were performed on PSS columns in a WGE Dr.Bures TAU 2010 column oven at 70 °C, using a WGE Dr.Bures Q-2010 HPLC pump and a Knauer Smartline 3800 autosampler. Detection was achieved using a WGE ETA-2020 RI-visco-detector and a Knauer Smartline 2500 UV-detector. Flow-rate was 1.0 mL/min. Columns were calibrated using a Polystyrene Calibration Kit S-L-10 LOT 79, using 2,4-Di-*tert*-butyl-4-methoxy-phenol as internal standard.

CEC was measured on a Hewlett Packard HP-3D-CE-System, using a 50 cm Fused Silica Capillary 50 µm i.d. Sample was loaded at 50 mbar, 1 s, 40 mmol phosphate-buffer, pH 3.0, potential 30 kV, 30 µA, 293 K, 220 nm.

Optical spectroscopy: UV/visible absorption and emission spectra were recorded in spectroscopic grade solvents, using Hellma quartz cuvettes of 1 cm for absorption and emission and 1 mm path length for absorption on a Cary 50 Spectrophotometer and a Cary Eclipse Fluorescence Spectrophotometer, respectively, both equipped with a Peltier thermostated cell holder ($T = 25 \pm 0.05$ °C). The fluorescence samples were excited at their respective absorbance maxima, slit was set to 5 nm bandpass for excitation and to 10 nm bandpass for emission. Circular dichroism spectra were recorded on a JASCO 710 Spectropolarimeter equipped with a JASCO PTC-423S/15 Peltier thermostated cell holder in spectroscopic grade solvents using Hellma quartz cuvettes of 1 cm and 1 mm path length. Prior to first use, the cuvettes were cleaned with 1:1 mixture of conc. H₂SO₄ / 30% H₂O₂, washed with water and acetonitrile, and a 10 vol-% solution of *silyl-501* (BSTFA: N,O-Bis(trimethylsilyl)acetamide,

1%TMSCl) in acetonitril added, stirred for 10 min at RT and 20 min at 50 °C, washed twice with acetonitrile and chloroform. After silylation, cuvettes were cleaned with aqueous Hellmanex II cuvette cleaning solutions. IR spectra were recorded on a Biorad Excalibur FTS30MX equipped with a Golden Gate ATR Specac.

3.3.2 General Procedures

General procedure for the deprotection of the Boc group: Peptide was dissolved in CH_2Cl_2 or in $\text{CH}_2\text{Cl}_2:\text{CH}_3\text{OH}$ 9:1 (depending on solubility) and cooled to 0 °C. TFA (same amount as the solvent) was added and the solution allowed to warm up to room temperature. After stirring at room temperature until starting material was consumed (TLC monitoring), the solution was concentrated i.vac. When the uncharged, neutralized peptide was the desired product, the solution was extracted with water, saturated aqueous NaHCO_3 -solution (in case of longer peptides (starting from octamer), CH_3OH was added to assure solubility of the peptide), water, and brine. The combined organic layers were dried over MgSO_4 , filtered, and evaporated i.vac. to yield the crude product in quantitative yield. In case of remaining protected peptide, procedure was repeated. When the amine salt was the desired product, the reaction mixture was evaporated i.vac. and wrapped several times with CH_2Cl_2 to give the product in quantitative yield.

General procedure for the deprotection of the methyl ester: To a solution of methyl ester protected peptide in water:THF 1:5, a 1 M aqueous solution of LiOH (water:LiOH:THF 1:1:5) was added and the reaction mixture stirred at room temperature until starting material was consumed (TLC monitoring). Acetic acid was added to give pH=5, and the product subsequently extracted with CH_2Cl_2 . The united organic layers were dried over MgSO_4 and the solvent evaporated i.vac. to give the product in quantitative yield.

General procedure for the deprotection of the Z group or benzyl ester: To a solution of Z or benzyl protected peptide in EE: CH_3OH (ratio depending on solubility), Pd/C was added and the solution stirred under hydrogen atmosphere at room temperature. The reaction mixture was filtered and evaporated i.vac. to give the product.

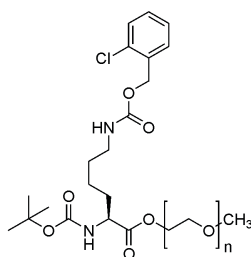
3 Linear D-(*alt*)-L-peptides

General procedure for the reduction of amino acids to amino alcohols with LAH: LAH (80 mmol) was suspended in dry THF (250 mL) and the suspension cooled to 0 °C. The amino acid (40 mmol) was added neat slowly (strong hydrogen formation). The mixture was allowed to warm up to room temperature and then refluxed for minimum 10 h. The reaction mixture was then cooled down to 0 °C and quenched by the addition of water or Baekstrom salt.^[38] The suspension was then filtered and the remaining solid washed extensively with THF. The organic layer was concentrated i.vac., dried over MgSO₄, filtered, and the solvents were evaporated i.vac. to give the crude product which was purified via bulb-to-bulb distillation i.vac.

General procedure for the superacidic cleavage of the 2Cl-Z protecting group: Peptide (0.02 – 0.03 mmol) in a round bottom flask with stirring bar was suspended in thioanisole/EDT (2:1) (0.75 mL) and cooled to 0 °C. The peptide was dissolved by the addition of TFA (5 mL). After 5 to 10 minutes at 0 °C, TFMSA (0.5 mL) was added dropwise under vigorous stirring. The solution was warmed to room temperature and stirred for 1 h. After 1 h, the mixture was precipitated in ice-cold Et₂O (70 mL). The solid was separated from the solution by centrifugation, was dissolved in TFA and precipitated again. Purification was achieved via preparative HPLC.

3.3.3 Synthetic Procedures

Boc-L-Lys(2Cl-Z)-MPEG (**1**):



MPEG 5000 was dried by wrapping with benzene and freeze drying in high vacuum. MPEG 5000 (30.0 g, 6.0 mmol), Boc-L-Lys(2Cl-Z) (5.0 g, 12.0 mmol) and DPTS (0.7 g, 2.4 mmol) were dissolved in anhydrous CH₂Cl₂ (70 mL) and cooled down to 0 °C. DIC (3.7 mL, 24.0 mmol) was added. After stirring over night, the solution was filtered through sintered glass to remove the solid, which precipitated during the reaction. The solvent of the filtered solution was

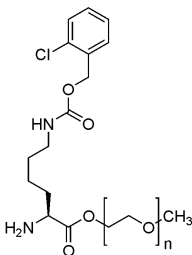
evaporated i.vac. to yield a white solid, which was dissolved in toluene. The solution was filtered to remove insoluble components. The solid was extensively washed with toluene. Toluene was evaporated i.vac. to yield a white solid which was dissolved in a minimal amount of CH_2Cl_2 . The solution was added dropwise to ice-cold, vigorously stirred Et_2O (500 mL). The appearing precipitate was filtered and washed with cold Et_2O . The remaining white solid was dried i.vac. and subjected to a second coupling procedure, in order to assure complete loading of the polymeric support (Boc-L-Lys(2Cl-Z) (1.2 g, 2.8 mmol), DPTS (0.17 g, 0.56 mmol), DIC (0.9 mL, 5.6 mmol)). The second coupling gave the desired product in quantitative yield.

Capping of unreacted polymer chain ends using acetic anhydride:

1 (31.4 g, 5.8 mmol), NEt_3 (20.4 mL, 145.0 mmol), and DMAP (0.07 g, 0.58 mmol) were dissolved in dry CH_2Cl_2 (100 mL) and cooled down to 0 °C. Acetic anhydride (13.7 mL, 145.0 mmol) was added to the cold solution, which was stirred at 0 °C for 30 minutes. The solution was allowed to warm up to room temperature and stirred for 1.5 h. The solution was diluted with CH_2Cl_2 and extracted with saturated aqueous NaHCO_3 -solution (3x50 mL). The aqueous layers were extracted with CH_2Cl_2 (3x100 mL). The combined organic layers were dried over MgSO_4 , filtered and concentrated i.vac. The concentrated solution was precipitated in ice-cold Et_2O . The white precipitate was filtered, washed extensively with Et_2O , and dried i.vac. to give the desired product in quantitative yield.

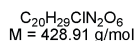
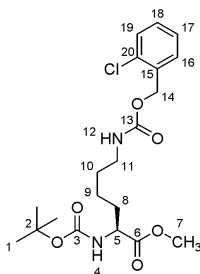
3 Linear D-(*alt*)-L-peptides

L-Lys(2Cl-Z)-MPEG (**2**):



1 (28.7 g, 5.3 mmol) was dissolved in dry CH_2Cl_2 (98 mL) and cooled down to 0 °C. TFA (98.4 mL) was added. The solution was allowed to warm up to room temperature and stirred for 1.5 h. The solution was concentrated i.vac. and added dropwise to ice-cold, vigorously stirred Et_2O (500 mL). The white precipitate was filtered, dried i.vac. and dissolved in CH_2Cl_2 . The solution was neutralized by the addition of piperidin and filtered. The solution was concentrated i.vac. and added to ice-cold, vigorously stirred Et_2O (500 mL). The white precipitate was filtered and dried i.vac. to give the desired product in quantitative yield.

Boc-L-Lys(2Cl-Z)-Me (**3**):



Synthesis via nucleophilic substitution on MeI:

A solution of Boc-L-Lys(2Cl-Z) (1.04 g, 2.5 mmol) in dry DMF (25.0 mL) was stirred overnight at room temperature with Cs_2CO_3 (0.82 g, 2.5 mmol) and MeI (0.31 mL, 5.0 mmol). The solvent was evaporated and the residue partitioned between toluene and H_2O . The toluene layer was extracted with H_2O (3x25 mL), dried over MgSO_4 , and evaporated to give a pale yellow oil. The oil was dissolved in CHCl_3 and wrapped several times.

ee-values were determined to be in the range of 80.64% and 96.49% by chiral HPLC (supported by ESI-MS).

HPLC (250 mm Chiracel OJ, 4.6 mm, *n*-heptane:2-propanol = 9:1, 0.5 mL/min, 2.1 MPa, 298 K): 34.83 min (9.63% peak area, Boc-D-Lys(2Cl-Z)-Me), 43.61 min (89.85% peak area, **3**).

Synthesis using DIC and MeOH:

Boc-L-Lys(2Cl-Z) (1.04 g, 2.50 mmol) and HOBt (0.37 g, 2.75 mmol) were dissolved in 10.0 mL solvent (CH₂Cl₂:MeOH 1:1) and cooled to 0 °C. To the cold solution, DIC (0.51 mL, 3.25 mmol) was added. The solution was allowed to warm up to room temperature and stirred for 2 h. The reaction mixture was filtered and extracted with 1 M aqueous citric acid solution (50 mL), water (50 mL), saturated aqueous NaHCO₃-solution (50 mL), water (50 mL), and brine (50 mL). The organic layer was dried over MgSO₄, filtered and evaporated i.vac. The pale yellow, gluelike liquid was dissolved in toluene and filtered. The filtrate was evaporated i.vac. to yield the crude product. Purification via column chromatography on silica (eluent: CH₂Cl₂:acetone 92:8) gave 1.06 g (yield: 98%) of **3** as a pale yellow oil.

ee-value was determined to be >99.9% by chiral HPLC.

HPLC (250 mm Chiracel OJ, 4.6 mm, *n*-heptane:2-propanol = 9:1, 0.5 mL/min, 2.0 MPa, 298 K): 42.13 min (99.01% peak area, **3**).

Synthesis using EDC and MeOH:

Boc-L-Lys(2Cl-Z) (2.07 g, 5.00 mmol) and HOBt (0.74 g, 5.50 mmol) were dissolved in 20.0 mL solvent (CH₂Cl₂:MeOH 1:1) and cooled to 0 °C. To the cold solution, a concentrated solution of EDC (1.25 g, 6.50 mmol) in CH₂Cl₂ was added. The solution was allowed to warm up to room temperature and stirred for 2 h. The reaction mixture was extracted with water (3x50 mL), 1 M aqueous citric acid solution (50 mL), water (50 mL), saturated aqueous NaHCO₃-solution (50 mL), water (50 mL), and brine (50 mL). The organic layer was dried over MgSO₄, filtered and evaporated i.vac. to give the crude product in quantitative yield.

ee-value was determined to be >99.9% by chiral HPLC.

3 Linear D-(*alt*)-L-peptides

HPLC (250 mm Chiracel OJ, 4.6 mm, *n*-heptane:2-propanol = 9:1, 0.5 mL/min, 2.2 MPa, 298 K): 43.79 min (99.73% peak area, **3**).

R_F = 0.66 (CH₂Cl₂:acetone 9:1)

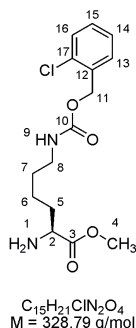
¹H NMR (300 MHz, DMSO-d₆, 20 °C): δ 7.49 - 7.31 (m, 5 H, C¹⁶⁻¹⁹H, N¹²H), 7.19 (d, ³J(H,H) = 7.5 Hz, 1 H, N⁴H), 5.08 (s, 2 H, C¹⁴H₂), 3.94 - 3.87 (m, 1 H, C⁵H), 3.61 (s, 3 H, C⁷H₃), 3.01 - 2.95 (m, 4 H, C¹¹H₂), 1.64 - 1.23 (m, 15 H, 3 C¹H₃, C⁸⁻¹⁰H₂).

¹³C NMR (DMSO-d₆): δ 174.07, 156.67, 156.45, 135.18, 133.18, 130.58, 130.54, 130.14, 128.16, 79.05, 63.43, 54.39, 52.53, 40.85, 31.18, 29.76, 29.05, 23.64.

EI-MS (135 °C): m/z = 428 (calcd 428 for C₂₀H₂₉ClN₂O₆⁺).

High-resolution ESI-MS: m/z = 451.108268 (calcd 451.160633 for C₂₀H₂₉ClN₂O₆ + 1 Na⁺).

L-Lys(2Cl-Z)-Me (**4**):



3 was reacted following the general procedure for the deprotection of the Boc group.

HPLC (125 mm Nucleodur, 4.0 mm, methanol/10 mmol TEAA pH7 = 60:40, 0.8 mL/min, 9.5 MPa, 308 K): 4.92 min (44.74% peak area (old solution), 77% peak area (fresh solution), **4**).

R_F = 0.15 (CH₂Cl₂:MeOH 92:8)

3 Linear D-(*alt*)-L-peptides

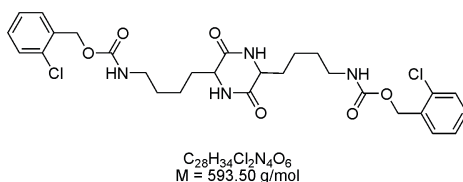
^1H NMR (300 MHz, DMSO- d_6 , 20 °C): δ 7.49 - 7.31 (m, 5 H, C^{13-16}H , N^9H), 5.08 (s, 2 H, C^{11}H_2), 3.30 - 3.24 (m, 1 H, C^2H), 3.60 (s, 3 H, C^4H_3), 3.01 - 2.95 (m, 4 H, C^8H_2), 1.72 (br. s, 2 H, N^1H_2), 1.64 - 1.23 (m, 6 H, C^{5-7}H_2).

^{13}C NMR (DMSO- d_6): δ 177.22, 156.69, 135.61, 133.19, 130.60, 130.57, 130.16, 128.21, 63.43, 54.78, 52.26, 41.10, 35.16, 30.07, 23.36.

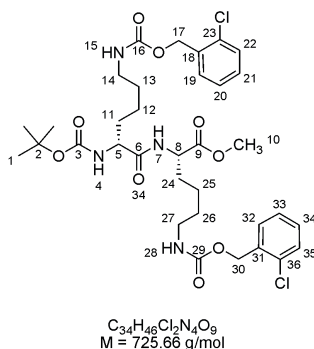
EI-MS (105 °C): m/z = 328 (calcd 328 for $\text{C}_{15}\text{H}_{21}\text{ClN}_2\text{O}_4^+$), 269 (calcd 269 for $\text{C}_{13}\text{H}_{18}\text{ClN}_2\text{O}_2^+$), 125 (calcd 125 for $\text{C}_7\text{H}_6\text{Cl}^+$).

High-resolution ESI-MS: m/z = 351.108268 (calcd 351.108207 for $\text{C}_{15}\text{H}_{21}\text{ClN}_2\text{O}_4 + 1 \text{ Na}^+$).

Important notice: When the deprotected amine was stored over a certain period of time (from days to months), it formed the diketopiperazine, which could be identified by mass spectrometry.



Boc-D-Lys(2Cl-Z)-L-Lys(2Cl-Z)-Me (**5**):



Synthesis using DIC:

4 (0.25 g, 0.77 mmol), Boc-D-Lys(2Cl-Z) (0.35 g, 0.85 mmol) and HOBT (0.11 g, 0.85 mmol) were dissolved in 2.50 mL CH_2Cl_2 and cooled to 0 °C. To the cold solution, DIC (0.16 mL, 1.00 mmol) was added. The solution was allowed to warm up to room temperature and stirred for 2 h. The reaction mixture was filtered and extracted with 1 M aqueous citric acid solution

3 Linear D-(*alt*)-L-peptides

(50 mL), water (50 mL), saturated aqueous NaHCO₃-solution (50 mL), water (50 mL) and brine (50 mL). The organic layer was dried over MgSO₄, filtered, and evaporated i.vac. The pale yellow, glue-like residue was redissolved in toluene and filtered. The filtrate was evaporated i.vac. to yield the crude product, which was purified via column chromatography on silica (eluent: CH₂Cl₂:acetone 92:8) to give 0.536 g (yield: 96%) of **5** as a white solid.

HPLC (125 mm Nucleodur 100-5-C18 ec, 4 mm, methanol/water = 65:35, 0.8 mL/min, 8.3 MPa, 308 K): 39.38 min (99.58% peak area, **5**).

Synthesis using EDC:

Boc-D-Lys(2Cl-Z) (4.07 g, 9.80 mmol), HOBT (1.46 g, 10.78 mmol) and **4** (3.22 g, 9.80 mmol) were dissolved in 40.0 mL CH₂Cl₂ and cooled to 0 °C. Then, a concentrated solution of EDC (2.44 g, 12.74 mmol) in CH₂Cl₂ (30.0 mL) was added. The reaction mixture was stirred over night, extracted with water (3x10 mL), aqueous 1 M citric acid solution (1x10 mL), water (1x10 mL), saturated aqueous NaHCO₃-solution (1x10 mL), water (1x10 mL), and brine (1x10 mL). The organic layer was dried over MgSO₄, filtered, and evaporated i.vac. to yield the crude product. Purification via column chromatography (eluent: CH₂Cl₂:acetone 9:1) gave 3.10 g (yield: 86%) of **5** as a white solid. Yields reach from 86% to 95%.

HPLC (125 mm Nucleodur 100-5-C18 ec, 4 mm, methanol/water = 65:35, 0.8 mL/min, 9.4 MPa, 308 K): 35.91 min (98.4% peak area, **5**).

R_f = 0.76 (CH₂Cl₂:MeOH 8:2)

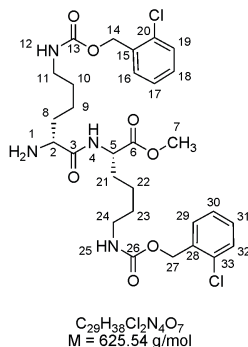
¹H NMR (300 MHz, DMSO-*d*₆, 20 °C): δ 8.09 (d, ³*J*(H,H) = 7.6 Hz, 1 H, N⁷H), 7.48 - 7.30 (m, 10 H, C¹⁹⁻²²H, C³²⁻³⁵H, N²⁸H, N¹⁵H), 6.72 (d, ³*J*(H,H) = 7.9 Hz, 1 H, N⁴H), 5.07 (s, 4 H, C¹⁷H₂, C³⁰H₂), 4.22 - 4.15 (m, 1 H, C⁸H), 3.96 - 3.91 (m, 1 H, C⁵H), 3.60 (s, 3 H, C¹⁰H₃), 2.98 - 2.94 (m, 4 H, C¹⁴H₂, C²⁷H₂), 1.71 - 1.14 (m, 21 H, 3 C¹H₃, C¹¹⁻¹³H₂, C²⁴⁻²⁶H₂).

¹³C NMR (DMSO-*d*₆): δ 173.41, 173.23, 156.68, 156.14, 135.54, 133.22, 130.60, 130.57, 130.17, 128.20, 78.94, 63.46, 55.05, 52.69, 52.61, 40.93, 32.71, 31.54, 29.95, 29.74, 29.08, 23.56, 23.37.

ESI-MS (245 °C): *m/z* = 747 (calcd 747 for C₃₄H₄₆Cl₂N₄O₉ + Na⁺).

High-resolution ESI-MS: $m/z = 747.254248$ (calcd 747.253401 for $C_{34}H_{46}Cl_2N_4O_9 + 1 Na^+$).

D-Lys(2Cl-Z)-L-Lys(2Cl-Z)-Me (**6**):



5 was reacted following the general procedure for the deprotection of the Boc group.

de-value was determined to be 97.4% by HPLC.

HPLC (150 mm YMC-Pack ODS-A, 4.6 mm, acetonitrile/10 mmol TEAA pH7 = 45:65, after 25 min in 10 min to 80:20, 0.8 mL/min, 7.8 MPa, 308 K): 20.07 min (70.97% peak area, **6**), 21.13 min (1.03% peak area, D-Lys(2Cl-Z)-D-Lys(2Cl-Z)-Me).

$R_F = 0.5$ (CH_2Cl_2 :MeOH 8:2)

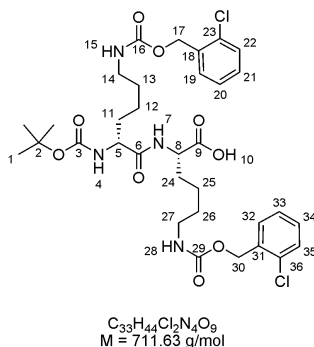
1H NMR (300 MHz, DMSO- d_6 , 20 °C): δ 8.12 (d, $^3J(H,H) = 7.6$ Hz, 1 H, N^4H), 7.48 - 7.30 (m, 10 H, $C^{16-19}H$, $C^{29-32}H$, $N^{12}H$, $N^{25}H$), 5.07 (s, 4 H, $C^{14}H_2$, $C^{27}H_2$), 4.23 - 4.18 (m, 1 H, C^5H), 3.60 (s, 3 H, C^7H_3), 3.16 - 3.14 (m, 1 H, C^2H), 2.98 - 2.94 (m, 4 H, $C^{14}H_2$, $C^{27}H_2$), 1.69 - 1.14 (m, 12 H, $C^{8-10}H_2$, $C^{21-23}H_2$).

^{13}C NMR (DMSO- d_6): δ 175.78, 172.97, 156.13, 134.97, 132.62, 130.00, 129.59, 127.63, 62.88, 54.72, 52.12, 51.88, 40.42, 35.13, 31.06, 29.64, 29.21, 22.86, 22.79.

High-resolution ESI-MS: $m/z = 625.219216$ (calcd 625.219033 for $C_{29}H_{39}Cl_2N_4O_7 + 1 H^+$).

3 Linear D-(*alt*)-L-peptides

Boc-D-Lys(2Cl-Z)-L-Lys(2Cl-Z) (**7**):



Deprotection using KOH:

To a solution of **5** (3.45 g, 4.75 mmol) in MeOH:water:THF 3:1:1 (75.0 mL), a 1 M aqueous KOH solution (38.0 mL, 38.0 mmol) was added and the reaction mixture was stirred at room temperature until starting material was consumed (TLC monitoring). Acetic acid was added to give pH=5, and the product subsequently extracted with CH₂Cl₂. The united organic layers were dried over MgSO₄ and the solvent evaporated i.vac. to yield 3.73 g (99% yield) of **7** as a white gluelike solid. The product was used without further purification.

de-value was determined to be 97.88% by HPLC.

HPLC (150 mm YMC-Pack ODS-A, 4.6 mm, methanol:TFA = 65:35, 0.8 mL/min, 10.0 MPa, 308 K): 50.50 min (98.94% peak area, **7**), 52.86 min (1.06% peak area, Boc-D-Lys(2Cl-Z)-D-Lys(2Cl-Z)).

Deprotection with LiOH:

5 was reacted following the general procedure for the deprotection of the methyl ester.

de-value was determined to be 99.24% by HPLC.

HPLC (150 mm YMC-Pack ODS-A, 4.6 mm, methanol:TFA = 65:35, 0.8 mL/min, 10.1 MPa, 308 K): 50.60 min (99.47% peak area, **7**), 52.86 min (0.38% peak area, Boc-D-Lys(2Cl-Z)-D-Lys(2Cl-Z)).

R_F = 0.16 (EE:acetone 1:1)

¹H NMR (300 MHz, DMSO-d₆, 20 °C): δ 7.90 (d, ³J(H,H) = 7.6 Hz, 1 H, N⁷H), 7.48 - 7.30 (m, 10 H, C¹⁹⁻²²H, C³²⁻³⁵H, N²⁸H, N¹⁵H), 6.73 (d, ³J(H,H) = 7.9 Hz, 1 H, N⁴H), 5.07 (s, 4 H, C¹⁷H₂, C³⁰H₂), 4.16 - 4.13 (m, 1 H, C⁸H), 3.94 - 3.91

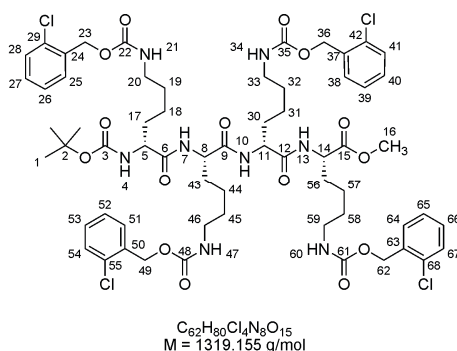
(m, 1 H, C^5H), 2.98 - 2.94 (m, 4 H, $C^{14}H_2$, $C^{27}H_2$), 1.71 - 1.14 (m, 21 H, 3 C^1H_3 , $C^{11-13}H_2$, $C^{24-26}H_2$).

^{13}C NMR (DMSO- d_6): δ 173.86, 172.43, 155.58, 155.11, 134.95, 132.60, 129.94, 129.56, 127.59, 78.35, 62.87, 54.50, 51.96, 40.47, 32.18, 31.24, 29.37, 29.24, 28.49, 23.02, 22.81.

ESI-MS: m/z = 711 (calcd 711 for $C_{33}H_{44}Cl_2N_4O_9 + 1 H^+$), 733 (calcd 733 for $C_{33}H_{44}Cl_2N_4O_9 + 1 Na^+$).

High-resolution ESI-MS: m/z = 733.237667 (calcd 733.237759 for $C_{33}H_{44}Cl_2N_4O_9 + 1 Na^+$).

Boc-(D-Lys(2Cl-Z)-L-Lys(2Cl-Z))₂-Me (**8**):



Synthesis using DIC:

6 (0.18 g, 0.25 mmol), **7** (0.16 g, 0.25 mmol) and HOBT (0.04 g, 0.28 mmol) were dissolved in 5.0 mL CH_2Cl_2 and cooled to 0 °C. To the cold solution, DIC (0.05 mL, 0.33 mmol) was added. The solution was allowed to warm up to room temperature and stirred for 2 h. After 2 h reaction time, TLC showed no complete conversion, so 0.01 mL DIC and 0.01 g HOBT were added. 1.5 h later, TLC still showed no complete conversion, so that further 0.01 mL DIC was added. After 4 h reaction time, the reaction mixture was extracted with 1 M aqueous citric acid solution (3x100 mL), water (3x100 mL), saturated aqueous $NaHCO_3$ -solution (3x100 mL), and water (3x100 mL). The organic layer was dried over $MgSO_4$, filtered, and evaporated i.vac. Purification of the pale yellow, glue-like liquid via column chromatography on silica (eluent: CH_2Cl_2 :acetone 9:1) gave 192 mg (58% yield) of **8**.

3 Linear D-(*alt*)-L-peptides

Final purification by preparative HPLC: (210 mm Nucleodur 100-16-C18/A, 25 mm, methanol:water = 80:20, 20.0 mL/min, 3.6 MPa, 308 K).

HPLC (100 mm Microsorb C18, 4.6 mm, methanol:water = 80:20, 0.8 mL/min, 15.1 MPa, 308 K): 23.99 min (>98.1% peak area, **8**).

Synthesis using EDC:

6 (2.35 g, 3.30 mmol), **7** (2.06 g, 3.30 mmol), and HOBT (0.49 g, 3.63 mmol) were dissolved in 100.0 mL CH₂Cl₂ and cooled to 0 °C. To the cold solution, a concentrated solution of EDC (0.82 g, 4.29 mmol) in CH₂Cl₂ was added. The solution was allowed to warm up to room temperature and was stirred for 12 h, extracted with water (3x100 mL), 1 M aqueous citric acid solution (3x100 mL), water (3x100 mL), saturated aqueous NaHCO₃-solution (3x100 mL), and water (3x100 mL). The organic layer was dried over MgSO₄, filtered and evaporated i.vac. The solid crude product was suspended in EE and filtered. The solid was extensively washed with EE and dried. Filtration gave 4.28 g (yield: 98%) of pure **8** as a white solid.

HPLC (100 mm Microsorb "Short-One", 4.6 mm, methanol:water = 80:20, 0.8 mL/min, 14.3 MPa, 308 K): 19.44 min (>99.9% peak area, **8**).

R_F = 0.4 (EE:acetone 9:1)

¹H NMR (300 MHz, DMSO-d₆, 20 °C): δ 8.09 (d, ³J(H,H) = 7.4 Hz, 1 H, N⁷H or N¹⁰H or N¹³H), 7.99 (d, ³J(H,H) = 8.0 Hz, 1 H, N⁷H or N¹⁰H or N¹³H), 7.86 (d, ³J(H,H) = 7.2 Hz, 1 H, N⁷H or N¹⁰H or N¹³H), 7.47 - 7.32 (m, 16 H, C²⁵⁻²⁸H, C³⁸⁻⁴¹H, C⁵¹⁻⁵⁴H, C⁶⁴⁻⁶⁷H), 7.29 - 7.24 (m, 4 H, N²¹H, N³⁴H, N⁴⁷H, N⁶⁰H), 6.75 (d, ³J(H,H) = 7.4 Hz, 1 H, N⁴H), 5.07 (s, 8 H, C²³H₂, C³⁶H₂, C⁴⁹H₂, C⁶²H₂), 4.30 - 4.19 (m, 3 H, C⁸H, C¹¹H, C¹⁴H), 3.93 - 3.87 (m, 1 H, C⁵H), 3.61 (s, 3 H, C¹⁶H₃), 2.97 - 2.94 (m, 8 H, C²⁰H₂, C³³H₂, C⁴⁶H₂, C⁵⁹H₂), 1.73 - 1.15 (m, 33 H, 3 C¹H₃, C¹⁷⁻¹⁹H₂, C³⁰⁻³²H₂, C⁴³⁻⁴⁵H₂, C⁵⁶⁻⁵⁸H₂).

¹³C NMR (DMSO-d₆): δ 173.30, 173.08, 172.40, 172.26, 156.67, 156.64, 135.51, 133.16, 130.51, 130.12, 128.14, 79.03, 63.42, 52.65, 52.59, 41.11, 40.91, 32.77, 32.55, 32.53, 31.49, 29.90, 29.87, 29.82, 29.65, 29.04, 23.62, 23.34, 23.30.

ESI-MS: m/z = 1339 (calcd 1339 for C₆₂H₈₀Cl₄N₈O₁₅ + 1 Na⁺).

High-resolution ESI-MS: $m/z = 1339.437227$ (calcd 1339.438944 for $C_{62}H_{80}Cl_4N_8O_{15} + 1 Na^+$).

2Cl-Z-deprotection attempts:

8 (0.100 g, 0.076 mmol) was dissolved in MeOH:EE 1:1 (20 mL). Pd/C (0.01 g, 10 mass-%) was added and the solution stirred under hydrogen atmosphere until reaction was finished (2 days, TLC monitoring). The solution was filtered through a pad of celite and evaporated i.vac. to give 0.075 g (yield: 153%) of the crude product as a pale yellow solid. High yield caused by rests of celite and charcoal. Attempts to purify product by extracting it with acidic/neutral/basic water failed. Product could not be recovered from aqueous layer.

R_F = baseline spot (CH_2Cl_2 :MeOH 9:1)

NMR was taken in $CDCl_3$: CD_3OD of unknown ratio. CD_3OD was impure. NMR not reproducible.

8 (0.050 g, 0.038 mmol) was dissolved in MeOH:EE 1:1 (10 mL), Pd/C (0.005 g) was added and the solution stirred under hydrogen atmosphere (ca. 2 bar) until the reaction was finished (TLC monitoring). The solution was filtered through celite and the solvents were evaporated i.vac. The remaining solid was dissolved in water and divided from solid by centrifugation. ESI-MS and NMR showed signals from partly deprotected **8**.

ESI-MS: $m/z = 545$ (calcd 545 for $C_{25}H_{52}N_8O_5 + 1 H^+$), 645 (calcd 645 for $C_{30}H_{60}N_8O_7 + 1 H^+$), 713 (calcd 713 for $C_{33}H_{57}ClN_8O_7 + 1 H^+$), 813 (calcd 813 for $C_{38}H_{65}ClN_8O_9 + 1 H^+$), 982 (calcd 982 for $C_{46}H_{70}Cl_2N_8O_{11} + 1 H^+$).

8 (0.020 g, 0.026 mmol) was dissolved in CH_2Cl_2 /MeOH 9:1 (20 mL), 4.4% formic acid was added and the solution stirred at room temperature. After 24 h, TLC showed no conversion, so more formic acid (2.4 mL) was added. After 6 days, the solution was filtered through celite and the solvents were evaporated i.vac. ESI-MS confirmed TLC and showed just signals from starting material.

ESI-MS: $m/z = 530$ (calcd 530 for $C_{24}H_{50}N_8O_5 + 1 H^+$), 545 (calcd 545 for $C_{25}H_{52}N_8O_5 + 1 H^+$), 630 (calcd 630 for $C_{29}H_{58}N_8O_7 + 1 H^+$), 645 (calcd 645 for

3 Linear D-(*alt*)-L-peptides

$C_{30}H_{60}N_8O_7 + 1 H^+$), 699 (calcd for $C_{32}H_{55}ClN_8O_7 + 1 H^+$), 713 (calcd 713 for $C_{33}H_{57}ClN_8O_7 + 1 H^+$), 798 (calcd 798 for $C_{37}H_{63}ClN_8O_9 + 1 H^+$), 813 (calcd 813 for $C_{38}H_{65}ClN_8O_9 + 1 H^+$), 880 (calcd. 880 for $C_{41}H_{62}Cl_2N_8O_9 + 1 H^+$), 982 (calcd 982 for $C_{46}H_{70}Cl_2N_8O_{11} + 1 H^+$), 1050 (calcd 1050 for $C_{49}H_{67}Cl_3N_8O_{11} + 1 H^+$), 1150 (calcd 1150 for $C_{54}H_{74}Cl_3N_8O_{13} + 1 H^+$), 1219 (calcd 1219 for $C_{57}H_{74}Cl_4N_8O_{13} + 1 H^+$).

8 (0.020 g, 0.026 mmol) was dissolved in CH_2Cl_2 :MeOH 1:1 (10 mL), ground ammonium formate (ca. 20 mg) was added and the solution stirred at room temperature. After 10 min, TLC showed no conversion, so the mixture was shortly heated to activate the ammonium formate. After 4 h, TLC showed no starting material, so more MeOH (5 mL) was added and the reaction stirred at room temperature. After 24 h, the solution was filtered through celite and the solvents were evaporated i.vac. Ammonium formate was removed under high vacuum. ESI-MS showed signals from product and completely *N*-deprotected **8** (Boc was also removed). NMR showed still some signals from partly deprotected **8**.

ESI-MS: $m/z = 545$ (calcd 545 for $C_{25}H_{52}N_8O_5 + 1 H^+$), 645 (calcd 645 for $C_{30}H_{60}N_8O_7 + 1 H^+$), 813 (calcd 813 for $C_{38}H_{65}ClN_8O_9 + 1 H^+$).

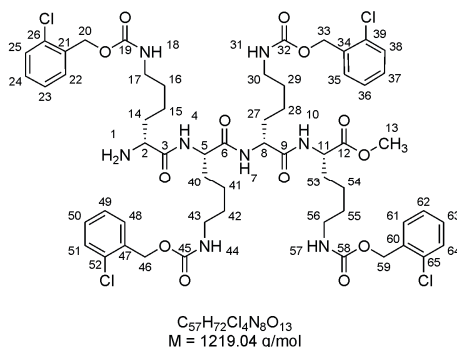
8 (0.020 g, 0.026 mmol) was dissolved in MeOH:EE 1:1 (14 mL), Pd/C (0.003 g) was added and the solution stirred under hydrogen atmosphere (30 bar) for 20 h. The solution was filtered through celite and the solvents were evaporated i.vac. The remaining solid was dissolved in water and separated from solid by centrifugation. ESI-MS showed signals from partly deprotected **8**.

ESI-MS: $m/z = 631$ (calcd 631 for $C_{29}H_{58}ClN_8O_7 + 1 H^+$), 681 (calcd 681 for **8** + 2 Na^+), 1150 (calcd 1150 for $C_{54}H_{74}Cl_3N_8O_{13} + 1 H^+$), 1171 (calcd 1171 for $C_{54}H_{74}Cl_3N_8O_{13} + 1 Na^+$), 1239 (calcd 1239 for $C_{57}H_{74}Cl_4N_8O_{13} + 1 Na^+$), 1339 (calcd 1339 for **8** + 1 Na^+).

8 (0.020 g, 0.026 mmol) was dissolved in MeOH:EE 1:1 (10 mL), Pd/C (0.003 g) and 1,4-cyclohexadiene (0.019 mL, 0.20 mmol) was added and the solution stirred at room temperature for 6 days. The solution was filtered through celite and the solvents evaporated i.vac. The remaining solid was dissolved in water and separated from solid by centrifugation. ESI-MS showed signals from partly deprotected **8**.

ESI-MS: $m/z = 631$ (calcd 631 for $C_{57}H_{74}Cl_4N_8O_{13} + 2 Na^+$), 681 (calcd 681 for **8** + 2 Na^+), 1239 (calcd 1239 for $C_{57}H_{74}Cl_4N_8O_{13} + 1 Na^+$), 1339 (calcd 1339 for **8** + 1 Na^+).

(D-Lys(2Cl-Z)-L-Lys(2Cl-Z))₂-Me (**9**):



8 was reacted following the general procedure for the deprotection of the Boc group.

HPLC (150 mm YMC-Pack ODS-A, 4.6 mm, acetonitrile/10 mmol TEAA pH7 = 60:40, 0.8 mL/min, 7.4 MPa, 308 K): 26.87 min (99.28% peak area, **9**).

$R_f = 0.34$ (CH_2Cl_2 :MeOH 9:1)

1H NMR (300 MHz, DMSO- d_6 , 20 °C): δ 8.23 (d, $^3J(H,H) = 7.5$ Hz, 1 H, N^4H or N^7H or $N^{10}H$), 8.14 (d, $^3J(H,H) = 8.2$ Hz, 1 H, N^4H or N^7H or $N^{10}H$), 8.08 - 8.04 (m, 1 H, N^4H or N^7H or $N^{10}H$), 7.48 - 7.29 (m, 20 H, $C^{22-25}H$, $C^{35-38}H$, $C^{48-51}H$, $C^{61-64}H$, $N^{18}H$, $N^{31}H$, $N^{44}H$, $N^{57}H$), 5.07 (s, 8 H, $C^{20}H_2$, $C^{33}H_2$, $C^{46}H_2$, $C^{59}H_2$), 4.31 - 4.18 (m, 3 H, C^5H , C^8H , $C^{11}H$), 3.61 (s, 3 H, $C^{13}H_3$), 3.20 - 3.14 (m, 1 H, C^2H), 3.03 - 2.90 (m, 8 H, $C^{17}H_2$, $C^{30}H_2$, $C^{43}H_2$, $C^{56}H_2$), 2.20 (br. s, 2 H, N^1H_2), 1.78 - 1.08 (m, 24 H, $C^{14-16}H_2$, $C^{27-29}H_2$, $C^{40-42}H_2$, $C^{53-55}H_2$).

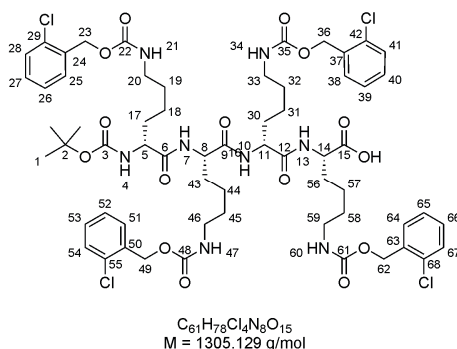
3 Linear D-(*alt*)-L-peptides

^{13}C NMR (DMSO- d_6): δ 173.33, 172.52, 172.45, 156.66, 135.53, 135.51, 133.16, 130.54, 130.51, 130.12, 128.14, 63.41, 52.66, 41.18, 40.91, 40.70, 40.49, 40.45, 32.82, 31.47, 30.19, 30.14, 29.93, 29.89, 29.81, 29.68, 23.49, 23.33.

ESI-MS: m/z = 1217 (calcd 1217 for $\text{C}_{57}\text{H}_{72}\text{Cl}_4\text{N}_8\text{O}_{13} + 1 \text{ H}^+$).

High-resolution ESI-MS: m/z = 1217.405464 (calcd 1217.404571 for $\text{C}_{57}\text{H}_{73}\text{Cl}_4\text{N}_8\text{O}_{13} + 1 \text{ H}^+$).

Boc-(D-Lys(2Cl-Z)-L-Lys(2Cl-Z))₂ (**10**):



8 was reacted following the general procedure for the deprotection of the methyl ester.

HPLC (150 mm YMC-Pack ODS-A, 4.6 mm, acetonitrile/0.1% TFA = 90:10, 0.8 mL/min, 7.5 MPa, 308 K): 4.85 min (98.73% peak area, **10**).

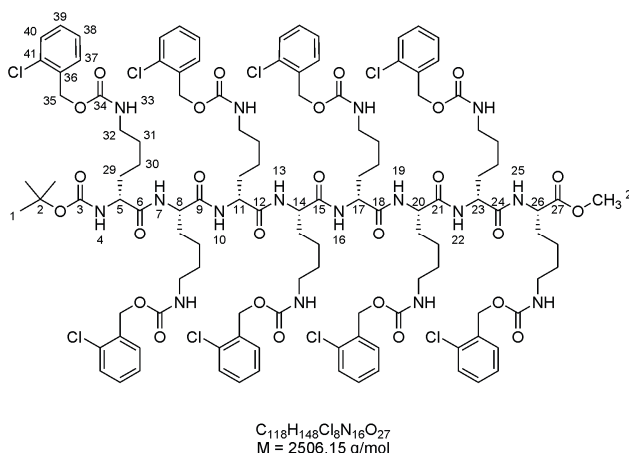
R_F = 0.05 (CH_2Cl_2 :MeOH 9:1)

^1H NMR (300 MHz, DMSO- d_6 , 20 °C): δ 12.40 (br. s, 1 H, O^{16}H), 8.05 (d, $^3J(\text{H,H}) = 7.6 \text{ Hz}$, 1 H, N^7H or N^{10}H or N^{13}H), 7.96 (d, $^3J(\text{H,H}) = 7.7 \text{ Hz}$, 1 H, N^7H or N^{10}H or N^{13}H), 7.83 (d, $^3J(\text{H,H}) = 7.4 \text{ Hz}$, 1 H, N^7H or N^{10}H or N^{13}H), 7.47 - 7.32 (m, 16 H, C^{25-28}H , C^{38-41}H , C^{51-54}H , C^{64-67}H), 7.29 - 7.24 (m, 4 H, N^{21}H , N^{34}H , N^{47}H , N^{60}H), 6.76 (d, $^3J(\text{H,H}) = 7.4 \text{ Hz}$, 1 H, N^4H), 5.07 (s, 8 H, C^{23}H_2 , C^{36}H_2 , C^{49}H_2 , C^{62}H_2), 4.30 - 4.14 (m, 3 H, C^8H , C^{11}H , C^{14}H), 3.93 - 3.87 (m, 1 H, C^5H), 2.97 - 2.94 (m, 8 H, C^{20}H_2 , C^{33}H_2 , C^{46}H_2 , C^{59}H_2), 1.70 - 1.14 (m, 33 H, 3 C^1H_3 , $\text{C}^{17-19}\text{H}_2$, $\text{C}^{30-32}\text{H}_2$, $\text{C}^{43-45}\text{H}_2$, $\text{C}^{56-58}\text{H}_2$).

ESI-MS: m/z = 1325 (calcd 1325 for $\text{C}_{61}\text{H}_{78}\text{Cl}_4\text{N}_8\text{O}_{15} + 1 \text{ Na}^+$).

High-resolution ESI-MS: $m/z = 1325.421773$ (calcd 1325.423299 for $C_{61}H_{78}Cl_4N_8O_{15} + 1 Na^+$).

Boc-(D-Lys(2Cl-Z)-L-Lys(2Cl-Z))₄-Me (**11**):



9 (0.914 g, 0.750 mmol), **10** (0.979 g, 0.750 mmol), and HOBt (0.111 g, 0.825 mmol) were dissolved in 100 mL CH_2Cl_2 :DMF (as less DMF as possible) and cooled to 0 °C. To the cold solution, a concentrated solution of EDC in CH_2Cl_2 (0.187 g, 0.975 mmol) was added. The solution was allowed to warm up to room temperature and stirred for 12 h. After TLC monitoring, CH_2Cl_2 was removed i.vac. and replaced by EE. The Solution was extracted with water (4x50 mL), 1 M aqueous citric acid solution (1x50 mL), water (1x50 mL), saturated aqueous $NaHCO_3$ -solution (3x50 mL), and water (1x50 mL). The organic layer was dried over $MgSO_4$, filtered and evaporated i.vac. The solid crude product was suspended in EE and filtered. The solid was extensively washed with EE and dried to give 1.60 g (yield: 85%) of **11** as a white solid. If necessary, product was further purified via column chromatography on silica (eluent: CH_2Cl_2 :MeOH 9:1).

HPLC (150 mm YMC-Pack ODS-A, 4.6 mm, acetonitrile/10 mmol TEAA pH7 = 90:10, 0.8 mL/min, 4.8 MPa, 308 K): 8.92 min (98.3% peak area, **11**).

$R_F = 0.64$ (CH_2Cl_2 :MeOH 9:1)

1H NMR (400 MHz, $DMSO-d_6$, 20 °C): δ 8.27 (d, $^3J(H,H) = 7.5$ Hz, 1 H, amide NH), 8.07 (d, $^3J(H,H) = 8.0$ Hz, 1 H, amide NH), 8.00 - 7.83 (m, 5 H, amide NH), 7.47 - 7.31 (m, 32 H, 8 $C^{34-37}H$), 7.29 - 7.22 (m, 8 H, 8 $N^{33}H$), 6.76 (d,

3 Linear D-(*alt*)-L-peptides

$^3J(\text{H,H}) = 7.1 \text{ Hz}$, 1 H, N^4H), 5.06 (s, 16 H, 8 C^{35}H_2), 4.38 - 4.16 (m, 7 H, C^8H , C^{11}H , C^{14}H , C^{17}H , C^{20}H , C^{23}H , C^{26}H), 3.93 - 3.88 (m, 1 H, C^5H), 3.60 (s, 3 H, C^{28}H_3), 2.99 - 2.92 (m, 16 H, 8 C^{32}H_2), 1.73 - 1.10 (m, 57 H, 3 C^1H_3 , 8 $\text{C}^{29-31}\text{H}_2$).

^{13}C NMR (DMSO- d_6): δ 173.44, 173.21, 172.57, 172.42, 172.35, 172.29, 156.73, 156.70, 156.29, 135.55, 133.23, 133.19, 130.54, 130.15, 128.17, 96.15, 79.06, 63.47, 55.84, 53.57, 53.53, 53.36, 52.84, 52.74, 52.63, 40.99, 40.92, 32.88, 32.85, 32.71, 32.56, 32.53, 32.49, 31.63, 31.59, 29.98, 29.93, 29.88, 29.72, 29.07, 23.67, 23.41.

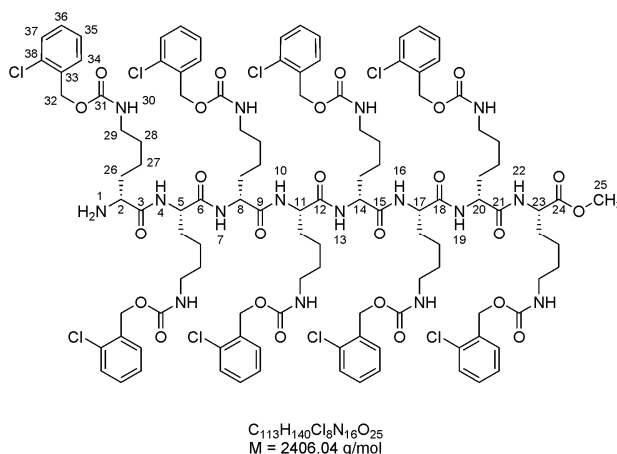
ESI-MS: $m/z = 2523$ (calcd 2523 for $\text{C}_{118}\text{H}_{148}\text{Cl}_8\text{N}_{16}\text{O}_{27} + 1 \text{ Na}^+$), 1273.4 (calcd 1273.4 for $\text{C}_{118}\text{H}_{148}\text{Cl}_8\text{N}_{16}\text{O}_{27} + 2 \text{ Na}^+$).

High-resolution ESI-MS: $m/z = 1273.403652$ (calcd 1273.399624 for $\text{C}_{118}\text{H}_{148}\text{Cl}_8\text{N}_{16}\text{O}_{27} + 2 \text{ Na}^+$).

2Cl-Z-deprotection attempts:

11 (0.05 g, 0.02 mmol) was dissolved in MeOH:EE 1:1 (20 mL), Pd/C (0.005 g) was added and the solution stirred under hydrogen atmosphere (ca. 2 bar). After 12 h, TLC showed no complete conversion, so MeOH (5 mL) was added. After 2 h, TLC still showed no complete conversion. 10 mL of the reaction mixture was filtered through celite and evaporated i.vac. To the remaining mixture, $\text{Pd}(\text{OH})_2$ (0.005 g) was added and the mixture stirred for 18 h. TLC showed no remaining starting material, so mixture was filtered through celite and evaporated i.vac. For both samples ESI-MS showed a variety of different peaks. Some could be assigned to different partly deprotected (D-Lys(2Cl-Z)-L-Lys(2Cl-Z))₄-Me, some could not. No peak for the desired product was found.

Boc deprotection of **11** to (D-Lys(2Cl-Z)-L-Lys(2Cl-Z))₄-Me:



11 was reacted following the general procedure for the deprotection of the Boc group.

HPLC (150 mm YMC-Pack ODS-A, 4.6 mm, acetonitrile/water = 80:20, 0.8 mL/min, 6.2 MPa, 308 K): 22.77 min (97.5% peak area, (D-Lys(2Cl-Z)-L-Lys(2Cl-Z))₄-Me).

R_F = 0.36 (CH₂Cl₂:MeOH 9:1)

¹H NMR (400 MHz, DMSO-d₆, 20 °C): δ 8.66 (br. s, 1 H, amide NH), 8.40 - 8.27 (m, 2 H, amide NH), 8.14 - 8.05 (m, 4 H, amide NH), 7.38 - 7.22 (m, 40 H, 8 N³⁰H), 8 C³⁴⁻³⁷H), 6.94 (br. s, 1 H, amide NH), 5.06 (s, 16 H, 8 C³²H₂), 4.47 - 4.15 (m, 7 H, C⁵H, C⁸H, C¹¹H, C¹⁴H, C¹⁷H, C²⁰H, C²³H), 3.78 - 3.56 (m, 1 H, C²H), 3.61 (s, 3 H, C²⁵H₃), 3.06 - 2.88 (m, 16 H, 8 C²⁹H₂), 1.77 - 1.10 (m, 48 H, 8 C²⁶⁻²⁸H₂).

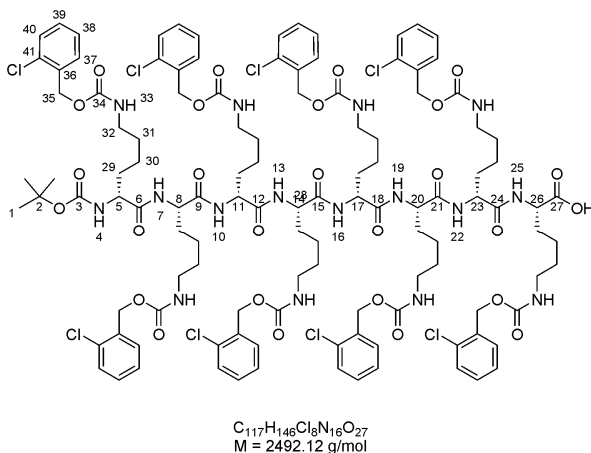
¹³C NMR (DMSO-d₆): δ 173.46, 172.65, 172.44, 156.72, 135.55, 135.52, 133.23, 133.18, 130.61, 130.53, 130.16, 128.19, 96.16, 63.48, 55.86, 53.46, 53.41, 53.39, 53.31, 52.99, 52.75, 52.70, 40.57, 33.16, 32.88, 32.84, 32.81, 31.54, 29.91, 29.72, 23.55, 23.51, 23.46.

ESI-MS: m/z = 2401 (calcd 2401 for C₁₁₃H₁₄₀Cl₈N₁₆O₂₅ + 1 H⁺), 2423 (calcd 2423 for C₁₁₃H₁₄₀Cl₈N₁₆O₂₅ + 1 Na⁺), 1212.4 (calcd 1212.4 for C₁₁₃H₁₄₀Cl₈N₁₆O₂₅ + 1 Na⁺ + 1 H⁺), 1223.4 (calcd 1223.4 for C₁₁₃H₁₄₀Cl₈N₁₆O₂₅ + 2 Na⁺).

High-resolution ESI-MS: m/z = 1201.391467 (calcd 1201.391467 for C₁₁₃H₁₄₀Cl₈N₁₆O₂₅ + 2 H⁺).

3 Linear D-(*alt*)-L-peptides

Deprotection of the Me ester on **11** to Boc-(D-Lys(2Cl-Z)-L-Lys(2Cl-Z))₄:



11 was reacted following the general procedure for the deprotection of the methyl ester.

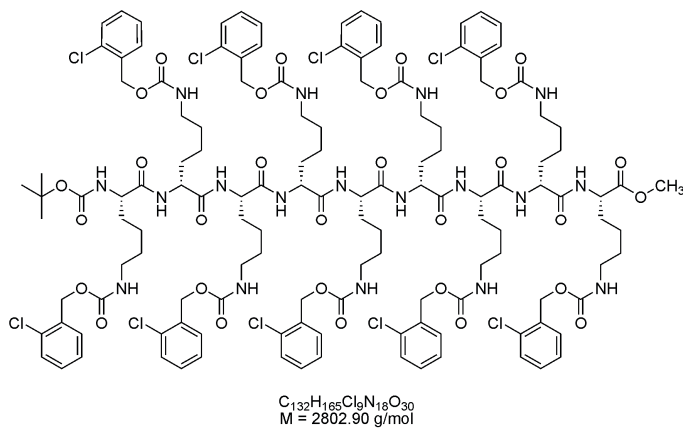
HPLC (150 mm YMC-Pack ODS-A, 4.6 mm, acetonitrile/0.1% TFA = 85:15, 0.8 mL/min, 4.6 MPa, 308 K): 13.69 min (97.20% peak area, Boc-(D-Lys(2Cl-Z)-L-Lys(2Cl-Z))₄).

R_F = 0.46 (CH₂Cl₂:MeOH 9:1)

ESI-MS: m/z = 2509 (calcd 2509 for $C_{117}H_{146}Cl_8N_{16}O_{27} + 1 Na^+$), 1266.4 (calcd 1256.4 for $C_{117}H_{146}Cl_8N_{16}O_{27} + 2 Na^+$).

High-resolution ESI-MS: m/z = 1266.389144 (calcd 1266.39179 for $C_{117}H_{146}Cl_8N_{16}O_{27} + 2 Na^+$).

Boc-L-Lys(2Cl-Z)-(D-Lys(2Cl-Z)-L-Lys(2Cl-Z))₄-Me (**33**):



(D-Lys(2Cl-Z)-L-Lys(2Cl-Z))₄-Me (0.029 g, 0.012 mmol), Boc-L-Lys(2Cl-Z) (0.006 g, 0.016 mmol), and HOBT (0.002 g, 0.016 mmol) were dissolved in CH₂Cl₂:DMF (5:1, 12 mL) and cooled to 0 °C. To the cold solution, a concentrated solution of EDC in CH₂Cl₂ (0.003 g, 0.016 mmol) was added and the solution allowed to warm up to room temperature. After 1 h, no product had been formed, so EDC (2 mg) and HOBT (1 mg) was added. After 4 h, there was still remaining (D-Lys(2Cl-Z)-L-Lys(2Cl-Z))₄-Me, so further EDC (10 mg) and HOBT (2 mg) was added. After stirring at room temperature over night (TLC monitoring), the solution was extracted with 1 M aqueous citric acid solution (1x10 mL), water (1x10 mL), saturated aqueous NaHCO₃-solution (3x10 mL), water (1x50 mL), and brine (1x10 mL). The organic layer was dried over MgSO₄, filtered and evaporated i.vac. The solid was suspended in EE, filtered and washed extensively with EE to give 0.030 g (Yield: 89%) of **33** as a white solid.

HPLC: (150 mm YMC-Pack ODS-A, 4.6 mm, acetonitrile/water = 85:15, 0.8 mL/min, 4.5 MPa, 308 K): 25.95 min (93.5% peak area, **33**).

Procedure see above, but with additional purification via column chromatography on silica (eluent: CH₂Cl₂:MeOH 95:5). Yield: 97%.

HPLC: (150 mm YMC-Pack ODS-A, 4.6 mm, acetonitrile/water = 85:15, 0.8 mL/min, 4.6 MPa, 308 K): 25.96 min (95.0% peak area, **33**).

(D-Lys(2Cl-Z)-L-Lys(2Cl-Z))₄-Me (0.962 g, 0.400 mmol), Boc-L-Lys(2Cl-Z) (0.216 g, 0.520 mmol), and HOBT (0.070 g, 0.520 mmol) were dissolved in DMF (15 mL) and cooled to 0 °C. To the cold solution, a concentrated solution of EDC in CH₂Cl₂ (0.199 g, 1.040 mmol) was added, the solution allowed to warm up to room temperature and stirred over night. Reaction mixture was concentrated i.vac., CH₂Cl₂ and water were added and the biphasic system stirred for 10 minutes. After phase separation, MeOH was added to the organic layer to assure solubility of the peptide, and organic layer was extracted with brine (1x30 mL). The organic layer was dried over MgSO₄, filtered and evaporated i.vac. The solid was suspended in EE (50 mL), hexane (50 mL) was added and the solid filtered and washed extensively with EE/hexane 1:1 to give 1.24 g of **33** as a white solid. But as TLC showed unreacted (D-Lys(2Cl-Z)-L-

3 Linear D-(*alt*)-L-peptides

Lys(2Cl-Z))₄-Me, coupling reaction was restarted in DMF with Boc-L-Lys(2Cl-Z) (0.040 g), HOBT (0.030 g) and EDC (0.060 g) and stirred for 60 h. Work-up was repeated and gave 1.12 g (Yield: 100%) of **33** as a white solid.

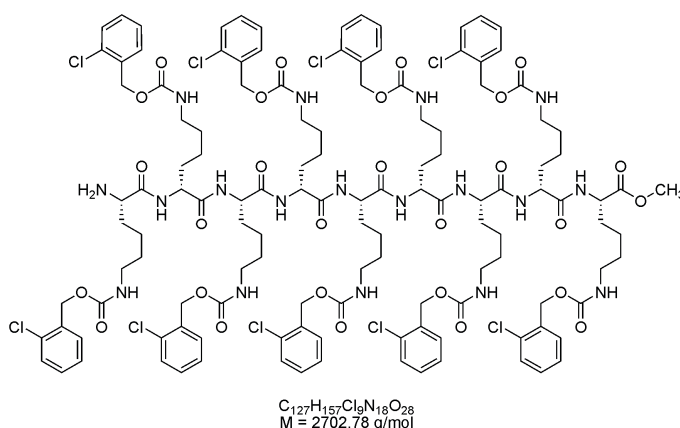
HPLC: (150 mm YMC-Pack ODS-A, 4.6 mm, acetonitrile/water = 85:15, 0.8 mL/min, 4.1 MPa, 308 K): 25.50 min (95.1% peak area, **33**).

R_F = 0.5 (CH₂Cl₂:MeOH 9:1)

ESI-MS: m/z = 1424 (calcd 1424 for C₁₃₂H₁₆₅Cl₉N₁₈O₃₀ + 2 Na⁺).

High-resolution ESI-MS: m/z = 1421.444430 (calcd 1421.446009 for C₁₃₂H₁₆₅Cl₉N₁₈O₃₀ + 2 Na⁺).

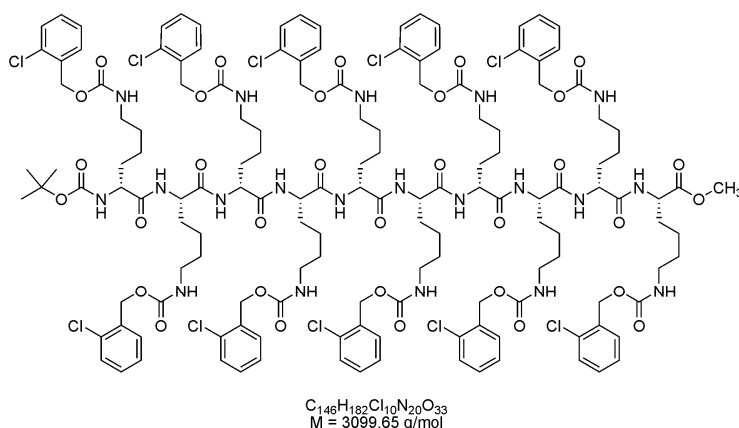
Boc deprotection of **33** to L-Lys(2Cl-Z)-(D-Lys(2Cl-Z)-L-Lys(2Cl-Z))₄-Me:



33 (1.12 g, 0.400 mmol) was reacted following the general procedure for the deprotection of the Boc group. TFA (20 mL), CH₂Cl₂:MeOH (9:1) (20 mL).

R_F = 0.32 (CH₂Cl₂:MeOH 9:1)

Boc-(D-Lys(2Cl-Z)-L-Lys(2Cl-Z))₅-Me (**13**):



Procedures starting from *N*-deprotected octamer:

(D-Lys(2Cl-Z)-L-Lys(2Cl-Z))₄-Me (0.205 g, 0.085 mmol), **7** (0.07 g, 0.098 mmol), and HOBt (0.013 g, 0.094 mmol) were dissolved in 80.0 mL CH₂Cl₂:DMF (as less DMF as possible) and cooled to 0 °C. To the cold solution, a concentrated solution of EDC in CH₂Cl₂ (0.02 g, 0.11 mmol) was added. The solution was allowed to warm up to room temperature and stirred for 12 h. After TLC monitoring, the solution was extracted with water (3x100 mL), 1 M aqueous citric acid solution (1x100 mL), water (1x100 mL), saturated aqueous NaHCO₃-solution (1x100 mL), water (1x100 mL), and brine (1x100 mL). The organic layer was dried over MgSO₄, filtered and evaporated i.vac. The crude product was suspended in EE, filtered, and the solid extensively washed with EE. The white solid was purified via column chromatography on silica (eluent: CH₂Cl₂:MeOH 95:5) to give 0.102 g (yield: 42%) of **13** as a white solid.

HPLC (150 mm YMC-Pack ODS-A, 4.6 mm, acetonitrile/water = 85:15, 0.8 mL/min, 4.8 MPa, 308 K): 41.78 min (15.8% peak area, probably diastereomer), 43.53 min (76.6% peak area, **13**).

The TFA-salt of (D-Lys(2Cl-Z)-L-Lys(2Cl-Z))₄-Me (0.030 g, 0.012 mmol), **7** (0.017 g, 0.024 mmol), DIPEA (0.01 M in CH₂Cl₂) (1.30 mL, 0.013 mmol), and HOBt (0.004 g, 0.030 mmol) were dissolved in 40.0 mL CH₂Cl₂:DMF (as less DMF as possible) and cooled to 0 °C. To the cold solution, a concentrated solution of EDC in CH₂Cl₂ (0.006 g, 0.030 mmol) was added. The solution was

3 Linear D-(*alt*)-L-peptides

allowed to warm up to room temperature and stirred for 12 h. After TLC monitoring, the solution was extracted with water (3x100 mL), 1 M aqueous citric acid solution (1x100 mL), water (1x100 mL), saturated aqueous NaHCO₃-solution (1x100 mL), water (1x100 mL), and brine (1x100 mL). The organic layer was dried over MgSO₄, filtered and evaporated i.vac. The crude product was suspended in EE, filtered and the solid extensively washed with EE to give **13** as a white solid in quantitative yield.

HPLC (150 mm YMC-Pack ODS-A, 4.6 mm, acetonitrile/water = 85:15, 0.8 mL/min, 4.4 MPa, 308 K): 40.96 min (9.2% peak area, probably diastereomer), 42.66 min (83.0% peak area, **13**).

7 (0.022 g, 0.030 mmol) and NHS (0.004 g, 0.036 mmol) were dissolved in CH₂Cl₂ (15 mL) and cooled to 0 °C. To the cold solution, a concentrated solution of EDC in CH₂Cl₂ (0.007 g, 0.036 mmol) was added and the solution allowed to warm up to room temperature. After formation of the NHS-ester (TLC monitoring, approx. 5 to 10 min), (D-Lys(2Cl-Z)-L-Lys(2Cl-Z))₄-Me (0.03 g, 0.012 mmol) in 20.0 mL CH₂Cl₂:DMF (as less DMF as possible) was added dropwise. The solution was stirred at room temperature until (D-Lys(2Cl-Z)-L-Lys(2Cl-Z))₄-Me was consumed. The solution was evaporated i.vac. The crude product was dissolved in THF:water to quench remaining NHS-ester. The solvent was evaporated i.vac. and the remaining solid suspended in EE, filtered and the solid extensively washed with EE to give 0.036 g (yield: 99%) of **13** as a white solid.

HPLC: (150 mm YMC-Pack ODS-A, 4.6 mm, acetonitrile/0.1% TFA = 85:15, 0.8 mL/min, 4.2 MPa, 308 K): 41.91 min (77.8% peak area, **13**).

7 (0.174 g, 0.240 mmol) and NHS (0.035 g, 0.300 mmol) were dissolved in CH₂Cl₂ (150 mL) and cooled to 0 °C. To the cold solution, a concentrated solution of EDC in CH₂Cl₂ (0.069 g, 0.360 mmol) was added and the solution allowed to warm up to room temperature. After formation of the NHS-ester (TLC monitoring, approx. 5 to 10 min), (D-Lys(2Cl-Z)-L-Lys(2Cl-Z))₄-Me (0.289 g, 0.120 mmol) in 42.0 mL CH₂Cl₂:DMF (40:12) was added dropwise over 15 min.

The solution was stirred at room temperature until (D-Lys(2Cl-Z)-L-Lys(2Cl-Z))₄-Me was consumed. The solution was evaporated i.vac. and wrapped twice with CH₂Cl₂. The solid was dissolved in CH₂Cl₂:MeOH and evaporated. The crude product (750 mg) was purified via column chromatography on silica (eluent: CH₂Cl₂:MeOH 95:5), to give 440 mg of crude product. The solid was suspended in EE and filtered. The solid was washed extensively with EE to give 0.270 g (yield: 73%) of **13** as a white solid.

HPLC: (150 mm YMC-Pack ODS-A, 4.6 mm, acetonitrile/0.1% TFA = 85:15, 0.8 mL/min, 4.2 MPa, 308 K): 41.71 min (83.7% peak area, **13**).

7 (1.161 g, 1.60 mmol) and NHS (0.230 g, 2.00 mmol) were dissolved in CH₂Cl₂ (500 mL) and cooled to 0 °C. To the cold solution, a concentrated solution of EDC in CH₂Cl₂ (0.383 g, 2.50 mmol) was added and the solution allowed to warm up to room temperature. After formation of the NHS-ester (TLC monitoring, approx. 5 to 10 min), (D-Lys(2Cl-Z)-L-Lys(2Cl-Z))₄-Me (1.925 g, 0.80 mmol) in CH₂Cl₂:DMF (as less DMF as possible) was added dropwise over 15 min. The solution was stirred at room temperature until (D-Lys(2Cl-Z)-L-Lys(2Cl-Z))₄-Me was consumed. After 2 h, there was still unconsumed detectable by TLC (D-Lys(2Cl-Z)-L-Lys(2Cl-Z))₄-Me, so EDC and NHS (200 mg each) was added. After 3 h, there was still unconsumed detectable by TLC (D-Lys(2Cl-Z)-L-Lys(2Cl-Z))₄-Me, so **7** (30 mg), was added. After 16 h, the solution was concentrated i.vac. to a total volume of approx. 20 mL. Then EE was added and the precipitate filtered. The solid was extensively washed with EE, to give the crude product as a white solid, which was dissolved in CH₂Cl₂:MeOH and extracted with water (1x200 mL), 1 M aqueous citric acid solution (1x200 mL), water (1x200 mL), saturated aqueous NaHCO₃-solution (1x200 mL), water (1x200 mL), and brine (1x200 mL). The organic layer was dried over MgSO₄, filtered and evaporated i.vac. to give the crude product as a white solid. The crude product (1.99 g) was purified in several batches via column chromatography on silica (eluent: CH₂Cl₂:MeOH 95:5), to give 770 mg (yield: 31%) of **13** as a white solid.

3 Linear D-(*a/t*)-L-peptides

HPLC: (150 mm YMC-Pack ODS-A, 4.6 mm, acetonitrile/0.1% TFA = 85:15, 0.8 mL/min, 4.5 MPa, 308 K): 41.38 min (93.4% peak area, **13**).

Procedures starting from C-deprotected octamer:

Boc-(D-Lys(2Cl-Z)-L-Lys(2Cl-Z))₄ (0.210 g, 0.085 mmol), the TFA-salt of **6** (0.104 g, 0.140 mmol), NEt₃ (0.024 mL, 0.170 mmol), and HOBT (0.023 g, 0.230 mmol) were dissolved in 50.0 mL CH₂Cl₂:DMF (as less DMF as possible) and cooled to 0 °C. To the cold solution, a concentrated solution of EDC in CH₂Cl₂ (0.033 g, 0.170 mmol) was added. The solution was allowed to warm up to room temperature and stirred for 12 h. After TLC monitoring, the solution was extracted with water (3x100 mL), 1 M aqueous citric acid solution (1x100 mL), water (1x100 mL), saturated aqueous NaHCO₃-solution (1x100 mL), water (1x100 mL) and brine (1x100 mL). The organic layer was dried over MgSO₄, filtered and evaporated i.vac. The crude product was suspended in EE, filtered and the solid extensively washed with EE. The white solid was purified via column chromatography on silica (eluent: CH₂Cl₂:MeOH 95:5) to give 0.25 g (yield: 95%) of **13** as a white solid.

HPLC (150 mm YMC-Pack ODS-A, 4.6 mm, acetonitrile/water = 85:15, 0.8 mL/min, 4.8 MPa, 308 K): 43.30 min (87.6% peak area, **13**), 45.61 min (6.4% peak area, probably diastereomer).

Procedure see above, but with use of DIPEA instead of NEt₃.

HPLC (150 mm YMC-Pack ODS-A, 4.6 mm, acetonitrile/water = 85:15, 0.8 mL/min, 4.5 MPa, 308 K): 42.97 min (83.6% peak area, **13**), 45.26 min (11.0% peak area, probably diastereomer).

Boc-(D-Lys(2Cl-Z)-L-Lys(2Cl-Z))₄ (0.030 g, 0.012 mmol), the TFA-salt of **6** (0.019 g, 0.025 mmol), and HOBT (0.002 g, 0.012 mmol) were dissolved in 40.0 mL CH₂Cl₂:DMF (as less DMF as possible) and cooled to 0 °C. To the cold solution, DIPEA (0.01 M in CH₂Cl₂) (1.30 mL, 0.013 mmol) and a concentrated solution of EDC in CH₂Cl₂ (0.003 g, 0.014 mmol) was added. The solution was

stirred at 0 °C for 1 h and then for 1 h at room temperature. After TLC monitoring, one half of the solution was extracted with water (3x100 mL), 1 M aqueous citric acid solution (1x100 mL), water (1x100 mL), saturated aqueous NaHCO₃-solution (1x100 mL), water (1x100 mL), and brine (1x100 mL). The organic layer was dried over MgSO₄, filtered and evaporated i.vac. The crude product was suspended in EE, filtered and the solid extensively washed with EE. The other half was evaporated to dryness, suspended in EE, filtered and extensively washed with EE to give **13** as a white solid.

HPLC: (150 mm YMC-Pack ODS-A, 4.6 mm, acetonitrile/0.1% TFA = 85:15, 0.8 mL/min, 4.2 MPa, 308 K): 13.25 min (31.6% peak area, Boc-(D-Lys(2Cl-Z)-L-Lys(2Cl-Z))₄), 41.71 min (48.7% peak area, **13**), 44.09 min (4.5% peak area, probably diastereomer).

Procedure see above, but with use of s-collidin (1.1 eq) instead of NEt₃.

HPLC (150 mm YMC-Pack ODS-A, 4.6 mm, acetonitrile/0.1% TFA = 85:15, 0.8 mL/min, 4.5 MPa, 308 K): 13.23 min (9.2% peak area, Boc-(D-Lys(2Cl-Z)-L-Lys(2Cl-Z))₄), 41.77 min (74.6% peak area, **13**), 44.06 min (11.8% peak area, probably diastereomer).

Procedure see above, but with use of TBTU (3.0 eq, 0.012 g) instead of EDC:HOBt as coupling reagent. Additionally, 4.0 eq instead of 1.1 eq of s-collidin was used. Reaction mixture was stirred at room temperature over night. Aqueous work-up was skipped, solvent was evaporated i.vac., slurry solid precipitated in EE.

HPLC: (150 mm YMC-Pack ODS-A, 4.6 mm, acetonitrile/0.1% TFA = 85:15, 0.8 mL/min, 4.2 MPa, 308 K): 13.34 min (6.2% peak area, Boc-(D-Lys(2Cl-Z)-L-Lys(2Cl-Z))₄), 17.25 min (14.5% peak area, **11**), 41.77 min (39.2% peak area, **13**), 44.41 min (4.5% peak area, probably diastereomer).

Procedure see above, but with use of NHS (1.2 eq, 0.022 mmol) instead of HOBt; s-collidin (1.5 eq) was used as base. Reaction mixture was stirred at

3 Linear D-(*alt*)-L-peptides

room temperature over night. Aqueous work-up was skipped, solvent was evaporated i.vac., slurry solid precipitated in EE.

HPLC: (150 mm YMC-Pack ODS-A, 4.6 mm, acetonitrile/0.1% TFA = 85:15, 0.8 mL/min, 4.2 MPa, 308 K): 13.52 min (67.5% peak area, Boc-(D-Lys(2Cl-Z)-L-Lys(2Cl-Z))₄), 41.88 min (13.0% peak area, **13**), 44.66 min (4.6% peak area, probably diastereomer).

Boc-(D-Lys(2Cl-Z)-L-Lys(2Cl-Z))₄ (0.03 g, 0.012 mmol), **6** (0.025 g, 0.040 mmol), and HOBT (0.003 g, 0.024 mmol) were dissolved in 20.0 mL CH₂Cl₂:DMF (as less DMF as possible) and cooled to 0 °C. To the cold solution, a concentrated solution of EDC in CH₂Cl₂ (0.005 g, 0.024 mmol) was added. The solution was allowed to warm up to room temperature and stirred for 2 h. Then, HOBT (2 mg) and EDC (3 mg) was added and the solution stirred over night. After TLC monitoring, the solution was evaporated i.vac. The crude product was suspended in EE, filtered and the solid extensively washed with EE. The white solid was purified via column chromatography on silica (eluent: CH₂Cl₂:MeOH 95:5) to give 0.025 g (yield: 67%) of **13** as a white solid.

HPLC: (150 mm YMC-Pack ODS-A, 4.6 mm, acetonitrile/0.1% TFA = 85:15, 0.8 mL/min, 4.2 MPa, 308 K): 42.08 min (80.6% peak area, **13**), 44.52 min (7.1% peak area, probably diastereomer).

Procedures starting from *N*-deprotected nonamer:

L-Lys(2Cl-Z)-(D-Lys(2Cl-Z)-L-Lys(2Cl-Z))₄-Me (1.856 g, 0.690 mmol) was dissolved in dry DMF (40 mL) and the solution diluted with dry CH₂Cl₂ (350 mL), Boc-D-Lys(2Cl-Z) (0.372 g, 0.897 mmol) and HOBT (0.186 g, 0.138 mmol) were added and the solution was cooled to 0 °C. To the cold solution, a concentrated solution of EDC in dry CH₂Cl₂ (0.661 g, 3.45 mmol) was added. The solution was allowed to warm up to room temperature and stirred over night. TLC monitoring showed no remaining L-Lys(2Cl-Z)-(D-Lys(2Cl-Z)-L-Lys(2Cl-Z))₄-Me, so the solution was extracted with water (1x200 mL). The organic layer was dried over MgSO₄, filtered and evaporated i.vac. The solid was suspended in EE,

precipitated and washed extensively with EE. The crude product was purified via column chromatography on silica (eluent: CH₂Cl₂:MeOH 9:1) to give 2.03 g (Yield:95%) of **13** as a white solid.

HPLC: (150 mm YMC-Pack ODS-A, 4.6 mm, acetonitrile/water = 85:15, 0.8 mL/min, 4.6 MPa, 308 K): 38.79 min (91.5% peak area, **13**).

L-Lys(2Cl-Z)-(D-Lys(2Cl-Z)-L-Lys(2Cl-Z))₄-Me (1.08 g, 0.400 mmol), Boc-D-Lys(2Cl-Z) (0.216 g, 0.520 mmol), and HOBT (0.070 g, 0.520 mmol) were dissolved in DMF (15 mL) and cooled to 0 °C. To the cold solution, a concentrated solution of EDC in CH₂Cl₂ (0.200 g, 1.04 mmol) was added. The solution was allowed to warm up to room temperature and stirred over night. TLC monitoring showed no remaining L-Lys(2Cl-Z)-(D-Lys(2Cl-Z)-L-Lys(2Cl-Z))₄-Me, so the solution was concentrated i.vac. The solid was suspended in EE and precipitated quantitatively by the addition of hexane. The solid was filtered, extensively washed with EE:hexane (1:1) and redissolved in CH₂Cl₂:MeOH. Water was added to the solution and the biphasic system stirred for 10 minutes. The organic layer was separated, dried over MgSO₄, filtered and evaporated i.vac. The TLC of the crude product showed remaining L-Lys(2Cl-Z)-(D-Lys(2Cl-Z)-L-Lys(2Cl-Z))₄-Me, so coupling was restarted (DMF (15 mL), EDC: (0.060 g), HOBT: (0.030 g), Boc-D-Lys(2Cl-Z) (0.040 g)). After stirring over night, work-up gave crude product, which was precipitated once more to give 1.18 g (Yield: 95%) of **13** as a white solid.

HPLC: (150 mm YMC-Pack ODS-A, 4.6 mm, acetonitrile/water = 85:15, 0.8 mL/min, 4.0 MPa, 308 K): 40.85 min (95.04% peak area, **13**).

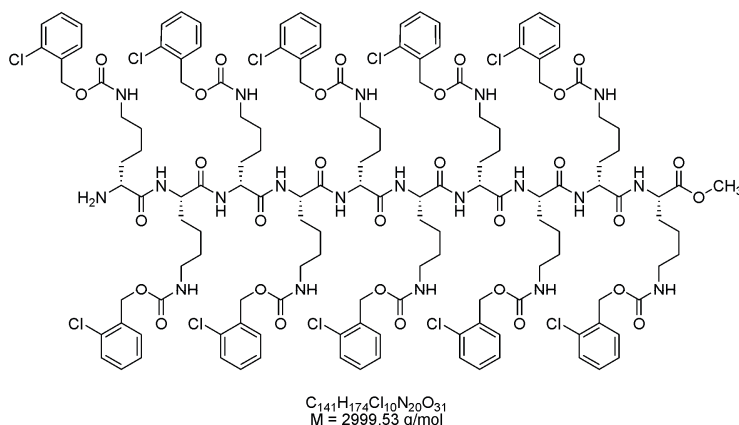
R_f = 0.54 (CH₂Cl₂:MeOH 9:1)

ESI-MS: m/z = 1572.5 (calcd 1572 for C₁₄₆H₁₈₂Cl₁₀N₂₀O₃₃ + 2 Na⁺), 1056.0 (calcd 1056 for C₁₄₆H₁₈₂Cl₁₀N₂₀O₃₃ + 3 Na⁺).

High-resolution ESI-MS: m/z = 1569.495343 (calcd 1569.492390 for C₁₄₆H₁₈₂Cl₁₀N₂₀O₃₃ + 2 Na⁺).

3 Linear D-(*alt*)-L-peptides

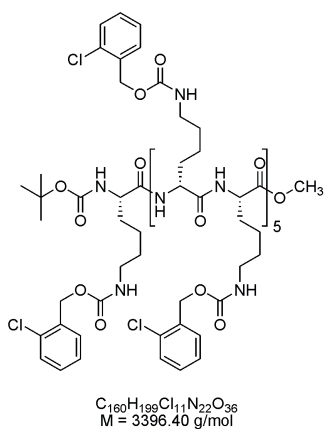
Boc deprotection of **13** to (D-Lys(2Cl-Z)-L-Lys(2Cl-Z))₅-Me:



13 (2.03 g, 0.66 mmol) was reacted following the general procedure for the deprotection of the Boc group. TFA (40 mL), CH₂Cl₂:MeOH (9:1) (40 mL).

R_F = 0.32 (CH₂Cl₂:MeOH 9:1)

Boc-L-Lys(2Cl-Z)-(D-Lys(2Cl-Z)-L-Lys(2Cl-Z))₅-Me:



(D-Lys(2Cl-Z)-L-Lys(2Cl-Z))₅-Me (1.97 g, 0.66 mmol) was dissolved in dry DMF (40 mL), the solution was diluted with dry CH₂Cl₂ (200 mL), Boc-L-Lys(2Cl-Z) (0.353 g, 0.85 mmol) and HOBt (0.177 g, 1.31 mmol) were added and the solution was cooled to 0 °C. To the cold solution, a concentrated solution of EDC in dry CH₂Cl₂ (0.377 g, 1.97 mmol) was added. The solution was allowed to warm up to room temperature and stirred over night. After TLC monitoring the solution was extracted with water (1x200 mL). The organic layer was dried over MgSO₄, filtered and evaporated i.vac. The solid was suspended in EE, filtered and washed extensively with EE. The crude product was purified via column

chromatography on silica (eluent: CH₂Cl₂:MeOH (9:1)) to give 2.09 g (Yield: 94%) of the desired product as a white solid.

HPLC (250 mm Asahipak C4P-50 ec, 4.6 mm, acetonitrile/water = 80:20, 0.8 mL/min, 6.1 MPa, 308 K): 10.87 min (90.7% peak area, (Boc-L-Lys(2Cl-Z)-(D-Lys(2Cl-Z)-L-Lys(2Cl-Z))₅-Me).

(D-Lys(2Cl-Z)-L-Lys(2Cl-Z))₅-Me (1.14 g, 0.38 mmol), Boc-L-Lys(2Cl-Z) (0.21 g, 0.50 mmol), and HOBt (0.067 g, 0.50 mmol) were dissolved in dry DMF (25 mL) and cooled to 0 °C. To the cold solution, a concentrated solution of EDC in CH₂Cl₂ (0.19 g, 0.99 mmol) was added. The solution was allowed to warm up to room temperature and stirred over night. After TLC monitoring, the solution was concentrated i.vac. The solid was suspended in EE, quantitatively precipitated by the addition of hexane, filtered and washed extensively with EE:hexane (1:1). The solid was dissolved in CH₂Cl₂:MeOH and extracted with water (1x100 mL). The organic layer was dried over MgSO₄, filtered and evaporated i.vac. The white solid was precipitated once more with EE:hexane to give 1.29 g (Yield: 100%) of Boc-L-Lys(2Cl-Z)-(D-Lys(2Cl-Z)-L-Lys(2Cl-Z))₅-Me as a white solid.

HPLC (250 mm Asahipak C4P-50 ec, 4.6 mm, acetonitrile/water = 80:20, 0.8 mL/min, 6.0 MPa, 308 K): 11.12 min (93.4% peak area, Boc-L-Lys(2Cl-Z)-(D-Lys(2Cl-Z)-L-Lys(2Cl-Z))₅-Me).

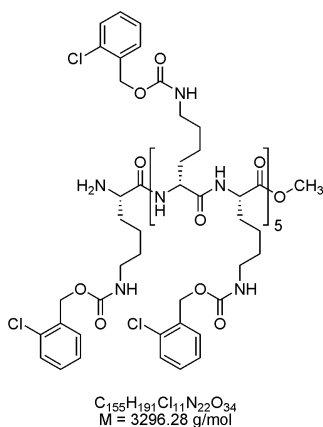
R_F = 0.52 (CH₂Cl₂:MeOH 9:1)

ESI-MS: m/z = 1720.5 (calcd 1720.0 for C₁₆₀H₁₉₉Cl₁₁N₂₂O₃₆ + 2 Na⁺), 1154.7 (calcd 1154.7 for C₁₆₀H₁₉₉Cl₁₁N₂₂O₃₆ + 3 Na⁺), 2287.4 (calcd 2287.4 for (C₁₆₀H₁₉₉Cl₁₁N₂₂O₃₆)₂ + 3 Na⁺).

High-resolution ESI-MS (calculated at the most abundance peak): m/z = 1720.542512 (calcd 1720.538080 for C₁₆₀H₁₉₉Cl₁₁N₂₂O₃₆ + 2 Na⁺).

3 Linear D-(*alt*)-L-peptides

Boc deprotection of Boc-L-Lys(2Cl-Z)-(D-Lys(2Cl-Z)-L-Lys(2Cl-Z))₅-Me to L-Lys(2Cl-Z)-(D-Lys(2Cl-Z)-L-Lys(2Cl-Z))₅-Me:

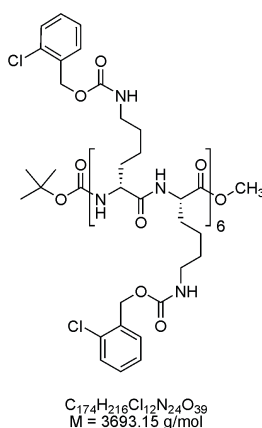


Boc-L-Lys(2Cl-Z)-(D-Lys(2Cl-Z)-L-Lys(2Cl-Z))₅-Me (1.97 g, 0.66 mmol) was reacted following the general procedure for the deprotection of the Boc group. TFA (50 mL), CH₂Cl₂:MeOH (9:1) (50 mL).

HPLC (250 mm Asahipak C4P-50 ec, 4.6 mm, acetonitrile/10 mmol TEAA pH6.8 = 75:15, 0.8 mL/min, 6.6 MPa, 308 K): 18.78 min (92.4% peak area, L-Lys(2Cl-Z)-(D-Lys(2Cl-Z)-L-Lys(2Cl-Z))₅-Me).

$R_F = 0.4$ (CH₂Cl₂:MeOH 9:1)

Boc-(D-Lys(2Cl-Z)-L-Lys(2Cl-Z))₆-Me (**26**):



L-Lys(2Cl-Z)-(D-Lys(2Cl-Z)-L-Lys(2Cl-Z))₅-Me (2.01 g, 0.61 mmol) was dissolved in dry DMF (40 mL), the solution was diluted with dry CH₂Cl₂ (200 mL), Boc-D-Lys(2Cl-Z) (0.51 g, 1.22 mmol) and HOBT (0.25 g, 1.83 mmol) were added and the solution was cooled to 0 °C. To the cold solution, a concentrated solution of

EDC in dry CH_2Cl_2 (0.70 g, 3.66 mmol) was added. The solution was allowed to warm up to room temperature and stirred over night. After TLC monitoring, the solution was evaporated i.vac. The solid was suspended in EE, filtered and extensively washed with EE. The crude product was purified via column chromatography on silica (eluent: CH_2Cl_2 :MeOH (9:1)) to give 1.86 g (Yield: 83%) of **26** as a white solid.

HPLC (250 mm Asahipak C4P-50 ec, 4.6 mm, acetonitrile/water = 75:25, 0.8 mL/min, 6.8 MPa, 308 K): 31.77 min (92.0% peak area, **26**).

L-Lys(2Cl-Z)-(D-Lys(2Cl-Z)-L-Lys(2Cl-Z))₅-Me (1.25 g, 0.38 mmol), Boc-D-Lys(2Cl-Z) (0.21 g, 0.49 mmol), and HOBT (0.067 g, 0.49 mmol) were dissolved in dry DMF (20 mL) and cooled to 0 °C. To the cold solution, a concentrated solution of EDC in CH_2Cl_2 (0.22 g, 1.14 mmol) was added. The solution was allowed to warm up to room temperature and stirred over night. After TLC monitoring, the solution was concentrated i.vac. The solid was suspended in EE, quantitatively precipitated by the addition of hexane, filtered and washed extensively with EE:hexane (1:1). The solid was dissolved in CH_2Cl_2 :MeOH, water was added and the biphasic system stirred for 10 min. After phase separation, the organic layer was dried over MgSO_4 , filtered and evaporated i.vac. The white solid was precipitated once more with EE:hexane to give 1.38 g (Yield: 98%) of **26** as a white solid.

HPLC (250 mm Asahipak C4P-50 ec, 4.6 mm, acetonitrile/water = 75:25, 0.8 mL/min, 6.5 MPa, 308 K): 31.90 min (96.4% peak area, **26**).

$R_F = 0.7$ (CH_2Cl_2 :MeOH 9:1)

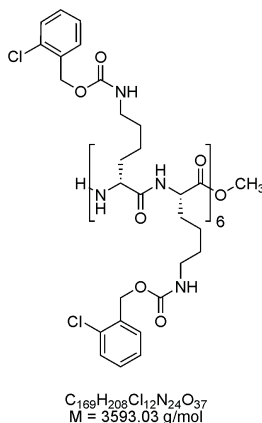
ESI-MS: $m/z = 1869.6$ (calcd 1869.6 for $\text{C}_{174}\text{H}_{216}\text{Cl}_{12}\text{N}_{24}\text{O}_{39} + 2 \text{Na}^+$), 1253.7 (calcd 1253.7 for $\text{C}_{174}\text{H}_{216}\text{Cl}_{12}\text{N}_{24}\text{O}_{39} + 3 \text{Na}^+$), 2485.1 (calcd 2485.1 for $(\text{C}_{174}\text{H}_{216}\text{Cl}_{12}\text{N}_{24}\text{O}_{39})_2 + 3 \text{Na}^+$).

High-resolution ESI-MS (calculated at the most abundance peak):

$m/z = 1869.579374$ (calcd 1869.584047 for $\text{C}_{174}\text{H}_{216}\text{Cl}_{12}\text{N}_{24}\text{O}_{39} + 2 \text{Na}^+$).

3 Linear D-(*alt*)-L-peptides

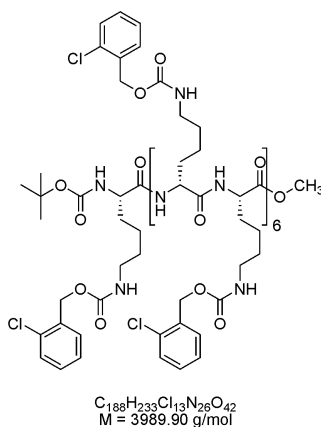
Boc deprotection of **26** to (D-Lys(2Cl-Z)-L-Lys(2Cl-Z))₆-Me:



26 (1.16 g, 0.32 mmol) was reacted following the general procedure for the deprotection of the Boc group. TFA (25 mL), CH₂Cl₂:MeOH (9:1) (25 mL).

R_F = varied from 0.16 to 0.4 (CH₂Cl₂:MeOH 9:1)

Boc-L-Lys(2Cl-Z)-(D-Lys(2Cl-Z)-L-Lys(2Cl-Z))₆-Me (**34**):



(D-Lys(2Cl-Z)-L-Lys(2Cl-Z))₆-Me (1.13 g, 0.32 mmol) was dissolved in dry DMF (40 mL), the solution was diluted with dry CH₂Cl₂ (200 mL), Boc-L-Lys(2Cl-Z) (0.11 g, 0.41 mmol) and HOBT (0.085 g, 0.63 mmol) were added and the solution was cooled to 0 °C. To the cold solution, a concentrated solution of EDC in dry CH₂Cl₂ (0.30 g, 1.58 mmol) was added. The solution was allowed to warm up to room temperature and stirred over night. After TLC monitoring, the solution was extracted with water (1x200 mL), 1 M aqueous citric acid solution (1x200 mL), water (2x200 mL), and brine (1x200 mL). The organic layer was dried over MgSO₄, filtered and evaporated i.vac. The solid was suspended in EE,

filtered and extensively washed with EE. The crude product was purified via column chromatography on silica (eluent: CH₂Cl₂/MeOH (9:1)) to give 1.12 g (Yield: 89%) of **34** as a white solid.

HPLC (250 mm Asahipak C4P-50 ec, 4.6 mm, acetonitrile/water = 75:25, 0.8 mL/min, 6.8 MPa, 308 K): 40.96 min (85.0% peak area, **34**).

(D-Lys(2Cl-Z)-L-Lys(2Cl-Z))₆-Me (1.33 g, 0.37 mmol), Boc-L-Lys(2Cl-Z) (0.20 g, 0.48 mmol), and HOBT (0.065 g, 0.48 mmol) were dissolved in dry DMF (20 mL) and cooled to 0 °C. To the cold solution, a concentrated solution of EDC in CH₂Cl₂ (0.21 g, 1.11 mmol) was added. The solution was allowed to warm up to room temperature and stirred over night. After TLC monitoring, the solution was concentrated i.vac. The solid was suspended in EE, quantitatively precipitated by the addition of hexane, filtered, and washed extensively with EE:hexane (1:1). The solid was dissolved in CH₂Cl₂:MeOH, water was added and the biphasic system stirred for 10 min. After phase separation, the organic layer was dried over MgSO₄, filtered and evaporated i.vac. The white solid was precipitated once more with EE:hexane to give 1.42 g (Yield: 96%) of **34** as a white solid.

HPLC (250 mm Asahipak C4P-50 ec, 4.6 mm, acetonitrile/water = 75:25, 0.8 mL/min, 6.6 MPa, 308 K): 40.96 min (96.5% peak area, **34**).

$R_F = 0.5$ (CH₂Cl₂:MeOH 9:1)

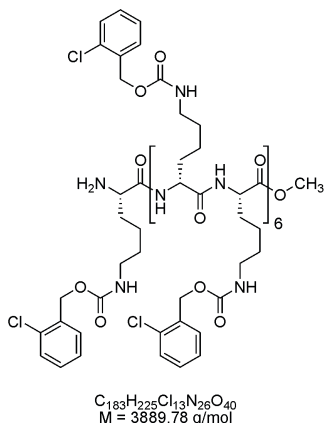
ESI-MS: $m/z = 2013.6$ (calcd 2013.6 for C₁₈₈H₂₃₃Cl₁₃N₂₆O₄₂ + 2 Na⁺), 1350.1 (calcd 1350.1 for C₁₈₈H₂₃₃Cl₁₃N₂₆O₄₂ + 3 Na⁺).

High-resolution ESI-MS (calculated at the most abundance peak):

$m/z = 2017.632350$ (calcd 2017.630543 for C₁₈₈H₂₃₃Cl₁₃N₂₆O₄₂ + 2 Na⁺).

3 Linear D-(*alt*)-L-peptides

Boc deprotection of **34** to L-Lys(2Cl-Z)-(D-Lys(2Cl-Z)-L-Lys(2Cl-Z))₆-Me:



34 (1.13 g, 0.28 mmol) was reacted following the general procedure for the deprotection of the Boc group. TFA (20 mL), CH₂Cl₂:MeOH (9:1) (20 mL).

HPLC (250 mm Asahipak C4P-50 ec, 4.6 mm, acetonitrile/10 mmol TEAA pH6.8 = 75:25, 0.8 mL/min, 6.7 MPa, 308 K): 31.88 min (86.7% peak area, L-Lys(2Cl-Z)-(D-Lys(2Cl-Z)-L-Lys(2Cl-Z))₆-Me).

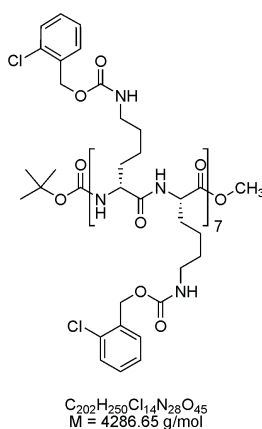
$R_F = 0.26$ (CH₂Cl₂:MeOH 9:1)

ESI-MS: $m/z = 1967.6$ (calcd 1967.6 for $C_{183}H_{225}Cl_{13}N_{26}O_{40} + 2 Na^+$).

High-resolution ESI-MS (calculated at the most abundance peak):

$m/z = 1967.600606$ (calcd 1967.604281 for $C_{183}H_{225}Cl_{13}N_{26}O_{40} + 2 Na^+$).

Boc-(D-Lys(2Cl-Z)-L-Lys(2Cl-Z))₇-Me (**27**):



L-Lys(2Cl-Z)-(D-Lys(2Cl-Z)-L-Lys(2Cl-Z))₆-Me (0.93 g, 0.31 mmol) was dissolved in dry DMF (30 mL), the solution was diluted with dry CH₂Cl₂ (150 mL), Boc-D-

Lys(2Cl-Z) (0.13 g, 0.31 mmol) and HOBT (0.065 g, 0.48 mmol) were added and the solution was cooled to 0 °C. To the cold solution, a concentrated solution of EDC in dry CH₂Cl₂ (0.23 g, 1.20 mmol) was added. The solution was allowed to warm up to room temperature and stirred over night. After TLC monitoring, the solution was evaporated i.vac. The solid was purified via column chromatography on silica (eluent: CH₂Cl₂:MeOH (9:1)). The solid was suspended in EE, filtered and extensively washed with EE. The product showed degradation on silica and in HPLC. Purification gave 0.99 g (Yield: 96%) of **27** as a white solid.

HPLC (250 mm Asahipak C4P-50 ec, 4.6 mm, acetonitrile/water = 75:25, 0.8 mL/min, 6.8 MPa, 308 K): Product peak showed strong tailing, hence no exact HPLC was possible.

L-Lys(2Cl-Z)-(D-Lys(2Cl-Z)-L-Lys(2Cl-Z))₆-Me (1.10 g, 0.28 mmol), Boc-D-Lys(2Cl-Z) (0.15 g, 0.37 mmol), and HOBT (0.05 g, 0.37 mmol) were dissolved in dry DMF (20 mL) and cooled to 0 °C. To the cold solution, a concentrated solution of EDC in CH₂Cl₂ (0.14 g, 0.73 mmol) was added. The solution was allowed to warm up to room temperature and stirred for 48 h. After TLC monitoring, the solution was concentrated i.vac. The solid was suspended in EE, quantitatively precipitated by the addition of hexane, filtered and washed extensively with EE:hexane (1:1). The solid was dissolved in CH₂Cl₂:MeOH, water was added and the biphasic system stirred for 10 min. After phase separation, the organic layer was dried over MgSO₄, filtered and evaporated i.vac. Precipitation and extracting procedure were repeated until TLC showed no impurities to give 1.21 g (Yield: 100%) of **27** as a white solid.

HPLC (250 mm Asahipak C4P-50 ec, 4.6 mm, acetonitrile/water = 80:20, 0.8 mL/min, 6.0 MPa, 308 K): Product peak showed strong tailing, hence no exact HPLC was possible.

$R_f = 0.76$ (CH₂Cl₂:MeOH 9:1)

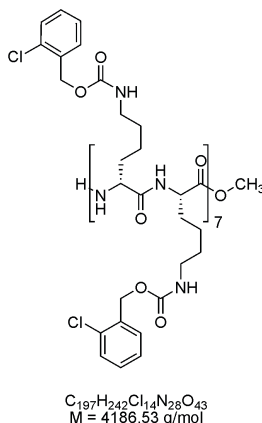
ESI-MS: $m/z = 2166.2$ (calcd 2166.2 for C₂₀₂H₂₅₀Cl₁₄N₂₈O₄₅ + 2 Na⁺).

3 Linear D-(*alt*)-L-peptides

High-resolution ESI-MS (calculated at the most abundance peak):

$m/z = 2017.632350$ (calcd 2017.630543 for $C_{188}H_{233}Cl_{13}N_{26}O_{42} + 2 Na^+$).

Boc deprotection of **27** to (D-Lys(2Cl-Z)-L-Lys(2Cl-Z))₇-Me:



27 (0.65 g, 0.15 mmol) was reacted following the general procedure for the deprotection of the Boc group. TFA (12 mL), CH_2Cl_2 :MeOH (9:1) (12 mL).

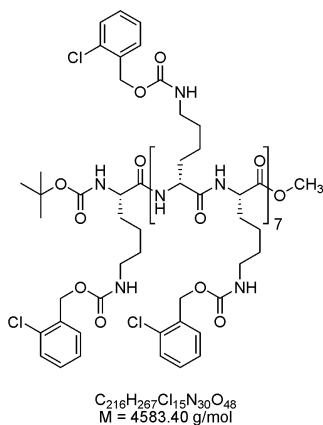
HPLC (250 mm Asahipak C4P-50 ec, 4.6 mm, acetonitrile/10 mmol TEAA pH6.8 = 75:25, 0.8 mL/min, 6.7 MPa, 308 K): No HPLC possible.

$R_F = 0.28$ (CH_2Cl_2 :MeOH 9:1)

High-resolution ESI-MS (calculated at the most abundance peak):

$m/z = 1967.600606$ (calcd 1967.604281 for $C_{183}H_{225}Cl_{13}N_{26}O_{40} + 2 Na^+$).

Boc-L-Lys(2Cl-Z)-(D-Lys(2Cl-Z)-L-Lys(2Cl-Z))₇-Me (**35**):



(D-Lys(2Cl-Z)-L-Lys(2Cl-Z))₇-Me (0.63 g, 0.15 mmol), Boc-L-Lys (81 mg, 0.20 mmol), and HOBt (27 mg, 0.20 mmol) were dissolved in dry DMF (10 mL) and cooled to 0 °C. To the cold solution, a concentrated solution of EDC in dry CH₂Cl₂ (87 mg, 0.45 mmol) was added. The solution was allowed to warm up to room temperature and stirred over night. After TLC monitoring, the solution was concentrated i.vac. The solid was suspended in EE, quantitatively precipitated by the addition of hexane, filtered and washed extensively with EE:hexane (1:1). The solid was dissolved in CH₂Cl₂:MeOH, water was added and the biphasic system stirred for 10 min. After phase separation, the organic layer was washed with water (1x50 mL), dried over MgSO₄, filtered and evaporated i.vac. Tedious precipitation and extracting procedure was repeated until TLC showed no impurities to give 0.65 g (Yield: 94%) of **35** as a white solid.

HPLC (250 mm Asahipak C4P-50 ec, 4.6 mm, acetonitrile/water = 80:20, 0.8 mL/min, 6.0 MPa, 308 K): No HPLC possible.

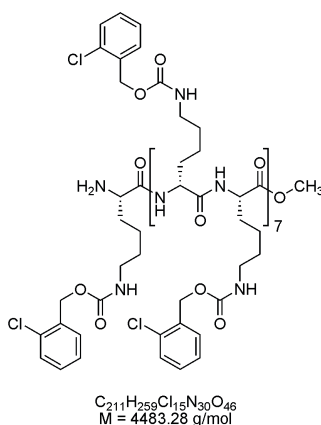
$R_f = 0.70$ (CH₂Cl₂:MeOH 9:1)

ESI-MS: $m/z = 4604.6$ (calcd 4604.6 for C₂₁₆H₂₆₇Cl₁₅N₃₀O₄₈ + 2 Na⁺).

High-resolution ESI-MS (calculated at the most abundance peak):

$m/z = 2314.219483$ (calcd 2314.223279 for C₂₁₆H₂₆₇Cl₁₅N₃₀O₄₈ + 2 Na⁺).

Boc deprotection of **35** to L-Lys(2Cl-Z)-(D-Lys(2Cl-Z)-L-Lys(2Cl-Z))₇-Me:



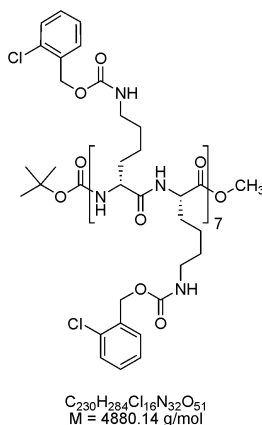
35 (0.46 g, 0.10 mmol) was reacted following the general procedure for the deprotection of the Boc group. TFA (15 mL), CH₂Cl₂:MeOH (9:1) (15 mL).

3 Linear D-(*alt*)-L-peptides

HPLC (250 mm Asahipak C4P-50 ec, 4.6 mm, acetonitrile/10 mmol TEAA pH6.8 = 75:25, 0.8 mL/min, 6.7 MPa, 308 K): No HPLC possible.

$R_F = 0.14$ (CH_2Cl_2 :MeOH 9:1)

Boc-(D-Lys(2Cl-Z)-L-Lys(2Cl-Z))₈-Me (**12**):



Procedure in divergent/convergent growth approach:

(D-Lys(2Cl-Z)-L-Lys(2Cl-Z))₄-Me (0.363 g, 0.135 mmol), Boc-(D-Lys(2Cl-Z)-L-Lys(2Cl-Z))₄ (0.325 g, 0.135 mmol), and HOBT (0.020 g, 0.149 mmol) were dissolved in 50.0 mL CH_2Cl_2 :DMF (as less DMF as possible) and cooled to 0 °C. To the cold solution, a concentrated solution of EDC in CH_2Cl_2 (0.034 g, 0.176 mmol) was added. The solution was allowed to warm up to room temperature and stirred for 12 h. After TLC monitoring the solution was extracted with water (4x50 mL), aqueous citric acid solution (1x50 mL), water (1x50 mL), saturated aqueous NaHCO_3 -solution (3x50 mL), and water (1x50 mL). The organic layer was dried over MgSO_4 , filtered and evaporated i.vac. The crude product was suspended in EE, precipitated in hexane, filtered and the solid extensively washed with EE to give 0.523 g (yield: 79%) of **12** as a white solid.

Procedure in linear growth approach:

L-Lys(2Cl-Z)-(D-Lys(2Cl-Z)-L-Lys(2Cl-Z))₇-Me (0.50 g, 0.10 mmol), Boc-D-Lys (54 mg, 0.13 mmol), and HOBT (18 mg, 0.13 mmol) were dissolved in dry DMF (15 mL) and cooled to 0 °C. To the cold solution, a concentrated solution of EDC

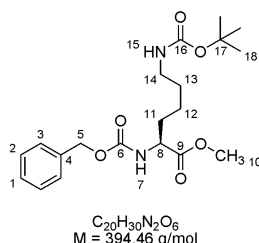
in dry CH_2Cl_2 (50 mg, 0.26 mmol) was added. The solution was allowed to warm up to room temperature and stirred for 72 h. After TLC monitoring, the solution was concentrated i.vac. The solid was suspended in EE, quantitatively precipitated by the addition of hexane, filtered and washed extensively with EE:hexane (1:1). The solid was dissolved in CH_2Cl_2 :MeOH, water was added and the biphasic system stirred for 10 min. After phase separation, the organic layer was washed with water (1x50 mL), dried over MgSO_4 , filtered and evaporated i.vac. Tedious precipitation and extracting procedure was repeated until TLC showed no impurities to give 0.47 g (Yield: 97%) of **12** as a white solid.

HPLC (250 mm Asahipak C4P-50 ec, 4.6 mm, acetonitrile/water = 80:20, 0.8 mL/min, 6.0 MPa, 308 K): No HPLC possible.

R_f = varies from 0.6 to 0.84 (CH_2Cl_2 :MeOH 9:1)

ESI-MS: m/z = 1649.5 (calcd 1649.5 for $\text{C}_{230}\text{H}_{284}\text{Cl}_{16}\text{N}_{32}\text{O}_{51} + 3 \text{ Na}^+$), 2462.3 (calcd 2462.3 for $\text{C}_{230}\text{H}_{284}\text{Cl}_{16}\text{N}_{32}\text{O}_{51} + 2 \text{ Na}^+$).

Z-L-Lys(Boc)-Me (**17**):



Z-L-Lys(Boc) (2.01 g, 5.27 mmol) and HOBT (0.71 g, 5.27 mmol) were dissolved in CH_2Cl_2 :MeOH (20:75) (95 mL) and cooled to 0 °C. To the cold solution, EDC (1.52 g, 7.91 mmol) in CH_2Cl_2 (55 mL) was added. The solution was allowed to warm up to room temperature and stirred for 29 h. The solution was evaporated i.vac. and the residue dissolved in EE. The solution was washed with water (1x100 mL), saturated aqueous NaHCO_3 -solution (1x100 mL), water (1x100 mL), aqueous 1 M citric acid solution (1x100 mL), water (1x100 mL), brine (1x100 mL), dried over MgSO_4 , filtered, and evaporated i.vac. to give the product as a colorless oil in quantitative yield. If necessary, product was purified via column chromatography on silica (eluent: CH_2Cl_2 :MeOH 95:5).

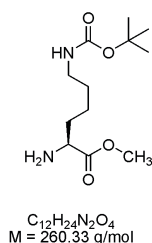
3 Linear D-(*alt*)-L-peptides

$R_F = 0.72$ (CH_2Cl_2 :MeOH 9:1)

^1H NMR (400 MHz, CDCl_3 , 20 °C): δ 7.27 - 7.20 (m, 5 H, C^1H , 2 C^2H , 2 C^3H), 5.44(d, $^3J(\text{H,H}) = 8.1$ Hz, 1 H, N^7H), 5.02 (s, 2 H, C^5H_2), 4.58 (br s, 1 H, N^{15}H), 4.29 - 4.14 (m, 1 H, C^8H), 3.64 (s, 3 H, C^{10}H_3), 3.15 - 2.95 (m, 2 H, C^{14}H_2), 1.82 - 1.50 (m, 2 H, C^{11}H_2), 1.40 - 1.18 (m, 13 H, C^{12}H_2).

^{13}C NMR (CDCl_3): δ 173.04, 156.17, 156.07, 136.31, 128.54, 128.20, 128.16, 79.20, 67.00, 53.77, 52.38, 40.09, 32.13, 29.60, 28.45, 22.39.

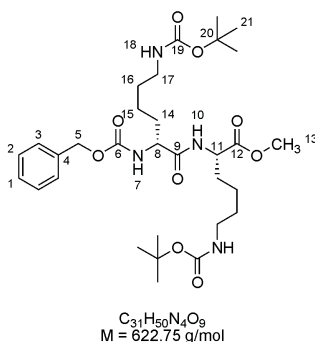
L-Lys(Boc)-Me (**18**):



17 (0.118 g, 0.300 mmol) was reacted following the general procedure for the deprotection of the Z group or benzyl ester. EE:MeOH (2:1) (15 mL), Pd/C (11 mg), reaction time: 1.5 h, hydrogen pressure: 5 bar. The product was used without further purification and analysis to avoid diketopiperazine formation.

$R_F = 0.34$ (CH_2Cl_2 :MeOH 9:1)

Z-D-Lys(Boc)-L-Lys(Boc)-Me (**19**):



Z-D-Lys(Boc) (0.12 g, 0.32 mmol), HOBT (0.05 g, 0.33 mmol), and **18** (0.08 g, 0.30 mmol) were dissolved in CH_2Cl_2 (15 mL) and cooled to 0 °C. To the cold solution, a concentrated solution of EDC (0.08 g, 0.39 mmol) in CH_2Cl_2 (5 mL)

was added. The reaction mixture was allowed to warm up to room temperature and stirred for 2.5 h. Water (20 mL) was added and the biphasic system stirred for 10 minutes. After phase separation, the organic layer was dried over MgSO_4 and evaporated i.vac. to give the crude product which was purified via column chromatography on silica (eluent: CH_2Cl_2 :MeOH 98:2 until the more unpolar impurity was removed, then CH_2Cl_2 :MeOH 9:1) to give 0.187 g (quantitative yield) of pure **19** as a white solid.

HPLC: (150 mm YMC-Pack ODS-A, 4.6 mm, acetonitrile:water = 60:40, 0.8 mL/min, 3.4 MPa, 308 K): 7.98 min (100% peak area, **19**). Purity of other batches always >98%.

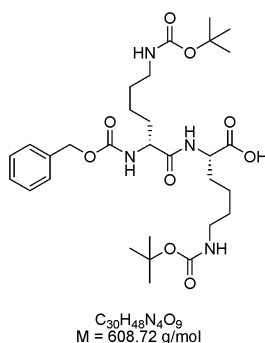
R_F = 0.70 (CH_2Cl_2 :MeOH 9:1)

^1H NMR (400 MHz, CDCl_3 , 20 °C): δ 7.30 - 7.20 (m, 5 H, C^1H , 2 C^2H , 2 C^3H), 6.94 (d, $^3J(\text{H,H})$ = 7.0 Hz, 1 H, N^{10}H), 5.75 (d, $^3J(\text{H,H})$ = 7.0 Hz, 1 H, N^7H), 5.03 (s, 2 H, C^5H_2), 4.96 - 4.61 (m, 2 H, 2 N^{18}H), 4.52 - 4.45 (m, 1 H, C^{11}H), 4.22 - 4.11 (m, 1 H, C^8H), 3.63 (s, 3 H, C^{13}H_3), 3.06 - 2.92 (m, 4 H, C^{17}H_2), 1.86 - 1.49 (m, 4 H, C^{14}H_2), 1.48 - 1.13 (m, 26 H, 2 C^{15}H_2 , 2 C^{16}H_2 , 6 C^{21}H_3).

^{13}C NMR (CDCl_3): δ 172.68, 171.81, 156.33, 156.20, 136.30, 128.53, 128.16, 128.02, 79.18, 67.00, 54.85, 52.41, 51.98, 40.24, 39.98, 31.16, 31.73, 29.69, 29.43, 28.45, 22.40.

High-resolution ESI-MS: m/z = 645.346728 (calcd 645.346995 for $\text{C}_{31}\text{H}_{50}\text{N}_4\text{O}_9$ + 1 Na^+).

Z-D-Lys(Boc)-L-Lys(Boc) (**21**):

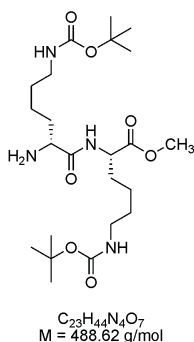


3 Linear D-(*alt*)-L-peptides

19 was reacted following the general procedure for the deprotection of the methyl ester. The product was used without further purification and analysis.

$R_F = 0.20$ (CH_2Cl_2 :MeOH 9:1)

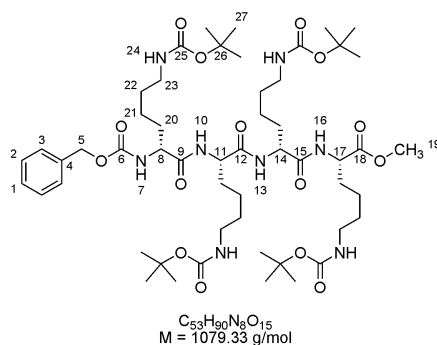
D-Lys(Boc)-L-Lys(Boc)-Me (**20**):



19 (0.084 g, 0.135 mmol) was reacted following the general procedure for the deprotection of the Z group or benzyl ester. EE:MeOH (2:1) (15 mL), Pd/C (9 mg), reaction time: 1.5 h, hydrogen pressure: 5 bar. The product was used without further purification and analysis.

$R_F = 0.30$ (CH_2Cl_2 :MeOH 9:1)

Z-(D-Lys(Boc)-L-Lys(Boc))₂-Me (**22**):



21 (0.16 g, 0.27 mmol), HOBT (0.040 g, 0.297 mmol), and **20** (0.13 g, 0.27 mmol) were dissolved in CH_2Cl_2 (30 mL) and cooled to 0 °C. To the cold solution, a concentrated solution of EDC (0.10 g, 0.54 mmol) in CH_2Cl_2 (20 mL) was added. The reaction mixture was allowed to warm up to room temperature and stirred for 20 h. Water (20 mL) was added and the biphasic system stirred

for 5 minutes. After phase separation, CH₂Cl₂ was removed i.vac. and replaced by EE. The organic layer was extracted with aqueous 1 M citric acid solution (1x100 mL), water (1x100 mL), saturated aqueous NaHCO₃-solution (1x100 mL), water (1x100 mL), brine (1x100 mL), dried over MgSO₄, filtered, and evaporated i.vac. to give the crude product, which was purified via column chromatography on silica (eluent: CH₂Cl₂:MeOH 98:2 until the more unpolar impurity was removed, then CH₂Cl₂:MeOH 95:5) to give 0.28 g (yield: 96%) of pure **22** as a white solid.

HPLC: (150 mm YMC-Pack ODS-A, 4.5 mm, acetonitrile:water = 70:30, 0.8 mL/min, 9.6 MPa, 308 K): 7.88 min (100% peak area, **22**).

R_F = 0.70 (CH₂Cl₂:MeOH 9:1)

¹H NMR (400 MHz, CDCl₃, 20 °C): δ 7.50 - 7.00 (m, 8 H, C¹H, 2 C²H, 2 C³H, N¹⁰H, N¹³H, N¹⁶H), 6.15 (br s, 1 H, N⁷H), 5.40 - 4.60 (m, 6 H, C⁵H₂, 4 N²⁴H), 4.53 - 4.24 (m, 3 H, C¹¹H, C¹⁴H, C¹⁷H), 4.23 - 4.11 (m, 1 H, C⁸H), 3.61 (s, 3 H, C¹⁹H₃), 3.06 (br s, 8 H, C²³H₂), 1.96 - 1.14 (m, 60 H, 4 C²⁰H₂, 4 C²¹H₂, 4 C²²H₂, 12 C²⁷H₃).

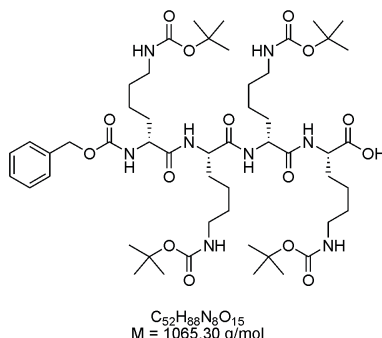
¹³C NMR (CDCl₃): δ 172.96, 172.18, 171.76, 156.33, 136.28, 128.56, 128.18, 127.92, 79.22, 67.12, 55.14, 53.81, 52.35, 40.38, 40.23, 31.71, 31.15, 29.76, 29.64, 29.43, 28.55, 28.53, 23.00, 22.58.

ESI-MS: m/z = 980 (calcd 980 for **22** - Boc + 1 H⁺), 1080 (calcd 1080 for **22** + 1 H⁺), 1102 (calcd 1102 for **22** + 1 Na⁺), 1118 (calcd 1118 for **22** + 1 K⁺).

High-resolution ESI-MS: m/z = 1101.641620 (calcd 1101.641780 for C₅₃H₉₀N₈O₁₅ + 1 Na⁺).

3 Linear D-(*alt*)-L-peptides

Z-(D-Lys(Boc)-L-Lys(Boc))₂ (**24**):



22 was reacted following the general procedure for the deprotection of the methyl ester. Even at 0 °C and with the shortest reaction time necessary for complete deprotection (TLC monitoring), TLC showed 3 spots after work-up. For HPLC-ESI-MS-investigation, 11 mg were purified via column chromatography on silica (eluent: CH₂Cl₂:MeOH 95:5 to 9:1). Longer Reaction-times (20 h) led to total degradation of the product. Nevertheless, the product was used without further purification.

HPLC after column: (150 mm YMC-Pack ODS-A, 4.6 mm, acetonitrile:0.1% TFA = 70:30, 0.8 mL/min, 5.5 MPa, 308 K): 5.67 min (100% peak area, **24**).

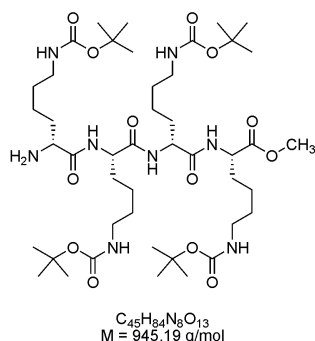
HPLC after degradation: (150 mm YMC-Pack ODS-A, 4.6 mm, acetonitrile:0.1% TFA = 70:30, 0.8 mL/min, 5.5 MPa, 308 K): 5.71 min (0.5% peak area, **24**).

R_F = 0.26 (CH₂Cl₂:MeOH 9:1)

ESI-MS: m/z = 1063 (calcd 1063 for **24** - 1 H⁺).

High-resolution ESI-MS: m/z = 1063.629492 (calcd 1063.629637 for C₅₂H₈₈N₈O₁₅ - 1 H⁺).

(D-Lys(Boc)-L-Lys(Boc))₂-Me (**23**):

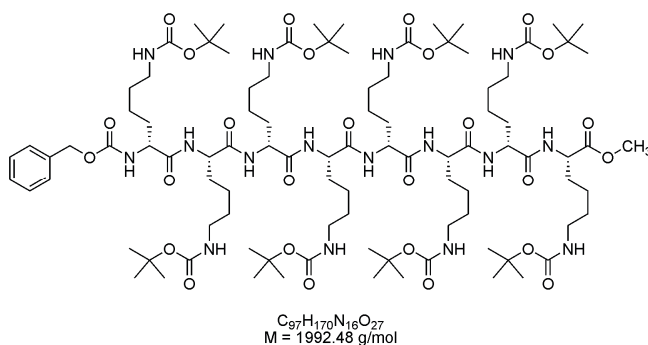


22 (0.062 g, 0.057 mmol) was reacted following the general procedure for the deprotection of the Z group or benzyl ester. EE:MeOH (2:1) (15 mL), Pd/C (17 mg), reaction time: 7.5 h, hydrogen pressure: 5 to 8 bar. TLC monitoring after 3.5 h (at 5 bar), 1.5 h (at 8 bar), 2.5 h (at 8 bar) The product was used without further purification.

R_F = 0.30 (CH₂Cl₂:MeOH 9:1)

ESI-MS: m/z = 945 (calcd 945 for **23** + 1 H⁺), 967 (calcd 967 for **23** + 1 Na⁺).

Z-(D-Lys(Boc)-L-Lys(Boc))₄-Me (**25**):



24 (0.061 g, 0.057 mmol), HOBT (0.008 g, 0.063 mmol), and **23** (0.054 g, 0.057 mmol) were dissolved in CH₂Cl₂ (15 mL) and cooled to 0 °C. To the cold solution, a concentrated solution of EDC (0.028 g, 0.145 mmol) in CH₂Cl₂ (10 mL) was added and the reaction mixture stirred for 16 h. Without any aqueous work-up, the reaction mixture was purified via column chromatography on silica (eluent: CH₂Cl₂:MeOH 98:2 to 95:5 to 9:1) to give 112 mg of impure product as a white solid. Purification via preparative HPLC failed.

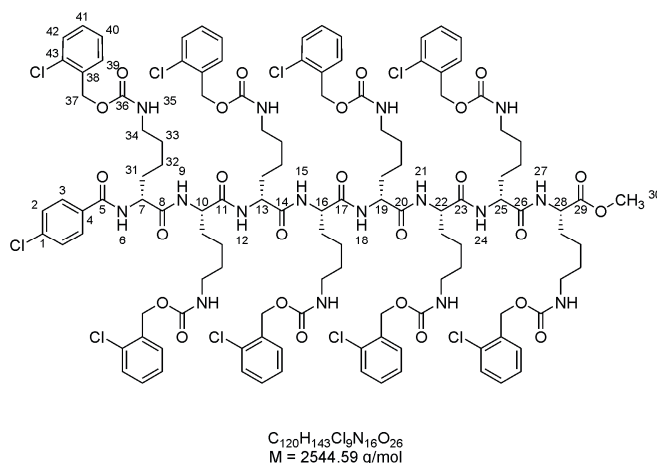
3 Linear D-(*alt*)-L-peptides

HPLC: (150 mm YMC-Pack ODS-A, 4.5 mm, acetonitrile:water = 80:20, 0.8 mL/min, 9.6 MPa, 308 K): 4.21 min (23.1% peak area, **22**), 11.24 min (56.7% peak area, **25**).

$R_F = 0.36$ (CH_2Cl_2 :MeOH 9:1)

ESI-MS: $m/z = 1018$ (calcd 1018 for **25** + 2 Na^+), 2013 (calcd 2013 for **25** + 1 Na^+), 2029 (calcd 2029 for **25** + 1 K^+) but also 1101 (calcd 1101 for **22** + 1 Na^+) and 1117 (calcd 1117 for **22** + 1 K^+).

p-Cl-benzoic acid-(D-Lys(2Cl-Z)-L-Lys(2Cl-Z))₄-Me (**14**):



(D-Lys(2Cl-Z)-L-Lys(2Cl-Z))₄-Me (0.096 g, 0.040 mmol), 4-chlorobenzoic acid (0.008 g, 0.052 mmol), and HOBT (0.007 g, 0.052 mmol) were dissolved in DMF (10 mL) and cooled to 0 °C. To the cold solution a concentrated solution of EDC in CH_2Cl_2 (0.020 g, 0.104 mmol) was added. The solution was allowed to warm up to room temperature and stirred for 16 h. TLC monitoring showed remaining (D-Lys(2Cl-Z)-L-Lys(2Cl-Z))₄-Me, so more EDC, HOBT and 4-chlorobenzoic acid were added until reaction was complete according to TLC. The solution was evaporated i.vac. and the remaining solid dissolved in CH_2Cl_2 :MeOH. Water was added and the biphasic system stirred for 10 min. After phase separation, the organic layer was dried over MgSO_4 , filtered and evaporated i.vac. The crude product was suspended in EE, quantitatively precipitated by the addition of hexane, filtered, and washed extensively with EE:hexane (1:1). The crude product was purified via column chromatography on

silica (eluent: CH₂Cl₂:MeOH (95:5)) to give **14** as a white solid in quantitative yield.

HPLC (150 mm YMC-Pack ODS-A, 4.6 mm, acetonitrile/water = 85:15, 0.8 mL/min, 4.5 MPa, 308 K): 17.11 min (97.7% peak area, **14**).

R_F = 0.54 (CH₂Cl₂:MeOH 9:1)

¹H NMR (400 MHz, DMSO-d₆, 20 °C): δ 8.60 - 8.56 (m, 1 H, NH), 8.31 - 8.29 (m, 2 H, 2 NH), 8.17 - 7.89 (m, 7 H, 2 C³H, 5 NH), 7.49 (d, ³J(H,H) = 8.7 Hz, 2 H, 2 C²H), 7.47 - 7.21 (m, 40 H, 8 C³⁹⁻⁴²H, 8 N³⁵H), 5.05 (s, 16 H, 8 C³⁷H), 4.43 - 4.12 (m, 8 H, C⁷H, C¹⁰H, C¹³H, C¹⁶H, C¹⁹H, C²²H, C²⁵H, C²⁸H), 3.59 (s, 3 H, C³⁰H₃), 3.02 - 2.83 (m, 16 H, 8 C³⁴H₂), 1.77 - 1.06 (m, 48 H, 8 C³¹⁻³³H₂).

ESI-MS: m/z = 2561 (calcd 2561 for C₁₂₀H₁₄₃Cl₉N₁₆O₂₆ + 1 Na⁺), 1292.8 (calcd 1292.8 for C₁₂₀H₁₄₃Cl₉N₁₆O₂₆ + 2 Na⁺).

2Cl-Z-deprotection attempts:

14 (0.030 g, 0.012 mmol) was dissolved in CH₂Cl₂:MeOH 1:1 (10 mL), ground ammonium formate (ca. 20 mg) was added and the solution stirred at room temperature. After 2 h, TLC showed no conversion, so the mixture was shortly heated to activate the ammonium formate. Then, more formate (ca 0.05 g) was added and the mixture heated to 50 °C. After stirring at this temperature for 2 days, TLC still showed starting material, so Pd/C (0.005 g) of a different provider and MeOH (3 mL) was added. After 12 h, the reaction mixture was filtered through celite and evaporated i.vac. TLC showed remaining starting material.

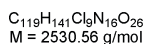
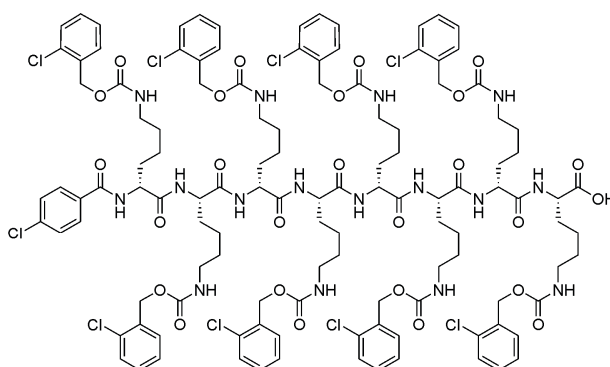
14 (0.020 g, 0.008 mmol) was dissolved in EE:MeOH:formic acid 9:9:2 (10 mL). Pd/C (0.02 g) was added and the solution stirred under nitrogen atmosphere at room temperature. After 20 min TLC showed no conversion, so reaction mixture was heated to 50 °C. After 2 h, TLC still showed no conversion, so mixture was heated to 60 °C. After 2 h, TLC showed no remaining starting material. The reaction mixture was filtered through celite (celite plug intensively washed with MeOH before!) and evaporated i.vac. NMR showed signals of

3 Linear D-(*alt*)-L-peptides

(partly) protected **14**, ESI-MS showed a variety of different signals. (ESI-positive showed lower molecular weights, ESI-negative showed many of higher molecular weights). Some could not be assigned. MALDI-TOF and CEC showed several peaks of (partly) cleaved product (6 to 1 remaining 2Cl-Z-protecting groups).

14 (0.030 g, 0.012 mmol) was dissolved in EE:MeOH:formic acid 9:9:2 (10 mL). Pd/C (0.03 g) was added and the solution stirred under nitrogen atmosphere at 60 °C. After 16 h, TLC showed no conversion, so Pd/C (0.03 g) from a freshly opened charge was added. After 10 min, TLC still showed no conversion, so MeOH:formic acid (2:1) was added. After 1 h, TLC showed no remaining starting material. More MeOH:formic acid (2:1) was added and the reaction stirred for 4 h. The reaction mixture was filtered through celite (celite plug intensively washed with MeOH before!) and evaporated i.vac. ¹H NMR showed small traces of protected **14**, ESI-MS showed a variety of different signals. (ESI-positive showed lower molecular weights, ESI-negative showed higher molecular weights). Some could not be assigned. Product signal was found in ESI-negative. MALDI-TOF and CEC showed several signals.

p-Cl-benzoic acid-(D-Lys-L-Lys)₄ (**16**):



14 (0.25 g, 0.10 mmol) was reacted following the general procedure for the deprotection of the methyl ester to give the desired product **16** in 97% yield.

HPLC (150 mm YMC-Pack ODS-A, 4.6 mm, acetonitrile/0.1% TFA = 80:20, 0.8 mL/min, 4.6 MPa, 308 K): 29.37 min (97.0% peak area, **16**).

$R_F = 0.28$ (CH_2Cl_2 :MeOH 9:1)

ESI-MS: $m/z = 2530.0$ (calcd 2530.0 for $\text{C}_{119}\text{H}_{141}\text{Cl}_9\text{N}_{16}\text{O}_{26} - \text{H}^+$).

High-resolution ESI-MS (calculated at the most abundance peak):

$m/z = 2529.730051$ (calcd 2529.730618 for $\text{C}_{119}\text{H}_{140}\text{Cl}_9\text{N}_{16}\text{O}_{26} - \text{H}^+$).

2Cl-Z-deprotection attempts:

16 (0.025 g, 0.010 mmol) was dissolved in MeOH:EE (2:1) (21.0 mL). Pd/C (0.025 g) was added and the solution stirred under hydrogen atmosphere (8 bar) at 75 °C. After 16 h, CEC showed 2 peaks. Reaction was continued for 4 h at 9 bar and 75 °C. CEC changed and showed one main peak. Reaction was restarted with Pd/C (8 mg), in MeOH:EE 14:1 under hydrogen atmosphere (9 bar) at 70 °C to drive it to completion. CEC chromatogram became worse, with longer reaction times. ^1H NMR showed no benzylic signals of the protecting group, but had two significant signals that could not be assigned to the product.

16 (0.025 g, 0.010 mmol) was dissolved in MeOH:EE (1:1). Formic acid (2.0 mL) and Pd/C (0.025 g) were added and the solution was stirred under argon atmosphere at 75 °C for 14 h. ^1H NMR showed uncleaved starting material, so the reaction was restarted with Pd/C (8 mg) and formic acid (2 mL) in MeOH at 75 °C. After 6 h, reaction mixture was filtered and evaporated i.vac. ^1H NMR showed less signals of uncleaved **16**, so reaction was restarted with $\text{Pd}(\text{OH})_2$ (10 mg) and formic acid (2.0 mL) in MeOH at 75 °C. After 18 h, ^1H NMR showed signals of uncleaved starting material, so reaction was restarted with $\text{Pd}(\text{OH})_2$ (10 mg) and formic acid (2.0 mL) in MeOH (10 mL) at 80 °C. After 24 h, reaction mixture was filtered and evaporated i.vac. ^1H NMR showed no benzylic signals of the protecting group, but had two significant signals that could not be assigned to the product. ESI-MS showed several signals, of which none could be assigned to the product.

3 Linear D-(*alt*)-L-peptides

16 (0.025 g, 0.010 mmol) was dissolved in DMF (10 mL). Pd/C (0.013 g) was added and the solution stirred under hydrogen atmosphere (9 bar) at 75 °C for 18 h. TLC monitoring showed starting material and very polar substances (possibly cleaved octapeptide). The reaction was restarted with Pd/C (10 mg) in DMF (15 mL) under hydrogen atmosphere 10 bar, at 75 °C. After 6 h, ¹H NMR showed signals of (partially) protected starting material, so reaction was restarted with Pd/C (10 mg) in DMF:MeOH 3:1 (20 mL) under hydrogen atmosphere (30 bar) at 75 °C for 20 h. The reaction conditions were hardly reproducible, because of an autoclave leakage and the resulting pressure decrease to 10 bar. ESI-MS of the filtered reaction mixture showed several signals, of which none could be assigned to the product. CEC showed 8 peaks. ¹H NMR showed no benzylic signals of the protecting group, but had two significant signals that could not be assigned to the product.

16 (0.025 g, 0.010 mmol) was dissolved in DMF (10 mL). Pd/C (0.012 g) and 1,4-cyclohexadiene (0.076 mL, 0.800 mmol) were added and the solution was stirred under argon atmosphere at 60 °C. Since TLC Monitoring after 2 h showed no conversion to the desired product, the temperature was raised to 70 °C. After 6 h at 70 °C, the solution was filtered and evaporated i.vac. TLC showed exclusively starting material.

16 (0.020 g, 0.008 mmol) was dissolved in DMF (9 mL). Formic acid (2.0 mL) and Pd/C (0.010 g) were added and the solution was stirred under argon atmosphere at 60 °C for 20 h. The solution was filtered and evaporated i.vac. Since TLC monitoring showed remaining uncleaved starting material, mixture was dissolved in CH₂Cl₂:MeOH 3:1 (20 mL). Most of CH₂Cl₂ was removed i.vac. without precipitation of the mixture. MeOH (5 mL) was added and the reaction restarted with Pd/C (13 mg) and formic acid (3.0 mL) at 70 °C for 17 h. The reaction mixture was filtered and evaporated i.vac. ¹H NMR showed signals of uncleaved **16** and 2 peaks that could not be assigned.

16 (0.025 g, 0.010 mmol) was dissolved in DMF (15 mL). Pd/C (0.015 g) and formic acid (0.1 mL) were added and the solution was stirred under hydrogen atmosphere (29 bar) at 70 °C. After 3 h, autoclave pressure decreased to 15 bar. Reaction was restarted with Pd/C (32 mg) in DMF (15 mL) under hydrogen atmosphere (29 bar) at 70 °C for 3 h. The reaction mixture was filtered and evaporated i.vac. ¹H NMR of the solid residue showed signals of uncleaved starting material and additional signals that could not be assigned.

16 (0.016 g, 0.007 mmol) was suspended in aqueous 1 M HCl. Pd/C (0.014 g) was added and the solution stirred under hydrogen atmosphere (30 bar) at 50 °C. After 24 h, reaction mixture was filtered and evaporated i.vac. ESI-MS and NMR analysis of the green-yellow residue was not possible. Attempts to remove colored impurities failed.

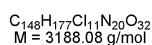
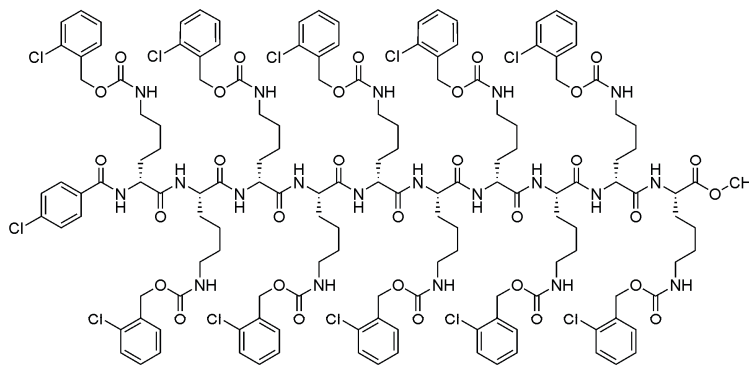
16 (0.016 g, 0.007 mmol) was suspended in aqueous 1 M HCl. Pd/C (0.014 g) was added and the solution stirred under hydrogen atmosphere (30 bar) at 60 °C for 3.5 h. The reaction mixture was filtered and evaporated i.vac. ESI-MS and NMR analysis of the green-yellow residue was not possible. Attempts to remove colored impurities failed.

16 (0.020 g, 0.008 mmol) was suspended in MeOH (10 mL). Formic acid (2.0 mL) and Pd/C (0.020 g) were added and the solution was stirred under argon atmosphere at 70 °C for 18 h. After TLC monitoring, formic acid (0.5 mL) was added and the reaction mixture stirred at 70 °C for 1 h. Reaction was stopped, worked up for ¹H NMR analysis and restarted 3 times. Overall reaction time: 50 h. Several attempts to purify product by precipitation and filtration failed. CEC showed several very small peaks and one main peak. ¹H NMR showed very small signals of uncleaved protecting groups.

Isolation and characterization of the desired product was not possible following the procedures described above.

3 Linear D-(*alt*)-L-peptides

p-Cl-benzoic acid-(D-Lys(2Cl-Z)-L-Lys(2Cl-Z))₅-Me (**15**):



4-Chlorobenzoic acid (10 mg, 0.066 mmol), (D-Lys(2Cl-Z)-L-Lys(2Cl-Z))₅-Me (99 mg, 0.033 mmol), and HOBT (6 mg, 0.043 mmol) were dissolved in dry DMF (10 mL) and cooled to 0 °C. To the cold solution, a concentrated solution of EDC in CH₂Cl₂ (19 mg, 0.99 mmol) was added. The solution was allowed to warm up to room temperature and stirred for 14 h. TLC monitoring showed remaining unreacted (D-Lys(2Cl-Z)-L-Lys(2Cl-Z))₅-Me, so more EDC (5 mg), 4-chlorobenzoic acid (3 mg) and HOBT (2 mg) were added. After 3 h, DMF was evaporated i.vac. to give a gelous solid, which was suspended in EE:hexane and chilled in the freezer for 1 h. The solid was filtered and dissolved in CH₂Cl₂:MeOH. Water was added to the solution and the biphasic system stirred for 10 minutes. After phase separation, the organic layer was washed with aqueous 1 M citric acid solution (1x20 mL), dried over MgSO₄, filtered and evaporated i.vac. The solid was suspended in EE, then diluted with hexane and filtered to give **15** as a white solid in 95% yield.

HPLC (150 mm YMC-Pack ODS-A, 4.6 mm, acetonitrile/water = 90:10, 0.8 mL/min, 3.7 MPa, 308 K): 16.19 min (93.4% peak area, **15**).

$R_f = 0.7$ (CH₂Cl₂:MeOH 9:1)

ESI-MS: $m/z = 1588.5$ (calcd 1588.5 for C₁₄₈H₁₇₇Cl₁₁N₂₀O₃₂ + 2 Na⁺), 1066.3 (calcd 1066.3 for C₁₄₈H₁₇₇Cl₁₁N₂₀O₃₂ + 3 Na⁺).

High-resolution ESI-MS (calculated at the most abundance peak):

$m/z = 1591.456678$ (calcd 1591.458998 for C₁₄₈H₁₇₇Cl₁₁N₂₀O₃₂ + 2 Na⁺).

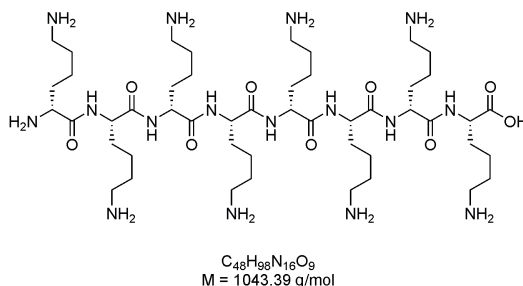
2Cl-Z-deprotection attempts:

15 (0.032 g, 0.010 mmol) was dissolved in MeOH:EE:formic acid (9:9:2) (10.0 mL). Pd/C (0.032 g) was added and the solution shortly heated for activation, then stirred under nitrogen atmosphere at 60 °C. After 30 min, MeOH:formic acid (2:1) was added, 1 h later more MeOH:formic acid (2:1) was added. 2 h later, reaction mixture was filtered and the solvent evaporated. ¹H NMR showed signals of remaining, uncleaved **15**. CEC showed several peaks. Reaction was restarted with Pd/C (10 mg) under the conditions described above. Reaction was stopped after 4 h. CEC showed several peaks, so reaction was restarted with Pd/C (20 mg) at 75 °C for 60 h. CEC looked comparable to the others. ESI-MS showed several peaks of partially uncleaved **15**. Eventually formed product could not be isolated from other partially uncleaved decapeptides.

15 (0.014 g, 0.005 mmol) was dissolved in MeOH:EE (2:1) (21.0 mL). Pd/C (0.014 g) was added and the solution stirred under hydrogen atmosphere (7 bar) at 60 °C. After 4 h, TLC monitoring showed remaining starting material, so reaction was continued under hydrogen atmosphere (8 bar) at 65 °C. After 2 h, reaction mixture was filtered and the solvents removed i.vac. It was attempted to purify the crude product by dissolving the solid in a small amount of MeOH, precipitating it by the addition of EE and filtering it. The ¹H NMR spectrum could be in concordance with the desired product. CEC showed one main peak and one small peak, but ESI-MS gave a Spectrum of several peaks, of which none could be assigned to the product.

3 Linear D-(*alt*)-L-peptides

(D-Lys-L-Lys)₄ (**28**):

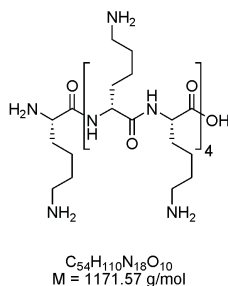


11 (0.075 g, 0.03 mmol) was reacted following the general procedure for the deprotection of the methyl ester. After aqueous work-up, the product was dried i.vac. and subsequently reacted according to the general procedure for the superacidic cleavage of the 2Cl-Z protecting group.

HPLC (C18 acetonitrile/water = 0:100 to 10:90 in 30 min): 6.49 min (>99.0% peak area).

MALDI-TOF: m/z = 1045.7 (calcd 1044.4 for $C_{48}H_{98}N_{16}O_9 + H^+$).

L-Lys-(D-Lys-L-Lys)₄ (**36**):

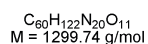
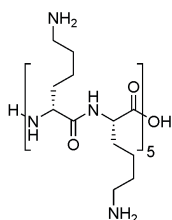


33 (0.084 g, 0.03 mmol) was reacted following the general procedure for the deprotection of the methyl ester. After aqueous work-up, the product was dried i.vac. and subsequently reacted according to the general procedure for the superacidic cleavage of the 2Cl-Z protecting group.

HPLC (C18 acetonitrile/water = 0:100 to 10:90 in 30 min): 9.86 min (>99.0% peak area).

MALDI-TOF: m/z = 1174.4 (calcd 1172.6 for $C_{54}H_{110}N_{18}O_{10} + H^+$).

(D-Lys-L-Lys)₅ (**29**):

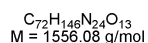
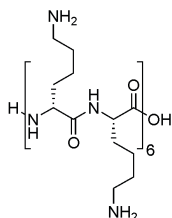


13 (0.093 g, 0.03 mmol) was reacted following the general procedure for the deprotection of the methyl ester. After aqueous work-up, the product was dried i.vac. and subsequently reacted according to the general procedure for the superacidic cleavage of the 2Cl-Z protecting group.

HPLC (C18 acetonitrile/water = 0:100 to 10:90 in 30 min): 11.35 min (>99.0% peak area).

MALDI-TOF: $m/z = 1303.1$ (calcd 1300.7 for $\text{C}_{60}\text{H}_{122}\text{N}_{20}\text{O}_{11} + \text{H}^+$).

(D-Lys-L-Lys)₆ (**30**):



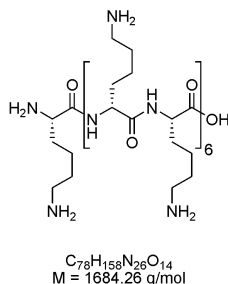
26 (0.092 g, 0.025 mmol) was reacted following the general procedure for the deprotection of the methyl ester. After aqueous work-up, the product was dried i.vac. and subsequently reacted according to the general procedure for the superacidic cleavage of the 2Cl-Z protecting group.

HPLC (C18 acetonitrile/water = 0:100 to 10:90 in 30 min): 14.22 min (>99.0% peak area).

MALDI-TOF: $m/z = 1560.2$ (calcd 1557.1 for $\text{C}_{72}\text{H}_{146}\text{N}_{24}\text{O}_{13} + \text{H}^+$).

3 Linear D-(*alt*)-L-peptides

L-Lys-(D-Lys-L-Lys)₆ (**37**):

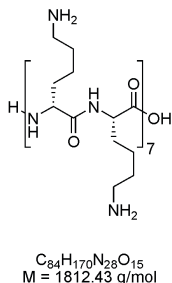


34 (0.068 g, 0.017 mmol) was reacted following the general procedure for the deprotection of the methyl ester. After aqueous work-up, the product was dried i.vac. and subsequently reacted according to the general procedure for the superacidic cleavage of the 2Cl-Z protecting group.

HPLC (C18 acetonitrile/water = 0:100 to 10:90 in 30 min): 15.15 min (>99.0% peak area).

MALDI-TOF: $m/z = 1689.6$ (calcd 1685.3 for $C_{78}H_{158}N_{26}O_{14} + H^+$).

(D-Lys-L-Lys)₇ (**31**):

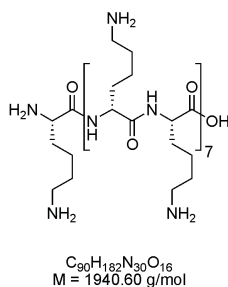


27 (0.073 g, 0.017 mmol) was reacted following the general procedure for the deprotection of the methyl ester. After aqueous work-up, the product was dried i.vac. and subsequently reacted according to the general procedure for the superacidic cleavage of the 2Cl-Z protecting group.

HPLC (C18 acetonitrile/water = 0:100 to 10:90 in 30 min): 16.09 min (>99.0% peak area).

MALDI-TOF: $m/z = 1817.4$ (calcd 1813.4 for $C_{84}H_{170}N_{28}O_{15} + H^+$).

L-Lys-(D-Lys-L-Lys)₇ (**38**):

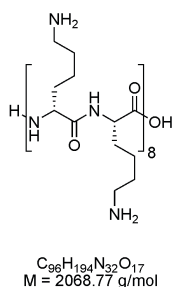


35 (0.069 g, 0.015 mmol) was reacted following the general procedure for the deprotection of the methyl ester. After aqueous work-up, the product was dried i.vac. and subsequently reacted according to the general procedure for the superacidic cleavage of the 2Cl-Z protecting group.

HPLC (C18 acetonitrile/water = 0:100 to 10:90 in 30 min): 17.21 min (>99.0% peak area).

MALDI-TOF: $m/z = 1946.7$ (calcd 1941.6 for $\text{C}_{90}\text{H}_{182}\text{N}_{30}\text{O}_{16} + \text{H}^+$).

(D-Lys-L-Lys)₈ (**32**):



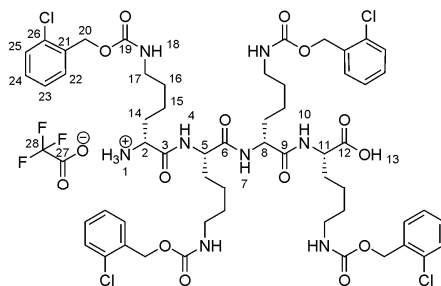
12 (0.068 g, 0.014 mmol) was reacted following the general procedure for the deprotection of the methyl ester. After aqueous work-up, the product was dried i.vac. and subsequently reacted according to the general procedure for the superacidic cleavage of the 2Cl-Z protecting group.

HPLC (C18 acetonitrile/water = 0:100 to 10:90 in 30 min): 18.28 min (>99.0% peak area).

MALDI-TOF: $m/z = 2074.6$ (calcd 2069.8 for $\text{C}_{96}\text{H}_{194}\text{N}_{32}\text{O}_{17} + \text{H}^+$).

3 Linear D-(*alt*)-L-peptides

(D-Lys(2Cl-Z)-L-Lys(2Cl-Z))₂ (**39**):



C₅₈H₇₁Cl₄F₃N₈O₁₅
M = 1319.04 g/mol

10 (0.195 g, 0.150 mmol) was reacted following the general procedure for the deprotection of the Boc group. TFA (6 mL), CH₂Cl₂ (6 mL).

HPLC (125 mm Nucleodur 100-5-C18 ec, 4 mm, methanol/0.1% TFA = 70:30, 0.8 mL/min, 9.6 MPa, 308 K): 18.04 min (96.9% peak area, **39**).

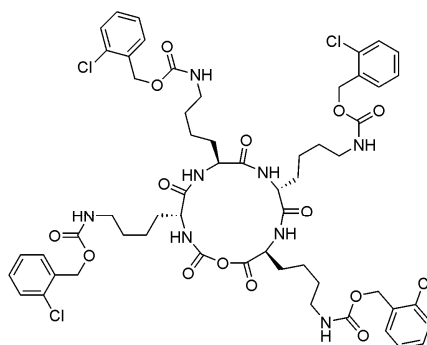
R_F = 0.2 (CH₂Cl₂:MeOH 9:1)

¹H NMR (400 MHz, DMSO-d₆, 20 °C): δ 8.66 (d, ³J(H,H) = 8.4 Hz, 1 H, NH), 8.34 (d, ³J(H,H) = 8.2 Hz, 2 H, 2 NH), 8.08 - 8.06 (m, 3 H, N¹H₃⁺), 7.50 - 7.28 (m, 20 H, 4 C²²⁻²⁵H, 4 N¹⁸H), 5.07 (2 s, 8 H, 4 C²⁰H₂), 4.58 - 4.48 (m, 1 H, C⁵H or C⁸H or C¹¹H), 4.47 - 4.37 (m, 1 H, C⁵H or C⁸H or C¹¹H), 4.19 - 4.09 (m, 1 H, C⁵H or C⁸H or C¹¹H), 3.85 - 3.75 (m, 1 H, C²H), 3.00 - 2.92 (m, 8 H, 4 C¹⁷H₂), 1.78 - 1.10 (m, 24 H, 4 C¹⁴⁻¹⁶H₂).

¹³C NMR (DMSO-d₆): δ 173.55, 171.51, 170.65, 168.24, 155.73, 155.72, 136.86, 134.54, 134.48, 132.27, 132.22, 129.68, 129.63, 129.59, 129.38, 129.21, 129.18, 127.21, 127.19, 62.54, 62.49, 51.96, 51.64, 51.62, 51.56, 51.52, 40.19, 32.54, 30.85, 30.77, 28.91, 28.81, 22.54, 22.43, 21.43.

ESI-MS: m/z = 1205 (calcd 1205 for C₅₈H₇₁Cl₄F₃N₈O₁₅ - TFA).

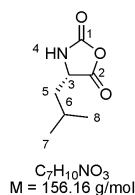
D-Lys(2Cl-Z)-L-Lys(2Cl-Z)₂-NCA (**40**):



C₅₇H₆₈Cl₄N₈O₁₄
Mol. Wt.: 1231.01

39 (0.13 g, 0.10 mmol) and dry NEt₃ (0.7 mL, 0.05 mmol) were dissolved in dry THF (200 mL). Starting material did not dissolve, so THF was removed by condensation and replaced by DMF (100 mL). Phosgene (20% in toluene) (0.53 mL, 1.0 mmol) was dissolved in dry THF (100 mL) and DMF-solution of Tetramer added within 15 min. After addition, the reaction mixture was stirred at room temperature for 20 h. The solvent was removed i.vac., the remaining solid was suspended in dry THF:dry pentane (3:2, 200 mL) and stored in the freezer over night. The solid was filtered and the solution chilled for 7 days to form crystals, but no crystallization took place. ESI-MS of filtered solid and solution showed no evidence for product formation.

L-Leu-*N*-carboxy anhydride (**43**):



C₇H₁₁NO₃
M = 156.16 g/mol

L-Leucin (3.15 g, 24.0 mmol) was dissolved in anhydrous EE (600.0 mL) and phosgene (20% in toluene, 12.8 mL, 24.0 mmol) was added. Then, NEt₃ (3.37 mL, 24.0 mmol) was added slowly under stirring at room temperature. After 20 h reaction time, the reaction mixture was filtered. The solid residue was washed extensively with EE. The solution was cooled to -5 °C and extracted quickly with ice-cold water (100 mL) and 0.5% aqueous NaHCO₃-solution (100 mL). The cold organic layer was dried over MgSO₄ and concentrated i.vac.

3 Linear D-(*alt*)-L-peptides

($T < 30\text{ }^{\circ}\text{C}$) to a volume of less than 20 mL. The concentrated solution was added to hexane (250 mL). The solution was stored in the freezer for 3 days to crystallize. The crystals were filtered, washed with ice-cold EE and dried i.vac. The remaining solution was concentrated again and added to hexane (250 mL) to crystallize again. The first crystallization afforded 0.39 g (Yield: 10%) of **43** as colorless crystals.

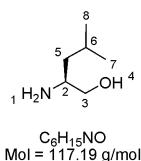
$R_F = 0.66$ (CH_2Cl_2 :acetone 7:3)

^1H NMR (300 MHz, DMSO-d_6 , $20\text{ }^{\circ}\text{C}$): δ 6.95 (br. s, 1 H, N^4H), 4.35 - 4.30 (m, 1 H, C^3H), 1.83 - 1.60 (m, 3 H, C^5H_2 , C^6H), 0.97 (t, $^3J(\text{H,H}) = 6.4\text{ Hz}$, 6 H, C^7H_3 , C^8H_3).

^{13}C NMR (DMSO-d_6): δ 169.89, 153.00, 56.11, 40.75, 24.98, 22.65, 21.46.

EI-MS ($45\text{ }^{\circ}\text{C}$): $m/z = 156$ (calcd 156 for $\text{C}_{34}\text{H}_{46}\text{Cl}_2\text{N}_4\text{O}_9^+$).

L-Leucinol (**41**):



L-Leu was reacted following the general procedure for the reduction of amino acids to amino alcohols with LAH. Bulb-to-bulb distillation at $140\text{ }^{\circ}\text{C}$ afforded **41** as colorless oil in 86% yield.

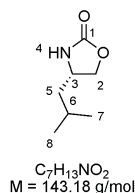
In one batch, the amino alcohol was transferred into the amine hydrochloride with HCl prior to THF removal. This procedure lowered the volatility of the product but afforded impure material which had to be used without further purification since distillation was impossible.

$R_F = 0.1$ (CH_2Cl_2 :MeOH 8:2)

^1H NMR (300 MHz, DMSO-d_6 , $20\text{ }^{\circ}\text{C}$): δ 3.24 (dd, $^3J(\text{H,H}) = 4.5\text{ Hz}$, $^3J(\text{H,H}) = 10.2\text{ Hz}$, 1 H, C^3H), 3.09 - 3.03 (m, 1 H, C^3H), 2.67 - 2.59 (m, 1 H, C^2H), 1.79 - 1.63 (m, 1 H, C^6H), 1.15 - 1.00 (m, 2 H, C^5H_2), 0.87 (d, $^3J(\text{H,H}) = 6.9\text{ Hz}$, 3 H, C^7H_3 or C^8H_3), 0.83 (d, $^3J(\text{H,H}) = 6.9\text{ Hz}$, 3 H, C^7H_3 or C^8H_3).

^{13}C NMR (DMSO- d_6): δ 67.72, 50.95, 43.53, 24.38, 23.95, 22.41.

(*S*)-4-isobutyloxazolidin-2-one (**42**):



A 25 mL flask equipped with a reflux-condenser was charged with freshly distilled **41** (2.93 g, 25.0 mmol), diethyl carbonate (3.79 mL, 31.3 mmol) and sodium methanolate (0.014 g, 0.25 mmol). The mixture was stirred and the flask heated in an oil bath maintained at 120 °C. After heating over night, the reaction mixture was allowed to cool down to 60 - 70 °C and was recrystallized in hexane to yield 0.96 g (yield: 60%) of pure **42** as colorless solid.

$R_F = 0.56$ (CH_2Cl_2 :MeOH 9:1)

^1H NMR (300 MHz, CDCl_3 , 20 °C): δ 6.53 (br. s, 1 H, N^1H), 4.48 - 4.43 (m, 1 H, C^2H or C^3H), 3.97 - 3.86 (m, 2 H, C^2H_2 or C^2H , C^3H), 1.69 - 1.49 (m, 2 H, C^5H_2 or C^6H , C^5H), 1.39 - 1.30 (m, 1 H, C^6H or C^5H), 0.90 (d, $^3J(\text{H},\text{H}) = 6.8 \text{ Hz}$, 3 H, C^7H_3 or C^8H_3), 0.89 (d, $^3J(\text{H},\text{H}) = 6.6 \text{ Hz}$, 3 H, C^7H_3 or C^8H_3).

^{13}C NMR (DMSO- d_6): δ 160.57, 71.11, 51.37, 44.84, 25.40, 23.32, 22.45.

EI-MS (35 °C): $m/z = 143$ (calcd 143 for $\text{C}_7\text{H}_{13}\text{NO}_2^+$), 86 (calcd 86 for $\text{C}_3\text{H}_4\text{NO}_2^+$).

GC (achiral, 6890N Agilent Technologies, 95% methyl-5% phenyl-polysiloxan, FID, split injector, 220/80 6 /min 300/350, 0.3 bar H_2): 99.3% peak area.

GC (chiral, HP 6890, 25 m dimethylpentyl β -cyclodextrin (30%) in PS086 (70%) 0.25/~ 0.25, FID, split injector, 220/135/320, 0.6 bar H_2): 99.2% peak area (probably L-enantiomer), 0.8% peak area (probably D-enantiomer).

Attempts of oxidation to L-Leu-*N*-carboxy anhydride **43**:

A solution of (**42**) (70.0 mg, 0.5 mmol) in acetone (10.0 mL) was cooled to -78 °C before KMnO_4 (0.79 g, 5.0 mmol) and FeCl_3 (0.50 g, 3.1 mmol) were added. After stirring for 2 h at -78 °C, the reaction mixture was allowed to

3 Linear D-(*alt*)-L-peptides

warm up to room temperature and stirred for another 12 h. The resulting suspension was diluted with CH₂Cl₂ (20 mL) and filtered (the residue was washed with CH₂Cl₂ (2x20 mL)). The combined organic layers were dried over MgSO₄, decolorized over charcoal and the solvent evaporated i.vac. Resulting yellow solid was analysed by ¹H NMR, which showed neither product, nor starting material signals. TLC showed several UV-inactiv spots.

A solution of (**42**) (70.0 mg, 0.5 mmol) in CH₂Cl₂ (10.0 mL) was cooled to –78 °C before KMnO₄ (0.79 g, 5.0 mmol) and FeCl₃ (0.50 g, 3.1 mmol) were added. After stirring for 2 h at –78 °C, the reaction mixture was allowed to warm up to room temperature and stirred for another 12 h. The resulting suspension was diluted with CH₂Cl₂ (20 mL) and filtered (the residue was washed with CH₂Cl₂ (2x20 mL)). The combined organic layers were dried over MgSO₄, decolorized over charcoal and the solvent evaporated i.vac. to give 70 mg of a solid. Resulting yellow solid was analysed by ¹H NMR, which was not interpretable. TLC showed several UV-inactiv spots.

AgNO₃ (0.093 g, 0.55 mmol) was added at 0 °C to a stirred solution of TMSCl (0.064 mL, 0.50 mmol) in dry acetonitrile (2.0 mL) and the resulting mixture stirred for 1 h. The resulting solution of TMSONO₂ was decanted from the precipitated AgCl and was added to a stirred mixture of CrO₃ (0.075 g, 1.50 mmol) in acetonitrile (1 mL). The mixture was stirred for 15 minutes and subsequently treated with a solution of (**42**) (0.072 g, 0.50 mmol) in acetonitrile (1.0 mL) under cooling in an ice-bath. Reaction was monitored by mass spectrometry. After 4 days at room temperature: no conversion of the starting material. After 2 days at 60 °C no conversion of starting material. After 2 days at 80 °C no conversion of starting material. Reaction failed.

3.4 Literature

- [1] B. A. Wallace, K. Ravikumar, *Science* **1988**, 241, 182.
- [2] B. A. Wallace, *Prog. Biophys. Mol. Biol.* **1992**, 57, 59.
- [3] D. A. Doyle, B. A. Wallace, *J. Mol. Biol.* **1997**, 266, 963.
- [4] D. A. Langs, *Science* **1988**, 241, 188.
- [5] D. A. Langs, G. D. Smith, C. Courseille, G. Precigoux, M. Hospital, *Proc. Natl. Acad. Sci. U. S. A.* **1991**, 88, 5345.
- [6] D. A. Langs, *Biopolymers* **1989**, 28, 259.
- [7] B. Lotz, F. Colonna-Cesari, F. Heitz, G. Spach, *J. Mol. Biol.* **1976**, 106, 915.
- [8] M. A. B. Block, C. Kaiser, A. Khan, S. Hecht, in *Functional Molecular Nanostructures, Vol. 245*, SPRINGER-VERLAG BERLIN, Berlin, **2005**, pp. 89.
- [9] D. T. Bong, T. D. Clark, J. R. Granja, M. R. Ghadiri, *Angew. Chem., Int. Ed.* **2001**, 40, 988.
- [10] G. P. Lorenzi, C. Gerber, H. Jaeckle, *Biopolymers* **1984**, 23, 1905.
- [11] G. P. Lorenzi, L. Tomasic, *Makromol. Chem.* **1988**, 189, 207.
- [12] G. P. Lorenzi, L. Tomasic, *J. Am. Chem. Soc.* **1977**, 99, 8322.
- [13] G. P. Lorenzi, L. Tomasic, F. Bangerter, P. Neuenschwander, B. Di Blasio, *Helv. Chim. Acta* **1983**, 66, 2129.
- [14] G. P. Lorenzi, L. Tomasic, H. Jaeckle, *Makromol. Chem. Rapid Commun.* **1980**, 1, 729.
- [15] G. P. Lorenzi, H. Jaeckle, L. Tomasic, V. Rizzo, C. Pedone, *J. Am. Chem. Soc.* **1982**, 104, 1728.
- [16] G. P. Lorenzi, H. Jaeckle, L. Tomasic, C. Pedone, B. Di Blasio, *Helv. Chim. Acta* **1983**, 66, 158.
- [17] L. Tomasic, A. Stefani, G. P. Lorenzi, *Helv. Chim. Acta* **1980**, 63, 2000.
- [18] E. Benedetti, B. Di Blasio, C. Pedone, G. P. Lorenzi, L. Tomasic, V. Gramlich, *Nature* **1979**, 282, 630.

- [19] B. Di Blasio, E. Benedetti, V. Pavone, C. Pedone, O. Spiniello, G. P. Lorenzi, *Biopolymers* **1989**, 28, 193.
- [20] G. P. Lorenzi, V. Muri-Valle, F. Bangerter, *Helv. Chim. Acta* **1984**, 67, 1588.
- [21] G. P. Lorenzi, T. Paganetti, *J. Am. Chem. Soc.* **1977**, 99, 1282.
- [22] G. P. Lorenzi, C. Gerber, H. Jaeckle, *Macromolecules* **1985**, 18, 154.
- [23] E. Navarro, R. Tejero, E. Fenude, B. Celda, *Biopolymers* **2001**, 59, 110.
- [24] E. Navarro, E. Fenude, B. Celda, *Biopolymers* **2002**, 64, 198.
- [25] E. Navarro, E. Fenude, B. Celda, *Biopolymers* **2004**, 73, 229.
- [26] T. Ozaki, A. Shoji, *Makromol. Chem. Rapid Commun.* **1982**, 3, 157.
- [27] R. Meudtner, Diplomarbeit, Freie Universität (Berlin), **2005**.
- [28] L. M. Berkowitz, P. N. Rylander, *J. Am. Chem. Soc.* **1958**, 80, 6682.
- [29] M. Bressan, A. Morvillo, G. Romanello, *Inorg. Chem.* **1990**, 29, 2976.
- [30] M. T. Reetz, K. Toellner, *Tetrahedron Lett.* **1995**, 36, 9461.
- [31] S. P. Shahi, A. Gupta, S. V. Pitre, M. V. R. Reddy, R. Kumareswaran, Y. D. Vankar, *J. Org. Chem.* **1999**, 64, 4509.
- [32] S. Wolfe, C. F. Ingold, *J. Am. Chem. Soc.* **1983**, 105, 7755.
- [33] S. Lai, D. G. Lee, *Tetrahedron* **2002**, 58, 9879.
- [34] M. Sasidharan, S. Suresh, A. Sudalai, *Tetrahedron Lett.* **1995**, 36, 9071.
- [35] N. C. Deno, N. H. Potter, *J. Am. Chem. Soc.* **1967**, 89, 3550.
- [36] L. Metsger, S. Bittner, *Tetrahedron* **2000**, 56, 1905.
- [37] Y. Ogata, K. Tomizawa, T. Ikeda, *J. Org. Chem.* **1980**, 45, 1320.
- [38] P. Baeckstrom, L. Li, M. Wickramaratne, T. Norin, *Synth. Commun.* **1990**, 20, 423.

4 Linear (Ester-[a/t]-urea)s

4.1 Linear Poly(ester-[a/t]-urea)s With Variable Stereochemistry

4.1.1 General Considerations

The generation and elucidation of peptide structures is of much interest since it is the key step for both understanding biological processes and developing biologically active materials suitable for pharmaceutical and medical applications. With this in mind, it becomes apparent that not only the development of new peptides is an important field of research, but also the integration of other functionalities into the polyamide backbone of a peptide is promising for a deeper understanding of the structure-function relationship, likely leading to improved properties.

One possibility of varying the backbone of a peptide is the replacement of amides with esters. For this ester incorporation into the sequence, an α -amino acid is exchanged by an α -hydroxy acid. This replacement maintains the direction of the peptide sequence (i.e. from *N*- to *C*-terminus) but eliminates one hydrogen bond donor site (see Figure 1 on the left). Intensive work in the field of depsipeptides has been carried out so far and for details, the reader is referred to Chapter 2.

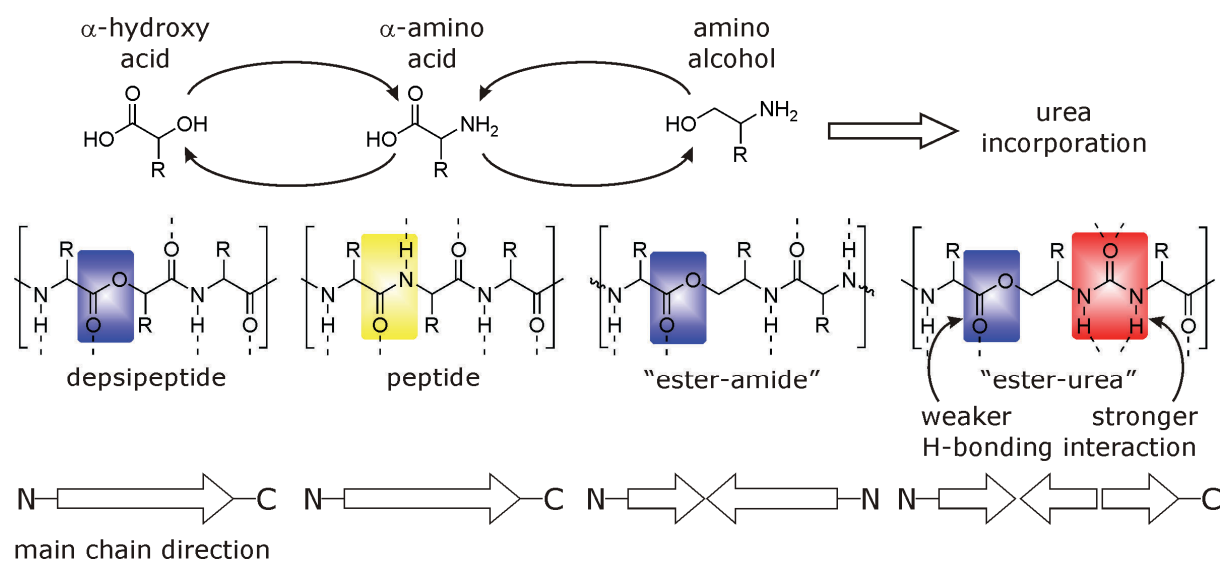


Figure 1: Peptide backbone modifications leading to depsipeptides, "ester-amides" and novel structural motifs such as "ester-ureas".

4 Linear (Ester-[*alt*]-urea)s

Another interesting possibility to exchange an amide by an ester is the replacement of an α -amino acid in the sequence by the corresponding amino alcohol (see Figure 1 in the middle). This exchange introduces an ester under elongation of the backbone by one atom and eliminates one hydrogen bond acceptor site. This amide-ester exchange goes in hand with a reversal of the main chain direction in the backbone.

One option to maintain the main chain direction of the peptide, is the further incorporation of a urea moiety into the backbone, so that altogether two adjacent amino acids in the peptide are replaced by an "ester-urea" moiety (see Figure 1 on the right). This urea incorporation elongates the backbone by one further atom and adds one hydrogen acceptor. The ester-urea structure has the same main chain direction as the original peptide and also the same number of hydrogen bond donors and acceptors. The location and the direction of these hydrogen bond donors and acceptors in the backbone differs significantly from those in peptides. The incorporation of an ester interrupts the highly ordered hydrogen bonding pattern of the peptide backbone, whereas the urea unit is a stronger hydrogen bonding interactor, which may be able to compensate this.^[1] This difference may result in a very interesting type of hydrogen bonding pattern and thereby in an interesting secondary structure. Consequent replacement of every amide in the main chain affords an ester-(*alt*)-urea backbone, which especially in the case of polymers would lead to an interesting and novel compound class. We expect these poly(ester-[*alt*]-urea)s to have interesting properties, such as a high biodegradability, since they are of a polyester backbone. Polyesters such as polylactide are highly biodegradable and are therefore very interesting for medicinal applications, such as surgery or temporary implants, which have to be degraded in the human body after the time they were needed. So it seems very interesting to investigate not only the structure of this new class of polymer but also its biological and physiological properties.

The goal of this project is the preparation of poly(ester-[*alt*]-urea)s with variable stereochemistry, which are well defined in length with narrow polydispersities.

4.1.2 Synthetic Considerations

A polymer should – if possible – result from a polymerization by which the length of the polymer can be determined by the reaction conditions and by which the polydispersity of the product is as narrow as possible. Starting from the approach of generating alternating polypeptides by the ring opening polymerization of macrocyclic *N*-carboxy anhydrides (NCAs), one can also think of following the path of ring opening polymerization to end up with the poly(ester-[*alt*]-urea)-structure. The macrocyclic monomer needed for this polymerization is depicted in Figure 2.

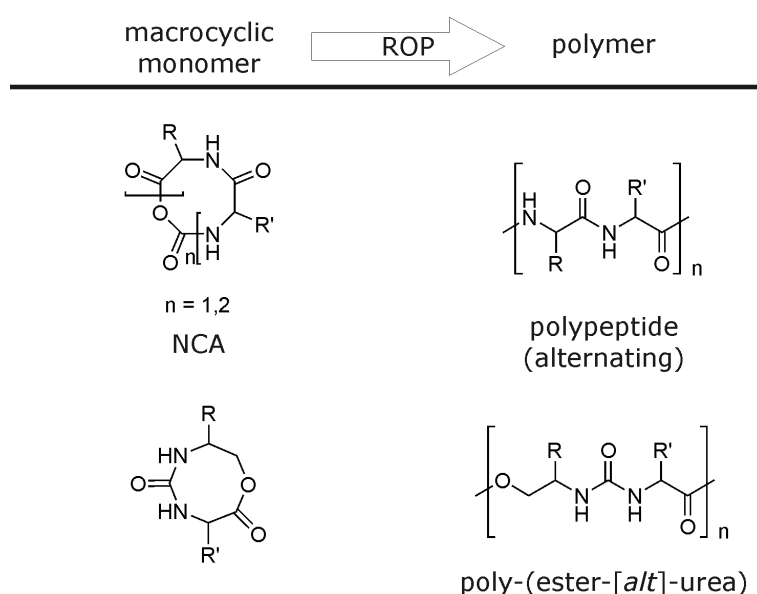
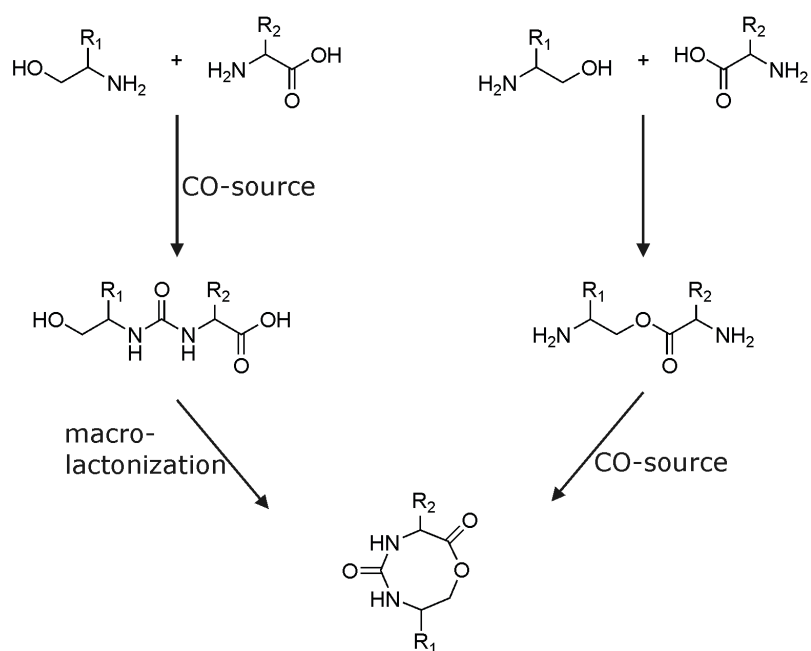


Figure 2: Macrocyclic monomers and resulting polymer after ring opening polymerization.

The polymerization of this monomer is expected to be comparable to the lactide polymerization and should proceed well under control of *N*-heterocyclic carbene catalysts.

The first step towards the polymer is the synthesis of the monomer. With regard to the structural motif to be generated in the polymer it seems reasonable to start the monomer synthesis from an amino alcohol and an amino acid. The missing urea link can be introduced with a C^1 -building block. With this in mind, the synthesis can in principle follow two routes as depicted in Scheme 1.

4 Linear (Ester-[*alt*]-urea)s



Scheme 1: Strategy for the synthesis of a macrocyclic monomer for poly(ester-[*alt*]-urea)s.

In the first approach (right pathway in Scheme 1), the first bond to be formed is the ester bond between the amino alcohol and the amino acid. The resulting ester is to be cyclized with a CO-source, such as triphosgene or phosgene to the desired macrocycle. In the second approach (left pathway in Scheme 1), the *N*-termini of the amino alcohol and of the amino acid are linked with a CO-source, such as 1,1'-carbonyldiimidazole (CDI) to the corresponding urea, and subsequently cyclized in a macrolactonization to the desired monomer.^[2,3]

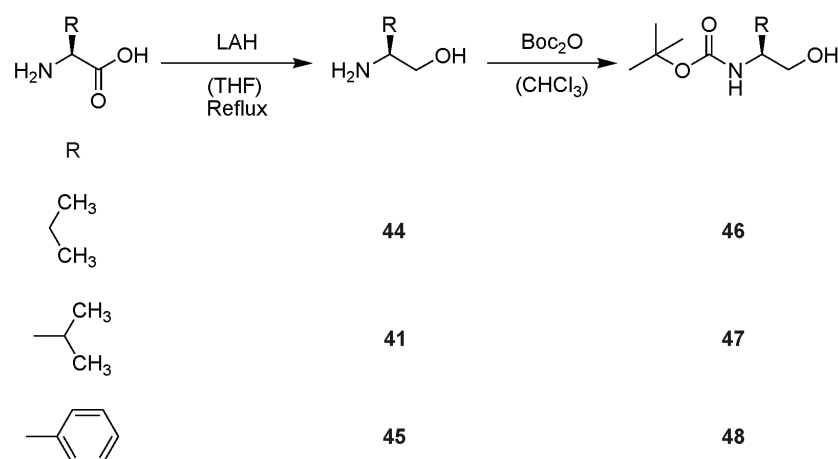
The macrocyclic monomer is expected to have a high ring strain. The rigid urea functionality with its preferred *all-trans*-conformation in the small eight membered ring dominates the ring conformation. Building up the urea functionality first (pathway two) bears the risk that the chain ends will not find each other in the macrolactonization step, since the rigid urea forces the molecule into an extended conformation. So it seems reasonable to build up the urea functionality in the last step of the synthesis. Additionally, the exothermic urea formation may enable the molecule to ring close, overcompensating for the build-up of ring strain. This consideration clearly favors pathway one. The major drawback of this pathway is the indistinguishability of both *N*-termini prior to cyclization. The open-chain-molecule has two reactive centers, which could both

react with the CO-source. In the case of phosgene, both chain ends are hence capable to form the isocyanate, in which case the ring closure could not occur. Therefore, adjusting the ratios and concentrations is of crucial importance.

In order to simplify the synthesis, only bifunctional amino acids, such as valine, leucine and phenylalanine were used. As throughout this thesis, the aim was to generate D-(*alt*)-L-structures and compare them with homo-L-structures.

4.1.3 Monomer Synthesis: Pathway One

The five step synthesis started with the reduction of an L-amino acid to the corresponding amino alcohol with lithium aluminium hydride in refluxing THF (Scheme 2). The crude product was purified via bulb-to-bulb distillation to give the pure amino alcohols **44**, **41** and **45**, respectively. The yields of this reaction were only moderate due to the volatility of the product. The subsequent Boc protection worked out satisfyingly.

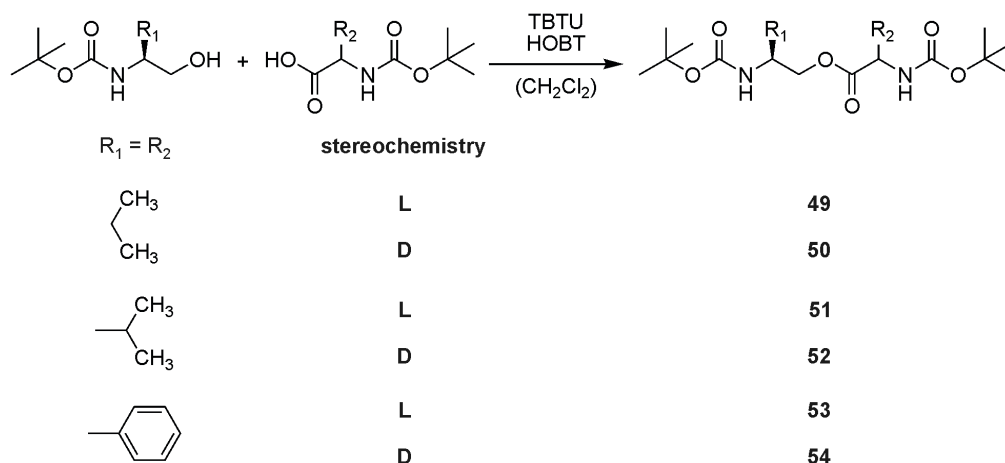


Scheme 2: Synthesis of Boc protected amino alcohols from the corresponding amino acids.

In the next step, the amino alcohol or its hydrochloride was converted to the Boc protected amino alcohol with Boc-anhydride. This *N*-protection was crucial, prohibiting the undesired reaction of the much more nucleophilic amine in the subsequent esterification reaction. Depending on the starting material (hydrochloride or neutral amino alcohol), the addition of triethylamine as a base was necessary. Since the yield of the hydrochloride could not be determined, the amount of Boc-anhydride was adapted to the reaction (addition of Boc-anhydride until TLC monitoring showed no remaining amino alcohol). This

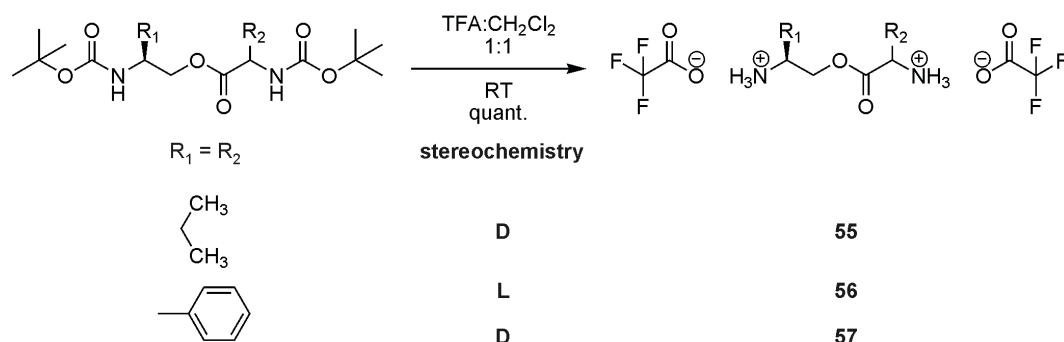
4 Linear (Ester-[*alt*]-urea)s

procedure worked smoothly and gave in the case of Boc-L-valinol (**46**) and Boc-L-leucinol (**47**) the pure product after column chromatography, whereas Boc-L-phenylalanine (**48**) was purified by recrystallization.



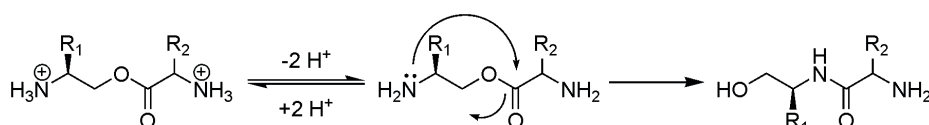
Scheme 3: Esterification of the different Boc protected amino alcohols with their corresponding Boc protected amino acids.

In the following sequence, the *N*-Boc-protected amino alcohol was condensed with the corresponding Boc protected D- and L-amino acid to the dimeric ester (Scheme 3). In order to limit the variability of the system, only the corresponding amino acids were condensed (i.e. leucinol with leucine). This reaction was first attempted with EDC/HOBT as coupling reagents, but gave in all cases unsatisfying yields. In every reaction, TLC monitoring showed remaining starting material. Attempts to drive the reaction to completion by changing the solvent from CH_2Cl_2 to more polar solvents, such as THF or DMF, as well as the addition of more EDC/HOBT and Boc-amino acid or even the addition of DPTS to the reaction mixture and long reaction times (76 h) failed. Once it was tried to convert the amino acid quantitatively into the active ester with EDC/HOBT prior to the addition of the nucleophile, but this conversion was not quantitative. So the reactions were aborted and the product was isolated in low yields (30 to 60 %), the Boc-amino alcohol was recovered and reacted once more. The change from EDC/HOBT to TBTU/HOBT was the breakthrough in this particular reaction, converting the amino acid into the ester in high yields. In this reaction, the addition of triethylamine was crucial, since the reaction just took place after the activation of TBTU with a base.



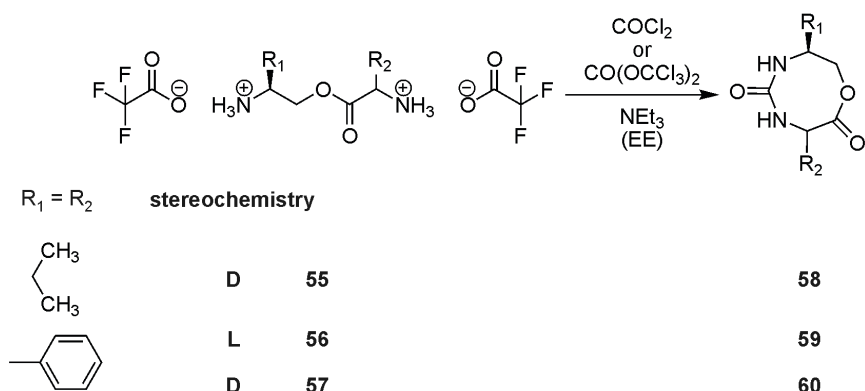
Scheme 4: Boc deprotection of some esters with TFA in methylene chloride.

The subsequent Boc-deprotections gave the TFA salt of the amine without further complications in less than 1 h. TLC monitoring within the first minutes of the reaction also showed both mono deprotected amines. The resulting ammonium trifluoroacetates were directly submitted to the ring closing reaction without further purification. It was important to isolate the product as TFA-salt in order to avoid rearrangement by intramolecular amidation of the ester (Scheme 5).



Scheme 5: Intramolecular amidation as undesired side reaction.

The last step of this route was the ring closure of the deprotected ester with phosgene or triphosgene to the macrocyclic monomer. Different reaction conditions have been tried (Scheme 6).



Scheme 6: Attempted cyclization to the macrocyclic monomers.

The problem with this reaction was the analysis of the product mixture. HPLC-MS of the crude mixtures gave no satisfying results, since the HPLC results turned out not to be reproducible and reliable and the ESI-coupling gave no interpretable results either. Only in one case the mol peak could be found. By employing compounds **56** and **57** it was anticipated that the resulting ring would be a solid, which could be isolated via precipitation. The most promising results were obtained, when the amine **57** was dissolved with triethylamine in high dilution and when triphosgene dissolved and diluted was added slowly using a syringe pump. Attempts to add the amine to a diluted solution of triphosgene or phosgene were not that promising probably due of the formation of the bis-isocyanate. The product of the most promising reaction was purified via precipitation. The HPLC-MS of the solid showed two main peaks in close proximity to each other both with the same mass of the desired macrocycle. It is unclear, if these two peaks belonged to two diastereomers resulting from epimerization during the reaction or if they belonged to two stable conformations of the rigid ring. NMR results were promising (Figure 3). The substance started to crystallize from solution in the NMR-tube. Unfortunately, the crystals were not large enough for X-ray analysis.

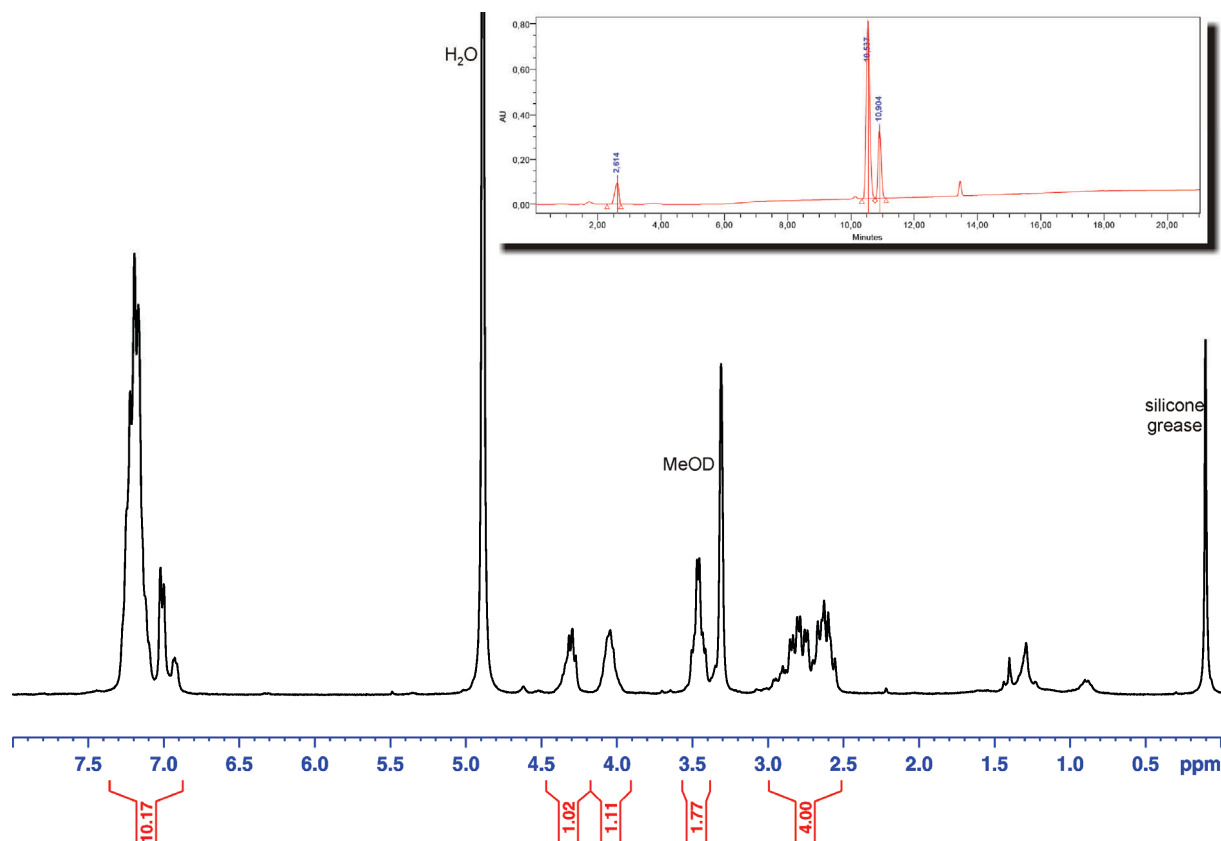


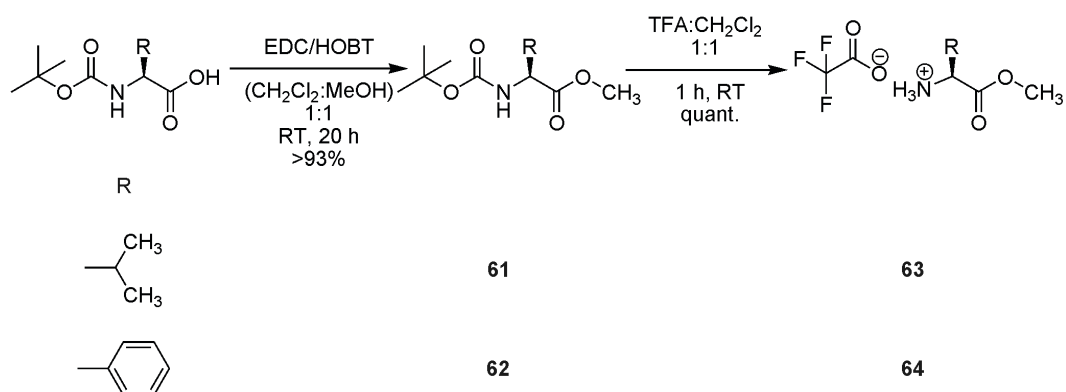
Figure 3: ^1H NMR spectrum and HPLC-trace of the cyclization of **57** to **60** ($\text{MeOH-}d_4$, 25 °C).

Although there were some promising indications, this synthetic strategy turned out not to be feasible for the synthesis of the macrocyclic monomer. In addition, the scale-up of the reaction would have caused problems, due to the extreme high dilution that was necessary to prevent intermolecular side reactions.

4.1.4 Monomer Synthesis: Pathway Two

This five step synthesis started with a simple esterification of the amino acids Boc-L-leucine and Boc-L-phenylalanine with methanol to the corresponding C-protected methyl esters Boc-L-Leu-Me (**61**) and Boc-L-Phe-Me (**62**) (Scheme 7). Both reactions proceeded smoothly and gave the desired products in high yields and purities.

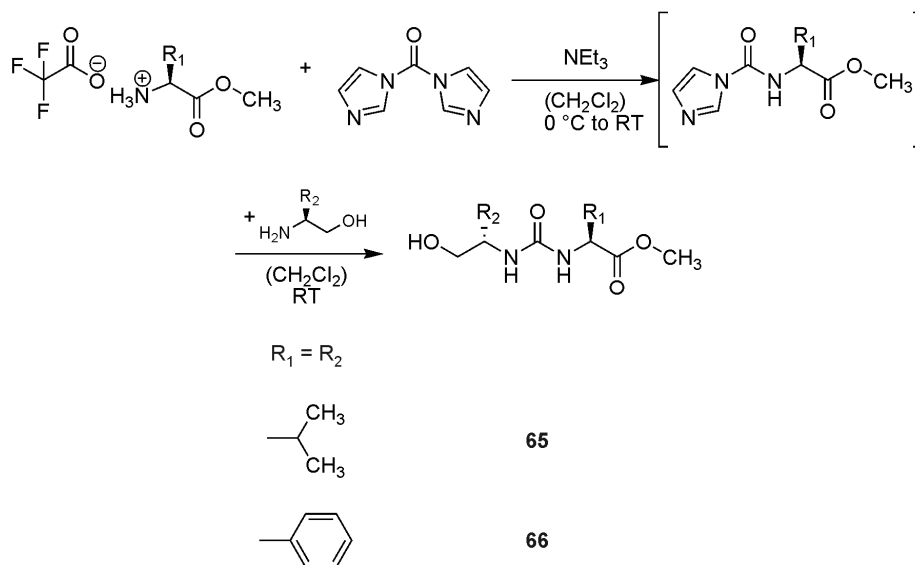
4 Linear (Ester-[*alt*]-urea)s



Scheme 7: Synthesis of amino acid methyl ester starting from Boc protected amino acids.

In the next step, the Boc protecting group was cleaved under standard protocol conditions. This reaction gave the TFA salt of the C-protected amino acids in quantitative yields.

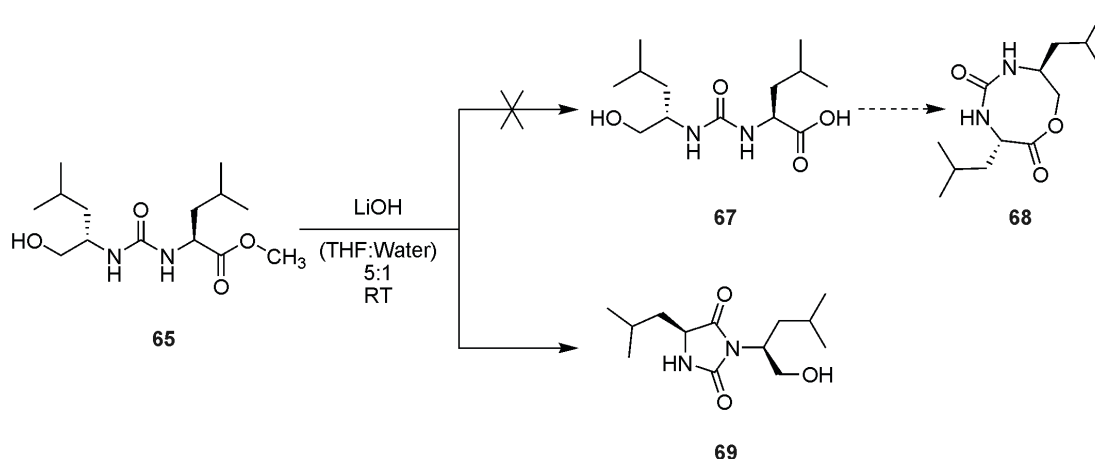
The Boc deprotected amino acids were then reacted with CDI and subsequently treated with the corresponding amino alcohols (Scheme 8).



Scheme 8: Coupling of the amino acid methyl esters with their corresponding amino alcohols to the resulting ureas, using CDI.

In this reaction, the TFA salt of the amino acid was dissolved in CH₂Cl₂ together with triethylamine to give the deprotonated and nucleophilic amine functionality. This solution was then added slowly to a chilled solution of CDI, using a syringe pump, in order to have a high excess of CDI in relation to the amino acid. This

was crucial since the amino acid had to react with CDI instead of building the homo-urea with an activated amino acid. The intermediate activated amino acid displayed decomposition on silica rendering TLC monitoring of the reaction impossible. The reaction was expected to be finished after the time given at room temperature. After aqueous work-up, the intermediate activated amino acid was dissolved in CH_2Cl_2 and treated with the freshly distilled amino alcohol to give the mixed ureas **65** (74% yield) and **66** (92% yield, but impure).



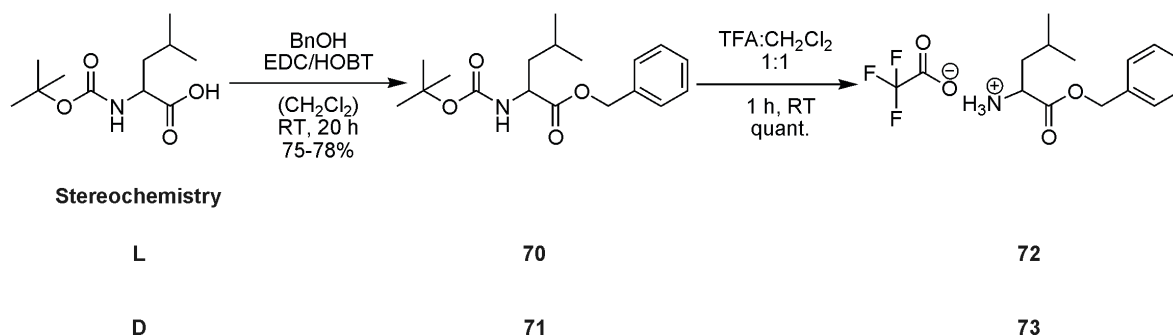
Scheme 9: Saponification and observed cyclization of **65**.

In the next step of the synthesis, the methyl ester **65** was saponified in order to give the free acid **67**, which should then be cyclized to **68** (Scheme 9). Under standard saponification conditions with subsequent acidification and aqueous work-up, HPLC-MS of the product mixture showed one major peak with the mass of dehydroxylated **67**. This could be explained by cyclization to either the five membered hydantoin **69** or to the desired eight membered ring **68**. 2D NMR confirmed the undesired formation of **69**. Deviating from the standard protocol, the basic solution was smoothly acidified with citric acid instead of acetic acid. The resulting HPLC-MS showed two peaks with ca. 10% peak area each, having the mass of **67**, and one peak with 5% peak area with the mass of **69**. This result showed that the formation of the hydantoin **69** could be suppressed to a certain amount, using a weaker acid during the work-up procedure, but it also showed that the desired product was formed under epimerization during the reaction, leading to two peaks with the same peak areas and masses. Since the synthesis of **67** was not possible by this synthetic

4 Linear (Ester-[*alt*]-urea)s

route, the methyl ester was replaced by the benzyl ester which could be cleaved under hydrogenation conditions (Pd/C/H₂).

Since a saponification of the methylester **65** or a transesterification was impossible without hydantoin formation, the benzyl ester had to be introduced in the first reaction of the sequence (Scheme 10).

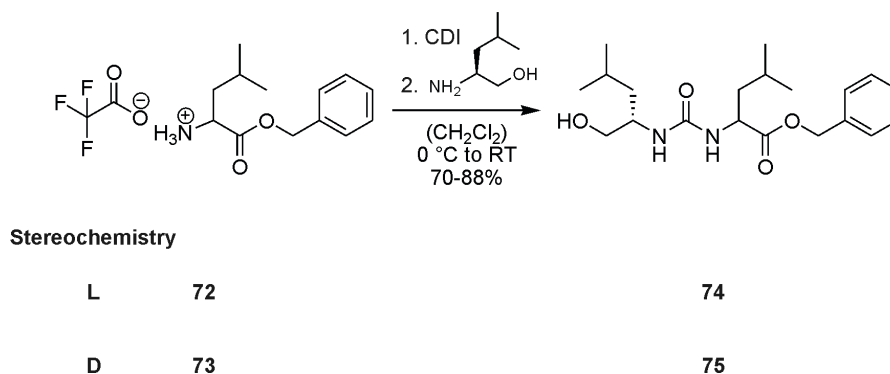


Scheme 10: Synthesis of L- and D-Leu-Bn.

For both enantiomers, this reaction proceeded in yields around 75%. Compared to the methyl esterification, the yields were much lower, what could be explained by the equivalents of alcohol used in the reaction. In case of the methyl ester, the alcohol was used in large excess (as solvent) and could be removed after the reaction by evaporation, whereas the benzyl alcohol had to be separated from the product via column chromatography and was hence used in only 2 equivalents. The purification of the bis-protected leucines **70** and **71** was achieved by repetitive column chromatography on silica. The main impurity was benzyl alcohol, which had to be removed by two to three column chromatographic purification steps. The following Boc deprotection was achieved using the standard protocol. The reaction proceeded smoothly, and gave the TFA-salt of the C-protected leucines **72** and **73** in quantitative yields.

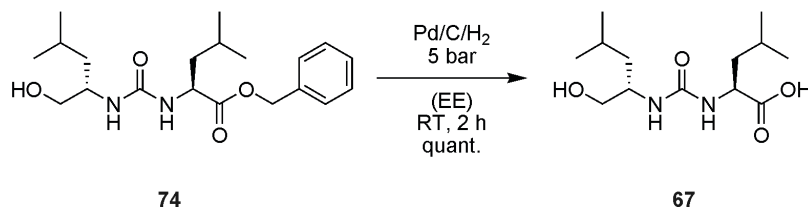
The TFA salts **72** and **73** were coupled with CDI to the corresponding imidazole-urea intermediates, which were then reacted with L-leucinol to the desired benzyl protected ureas **74** and **75**, respectively (Scheme 11). These reactions proceeded in satisfying yields and the products could be isolated in high purity according to HPLC. The purification of the L,L-isomer **74** was achieved via repetitive column chromatography on silica (two to three columns), since it was not possible to crystallize the compound. The L,D-isomer **75** could easily be

crystallized from CH₂Cl₂:PE and was obtained in high purity. All following experiments concerning deprotection, ring closure or extension have exclusively been performed with the L,L-isomer to improve the synthesis prior to react the more precious L,D-isomer.



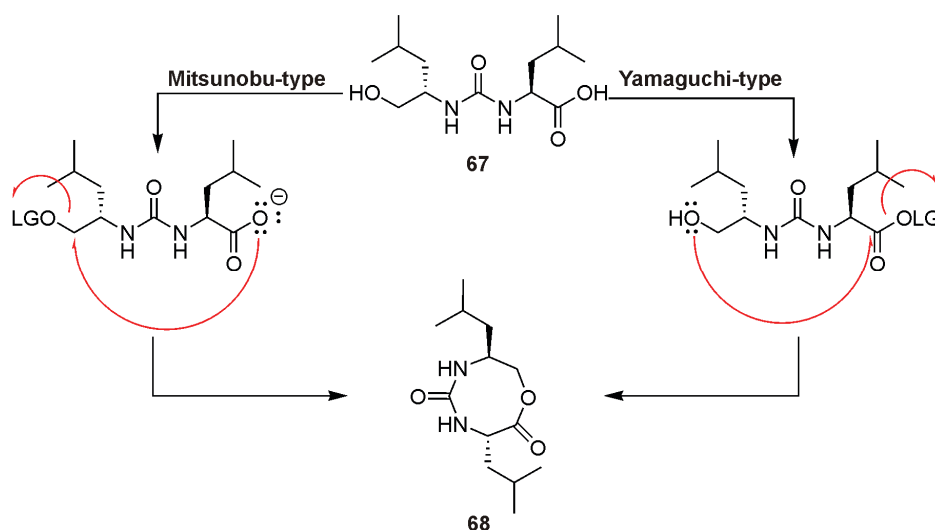
Scheme 11: Synthesis of the two benzyl protected leucine ureas **74** and **75**.

The debenzylation with Pd/C/H₂ was carried out in an autoclave at 5 bar hydrogen pressure and was finished after 1 h (Scheme 12). The deprotected urea **67** was isolated in high purity and quantitative yield by simple filtration and evaporation.



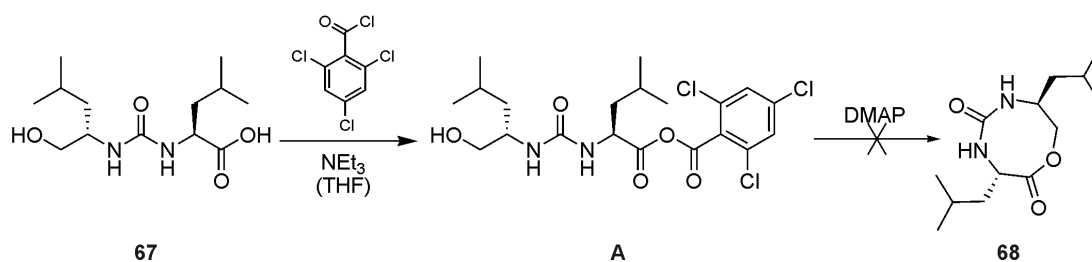
Scheme 12: Debenzylation of the L,L-leucine urea **74**.

The last step of the synthesis was the cyclization of the deprotected urea **67** to the desired macrocycle **68**. In general, there are two possible options to ring close **67** (Scheme 13).^[4] One possibility is the transfer of the alcohol into a leaving group, rendering the alcohol carbon atom accessible to nucleophilic attack of the carboxylate (Mitsunobu-type).^[5-7] On the other hand, one could activate the carboxyl functionality, which is then attacked by the alcohol (Yamaguchi-type).^[8]



Scheme 13: Cyclization via nucleophilic attack of the carboxylate on the alcohol carbon atom (Mitsunobu-type) or via nucleophilic attack of the alcohol on the activated carboxyl carbon atom (Yamaguchi-type). Leaving group is abbreviated by LG.

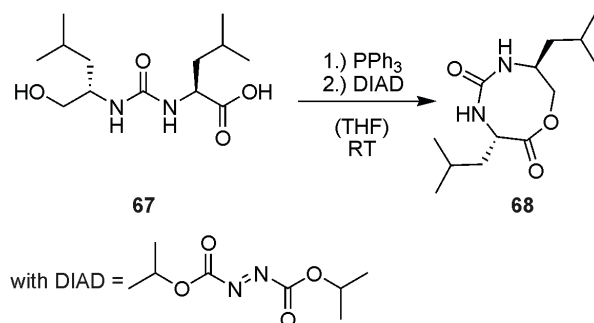
There are several possibilities to perform this reaction, and one of the most popular is the Yamaguchi macrolactonization, transferring the acid into a mixed anhydride **A** with 2,4,6-trichlorobenzoylchloride, which is then treated with excess DMAP. This reaction has widely been used for the synthesis of complex cyclic compounds.^[9-12]



Scheme 14: Attempted macrolactonization with Yamaguchi reagent.

In the first attempt, **67** was transferred into the mixed anhydride which was then added slowly to a solution of excess DMAP. Main problem in these reactions was the analysis of the product mixture. HPLC-MS showed DMAP as main component of the reaction mixture, rendering reaction monitoring impossible. It was also tried to avoid aqueous work-up, in order not to lose any information by i.e. decomposing the product, yet rendering a removal of DMAP impossible. HPLC-MS showed DMAP as major component. The other peak with a remarkable

peak area showed an isotope pattern in ESI(-), which could result from chlorine substitution. The mass of 179 g/mol could be assigned to a trichlorobenzene fragment. The mass of the desired cyclic product was found in ESI(+) but had no detectable peak area in the elugram. For that reason, the Mitsunobu-conditions were tried out (Scheme 15).



Scheme 15: Macrolactonization under Mitsunobu conditions.

It turned out that the major problem of this reaction was of technical origin, since the very slow addition of one reagent (within 24 h), dissolved in THF was hardly possible. In the first reaction, PPh_3 and **67** were dissolved in THF and excess DIAD, dissolved in THF was added. HPLC-MS of the reaction showed one peak with the mass of triphenylphosphineoxide (278 g/mol). When DIAD and PPh_3 were dissolved in THF and **67**, dissolved in THF was added slowly, HPLC-MS looked comparable.

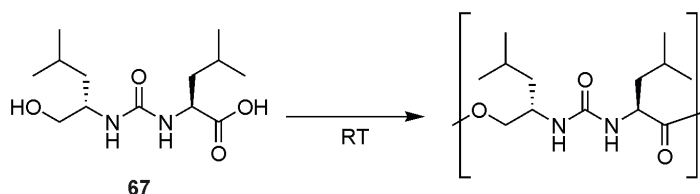
Summarizing the results of the ring closing reactions of **67**, it turned out that the eight membered ring could not be synthesized or isolated. It was not possible to synthesize the desired macrocycle by both pathways. This is in congruence with the difficulties concerning the synthesis of small cyclic peptoids and peptides described in literature.^[13-15]

4.1.5 Polymerization Of Linear Monomer

Since all attempts to synthesize a cyclic monomer for the ring opening polymerization failed, it was tried to polymerize **67** directly. The results of the polymerization experiments are summarized in Table 1. Best results are highlighted in yellow. All polymerizations were performed under non-dry conditions.

4 Linear (Ester-[*alt*]-urea)s

Table 1: Comparison of different polymerization conditions and different work-up procedures. Best results are highlighted in yellow.



Entry	solvent	Conc. [mol/L]	Coupling reagent ¹	Coupling catalyst ²	Time	work up ³	Mp [g/mol] ⁴	Mw [g/mol] ⁴	Mn [g/mol] ⁴
1	DMF	0.1	TBTU ⁵	HOBT	14 d	1	544	715	660
2	DMF	0.4	EDC ⁵	HOBT	4 d	1	730	851	822
3	DMF	0.4	EDC	HOBT	7 d	1	723	1130	809
4	DMF	0.4	EDC	HOBT	7 d	2	729	874	775
5	DMF	0.4	EDC	HOBT	14 d	1	692	856	756
6	DMF	0.4	EDC	HOBT	14 d	3	761 ⁷	875 ⁷	772 ⁷
7	CH ₂ Cl ₂	0.4	EDC ⁵	HOBT	4 d	1	723	820	790
8	CH ₂ Cl ₂	0.4	EDC	HOBT	7 d	1	434	869	654
9	CH ₂ Cl ₂	0.4	EDC	HOBT	7 d	2	724	923	758
10	CH ₂ Cl ₂	0.4	EDC	HOBT	14 d	1	735	828	717
11	CH ₂ Cl ₂	0.4	EDC	HOBT	14 d	2	744 ⁷	917 ⁷	753 ⁷
12	CH ₂ Cl ₂	0.4	EDC	HOBT	14 d	2, 3	745 ⁷	932 ⁷	787 ⁷
13	DMF	0.4	EDC ⁵	DMAP	4 d	1	1081	2650	1876
14	DMF	0.4	EDC	DMAP	7 d	1	1075	2418	1490
15	DMF	0.4	EDC	DMAP	7 d	2	1059	2175	1400
16	DMF	0.4	EDC	DMAP	11 d	3	1224	2697	1582
17	DMF	0.4	EDC	DMAP	14 d	1	1185 ⁷	2669 ⁷	1602 ⁷
18	DMF	0.4	EDC	DMAP	14 d	3	1334	3094	1634
19	CH ₂ Cl ₂	0.4	EDC ⁵	DMAP	4 d	1	1007	1231	1126
20	CH ₂ Cl ₂	0.4	EDC	DMAP	7 d	1	1031 ⁷	1313 ⁷	1207 ⁷
21	CH ₂ Cl ₂	0.4	EDC	DMAP	7 d	2	1084	1547	1148
22	CH ₂ Cl ₂	0.4	EDC	DMAP	14 d	1	842	1457	1163
23	CH ₂ Cl ₂	0.4	EDC	DMAP	14 d	3	1148	1792	1258
24	CH ₂ Cl ₂	0.3	EDC	DPTS ⁶	2 d	1	743	927	768
25	CH ₂ Cl ₂	0.3	EDC	DPTS ⁶	2 d	2	726 ⁷	1034 ⁷	834 ⁷
26	CH ₂ Cl ₂	0.3	EDC	DPTS ⁶	2 d	2, 3	726 ⁷	1001 ⁷	821 ⁷
27	DMF	3.0	EDC	DMAP	6 d	3	3496	2448	1520
28	DMF	2.0	EDC	DMAP:DPTS 1:1	6 d	3	2627	2289	1455
29	DMF	2.0	DIC	DMAP	6 d	3	3392	2576	1653
30	DMF	2.0	DIC	DPTS	6 d	3	500	1351	945

¹ 4 eq of coupling reagent were used; ² 1 eq of coupling catalyst was used; ³ work-up-procedures: 1: solvent evaporated; 2: aqueous work-up with acidic and basic washing; 3: precipitation in water; ⁴ detection by UV; ⁵ 2 eq of coupling reagent were used; ⁶ 0.2 eq of coupling catalyst was used; ⁷ GPC-analysis (in DMF at 70 °C, calibrated with polystyrene standards, detection by RI).

To give a short summary of the data, one can compare different factors, such as the concentration of the reaction solution, the employed coupling reagents, the solvent used and the work-up procedure applied. Starting with the concentration of the solution, one can easily see that the molecular weight of the resulting polymer (compare entries 1, 13, 24, 27, 28) increased with increasing concentration.

Concerning the coupling, one can see that DMAP or DPTS catalyzed the reaction much better than HOBT (compare entries 2, 13 and 7, 19). This result went in line with the experiences made in esterification reactions with HOBT (*vide infra*). The problem with DPTS was its poor solubility in such highly concentrated mixtures. For that reason, DMAP seemed to be the coupling catalyst of choice.

Discussing the coupling reagent in this reaction, EDC and DIC gave comparable results (entries 27 and 29), with a slight preference for DIC, which gave similar results at lower concentrations. But since the urea formed in the reaction with DIC was hardly separable from the product, EDC seemed to be the coupling reagent of choice. TBTU was excluded from this considerations, since its use was only meaningful in combination with HOBT.

The used solvent had less influence on the reaction as perhaps expected. CH₂Cl₂ and DMF afforded comparable results with a slight preference for DMF (compare entries 1-6 with 7-12 and 13-18 with 19-23). And since the precipitation in water only worked with DMF, it was the solvent of choice.

The work-up procedure applied to the polymer had no notable influence on the polymeric mixture and its distribution. No matter if the solvent was evaporated, if an aqueous work-up procedure was performed or if the polymer was precipitated in water, the results were comparable. GPC measurements with the evaporated solutions were troublesome due to the remaining coupling reagents, and since the aqueous work-up was the most complex and only worked with CH₂Cl₂ solutions, the precipitation in water was the work-up procedure of choice.

Summarizing the results, the best polymerization condition are a highly concentrated DMF solution, using an EDC/DMAP- (or DIC/DMAP-) coupling system with subsequent precipitation of the polymer in water.

Besides all, the resulting polymers were relatively short, with very broad polydispersities and the GPC traces had no ideal shape. Of course, the real molecular weight might be higher due to the necessary use of polystyrene standards for GPC calibration, however even if this is taken into consideration, molecular weights are low. Also important to mention is the possible racemization during the polymerizations (especially when using DMAP-based coupling catalysts). For more convenient and milder polymerizations, much more effort has to be spent into the optimization of the reaction. Instead of doing so, short oligomers with variable stereochemistry and variable amount of amide content were synthesized, in order to get access to discrete, well defined structures.

4.2 Linear Oligo(ester-[*alt*]-urea)s With Variable Stereochemistry And Isostere Incorporation

4.2.1 General Considerations

The variation of a peptide backbone is not only interesting for polymeric structures, but also for small oligomers. In comparison to polymers, oligomers are discrete molecules with a defined length. The exact elucidation of folding and aggregation behavior as function of chain length, stereochemistry and isostere incorporation is only possible when investigating discrete oligomers. Additionally, the synthesis can be much more versatile, leading to more diverse compounds. All these points encouraged us to synthesize oligomers with the structural diversity shown in Figure 4. In addition to stereochemistry, also the degree of isostere incorporation was systematically varied.

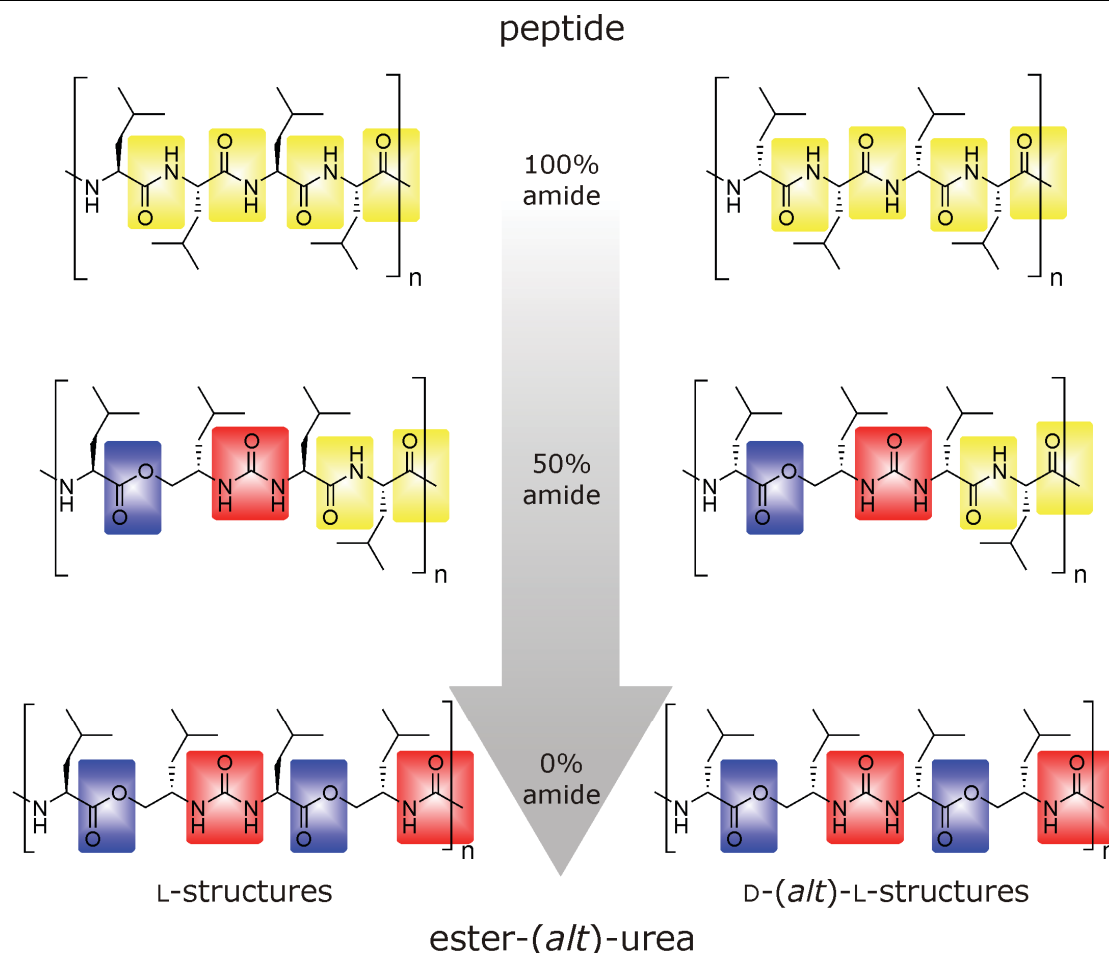


Figure 4: Two neighboring amide bonds in the peptide backbone (highlighted in yellow) are successively replaced by an ester-(*alt*)-urea moiety (ester highlighted in blue, urea highlighted in red).

Oligo-L- and oligo-D-(*alt*)-L-leucine is shown on top. The amide content in the peptide is 100%. In the middle, half of the peptide backbone's amide bonds has been replaced by an ester-(*alt*)-urea moiety, still allowing for variation of the stereochemistry, leading to L- and D-(*alt*)-L-structures. In the L- and D-(*alt*)-L-oligomers shown on the bottom, every amide bond has been replaced by ester-(*alt*)-urea moieties, leading to an amide content in the pseudopeptide of 0%. It is now very interesting to investigate the properties of these structures in dependence on the stereochemistry and on the degree of amide replacement. The backbone motif of the structures with 50% and 0% amide content is unique and to the best of our knowledge has not been reported so far.

4.2.2 Synthetic Considerations

The synthesis of these different series of compounds with variable stereochemistry requires a straightforward strategy, in order to minimize the synthetic effort. The pure peptides are readily accessible via a divergent/convergent synthesis. It would be desirable to identify a key building block in the structure of the two pseudopeptide backbones, which could be used in the synthesis of both. As illustrated in Figure 5, the common structural fragment in 50% and 0% amide containing pseudopeptides can be derived from the ureas **74** and **75**, which therefore serve as key building blocks in the synthesis of the corresponding oligopseudopeptides. Their synthesis has been described in 4.1.4.

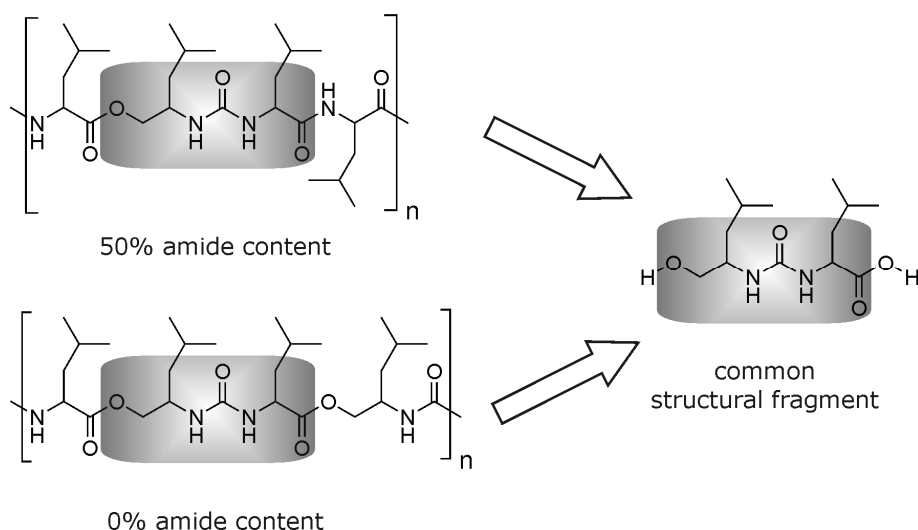
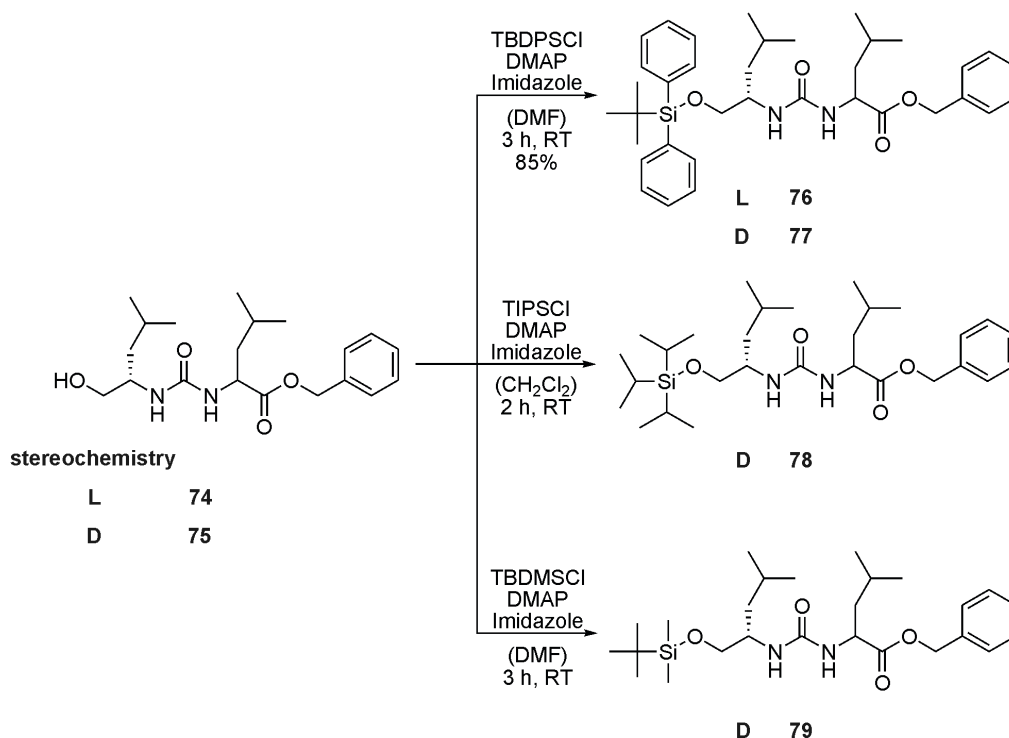


Figure 5: Identification of the key building block for pseudopeptide synthesis.

4.2.3 Synthesis Of 0% Amide Containing Pseudopeptide

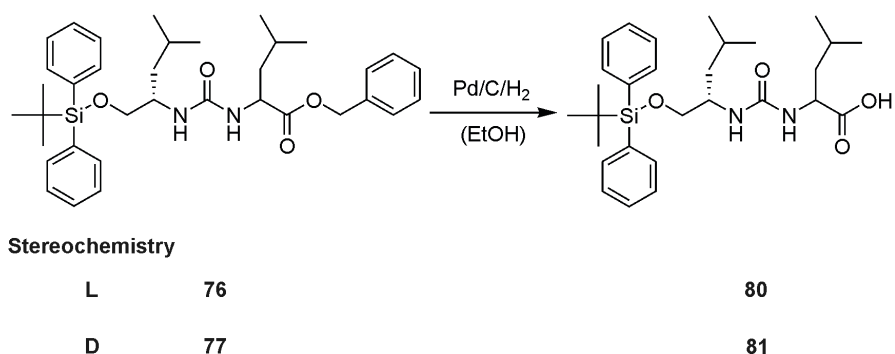
With the key building blocks **74** and **75**, the pseudopeptide with 0% amide content can be synthesized via divergent/convergent synthesis. One requirement for divergent/convergent synthesis is the protection of both reactive chain ends with orthogonal protecting groups, in order to prevent undesired polymerization. First, the alcohol functionality had to be protected with a suitable protecting group and a silyl protecting group was chosen since it can easily be cleaved with fluoride.



Scheme 16: Synthesis of different silyl-protected key building blocks.

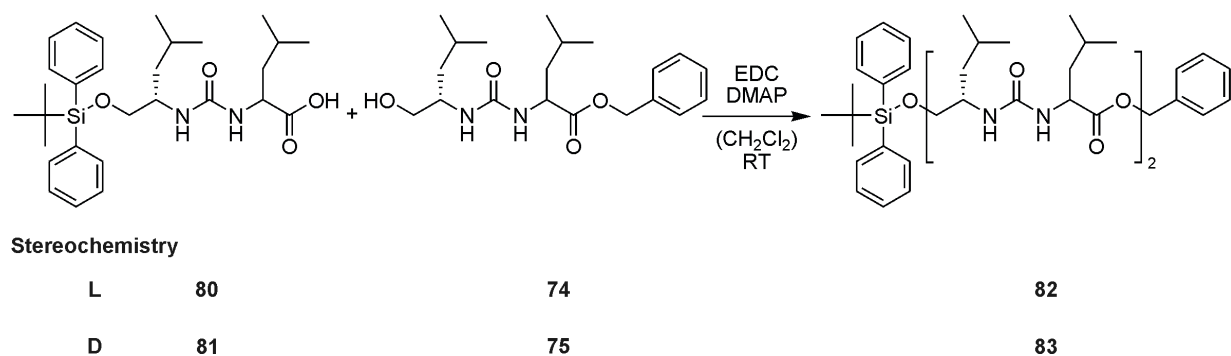
In a first attempt, urea **75** was reacted with triisopropylsilyl chloride in the presence of DMAP, to give the TIPS-protected compound **78**. The compound was stable under aqueous work-up conditions but decomposed on silica, so that urea **75** was obtained after column chromatography of the crude product. In a second attempt, **75** was protected using *tert*-butyldimethylsilyl chloride to give the protected urea **79**, which immediately started to decompose and could not be isolated. The protection of **74** and **75** using *tert*-butyldiphenylsilyl chloride gave the stable TBDPSCI protected ureas **76** and **77**, which could be isolated and purified, rendering it the protecting group of choice for further divergent/convergent synthesis.

4 Linear (Ester-[*alt*]-urea)s



Scheme 17: Benzyl deprotection of fully protected L,L- and L,D-urea.

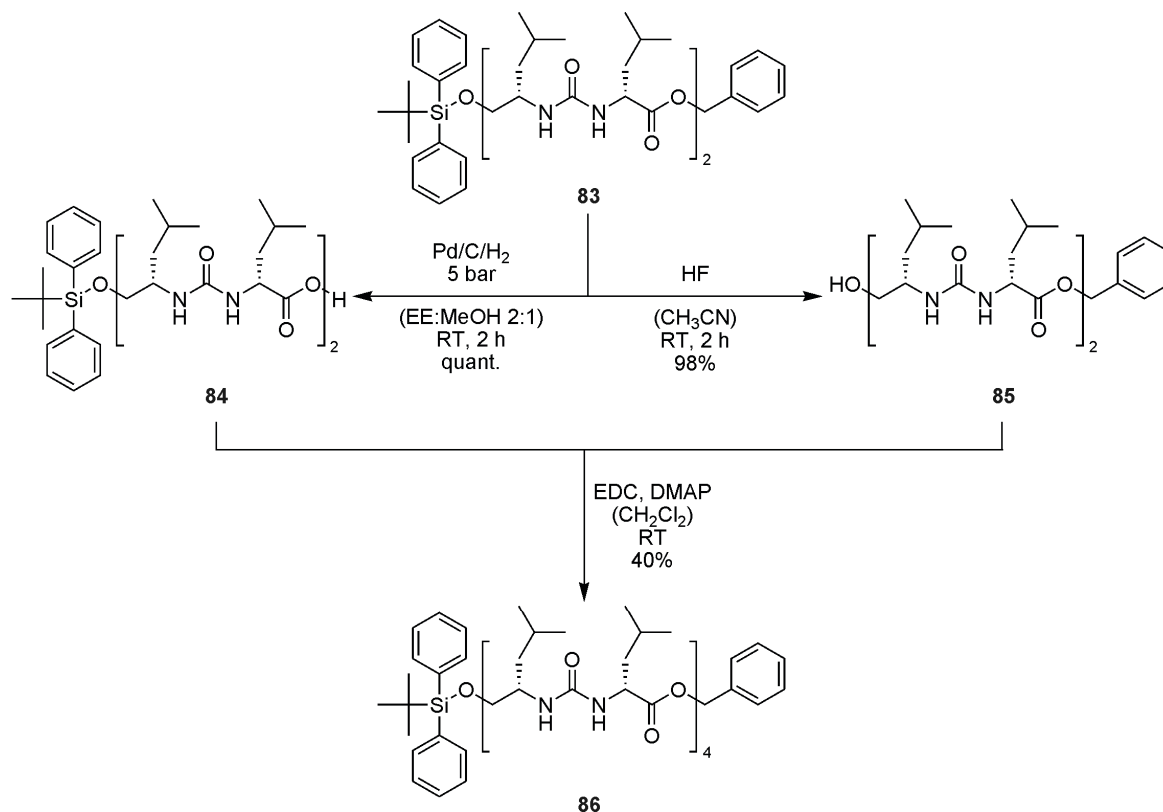
In the first reaction of the divergent/convergent synthesis, the benzyl protecting group at the C-terminus was cleaved under hydrogenolysis to give the TBDPS protected ureas **80** and **81** in moderate yields around 60% (Scheme 17). The crude product was used without further purification and immediately coupled with the corresponding urea **74** or **75** to give tetramers **82** and **83** (Scheme 18).



Scheme 18: Coupling to the tetramers **82** and **83**.

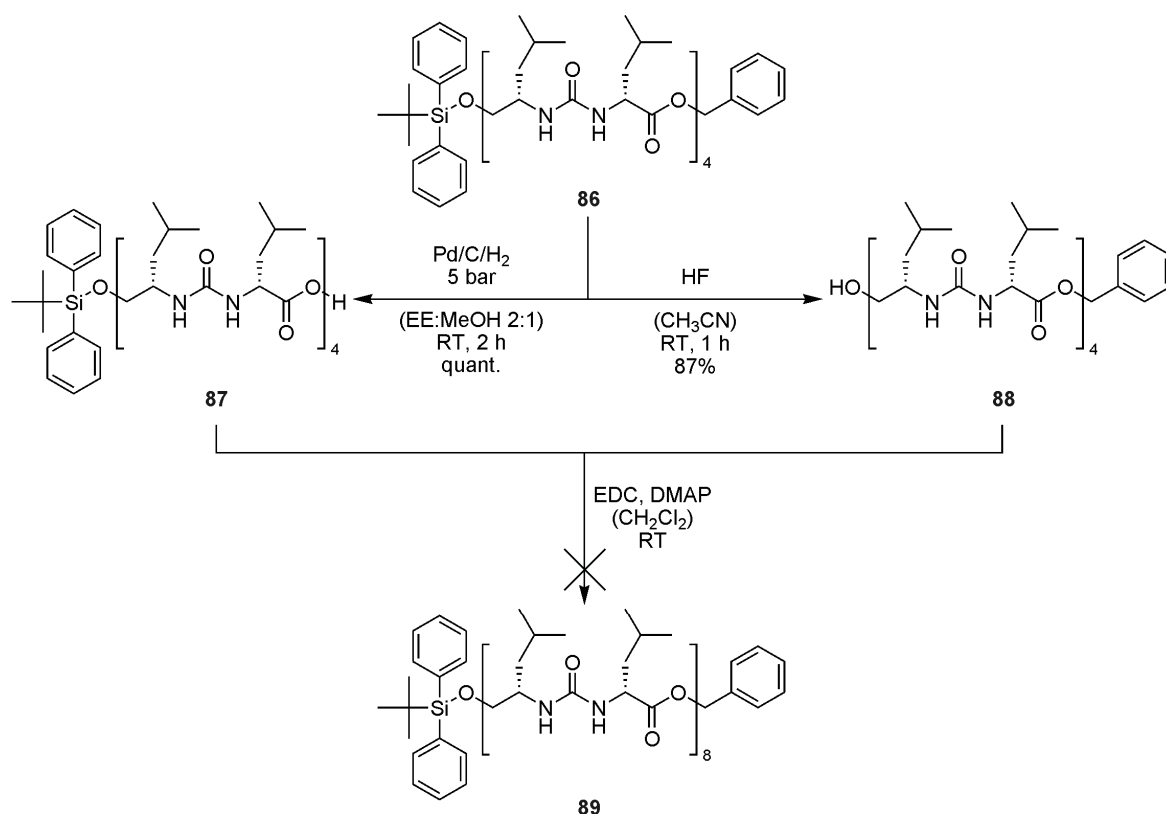
The reaction proceeded in moderate yields of around 50% after isolation by column chromatography. DMAP was used as coupling catalyst, since it turned out to be more potent than HOBT in esterification reactions (*vide infra*).

Further synthesis to higher oligomers was attempted with the L,D-urea **83** (Scheme 19). Both deprotection reactions proceeded smoothly and gave the partly deprotected ureas in quantitative yields. **85** had to be purified via column chromatography in order to remove nonpolar silyl impurities. The subsequent coupling gave the product **86** in poor yields after purification via column chromatography.



Scheme 19: Divergent/convergent synthesis to L,D-urea octamer **86**.

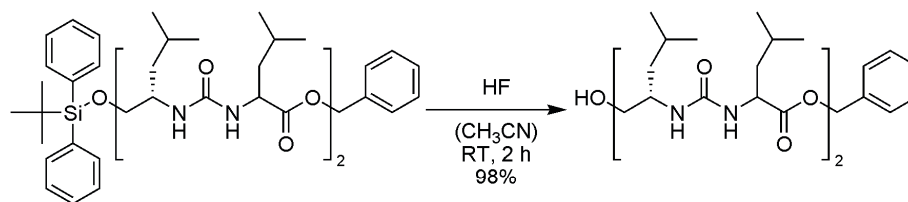
In order to check how far the synthesis can be driven, fully protected urea **86** was subjected to one further deprotection/coupling cycle (Scheme 20). Both deprotection reactions proceeded in very good yields around 90% and gave the resulting partly deprotected ureas **87** and **88**. The latter one had to be purified via column chromatography prior to the subsequent coupling. The coupling of both fragments to the L,D-urea hexadecamer led to a complex product mixture, which could not be purified.



Scheme 20: Attempted divergent/convergent synthesis to L,D-urea hexadecamer **89**.

In summary, it was possible to synthesize both urea tetramers **82** and **83** in moderate yields. Further synthesis to the octamers was in principle possible, but proceeded in poor yields. A further cycle in the divergent/convergent synthesis did not afford the desired hexadecamer. Therefore synthesis of longer oligomers than the tetramer was not performed with both stereoisomers.

For further investigations of the tetramers, the TBDPS-protecting group was removed (Scheme 21). Both deprotections proceeded smoothly using HF in acetonitrile and gave the desired deprotected ureas **90** and **85** in high yields after column chromatography.



Stereochemistry

L 82

90

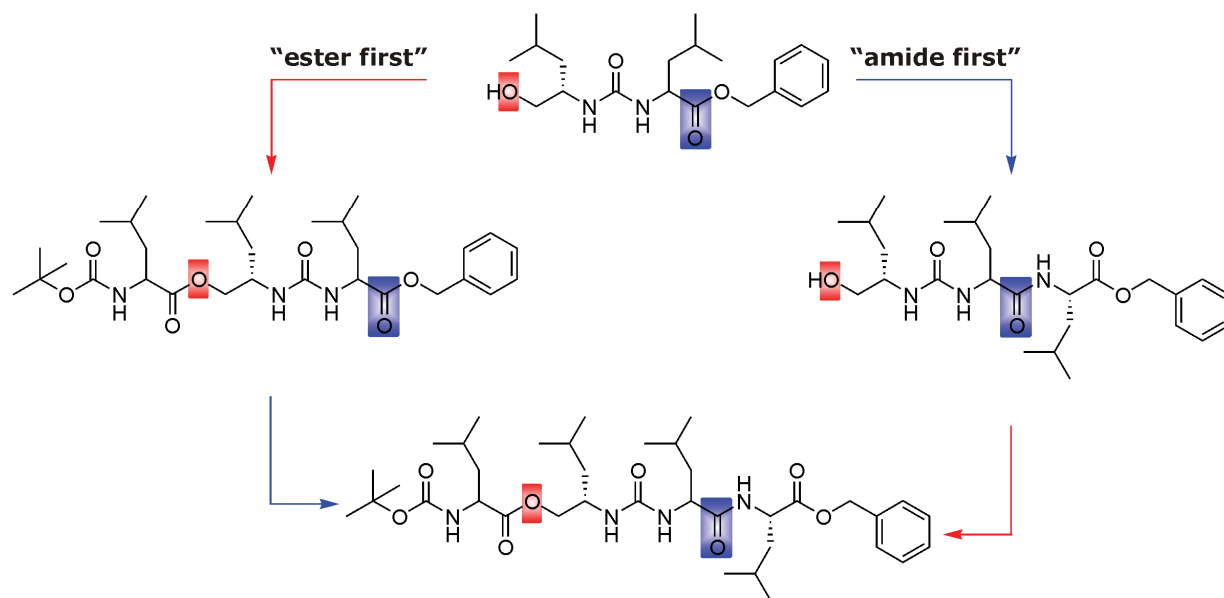
D 83

85

Scheme 21: TBDPS-deprotection of L,L- and L,D-ureas **82** and **83**.

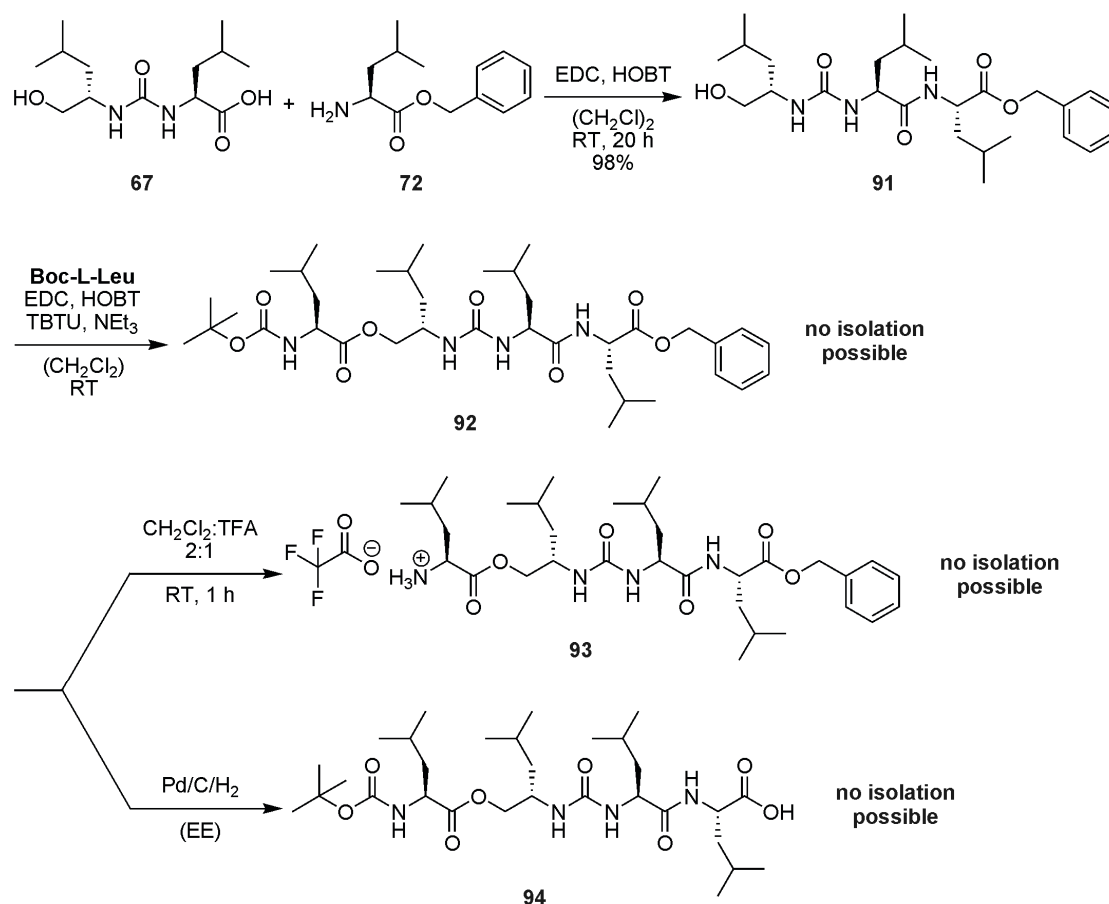
4.2.4 Synthesis Of 50% Amide Containing Pseudopeptides

Starting the synthesis from the building blocks **74** and **75**, the target structure for the 50% amide containing pseudopeptides can be reached via two pathways. The building blocks can in general be extended in both directions (Figure 6). On the one hand, the first extension can take place at the alcohol so that the ester bond is made first, and the amide last. On the other hand, the amide bond can be made first and the ester last. It turns out that the extension direction strongly influences the feasibility of the synthesis.

**Figure 6:** Extension pathways of the key building block. Ester bond formation reactions indicated with red arrows, amide bond formation indicated with blue arrows.

In a first attempt, the “amide first” pathway was followed to reach the target structure. The synthetic route was explored exclusively with the L,L-isomer and

starts with the totally deprotected urea **67**, which was coupled with the benzyl protected leucine **72** to the trimer **91** (Scheme 22). In the reaction, there was no need for an alcohol protecting group, since the much more nucleophilic amino group was expected to react prior to the alcohol function. This reaction proceeded in 98% yield and gave the product after precipitation in PE and short chromatography in very high purity (>99% according to HPLC). However, the subsequent esterification with Boc-L-Leu was troublesome. TLC monitoring during the reaction showed incomplete conversion of **91**, even after the addition of more coupling reagents and amino acid. Bearing in mind that TBTU once solved the issue of incomplete conversion in an esterification, TBTU/ NEt_3 was added instead of EDC. The use of a large excess of coupling reagents led to higher conversion of the starting material. After work-up, the product could not be precipitated, so the purification had to proceed via column chromatography. The isolated product fractions consisted of two spots in TLC and three peaks in HPLC, which could not be separated. For that reason, the impure tetramer **92** was deprotected at the C-terminus and at the N-terminus separately to check if the more polar substances **93** and **94** could be purified via column chromatography or precipitation. This was not the case, so that the “amide first” pathway turned out not to be feasible for the extension of the building block.

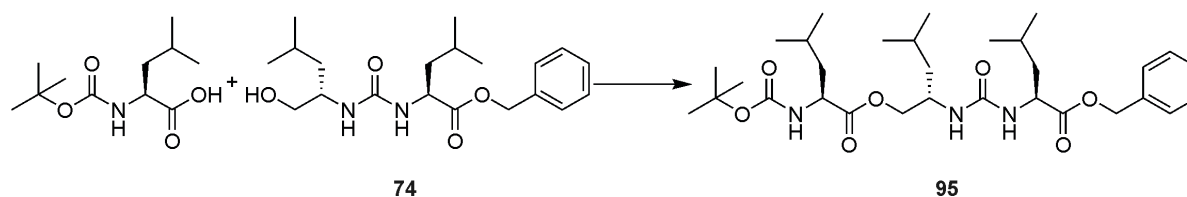


Scheme 22: Attempts to extend the building block by the “amide first” pathway.

The alternative “ester first” approach starts with the formation of the ester bond. Since first attempts suffered from poor yields and impure product, which could not be purified, the reaction was screened extensively in order to elaborate the best coupling conditions and work-up procedures. The esterification was optimized with the L,L-isomer **74** and Boc-L-leucine. The results of this screening are summarized in Table 2. The esterification reaction was performed in CH_2Cl_2 using different coupling reagents, different coupling catalysts, and different work-up procedures.

4 Linear (Ester-[*alt*]-urea)s

Table 2: Screening different reaction conditions and work-up procedures for the esterification of **74** with Boc-L-leucine.



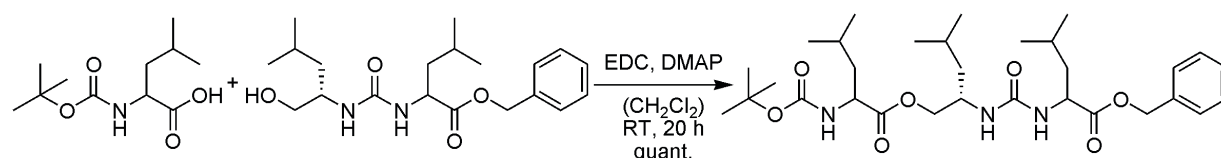
Entry	Coupling reagent	Coupling catalyst	Temperature	work-up	Conversion	Product isolation
1	TBTU	HOBT	RT	aqueous ²	incomplete ⁴	not possible ⁴
2	EDC	HOBT	80-100 °C ¹	-	incomplete ⁴	not possible ⁴
3	EDC	DMAP	RT	aqueous ²	complete ⁴	89% pure ⁵
4	EDC	DPTS	RT	silica ³	complete ⁴	possible ⁴
5	DIC	DMAP	RT	silica ³	complete ⁴	possible ⁴
6	DIC	DPTS	RT	silica ³	complete ⁴	>99% ⁵
7	CDI	-	RT	-	incomplete ⁴	possible ⁴
8	EDC	DMAP	RT	silica ³	complete ⁴	>99% ⁵

¹ Microwave assisted (for details see experimental part); ² including acidic and basic washing; ³ reaction mixture was quenched by addition of and stirring over silica gel. Filtration or drying and adding silica to a column gave the product; ⁴ according to TLC; ⁵ according to HPLC-MS.

Using TBTU/HOBT at room temperature combined with an aqueous work-up did not convert all **74** into the product **95**, which could not be isolated from the resulting mixture, since precipitation was not possible and TLC indicated a separation problem for column chromatography (entry 1). In the next attempt, EDC/HOBT was used under microwave assistance. This procedure gave no complete conversion, but decomposition and a very complex mixture, which was not worked up (entry 2). Entries 3 to 8 were carried out on a small 11 mg scale. It turned out that best results were obtained using DMAP or DPTS as coupling catalysts in combination with a "silica work-up" (entries 4, 5, 6, 8). Therefore, silica gel was added to the reaction mixture when **74** was consumed, and the suspension was stirred for 1 day. Following the optimized procedure (entries 6, 8), the suspension was evaporated, the dry silica was given on a packed column (eluent: Et₂O) and the pure product was eluted from the column. In entry 3, the TLC prior to the aqueous work-up looked better than after, so that the product could just be isolated in 89% purity.

For that reason, the reaction was repeated under similar conditions but with “silica-work-up” and gave absolutely satisfying results. Concerning the coupling reagent, there was no remarkable difference detectable using EDC or DIC, but for reasons of separation from the formed urea (especially when the reaction was scaled up), EDC was still the preferred coupling reagent. The coupling with CDI did also yield the product **95**, but no complete consumption of **74** could be observed and TLC showed a complex mixture, which was not worked up.

Summarizing the results from this screening, it is important to point out the role of the coupling catalysts in this esterification. HOBt, which is one of the coupling catalysts of choice for peptide bond formation, because of its high reactivity and its low degree of peptide epimerization, was by far not the best coupling catalyst for these esterifications. It turned out that DMAP and DPTS gave much better results, quite independently from the coupling reagent. Furthermore, the typically performed aqueous work-up procedure in this reaction was not the method of choice, and could be replaced by an alternative method involving stirring the mixture over silica gel followed by chromatography. With these results, the esterification could be transferred to preparative scales and both isomers (Scheme 23). The reaction could be performed on gram scales and afforded the resulting products **95** and **96** in quantitative yields and in high purity, when the elaborated procedures were applied.



Stereochemistry

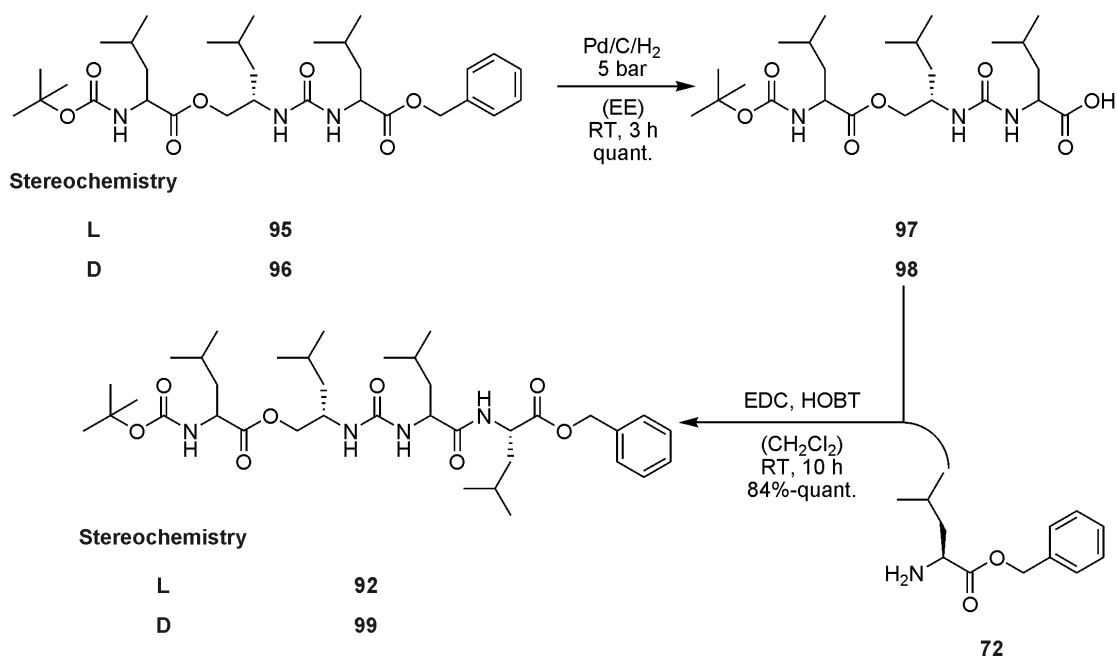
L	74	95
D	75	96

Scheme 23: Coupling of key building blocks **74** and **75** to the extended ureas **95** and **96**.

In the next step, the trimers **95** and **96** were deprotected at the C-terminus via hydrogenolysis (Scheme 24). The reaction proceeded smoothly and gave the desired products **97** and **98** in quantitative yields after purification via column chromatography on silica. Subsequent coupling with C-protected leucine **72**

4 Linear (Ester-[*alt*]-urea)s

gave the *all*-L- and L-(*alt*)-D-ester-(*alt*)-urea-tetramers **92** and **99** in high yields and purities.

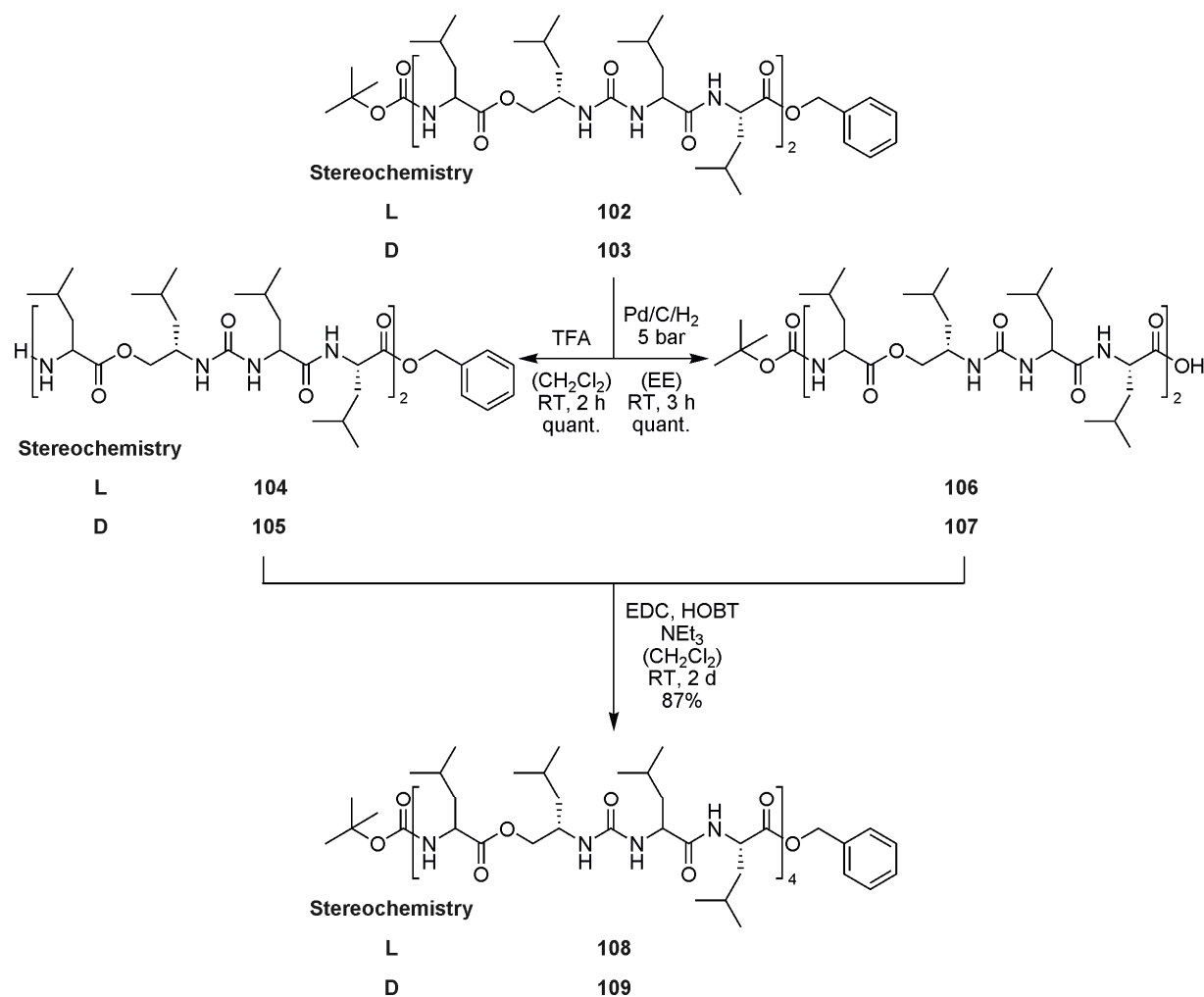


Scheme 24: Extension to protected L-(*alt*)-D- and *all*-L-ester-(*alt*)-urea-tetramer.

The tetramers **92** and **99** include the repeat unit of the 50% amide containing structures, protected with two orthogonal protecting groups, rendering the elongation of the tetramers via a divergent/convergent synthesis possible (Scheme 25).

Both deprotections proceeded smoothly and gave the resulting L-(*alt*)-D- and *all*-L-ester-(*alt*)-urea-tetramers **93**, **94**, **100**, and **101** in quantitative yields and high purity. The subsequent coupling of the fragments with EDC and HOBT gave the desired octamers **102** and **103** in high yields and purity after precipitation and column chromatography. The octamers were now subjected to another split/pool-synthesis cycle to yield the hexadecamers (Scheme 26).

4 Linear (Ester-[*alt*]-urea)s

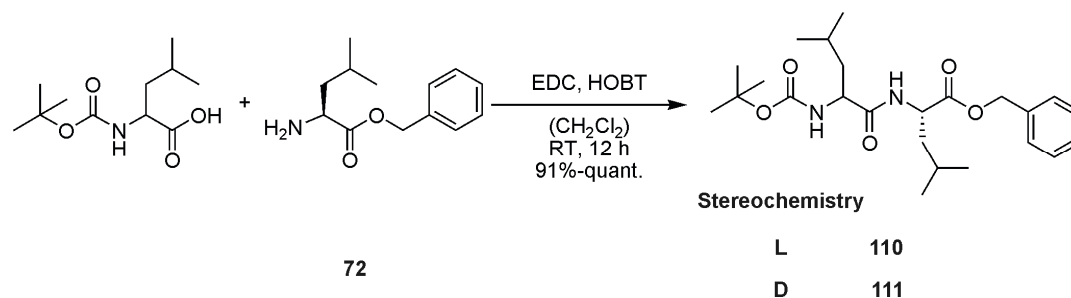


Scheme 26: Divergent/convergent synthesis to L-(*alt*)-D- and *all*-L-ester-(*alt*)-urea-hexadecamers **108** and **109**.

The cleavage of the benzyl ester proceeded smoothly to the octamers **106** and **107**. The Boc cleavage in methylene chloride also gave the desired product. In order to couple both fragments, excess triethylamine had to be added to neutralize the solution as some residual TFA remained. By this route both hexadecamers could be isolated in good yields.

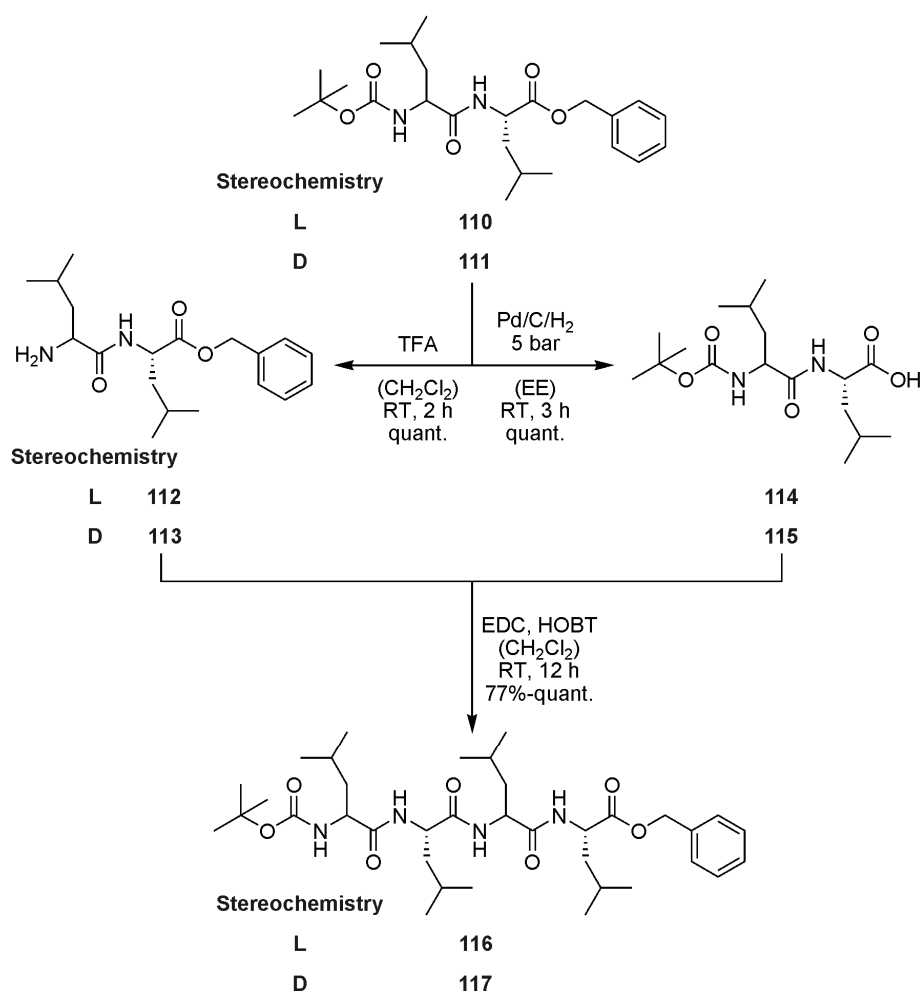
4.2.5 Synthesis Of The Peptide

To complete the series of pseudopeptides and peptides with varying stereochemistry and degree of isostere incorporation, D-(*alt*)-L- and *all*-L-leucine oligomers were synthesized. Encouraged by the experiences in the synthesis of D-(*alt*)-L-lysine octapeptide, the divergent/convergent synthesis in solution was chosen for the synthesis of leucine oligopeptides.



Scheme 27: Synthesis of Boc-L-Leu-L-Leu-Bn (**110**) and Boc-D-Leu-L-Leu-Bn (**111**).

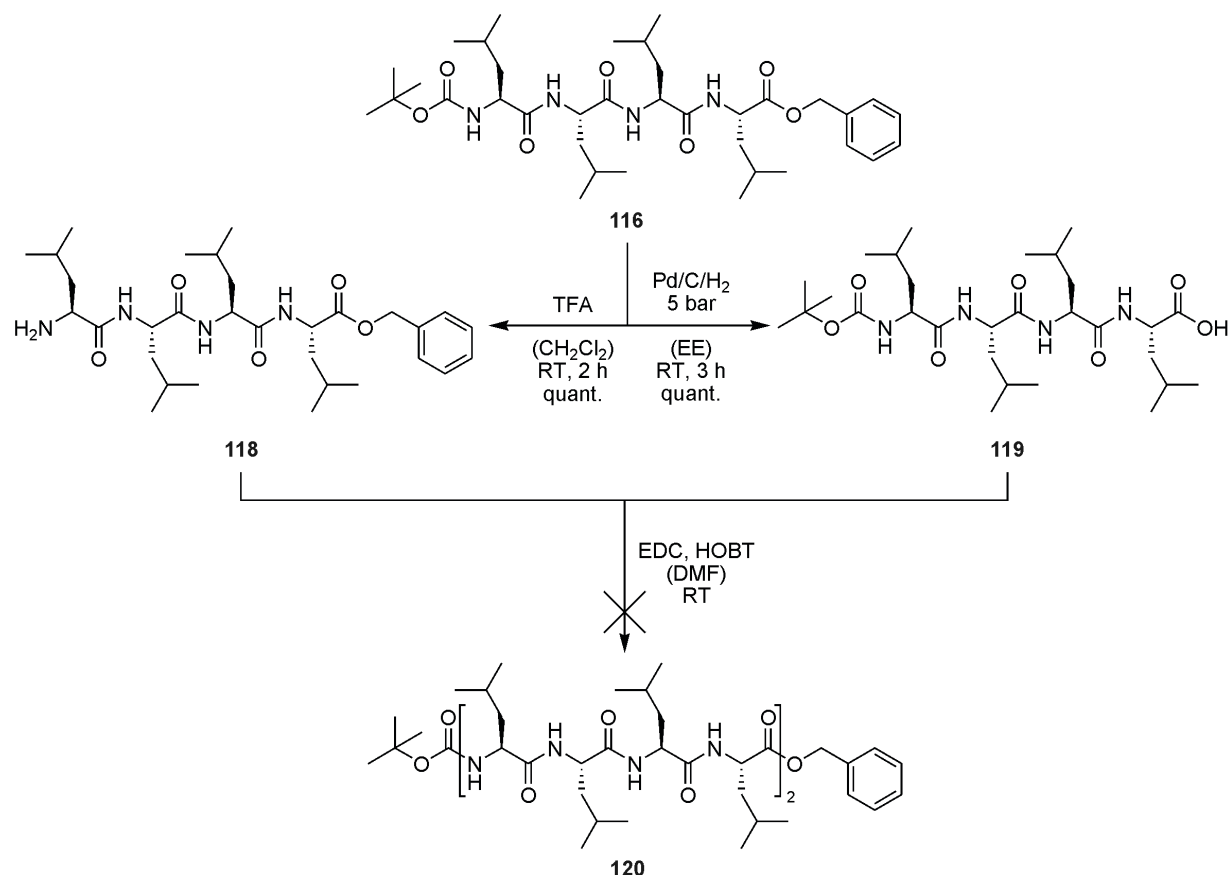
In the first reaction of the synthesis, L-Leu-Bn **72** was coupled with Boc-L-Leu or Boc-D-Leu to give the dipeptides Boc-L-Leu-L-Leu-Bn (**110**) and Boc-D-Leu-L-Leu-Bn (**111**) in high yields and purity after column chromatography. The protected dipeptides were then selectively deprotected and coupled to the tetrapeptides (Scheme 28).



Scheme 28: Divergent/convergent synthesis to Boc-L- and Boc-D-(*alt*)-L-Leu-Bn tetrapeptides **116** and **117**.

4 Linear (Ester-[*alt*]-urea)s

The deprotection reactions gave the desired dipeptides in quantitative yields. Subsequent coupling to the tetrapeptides proceeded smoothly and gave the resulting peptides in good to quantitative yields and high purities. Further growth of the peptide chain was first explored with the L-isomer **116** (Scheme 29).



Scheme 29: Divergent/convergent synthesis attempt of Boc-L-Leu-Bn octapeptide.

Both deprotections yielded the desired peptides (L-Leu)₄-Bn (**118**) and Boc-(L-Leu)₄ (**119**) in quantitative yields. Since both fragments were insoluble in methylene chloride, the solvent for the coupling reaction had to be changed to DMF. TLC monitoring of the reaction was not possible due to the use of DMF. Aqueous work-up was tedious, due to extensive emulsion formation. The resulting crude product was fractionated by column chromatography. Since the product fractions were hardly soluble, their handling was unpleasant. No pure fraction could be isolated and in no fraction, the product mass could be detected by ESI-MS. For these reasons, no further growth of the peptide chain was

attempted. Final products of the synthesis are the peptides Boc-(L-Leu-L-Leu)₂-Bn and Boc-(D-Leu-L-Leu)₂-Bn.

4.2.6 Aggregation Studies

All compounds synthesized are small, leucine based oligomers, differing in the stereochemistry of the neighboring units and in the connectivity of the building blocks. Compounds **116** and **117** are leucine tetrapeptides with *all*-L- and D-(*alt*)-L-stereochemistry. In compounds **92** and **99**, 50% of the amide bonds are replaced by an ester-(*alt*)-urea moiety, resulting in a unique backbone structure that has not been reported so far. In these compounds, the stereochemistry varies from *all*-L- to D-(*alt*)-L. In compounds **90** and **85**, every amide bond was replaced by an ester-(*alt*)-urea moiety, resulting in a unique backbone structure that has not been reported so far either. The stereochemistry in the backbone was varied as in the other compounds. The replacement of amide bonds by ester-(*alt*)-urea moieties was expected to significantly change the hydrogen bonding pattern in the compound. Since the oligomers are expected to be too short for intramolecular secondary structure formation, the aim of these studies was the investigation of their aggregation. The eminent differences of these compounds, regarding stereochemistry and connectivity were expected to display a significant change in aggregation behavior.

4.2.6.1 NMR Studies

Proton NMR spectroscopy is a versatile tool for aggregation studies of small oligomers, since the protons involved in hydrogen bonding interactions are expected to display a detectable downfield shift in the spectrum. Aggregation as such is a concentration dependent process.^[16-19] Once, every relevant proton in the spectrum has correctly been attributed to the corresponding signal, aggregation can be monitored as function of the concentration dependent downfield shift of the amide or urea protons.

The choice of the solvent for these studies was crucial for several reasons. The protons involved in aggregation processes were all exchanging protons. This fact excluded all protic solvents such as water or alcohols, since they would have undergone fast proton exchange, vanishing all relevant signals. The solvent had to dissolve all six compounds. This further eliminated acetonitrile

4 Linear (Ester-[*alt*]-urea)s

and all apolar solvents, such as hexane or toluene. On the other hand, the solvation of the compounds in the solvent should not disfavor the aggregation process. This excluded strong solvating solvents, such as DMF or DMSO. All these restrictions limited the number of possible solvents to only a few. One possible solvent is CDCl_3 , however, due to its potential decomposition, liberating HCl, CDCl_3 is not suitable as the aggregation process is also pH-dependent. For this reason, CD_2Cl_2 was chosen as the solvent for the aggregation studies. Major drawbacks of CD_2Cl_2 are its low boiling point, excluding experiments at temperatures higher than 25 °C.

All compounds were measured at concentrations of 7.5, 15, 30, 60 and 120 mmol/L. The assignment of all signals was achieved via COSY and NOESY measurements at a concentration of 7.5 mmol/L, where no significant aggregation was expected to occur.

The dilution series of the *all*-L-tetrapeptide **116** is shown in Figure 7.

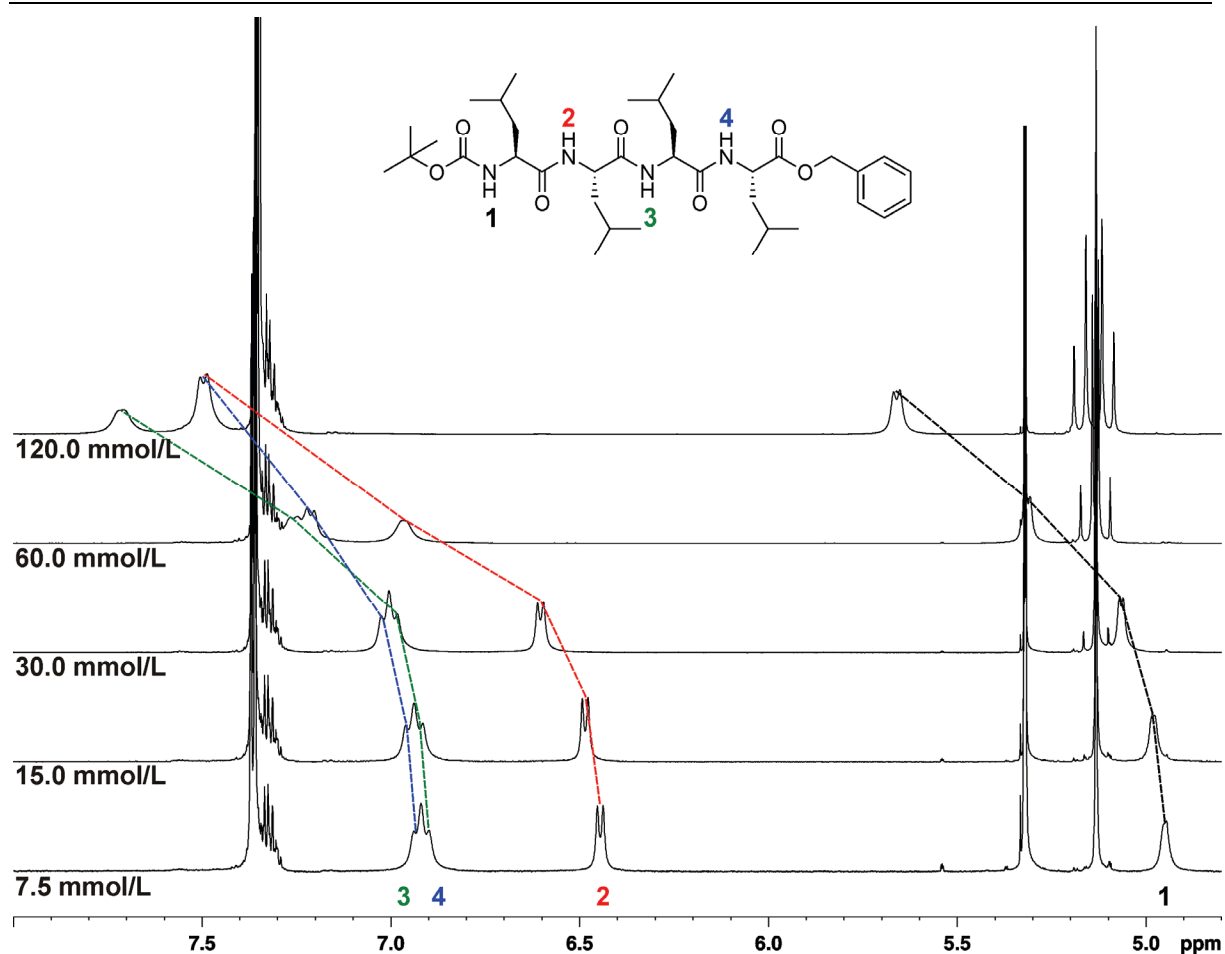


Figure 7: ^1H NMR dilution series of the *all*-L-tetrapeptide **116** (CD_2Cl_2 , 25 $^\circ\text{C}$).

The four protons of interest were numbered from *N*- to *C*-terminus. Proton #1 is the *N*-terminal, Boc protected carbamate proton, which is expected to appear at highest field in the spectrum. The resonance appears at 4.95 ppm as a broad singlet. Proton #2 is attributed to the sharp doublet appearing at 6.45 ppm. The resonances of protons #3 and #4 are overlapping and display a signal with a broad triplet shape at 6.92 ppm. Doubling the concentration to 15.0 mmol/L leads to a slight downfield shift of the signals. Proton #1 is shifted by 0.03 ppm (all shifts are calculated to the signal at lowest concentration), displaying a very small change of the signal shape from a broad singlet to a broad and structureless doublet. Proton #2 is shifted by 0.04 ppm, protons #3 and #4 by 0.02 ppm. Doubling the concentration to 30.0 mmol/L leads to a further downfield shift of the signals. Proton #1 is shifted by 0.12 ppm, proton #2 by 0.15 ppm and protons #3 and #4 by 0.09 ppm. The resolution of proton #1 is increasing, displaying a doublet, whereas the resolution of proton #2 is

decreasing. Further doubling of the concentration to 60.0 mmol/L results in a notable change of the spectrum. Proton #1 is shifted by 0.36 ppm under increasing resolution of the signal shape. Proton #2 is shifted by 0.52 ppm, under a significant decrease of resolution. The former doublet is transformed into a very broad singlet. Proton #3 is shifted by 0.34 ppm, proton #4 by 0.29 ppm. This different downfield shift leads to a visible separation of both signals into two broad doublets. Doubling the concentration to 120.0 mmol/L leads to a further downfield shift of all signals. Under increasing resolution of the signal, proton #1 is shifted by 0.71 ppm. Proton #2 is shifted by 1.05 ppm. The resonance of proton #2 is overlapping with the one of proton #4, which is shifted by 0.58 ppm to give a signal with the shape of a broad doublet. Proton #3 is shifted by 0.79 ppm and displays a resonance with the shape of a broad doublet. Very interesting is the significant change of the signal at 5.16 ppm, which is assigned to the benzyl protons of the C-terminal benzyl ester. With increasing concentration, the singlet splits into a doublet of a doublet with increasing coupling constants.

The D-(*alt*)-L-tetrapeptide **117** was subjected to an identical dilution experiment (Figure 8). Proton #1 is assigned to the resonance at highest field (5.03 ppm), which has the shape of a broad doublet. Proton #2 is assigned to the broad doublet at 6.53 ppm, proton #3 to the broad doublet at 6.68 ppm, proton #4 to the sharp doublet at 6.90 ppm. In contrast to compound **116**, the protons #3 and #4 in compound **117** are well separated. Increasing the concentration by a factor of 16 to 120 mmol shifts protons #1 and #4 by 0.23 ppm, proton #2 by 0.26 ppm and proton #3 by 0.25 ppm. The signals at this concentration display the shape of a broad doublet. Interestingly, the benzyl protons of the C-terminal benzyl ester display a doublet of a doublet even at the lowest concentration, which remains unchanged with increasing concentration.

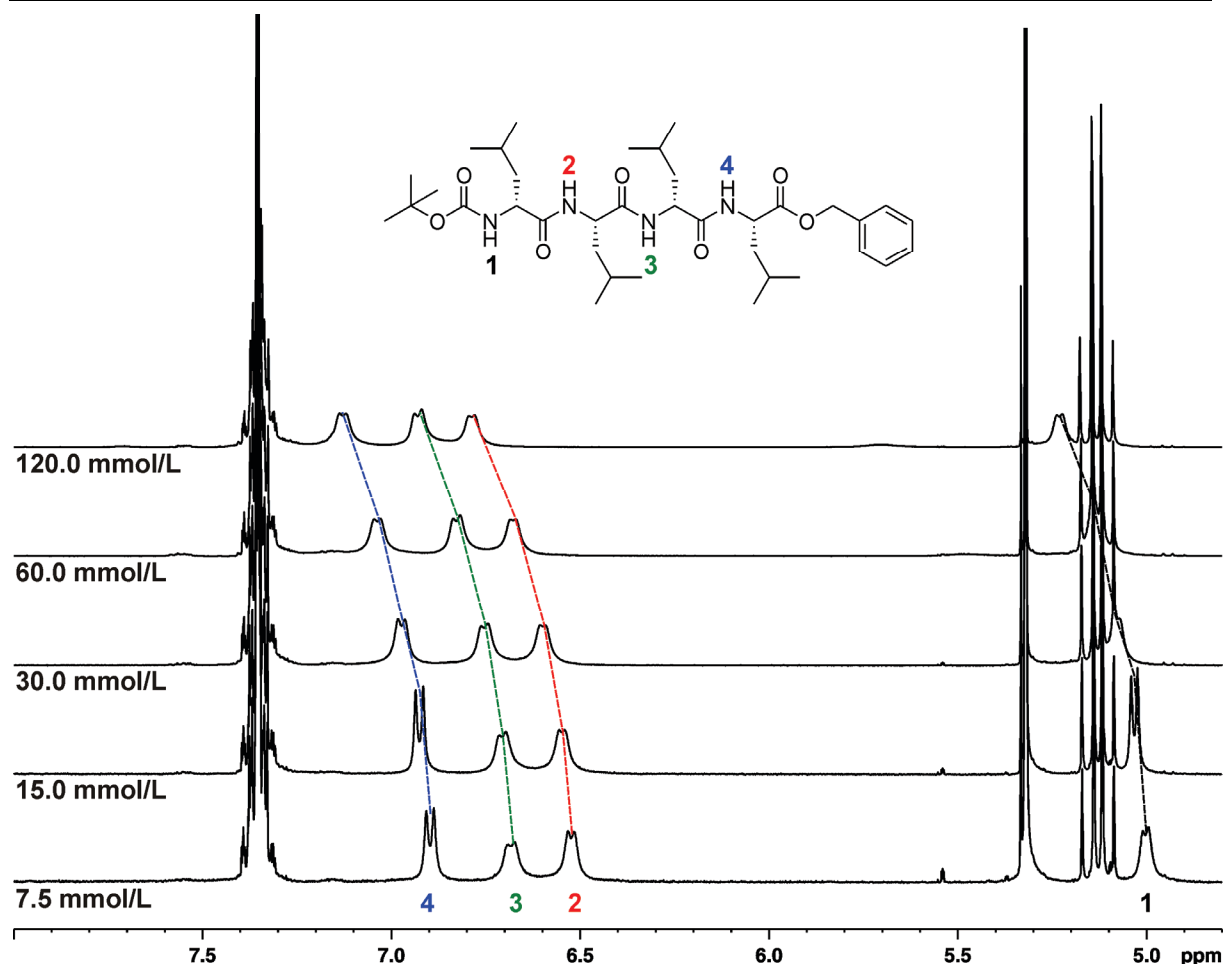


Figure 8: ^1H NMR dilution series of the D-(*alt*)-L-tetrapeptide **117** (CD_2Cl_2 , 25 $^\circ\text{C}$).

To analyze data from NMR experiments, the different proton shifts were plotted against sample concentration. The resulting graphs for **116** and **117** are shown in Figure 9. In compound **116**, proton #2 displays the most significant downfield shift. The least shifted proton is proton #4. With regard to aggregation, proton #2 is probably most involved into intermolecular hydrogen bonding. In compound **117**, all protons display a similar downfield shift. The proton shifts of **116** are by a factor 3 to 4 more intense than the shifts of **117**. With regard to aggregation, the downfield shifts indicate a much stronger, intermolecular hydrogen bonding interaction in **116** than in **117**.

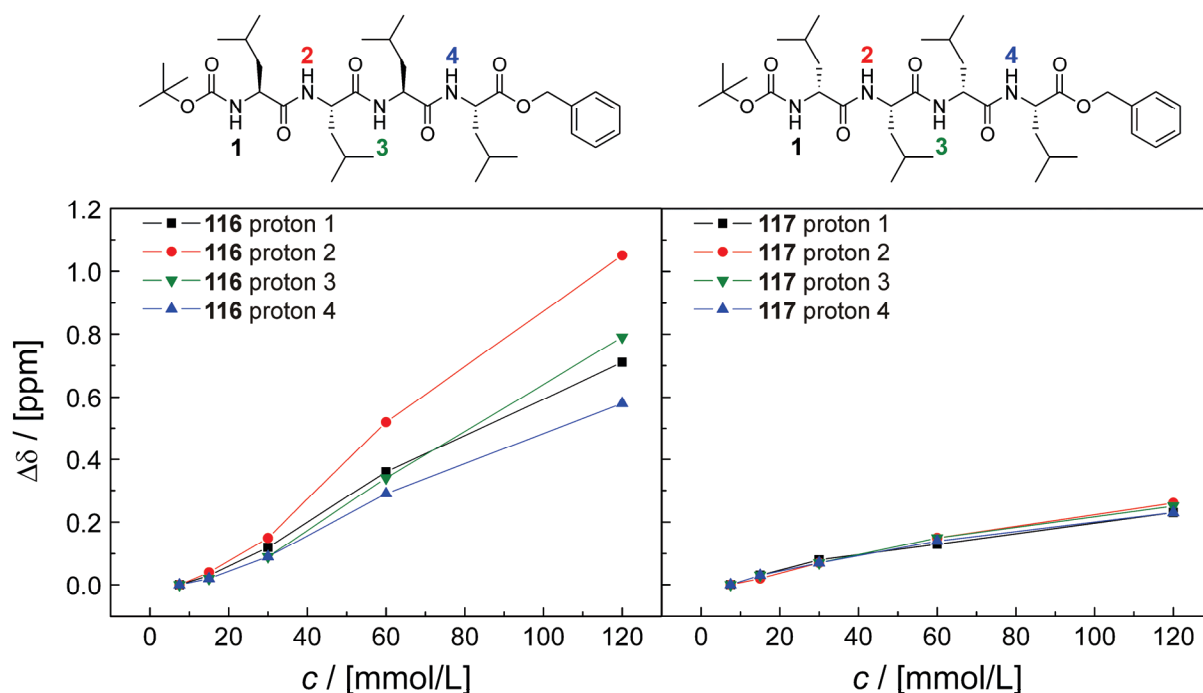


Figure 9: Proton resonance shifts plotted against sample concentration for peptides **116** and **117** (CD_2Cl_2 , 25 °C).

Since the only structural difference between **116** and **117** is the stereochemistry of the backbone $\text{C}\alpha$'s, the weaker aggregation of **117** is attributed to sterical hindrance of the side chains during the aggregation process. This is in line with β -sheet type aggregation, where in **116** side chains could be placed on opposite faces of the sheet, while in **117** the residues would be forced onto the same side, causing steric repulsion and hence destabilization of the aggregate.

The dilution series of the 50% amide containing pseudopeptide **92** is shown in Figure 10. The four protons of interest were numbered from *N*- to *C*-terminus. Proton #1 is the *N*-terminal Boc protected carbamate proton, which is expected to display a similar chemical shift than in compounds **116** or **117**. The resonance of proton #1 appears at 5.07 ppm as a sharp doublet. Protons #2 and #3 are located in the urea group and are attributed to the broad, structureless multiplet at 4.88 ppm. Proton #4 is located at the *C*-terminal amide and is attributed to the sharp doublet at 6.74 ppm. Doubling the concentration of the sample to 15.0 mmol/L leads to no detectable downfield shift of the protons. Increasing the concentration to 30.0 mmol/L shifts proton

#1 by 0.03 ppm, proton #2 by 0.07 ppm, proton #3 by 0.17 ppm, and proton #4 by 0.08 ppm. The different downfield shifts of protons #2 and #3 leads to a separation of the broad, structureless multiplet into two doublets. Doubling of the concentration to 60.0 mmol/L further shifts the protons. Proton #1 was shifted by 0.08 ppm, proton #2 by 0.19 ppm, proton #3 by 0.38 ppm and proton #4 by 0.2 ppm. Increasing the concentration to 120.0 mmol/L shifts proton #1 by 0.13 ppm, proton #2 by 0.32 ppm, proton #3 by 0.61 ppm and proton #4 by 0.36 ppm. Even at the highest concentration, the resonances of protons #3 and #4 are sharp doublets. The signals of protons one and two are overlapping with each other and with the benzylic protons of the C-terminal protecting group.

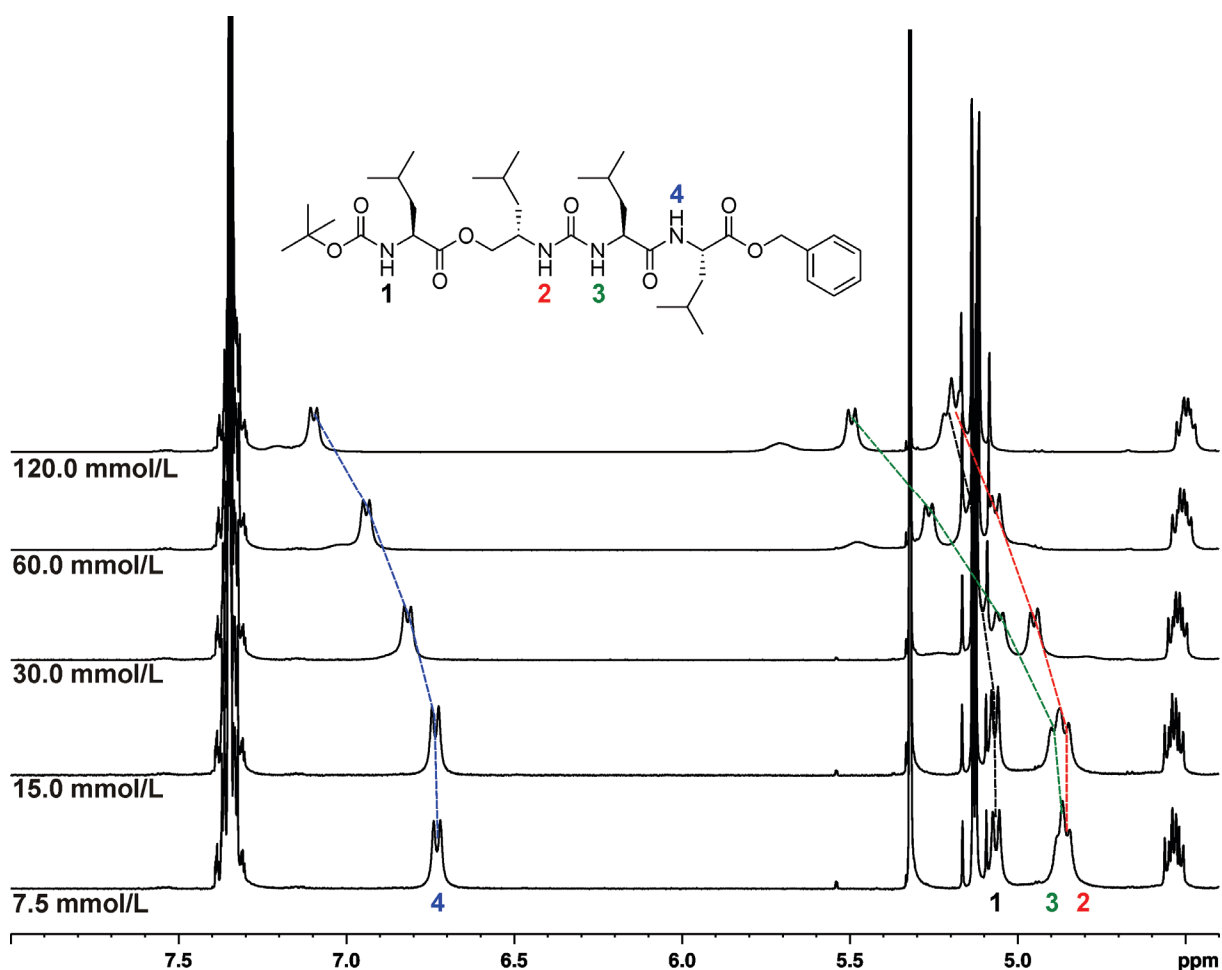


Figure 10: ^1H NMR dilution series of the *all*-L-configured, 50% amide containing pseudotetrapeptide **92** (CD_2Cl_2 , 25 °C).

4 Linear (Ester-[*alt*]-urea)s

The proton NMR spectra of the dilution series of pseudotetrapeptide **99** are shown in Figure 11. Proton #1 is attributed to the poorly resolved doublet at 5.04 ppm. The urea proton #2 is assigned to the well resolved doublet at highest field (4.81 ppm), urea proton #3 to the well resolved doublet at 4.90 ppm. In contrast to compound **92**, the resonances of urea protons are separated. Proton #4 is attributed to the poorly resolved doublet at 7.15 ppm. Increasing the concentration by a factor of 16 to the highest measured concentration shifts proton #1 by 0.12 ppm, proton #2 by 0.16 ppm, proton #3 by 0.26 ppm, and proton #4 by 0.11 ppm. The shape of the signals does not change notably. At the highest concentration, the resonances of protons #1 and #3 are overlapping with each other and with the benzylic protons of the C-terminal protecting group.

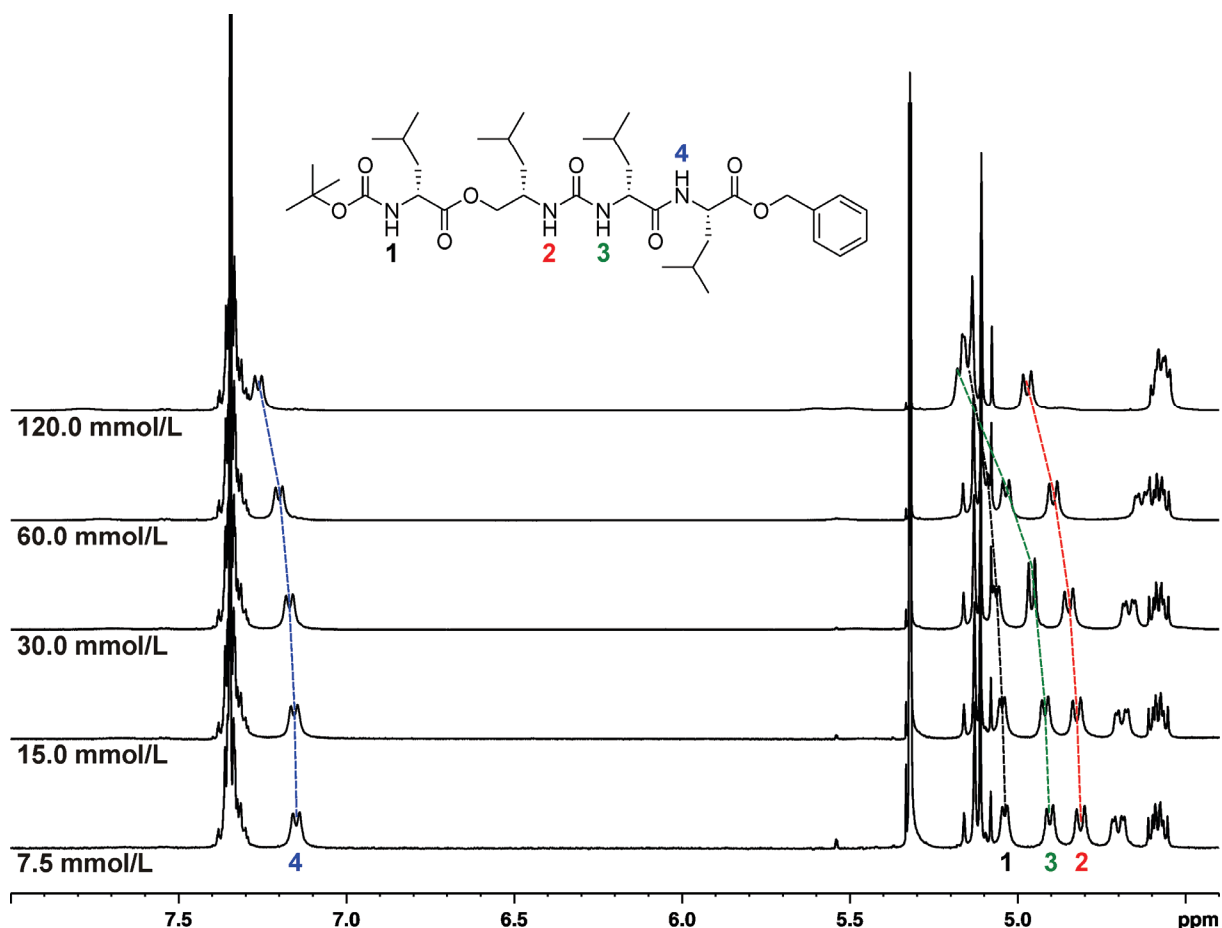


Figure 11: ^1H NMR dilution series of the D-(*alt*)-L-configured, 50% amide containing pseudotetrapeptide **99** (CD_2Cl_2 , 25 °C).

The different proton shifts were plotted against sample concentration. The resulting graphs for **92** and **99** are shown in Figure 12. In compound **92**, the protons of interest display no detectable shift, when the concentration is increased from 7.5 to 15 mmol/L. Aggregation of this compound though sets in at a concentration higher than 15.0 mmol/L. Proton #2 is most affected by the aggregation process, displaying the most significant downfield shift. Proton #2 shows the smallest shift and hence is least involved into the intermolecular hydrogen bonding. In compound **99**, the proton shifts are by approximately a factor two smaller than in compound **92**. As in compound **92**, the most intense shift is recorded for proton #3.

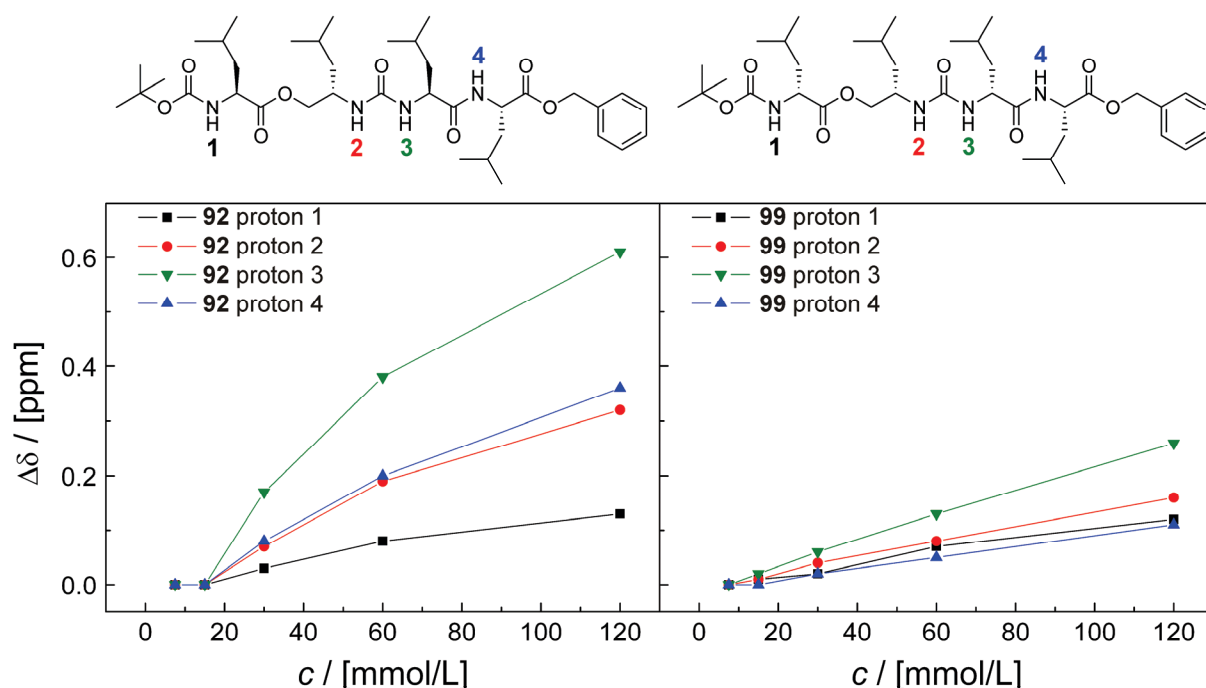


Figure 12: Proton resonance shifts plotted against sample concentration for the 50% amide containing pseudotetrapeptides **92** and **99** (CD_2Cl_2 , 25 °C).

The structural difference between compounds **92** and **99** is the configuration of the building blocks. In analogy to compounds **116** and **117**, **92** and **99** display a significant influence of the stereochemistry on aggregation behavior. The *all*-L-configured compound **92** shows more intense downfield shifts than the D-(*alt*)-L-pseudotetrapeptide **99**. This trend can also be observed for **116** and **117**. Most probably, the D,L-alternating stereochemistry leads to an unfavorable steric

interaction of the leucine residues during the aggregation process and hence inhibit it.

In the compounds **116**, **117**, **92**, and **99**, the shifts of four protons are evaluated. In the ester-(*alt*)-urea compounds **90** and **85**, the number of exchanging protons is increased by the alcohol proton. The proton spectra of the *all*-L-configured ester-(*alt*)-urea pseudotetrapeptide **90** at different concentrations are shown in Figure 13. The protons of interest were numbered starting with the alcohol, which is attributed to the broad multiplet at 3.36 ppm. Urea proton #2 is attributed to the well resolved doublet at 4.74 ppm. Proton #3 is attributed to the broad, structureless multiplet at 5.44 ppm. Proton #4 is attributed to the doublet at 5.27 ppm, which is partially overlapping with the solvent signal. The doublet of proton #5, located at 5.34 ppm is also overlapping with the solvent signal. Increasing the sample concentration leads to downfield shifts of all protons. At the final concentration of 120.0 mmol/L, the resonance of proton #1 is shifted by 0.55 ppm. The broad, structureless shape of the signal remains unchanged. The doublet of proton #2 is shifted by 0.64 ppm and displays a broad, structureless shape, already at a concentration of 30.0 mmol/L. Proton #3 is shifted by 0.41 ppm, proton #4 is shifted by 0.32 ppm, and proton #5 by 0.31 ppm, displaying sharp doublets at this concentration. Interestingly, the singlet of the benzylic protons splits into the doublet of a doublet with increasing concentration.

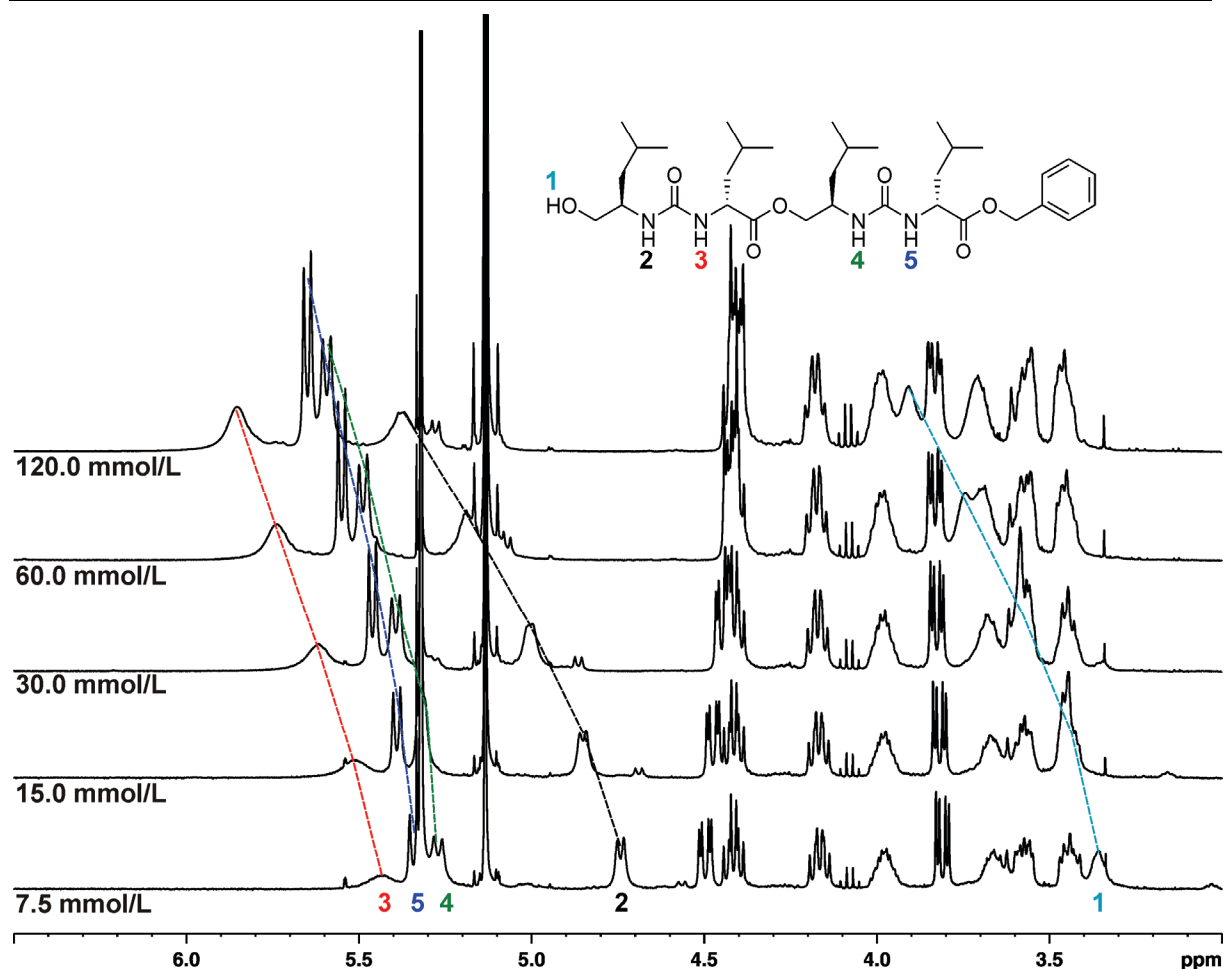


Figure 13: ^1H NMR dilution series of the *all*-L-configured, ester-(*alt*)-urea pseudotetrapeptide **90** (CD_2Cl_2 , 25 °C).

The proton NMR spectra of the D,L-alternating ester-(*alt*)-urea pseudotetrapeptide **85** at different concentrations are shown in Figure 14. The alcohol proton is attributed to the poorly resolved triplet at 4.23 ppm. The urea proton #2 is attributed to the sharp doublet at 4.87 ppm. Proton #3 displays a doublet at 5.08 ppm, which is overlapping with the benzyl proton signal of the C-terminal protecting group. The sharp doublet at 4.81 ppm is assigned to proton #4, the sharp doublet at 5.13 ppm is also overlapping with the benzyl proton signal and is attributed to proton #5. Increasing the concentration to 120.0 mmol/L leads to a downfield shift of all protons. The shape of all signals remains unchanged. Proton #1 is shifted by 0.36 ppm, proton #2 by 0.43 ppm, proton #3 by 0.45 ppm, proton #4 by 0.58 ppm, and proton #5 by 0.54 ppm. Interestingly, the benzylic protons of the C-terminal protecting group display a

4 Linear (Ester-[*alt*]-urea)s

highly split doublet of a doublet, of which the coupling constants remain constant at all concentrations.

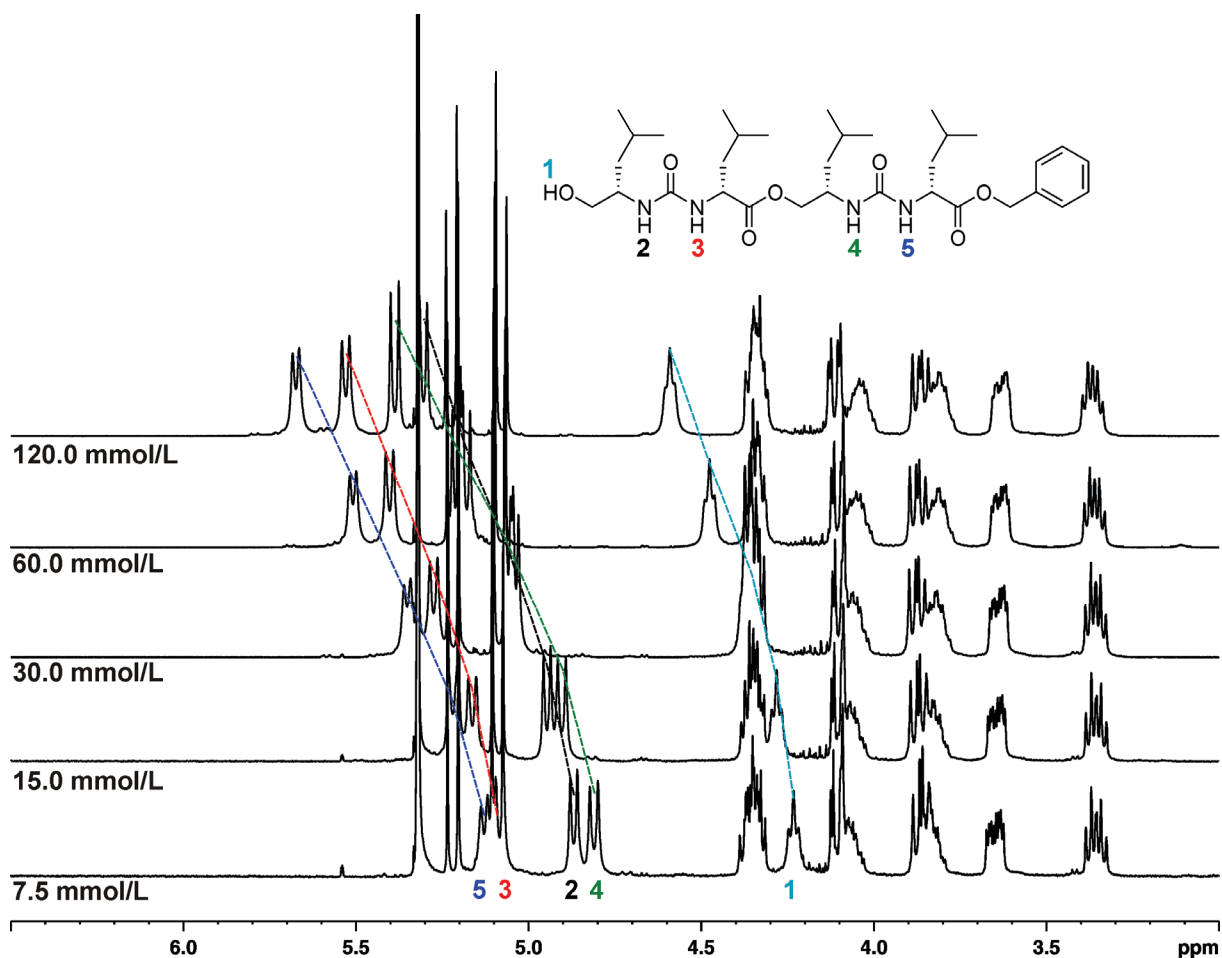


Figure 14: ^1H NMR dilution series of the D-(*alt*)-L-configured, ester-(*alt*)-urea pseudotetrapeptide **85** (CD_2Cl_2 , 25 °C).

The resulting graphs of the dilution experiments are shown in Figure 15. In both compounds, the downfield shift sets in, with the first doubling of the concentration and slightly levels off at the highest concentration. In compound **90**, proton #2 is most shifted, protons #4 and #5 least. With regard to aggregation, proton #2 is most involved into intermolecular hydrogen bonding. In compound **85**, protons #4 and #5 were most shifted and though most involved into intermolecular hydrogen bonding. In contrast to the compounds **116**, **117**, **92**, and **99**, the intensity of the downfield shift is comparable for both compounds, pointing to an aggregation mode, in which steric hindrance between side chains does not occur, as the stereochemistry has a negligible

influence on the aggregation process. Probably, the hydrogen bond network in the ester-(*alt*)-urea aggregate structure is less affected by the orientation of the leucine residues.

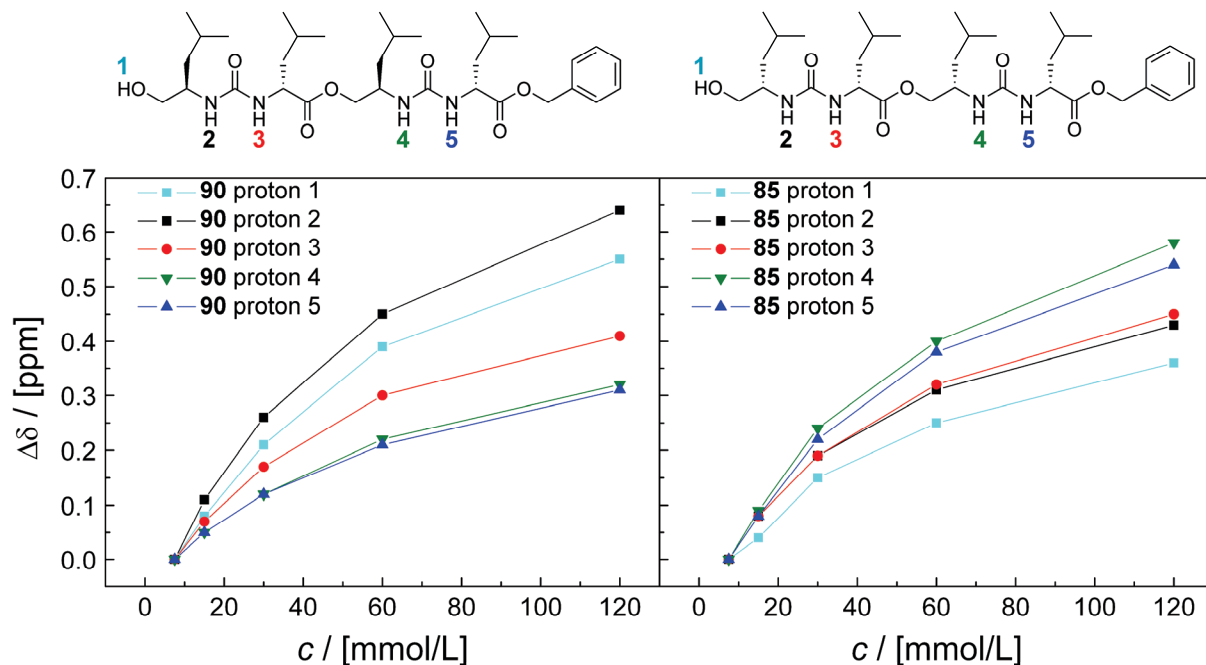


Figure 15: Proton resonance shifts plotted against sample concentration for the ester-(*alt*)-urea pseudotetrapeptides **90** and **85** (CD_2Cl_2 , 25 °C).

An overlay of the proton shifts of all compounds is shown in Figure 16. The protons with the most intense shifts are displayed on top, the average shifts of all compounds are displayed on the bottom. The *all*-L-configured compounds **116**, **92**, and **90** are shown on the left, the D-(*alt*)-L-compounds **117**, **99**, and **85** on the right. Comparing the strongest shifting protons of the *all*-L-compounds, peptide **116** displays the most intense shift, followed by the ester-(*alt*)-urea-compound **90**. Interestingly, the aggregation of **90** immediately sets in, whereas compounds **92** and **116** start to aggregate upon a concentration of 30 mmol/L. This is also valid for the average shifts of all three compounds. Comparing the strongest shifting protons of the D-(*alt*)-L-compounds, the ester-(*alt*)-urea compound **85** displays the most intense shift. This is also valid for the average shifts.

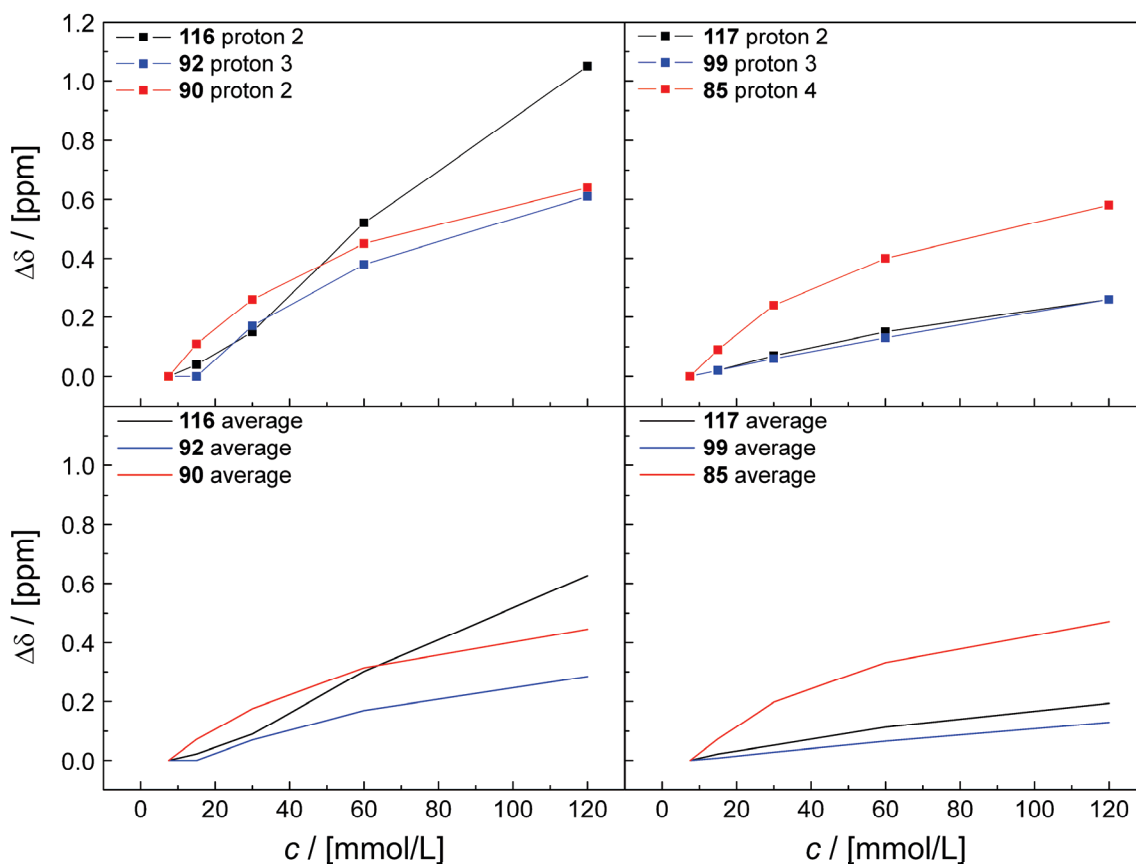


Figure 16: Overlay of proton shifts: Strongest shifting protons of all *L,L*-compounds (top left) and all *D,L*-compounds (top right) and average shifts of all *L,L*-compounds (bottom left) and all *D,L*-compounds (bottom right) (CD_2Cl_2 , 25 °C).

The aggregation tendencies of the compounds could be summarized as follows: The pure, natural peptide shows the most intense aggregation. Changing the stereochemistry from *all*-L to D-(*alt*)-L leads to a significantly reduced aggregation of the peptide by a factor of 3.2^a. Replacing two amide bonds of the natural peptide by an ester-(*alt*)-urea-moiety lowers the aggregation tendency of the naturally configured compound by a factor of 2.2^a. Changing the stereochemistry from *all*-L to D-(*alt*)-L leads to a notable drop of aggregation by a factor of 1.5^a. Replacing all amide bonds by ester-(*alt*)-urea moieties leads to a decrease of aggregation by a factor of 1.3^a. Changing the stereochemistry

^a Quantitative parameter based on average shift differences.

leads to a negligible increase of aggregation. Hence, replacing amide bonds by ester-(*alt*)-urea isostere units decreases significantly the influence of stereochemistry on the aggregation behavior of the compound.

4.2.7 Tentative Structural Proposal

The aggregation tendencies of the different compounds are the direct result of their primary structure and are influenced by stereochemistry and hydrogen bonding pattern. In the following, the results obtained in the NMR experiments are explained by considering possible aggregate structures. It should be pointed out that these structural proposals are very tentative and by no means substantiated by theoretical calculations. Structural proposals are given for peptide aggregates (Figure 17) and ester-(*alt*)-urea aggregates (Figure 18). Assuming aggregation in a β -sheet pattern, the structural proposals display parallel and antiparallel orientation. Furthermore, a dimer structure for ester-(*alt*)-urea compounds is proposed (Figure 19).

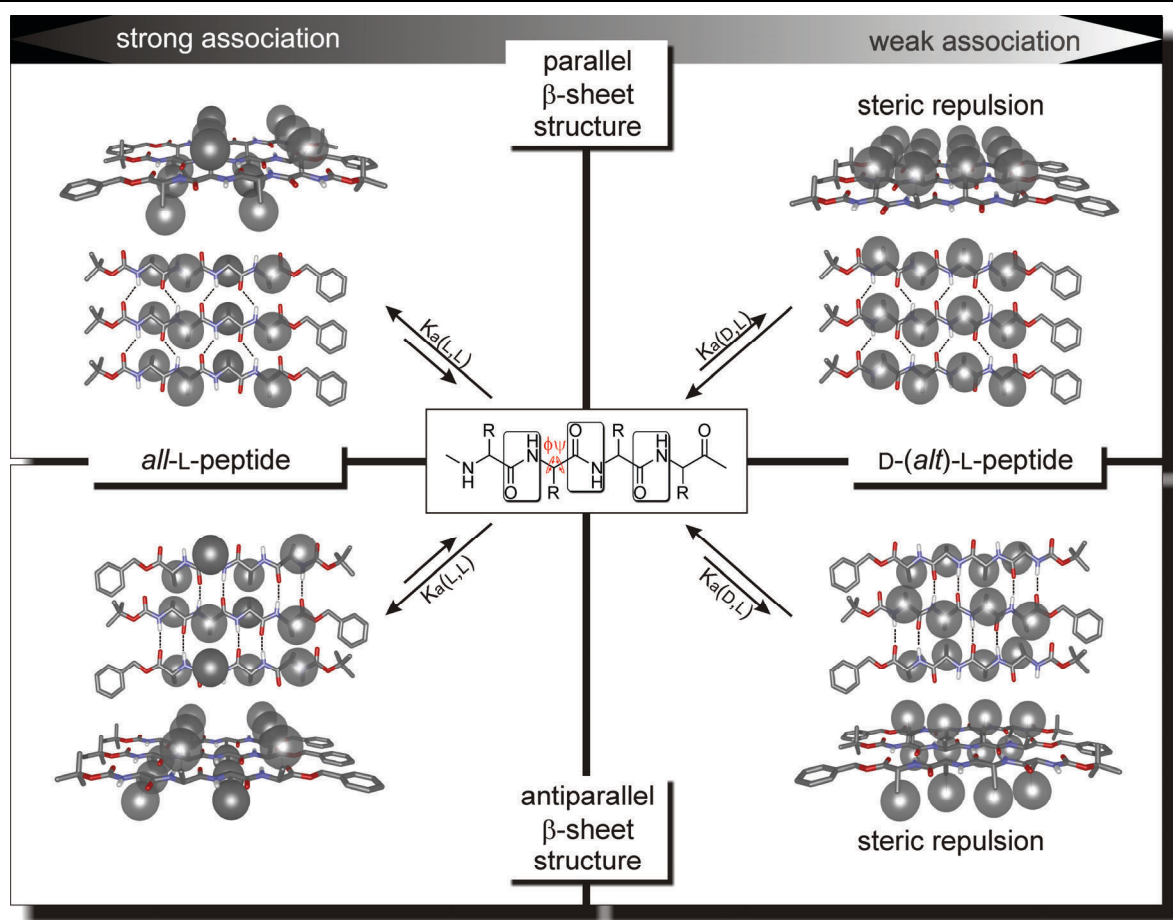


Figure 17: Tentative proposal of peptide aggregation structures. *All*-L-peptide aggregates are shown on the left, D-(*alt*)-L-peptide aggregates on the right. Parallel β -sheet structural proposals are shown on top, antiparallel β -sheet structural proposals at the bottom. Side chain residues are replaced by spheres for clarity. Rotational angles ϕ and ψ are displayed in red, fixed angles of the amide bond are indicated with planes. Hydrogen bonds are indicated with dotted lines. Aggregation tendencies are indicated with arrows.

A structural proposal for the peptide aggregates is shown in Figure 17. The *all*-L-peptide displayed stronger proton shifts in the NMR studies than the D-(*alt*)-L-peptide, indicating a higher association tendency. Assuming a similar β -sheet aggregate structure for both compounds, this difference has to result from different steric interactions of the side chain residues. As indicated in Figure 17, the *all*-L-peptide aggregate experiences much weaker steric interactions than the D-(*alt*)-L-peptide, resulting in a stronger association. In the antiparallel and in the parallel β -sheet, the side chain residues of the *all*-L-peptide are located above and underneath the plane of the sheet, leading to a reduced side chain

interaction as compared to the D-(*alt*)-L-peptide. The parallel sheet orientation of the D-(*alt*)-L-peptide projects the side chain residues all on one side of the β -sheet plane (enabling the generation of an amphiphilic β -sheet). The steric repulsion of the side chain residues is most likely preventing or at least hindering the aggregation process. The rotational freedom of the peptide backbone is given only by the two angles ϕ and ψ , since the preferred *anti* conformation of the amide bond fixes this angle to 180° (indicated by planes). Intramolecular steric repulsion of the side chain residues in the D-(*alt*)-L-peptide may lead to a distortion of the molecule. The limited rotational freedom of the backbone may inhibit the formation of a structure with reduced steric interaction, which is still able to associate in a sheet structure. This could explain the notable differences in proton shifts for *all*-L and D-(*alt*)-L-peptides.

4 Linear (Ester-[*alt*]-urea)s

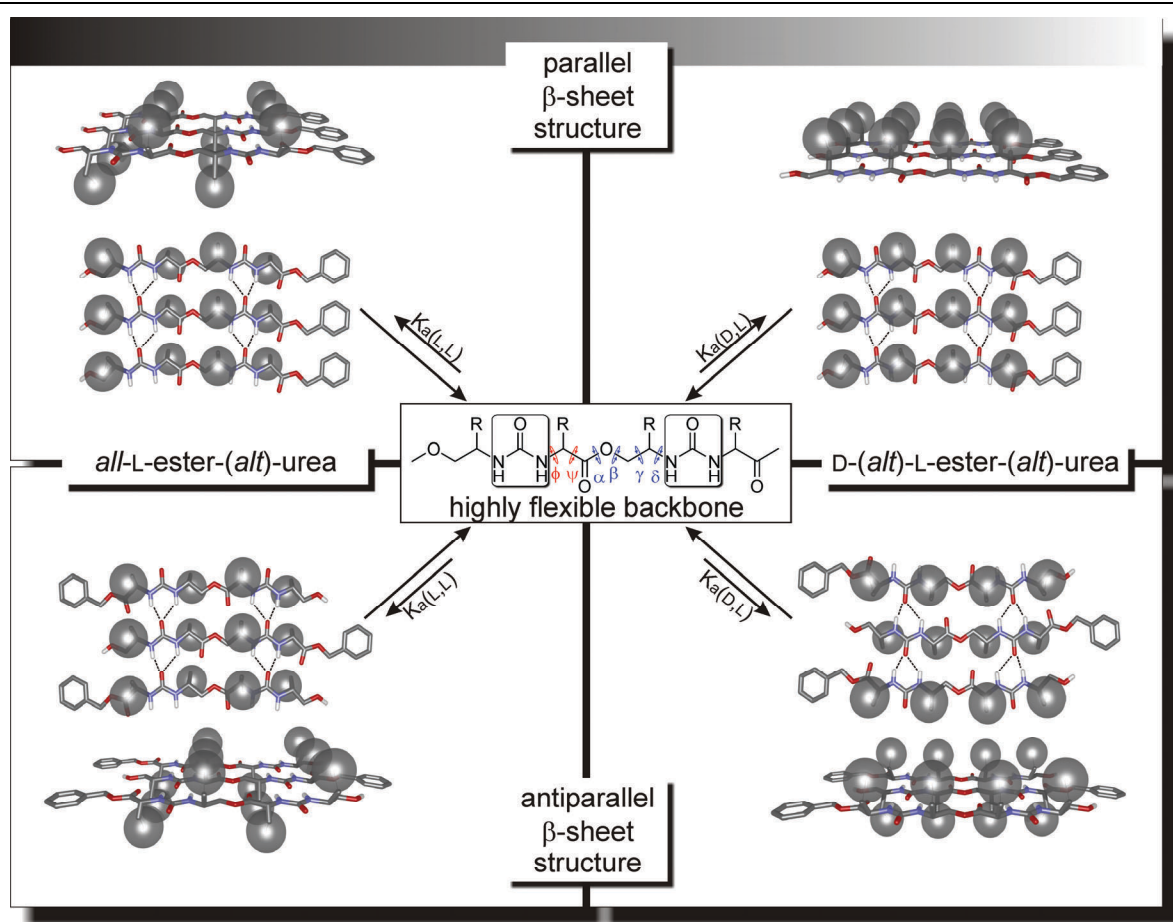


Figure 18: Tentative proposal of ester-(*alt*)-urea pseudopeptide aggregation structures. *All*-L-compound aggregates are shown on the left, D-(*alt*)-L-compound aggregates on the right. Parallel β -sheet structural proposals are shown on top, antiparallel β -sheet structural proposals at the bottom. Side chain residues are replaced by spheres for clarity. Rotational angles ϕ and ψ are displayed in red, additional rotational freedom is indicated by further rotational angles α , β , γ , and δ (displayed in blue), fixed angles of the amide bond are indicated with planes. Hydrogen bonds are indicated with dotted lines. Aggregation tendencies are indicated with arrows.

A structural proposal for the ester-(*alt*)-urea compounds with 0% amide content, based on a β -sheet association of the molecules is displayed in Figure 18. The *all*-L-ester-(*alt*)-urea and the D-(*alt*)-L-ester(*alt*)-urea displayed similar proton shifts in the NMR studies, indicating a reduced influence of the stereochemistry on the aggregation process. The proposed structures display a comparable steric interaction of the side chain residues as in the case of the peptides. The major difference to the peptide structures is the enhanced

rotational freedom in the backbone. As displayed, four additional variable rotational angles (α , β , γ , and δ) allow an increased backbone flexibility. The deformation of the molecule, in order to avoid an unfavorable steric interaction may hence not necessarily lead to a conformation, where a sheet-type association is not possible. This may explain the vanishing difference in association tendencies of *all*-L-ester-(*alt*)-urea and the D-(*alt*)-L-ester(*alt*)-urea compounds.

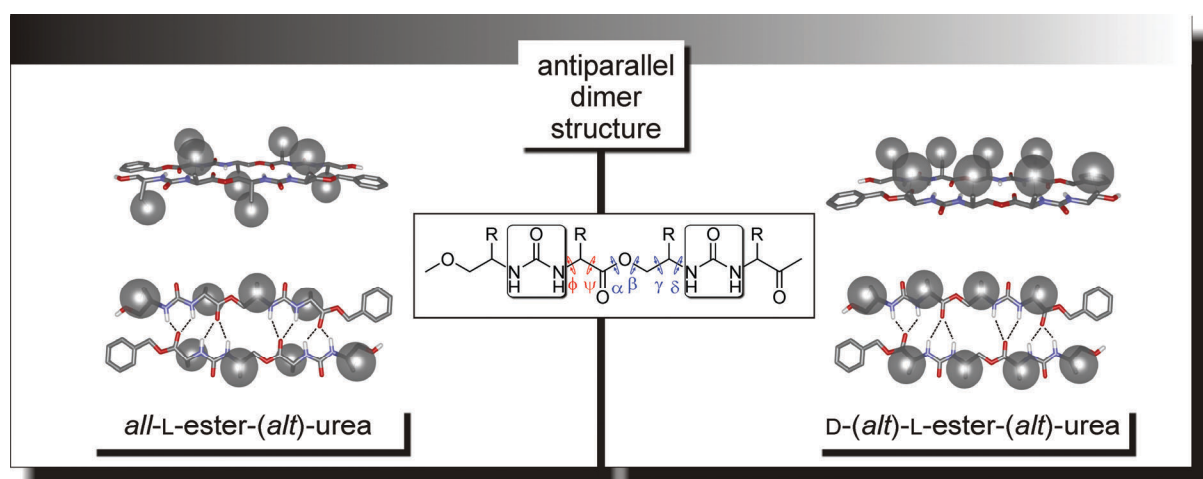


Figure 19: Tentative proposal of an ester-(*alt*)-urea dimer structure. *All*-L-compound aggregates are shown on the left, D-(*alt*)-L-compound aggregates on the right. Side chain residues are replaced by spheres for clarity. Rotational angles ϕ and ψ are displayed in red, additional rotational freedom is indicated by further rotational angles α , β , γ , and δ (displayed in blue), fixed angles of the amide bond are indicated with planes. Hydrogen bonds are indicated with dotted lines.

A tentative structural proposal for the formation of an ester-(*alt*)-urea dimer is given in Figure 19. The number of possible intermolecular hydrogen bonding interactions in this dimer structure would be twice of that in the structures proposed in Figure 18. Further aggregation to sheet structures would be unlikely, as all hydrogen bond donor sites are involved in this hydrogen bonding pattern.

In all cases, these structural proposals are speculative and should be treated with caution. For example, one may not exclude the probability of intramolecular secondary structure formation, i.e. loop structures, also inhibiting the formation of aggregates.

4.3 Experimental Part

4.3.1 General

General Methods: Starting materials were commercial and used as received. All solvents used at FU Berlin and HU Berlin were distilled once prior to usage, all solvents used at MPI were used without further purification. THF was in all cases stored over KOH and freshly distilled prior to usage. Dry solvents were kindly provided by the respective facility of the MPI. Dry DMF was purchased from Acros. If mentioned, solvents were degassed by freeze drying or by purging with argon. Column chromatography was carried out with 130 – 140 mesh silica gel. Dialysis of the compounds was achieved using regenerated cellulose dialysis tubes Spectra/Por Dialysis Membrane MWCO:1000 or MWCO:25000. Slow compound addition was achieved using a Harvard Apparatus 11Plus syringe pump. Compound lyophilization was performed using Christ Alpha 2-4 LDC-1m apparatus. Microwave assisted reactions were performed in a CEM-Discover monomode microwave reactor having a continuous microwave power delivery system from 0 to 300 W. The reactions were carried out in 10 mL sealed glass vials. The temperature was monitored by an IR sensor on the outer surface of the reaction vessel. All the reactions were performed with max. power and super-cooling.

Analytic Methods:

NMR (^1H and ^{13}C , respectively) were recorded on Bruker DPX 300 (300.1 and 75 MHz for ^1H and ^{13}C , respectively), Bruker AV400 (400.1 and 100.6 MHz for ^1H and ^{13}C , respectively) spectrometers at 23 \pm 2 $^\circ\text{C}$ using residual protonated solvent signals as internal standard (^1H : $\delta(\text{CHCl}_3)$ = 7.26 ppm, $\delta(\text{DMSO})$ = 2.50 ppm, $\delta(\text{CH}_3\text{OH})$ = 3.31 ppm, $\delta(\text{H}_2\text{O})$ = 4.79 ppm, $\delta(\text{CH}_3\text{CN})$ = 4.79 ppm, $\delta(\text{CH}_2\text{Cl}_2)$ = 5.32 ppm, and ^{13}C : $\delta(\text{CHCl}_3)$ = 77.16 ppm, $\delta(\text{DMSO})$ = 39.52 ppm, $\delta(\text{CH}_3\text{OH})$ = 49.00 ppm, $\delta(\text{CH}_3\text{CN})$ = 1.32 ppm and 118.26 ppm, $\delta(\text{CH}_2\text{Cl}_2)$ = 53.80 ppm).

Mass spectrometry was performed on a Bruker APEX III Fourier Transform Ion Cyclotron Resonance Mass Spectrometer (FTICR-MS) or on a Waters LCT Premier XE.

TLC was performed on Merck Silica Gel 60 F254 TLC plates with a fluorescent indicator with a 254 nm excitation wavelength. Compounds were visualized under UV light at 254 nm and developed with ninhydrin solution.

HPLC/UPLC was performed with a Waters UPLC Acquity equipped with a Waters LCT Premier XE Mass detector for UPLC-HR-MS, with Waters Alliance systems (consisting of a Waters Separations Module 2695, a Waters Diode Array detector 996 and a Waters Mass Detector ZQ 2000) equipped with the columns described with the corresponding substances, with Shimadzu LC-10A systems equipped with a photodiode array detector (PAD or DAD).

GPC measurements in DMF as the mobile phase were performed on PSS columns in a WGE Dr.Bures TAU 2010 column oven at 70 °C, using a WGE Dr.Bures Q-2010 HPLC pump and a Knauer Smartline 3800 autosampler. Detection was achieved using a WGE ETA-2020 RI-visco-detector and a Knauer Smartline 2500 UV-detector. Flow-rate was 1.0 mL/min. Columns were calibrated using a Polystyrene Calibration Kit S-L-10 LOT 79, using 2,4-Di-*tert*-butyl-4-methoxy-phenol as internal standard.

4.3.2 General Procedures

General procedure for the deprotection of the Boc group: Peptide was dissolved in CH₂Cl₂ or in CH₂Cl₂:CH₃OH 9:1 (depending on solubility) and cooled to 0 °C. TFA (same amount as the solvent) was added and the solution allowed to warm up to room temperature. After stirring at room temperature until starting material was consumed (TLC monitoring), the solution was concentrated i.vac. When the uncharged, neutralized peptide was the desired product, the solution was extracted with water, saturated aqueous NaHCO₃-solution (in case of longer peptides (starting from octamer), CH₃OH was added to assure solubility of the peptide), water, and brine. The combined organic layers were dried over MgSO₄, filtered, and evaporated i.vac. to yield the crude product in quantitative yield. In case of remaining protected peptide, procedure was repeated. When the amine salt was the desired product, the reaction mixture was evaporated i.vac. and wrapped several times with CH₂Cl₂ to give the product in quantitative yield.

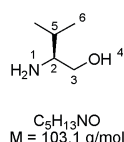
General procedure for the deprotection of the methyl ester: To a solution of methyl ester protected peptide in water:THF 1:5, a 1 M aqueous solution of LiOH (water:LiOH:THF 1:1:5) was added and the reaction mixture stirred at room temperature until starting material was consumed (TLC monitoring). Acetic acid was added to give pH=5, and the product subsequently extracted with CH₂Cl₂. The united organic layers were dried over MgSO₄ and the solvent evaporated i.vac. to give the product in quantitative yield.

General procedure for the deprotection of the Z group or benzyl ester: To a solution of Z- or benzyl protected peptide in EE:CH₃OH (ratio depending on solubility), Pd/C was added and the solution stirred under hydrogen atmosphere at room temperature. The reaction mixture was filtered and evaporated i.vac. to give the product.

General procedure for the reduction of amino acids to amino alcohols with LAH: LAH (80 mmol) was suspended in dry THF (250 mL) and the suspension cooled to 0 °C. The amino acid (40 mmol) was added neat slowly (strong hydrogen formation). The mixture was allowed to warm up to room temperature and then refluxed for minimum 10 h. The reaction mixture was then cooled down to 0 °C and quenched by the addition of water or Baekstrom salt.^[20] The suspension was then filtered and the remaining solid washed extensively with THF. The organic layer was concentrated i.vac., dried over MgSO₄, filtered, and the solvents were evaporated i.vac. to give the crude product which was purified via bulb-to-bulb distillation i.vac.

4.3.3 Synthetic Procedures

L-Valinol (**44**):

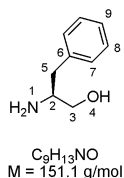


L-Valine was reacted following the general procedure for the LAH-reduction of amino acids. In one batch, the amino alcohol was transferred into the amine-hydrochloride with HCl prior to THF removal. This procedure lowered the volatility of the product but gave impure material which had to be used without further purification since distillation was not possible.

$R_F = 0.1$ (CH_2Cl_2 :MeOH 9:1)

^1H NMR and ^{13}C NMR agreed very well with the literature.^[21]

L-Phenylalaninol (**45**):



L-Phenylalanine was reacted following the general procedure for the LAH-reduction of amino acids. In one batch, the amino alcohol was transferred into the amine-hydrochloride with HCl prior to THF removal. This procedure lowered the volatility of the product but gave impure material which had to be used without further purification since distillation was not possible.

R_F , ^1H NMR and ^{13}C NMR agreed very well with the literature.^[21]

Boc-L-Valinol (**46**):



Reaction starting from L-Valinol hydrochloride:

To a chilled (0 °C) and stirred solution of **44** hydrochloride (4.19 g, 30 mmol) and NEt_3 (8.33 mL, 60 mmol) in CHCl_3 , neat Boc_2O (6.55 g, 30 mmol) was added. The solution was stirred for 30 minutes at 0 °C and then allowed to warm up to room temperature. After stirring for 24 h, the solution was extracted with 1 M aqueous citric acid solution (1x100 mL), saturated aqueous NaHCO_3 -solution (1x100 mL), water (1x100 mL), and brine (1x100 mL). The organic layer was dried over MgSO_4 , filtered and evaporated to give the crude product, which was purified via column chromatography on silica (eluent: EE/PE 3:7) to give 5.6 g (56% yield) of **46** as a yellow oil.

HPLC (2x150 mm Luna Phenyl-Hexyl 3 μm , acetonitrile:water = 1:1): 6.04 min (>99% peak area, **46**).

4 Linear (Ester-[*alt*]-urea)s

Reaction starting from L-Valinol:

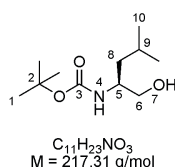
To a chilled (0 °C) and stirred solution of **44** (8.77 g, 85.0 mmol) in CHCl₃, neat Boc₂O (18.55 g, 85.0 mmol) was added and the solution stirred at 0 °C for 30 minutes. The solution was then allowed to warm up to room temperature and stirred for 72 h. The reaction mixture was then extracted with water (1x100 mL), 1 M aqueous citric acid solution (1x100 mL), water (1x100 mL), saturated aqueous NaHCO₃-solution (1x100 mL), water (1x100 mL), and brine (1x100 mL). The organic layer was dried over MgSO₄, filtered and evaporated i.vac. to give the crude product which was purified via column chromatography on silica (eluent: EE:PE 3:7) to give **46** as a yellow oil (16.5 g, 95% yield).

R_F = 0.20 (EE:PE 3:7)

¹H NMR (300 MHz, CDCl₃, 20 °C): δ 4.82 (d, ³ $J(H,H)$ = 8.0 Hz, 1 H, N⁴H), 3.70 - 3.48 (m, 2 H, C⁵H, C⁶H or C⁶H₂), 3.45 - 3.30 (m, 1 H, C⁵H or C⁶H), 3.20 - 2.98 (m, 1 H, O⁷H), 1.90 - 1.70 (m, 1 H, C⁸H), 1.41 (s, 9 H, 3 C¹H₃), 0.90 (t, ³ $J(H,H)$ = 6.7 Hz, 6 H, 2 C⁹H₃).

¹³C NMR (CDCl₃): δ 156.91, 79.51, 63.94, 58.05, 29.33, 28.45, 19.59, 18.57.

Boc-L-Leucinol (**47**):



To a chilled (0 °C) and stirred solution of **41** hydrochloride (14 g, guessed amount of 68 mmol) and NEt₃ (13.7 mL, 99.0 mmol) in CHCl₃, neat Boc₂O (6.0 g, 27.5 mmol) was added. The solution was stirred for 30 minutes at 0 °C and then allowed to warm up to room temperature. According to TLC monitoring, Boc₂O was added until all amino alcohol was consumed (altogether 14.84 g, 68 mmol). After 72 h reaction time, the solution was extracted with 1 M aqueous citric acid solution (3x50 mL), saturated aqueous NaHCO₃-solution (1x50 mL), water (1x50 mL), and brine (1x50 mL). The organic layer was dried over MgSO₄ and evaporated i.vac. to give 16.17 g of the crude product which

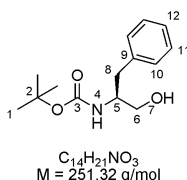
was purified via column chromatography on silica (eluent: PE:EE: 9:1 to 7:3) to give 12.84 g (87% yield) of **47** as an yellow oil.

$R_F = 0.26$ (EE:PE 3:7)

^1H NMR (300 MHz, CDCl_3 , 20 °C): δ 4.80 (d, $^3J(\text{H},\text{H}) = 7.1$ Hz, 1 H, N^4H), 3.75 - 3.50 (m, 2 H, C^5H , C^6H or C^6H_2), 3.48 - 3.36 (m, 1 H, C^5H or C^6H), 3.27 (br s, 1 H, O^7H), 1.75 - 1.50 (m, 1 H, C^9H), 1.40 (s, 9 H, 3 C^1H_3), 1.32 - 1.20 (m, 2 H, C^8H_2), 0.88 (d, $^3J(\text{H},\text{H}) = 6.5$ Hz, 6 H, 2 C^{10}H_3).

^{13}C NMR (CDCl_3): δ 156.59, 79.50, 66.12, 50.90, 40.62, 28.45, 24.84, 23.11, 22.27.

Boc-L-Phenylalaninol (**48**):



To a chilled (0 °C) and stirred solution of **45** hydrochloride (14 g, guessed amount of 70 mmol) and NEt_3 (19.4 mL, 140 mmol) in CHCl_3 , neat Boc_2O (15.28 g, 70.0 mmol) was added. The solution was stirred for 30 minutes at 0 °C and then allowed to warm up to room temperature. After 24 h reaction time, the solution was extracted with 1 M aqueous citric acid solution (3x50 mL), saturated aqueous NaHCO_3 -solution (3x50 mL), water (1x100 mL), and brine (1x100 mL). The organic layer was dried over MgSO_4 and evaporated i.vac. to give the crude product which was purified via recrystallization from CH_2Cl_2 :PE to give the product as white crystals with a slightly brown color. Attempts to further purify the crystalline product via recrystallization failed, since it immediately decomposed in solution to a dark brown substance. Attempts to purify the crystalline product via column chromatography on silica (eluent: EE:MeOH 98:2) also failed. So the once recrystallized, slightly brown colored product was used without further purification. Yield could not be determined because of unsatisfying isolation of the product and decomposition.

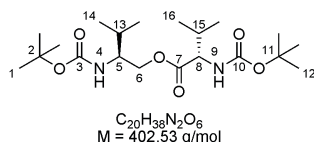
$R_F = 0.40$ (EE:PE 1:1)

4 Linear (Ester-[*alt*]-urea)s

^1H NMR (300 MHz, CDCl_3 , 20 °C): δ 7.34 - 7.22 (m, 5 H, 2 C^{10}H , 2 C^{11}H , C^{12}H), 4.90 (br s, 1 H, N^4H), 3.90 - 3.70 (m, 1 H, C^5H), 3.66 (dd, $^2J(\text{H},\text{H}) = 11.1$ Hz, $^3J(\text{H},\text{H}) = 3.9$ Hz, 1 H, C^6H), 3.55 (dd, $^2J(\text{H},\text{H}) = 11.1$ Hz, $^3J(\text{H},\text{H}) = 5.3$ Hz, 1 H, C^6H), 2.85 (d, $^3J(\text{H},\text{H}) = 7.1$ Hz, 2 H, C^8H_2), 2.75 (br s, 1 H, O^7H), 1.42 (s, 9 H, 3 C^1H_3).

^{13}C NMR (CDCl_3): δ 156.30, 137.99, 129.43, 128.63, 126.60, 79.86, 64.23, 53.93, 37.65, 28.45.

Boc-L-Valinol-ester-L-Valine-Boc (**49**):



Boc-L-Val (2.97 g, 13.65 mmol), HOBT (1.93 g, 14.30 mmol), and **46** (2.64 g, 13.00 mmol) were dissolved in CH_2Cl_2 (70 mL) and cooled to 0 °C. To the cold solution, EDC (3.74 g, 19.50 mmol), dissolved in CH_2Cl_2 (30 mL) was added. The reaction mixture was allowed to warm up to room temperature and stirred for 16 h. TLC monitoring showed no complete conversion even if more HOBT (0.42 g), Boc-L-Val (0.55 g) and EDC (1.3 g) were added. After 20 h reaction time, the solution was evaporated i.vac. and the residue dissolved in EE. Water was added to the organic layer and the biphasic system stirred for 10 minutes. After phase separation, the organic layer was extracted with 1 M aqueous citric acid solution (1x100 mL), saturated aqueous NaHCO_3 -solution (1x100 mL), water (1x100 mL), and brine (1x100 mL). The organic layer was dried over MgSO_4 and evaporated i.vac. to give 6.29 g of the crude product, which was purified via column chromatography on silica (eluent: CH_2Cl_2 :MeOH 98:2) to give 2.06 g (yield: 39%) of **49** as a yellow oil.

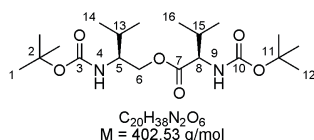
$R_F = 0.76$ (CH_2Cl_2 :MeOH 9:1)

^1H NMR (300 MHz, CDCl_3 , 20 °C): δ 5.01 (d, $^3J(\text{H},\text{H}) = 8.7$ Hz, 1 H, N^9H), 4.60 (d, $^3J(\text{H},\text{H}) = 9.5$ Hz, 1 H, N^4H), 4.30 - 4.00 (m, 3 H, C^6H_2 , C^8H), 3.75 - 3.50 (m, 1 H, C^5H), 2.20 - 2.00 (m, 1 H, C^{16}H), 1.90 - 1.70 (m, 1 H, C^{13}H), 1.44 and 1.43 (2 s, 18 H, 3 C^1H_3 , 3 C^{12}H_3), 1.05 - 0.80 (m, 12 H, 2 C^{14}H_3 , 2 C^{16}H_3).

^{13}C NMR (CDCl_3): δ 172.62, 155.73, 79.96, 79.52, 65.47, 58.69, 54.78, 31.36, 29.84, 28.49, 28.44, 19.49, 19.16, 18.60, 17.66.

High-resolution ESI-MS: m/z = 403.2803 (calcd 403.2811 for $\text{C}_{20}\text{H}_{38}\text{N}_2\text{O}_6$ + 1 H^+), 425.2622 (calcd 425.2631 for $\text{C}_{20}\text{H}_{38}\text{N}_2\text{O}_6$ + 1 Na^+), 441.2361 (calcd 441.2371 for $\text{C}_{20}\text{H}_{38}\text{N}_2\text{O}_6$ + 1 K^+), 805.5533 (calcd 805.5547 for $(\text{C}_{20}\text{H}_{38}\text{N}_2\text{O}_6)_2$ + 1 H^+), 827.5352 (calcd 827.5370 for $(\text{C}_{20}\text{H}_{38}\text{N}_2\text{O}_6)_2$ + 1 Na^+), 843.5091 (calcd 843.5106 for $(\text{C}_{20}\text{H}_{38}\text{N}_2\text{O}_6)_2$ + 1 K^+).

Boc-L-Valinol-ester-D-Valine-Boc (**50**):



Boc-D-Val (2.97 g, 13.65 mmol), HOBT (1.93 g, 14.30 mmol), and **46** (2.64 g, 13.00 mmol) were dissolved in CH_2Cl_2 (70 mL) and cooled to 0 °C. To the cold solution, EDC (3.74 g, 19.50 mmol), dissolved in CH_2Cl_2 (30 mL) was added. The reaction mixture was allowed to warm up to room temperature and stirred for 16 h. TLC monitoring showed no complete conversion even if more HOBT (0.42 g), Boc-D-Val (0.55 g) and EDC (1.3 g) was added. After 20 h reaction time, the solution was evaporated i.vac. and the residue was dissolved in EE. Water was added to the organic layer and the biphasic system stirred for 10 minutes. After phase separation, the organic layer was extracted with 1 M aqueous citric acid solution (1x100 mL), saturated aqueous NaHCO_3 -solution (1x100 mL), water (1x100 mL), and brine (1x100 mL). The organic layer was dried over MgSO_4 and evaporated i.vac. to give 6.83 g of the crude product, which was purified via column chromatography on silica (eluent: CH_2Cl_2 :MeOH 98:2) to give 3.02 g (yield: 56%) of **50** as a yellow oil.

R_f = 0.76 (CH_2Cl_2 :MeOH 9:1)

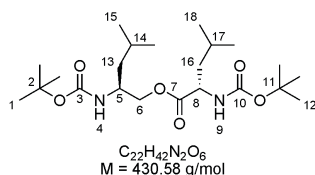
^1H NMR (300 MHz, CDCl_3 , 20 °C): δ 5.01 (d, $^3J(\text{H},\text{H})$ = 8.7 Hz, 1 H, N^9H), 4.54 (d, $^3J(\text{H},\text{H})$ = 9.3 Hz, 1 H, N^4H), 4.27 - 4.03 (m, 3 H, C^6H_2 , C^8H), 3.71 - 3.45 (m, 1 H, C^5H), 2.20 - 2.03 (m, 1 H, C^{15}H), 1.88 - 1.68 (m, 1 H, C^{13}H), 1.43 and 1.42 (2 s, 18 H, 3 C^1H_3 , 3 C^{12}H_3), 1.00 - 0.75 (m, 12 H, 2 C^{14}H_3 , 2 C^{16}H_3).

4 Linear (Ester-[*alt*]-urea)s

^{13}C NMR (CDCl_3): δ 172.36, 155.77, 79.90, 79.48, 65.36, 58.79, 54.73, 31.33, 29.79, 28.46, 28.43, 19.48, 19.17, 18.43, 17.67.

High-resolution ESI-MS: m/z = 403.2803 (calcd 403.2811 for $\text{C}_{20}\text{H}_{38}\text{N}_2\text{O}_6$ + 1 H^+), 425.2622 (calcd 425.2631 for $\text{C}_{20}\text{H}_{38}\text{N}_2\text{O}_6$ + 1 Na^+), 441.2361 (calcd 441.2371 for $\text{C}_{20}\text{H}_{38}\text{N}_2\text{O}_6$ + 1 K^+), 805.5533 (calcd 805.5548 for $(\text{C}_{20}\text{H}_{38}\text{N}_2\text{O}_6)_2$ + 1 H^+), 827.5352 (calcd 827.5371 for $(\text{C}_{20}\text{H}_{38}\text{N}_2\text{O}_6)_2$ + 1 Na^+), 843.5091 (calcd 843.5107 for $(\text{C}_{20}\text{H}_{38}\text{N}_2\text{O}_6)_2$ + 1 K^+).

Boc-L-Leucinol-ester-L-Leucine-Boc (**51**):



Boc-L-Leu monohydrate (3.38 g, 13.55 mmol), HOBT (1.92 g, 14.19 mmol), and **47** (2.80 g, 12.90 mmol) were dissolved in CH_2Cl_2 (70 mL) and cooled to 0 °C. To the cold solution, EDC (3.71 g, 19.35 mmol), dissolved in CH_2Cl_2 (30 mL) was added. The reaction mixture was allowed to warm up to room temperature and stirred for 72 h. TLC monitoring showed no complete conversion to the product. TLC after the addition of DPTS (10 mg) remained unchanged. The solution was concentrated i.vac. and dry THF (50 mL) was added, but TLC remained unchanged. After 76 h reaction time, the solution was evaporated i.vac. and the residue was dissolved in EE. Water was added to the organic layer and the biphasic system stirred for 10 minutes. After phase separation, the organic layer was extracted with 1 M aqueous citric acid solution (1x100 mL), saturated aqueous NaHCO_3 -solution (1x100 mL), water (1x100 mL), and brine (1x100 mL). The organic layer was dried over MgSO_4 and evaporated i.vac. to give the crude product, which was purified via column chromatography on silica (eluent: CH_2Cl_2 :MeOH 98:2) to give 2.55 g (yield: 46%) of **51** as a yellow solid.

Boc-L-Leu monohydrate (3.38 g, 13.55 mmol) and HOBT (1.92 g, 14.19 mmol) were dissolved in CH_2Cl_2 (70 mL) and cooled to 0 °C. To the cold solution, EDC

(3.71 g, 19.35 mmol), dissolved in CH₂Cl₂ (30 mL) was added. The reaction mixture was allowed to warm up to room temperature and stirred for 2 h to convert the amino acid into the active ester. According to TLC, this reaction was not quantitative. Nevertheless, **47** (2.80 g, 12.90 mmol) was added to the solution and the reaction was stirred for 5 h. TLC monitoring showed no complete conversion to the product, so the solution was concentrated i.vac. and DMF (15 mL) was added. After stirring at room temperature for 72 h, TLC remained unchanged. The organic layer was extracted with water (1x100 mL), 1 M aqueous citric acid solution (1x100 mL), saturated aqueous NaHCO₃-solution (1x100 mL), water (1x100 mL), and brine (1x100 mL). The organic layer was dried over MgSO₄ and evaporated i.vac. to give the crude product, which was purified via column chromatography on silica (eluent: CH₂Cl₂:MeOH 98:2) to give 1.42 g (yield: 51%) of **51** as an yellow solid.

R_F = 0.78 (CH₂Cl₂:MeOH 9:1)

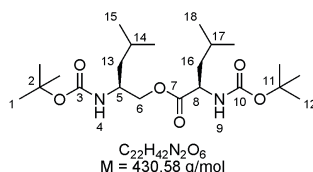
¹H NMR (300 MHz, CDCl₃, 20 °C): δ 4.90 (d, ³*J*(*H*,*H*) = 8.2 Hz, 1 H, N⁹*H*), 4.56 (d, ³*J*(*H*,*H*) = 7.7 Hz, 1 H, N⁴*H*), 4.35 - 4.25 (m, 1 H, C⁸*H*), 4.20 - 4.04 (m, 2 H, C⁶*H*₂ or C⁶*H*, C⁵*H*), 4.00 - 3.80 (m, 1 H, C⁶*H* or C⁵*H*), 1.79 - 1.18 (m, 24 H, 3 C¹*H*₃, 3 C¹²*H*₃, C¹³*H*₂, C¹⁴*H*, C¹⁶*H*₂, C¹⁷*H*), 0.96 - 0.90 (m, 12 H, 2 C¹⁵*H*₃, 2 C¹⁸*H*₃).

¹³C NMR (CDCl₃): δ 173.63, 155.59, 155.46, 80.03, 79.52, 67.26, 52.28, 47.89, 41.87, 41.03, 28.53, 28.47, 24.95, 24.86, 23.00, 22.93, 22.37, 22.09.

High-resolution ESI-MS: *m/z* = 431.3116 (calcd 431.3125 for C₂₂H₄₂N₂O₆ + 1 H⁺), 453.2935 (calcd 453.2945 for C₂₂H₄₂N₂O₆ + 1 Na⁺), 469.2674 (calcd 469.2685 for C₂₂H₄₂N₂O₆ + 1 K⁺), 861.6159 (calcd 861.6176 for (C₂₂H₄₂N₂O₆)₂ + 1 H⁺), 883.5978 (calcd 883.5592 for (C₂₂H₄₂N₂O₆)₂ + 1 Na⁺), 899.5717 (calcd 899.5734 for (C₂₂H₄₂N₂O₆)₂ + 1 K⁺).

4 Linear (Ester-[*alt*]-urea)s

Boc-L-Leucinol-*ester*-D-Leucine-Boc (**52**):



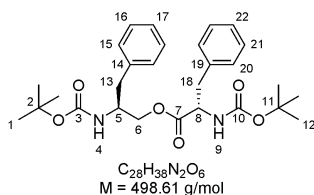
Boc-D-Leu monohydrate (3.19 g, 12.81 mmol), HOBt (1.83 g, 13.42 mmol), and **47** (2.65 g, 12.20 mmol) were dissolved in CH_2Cl_2 (70 mL) and cooled to 0 °C. To the cold solution, EDC (3.51 g, 18.30 mmol), dissolved in CH_2Cl_2 (30 mL) was added. The reaction mixture was allowed to warm up to room temperature and stirred for 72 h. TLC monitoring showed no complete conversion to the product. The solution was evaporated i.vac. and the residue was dissolved in EE. Water was added to the organic layer and the biphasic system stirred for 10 minutes. After phase separation, the organic layer was extracted with water (1x100 mL), 1 M aqueous citric acid solution (1x100 mL), saturated aqueous NaHCO_3 -solution (1x100 mL), water (1x100 mL), and brine (1x100 mL). The organic layer was dried over MgSO_4 and evaporated i.vac. to give the crude product, which was purified via column chromatography on silica (eluent: CH_2Cl_2 :MeOH 98:2) to give 2.20 g (yield: 42%) of **52** as a yellow solid.

$R_f = 0.78$ (CH_2Cl_2 :MeOH 9:1)

^1H NMR (300 MHz, CDCl_3 , 20 °C): δ 4.90 (d, $^3J(\text{H},\text{H}) = 7.9 \text{ Hz}$, 1 H, N^9H), 4.51 (d, $^3J(\text{H},\text{H}) = 7.1 \text{ Hz}$, 1 H, N^4H), 4.35 - 4.25 (m, 1 H, C^8H), 4.22 - 4.00 (m, 2 H, C^6H_2 or C^6H , C^5H), 3.99 - 3.72 (m, 1 H, C^6H or C^5H), 1.77 - 1.19 (m, 24 H, 3 C^1H_3 , 3 C^{12}H_3 , C^{13}H_2 , C^{14}H , C^{16}H_2 , C^{17}H), 1.01 - 0.78 (m, 12 H, 2 C^{15}H_3 , 2 C^{18}H_3).

^{13}C NMR (CDCl_3): δ 173.47, 155.60, 155.44, 80.00, 79.50, 67.34, 52.36, 47.93, 41.74, 41.08, 28.51, 28.46, 24.92, 24.82, 23.07, 22.89, 22.27, 22.06.

High-resolution ESI-MS: $m/z = 431.3116$ (calcd 431.3125 for $\text{C}_{22}\text{H}_{42}\text{N}_2\text{O}_6 + 1 \text{ H}^+$), 453.2935 (calcd 453.2945 for $\text{C}_{22}\text{H}_{42}\text{N}_2\text{O}_6 + 1 \text{ Na}^+$), 469.2674 (calcd 469.2685 for $\text{C}_{22}\text{H}_{42}\text{N}_2\text{O}_6 + 1 \text{ K}^+$), 861.6159 (calcd 861.6177 for $(\text{C}_{22}\text{H}_{42}\text{N}_2\text{O}_6)_2 + 1 \text{ H}^+$), 883.5978 (calcd 883.5592 for $(\text{C}_{22}\text{H}_{42}\text{N}_2\text{O}_6)_2 + 1 \text{ Na}^+$), 899.5717 (calcd 899.5734 for $(\text{C}_{22}\text{H}_{42}\text{N}_2\text{O}_6)_2 + 1 \text{ K}^+$).

Boc-L-Phenylalaninol-ester-L-Phenylalanine-Boc (**53**):

Boc-L-Phe (1.37 g, 5.17 mmol) and **48** (1.18 g, 4.70 mmol) were dissolved in CH₂Cl₂ (100 mL) and cooled to 0 °C. To the cold solution, TBTU (3.02 g, 9.40 mmol) and HOBT (0.64 g, 4.70 mmol) suspended in CH₂Cl₂ (50 mL) was added. The reaction mixture was allowed to warm up to room temperature and stirred for 16 h. TBTU did not dissolve. TLC monitoring showed no conversion to the product. After the addition of NEt₃ (2.61 mL, 18.80 mmol), TBTU dissolved completely within one hour and TLC showed conversion to one main product. TBTU (0.20 g, 0.65 mmol) was added and the solution stirred for 2 h. Water was added to the organic layer and the biphasic system stirred for 10 minutes. After phase separation, the organic layer was extracted with water (1x50 mL), 1 M aqueous citric acid solution (1x50 mL), saturated aqueous NaHCO₃-solution (1x50 mL), water (1x50 mL), and brine (1x50 mL). The organic layer was dried over MgSO₄ and evaporated i.vac. to give the crude product, which was purified via column chromatography on silica (eluent: toluene:EE 95:5) to give **53** as a white solid. The Purification of all fractions has not been completed, so that the yield could not be determined.

Boc-L-Phe (1.37 g, 5.17 mmol), HOBT (0.64 g, 4.70 mmol), and **48** (1.18 g, 4.70 mmol) were dissolved in CH₂Cl₂ (100 mL) and cooled to 0 °C. To the cold solution, neat TBTU (3.02 g, 9.40 mmol) and NEt₃ (2.60 mL, 18.80 mmol) was added. The reaction mixture was allowed to warm up to room temperature and stirred for 16 h. Water was added to the organic layer and the biphasic system stirred for 10 minutes. After phase separation, the organic layer was extracted with water (1x50 mL), 1 M aqueous citric acid solution (1x50 mL), saturated aqueous NaHCO₃-solution (1x50 mL), water (1x50 mL), and brine (1x50 mL). The organic layer was dried over MgSO₄ and evaporated i.vac. to give the crude

4 Linear (Ester-[*alt*]-urea)s

product, which was purified via column chromatography on silica (eluent: CH₂Cl₂:MeOH 98:2) to give 2.25 g (quantitative yield) of **53** as a white solid.

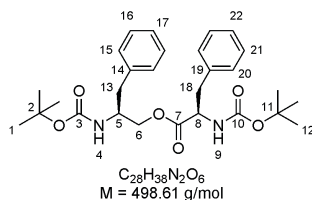
R_F = 0.26 (toluene:EE 9:1)

¹H NMR (300 MHz, CDCl₃, 20 °C): δ 7.36 - 7.08 (m, 10 H, C¹⁵H - C¹⁷H, C²⁰H - C²²H), 4.98 (d, ³J(H,H) = 7.8 Hz, 1 H, N⁹H), 4.70 (d, ³J(H,H) = 7.0 Hz, 1 H, N⁴H), 4.62 - 4.55 (m, 1 H, C⁸H), 4.24 - 3.83 (m, 3 H, C⁶H₂, C⁵H), 3.20 - 2.60 (m, 4 H, C¹³H, C¹⁸H), 1.43 and 1.41 (2 s, 18 H, 3 C¹H₃, 3 C¹²H₃).

¹³C NMR (CDCl₃): δ 172.12, 155.28, 137.31, 136.05, 129.40, 129.39, 128.82, 128.71, 127.30, 126.78, 80.34, 79.74, 65.76, 54.86, 50.81, 38.44, 37.92, 28.49, 28.44.

High-resolution ESI-MS: m/z = 499.2803 (calcd 499.2813 for C₂₈H₃₈N₂O₆ + 1 H⁺), 521.2622 (calcd 521.2634 for C₂₈H₃₈N₂O₆ + 1 Na⁺), 537.2361 (calcd 537.2373 for C₂₈H₃₈N₂O₆ + 1 K⁺), 997.5533 (calcd 997.5545 for (C₂₈H₃₈N₂O₆)₂ + 1 H⁺), 1019.5332 (calcd 1019.5366 for (C₂₈H₃₈N₂O₆)₂ + 1 Na⁺), 1035.5091 (calcd 1035.5107 for (C₂₈H₃₈N₂O₆)₂ + 1 K⁺).

Boc-L-Phenylalaninol-ester-D-Phenylalanine-Boc (**54**):



Boc-D-Phe (2.74 g, 10.34 mmol), HOBT (1.27 g, 9.40 mmol), and **48** (2.36 g, 9.40 mmol) were dissolved in CH₂Cl₂ (100 mL) and cooled to 0 °C. To the cold solution, neat TBTU (6.04 g, 18.80 mmol) and NEt₃ (5.20 mL, 37.60 mmol) was added. The reaction mixture was allowed to warm up to room temperature and stirred for 16 h. Water was added to the organic layer and the biphasic system stirred for 10 minutes. After phase separation, the organic layer was extracted with water (1x50 mL), 1 M aqueous citric acid solution (1x50 mL), saturated aqueous NaHCO₃-solution (1x50 mL), water (1x50 mL), and brine (1x50 mL). The organic layer was dried over MgSO₄ and evaporated i.vac. to give the crude

product, which was purified via column chromatography on silica (eluent: CH₂Cl₂:MeOH 98:2) to give 4.66 g (quantitative yield) of **54** as a white solid.

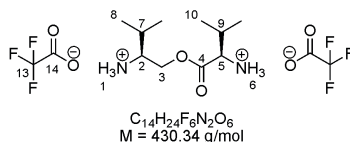
R_F = 0.26 (toluene:EE 9:1)

¹H NMR (300 MHz, CDCl₃, 20 °C): δ 7.36 - 7.09 (m, 10 H, C¹⁵H - C¹⁷H, C²⁰H - C²²H), 5.05 - 4.96 (m, 1 H, N⁹H), 4.70 - 4.40 (m, 2 H, N⁴H, C⁸H), 4.16 - 3.88 (m, 3 H, C⁶H₂, C⁵H), 3.18 - 2.99 (m, 2 H, C¹⁸H₂), 2.82 - 2.57 (m, 2 H, C¹³H₂), 1.44 - 1.41 (m, 18 H, 3 C¹H₃, 3 C¹²H₃).

¹³C NMR (CDCl₃): δ 172.02, 155.27, 137.29, 136.22, 129.39, 129.32, 128.84, 128.69, 127.32, 126.76, 80.24, 79.69, 65.78, 54.85, 50.68, 38.64, 37.79, 28.48, 28.44.

High-resolution ESI-MS: m/z = 499.2803 (calcd 499.2814 for C₂₈H₃₈N₂O₆ + 1 H⁺), 521.2622 (calcd 521.2634 for C₂₈H₃₈N₂O₆ + 1 Na⁺), 537.2361 (calcd 537.2374 for C₂₈H₃₈N₂O₆ + 1 K⁺), 997.5533 (calcd 997.5548 for (C₂₈H₃₈N₂O₆)₂ + 1 H⁺), 1019.5332 (calcd 1019.5367 for (C₂₈H₃₈N₂O₆)₂ + 1 Na⁺), 1035.5091 (calcd 1035.5108 for (C₂₈H₃₈N₂O₆)₂ + 1 K⁺).

L-Valinol-ester-D-Valine (**55**):



50 (0.10 g, 0.25 mmol) was reacted following the general procedure for the deprotection of the Boc group. The product was obtained in quantitative yield and was used without further purification.

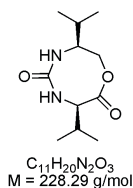
R_F = 0.26 (CH₂Cl₂:MeOH 9:1)

¹H NMR (300 MHz, MeOD, 20 °C): δ 4.54 - 4.43 (m, 2 H, C³H₂), 4.01 (d, ³J(*H,H*) = 4.7 Hz, 1 H, C⁵H), 3.38 - 3.29 (m, 1 H, C²H), 2.46 - 2.28 (m, 1 H, C⁹H), 2.14 - 2.00 (m, 1 H, C⁷H), 1.16 - 1.01 (m, 12 H, 2 C⁸H₃, 2 C¹⁰H₃).

¹³C NMR (MeOD): δ 169.45, 64.91, 59.49, 56.91, 30.84, 29.40, 18.88, 18.57, 18.47, 18.09.

4 Linear (Ester-[*alt*]-urea)s

Attempted cyclization of **55** to **58**:



Triphosgene (82 mg, 0.28 mmol) and NEt_3 (0.10 mL, 0.75 mmol) were dissolved in dry THF (200 mL). **55** (108 mg, 0.25 mmol), dissolved in dry THF (20 mL) was added dropwise within 10 h using a syringe pump. After 14 h, TLC monitoring showed remaining starting material, so triphosgene (5 mg) was added and the solution smoothly heated to 40 °C for 2 h. Then, water (20 mL) and EE (50 mL) were added. The solution was concentrated i.vac. prior to the addition of EE (50 mL). After phase separation, the organic layer was extracted with water (2x200 mL) and brine (1x100 mL), dried over $MgSO_4$, filtered and evaporated i.vac. The crude product was removed from most polar impurities via column chromatography (eluent: EE:PE 7:3). The resulting product mixture was given to HPLC-MS.

HPLC-MS ((2x150 mm Luna Phenyl-Hexyl 3 μ m, acetonitrile:water Grad 40 95A): 6.26 min (4.7% peak area, ESI(+): 142.01, 363.13), 9.93 min (1.5% peak area, ESI(+): 135.90), 12.79 min (19.2% peak area, ESI(+): 182.11, 200.12, 417.05; ESI(-): 212.01), 14.67 min (4.2% peak area, ESI(+): 182.11; ESI(-): 141.83), 14.93 min (3.3% peak area, ESI(+): 129.95, 182.15); ESI(-): 127.83, 141.84, 193.98, 324.04), 19.55 min (58% peak area, ESI(+): 180.18).

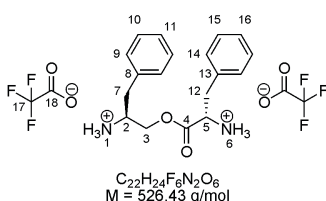
Phosgene (20% in toluene) (0.15 mL, 0.28 mmol) and NEt_3 (0.10 mL, 0.75 mmol) were dissolved in CH_2Cl_2 (200 mL). **55** (108 mg, 0.25 mmol) and NEt_3 (0.07 mL, 0.50 mmol), dissolved in CH_2Cl_2 (20 mL) were added within 10 h using a syringe pump. The reaction mixture was stirred for 48 h. Water was added to quench remaining phosgene. After phase separation, the organic layer was extracted with water (1x100 mL), dried over $MgSO_4$, filtered and evaporated i.vac. The resulting product mixture was given to HPLC-MS.

HPLC-MS ((2x150 mm Luna Phenyl-Hexyl 3 μ m, acetonitrile:water Grad 40 95A): 2.25 min (80.2% peak area, ESI(+): 71.68, 103.83, 204.24); ESI(-):

227.13, 271.13, 300.15), 4.67 min (11.8% peak area, ESI(+): 171.22, 199.24, 302.34, 324.32; ESI(-): 68.39, 112.63, 300.16), 9.98 min (4.9% peak area, ESI(+): 135.94; ESI(-): 112.62, 147.83, 215.13).

The formation of the desired product could not be proven by the means of HPLC-MS.

L-Phenylalaninol-ester-L-Phenylalanine (**56**):



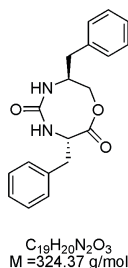
53 (0.11 g, 0.22 mmol) was reacted following the general procedure for the deprotection of the Boc group. The product was obtained in quantitative yield and was used without further purification.

R_F = 0.22 (CH₂Cl₂:MeOH 9:1)

¹H NMR (300 MHz, MeOD, 20 °C): δ 7.44 - 7.20 (m, 10 H, C⁸⁻¹¹H, C¹³⁻¹⁶H), 4.54 - 4.43 (m, 2 H, C³H₂), 4.10 (dd, ³J(*H,H*) = 12.2 Hz, ³J(*H,H*) = 6.2 Hz, 1 H, C⁵H), 3.80 - 3.76 (m, 1 H, C²H), 3.38 - 3.21 (m, 2 H, C¹²H), 3.05 - 2.87 (m, 1 H, C⁷H).

¹³C NMR (MeOD): δ 169.64, 136.17, 135.25, 130.43, 130.30, 130.20, 130.12, 128.98, 128.63, 65.27, 55.21, 52.64, 37.27, 36.38.

Attempted cyclization of **56** to **59**:



Triphosgene (82 mg, 0.28 mmol) and NEt₃ (0.03 mL, 0.22 mmol) were dissolved in CH₂Cl₂ (200 mL). **56** (116 mg, 0.22 mmol) and NEt₃ (0.06 mL,

4 Linear (Ester-[*alt*]-urea)s

0.44 mmol), dissolved in CH₂Cl₂ (20 mL) were added dropwise within 10 h using a syringe pump. The reaction mixture was stirred for 6 h. Water was added to quench remaining phosgene. After phase separation, the organic layer was extracted with water (1x100 mL), dried over MgSO₄, filtered and evaporated. The resulting product mixture was given to HPLC-MS.

HPLC-MS ((2x150 mm Luna Phenyl-Hexyl 3um, acetonitrile:water Grad 40 95A): 9.61 min (20.1% peak area, ESI(+): 152.11, 377.20, 395.16, 417.13; ESI(-): 323.06, 392.96), 13.12 min (75.0% peak area, ESI(+): 230.18, 248.18, 513.05; ESI(-): 260.01).

56 (116 mg, 0.22 mmol) and NEt₃ (0.12 mL, 0.88 mmol) were dissolved in dry THF (200 mL). Triphosgene (20 mg, 0.07 mmol) dissolved in dry THF (20 mL) was added within 15 h using a syringe pump. After 18 h, water (10 mL) was added to quench remaining phosgene. The solution was evaporated i.vac. to give HSE-HC-027-00 (first HPLC). The white solid was suspended in EE and filtered (solid: HSE-HC-027-11, second HPLC). The organic layer was extracted with water (2x20 mL) and brine (1x20 mL), dried over MgSO₄, filtered and evaporated to give HSE-HC-027-10 (third HPLC).

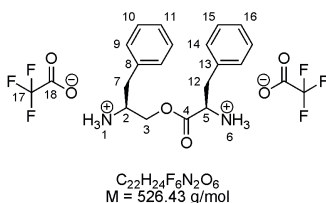
HSE-HC-027-00: HPLC-MS ((2x150 mm Luna Phenyl-Hexyl 3um, acetonitrile:water Grad 40 95A): 8.25 min (9.5% peak area, ESI(+): 307.25, 325.25, 347.19; ESI(-): 323.06), 9.97 min (23.6% peak area, ESI(+): 472.16, 623.26, 645.30; ESI(-): 621.16, 667.10), 15.33 min (61.1% peak area, ESI(+): 180.24, 282.40, 735.47; ESI(-): 392.94, 539.12, 621.09).

HSE-HC-027-10: HPLC-MS ((2x150 mm Luna Phenyl-Hexyl 3um, acetonitrile:water Grad 40 95A): 8.22 min (10.3% peak area, ESI(+): 307.25, 325.25, 347.19; ESI(-): 323.05), 9.95 min (19.0% peak area, ESI(+): 472.16, 623.26, 645.26; ESI(-): 621.18, 667.10), 15.33 min (67.8% peak area, ESI(+): 180.24, 282.40).

HSE-HC-027-11: HPLC-MS ((2x150 mm Luna Phenyl-Hexyl 3um, acetonitrile:water Grad 40 95A): 9.96 min (89.1% peak area, ESI(+): 472.16, 623.26, 645.26; ESI(-): 621.18, 667.10).

The formation of the desired product could not be proven by the means of HPLC-MS.

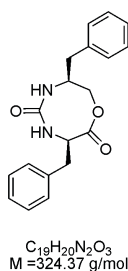
L-Phenylalaninol-*ester*-D-Phenylalanine (**57**):



54 (0.11 g, 0.22 mmol) was reacted following the general procedure for the deprotection of the Boc group. The product was obtained in quantitative yield and was used without further purification and characterization.

R_F = 0.22 (CH_2Cl_2 :MeOH 9:1)

Attempted cyclization of **57** to **60**:



57 (116 mg, 0.22 mmol) and NEt_3 (0.12 mL, 0.88 mmol) were dissolved in dry THF (200 mL). Triphosgene (20 mg, 0.07 mmol) dissolved in dry THF (20 mL) was added within 15 h using a syringe pump. After 26 h, water (10 mL) was added to quench remaining phosgene. The solution was evaporated i.vac. to give HSE-HC-029-00 (first HPLC). The white solid was suspended in CH_2Cl_2 and extracted with water (2x20 mL) and brine (1x20 mL) (each aqueous layer was extracted with CH_2Cl_2), dried over $MgSO_4$, filtered and evaporated i.vac. The solid was suspended in EE and filtered to give HSE-HC-029-10 (second HPLC).

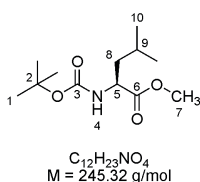
HSE-HC-029-00: HPLC-MS ((2x150 mm Luna Phenyl-Hexyl 3 μ m, acetonitrile:water Grad 40 95A): 5.75 min (4.1% peak area, ESI(+): 101.89, 219.31, 320.40, 623.32), 8.37 min (6.6% peak area, ESI(+): 119.92, 191.21, 307.25, 325.25, 347.23); ESI(-): 96.90, 232.09, 323.09), 10.64 min (21.0%

4 Linear (Ester-[*alt*]-urea)s

peak area, ESI(+): 472.16, 623.29); ESI(-): 162.99, 297.09, 323.06), 10.82 min (8.3% peak area, ESI(+):472.16, 623.29); ESI(-): 162.99, 297.09, 323.06), 13.00 min (3.2% peak area, ESI(+): 947.49; ESI(-): 470.08), 13.36 min (4.5% peak area, ESI(+):947.49; ESI(-): 470.08), 14.12 min (9.7% peak area, ESI(+): 947.49; ESI(-): 470.08), 15.32 min (33.1% peak area, ESI(+): 56.61, 180.24, 282.41, 735.48, 973.48; ESI(-): 337.01, 470.05, 647.09, 794.30).

HSE-HC-029-10: HPLC-MS ((2x150 mm Luna Phenyl-Hexyl 3um, acetonitrile:water Grad 40 95A): 10.54 min (67.5% peak area, ESI(+): 472.16, 623.26); ESI(-): 323.01), 10.90 min (23.1% peak area, ESI(+):472.16, 623.26); ESI(-): 323.06).

Boc-L-Leu-Me (**61**):



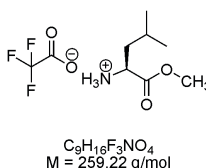
Boc-L-Leu monohydrate (3.74 g, 15.00 mmol) and HOBt (2.03 g, 15.00 mmol) were dissolved in MeOH (75 mL) and cooled to 0 °C. To the cold solution, EDC (4.31 g, 22.50 mmol), dissolved in CH₂Cl₂ (75 mL) was added. The reaction mixture was allowed to warm up to room temperature and stirred for 1 h. TLC monitoring showed an UV-active spot in the region of product and starting material, so further EDC (0.65 g) was added. After 3 h, water was added and the biphasic system stirred for 10 minutes. After phase separation, the organic layer was extracted with 1 M aqueous citric acid solution (1x100 mL), saturated aqueous NaHCO₃-solution (1x100 mL), water (1x100 mL), and brine (1x100 mL). The organic layer was dried over MgSO₄ and evaporated i.vac. to give 6.29 g of the crude product, which was purified via column chromatography on silica (eluent: PE:EE 9:1) to give 3.43 g (yield: 93%) of **61**.

R_F = 0.26 (PE:EE 9:1)

^1H NMR (300 MHz, CDCl_3 , 20 °C): δ 4.95 (d, $^3J(\text{H},\text{H}) = 8.3$ Hz, 1 H, N^4H), 4.29 - 4.22 (m, 1 H, C^5H), 3.67 (s, 3 H, C^7H_3), 1.72 - 1.31 (m, 12 H, 3 C^1H_3 , C^8H_2 , C^9H), 0.90 - 0.87 (m, 6 H, 2 C^{10}H).

^{13}C NMR (CDCl_3): δ 174.05, 155.48, 79.77, 52.15, 41.81, 28.33, 24.79, 22.86, 21.89.

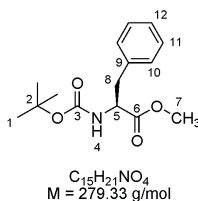
L-Leu-Me (**63**):



61 was reacted following the general procedure for the deprotection of the Boc group. The product was obtained in quantitative yield and was used without further purification and characterization.

$R_F = 0.24$ (CH_2Cl_2 :MeOH 95:5)

Boc-L-Phe-Me (**62**):



Boc-L-Phe (3.98 g, 15.00 mmol) and HOBt (2.03 g, 15.00 mmol) were dissolved in MeOH (75 mL) and cooled to 0 °C. To the cold solution, EDC (4.31 g, 22.50 mmol), dissolved in CH_2Cl_2 (75 mL) was added. The reaction mixture was allowed to warm up to room temperature and stirred for 18 h. Water was added and the biphasic system stirred for 10 minutes. After phase separation, the organic layer was extracted with 1 M aqueous citric acid solution (1x100 mL), saturated aqueous NaHCO_3 -solution (1x100 mL), water (1x100 mL), and brine (1x100 mL). The organic layer was dried over MgSO_4 and evaporated i.vac. to give the crude product which was purified via column chromatography on silica (eluent: PE:EE 9:1) to give 3.95 g (yield: 94%) of **62**.

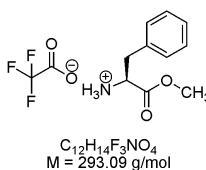
4 Linear (Ester-[*alt*]-urea)s

$R_F = 0.28$ (PE:EE 9:1)

^1H NMR (300 MHz, CDCl_3 , 20 °C): δ 7.30 - 7.10 (m, 5 H, 2 C^{10}H , 2 C^{11}H , C^{12}H), 5.05(d, $^3J(\text{H},\text{H}) = 7.9$ Hz, 1 H, N^4H), 4.62 - 4.52 (m, 1 H, C^5H), 3.69 (s, 3 H, C^7H_3), 3.16 - 2.98 (m, 2 H, C^8H_2), 1.41 (s, 9 H, 3 C^1H_3).

^{13}C NMR (CDCl_3): δ 172.35, 155.10, 136.29, 129.29, 128.53, 127.00, 79.84, 54.45, 52.17, 38.32, 28.29.

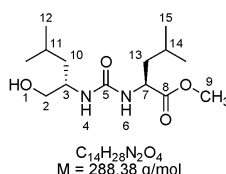
L-Phe-Me (**64**):



62 was reacted following the general procedure for the deprotection of the Boc group. The product was obtained in quantitative yield and was used without further purification and characterization.

$R_F = 0.04$ (Et_2O)

L-Leucinol-*urea*-L-Leucine-Me (**65**):



63 (3.62 g, 13.95 mmol) and NEt_3 (1.94 mL, 13.95 mmol) were dissolved in CH_2Cl_2 (20 mL) and added to a solution of CDI (4.52 g, 27.90 mmol) in CH_2Cl_2 (100 mL) at 0 °C. After the addition, the mixture was stirred at 0 °C for 1 h, then, the mixture was allowed to warm up to room temperature and stirred for 1 h. The reaction mixture was extracted with water (2x100 mL) and brine (1x100 mL). The organic layer was evaporated i.vac. to give the intermediate imidazole-urea.

41 (1.64 g, 13.95 mmol), dissolved in CH_2Cl_2 (100 mL) was cooled to 0 °C and the intermediate imidazole-urea, dissolved in CH_2Cl_2 (20 mL) was added within

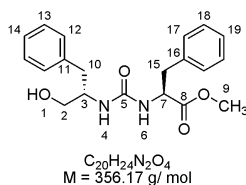
20 minutes. The mixture was allowed to warm up to room temperature and stirred for 10 days. The reaction mixture was extracted with water (1x50 mL), 1 M aqueous citric acid solution (1x100 mL), saturated aqueous NaHCO₃-solution (1x100 mL), water (1x100 mL), and brine (1x100 mL). The organic layer was dried over MgSO₄ and evaporated i.vac. to give 3.9 g of the crude product, which was purified via column chromatography on silica (eluent: EE:PE 1:1 to 9:1) to give 2.54 g (yield: 74%) of **65**.

$R_F = 0.24$ (PE:EE 1:1)

¹H NMR (300 MHz, CDCl₃, 20 °C): δ 5.74 (d, ³ $J(H,H) = 8.0$ Hz, 1 H, N⁶H), 5.32 (d, ³ $J(H,H) = 6.0$ Hz, 1 H, N⁴H), 4.43 - 4.33 (m, 1 H, C⁷H), 3.72 - 3.63 (m, 7 H, O¹H, C³H, C⁹H₃), 3.60 (dd, ² $J(H,H) = 11.0$ Hz, ³ $J(H,H) = 3.3$ Hz, 1 H, 1 C²H₂), 3.46 (dd, ² $J(H,H) = 11.0$ Hz, ³ $J(H,H) = 6.8$ Hz, 1 H, 1 C²H₂), 1.68 - 1.40 (m, 6 H, C¹⁰H, C¹¹H₂, C¹³H, C¹⁴H₂), 0.93 - 0.85 (m, 12 H, 2 C¹²H₃, 2 C¹⁵H₃).

¹³C NMR (CDCl₃): δ 175.44, 159.16, 67.16, 52.27, 51.87, 51.28, 41.78, 40.58, 24.92, 24.87, 23.10, 22.91, 22.29, 22.03.

L-Phenylalaninol-*urea*-L-Phenylalanine (**66**):



64 (1.17 g, 4.00 mmol) and NEt₃ (0.56 mL, 4.00 mmol) were dissolved in CH₂Cl₂ (20 mL) and added to a solution of CDI (1.30 g, 8.00 mmol) in CH₂Cl₂ (100 mL) at 0 °C within 1 h. After the addition, the mixture was stirred at 0 °C for 1 h, then, the mixture was allowed to warm up to room temperature and stirred for 1 h. The reaction mixture was extracted with water (2x100 mL) and brine (1x100 mL). The organic layer was evaporated i.vac. to give the intermediate imidazole-urea.

45 (0.47 g, 4.00 mmol), dissolved in CH₂Cl₂ (30 mL) was cooled to 0 °C and the intermediate imidazole-urea, dissolved in CH₂Cl₂ (20 mL) was added within 20 minutes using a syringe pump. The mixture was allowed to warm up to room

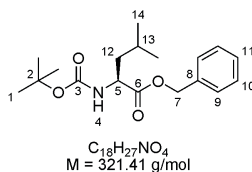
4 Linear (Ester-[*alt*]-urea)s

temperature and stirred for 3 days. The reaction mixture was extracted with water (1x50 mL), 1 M aqueous citric acid solution (2x100 mL), water (1x50 mL), saturated aqueous NaHCO₃-solution (1x100 mL), water (1x50 mL), and brine (1x50 mL). The organic layer was dried over MgSO₄ and evaporated i.vac. to give the crude product, which was recrystallized from EE:PE. Filtrate and solid were purified via column chromatography on silica (eluent: CH₂Cl₂:MeOH 95:5) to give 0.90 g (yield: 92%) of **66**. Despite all efforts, it was not possible to obtain a pure NMR spectrum and a pure HPLC of the compound.

$R_F = 0.44$ (CH₂Cl₂:MeOH 95:5)

High-resolution ESI-MS: $m/z = 357.1809$ (calcd 357.1813 for C₂₀H₂₄N₂O₄ + 1 H⁺), 379.1628 (calcd 379.1634 for C₂₀H₂₄N₂O₄ + 1 Na⁺), 395.1368 (calcd 395.1368 for C₂₀H₂₄N₂O₄ + 1 K⁺).

Boc-L-Leu-Bn (**70**):



Boc-L-Leu monohydrate (3.74 g, 15.00 mmol), benzyl alcohol (3.11 mL, 30.00 mmol), and HOBT (2.03 g, 15.00 mmol) were dissolved in CH₂Cl₂ (30 mL) and cooled to 0 °C. To the cold solution, EDC (4.31 g, 22.5 mmol) in CH₂Cl₂ (50 mL) was added and CH₂Cl₂ was added to give a suspension of a total volume of 130 mL. The suspension was allowed to warm up to room temperature and stirred. After 16 h, water was added to the solution and the biphasic system stirred for 10 minutes. After phase separation, the organic layer was extracted with 1 M aqueous citric acid solution (1x100 mL), water (1x100 mL), saturated aqueous NaHCO₃-solution (1x100 mL), water (1x100 mL) and brine (1x50 mL). The organic layer was dried over MgSO₄, filtered and evaporated i.vac. to give 5.96 g of the crude product, which was purified via column chromatography on silica (eluent: PE:EE 95:5) to give 3.60 g (75% yield) of pure **70**.

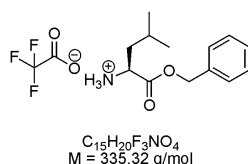
HPLC-MS ((2x150 mm Luna Phenyl-Hexyl 3 μ m, acetonitrile:water Grad 5 95A): 21.60 min (>99.0% peak area, ESI(+): 222.31 (**70** - (Boc) + 1 H⁺), 344.26 (**70** + 1 Na⁺).

R_F = 0.30 (PE:EE 9:1)

¹H NMR (300 MHz, CDCl₃, 20 °C): δ 7.35 - 7.32 (m, 5 H, C⁹⁻¹¹H), 5.21 - 5.10 (m, 2 H, C⁷H), 4.95 (d, ³J(H,H) = 8.2 Hz, 1 H, N⁴H), 4.40 - 4.32 (m, 1 H, C⁵H), 1.78 - 1.33 (m, 12 H, 3 C¹H₃, C¹²H₂, C¹³H), 0.93 - 0.90 (m, 6 H, 2 C¹⁴H₃).

¹³C NMR (CDCl₃): δ 173.42, 155.49, 135.60, 128.63, 128.38, 128.24, 79.86, 66.94, 52.27, 41.76, 28.39, 24.83, 22.91, 21.95.

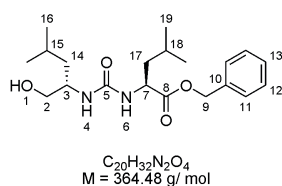
L-Leu-Bn (**72**):



70 (0.96 g, 3.00 mmol) was reacted following the general procedure for the deprotection of the Boc group. The product was obtained in quantitative yield and was used without further purification and characterization.

R_F = 0.06 (PE:EE 9:1)

L-Leucinol-*urea*-L-Leucine-Bn (**74**):



72 (1.01 g, 3.00 mmol) and NEt₃ (0.42 mL, 3.00 mmol) were dissolved in CH₂Cl₂ (20 mL) and added to a solution of CDI (0.97 g, 6.00 mmol) in CH₂Cl₂ (50 mL) at 0 °C within 1 h. After the addition, the mixture was stirred at 0 °C for 1 h, then the mixture was allowed to warm up to room temperature and stirred for 1 h. The reaction mixture was extracted with water (2x100 mL) and

4 Linear (Ester-[*alt*]-urea)s

brine (1x100 mL). The organic layer was dried over MgSO_4 , filtered and evaporated i.vac. to give the intermediate imidazole-urea.

41 (0.35 g, 3.00 mmol), dissolved in CH_2Cl_2 (100 mL) was cooled to 0 °C and the intermediate imidazole-urea, dissolved in CH_2Cl_2 (20 mL) was added within 20 minutes. The mixture was allowed to warm up to room temperature and stirred for 16 h. The reaction mixture was extracted with water (1x50 mL), 1 M aqueous citric acid solution (1x50 mL), water (1x50 mL), saturated aqueous NaHCO_3 -solution (1x50 mL), water (1x50 mL), and brine (1x50 mL). The organic layer was dried over MgSO_4 , filtered and evaporated i.vac. to give 1.16 g of the crude product which was purified via column chromatography on silica (eluent: PE:EE 1:1). The Second column gave 900 mg (82%) of pure product as colorless crystals.

HPLC-MS ((2x150 mm Luna Phenyl-Hexyl 3 μm , acetonitrile:water Grad 5 95A): 18.57 min (>99.0% peak area, ESI(+): 365.28 (**74** + 1 H^+), 387.30 (**74** + 1 Na^+)).

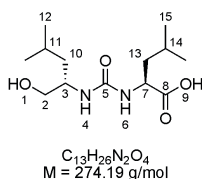
R_f = 0.50 (PE:EE 2:8)

^1H NMR (300 MHz, CDCl_3 , 20 °C): δ 7.36 - 7.31 (m, 5 H, C^{11-13}H), 5.99 - 5.94 (m, 1 H, N^6H), 5.59 - 5.54 (m, 1 H, N^4H), 5.19 - 5.07 (m, 2 H, C^9H_2), 4.48 - 4.42 (m, 1 H, C^7H), 4.00 (br s, 1 H, O^1H), 3.76 - 3.71 (m, 1 H, C^3H), 3.58 (dd, $^2J(\text{H},\text{H}) = 11.0$ Hz, $^3J(\text{H},\text{H}) = 3.4$ Hz, 1 H, 1 C^2H_2), 3.46 (dd, $^2J(\text{H},\text{H}) = 11.0$ Hz, $^3J(\text{H},\text{H}) = 6.5$ Hz, 1 H, 1 C^2H_2), 1.72 - 1.46 (m, 4 H, C^{14}H_2 , C^{17}H_2), 1.44 - 1.23 (m, 2 H, C^{15}H , C^{18}H), 0.93 - 0.87 (m, 12 H, 2 C^{16}H_3 , 2 C^{19}H_3).

^{13}C NMR (CDCl_3): δ 174.56, 159.16, 135.50, 128.54, 128.28, 128.04, 66.90, 66.84, 51.96, 51.06, 41.55, 40.48, 24.81, 24.78, 23.06, 22.82, 22.25, 21.98.

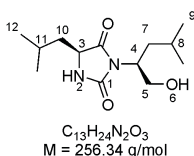
High-resolution ESI-MS: m/z = 365.2435 (calcd 365.2443 for $\text{C}_{20}\text{H}_{32}\text{N}_2\text{O}_4$ + 1 H^+), 387.2254 (calcd 387.2263 for $\text{C}_{20}\text{H}_{32}\text{N}_2\text{O}_4$ + 1 Na^+), 751.4616 (calcd 751.4634 for $(\text{C}_{20}\text{H}_{32}\text{N}_2\text{O}_4)_2$ + 1 Na^+), 767.4356 (calcd 767.4375 for $(\text{C}_{20}\text{H}_{32}\text{N}_2\text{O}_4)_2$ + 1 K^+), 1093.7159 (calcd 1093.7176 for $(\text{C}_{20}\text{H}_{32}\text{N}_2\text{O}_4)_3$ + 1 H^+).

L-Leucinol-*urea*-L-Leucine(**67**):



Synthesis via saponification of **65**:

65 (0.24 g, 0.84 mmol) was reacted following the general procedure for the deprotection of the methyl ester. In addition to the protocol, the aqueous layer was also extracted with EE. Reaction-time: 1.5 h. The analytical data did not fit with the structure of the desired product. Attempts to recrystallize the crude product failed. HPLC-MS-data and ¹H NMR, COSY and NOESY suggest the quantitative formation of **69**.



HPLC-MS ((2x150 mm Luna Phenyl-Hexyl 3um, acetonitrile:water Grad 5 95A): 17.58 min (94.8% peak area, ESI(+): 257.34).

¹H NMR (400 MHz, CDCl₃, 20 °C): δ 6.51 (br s, 1 H, N²H), 4.29 - 4.20 (m, 1 H, C⁴H), 4.09 - 4.02 (m, 1 H, C³H), 3.94 (dd, ²J(*H,H*) = 12.0 Hz, ³J(*H,H*) = 7.7 Hz, 1 H, 1 C⁵H₂), 3.74 (dd, ²J(*H,H*) = 12.0 Hz, ³J(*H,H*) = 3.4 Hz, 1 H, 1 C⁵H₂), 2.50 (br s, 1 H, O⁶H), 1.90 - 1.73 (m, 3 H, 1 C⁷H₂, C⁸H or C¹¹H, 1 C¹⁰H₂), 1.56 - 1.41 (m, 3 H, 1 C⁷H₂, C⁸H or C¹¹H, 1 C¹⁰H₂), 1.02 - 0.86 (m, 12 H, 2 C⁹H₃, 2 C¹²H₃).

To a solution of **65** (0.058 g, 0.200 mmol) in acetonitrile (5 mL), formic acid (0.05 mL) was added and the solution stirred for 1 h. The solution was evaporated i.vac. and directly given to HPLC-MS.

HPLC-MS ((2x150 mm Luna Phenyl-Hexyl 3um, acetonitrile:water Grad 5 95A): 15.33 min (33.9% peak area, ESI(+): 289.32, **65**), 15.79 min (62.5% peak area, ESI(+): 257.32).

4 Linear (Ester-[*alt*]-urea)s

65 was reacted following the general procedure for the deprotection of the methyl ester. Different from the protocol, the reaction mixture was not acidified prior to extraction with CH₂Cl₂ and EE. Since the product could not be extracted from the aqueous layer, the latter one was acidified by the addition of citric acid.

HPLC-MS ((2x150 mm Luna Phenyl-Hexyl 3 μ m, acetonitrile:water Grad 5 95A): 13.50 min (10.1% peak area, ESI(+): 275.32), 14.41 min (9.7% peak area, ESI(+): 275.32), 15.76 min (4.9% peak area, ESI(+): 257.32).

Synthesis via reductive cleavage on **74**:

74 (87 mg, 0.24 mmol) was reacted following the general procedure for the deprotection of the Z group or benzyl ester. EE (20 mL), Pd/C (9 mg), reaction time: 1.5 h, hydrogen pressure: 5 bar.

HPLC-MS ((2x150 mm Luna Phenyl-Hexyl 3 μ m, acetonitrile:water Grad 5 95A): 14.06 min (13.5% peak area, ESI(-): 273.20 (**67** - 1 H⁺), 547.25 ((**67**)₂ - 1 H⁺), ESI(+): 275.36, (**67** + 1 H⁺)). Peak area calculation also included solvent peaks. Elugram was very pure.

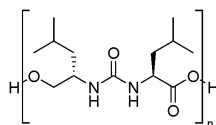
R_f = 0.16 (PE:EE 2:8)

¹H NMR (300 MHz, MeOD, 20 °C): δ 4.28 (dd, ³ $J(H,H)$ = 9.5 Hz, ³ $J(H,H)$ = 5.2 Hz, 1 H, C⁷H), 3.77 - 3.71 (m, 1 H, C³H), 3.52 - 3.40 (m, 2 H, C²H₂), 1.84 - 1.46 (m, 4 H, C¹⁰H₂, C¹³H₂), 1.39 - 1.25 (m, 2 H, C¹¹H, C¹⁴H), 0.98 - 0.89 (m, 12 H, C¹²H₃, C¹⁵H₃).

¹³C NMR (MeOD): δ 177.41, 160.57, 66.23, 52.69, 50.97, 42.56, 41.92, 25.96, 25.82, 23.78, 23.42, 22.48, 22.05.

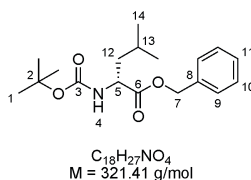
High-resolution ESI-MS: m/z = 275.1965 (calcd 275.1967 for C₁₃H₂₆N₂O₄ + 1 H⁺), 297.1785 (calcd 297.1787 for C₁₃H₂₆N₂O₄ + 1 Na⁺), 313.1524 (calcd 313.1527 for C₁₃H₂₆N₂O₄ + 1 K⁺).

Attempted polymerizations of L-Leucinol-*urea*-L-Leucine(**67**):



In a typical procedure, **67** and coupling catalyst (HOBT, DMAP or DPTS) (1 eq.) were dissolved in the respective solvent. Under stirring, neat coupling reagent (EDC, DIC or TBTU) (2 to 4 eq.) was added and the mixture stirred. All details (reaction time, work-up etc..) are displayed in Special Part chapter 2, table 1.

Boc-D-Leu-Bn (**71**):



Boc-D-Leu monohydrate (12.47 g, 50.00 mmol), benzyl alcohol (5.18 mL, 50.00 mmol), and HOBT (6.76 g, 50.00 mmol) were dissolved in CH_2Cl_2 (200 mL) and cooled to 0 °C. To the cold solution, EDC (14.38 g, 75.00 mmol) in CH_2Cl_2 (200 mL) was added. CH_2Cl_2 was added to give a suspension with a total volume of 500 mL. The suspension was allowed to warm up to room temperature and stirred for 4 h. TLC monitoring showed remaining alcohol and remaining acid, so EDC (1.0 g) was added. After 18 h, TLC monitoring still showed starting material, so benzyl alcohol (4.0 mL) and EDC (1.75 g) were added. After 20 h, the solution was concentrated i.vac. to a volume of 150 mL and stirred. After 24 h, the reaction mixture was concentrated i.vac. and redissolved in EE (200 mL). Water was added to the solution and the biphasic system stirred for 10 minutes. After phase separation, the organic layer was extracted with water (3x150 mL), 1 M aqueous citric acid solution (2x100 mL), water (1x100 mL), saturated aqueous $NaHCO_3$ -solution (1x100 mL), water (1x100 mL), and brine (1x50 mL). The organic layer was dried over $MgSO_4$, filtered and evaporated i.vac. to give 17.2 g of the crude product which was purified via column chromatography on silica (eluent: PE:Et₂O 2:1) to give 12.54 g (78% yield) of pure **71** after 3 columns.

4 Linear (Ester-[*alt*]-urea)s

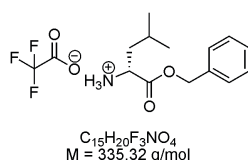
HPLC-MS ((2x150 mm Luna Phenyl-Hexyl 3 μ m, acetonitrile:water Grad 5 95A): 21.70 min (>99.0% peak area, ESI(+): 222.32 (**71** - (Boc) + 1 H⁺), 344.28 (**71** + 1 Na⁺).

R_F = 0.54 (PE:Et₂O 1:1)

¹H NMR (300 MHz, CDCl₃, 20 °C): δ 7.35 - 7.32 (m, 5 H, C⁹⁻¹¹H), 5.21 - 5.10 (m, 2 H, C⁷H), 4.97 (d, ³J(H,H) = 7.8 Hz, 1 H, N⁴H), 4.39 - 4.33 (m, 1 H, C⁵H), 1.79 - 1.31 (m, 12 H, 3 C¹H₃, C¹²H₂, C¹³H), 0.93 - 0.90 (m, 6 H, 2 C¹⁴H₃).

¹³C NMR (CDCl₃): δ 173.39, 155.48, 135.60, 128.60, 128.36, 128.22, 79.83, 66.90, 52.27, 41.72, 28.37, 24.81, 22.88, 21.93.

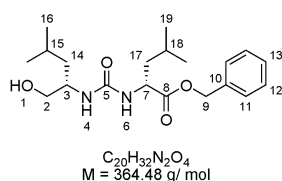
D-Leu-Bn (**73**):



71 (12.54 g, 39.00 mmol) was reacted following the general procedure for the deprotection of the Boc group. The product was obtained in quantitative yield and was used without further purification and characterization.

R_F = 0.16 (Et₂O)

L-Leucinol-urea-D-Leucine-Bn (**75**):



73 (13.08 g, 39.00 mmol) and NEt₃ (7.59 mL, 54.60 mmol) were dissolved in CH₂Cl₂ (100 mL) and added to a solution of CDI (12.65 g, 78.00 mmol) in CH₂Cl₂ (400 mL) at 0 °C within 1 h. After the addition, the mixture was stirred for 1 h at 0 °C, then for 2 h at room temperature. The reaction mixture was extracted with water (2x100 mL). The organic layer was dried over MgSO₄, filtered and evaporated i.vac. to give the intermediate imidazole-urea.

41 (4.80 g, 40.95 mmol), dissolved in CH₂Cl₂ (400 mL) was cooled to 0 °C and the intermediate imidazole-urea, dissolved in CH₂Cl₂ (100 mL) was added within 1 h. The mixture was allowed to warm up to room temperature and stirred for 16 h. Water was added to the reaction mixture and the biphasic system was stirred for 30 minutes. After phase separation, the organic layer was evaporated i.vac. and CH₂Cl₂ was replaced by EE. The organic layer was extracted with water (2x100 mL), 1 M aqueous citric acid solution (2x50 mL), water (1x50 mL), saturated aqueous NaHCO₃-solution (1x50 mL), water (1x50 mL), and brine (1x50 mL). The organic layer was dried over MgSO₄, filtered and evaporated i.vac. to give the crude product which was purified via recrystallization from PE:CH₂Cl₂ to give 12.51 g (88%) of pure **75** as colorless crystals.

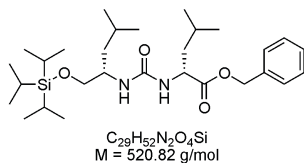
HPLC-MS ((2x150 mm Luna Phenyl-Hexyl 3um, acetonitrile:water Grad 5 95A): 18.82 min (>99.0% peak area, ESI(+): 365.29 (**75** + 1 H⁺), 387.30 (**75** + 1 Na⁺)).

R_F = 0.50 (PE:EE 2:8)

¹H NMR (300 MHz, CDCl₃, 20 °C): δ 7.34 - 7.30 (m, 5 H, C¹¹⁻¹³H), 6.01 (d, ³J(H,H) = 6.7 Hz, 1 H, N⁶H), 5.66 - 5.60 (m, 1 H, N⁴H), 5.20 - 5.05 (m, 2 H, C⁹H₂), 4.56 - 4.44 (m, 1 H, C⁷H), 4.17 (br s, 1 H, O¹H), 3.85 - 3.70 (m, 1 H, C³H), 3.60 (dd, ²J(H,H) = 11.0 Hz, ³J(H,H) = 3.2 Hz, 1 H, 1 C²H₂), 3.41 (dd, ²J(H,H) = 11.0 Hz, ³J(H,H) = 5.8 Hz, 1 H, 1 C²H₂), 1.79 - 1.46 (m, 4 H, C¹⁴H₂, C¹⁷H₂), 1.44 - 1.17 (m, 2 H, C¹⁵H, C¹⁸H), 0.93 - 0.87 (m, 12 H, C¹⁶H₃, C¹⁹H₃).

¹³C NMR (CDCl₃): δ 175.21, 158.86, 135.38, 128.50, 128.25, 128.00, 66.89, 66.09, 51.77, 50.48, 41.47, 40.79, 24.79, 23.03, 22.79, 22.27, 21.87.

TIPS-L-Leucinol-urea-D-Leucine-Bn (**78**):

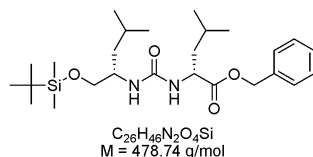


75 (0.21 g, 0.56 mmol), imidazole (0.08 g, 1.12 mmol), and DMAP (0.007 g, 0.056 mmol) were dissolved in CH₂Cl₂ (10 mL). TIPSCI (0.24 mL, 1.12 mmol)

4 Linear (Ester-[*alt*]-urea)s

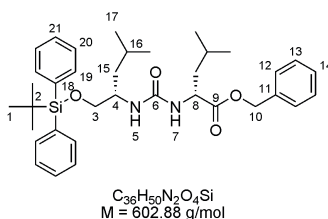
was added and the solution stirred for 1 h. A white precipitate was formed quickly. TIPSCl (0.06 mL) and imidazole (20 mg) were added until TLC monitoring showed no unreacted **75**. The suspension was diluted with CH₂Cl₂ and water. The organic layer was extracted with water (1x50 mL). The aqueous layers were extracted with CH₂Cl₂. The combined organic layers were dried over MgSO₄ and evaporated i.vac. The residue was suspended in PE:CH₂Cl₂ and filtered to remove very polar impurities. The remaining oily substance (210 mg) was purified via column chromatography on silica. Product decomposed on silica to form **75**. Isolation of the desired product was not possible.

TBDMS-L-Leucinol-*urea*-D-Leucine-Bn (**79**):



75 (0.21 g, 0.56 mmol), imidazole (0.08 g, 1.12 mmol), and DMAP (0.007 g, 0.056 mmol) were dissolved in CH₂Cl₂ (10 mL). TBDMSCl (0.17 g, 1.12 mmol) was added and the solution stirred for 1 h. The suspension was diluted with CH₂Cl₂ and water. The organic layer was extracted with water (1x50 mL). The aqueous layers were extracted with CH₂Cl₂. The combined organic layers were dried over MgSO₄ and evaporated i.vac. TLC monitoring confirmed quick decomposition to **75**. The desired product could not be isolated.

TBDPS-L-Leucinol-*urea*-D-Leucine-Bn (**77**):



75 (5.45 g, 14.95 mmol), imidazole (2.04 g, 29.90 mmol), and TBDPSCl (0.17 g, 1.12 mmol) were dissolved in DMF (50 mL) and stirred for 3 h. The solution was poured on ice, the aqueous layer extracted with Et₂O, dried over

MgSO₄, and evaporated i.vac. The crude product was purified via column chromatography on silica (eluent: PE:EE 10:1) to give 7.63 g (yield: 85%) of the desired product. NMR sample in CDCl₃ showed decomposition. Product could be stored in freezer without decomposition.

HPLC-MS ((2x150 mm Luna Phenyl-Hexyl 3um, acetonitrile:water Grad 40 95A): 20.02 min (>99.0% peak area, ESI(+): 603.33 (**77** + 1 H⁺)).

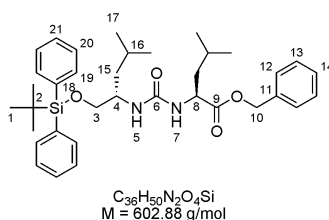
R_F = 0.70 (PE:EE 10:1)

¹H NMR (300 MHz, CD₃CN, 20 °C): δ 7.70 - 7.67 (m, 4 H, 4 C¹⁹H), 7.45 - 7.34 (m, 11 H, C¹²⁻¹⁴H, 2 C²⁰⁻²¹H), 5.31 (d, ³J(H,H) = 8.3 Hz, 1 H, N⁷H), 5.12 (s, 2 H, C¹⁰H₂), 5.05 (d, ³J(H,H) = 8.3 Hz, 1 H, N⁵H), 4.39 - 4.31 (m, 1 H, C⁵H), 3.86 - 3.82 (m, 1 H, C⁴H), 3.61 - 3.58 (m, 1 H, C³H₂), 1.66 - 1.37 (m, 6 H, 2 C¹⁵H₂, 2 C¹⁶H), 1.06 (s, 9 H, 3 C¹H₃), 0.98 - 0.83 (m, 12 H, 4 C¹⁷H₃).

¹³C NMR (CD₃CN): δ 174.64, 158.24, 137.27, 136.44, 134.55, 134.47, 130.79, 130.74, 129.43, 129.03, 128.87, 128.76, 67.52, 67.98, 52.65, 50.35, 42.11, 41.81, 27.25, 25.60, 25.58, 23.49, 23.13, 22.56, 22.06, 19.85.

High-resolution ESI-MS: m/z = 603.3604 (calcd 603.3613 for C₃₆H₅₁N₂O₄Si₁ + 1 H⁺), 625.3426 (calcd 625.3432 for C₃₆H₅₀N₂O₄Si₁ + 1 Na⁺).

TBDPS-L-Leucinol-*urea*-L-Leucine-Bn (**76**):



74 (5.45 g, 14.95 mmol), imidazole (2.04 g, 29.90 mmol), and TBDPSCI (0.17 g, 1.12 mmol) were dissolved in DMF (50 mL) and stirred for 3 h. The solution was poured on ice, the aqueous layer extracted with Et₂O, dried over MgSO₄, and evaporated i.vac. The crude product was purified via column chromatography on silica (eluent: PE:EE 10:1) to give 7.63 g (yield: 85%) of the desired product. NMR sample in CDCl₃ showed decomposition. Product could be stored in freezer without decomposition.

4 Linear (Ester-[*alt*]-urea)s

UPLC-MS ((2.1x100 mm BEH Phenyl 1.7um, acetonitrile:water Grad 40 95A):: 4.60 min (86.1% peak area, ESI(+): 603.35 (**76** + 1 H⁺), 625.32 (**76** + 1 Na⁺)).

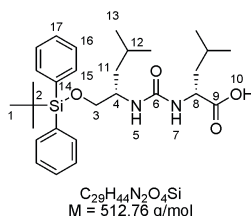
R_F = 0.70 (PE:EE 10:1)

¹H NMR (300 MHz, CD₂Cl₂, 20 °C): δ 7.72 - 7.56 (m, 4 H, C¹⁹H), 7.38 - 7.25 (m, 11 H, C¹²⁻¹⁴H, C²⁰⁻²¹H), 5.10 (s, 2 H, C¹⁰H₂), 4.67 (d, ³J(H,H) = 8.7 Hz, 1 H, N⁷H), 4.46 (d, ³J(H,H) = 9.1 Hz, 1 H, N⁵H), 4.43 - 4.34 (m, 1 H, C⁵H), 3.84 - 3.71 (m, 1 H, C⁴H), 3.65 - 3.51 (m, 1 H, C³H₂), 1.67 - 1.25 (m, 6 H, 2 C¹⁵H₂, 2 C¹⁶H), 1.00 (s, 9 H, 3 C¹H₃), 0.91 - 0.74 (m, 12 H, 4 C¹⁷H₃).

¹³C NMR (CD₂Cl₂): δ 173.98, 156.94, 135.90, 135.58, 133.62, 133.47, 129.72, 129.69, 128.48, 128.17, 128.02, 127.69, 66.63, 66.53, 51.77, 49.84, 41.82, 41.22, 26.68, 24.77, 24.74, 22.81, 22.65, 21.61, 20.79, 19.18.

High-resolution ESI-MS: m/z = 603.3449 (calcd 603.3618 for C₃₆H₅₁N₂O₄Si₁ + 1 H⁺).

TBDPS-L-Leucinol-*urea*-D-Leucine (**81**):



TBDPS-L-Leucinol-*urea*-D-Leucine-Bn (1.00 g, 1.60 mmol) was reacted following the general procedure for the deprotection of the Z group or benzyl ester. EtOH (50 mL), Pd/C (120 mg), reaction time: 12 h, hydrogen pressure: 1 bar. Yield: 58%.

HPLC-MS ((2x150 mm Luna Phenyl-Hexyl 3um, acetonitrile:water Grad 40 95A): 17.18 min (>99.9% peak area, ESI(-): 511.13 (**81** - 1 H⁺)).

R_F = 0.50 (CH₂Cl₂:MeOH 100:5)

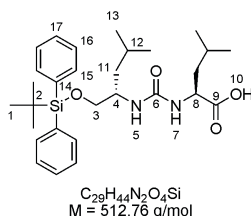
¹H NMR (300 MHz, CD₃CN, 20 °C): δ 7.70 - 7.66 (m, 4 H, C¹⁵H), 7.45 - 7.42 (m, 6 H, C¹⁶⁻¹⁷H), 5.42 (d, ³J(H,H) = 7.1 Hz, 1 H, N⁷H), 5.29 (d, ³J(H,H) = 8.3 Hz, 1 H, N⁵H), 4.20 - 4.16 (m, 1 H, C⁵H), 3.80 - 3.77 (m, 1 H,

C^4H), 3.63 - 3.60 (m, 1 H, C^3H_2), 1.81 - 1.31 (m, 6 H, 2 $C^{11}H_2$, 2 $C^{12}H$), 1.06 (s, 9 H, 3 C^1H_3), 0.91 - 0.86 (m, 12 H, 4 $C^{13}H_3$).

^{13}C NMR (CD_3CN): δ 174.55, 158.66, 135.47, 129.85, 129.79, 127.81, 66.41, 52.15, 49.73, 40.61, 40.31, 26.27, 24.61, 24.58, 22.46, 22.26, 21.56, 20.99, 18.88.

High-resolution ESI-MS: m/z = 513.3134 (calcd 513.3143 for $C_{29}H_{45}N_2O_4Si_1 + 1 H^+$), 535.2957 (calcd 535.2963 for $C_{29}H_{44}N_2O_4Si_1 + 1 Na^+$).

TBDPS-L-Leucinol-*urea*-L-Leucine (**80**):



TBDPS-L-Leucinol-*urea*-L-Leucine-Bn (1.00 g, 1.60 mmol) was reacted following the general procedure for the deprotection of the Z group or benzyl ester. EtOH (50 mL), Pd/C (120 mg), reaction time: 12 h, hydrogen pressure: 1 bar. Yield: 58%.

UPLC-MS ((2.1x100 mm BEH Phenyl 1.7 μ m, acetonitrile:water Grad 40 95A): 4.86 min (68.0% peak area, ESI(+): 513.33 (**80** + 1 H^+)).

R_F = 0.50 (CH_2Cl_2 :MeOH 100:5)

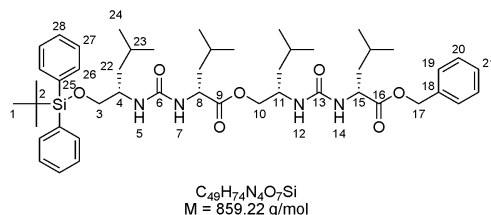
1H NMR (300 MHz, CD_2Cl_2 , 20 $^\circ C$): δ 7.71 - 7.65 (m, 4 H, $C^{15}H$), 7.50 - 7.37 (m, 6 H, $C^{16-17}H$), 5.34 - 5.24 (m, 1 H, N^7H), 5.20 - 5.07 (m, 1 H, N^5H), 4.30 - 4.20 (m, 1 H, C^5H), 3.90 - 3.75 (m, 1 H, C^4H), 3.71 - 3.59 (m, 1 H, C^3H_2), 1.81 - 1.31 (m, 6 H, 2 $C^{11}H_2$, 2 $C^{12}H$), 1.09 (s, 9 H, 3 C^1H_3), 1.04 - 0.88 (m, 12 H, 4 $C^{13}H_3$).

^{13}C NMR (CD_2Cl_2): δ 175.70, 158.96, 135.57, 133.38, 133.23, 129.78, 128.48, 128.03, 127.75, 66.70, 60.33, 40.83, 40.39, 26.68, 24.72, 24.68, 22.76, 22.76, 21.99, 21.52, 19.98.

High-resolution ESI-MS: m/z = 513.3134 (calcd 513.3143 for $C_{29}H_{45}N_2O_4Si_1 + 1 H^+$), 535.2957 (calcd 535.2963 for $C_{29}H_{44}N_2O_4Si_1 + 1 Na^+$).

4 Linear (Ester-[*alt*]-urea)s

TBDPS-(L-Leucinol-*urea*-D-Leucine)₂-Bn (**83**):



75 (1.50 g, 4.12 mmol), TBDPS-L-Leucinol-*urea*-D-Leucine (2.32 g, 4.53 mmol), and DMAP (0.50 g, 4.12 mmol) were dissolved in CH_2Cl_2 (100 mL) and cooled to 0 °C. EDC (1.74 g, 9.05 mmol), dissolved in CH_2Cl_2 (5 mL) was added slowly. The reaction mixture was allowed to warm up to room temperature, stirred for 5 h and evaporated i.vac. The residue was purified via column chromatography on silica (eluent: PE:EE 4:2) to give 1.88 g (yield: 53%) of the desired product. HPLC-MS ((2x150 mm Luna Phenyl-Hexyl 3 μ m, acetonitrile:water Grad 70 95A): 15.75 min (95.8% peak area, ESI(+): 859.52 (**83** + 1 H^+)).

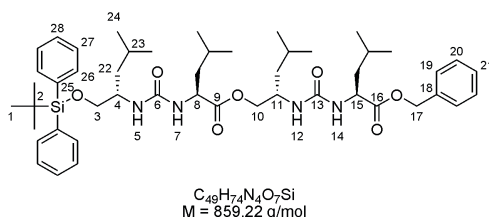
$R_F = 0.50$ (PE:EE 2:1)

1H NMR (300 MHz, CD_3CN , 20 °C): δ 7.70 - 7.64 (m, 4 H, $C^{26}H$), 7.45 - 7.37 (m, 10 H, $C^{19-21}H$, $C^{27-28}H$), 5.43 (d, $^3J(H,H) = 7.2 \text{ Hz}$, 1 H, NH), 5.32 (d, $^3J(H,H) = 7.6 \text{ Hz}$, 1 H, NH), 5.23 - 5.04 (m, 4 H, $C^{17}H_2$, 2 NH), 4.35 - 4.12 (m, 3 H, C^8H , $C^{11}H$, $C^{15}H$), 3.95 - 3.76 (m, 3 H, C^4H , $C^{10}H_2$), 3.64 - 3.51 (m, 1 H, C^3H_2), 1.72 - 1.16 (m, 12 H, 4 $C^{22}H_2$, 4 $C^{23}H$), 1.04 (s, 9 H, 3 C^1H_3), 0.94 - 0.74 (m, 24 H, 8 $C^{24}H_3$).

^{13}C NMR (CD_3CN): δ 173.67, 173.30, 157.77, 157.57, 136.27, 135.49, 133.50, 133.45, 129.82, 129.79, 128.50, 128.10, 127.94, 127.80, 117.33, 66.83, 66.47, 66.18, 52.14, 51.70, 49.39, 47.02, 41.05, 40.98, 40.94, 40.74, 26.31, 24.64, 24.59, 24.48, 22.57, 22.42, 22.18, 21.65, 21.37, 21.15, 21.09, 18.89.

High-resolution ESI-MS: $m/z = 859.5402$ (calcd 859.5400 for $C_{49}H_{75}N_4O_7Si_1 + 1 H^+$).

TBDPS-(L-Leucinol-*urea*-L-Leucine)₂-Bn (**82**):



74 (1.50 g, 4.12 mmol), TBDPS-L-Leucinol-*urea*-L-Leucine (2.32 g, 4.53 mmol), and DMAP (0.50 g, 4.12 mmol) were dissolved in CH₂Cl₂ (100 mL) and cooled to 0 °C. EDC (1.74 g, 9.05 mmol), dissolved in CH₂Cl₂ (5 mL) was added slowly. The reaction mixture was allowed to warm up to room temperature, stirred for 5 h and evaporated i.vac. The residue was purified via column chromatography on silica (eluent: PE:EE 4:2) to give 1.88 g (yield: 53%) of the desired product.

UPLC-MS ((2.1x100 mm BEH Phenyl 1.7μm, acetonitrile:water Grad 40 95A): 5.61 min (84.0% peak area, ESI(+): 860.51 (**82** + 1 H⁺), 882.50 (**82** + 1 Na⁺)).

R_F = 0.50 (PE:EE 2:1)

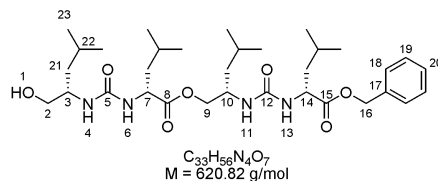
¹H NMR (300 MHz, CDCl₃, 20 °C): δ 7.67 - 7.62 (m, 4 H, C²⁶H), 7.43 - 7.28 (m, 10 H, C¹⁹⁻²¹H, C²⁷⁻²⁸H), 5.42 - 5.26 (m, 2 H, 2 NH), 5.15 - 4.90 (m, 3 H, C¹⁷H₂, NH), 4.73 - 4.60 (m, 1 H, NH), 4.57 - 4.42 (m, 2 H, C⁸H, C¹⁵H), 4.35 - 4.24 (m, 1 H, C¹¹H), 4.07 - 3.93 (m, 1 H, C⁴H), 3.95 - 3.57 (m, 4 H, C³H₂, C¹⁰H₂), 1.73 - 1.24 (m, 12 H, 4 C²²H₂, 4 C²³H), 1.07 (s, 9 H, 3 C¹H₃), 0.98 - 0.82 (m, 24 H, 8 C²⁴H₃).

¹³C NMR (CD₃CN): δ 173.67, 173.30, 157.77, 157.57, 136.27, 135.49, 133.50, 133.45, 129.82, 129.79, 128.50, 128.10, 127.94, 127.80, 117.33, 66.83, 66.47, 66.18, 52.14, 51.70, 49.39, 47.02, 41.05, 40.98, 40.94, 40.74, 26.31, 24.64, 24.59, 24.48, 22.57, 22.42, 22.18, 21.65, 21.37, 21.15, 21.09, 18.89.

High-resolution ESI-MS: m/z = 859.5394 (calcd 859.5400 for C₄₉H₇₅N₄O₇Si₁ + 1 H⁺).

4 Linear (Ester-[*alt*]-urea)s

(L-Leucinol-*urea*-D-Leucine)₂-Bn (**85**):



83 (0.22 g, 0.26 mmol) was dissolved in acetonitrile (10 mL) and HF (0.10 mL) was added. The reaction mixture was stirred for 2 h. K₂CO₃ was added and the solution filtered and evaporated i.vac. The residue was purified via column chromatography on silica (eluent: CH₂Cl₂:MeOH 10:1) to give 0.16 g (yield: 98%) of the desired product.

HPLC-MS ((2x150 mm Luna Phenyl-Hexyl 3um, acetonitrile:water Grad 40 95A): 14.80 min (>99.9% peak area, ESI(+): 621.35 (**85** + 1 H⁺)).

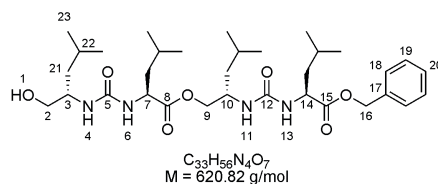
R_F = 0.50 (CH₂Cl₂:MeOH 10:1)

¹H NMR (400 MHz, CD₂Cl₂, 20 °C): δ 7.40 - 7.31 (m, 5 H, C¹⁸⁻²⁰H), 5.16 (d, ³J(H,H) = 7.8 Hz, 1 H, N¹³H), 5.11 (d, ³J(H,H) = 8.2 Hz, 1 H, N⁶H), 5.15 (dd, ²J(H,H) = 51.3 Hz, ³J(H,H) = 12.4 Hz, 2 H, C¹⁶H₂), 4.89 (d, ³J(H,H) = 8.0 Hz, 1 H, N⁴H), 4.84 (d, ³J(H,H) = 9.4 Hz, 1 H, N¹¹H), 4.39 - 4.31 (m, 2 H, C⁷H, C¹⁴H), 4.25 - 4.20 (m, 1 H, O¹H), 4.13 - 4.02 (m, 2 H, 1 C⁹H₂, C¹⁰H), 3.89 - 3.81 (m, 2 H, C³H, 1 C⁹H₂), 3.67 - 3.61 (m, 1 H, 1 C²H₂), 3.39 - 3.32 (m, 1 H, 1 C²H₂), 1.81 - 1.18 (m, 12 H, 4 C²¹H₂, 4 C²²H), 0.97 - 0.87 (m, 24 H, 8 C²³H₃).

¹³C NMR (CD₂Cl₂): δ 174.67, 173.40, 159.65, 158.15, 135.61, 128.52, 128.03, 67.91, 66.86, 66.59, 53.79, 53.43, 53.06, 50.67, 47.23, 40.84, 40.79, 40.60, 40.52, 24.82, 24.71, 22.88, 22.78, 22.75, 22.60, 22.09, 21.77.

High-resolution ESI-MS: m/z = 621.4230 (calcd 621.4222 for C₃₃H₅₆N₄O₇ + 1 H⁺), 643.4049 (calcd 643.4041 for C₃₃H₅₆N₄O₇ + 1 Na⁺), 1241.8374 (calcd 1241.8371 for C₆₆H₁₁₂N₈O₁₄ + 1 H⁺), . 1263.8182 (calcd 1263.8190 for C₆₆H₁₁₂N₈O₁₄ + 1 Na⁺).

(L-Leucinol-*urea*-L-Leucine)₂-Bn (**90**):



82 (0.22 g, 0.26 mmol) was dissolved in acetonitrile (10 mL) and HF (0.10 mL) was added. The reaction mixture was stirred for 2 h. K₂CO₃ was added and the solution filtered and evaporated i.vac. The residue was purified via column chromatography on silica (eluent: CH₂Cl₂:MeOH 10:1) to give 0.16 g (yield: 98%) of the desired product.

UPLC-MS ((2.1x100 mm BEH Phenyl 1.7μm, acetonitrile:water Grad 40 95A): 3.45 min (>99.9% peak area, ESI(+): 621.38 (**90** + 1 H⁺), 643.38 (**90** + 1 Na⁺)).

R_F = 0.50 (CH₂Cl₂:MeOH 10:1)

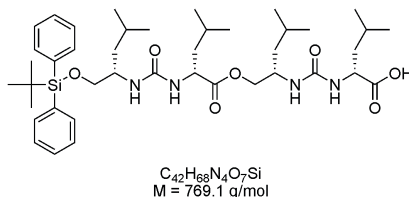
¹H NMR (400 MHz, CD₂Cl₂, 20 °C): δ 7.40 - 7.29 (m, 5 H, C¹⁸⁻²⁰H), 5.46 (br s, 1 H, N⁶H), 5.35 (d, ³J(*H,H*) = 8.2 Hz, 1 H, N¹³H), 5.27 (d, ³J(*H,H*) = 9.0 Hz, 1 H, N¹¹H), 5.12 (s, 2 H, C¹⁶H₂), 4.78 (d, ³J(*H,H*) = 7.5 Hz, 1 H, N⁴H), 4.48 (dd, ²J(*H,H*) = 10.8 Hz, ³J(*H,H*) = 3.4 Hz, 1 H, 1 C⁹H₂), 4.41 (dt, ³J(*H,H*) = 8.5 Hz, ³J(*H,H*) = 6.0 Hz, 1 H, C¹⁴H), 4.16 (dt, ³J(*H,H*) = 8.5 Hz, ³J(*H,H*) = 6.0 Hz, 1 H, C⁷H), 4.02 - 3.92 (m, 1 H, C¹⁰H), 3.81 (dd, ²J(*H,H*) = 10.8 Hz, ³J(*H,H*) = 4.0 Hz, 1 H, 1 C⁹H₂), 3.70 - 3.61 (m, 1 H, C³H), 3.60 - 3.54 (m, 1 H, 1 C²H₂), 3.47 - 3.34 (m, 2 H, 1 C²H₂, O₁H), 1.74 - 1.19 (m, 12 H, 4 C²¹H₂, 4 C²²H), 0.97 - 0.87 (m, 24 H, 8 C²³H₃).

¹³C NMR (CD₂Cl₂): δ 174.67, 173.40, 159.65, 158.15, 135.61, 128.52, 128.03, 67.91, 66.86, 66.59, 53.79, 53.43, 53.06, 50.67, 47.23, 40.84, 40.79, 40.60, 40.52, 24.82, 24.71, 22.88, 22.78, 22.75, 22.60, 22.09, 21.77.

High-resolution ESI-MS: *m/z* = 621.4229 (calcd 621.4222 for C₃₃H₅₆N₄O₇ + 1 H⁺).

4 Linear (Ester-[*alt*]-urea)s

TBDPS-(L-Leucinol-*urea*-D-Leucine)₂ (**84**):



83 (0.30 g, 0.39 mmol) was reacted following the general procedure for the deprotection of the Z group or benzyl ester. EtOH (30 mL), Pd/C (30 mg), reaction time: 12 h, hydrogen pressure: 1 bar. Yield: quantitative. TLC monitoring not possible due to decomposition on silica.

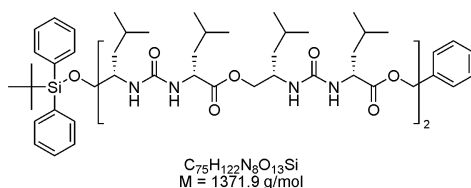
HPLC-MS ((2x150 mm Luna Phenyl-Hexyl 3μm, acetonitrile:water Grad 40 95A): 18.89 min (90.1% peak area, ESI(+): 769.47 (**84** + 1 H⁺)).

R_F = 0.20 (CH₂Cl₂:MeOH 10:1)

¹H NMR (300 MHz, CD₂Cl₂, 20 °C): δ 7.72 - 7.66 (m, 4 H, Ar-*H*), 7.50 - 7.40 (m, 6 H, Ar-*H*), 5.78 - 5.47 (m, 2 H, 2 NH), 5.33 - 4.99 (m, 2 H, 2 NH), 4.40 - 4.18 (m, 3 H), 4.05 - 3.57 (m, 5 H), 1.81 - 1.16 (m, 12 H), 1.10 (s, 9 H, Boc-H), 0.98 - 0.79 (m, 24 H).

High-resolution ESI-MS: m/z = 769.4941 (calcd 769.4936 for C₄₂H₆₈N₄O₇Si + 1 H⁺), 791.4762 (calcd 791.4750 for C₄₂H₆₈N₄O₇Si + 1 Na⁺).

TBDPS-(L-Leucinol-*urea*-D-Leucine)₄-Bn (**86**):



84 (0.20 g, 0.26 mmol), **85** (0.16 g, 0.26 mmol), DMAP (0.03 g, 0.25 mmol), and EDC (0.1 g, 0.51 mmol) were dissolved in CH₂Cl₂ (20 mL). The reaction mixture was stirred for 24 h and evaporated i.vac. The residue was purified via column chromatography on silica (eluent: PE:EE 1:1) to give 0.22 g (yield: 62%) of the desired product.

HPLC-MS ((2x150 mm Luna Phenyl-Hexyl 3μm, acetonitrile:water Grad 40 95A): 22.31 min (92.3% peak area, ESI(+): 686.68 (**86** + 2 H⁺)), 1372.10 (**86** + 1 H⁺)).

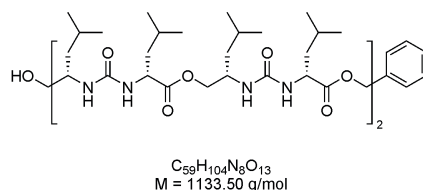
$R_F = 0.20$ (CH_2Cl_2 :MeOH 10:1)

^1H NMR (300 MHz, CD_2Cl_2 , 20 °C): δ 7.73 - 7.66 (m, 4 H, Ar-*H*), 7.48 - 7.35 (m, 6 H, Ar-*H*), 5.80 - 5.51 (m, 5 H), 5.26 - 5.02 (m, 4 H), 4.68 - 4.50 (m, 2 H), 4.46 - 3.58 (m, 15 H), 1.77 - 1.24 (m, 24 H), 1.10 (s, 9 H, Boc-*H*), 1.00 - 0.77 (m, 48 H).

^{13}C NMR (CD_2Cl_2): δ 173.79, 173.63, 173.58, 173.27, 158.14, 158.08, 157.99, 157.73, 136.07, 135.62, 135.58, 133.16, 129.81, 128.43, 128.05, 127.98, 127.79, 67.32, 67.21, 66.42, 60.27, 53.28, 52.90, 52.55, 51.83, 47.21, 46.95, 41.74, 41.55, 41.34, 41.20, 40.94, 40.58, 26.72, 24.93, 24.88, 24.77, 24.69, 22.91, 22.70, 22.65, 22.60, 22.49, 22.21, 22.12, 22.03, 21.81.

High-resolution ESI-MS: $m/z = 1393.8771$ (calcd 1393.8793 for $\text{C}_{75}\text{H}_{122}\text{N}_8\text{O}_{13}\text{Si} + 1 \text{ Na}^+$).

(L-Leucinol-*urea*-D-Leucine)₄-Bn (**88**):



86 (0.26 g, 0.19 mmol) was dissolved in acetonitrile (10 mL) and HF (0.10 mL) was added. The reaction mixture was stirred for 1 h. K_2CO_3 was added and the solution filtered and evaporated i.vac. The residue was purified via column chromatography on silica (eluent: CH_2Cl_2 :MeOH 100:5) to give 0.19 g (yield: 87%) of the desired product.

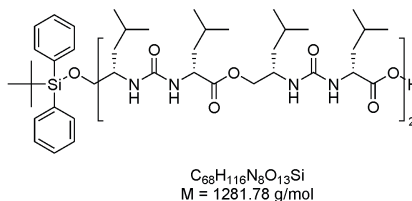
$R_F = 0.40$ (CH_2Cl_2 :MeOH 100:5)

^1H NMR (300 MHz, CD_2Cl_2 , 20 °C): δ 7.42 - 7.32 (m, 5 H, Ar-*H*), 6.01 - 5.30 (m, 8 H), 5.15 (dd, $^2J(\text{H},\text{H}) = 31.1 \text{ Hz}$, $^3J(\text{H},\text{H}) = 12.3 \text{ Hz}$, 2 H, Bn-*H*₂), 4.45 - 3.79 (m, 14 H), 3.73 - 3.64 (m, 1 H), 3.48 - 3.34 (m, 1 H), 1.79 - 1.20 (m, 24 H), 1.00 - 0.87 (m, 48 H).

High-resolution ESI-MS: $m/z = 1133.7836$ (calcd 1133.7801 for $\text{C}_{59}\text{H}_{104}\text{N}_8\text{O}_{13} + 1 \text{ H}^+$).

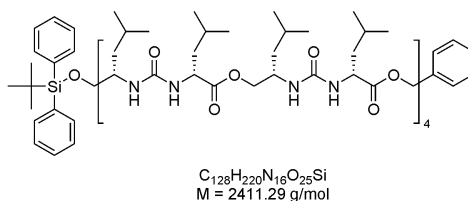
4 Linear (Ester-[*alt*]-urea)s

TBDPS-(L-Leucinol-*urea*-D-Leucine)₄ (**87**):



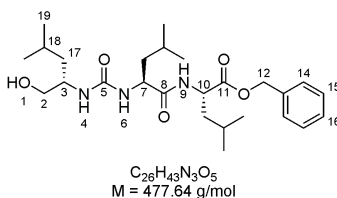
86 (0.26 g, 0.19 mmol) was reacted following the general procedure for the deprotection of the Z group or benzyl ester. EE (20 mL), Pd/C (30 mg), reaction time: 12 h, hydrogen pressure: 1 bar. Yield: quantitative. TLC monitoring not possible due to decomposition on silica. UPLC showed many byproducts. No further analysis.

TBDPS-(L-Leucinol-*urea*-D-Leucine)₈-Bn (**89**):



TBDPS-(L-Leucinol-*urea*-D-Leucine)₄ (0.19 g, 0.15 mmol), (L-Leucinol-*urea*-D-Leucine)₄-Bn (0.17 g, 0.15 mmol), DMAP (0.02 g, 0.15 mmol), and EDC (0.06 g, 0.30 mmol) were dissolved in CH₂Cl₂ (15 mL). The reaction mixture was stirred for 24 h. According to TLC monitoring, no reaction to the desired product took place.

L-Leucinol-*urea*-L-Leucine-*amide*-L-Leucine-Bn (**91**):



67 (0.17 g, 0.60 mmol), **72** (neutral compound) (0.14 g, 0.62 mmol) and HOBT (0.08 g, 0.60 mmol) were dissolved in DMF (3 mL). CH₂Cl₂ was added to a total volume of 30 mL and the solution cooled to 0 °C. To the cold solution, EDC

(0.21 g, 1.08 mmol) in CH_2Cl_2 (20 mL) was added. The solution was allowed to warm up to room temperature and stirred for 30 minutes. TLC monitoring showed remaining starting material, so EDC (0.21 g) was added. After 48 h, water was added to the solution and the biphasic system was stirred for 10 minutes. After phase separation, the organic layer was extracted with 1 M aqueous citric acid solution (2x50 mL), water (1x50 mL), saturated aqueous NaHCO_3 -solution (1x50 mL), water (1x50 mL), and brine (1x50 mL). The organic layer was dried over MgSO_4 , filtered and evaporated i.vac. to give 0.38 g of the crude product, which was dissolved in Et_2O and precipitated in PE. The obtained colorless solid was purified via column chromatography on silica (eluent: PE:EE 2:8) to give 0.28 g (98% yield) of pure **91**.

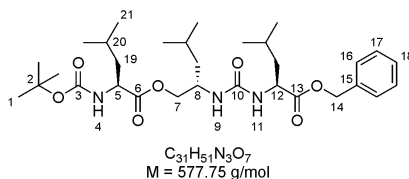
HPLC-MS ((2x150 mm Luna Phenyl-Hexyl 3 μm , acetonitrile:water Grad 5 95A): 19.71 min (>99.0% peak area, ESI(-): 476.40 (**91** - 1 H^+), ESI(+): 478.44 (**91** + 1 H^+)).

R_f = 0.10 (PE:EE 1:1)

^1H NMR (300 MHz, CDCl_3 , 20 $^\circ\text{C}$): δ 7.39 - 7.27 (m, 6 H, C^{14-16}H , N^9H), 6.21 (br s, 1 H, N^6H), 5.51 (br s, 1 H, N^4H), 5.17 - 5.07 (m, 2 H, C^{12}H_2), 4.57 - 4.45 (m, 1 H, C^{10}H), 4.39 - 4.28 (m, 1 H, C^7H), 3.84 - 3.20 (br s, 1 H, O^1H), 3.83 - 3.71 (m, 1 H, C^3H), 3.58 (dd, $^2J(\text{H},\text{H}) = 11.0$ Hz, $^3J(\text{H},\text{H}) = 3.3$ Hz, 1 H, 1 C^2H_2), 3.44 (dd, $^2J(\text{H},\text{H}) = 11.0$ Hz, $^3J(\text{H},\text{H}) = 6.2$ Hz, 1 H, 1 C^2H_2), 1.73 - 1.25 (m, 9 H, 3 C^{17}H_2 , 3 C^{18}H), 0.89 - 0.85 (m, 18 H, 6 C^{19}H_3).

^{13}C NMR (CDCl_3): δ 174.27, 172.69, 159.01, 135.39, 128.70, 128.53, 128.34, 67.19, 66.85, 52.72, 51.30, 50.97, 41.84, 40.75, 40.61, 24.97, 24.84, 24.80, 23.05, 22.91, 22.86, 22.51, 22.44, 21.98.

Boc-L-Leucine-ester-L-Leucinol-urea-L-Leucine-Bn (**95**):



4 Linear (Ester-[*alt*]-urea)s

74 (0.11 g, 0.30 mmol), Boc-L-Leu (0.079 g, 0.315 mmol), and HOBT (0.04 g, 0.30 mmol) were dissolved in CH₂Cl₂ (10 mL) and cooled to 0 °C. To the cold solution, TBTU (0.19 g, 0.60 mmol) and NEt₃ (0.17 mL) were added. The solution was allowed to warm up to room temperature and stirred for 7 h. TLC monitoring showed remaining **74**, so TBTU (100 mg) NEt₃ (0.08 mL) and Boc-L-Leu (20 mg) were added until the reaction was finished according to TLC. Water was added to the solution and the biphasic system stirred for 10 minutes. After phase separation, the organic layer was extracted with 1 M aqueous citric acid solution (1x20 mL), water (1x20 mL), saturated aqueous NaHCO₃-solution (1x20 mL), water (1x20 mL), and brine (1x20 mL), dried over MgSO₄, filtered and evaporated i.vac. The TLC of the crude product showed a complex mixture which was not separable via column chromatography on silica. Precipitation attempts in Et₂O and PE failed. The isolation of **95** was not possible following this procedure.

74 (0.07 g, 0.20 mmol), Boc-L-Leu (0.05 g, 0.21 mmol), HOBT (0.03 g, 0.20 mmol), and EDC (0.08 g, 0.40 mmol) were dissolved in CH₂Cl₂ (3 mL) and heated in the microwave. First run: 80 °C, 1 minute ramp, 10 minutes reaction time. TLC monitoring showed unreacted **74**, so EDC (70 mg) was added and the second run was started: 100 °C, 1 minute ramp, 10 minutes reaction time. TLC monitoring still showed remaining **74**, so EDC (70 mg) and Boc-L-Leu (52 mg) was added prior to the third run: 80 °C, 1 minute ramp, 30 minutes reaction time. TLC showed a complex mixture with remaining **74**, which was not separable via column chromatography on silica.

74 (0.01 g, 0.03 mmol), Boc-L-Leu (0.01 g, 0.04 mmol), and DMAP (0.004 g, 0.030 mmol) were dissolved in CH₂Cl₂ (3 mL) and cooled to 0 °C. To the cold solution, EDC (0.012 g, 0.060 mmol) was added. The solution was allowed to warm up to room temperature and stirred for 2 h. Under TLC monitoring, Boc-L-Leu (3 mg) and EDC (10 mg) was added until all **74** was consumed. Water was added to the solution and the biphasic system stirred for 10 minutes. After phase separation, the organic layer was extracted with 1 M aqueous citric acid

solution (1x20 mL), water (1x20 mL), saturated aqueous NaHCO_3 -solution (1x20 mL), water (1x20 mL), and brine (1x20 mL), dried over MgSO_4 , filtered and evaporated i.vac. The crude product was purified via column chromatography on silica (eluent: CH_2Cl_2 :MeOH 99.5:0.5) to give 0.013 g (75%) of **95**.

74 (0.01 g, 0.03 mmol), Boc-L-Leu (0.009 g, 0.036 mmol) and DPTS (0.009 g, 0.030 mmol) were dissolved in CH_2Cl_2 (3 mL) and cooled to 0 °C. To the cold solution, EDC (0.012 g, 0.060 mmol) was added. The solution was allowed to warm up to room temperature and stirred for 72 h. Silica was added to the reaction mixture, the mixture stirred for 12 h, the silica removed by centrifugation, and the solvent evaporated i.vac. The TLC of the crude product showed a mixture which was not purified.

74 (0.01 g, 0.03 mmol), Boc-L-Leu (0.009 g, 0.036 mmol), and DMAP (0.004 g, 0.030 mmol) were dissolved in CH_2Cl_2 (3 mL) and cooled to 0 °C. To the cold solution, DIC (0.009 mL, 0.060 mmol) was added. The solution was allowed to warm up to room temperature and stirred for 72 h. After the addition of Boc-L-Leu and EDC until the remaining traces of urea disappeared, the reaction mixture was quenched by the addition of silica gel. After stirring the mixture over night, silica was removed by centrifugation and the solvent evaporated i.vac. The TLC of the crude product showed a mixture which was not purified.

74 (0.01 g, 0.03 mmol), Boc-L-Leu (0.009 g, 0.036 mmol) and DPTS (0.009 g, 0.030 mmol) were dissolved in CH_2Cl_2 (3 mL) and cooled to 0 °C. To the cold solution, DIC (0.009 mL, 0.060 mmol) was added. The solution was allowed to warm up to room temperature and stirred for 72 h. After the addition of Boc-L-Leu and EDC until the remaining traces of urea disappeared, the reaction mixture was quenched by the addition of silica gel. After stirring the mixture for 48 h, the mixture was evaporated i.vac. given on a column and purified via column chromatography on silica (eluent: Et_2O) to give 0.015 g (87%).

4 Linear (Ester-[*alt*]-urea)s

HPLC-MS ((2x150 mm Luna Phenyl-Hexyl 3 μ m, acetonitrile:water Grad 5 95A): 23.07 min (>99.0% peak area, ESI(+): 578.46 (**95** + 1 H⁺), 478.41 (**95** - (Boc) + 1 H⁺)).

Boc-L-Leu (0.009 g, 0.036 mmol) was dissolved in CH₂Cl₂ (3 mL) and cooled to 0 °C. To the cold solution, CDI (0.006 g, 0.030 mmol) was added. After the effervescence had ceased, the solution was stirred at room temperature for 1 h. Then, **74** (11 mg, 0.03 mmol) was added and the solution stirred under TLC monitoring. After 72 h, CDI (5 mg) and Boc-L-Leu (3 mg) was added until all **74** was consumed. Water was added to the solution and the biphasic system stirred for 10 minutes. After phase separation, the organic layer was extracted with 1 M aqueous citric acid solution (1x20 mL), water (1x20 mL), saturated aqueous NaHCO₃-solution (1x20 mL), water (1x20 mL), and brine (1x20 mL), dried over MgSO₄, filtered and evaporated i.vac. The TLC of the crude product showed a complex mixture which was not separable via column chromatography on silica. Precipitation attempts in Et₂O and PE failed. The isolation of **95** was not possible following this procedure.

74 (1.09 g, 3.00 mmol), Boc-L-Leu (0.90 g, 3.60 mmol) and DMAP (0.37 g, 3.00 mmol) were dissolved in CH₂Cl₂ (250 mL) and cooled to 0 °C. To the cold solution, EDC (1.73 g, 1.80 mmol) was added. The solution was allowed to warm up to room temperature and stirred for 2 h. The reaction mixture was quenched by the addition of silica gel. After stirring the mixture for 2 h, the solvent was evaporated i.vac. given on a column and purified via column chromatography on silica (eluent: Et₂O). The crude product (1.74 g) was purified via column chromatography on silica (eluent: PE:EE) to remove more unpolar substances to give 1.72 g of pure **95**.

HPLC-MS ((2x150 mm Luna Phenyl-Hexyl 3 μ m, acetonitrile:water Grad 5 95A): 23.07 min (>99.0% peak area, ESI(+): 578.39 (**95** + 1 H⁺), 478.34 (**95** - (Boc) + 1 H⁺)).

R_F = 0.28 (PE:EE 4:1)

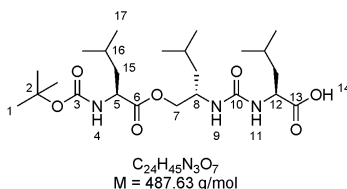
¹H NMR (300 MHz, MeOD, 20 °C): δ 7.36 - 7.30 (m, 5 H, C¹⁶⁻¹⁸H), 5.14 (dd, $J(H,H)$ = 12.4 Hz, $J(H,H)$ = 13.5 Hz, 2 H, C¹⁴H₂), 4.35 (dd, $J(H,H)$ = 5.8 Hz, $J(H,H)$ = 9.1 Hz, 1 H, C⁵H or C¹²H), 4.17 (t, $^3J(H,H)$ = 7.5 Hz, 1 H, C⁵H or C¹²H)

or 1 C⁷H₂), 4.06 - 3.97 (m, 3 H, 1 C⁷H₂, C⁸H, 1 C⁷H₂ or C⁵H or C¹²H), 1.78 - 1.24 (m, 18 H, 3 C¹H₃, 3 C¹⁹H₂, 3 C²⁰H), 0.97 - 0.89 (m, 18 H, 6 C²¹H₃).

¹³C NMR (MeOD): δ 175.07, 174.76, 159.92, 158.06, 135.25, 129.48, 129.20, 129.17, 80.48, 68.32, 67.65, 53.44, 52.96, 48.09, 42.24, 42.03, 41.59, 28.74, 25.92, 25.88, 25.73, 23.60, 23.29, 23.25, 22.44, 22.20, 21.93.

High-resolution ESI-MS: m/z = 578.3817 (calcd 578.3805 for C₃₁H₅₁N₃O₇ + 1 H⁺).

Boc-L-Leucine-ester-L-Leucinol-urea-L-Leucine (**97**):



95 (1.73 g, 3.00 mmol) was reacted following the general procedure for the deprotection of the Z group or benzyl ester. EE (50 mL), Pd/C (170 mg), reaction time: 1.0 h, hydrogen pressure: 6 bar.

HPLC-MS ((2x150 mm Luna Phenyl-Hexyl 3μm, acetonitrile:water Grad 5 95A): 19.84 min (>99.0% peak area, ESI(+): 488.38 (**97** + 1 H⁺), 388.37 (**97** - (Boc) + 1 H⁺)).

R_F = 0.40 (Et₂O)

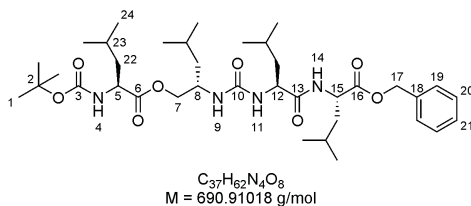
¹H NMR (300 MHz, MeOD, 20 °C): δ 4.29 (dd, J(H,H) = 5.2 Hz, J(H,H) = 9.3 Hz, 1 H, C⁵H or C¹²H), 4.17 (t, ³J(H,H) = 7.5 Hz, 1 H, C⁵H or C¹²H or 1 C⁷H₂), 4.11 - 3.96 (m, 3 H, 1 C⁷H₂, C⁸H, 1 C⁷H₂ or C⁵H or C¹²H), 1.83 - 1.25 (m, 18 H, 3 C¹H₃, 3 C¹⁵H₂, 3 C²⁶H), 0.97 - 0.91 (m, 18 H, 6 C¹⁷H₃).

¹³C NMR (MeOD): δ 177.23, 174.84, 160.09, 158.13, 80.54, 68.38, 53.50, 52.69, 48.15, 42.60, 42.09, 41.63, 28.76, 25.99, 25.77, 23.60, 23.42, 23.31, 22.46, 22.22, 21.94.

High-resolution ESI-MS: m/z = 488.3347 (calcd 488.3336 for C₂₄H₄₅N₃O₇ + 1 H⁺).

4 Linear (Ester-[*alt*]-urea)s

Boc-L-Leucine-*ester*-L-Leucinol-*urea*-L-Leucine-*amide*-L-Leucine-Bn (**92**):



Attempted synthesis starting from **91**:

91 (0.14 g, 0.30 mmol), Boc-L-Leu (0.08 g, 0.32 mmol), and HOBT (0.04 g, 0.30 mmol) were dissolved in CH_2Cl_2 (10 mL) and cooled to 0 °C. To the cold solution, EDC (0.12 g, 0.60 mmol) in CH_2Cl_2 (10 mL) was added. The solution was allowed to warm up to room temperature and stirred for 24 h. TLC monitoring showed unreacted **91**, so EDC (100 mg) and Boc-L-Leu (79 mg) were added. After 48 h, TLC showed remaining **91**, so TBTU (128 mg), NEt_3 (0.06 mL) and Boc-L-Leu (35 mg) were added. After 3 h, water was added to the solution and the biphasic system stirred for 10 minutes. After phase separation, the organic layer was extracted with 1 M aqueous citric acid solution (2x50 mL), water (1x50 mL), saturated aqueous $NaHCO_3$ -solution (1x50 mL), water (1x50 mL), and brine (1x50 mL). The organic layer was dried over $MgSO_4$, filtered and evaporated i.vac. to give 0.38 g of the crude product, which was dissolved in Et_2O and precipitated in PE. Precipitation did not work, so product was purified via column chromatography on silica (eluent: PE:EE 2:1) to give 0.29 g of impure **92**. TLC showed two overlaying spots, HPLC showed three peaks. Despite all efforts, **92** could not be isolated.

Synthesis starting from **97**:

97 (1.27 g, 2.61 mmol), **72** (0.60 g, 2.70 mmol) and DMAP (0.32 g, 2.61 mmol) were dissolved in CH_2Cl_2 (30 mL) and cooled to 0 °C. To the cold solution, EDC (1.00 g, 5.22 mmol) was added. The solution was allowed to warm up to room temperature and stirred for 24 h. The reaction mixture was quenched by the addition of silica gel. After stirring the mixture for 4 h, the solvent was evaporated i.vac. given on a column and purified via column chromatography on silica (eluent: PE:EE 5:1 to 3:1) to give 1.52 g (84%) of pure **92**.

HPLC-MS ((2x150 mm Luna Phenyl-Hexyl 3 μ m, acetonitrile:water Grad 5 95A): 19.84 min (97.0% peak area, ESI(+): 691.53 (**92** + 1 H⁺), 591.43 (**92** - (Boc) + 1 H⁺)).

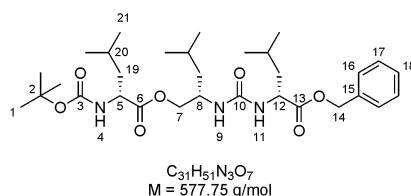
R_F = 0.34 (PE:EE 1:1)

¹H NMR (400 MHz, CD₂Cl₂, 20 °C): δ 7.40 - 7.30 (m, 5 H, C¹⁹⁻²¹H), 6.74 (d, ³ $J(H,H)$ = 7.6 Hz, 1 H, N¹⁴H), 5.13 (dd, $J(H,H)$ = 12.8 Hz, $J(H,H)$ = 16.6 Hz, 2 H, C¹⁷H₂), 5.07 (d, ³ $J(H,H)$ = 7.6 Hz, 1 H, N⁴H), 4.88 (m, 2 H, N⁹H, N¹¹H), 4.57 - 4.50 (m, 1 H, C¹⁵H), 4.34 - 4.26 (m, 1 H, 1 C⁷H₂), 4.24 - 4.13 (m, 2 H, C⁵H, C¹²H), 4.05 - 3.93 (m, 2 H, C⁸H, 1 C⁷H₂), 1.74 - 1.25 (m, 21 H, 3 C¹H₃, 4 C²²H₂, 4 C²³H), 0.96 - 0.85 (m, 24 H, 8 C²³H₃).

¹³C NMR (MeOD): δ 175.92, 174.85, 173.72, 159.71, 158.13, 137.18, 129.57, 129.38, 129.35, 80.54, 68.37, 67.88, 53.50, 53.20, 52.12, 48.12, 42.86, 42.13, 41.63, 41.37, 28.75, 25.98, 25.76, 23.63, 23.39, 23.36, 23.31, 22.47, 21.93, 21.86.

High-resolution ESI-MS: m/z = 691.4612 (calcd 691.4646 for C₃₇H₆₂N₄O₈ + 1 H⁺).

Boc-D-Leucine-ester-L-Leucinol-urea-D-Leucine-Bn (**96**):



75 (1.09 g, 3.00 mmol), Boc-D-Leu (0.90 g, 3.60 mmol), and DMAP (0.37 g, 3.00 mmol) were dissolved in CH₂Cl₂ (250 mL) and cooled to 0 °C. To the cold solution, EDC (1.73 g, 1.80 mmol) was added. The solution was allowed to warm up to room temperature and stirred for 5 h. The reaction mixture was quenched by the addition of silica gel. After stirring the mixture for 1 h, the solvent was evaporated i.vac. given on a column and purified via column chromatography on silica (eluent: Et₂O). The crude product (1.80 g) was recrystallized from PE:CH₂Cl₂ to give 1.73 g of pure **96**.

4 Linear (Ester-[*alt*]-urea)s

HPLC-MS ((2x150 mm Luna Phenyl-Hexyl 3 μ m, acetonitrile:water Grad 5 95A): 23.07 min (>99.0% peak area, ESI(+): 578.43 (**96** + 1 H⁺), 478.34 (**96** - (Boc) + 1 H⁺)).

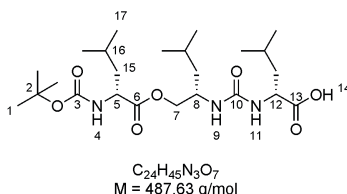
R_F = 0.30 (PE:EE 4:1)

¹H NMR (300 MHz, MeOD, 20 °C): δ 7.36 - 7.29 (m, 5 H, C¹⁶⁻¹⁸H), 5.14 (dd, $J(H,H)$ = 12.3 Hz, $J(H,H)$ = 25.1 Hz, 2 H, C¹⁴H₂), 4.38 (dd, $J(H,H)$ = 5.6 Hz, $J(H,H)$ = 9.1 Hz, 1 H, C⁵H or C¹²H), 4.18 (t, $^3J(H,H)$ = 7.5 Hz, 1 H, C⁵H or C¹²H or 1 C⁷H₂), 4.08 - 4.00 (m, 3 H, 1 C⁷H₂, C⁸H, 1 C⁷H₂ or C⁵H or C¹²H), 1.78 - 1.26 (m, 18 H, 3 C¹H₃, 3 C¹⁹H₂, 3 C²⁰H), 0.95 - 0.90 (m, 18 H, 6 C²¹H₃).

¹³C NMR (MeOD): δ 174.87, 174.58, 159.81, 158.00, 137.16, 129.49, 129.22, 129.17, 80.35, 68.27, 67.61, 53.46, 52.81, 48.10, 42.35, 41.90, 41.31, 28.77, 25.88, 25.84, 25.77, 23.64, 23.35, 23.28, 22.38, 22.15, 21.84.

High-resolution ESI-MS: m/z = 578.3817 (calcd 578.3805 for C₃₁H₅₁N₃O₇ + 1 H⁺).

Boc-D-Leucine-*ester*-L-Leucinol-*urea*-D-Leucine (**98**):



96 (1.73 g, 3.00 mmol) was reacted following the general procedure for the deprotection of the Z group or benzyl ester. EE (50 mL), Pd/C (170 mg), reaction time: 3.0 h, hydrogen pressure: 6 bar.

HPLC-MS ((2x150 mm Luna Phenyl-Hexyl 3 μ m, acetonitrile:water Grad 5 95A): 20.15 min (>99.0% peak area, ESI(+): 488.35 (**98** + 1 H⁺), 388.36 (**98** - (Boc) + 1 H⁺)).

R_F = 0.30 (Et₂O)

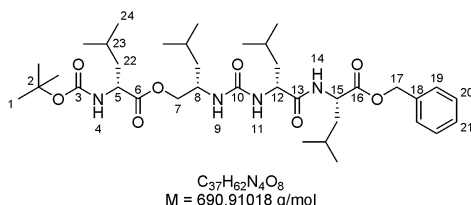
¹H NMR (300 MHz, MeOD, 20 °C): δ 4.32 (dd, $J(H,H)$ = 5.1 Hz, $J(H,H)$ = 9.3 Hz, 1 H, C⁵H or C¹²H), 4.16 (t, $^3J(H,H)$ = 7.5 Hz, 1 H, C⁵H or C¹²H or 1 C⁷H₂), 4.06 -

4.01 (m, 3 H, 1 C⁷H₂, C⁸H, 1 C⁷H₂ or C⁵H or C¹²H), 1.82 - 1.25 (m, 18 H, 3 C¹H₃, 3 C¹⁵H₂, 3 C²⁶H), 0.97 - 0.91 (m, 18 H, 6 C¹⁷H₃).

¹³C NMR (MeOD): δ 177.05, 174.66, 159.92, 158.08, 80.41, 68.37, 53.49, 52.58, 48.13, 42.77, 41.95, 41.35, 28.75, 25.98, 25.87, 25.82, 23.63, 23.42, 23.32, 22.37, 22.18, 21.82.

High-resolution ESI-MS: m/z = 488.3347 (calcd 488.3336 for C₂₄H₄₅N₃O₇ + 1 H⁺).

Boc-D-Leucine-*ester*-L-Leucinol-*urea*-D-Leucine-*amide*-L-Leucine-Bn (**99**):



98 (1.46 g, 3.00 mmol), **72** (0.69 g, 3.11 mmol), and DMAP (0.37 g, 3.00 mmol) were dissolved in CH₂Cl₂ (50 mL) and cooled to 0 °C. To the cold solution, EDC (0.86 g, 4.50 mmol) was added. The solution was allowed to warm up to room temperature and stirred for 60 h. The reaction mixture was quenched by the addition of silica gel. After stirring the mixture for 4 h, the solvent was evaporated i.vac. and the solid given on a column and purified via column chromatography on silica (eluent: Et₂O). The crude product (2.20 g) was recrystallized from PE:CH₂Cl₂ to give 1.98 g (96%) of pure **99**.

HPLC-MS ((2x150 mm Luna Phenyl-Hexyl 3μm, acetonitrile:water Grad 5 95A): 23.55 min (>99.0% peak area, ESI(+): 691.53 (**99** + 1 H⁺), 591.43 (**99** - (Boc) + 1 H⁺)).

R_F = 0.10 (PE:EE 4:1)

¹H NMR (400 MHz, CD₂Cl₂, 20 °C): δ 7.39 - 7.29 (m, 5 H, C¹⁹⁻²¹H), 7.15 (d, ³J(H,H) = 7.8 Hz, 1 H, N¹⁴H), 5.12 (dd, J(H,H) = 12.2 Hz, J(H,H) = 19.5 Hz, 2 H, C¹⁷H₂), 5.05 (d, ³J(H,H) = 5.6 Hz, 1 H, N⁴H), 4.92 (d, ³J(H,H) = 7.3 Hz, 1 H, N⁹H), 4.82 (d, ³J(H,H) = 9.2 Hz, 1 H, N¹¹H), 4.72 - 4.66 (m, 1 H, 1 C⁷H₂), 4.62 - 4.55 (m, 1 H, C¹⁵H), 4.20 - 4.09 (m, 2 H, C⁵H, C¹²H), 4.09 - 4.03 (m,

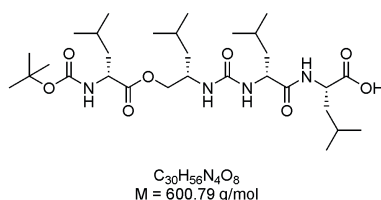
4 Linear (Ester-[*alt*]-urea)s

1 H, C⁸H), 3.76 (d, $J(H,H) = 9.6$ Hz, 1 H, 1 C⁷H₂), 1.75 - 1.21 (m, 21 H, 3 C¹H₃, 4 C²²H₂, 4 C²³H), 0.97 - 0.83 (m, 24 H, 8 C²³H₃).

¹³C NMR (MeOD): δ 175.94, 174.89, 173.70, 159.59, 158.22, 137.20, 129.56, 129.28, 129.20, 80.59, 67.88, 67.81, 53.73, 53.68, 52.19, 48.55, 42.88, 41.75, 41.35, 41.23, 28.82, 25.98, 25.93, 25.87, 23.58, 23.54, 23.35, 23.31, 22.35, 23.31, 22.35, 22.10, 21.91, 21.77.

High-resolution ESI-MS: $m/z = 691.4651$ (calcd 691.4646 for C₃₇H₆₂N₄O₈ + 1 H⁺), 713.4464 (calcd 713.4465 for C₃₇H₆₂N₄O₈ + 1 Na⁺).

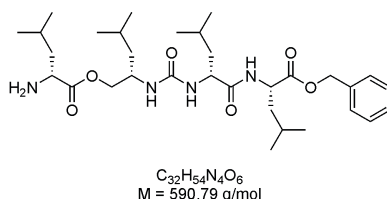
Boc-D-Leucine-ester-L-Leucinol-urea-D-Leucine-amide-L-Leucine (**101**):



99 (0.25 g, 0.37 mmol) was reacted following the general procedure for the deprotection of the Z group or benzyl ester. EE (20 mL), Pd/C (30 mg), reaction time: 3 h, hydrogen pressure: 5 bar. Yield: quantitative.

$R_F = 0.10$ (Et₂O)

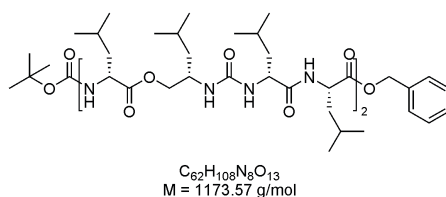
D-Leucine-ester-L-Leucinol-urea-D-Leucine-amide-L-Leucine-Bn (**100**):



99 (0.25 g, 0.37 mmol) was reacted following the general procedure for the deprotection of the Boc group. The product was obtained in quantitative yield and was used without further purification and characterization.

$R_F = 0.10$ (Et₂O)

Boc-(D-Leucine-*ester*-L-Leucinol-*urea*-D-Leucine-*amide*-L-Leucine)₂-Bn (**103**):



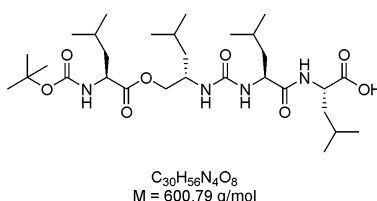
101 (0.22 g, 0.37 mmol), **100** (0.22 g, 0.37 mmol), and HOBT (0.05 g, 0.37 mmol) were dissolved in CH₂Cl₂ (20 mL) and cooled to 0 °C. EDC (0.11 g, 0.55 mmol) was added to the cold solution. The reaction mixture was allowed to warm up to room temperature, stirred for 12 h, and subsequently extracted with 1 M aqueous citric acid solution (2x50 mL), water (1x50 mL), saturated aqueous NaHCO₃-solution (1x50 mL), water (1x50 mL), and brine (1x50 mL). The crude product was filtered through a silica plug (eluent: Et₂O), to give 0.40 g (yield: 93%) of the desired product in high purity according to HPLC.

HPLC-MS ((2x150 mm Luna Phenyl-Hexyl 3μm, acetonitrile:water Grad 5 95A): 26.23 min (>99.9% peak area, ESI(+): 1174.08 (**103** + 1 H⁺), 1196.06 (**103** + 1 Na⁺)).

R_F = 0.70 (Et₂O)

High-resolution ESI-MS: m/z = 1195.7773 (calcd 1195.7943 for C₆₂H₁₀₈N₈O₁₃ + 1 Na⁺).

Boc-L-Leucine-*ester*-L-Leucinol-*urea*-L-Leucine-*amide*-L-Leucine (**94**):



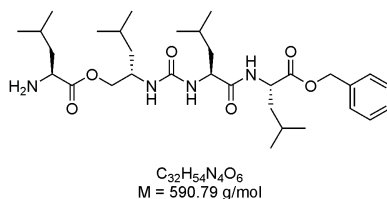
92 (0.25 g, 0.37 mmol) was reacted following the general procedure for the deprotection of the Z group or benzyl ester. EE (20 mL), Pd/C (30 mg), reaction time: 3 h, hydrogen pressure: 5 bar. Yield: quantitative.

The deprotection of **92**, derived from the "amide-first"-pathway afforded impure material. The pure product could not be isolated.

R_F = 0.10 (Et₂O)

4 Linear (Ester-[*alt*]-urea)s

L-Leucine-*ester*-L-Leucinol-*urea*-L-Leucine-*amide*-L-Leucine-Bn (**93**):

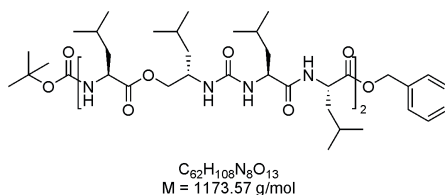


92 (0.25 g, 0.37 mmol) was reacted following the general procedure for the deprotection of the Boc group. The product was obtained in quantitative yield and was used without further purification and characterization.

The deprotection of **92**, derived from the "amide-first"-pathway afforded impure material. The pure product could not be isolated.

R_F = 0.05 (Et₂O)

Boc-(L-Leucine-*ester*-L-Leucinol-*urea*-L-Leucine-*amide*-L-Leucine)₂-Bn (**102**):



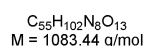
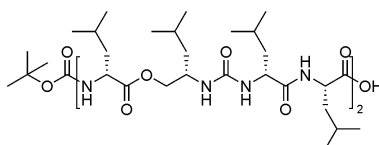
94 (0.22 g, 0.37 mmol), **93** (0.22 g, 0.37 mmol), and HOBt (0.05 g, 0.37 mmol) were dissolved in CH₂Cl₂ (20 mL) and cooled to 0 °C. EDC (0.11 g, 0.55 mmol) was added to the cold solution. The reaction mixture was allowed to warm up to room temperature, stirred for 12 h. The reaction mixture was evaporated i.vac., the residue dissolved in EE, and subsequently extracted with 1 M aqueous citric acid solution (2x50 mL), water (1x50 mL), saturated aqueous NaHCO₃-solution (1x50 mL), water (1x50 mL), and brine (1x50 mL). The crude product was dissolved in CH₂Cl₂ and precipitated by the addition of PE. The residue was purified via column chromatography on silica (eluent: CH₂Cl₂:acetone 9:1), to give the desired product in quantitative yield.

UPLC-MS ((2.1x100 mm BEH Phenyl 1.7μm, acetonitrile:water Grad 40 95A): 5.21 min (>99.9% peak area, ESI(+): 1195.754 (**102** + 1 Na⁺)).

R_F = 0.50 (Et₂O)

High-resolution ESI-MS: $m/z = 1173.8180$ (calcd 1173.8114 for $C_{62}H_{108}N_8O_{13} + 1 H^+$), 1195.7679 (calcd 1195.7943 for $C_{62}H_{108}N_8O_{13} + 1 Na^+$).

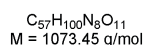
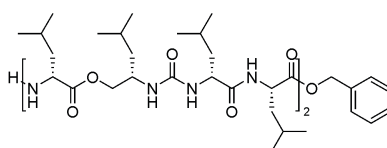
Boc-(D-Leucine-*ester*-L-Leucinol-*urea*-D-Leucine-*amide*-L-Leucine)₂ (**107**):



103 (0.12 g, 0.10 mmol) was reacted following the general procedure for the deprotection of the Z group or benzyl ester. EE (20 mL), Pd/C (12 mg), reaction time: 3 h, hydrogen pressure: 5 bar. Yield: quantitative.

$R_F = 0.30$ (Et₂O)

(D-Leucine-*ester*-L-Leucinol-*urea*-D-Leucine-*amide*-L-Leucine)₂-Bn (**105**):

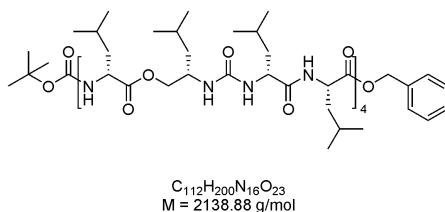


103 (0.12 g, 0.10 mmol) was reacted following the general procedure for the deprotection of the Boc group. Despite extensive extraction of the organic layer with saturated aqueous NaHCO₃-solution, TFA could not be removed quantitatively. The product was obtained in quantitative yield and was used without further purification and characterization.

$R_F = 0.20$ (Et₂O)

4 Linear (Ester-[*alt*]-urea)s

Boc-(D-Leucine-*ester*-L-Leucinol-*urea*-D-Leucine-*amide*-L-Leucine)₄-Bn (**109**):



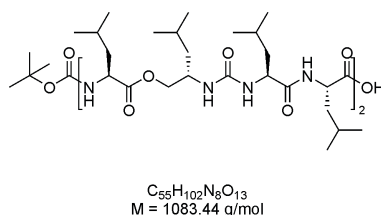
107 (0.11 g, 0.10 mmol), **105** (0.11 g, 0.10 mmol), and HOBT (0.14 g, 0.10 mmol) were dissolved in CH₂Cl₂ (10 mL) and cooled to 0 °C. EDC (0.40 g, 0.20 mmol) was added to the cold solution. The reaction mixture was allowed to warm up to room temperature, stirred for 1 h. TLC monitoring showed no conversion to the product. NEt₃ (0.04 mL) and EDC (100 mg) were added and the mixture was stirred for 3 days. Water was added to the reaction mixture and the biphasic system stirred for 10 minutes. After phase separation, the organic layer was extracted with 1 M aqueous citric acid solution (2x50 mL), water (1x50 mL), saturated aqueous NaHCO₃-solution (1x50 mL), water (1x50 mL), and brine (1x50 mL), dried over MgSO₄, filtered and evaporated i.vac. The crude product was purified via column chromatography on silica (eluent: PE:EE 2:1) to give 0.19 g (yield: 87%) of the desired product as a white solid.

HPLC-MS ((2x150 mm Luna Phenyl-Hexyl 3μm, acetonitrile:water Grad 60 95A): 23.07 min (>99.9% peak area, ESI(+): 1070.38 (**109** + 2 H⁺), 1081.42 (**109** + 1 H⁺, + 1 Na⁺), 1092.50 (**109** + 2 Na⁺)).

R_F = 0.50 (PE:EE 1:1)

High-resolution ESI-MS: m/z = 2160.4850 (calcd 2160.4870 for C₁₁₂H₂₀₀N₁₆O₂₃ + 1 Na⁺).

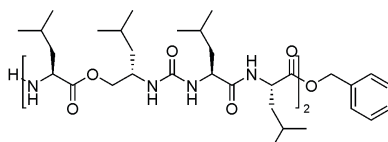
Boc-(L-Leucine-*ester*-L-Leucinol-*urea*-L-Leucine-*amide*-L-Leucine)₂ (**106**):



102 (0.13 g, 0.11 mmol) was reacted following the general procedure for the deprotection of the Z group or benzyl ester. EE (20 mL), Pd/C (12 mg), reaction time: 3 h, hydrogen pressure: 5 to 12 bar. Yield: quantitative.

$R_F = 0.05$ (Et₂O)

(L-Leucine-*ester*-L-Leucinol-*urea*-L-Leucine-*amide*-L-Leucine)₂-Bn (**104**):

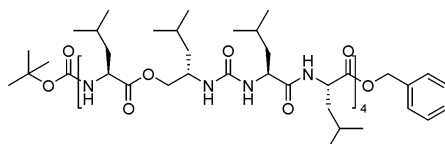


C₅₇H₁₀₀N₈O₁₁
M = 1073.45 g/mol

102 (0.13 g, 0.11 mmol) was reacted following the general procedure for the deprotection of the Boc group. Despite extensive extraction of the organic layer with saturated aqueous NaHCO₃-solution, TFA could not be removed quantitatively. The product was obtained in quantitative yield and was used without further purification and characterization.

$R_F = 0.05$ (Et₂O)

Boc-(L-Leucine-*ester*-L-Leucinol-*urea*-L-Leucine-*amide*-L-Leucine)₄-Bn (**108**):



C₁₁₂H₂₀₀N₁₆O₂₃
M = 2138.88 g/mol

106 (0.11 g, 0.10 mmol), **104** (0.11 g, 0.10 mmol), and HOBT (0.14 g, 0.10 mmol) were dissolved in CH₂Cl₂ (5 mL) and cooled to 0 °C. EDC (0.40 g, 0.20 mmol) was added to the cold solution. The reaction mixture was allowed to warm up to room temperature, stirred for 1 h. TLC monitoring showed no conversion to the product. NEt₃ (0.04 mL) and EDC (100 mg) were added and the mixture was stirred for 18 h. Water was added to the reaction mixture and the biphasic system stirred for 10 minutes. After phase separation, the organic layer was extracted with 1 M aqueous citric acid solution (2x50 mL), water

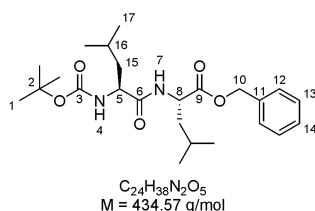
4 Linear (Ester-[*alt*]-urea)s

(1x50 mL), saturated aqueous NaHCO₃-solution (1x50 mL), water (1x50 mL), and brine (1x50 mL), dried over MgSO₄, filtered and evaporated i.vac., to give the desired product in quantitative yield. TLC analysis of the product was impossible.

HPLC-MS ((2x150 mm Luna Phenyl-Hexyl 3 μ m, acetonitrile:water Grad 5 95A): 24.86 min (>99.9% peak area, ESI(+): 1070.09 (**108** + 2 H⁺)).

High-resolution ESI-MS: m/z = 2160.4880 (calcd 2160.4870 for C₁₁₂H₂₀₀N₁₆O₂₃ + 1 Na⁺).

Boc-L-Leu-L-Leu-Bn (**110**):



Boc-L-Leu monohydrate (3.02 g, 11.55 mmol), **72** (2.43 g, 11.00 mmol), and HOBT (1.49 g, 11.00 mmol) were dissolved in CH₂Cl₂ (50 mL) and cooled to 0 °C. To the cold solution, EDC (3.16 g, 16.50 mmol) was added. The solution was allowed to warm up to room temperature and stirred for 72 h. The solution was evaporated i.vac. and the residue redissolved in EE. Water was added to the suspension and the biphasic system stirred for 60 minutes. After phase separation, the organic layer was extracted with 1 M aqueous citric acid solution (1x50 mL), water (1x50 mL), saturated aqueous NaHCO₃-solution (1x50 mL), water (1x50 mL), brine (1x50 mL), dried over MgSO₄, filtered, and evaporated i.vac. The crude product (4.98 g) was purified via column chromatography on silica (eluent: PE:EE 4:1) to give pure **110** in quantitative yield.

UPLC-HRMS ((2.1x100 mm BEH Phenyl 1.7 μ m, acetonitrile:water Grad 40 95A): 2.83 min (>99.0% peak area, AP(+): 435.28 (**110** + 1 H⁺), 891.52 ((**110**)₂ + 1 Na⁺)).

R_F = 0.36 (PE:EE 4:1)

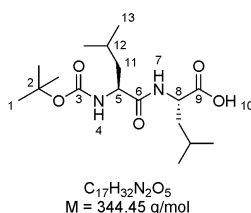
¹H NMR (300 MHz, MeOD, 20 °C): δ 7.34 - 7.29 (m, 5 H, 2 C¹²H, 2 C¹³H, C¹⁴H), 5.12 (dd, $J(H,H) = 12.3$ Hz, $J(H,H) = 18.0$ Hz, 2 H, C¹⁰H), 4.58 - 4.54 (m, 1 H,

C^8H), 4.22 - 4.17 (m, 1 H, C^5H), 1.80 - 1.34 (m, 15 H, 3 C^1H_3 , 2 $C^{15}H_2$, 2 $C^{16}H$), 0.97 - 0.79 (m, 12 H, 4 $C^{17}H_3$).

^{13}C NMR (MeOD): δ 175.23, 173.39, 157.34, 136.89, 129.41, 129.15, 80.09, 67.63, 53.87, 51.98, 42.03, 41.23, 28.77, 25.54, 23.41, 23.38, 22.28, 22.00.

High-resolution ESI-MS: m/z = 435.2855 (calcd 435.2853 for $C_{24}H_{38}N_2O_5 + 1 H^+$), 891.5464 (calcd 891.5475 for $(C_{24}H_{38}N_2O_5)_2 + 1 Na^+$).

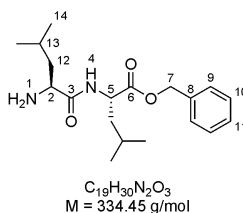
Boc-L-Leu-L-Leu (**114**):



110 (1.24 g, 2.85 mmol) was reacted following the general procedure for the deprotection of the Z group or benzyl ester. EE (20 mL), Pd/C (60 mg), reaction time: 2.5 h, hydrogen pressure: 5 bar.

R_F = 0.20 (Et_2O)

L-Leu-L-Leu-Bn (**112**):

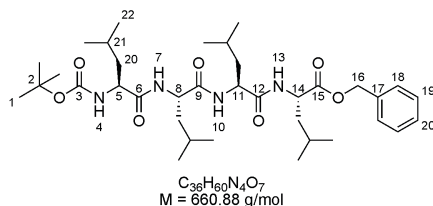


110 (1.24 g, 2.85 mmol) was reacted following the general procedure for the deprotection of the Boc group. The product was obtained in quantitative yield and was used without further purification and characterization.

R_F = 0.16 (Et_2O)

4 Linear (Ester-[*alt*]-urea)s

Boc-(L-Leu-L-Leu)₂-Bn (**116**):



114 (0.98 g, 2.85 mmol), HOBT (0.39 g, 2.85 mmol), and **112** (0.95 g, 2.85 mmol) were dissolved in CH_2Cl_2 (20 mL) and cooled to 0 °C. To the cold solution, EDC (1.09 g, 5.70 mmol) was added. The solution was allowed to warm up to room temperature and stirred for 72 h. The solution was evaporated i.vac. and the residue redissolved in EE. Water was added to the suspension and the biphasic system stirred for 60 minutes. After phase separation, the organic layer was extracted with 1 M aqueous citric acid solution (1x50 mL), water (1x50 mL), saturated aqueous NaHCO_3 -solution (1x50 mL), water (1x50 mL), brine (1x50 mL), dried over MgSO_4 , filtered, and evaporated i.vac. The crude product (1.90 g) was purified via column chromatography on silica (eluent: PE:EE 2:1). The impure product was further purified via precipitation and centrifugation in PE to give 1.74 g of pure **116**.

HPLC-MS ((2x150 mm Luna Phenyl-Hexyl 3 μm , acetonitrile:water Grad 5 95A): 22.98 min (>99.0% peak area, ESI(+): 661.58 (**116** + 1 H^+), 561.48 (**116** - (Boc) + 1 H^+), 1322.34 ((**116**)₂ + 1 H^+)).

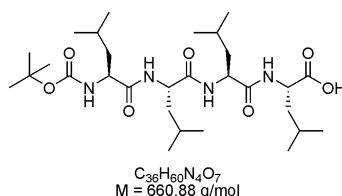
$R_f = 0.20$ (PE:EE 2:1)

^1H NMR (400 MHz, CD_2Cl_2 , 20 °C): δ 7.39 - 7.29 (m, 5 H, C^{18-20}H), 6.94 (m, 2 H, N^{10}H , N^{13}H), 6.49 (d, $^3J(\text{H},\text{H}) = 5.6 \text{ Hz}$, 1 H, N^7H), 5.13 (s, 2 H, C^{16}H_2), 4.98 (m, 1 H, N^4H), 4.55 - 4.41 (m, 2 H, C^{11}H , C^{14}H), 4.28 - 4.21 (m, 1 H, C^8H), 3.95 - 3.89 (m, 1 H, C^5H), 1.82 - 1.39 (m, 21 H, 3 C^1H_3 , 4 C^{20}H_2 , 4 C^{21}H), 0.98 - 0.84 (m, 24 H, 8 C^{22}H_3).

^{13}C NMR (MeOD): δ 172.75, 172.09, 171.99, 155.81, 135.70, 128.52, 128.25, 79.20, 66.90, 52.91, 51.59, 51.38, 50.72, 42.45, 42.16, 41.14, 40.73, 29.74, 28.50, 24.83, 24.76, 24.74, 23.11, 23.05, 22.77, 22.58, 22.43, 21.85.

High-resolution ESI-MS: $m/z = 661.4537$ (calcd 661.4535 for $C_{36}H_{60}N_4O_7 + 1 H^+$), 1321.8980 (calcd 1321.8997 for $(C_{36}H_{60}N_4O_7)_2 + 1 H^+$), 1343.8805 (calcd 1343.8816 for $(C_{36}H_{60}N_4O_7)_2 + 1 Na^+$).

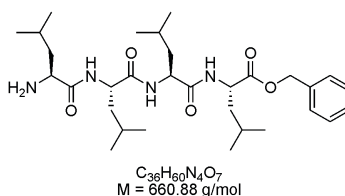
Boc-(L-Leu-L-Leu)₂ (**119**):



116 (0.38 g, 0.57 mmol) was reacted following the general procedure for the deprotection of the Z group or benzyl ester. EE (20 mL), Pd/C (30 mg), reaction time: 2.5 h, hydrogen pressure: 5 bar.

$R_F = 0.10$ (Et₂O)

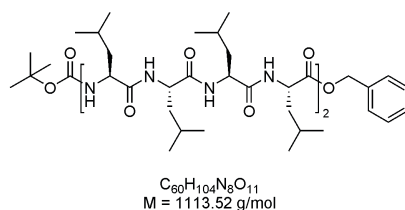
(L-Leu-L-Leu)₂-Bn (**118**):



116 (0.38 g, 0.57 mmol) was reacted following the general procedure for the deprotection of the Boc group. The product was obtained in quantitative yield and was used without further purification and characterization.

$R_F = 0.0$ (Et₂O)

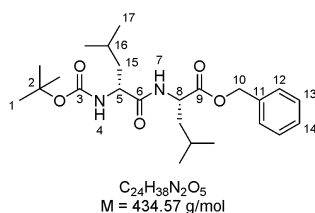
Boc-(L-Leu-L-Leu)₄-Bn (**120**):



4 Linear (Ester-[*alt*]-urea)s

119 (0.32 g, 0.57 mmol), HOBT (0.08 g, 0.57 mmol), and **118** (0.32 g, 0.57 mmol) were dissolved in DMF (20 mL) and cooled to 0 °C. To the cold solution, EDC (0.22 g, 0.14 mmol) was added. The solution was allowed to warm up to room temperature and stirred for 72 h. The solution was extracted with 1 M aqueous citric acid solution (1x50 mL), water (1x50 mL), saturated aqueous NaHCO₃-solution (1x50 mL), water (1x50 mL), brine (1x50 mL), dried over MgSO₄, filtered, and evaporated i.vac. The extraction procedure was tedious (emulsion) and required the addition of MeOH for solubility reasons. The crude product was suspended in water and filtered. A part of the residue was not soluble in MeOH, CH₂Cl₂, EE, PE, Et₂O or their mixtures. The soluble residue was fractioned via column chromatography on silica (eluent: CH₂Cl₂:MeOH 95:5). In no fraction, the desired product could not be detected by UPLC-MS. The reaction failed.

Boc-D-Leu-L-Leu-Bn (**111**):



Boc-D-Leu monohydrate (3.02 g, 11.55 mmol), **72** (2.43 g, 11.00 mmol), and HOBT (1.49 g, 11.00 mmol) were dissolved in CH₂Cl₂ (50 mL) and cooled to 0 °C. To the cold solution, EDC (3.16 g, 16.50 mmol) was added. The solution was allowed to warm up to room temperature and stirred for 12 h. Water was added to the solution and the biphasic system stirred for 10 minutes. After phase separation, the organic layer was extracted with 1 M aqueous citric acid solution (1x50 mL), water (1x50 mL), saturated aqueous NaHCO₃-solution (1x50 mL), water (1x50 mL), brine (1x50 mL), dried over MgSO₄, filtered, and evaporated i.vac. The crude product was purified via column chromatography on silica (eluent: PE:EE 4:1) to give pure **111** in quantitative yield.

UPLC-HRMS ((2.1x100 mm BEH Phenyl 1.7um, acetonitrile:water Grad 40 95A): 4.68 min (>99.9% peak area, AP(+): 435.29 (**111** + 1 H⁺), 335.24 (**111** - (Boc) + 1 H⁺), 868.55 ((**111**)₂ + 1 H⁺)).

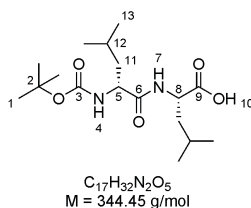
$R_F = 0.50$ (PE:EE 2:1)

^1H NMR (300 MHz, MeOD, 20 °C): δ 7.37 - 7.29 (m, 5 H, 2 C^{12}H , 2 C^{13}H , C^{14}H), 5.14 (dd, $J(\text{H},\text{H}) = 12.3$ Hz, $J(\text{H},\text{H}) = 18.9$ Hz, 2 H, C^{10}H), 4.54 - 4.41 (m, 1 H, C^8H), 4.16 - 3.99 (m, 1 H, C^5H), 1.79 - 1.33 (m, 15 H, 3 C^1H_3 , 2 C^{15}H_2 , 2 C^{16}H), 1.01 - 0.78 (m, 12 H, 4 C^{17}H_3).

^{13}C NMR (MeOD): δ 175.94, 173.62, 157.55, 137.20, 129.55, 129.27, 129.23, 80.56, 67.84, 54.73, 52.13, 42.29, 41.14, 28.69, 25.87, 23.37, 21.98, 21.65.

High-resolution ESI-MS: $m/z = 435.2856$ (calcd 435.2853 for $\text{C}_{24}\text{H}_{38}\text{N}_2\text{O}_5 + 1 \text{ H}^+$), 457.2679 (calcd 457.2673 for $\text{C}_{24}\text{H}_{38}\text{N}_2\text{O}_5 + 1 \text{ Na}^+$), 869.5626 (calcd 868.5634 for $(\text{C}_{24}\text{H}_{38}\text{N}_2\text{O}_5)_2 + 1 \text{ H}^+$).

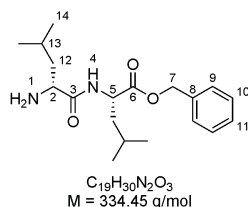
Boc-D-Leu-L-Leu (**115**):



111 (0.96 g, 2.20 mmol) was reacted following the general procedure for the deprotection of the Z group or benzyl ester. EE (20 mL), Pd/C (95 mg), reaction time: 2.5 h, hydrogen pressure: 5 bar.

$R_F = 0.20$ (Et_2O)

D-Leu-L-Leu-Bn (**113**):

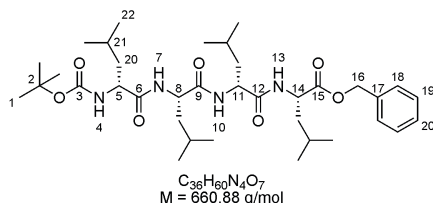


111 (0.96 g, 2.20 mmol) was reacted following the general procedure for the deprotection of the Boc group. The product was obtained in quantitative yield and was used without further purification and characterization.

4 Linear (Ester-[*alt*]-urea)s

$R_F = 0.16$ (Et₂O)

Boc-(D-Leu-L-Leu)₂-Bn (**117**):



115 (0.76 g, 2.20 mmol), HOBT (0.30 g, 2.20 mmol), and **113** (0.74 g, 2.20 mmol) were dissolved in CH₂Cl₂ (20 mL) and cooled to 0 °C. To the cold solution, EDC (0.84 g, 4.40 mmol) was added. The solution was allowed to warm up to room temperature and stirred for 12 h. The solution was evaporated i.vac. and the residue redissolved in EE. Water was added to the suspension and the biphasic system stirred for 60 minutes. After phase separation, the organic layer was extracted with 1 M aqueous citric acid solution (1x50 mL), water (1x50 mL), saturated aqueous NaHCO₃-solution (1x50 mL), water (1x50 mL), brine (1x50 mL), dried over MgSO₄, filtered, and evaporated i.vac. The crude product (1.55 g) was purified via column chromatography on silica (eluent: CH₂Cl₂:MeOH 95:5). The impure fractions were further purified via column chromatography and precipitation in PE to give pure **117** in quantitative yield.

HPLC-MS ((2x150 mm Luna Phenyl-Hexyl 3μm, acetonitrile:water Grad 40 95A): 16.35 min (>99.0% peak area, ESI(+): 661.42 (**117** + 1 H⁺), 561.35 (**117** - (Boc) + 1 H⁺). ESI(-): 659.21 (**117** - 1 H⁺)).

$R_F = 0.40$ (PE:EE 2:1)

¹H NMR (400 MHz, CD₂Cl₂, 20 °C): δ 7.40 - 7.30 (m, 5 H, C¹⁸⁻²⁰H), 6.90 (d, ³J(*H,H*) = 7.8 Hz, 1 H, N¹³H), 6.68 (d, ³J(*H,H*) = 7.2 Hz, 1 H, N¹⁰H), 6.53 (d, ³J(*H,H*) = 6.7 Hz, 1 H, N⁷H), 5.13 (dd, *J*(*H,H*) = 12.4 Hz, *J*(*H,H*) = 21.3 Hz, 2 H, C¹⁶H₂), 5.00 (d, ³J(*H,H*) = 6.2 Hz, 1 H, N⁴H), 4.56 - 4.49 (m, 1 H, C¹⁴H), 4.43 - 4.34 (m, 1 H, C¹⁴H), 4.28 - 4.19 (m, 1 H, C⁸H), 4.03 - 3.96 (m, 1 H, C⁵H), 1.77 - 1.36 (m, 21 H, 3 C¹H₃, 4 C²⁰H₂, 4 C²¹H), 0.98 - 0.83 (m, 24 H, 8 C²²H₃).

¹³C NMR (MeOD): δ 175.73, 174.58, 174.52, 173.51, 157.58, 137.12, 129.48, 129.20, 129.13, 80.50, 67.72, 54.85, 53.46, 53.03, 52.27, 42.07, 41.57,

41.24, 41.11, 28.77, 25.81, 25.75, 23.51, 23.48, 23.38, 22.16, 21.94, 21.84, 21.74.

High-resolution ESI-MS: $m/z = 661.4539$ (calcd 661.4535 for $C_{36}H_{60}N_4O_7 + 1 H^+$), 683.4361 (calcd 683.4354 for $C_{36}H_{60}N_4O_7 + 1 Na^+$), 1321.9009 (calcd 1321.8997 for $(C_{36}H_{60}N_4O_7)_2 + 1 H^+$), 1343.8816 (calcd 1343.8816 for $(C_{36}H_{60}N_4O_7)_2 + 1 Na^+$).

4.4 Literature

- [1] F. Fages, F. Vogtle, M. Zinic, in *Low Molecular Mass Gelators: Design, Self-Assembly, Function*, Vol. 256, SPRINGER-VERLAG BERLIN, Berlin, **2005**, pp. 77.
- [2] Y. Murakami, H. Hara, T. Okada, H. Hashizume, M. Kii, Y. Ishihara, M. Ishikawa, M. Shimamura, S.-i. Mihara, G. Kato, K. Hanasaki, S. Hagishita, M. Fujimoto, *J. Med. Chem.* **1999**, 42, 2621.
- [3] T. Fujisawa, S.-I. Katakura, S. Odake, Y. Morita, J. Yasuda, I. Yasumatsu, T. Morikawa, *Chem. Pharm. Bull.* **2001**, 49, 1272.
- [4] A. Parenty, X. Moreau, J. M. Campagne, *Chem. Rev.* **2006**, 106, 911.
- [5] G. W. Starkey, J. J. Parlow, D. L. Flynn, *Bioorg. Med. Chem. Lett.* **1998**, 8, 2385.
- [6] R. Dembinski, *Eur. J. Org. Chem.* **2004**, 2763.
- [7] K. Wisniewski, A. S. Koldziejczyk, B. Falkiewicz, *J. Pep. Sci.* **1998**, 4, 1.
- [8] J. Inanaga, K. Hirata, H. Saeki, T. Katsuki, M. Yamaguchi, *Bull. Chem. Soc. Jpn.* **1979**, 52, 1989.
- [9] M. Sasaki, M. Ishikawa, H. Fuwa, K. Tachibana, *Tetrahedron* **2002**, 58, 1889.
- [10] B. M. Bachmann, D. Seebach, *Helv. Chim. Acta* **1998**, 81, 2430.
- [11] M. Hikota, H. Tone, K. Horita, O. Yonemitsu, *J. Org. Chem.* **1990**, 55, 7.
- [12] K.-I. Takao, H. Saegusa, G. Watanabe, K.-I. Tadano, *Tetrahedron: Asymmetry* **2000**, 11, 453.
- [13] U. Kizmaier, C. Hebach, A. Watzke, S. Maier, H. Mues, V. Huch, *Org. Biomol. Chem.* **2005**, 3, 136.
- [14] V. S. Au, J. B. Bremner, J. Coates, P. A. Keller, S. G. Pyne, *Tetrahedron* **2006**, 62, 9373.
- [15] S. B. Y. Shin, B. Yoo, L. J. Todaro, K. Kirshenbaum, *J. Am. Chem. Soc.* **2007**, 129, 3218.
- [16] P. A. Raj, P. Balaram, *Biopolymers* **1985**, 24, 1131.

- [17] T. Higashijima, M. Tasumi, T. Miyazawa, M. Miyoshi, *Eur. J. Biochem.* **1978**, 89, 543.
- [18] M. Iqbal, P. Balaram, *Biochemistry* **1981**, 20, 7278.
- [19] M. Iqbal, P. Balaram, *Biopolymers* **1982**, 21, 1427.
- [20] P. Baeckstrom, L. Li, M. Wickramaratne, T. Norin, *Synth. Commun.* **1990**, 20, 423.
- [21] D. A. Quagliato, P. M. Andrae, E. M. Matelan, *J. Org. Chem.* **2000**, 65, 5037.

5 Linear Triazole Containing Polypseudopeptides

5.1 Linear Triazole Containing Polypseudopeptides With Variable Stereochemistry

5.1.1 General Considerations

The successful incorporation of triazole isosteres into a peptide, as demonstrated by Ghadiri,^[1,2] and the synthesis of nonpeptidic foldamers, as shown by Arora,^[3] point out the synthetic feasibility and structural versatility of these pseudopeptides and imposed the idea of incorporating them into polypeptide backbones. The focus of this work always was on the influence of stereochemistry in the peptide backbone on its secondary structure. In all projects, the variation of the stereochemistry from *all*-L- to D-(*alt*)-L-configuration and its influence on the structure was the key interest. With regard to the interesting secondary structure of oligo-D-(*alt*)-L-peptides,^[4-6] polypeptides with D,L-alternating stereochemistry are a desirable target structure. Unfortunately, no satisfying technique to synthesize poly-D-(*alt*)-L-peptides has been reported so far. The polycondensation of D-(*alt*)-L-di- or tetrapeptides results in polymers with broad polydispersities.^[7,8] The main shortcoming of their synthesis is the degree of epimerization, leading to optically impure material. This epimerization is a result of racemization at the C α of the activated acid during the fragment condensation and is to a certain degree intrinsic for this type of polypeptide synthesis. With the incorporation of triazole isosteres into the polypeptide backbone, one could generate a new type of backbone with new structural preferences and properties and meanwhile use the highly efficient and regioselective "Click" reaction to replace the amide coupling, which is susceptible to racemization, to link the peptide monomers to the polypseudopeptide. The elaboration of a versatile monomer synthesis, which enables the racemization-free polymerization to polypseudopeptides containing the triazole isostere is an attractive task and described here.

5.1.2 Synthetic Considerations I

A triazole isostere containing polypeptide can in general be described as peptide segments, which are somehow connected via triazole units (Figure 1 on top). A closer look to the sequence of the polymer reveals the possible connectivity

5 Linear Triazole Containing Polypseudopeptides

differences of the segments. On the one hand, one peptide segment is at one side connected with the triazole via the 1-position and at the other side via the 4-position (Figure 1 middle, right). On the other hand, one peptide segment can be connected with the triazole via the 1-position at both sides, therefore, the next peptide segment is connected with the triazoles via the 4-position at both sides (Figure 1 middle, left). These patterns can be obtained via two different synthetic strategies and three different monomers (Figure 1 bottom). The 1,1,4,4-triazole-sequence can be achieved by copolymerization of an A_2 -monomer with a B_2 -monomer, the 1,4,1,4-triazole-sequence is obtained, when an AB-monomer is polymerized.

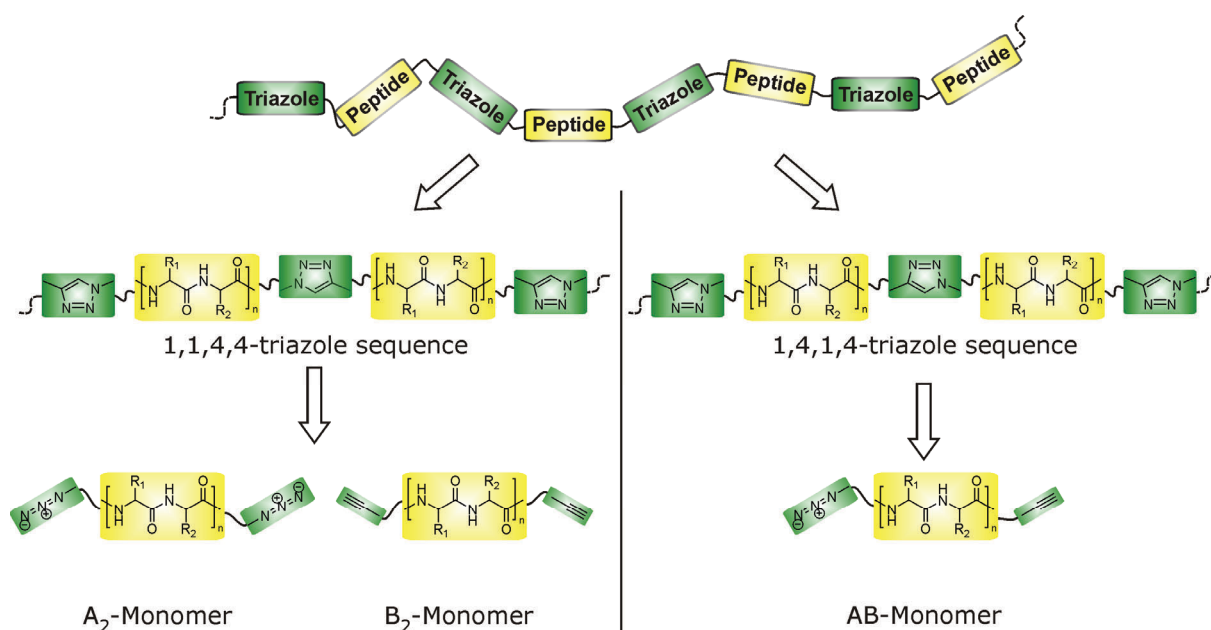


Figure 1: Schematic representation of a polypeptide with triazole incorporation into the backbone (on top), possible triazole directions in the sequence (middle) and resulting monomers (bottom).

Following the copolymerization pathway, several things have to be taken into consideration. The synthetic effort is high, since two different monomers have to be synthesized. In the polymerization reaction, the monomer ratios has to be abided very precisely, since a minimal change can significantly reduce the polymer length. The peptide segments have a certain chirality and chain direction, but the ends of the monomers are indistinguishable, so that the main chain direction can not be transferred into the polymer. Instead, the polymer main chain direction will be statistically scrambled (Figure 2).

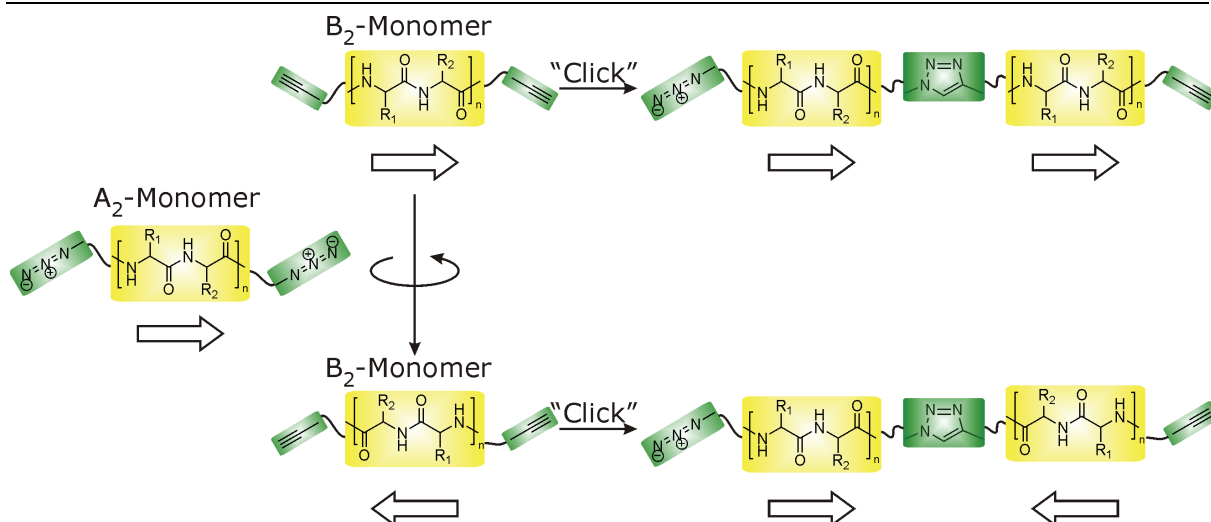


Figure 2: Indistinguishability of the monomer chain ends leads to scrambling in the main chain direction (main chain direction is symbolized with arrows).

These disadvantages can be circumvented, when the pathway of polymerizing an AB-monomer is followed. The synthetic effort is not as high as only one monomer has to be synthesized. The ends of the AB-monomer are distinguishable, what prevents a scrambling of the main chain direction. By this, the synthesis of a fully chiral polypseudopeptide with defined backbone structure should be possible.

For the design of an AB-monomer, two major questions have to be answered: How long are the peptide segments? In what manner are the azide and the acetylene attached to the chain ends of the peptide segment? The length of the peptide segment is determined by two factors. On the one hand, the synthetic effort should be kept as minimal as possible, favoring short segments. On the other hand, the information that should be transferred into the polymer has to be implemented into the repeat unit and hence into the monomer. The more complex the information, the longer the peptide segment has to be. In order to mimic the D,L-alternating stereochemistry of Gramicidin, the information of an alternating stereochemistry has to be incorporated into the monomer. When only homo-structures consisting of one amino acid are taken into consideration, a D-(*alt*)-L-dipeptide is sufficient to transfer the alternating stereochemistry into the polymer. The attachment of the azide to the chain end can readily be achieved by converting the amine at the N-terminus into an azide. This reaction proceeds smoothly and yields the azide under retention of the absolute

5 Linear Triazole Containing Polypseudopeptides

configuration.^[9] The acetylene can be introduced by coupling propargylamine to the C-terminus of the segment. The subsequent polymerization of the AB-“Click”-monomer should then yield a D-(*alt*)-L-polypseudopeptide (Figure 3).

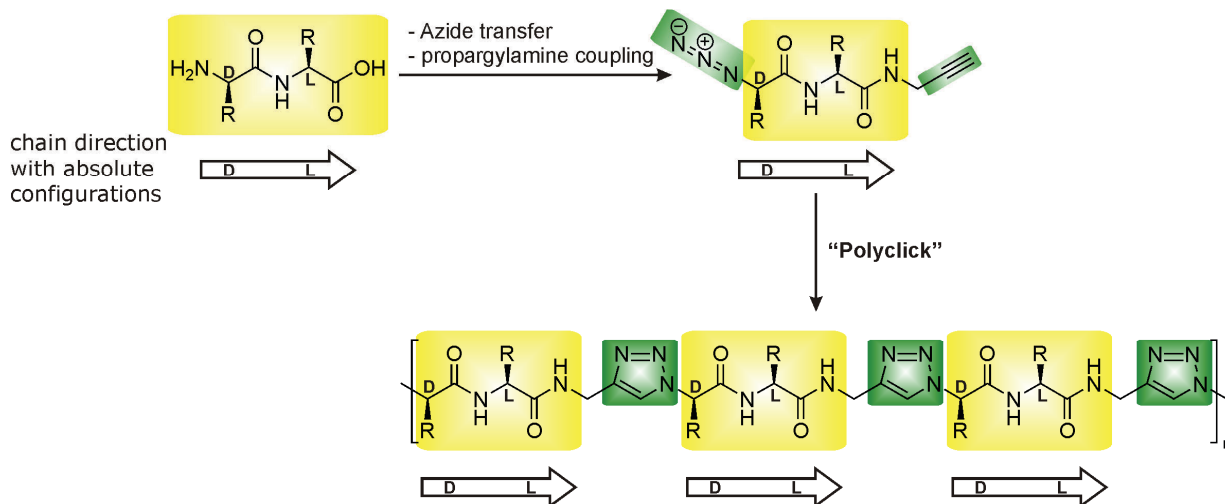
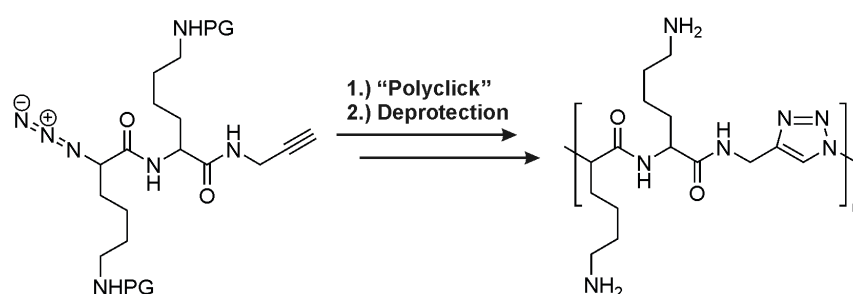


Figure 3: Transfer of a D-(*alt*)-L-dipeptide into an AB-“Click”-monomer and subsequent polymerization to D-(*alt*)-L-polypseudopeptide.

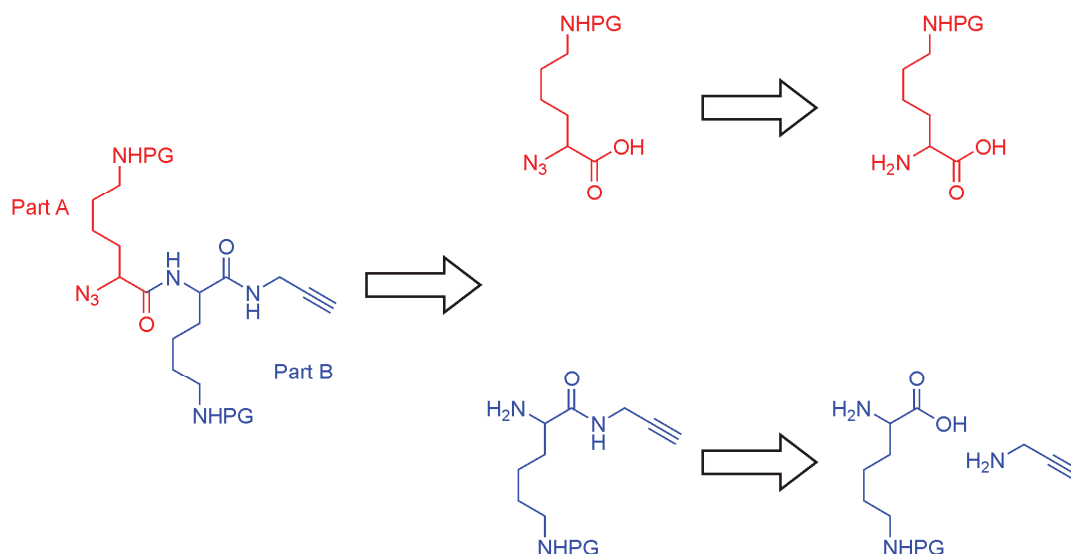
In analogy to the studies on oligo-D-(*alt*)-L-lysines (see Chapter 3) and the potential pH-dependent secondary structure switching behavior of peptides with chargeable side chain functionalities, polypseudopeptides consisting of D-(*alt*)-L-lysine dipeptide segments, connected via triazole units are the target structure (Scheme 1). The structure of the required AB-“Click”-monomer and hence the target structure of the monomer synthesis is also shown in Scheme 1.



Scheme 1: Targeted monomer structure (left) and resulting polypseudopeptide structure (right) (PG denotes protecting group).

The desired *N*_ε-protected monomer can be derived from a *N*_ε-protected azido-lysine (Part A) and *N*_ε-protected lysine propargylamide (Part B) (Scheme 2). Azido-lysine can be obtained from the conversion of *N*_ε-protected lysine, the

lysine propargylamide can be derived from *N* ϵ -protected lysine and propargylamine.



Scheme 2: Retrosynthesis of a protected AB-Click-monomer (PG denotes protecting group).

In a first approach to the synthesis of the desired monomer, 2Cl-Z was chosen as *N* ϵ -protecting group. Due to the robustness of this protecting group, it was supposed to overcome the reaction conditions of the azido transfer. Since the azido transfer was supposed to be the yield limiting step in the synthesis, only L-lysine was subjected to it, fixing the stereochemistry of the dipeptide to be L-(*alt*)-D.

5.1.3 Monomer Synthesis I

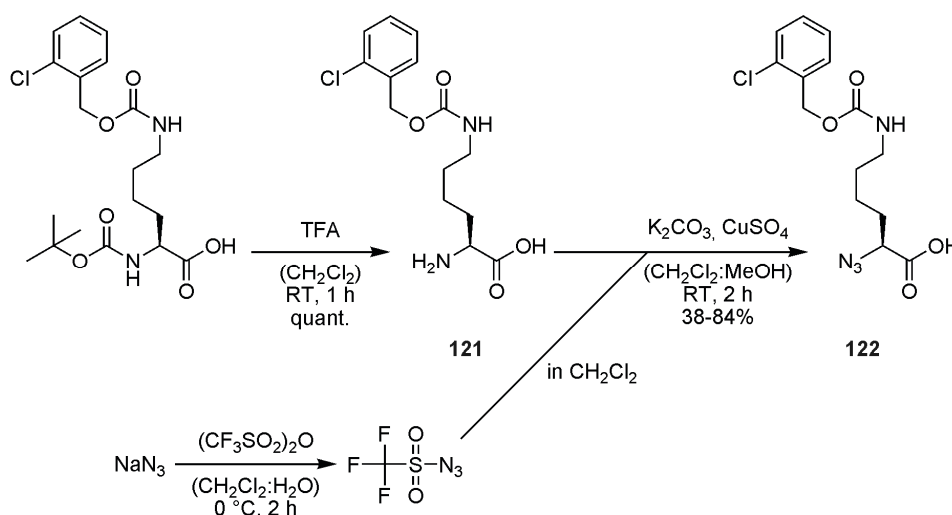
The synthesis of the monomer can be divided into the synthesis of part A, the synthesis of part B and the junction of both parts.

5.1.3.1 Synthesis Of Part A

The synthesis of part A is shown in Scheme 3. The sequence started with the Boc deprotection of Boc-L-Lys(2Cl-Z) to L-Lys(2Cl-Z) (**121**). This reaction proceeded in quantitative yield. Due to the possible water solubility of **121**, the aqueous work-up was skipped and the solvent simply evaporated *in vacuo* to give the TFA-salt of L-Lys(2Cl-Z). In the last step, **121** was transferred to the azido amino acid **122** using triflyl azide. This metal-catalyzed diazo transfer has already been described in the literature.^[9] First, NaN₃ was reacted with triflyl

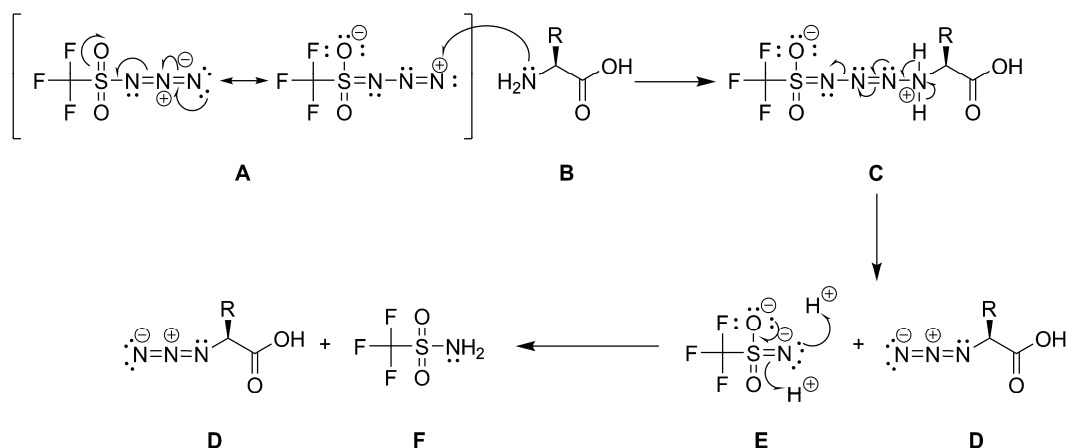
5 Linear Triazole Containing Polypseudopeptides

anhydride to give triflyl azide, which was added to **121**. The copper-catalyzed diazo transfer proceeded smoothly and gave the product in moderate 38% yield. With the addition of more, freshly synthesized triflyl azide after 2 h reaction time, the yield of the diazo transfer could be increased to more than 80% after column chromatography.



Scheme 3: Synthesis of part A of the AB-“Click”-monomer.

The diazo transfer gave pure **122** under retention of the absolute configuration. In the case of a nucleophilic displacement on C_α of the amino acid with N_3^- as nucleophile, one would expect – at least partial - inversion of the configuration. That this is not happening can easily be explained by the mechanism of the reaction, which is shown very simplified in Scheme 4.

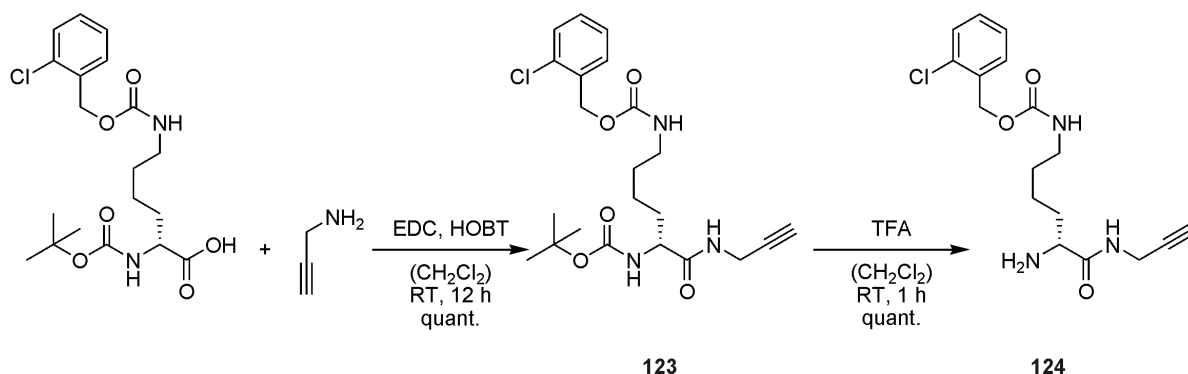


Scheme 4: Schematic representation of the diazo transfer mechanism.

The first step of the reaction is a nucleophilic attack of the amine of the amino acid on the azide nitrogen to give structure **C**. The electrophilic character of the azide group in triflyl azide can be realized by one resonance structure of **A** (on the right). Structure **C** splits into the desired product **D** and structure **E**, which is protonated in the next step to give trifluoromethanesulfonic acid amide **F**.

5.1.3.2 Synthesis Of Part B

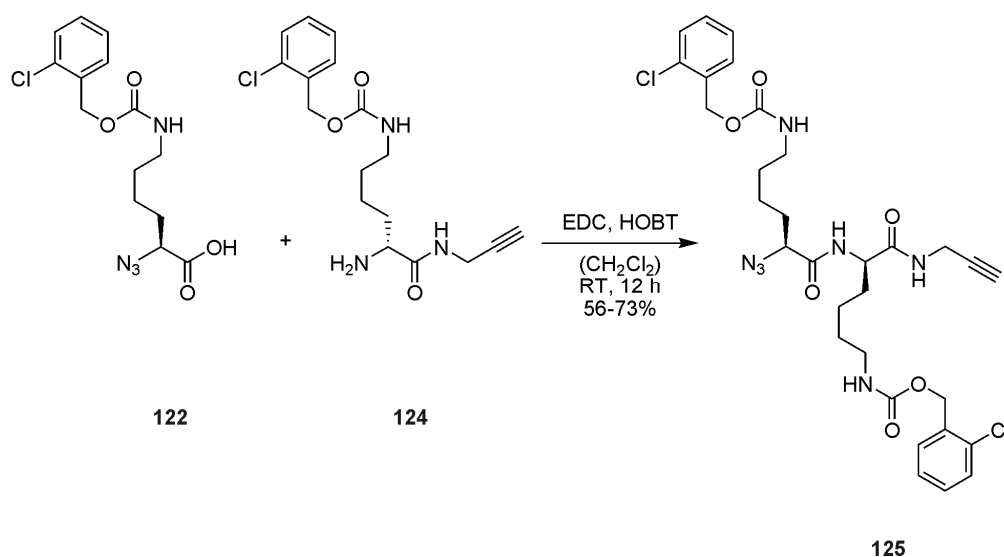
The synthesis of the building block **124** was straightforward and high yielding (Scheme 5). Boc-D-Lys(2Cl-Z) was coupled with propargylamine to give the lysine propargylamide **123** in quantitative yield after column chromatography. The Boc protecting group of **123** was removed with TFA in methylene chloride to give pure **124** after aqueous work-up.



Scheme 5: Synthesis of part B of the AB-“Click”-monomer.

5.1.3.3 Coupling Of Part A And Part B

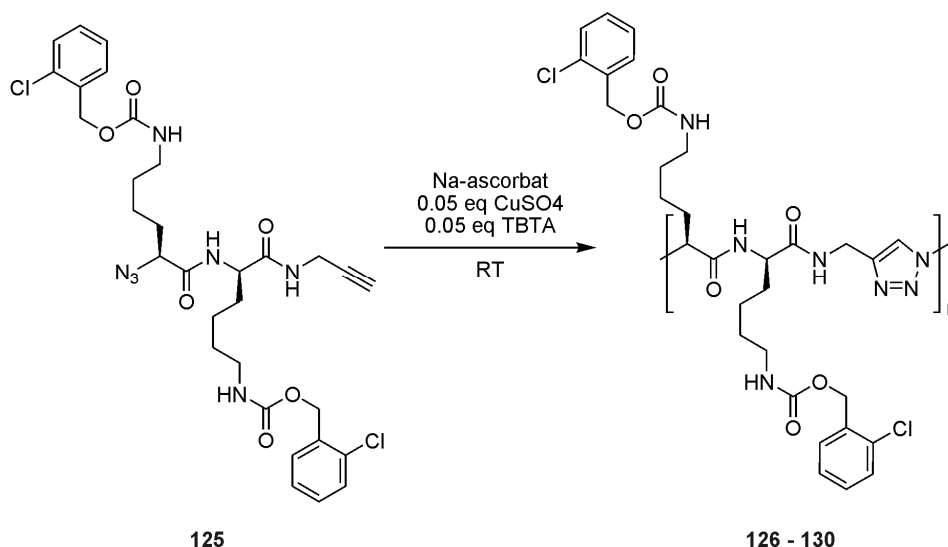
The coupling of the two fragments **122** and **124** was achieved in methylene chloride with EDC and HOBT as coupling reagents. Despite the very good experiences with EDC and HOBT, this coupling gave the desired product only in moderate yields.



Scheme 6: Coupling of part A (**122**) and part B (**124**) to the desired AB-“Click”-monomer **125**.

5.1.4 Polymerization I

The monomer was then subjected to polymerization in order to obtain high molecular weight polymers. The polydispersity of the resulting polymer was expected to be broad, due to the fact that a polycondensation reaction was used for polymerization. Monomer **125** was polymerized under well established conditions, using sodium ascorbate as reducing agent, copper sulfate as catalyst precursor and tris[(1-benzyl-1H-1,2,3-triazol-4-yl)methyl] amine (TBTA) as ligand. In the reaction, Cu(II) is reduced by sodium ascorbate to Cu(I), which is the catalytically active species. The general thermodynamic instability of Cu(I) however, results in easy oxidation to Cu(II) and disproportionation to Cu(0) and Cu(II). TBTA complexes Cu(I) and inhibits these processes. The use of CuSO₄ as catalyst precursor requires the addition of water to the reaction in order to dissolve it. The polymerization was done in different solvent systems. The results of the polymerizations are summarized in Table 1.

Table 1: Polymerization of AB-“Click”-monomer **125**.

Entry	Product	Solvent	Reaction time	Polymer length ¹
1	126	DMF:H ₂ O 1:1	2 d	dimer-nonamer ²
2	127	DMF ³	6 d	dimer
3	128	THF:H ₂ O 2:1	2 d	dimer-hexamer
4	129	DMSO:H ₂ O 4:1	13 d	dimer-tetramer
5	130	CH ₂ Cl ₂ :DMF:H ₂ O 1:1:1	14 d	dimer-tetramer

¹ As determined by MALDI-TOF; ² ESI-MS and GPC only detected dimer and trimer; ³ only minimum amount of water was added in order to dissolve CuSO₄.

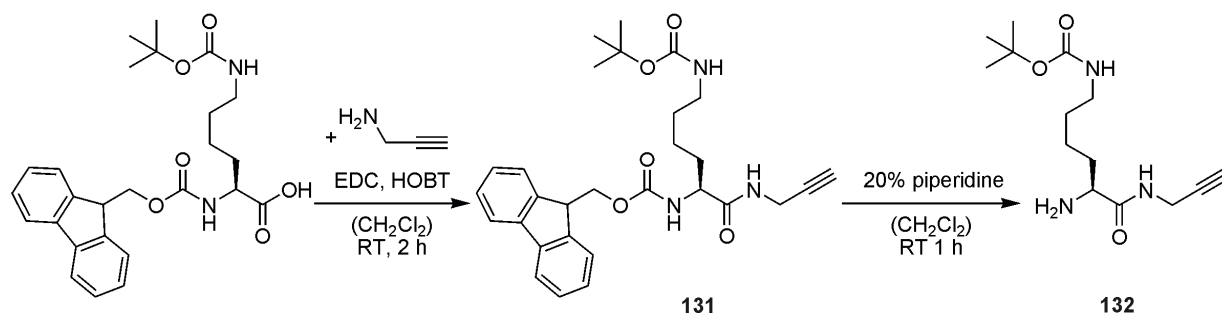
In a first attempt, the polymerization was accomplished in a DMF:H₂O (1:1) system (entry 1). After stirring for one day, a white precipitate was visible. After stirring the reaction mixture for one more day, it was subjected to the general work-up procedure, which consisted of its precipitation in water and subsequent washing of the solid with aqueous EDTA-solution in order to remove remaining copper ions. The product was analyzed by ESI-MS, MALDI-TOF, and GPC. GPC and ESI-MS were in good agreement and confirmed the existence of products with molecular masses that referred to dimer and trimer. MALDI-TOF also showed traces of higher oligomers (up to nonamer), but since MALDI is no quantitative analysis, the GPC results probably reflected the real product distribution much better. According to GPC and ESI-MS, the main product of this reaction was dimer and trimer, what referred to only one to two “Click”-reactions. The “Click”-reaction as such is a very potent reaction, hence the low conversion in the polymerization was probably due to solubility issues in

agreement with the poor solubility of the product and the appearance of a precipitate during the reaction. In order to increase the solubility of the oligomers, different solvent systems were tried.

In a second attempt, DMF with the minimal amount of water, necessary for the dissolution of copper sulfate was used (entry 2). After two days, no conversion was detectable, and more water was added. With the addition of more water, a white solid was immediately precipitating. Standard work-up after six days altogether yielded a white solid. MALDI-TOF only detected dimer. The use of THF:H₂O (2:1) (entry 3), DMSO: H₂O (4:1) (entry 4) and CH₂Cl₂:DMF:H₂O 1:1:1 (entry 5) in combination with long reaction times did not improve the situation, so that no further effort was invested into the polymerization of monomer **125**. As already experienced in the synthesis of *N*_ε-2Cl-Z-protected oligolysines, the solubility decreased remarkably with longer chain lengths. Especially in the presence of water, the oligopeptides or oligopseudopeptides were not soluble. The poor solubility of the peptides and pseudopeptides was referred to the 2Cl-Z protecting group. In order to increase solubility and chain length of the polymers, the 2Cl-Z protecting group had to be replaced by another protecting group, such as Boc. This resulted in a new protecting group strategy and a new synthesis to a monomer with different permanent protecting groups.

5.1.5 Synthetic Considerations II

To increase the solubility of the polymer, the 2Cl-Z group was replaced by the Boc group. As experienced in the oligolysine synthesis (Chapter 3), the shortcoming of hampered compound solubility, caused by the 2Cl-Z protecting group could be overcome with its replacement by the Boc group. This replacement required a new monomer synthesis with different protecting group strategy. Instead, Fmoc-Lys(Boc) or Z-Lys(Boc) could be used as starting material. Since Fmoc could be cleaved under mildly basic conditions, no change in the general synthetic concept was necessary. In a first attempt, Fmoc-L-Lys(Boc) was coupled to propargylamine (Scheme 7).



Scheme 7: Attempt to the synthesis of AB-"Click"-monomer starting from Fmoc-L-Lys(Boc).

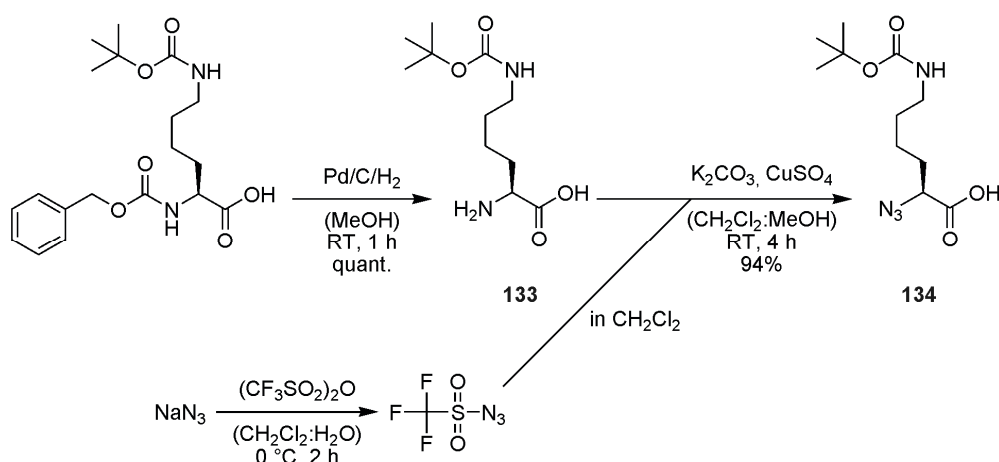
This coupling proceeded smoothly and gave the product **131** in high yields after tedious purification via column chromatography. Despite the nonpolar character of **131**, purification via a short column with CH₂Cl₂ (under addition of MeOH) was very time and solvent consuming and gave only impure material. The subsequent Fmoc cleavage proceeded smoothly in methylene chloride under addition of 20% piperidine. However, it was impossible to isolate product **132** from piperidine and the fluorene impurities, since column chromatography of the product was not feasible due to its high polarity. Hence, it turned out that Fmoc-Lys(Boc) could not be used as starting material for the monomer synthesis. The alternative was the use of Z-Lys(Boc) instead. The change from the temporary Boc or Fmoc group, which could be cleaved under acidic or basic conditions to the temporary Z group had an impact on the synthesis of the monomer, since the Z group had to be cleaved using Pd/C/H₂. These conditions were not compatible with acetylenes, hence the acetylene had to be introduced in the last step of the synthesis. Nevertheless, in analogy to Scheme 2 the synthesis can be divided into the synthesis of part A and part B and the coupling of both parts. The Boc protected monomer was synthesized with D-(*alt*)-L- and also with *all*-L-configuration in order to obtain polymers with alternating and with non alternating stereochemistry.

5.1.6 Monomer Synthesis II

5.1.6.1 Synthesis Of Part A

The synthesis of part A is shown in Scheme 8 and started with the reductive cleavage of the Z group on Z-L-Lys(Boc) to give L-Lys(Boc) (**133**) in quantitative

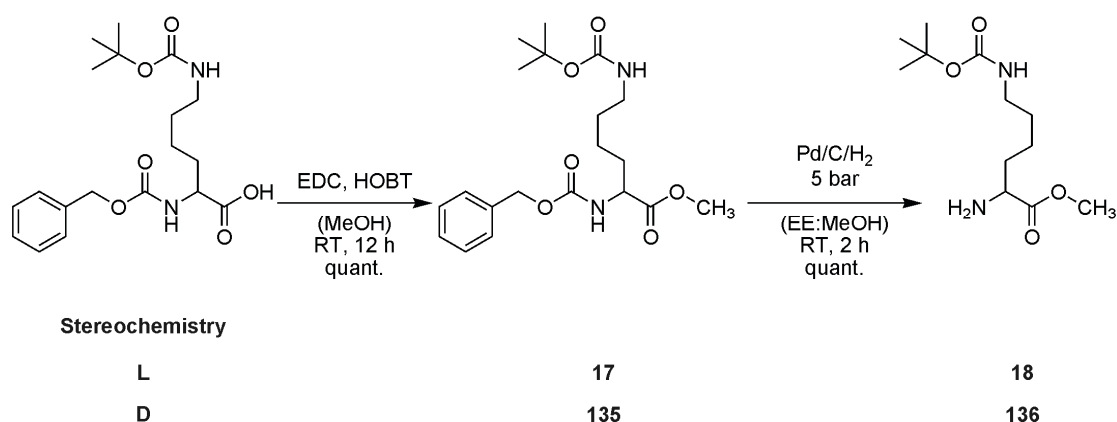
yield. Subsequent diazo transfer under optimized conditions gave the resulting azido amino acid **134** in 94% yield after column chromatography.



Scheme 8: Synthesis of Part A of the AB-“Click”-monomer.

5.1.6.2 Synthesis Of Part B

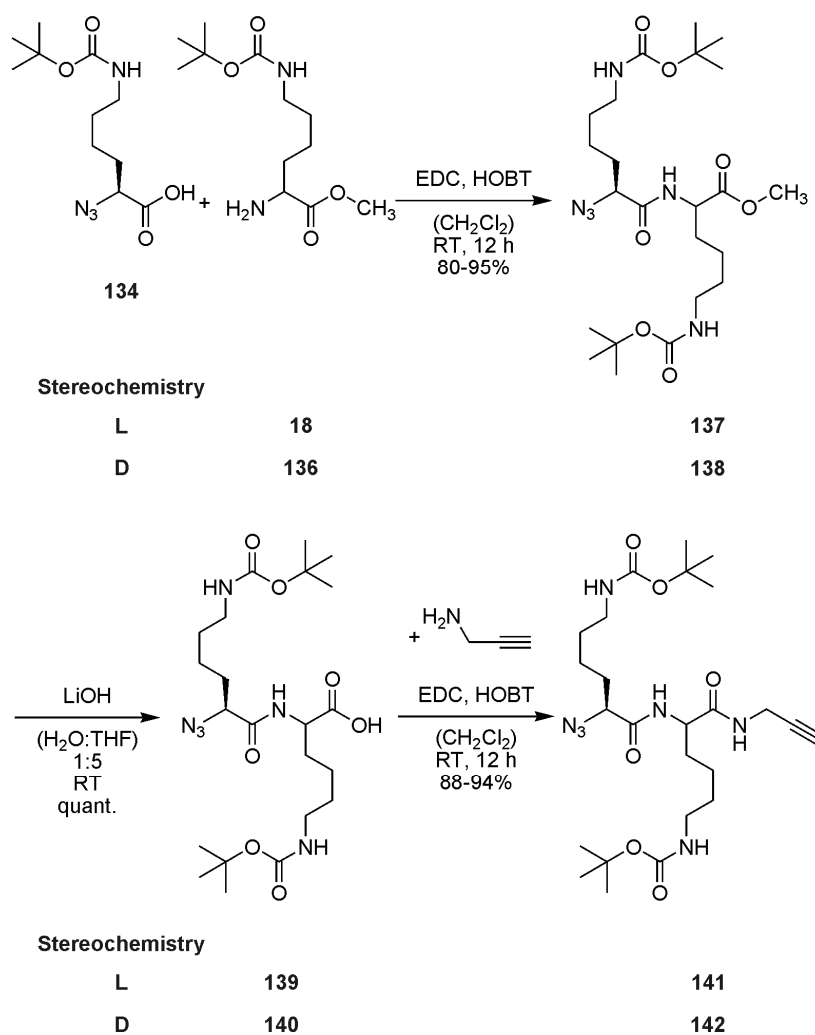
In order to obtain the monomer with D-(*alt*)-L- and also with *all*-L-configuration, Z-L-Lys(Boc) and Z-D-Lys(Boc) were used as starting material. Different from the synthesis of part B of the 2Cl-Z protected monomer, Z-Lys(Boc) could not directly be converted into the propargylamide, since the subsequent Z-deprotection was not compatible with the acetylene. Instead, Z-Lys(Boc) was transferred into the methylesters **17** and **135** first (Scheme 9). This reaction gave the products in quantitative yields after column chromatography. The subsequent reductive cleavage of the Z group proceeded smoothly and gave the desired products **18** and **136** in quantitative yields.



Scheme 9: Synthesis of Part B of the AB-“Click”-monomer.

5.1.6.3 Coupling Of Parts A And B And Conversion To The AB-"Click"-monomer

The coupling of azido-L-Lys(Boc) (**134**) with L- and D-Lys(Boc)-Me (**18** and **136**) proceeded smoothly and gave the resulting dipeptides **137** and **138** in good to excellent yields after purification via column chromatography.

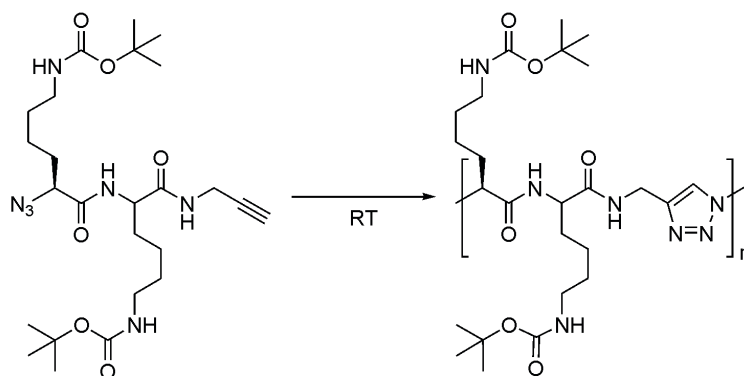


Scheme 10: Coupling to the azido dipeptide and conversion to the AB-"Click"-monomer.

Subsequent saponification of the methyl ester gave the free acids **139** and **140** in quantitative yields. The acids were then coupled with propargylamine to give the desired AB-"Click"-Monomers azido-L-Lys(Boc)-L-Lys(Boc)-propargylamide (**141**) and azido-L-Lys(Boc)-D-Lys(Boc)-propargylamide (**142**) in good to excellent yields after column chromatography.

5.1.7 Polymerization II

The pure monomers **141** and **142** were subjected to polymerization. In all reactions, the monomer was dissolved in the minimum amount DMF necessary to obtain a stirrable solution. When the copper catalyst was derived from CuSO₄, highly concentrated aqueous solutions of sodium ascorbate and CuSO₄ were added. When tetrakis(acetonitrile)copper(I) hexafluorophosphate was used as copper catalyst, the addition of water was unnecessary. The ligand TBTA, which was used in the polymerization of **125** was replaced by *N,N'*-dimethylethylenediamine, since in other reactions, TBTA turned out to be hardly separable from the products. In all reactions, copper wire was added. In contrast to the polymerization attempts with the 2Cl-Z protected monomer **125**, no precipitation occurred, even in the presence of water. Instead, the reaction mixtures started to become highly viscous after approximately 6 h. The reaction times were varied from 3 days to 2 weeks. Monitoring of the reaction via GPC revealed that once the reaction mixture had become highly viscous, longer stirring (even under dilution of the sample) led to no significant change in polymer length. The general work-up procedure was a repetitive precipitation in aqueous EDTA-solution and filtration. The crude product was swollen in MeOH and dialyzed in MeOH using a dialysis tube with a molecular weight cut-off (MWCO) of 25000 g/mol. In most cases, dialysis yielded pure high molecular weight material, which was analyzed by GPC analysis. The effect of purification could be monitored by GPC (Figure 4, left). The results of the polymerization reactions are shown in Table 2.

Table 2: Polymerization of AB-“Click”-monomers **141** and **142**.

Stereochemistry

L 141

143 - 149

D 142

150 - 153

Entry	Product (config.)	Solvent (Conc. [mol/L])	Mn [g/mol] ³	Mw [g/mol] ³	PDI	Mp [g/mol] ³
1 ¹	143 (L,L)	DMF:H ₂ O 2:1 (0.66)	120000	180000	1.5	170000
2 ¹	144 (L,L)	DMF:H ₂ O 5:1 (0.44)	24000	45000	1.9	56000
3 ¹	145 (L,L)	DMF:H ₂ O 5:1 (0.44)	13000	25000	1.9	22000
4 ¹	146 (L,L)	DMF:H ₂ O 5:1 (0.44)	3700	19000	5.1	20000
5 ¹	147 (L,L)	DMF:H ₂ O 5:1 (0.44)	9800	76000	7.8	20000
6 ¹	148 (L,L)	DMF:H ₂ O 5:1 (0.44)	8300	22000	2.7	21000
7 ¹	149 (L,L)	DMF:H ₂ O 5:1 (0.44)	12000	30000	2.4	43000
8 ¹	150 (L,D)	DMF:H ₂ O 1:1 (0.66)	50000	88000	1.8	86000
9 ²	151 (L,D)	DMF (1.4)	21000	46000	1.8	60000
10 ²	152 (L,D)	DMF (0.66)	13000	20000	1.8	18000
11 ¹	153 (L,D)	DMF:H ₂ O 3:1 (0.44)	72000	170000	2.3	140000

¹ Reaction Conditions: 0.2 eq. CuSO₄, 0.4 eq. sodium ascorbate, 2.0 eq. *N,N*-dimethylethylenediamine, 1.5 eq. copper wire; ² Reaction Conditions: 0.2 eq. tetrakis(acetonitrile)copper(I) hexafluorophosphate, 0.4 eq. *N,N'*-dimethylethylenediamine, 0.5 eq. copper wire; ³ GPC-analysis (in DMF at 70 °C, calibrated with polystyrene standards, detection by RI).

The polymerization of the Boc protected monomers yielded in all reactions much higher molecular weights than the polymerization of 2Cl-Z protected monomer **125**. This was in good agreement with the observed solubility of the protected pseudopeptides. In the polymerization of **125**, the oligopseudopeptides could not be kept in solution and precipitated immediately, whereas the polymeric products of the polymerizations of **141** and **142** were soluble, forming gels instead. In the polymerizations of **125**, water acted as precipitating solvent. For this reason, the reactions under water free conditions (entries 9 and 10) were

expected to yield higher molecular weight polymers than under standard conditions. In the two test reactions, this was not the case. The polymers were comparable in size with the polymers obtained under standard conditions. For this reason, further polymerizations were done under standard conditions. There was no influence of the stereochemistry on the polymer length observable. L,L-monomer (**141**) and L,D-monomer (**142**) yielded polymers in comparable lengths. There was also no remarkable trend observable concerning the influence of the concentration of the monomer in solution on polymer length. Polymer **143** (entry 1) had a Mp of 170000 g/mol and was obtained from a highly concentrated solution (0.66 mmol/L). Polymer **144** (entry 2) had a Mp of 56000 g/mol and was obtained from a lower concentrated solution (0.44 mmol/L). Despite the much higher water content in the first reaction, the molecular weight of **143** was ca. three times higher than that of **144**. This clearly spoke in favor of higher concentrated polymerization solutions. In contrast, **153** (Mp = 140000 g/mol) was obtained from a lower concentrated solution than **150** (Mp = 86000 g/mol). Entries 4 to 7 reflect four polymerizations under similar conditions and under comparable conditions than the polymerization to **153**. The resulting polymers were shorter than **153** and hardly comparable in size and PDI. In summary, the polymerization reactions were yielding polymers with remarkably higher molecular weights than the polymerizations of **125**. The polymerization reaction is very sensible to several external factors, what is well reflected in Table 2, where polymerizations under similar conditions yield different results. Marginal deviations in the reaction conditions can lead to significant changes in polymer length and PDI. Hence, future effort has to be invested into the fine tuning of the reaction conditions, in order to improve the reproducibility of the polymerization. GPC-traces of the products of the three best polymerization reactions are shown in Figure 4 (right).

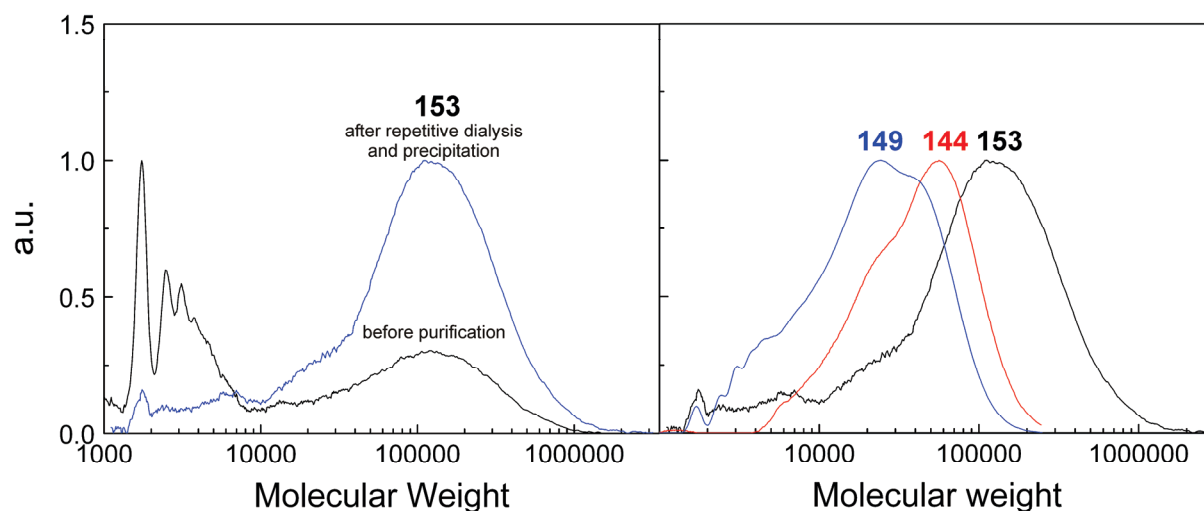


Figure 4: GPC-traces of polymer **153** before and after purification via precipitation and repetitive dialysis (left). GPC-traces of polypseudopeptides **144**, **149**, and **153** (all values are normalized) (GPC in DMF at 70 °C, calibrated with polystyrene standards).

5.1.8 Boc Deprotection Of Polymers

For further studies, the polymers **144**, **149**, and **153** were Boc deprotected. The Boc deprotection proceeded smoothly and yielded the polymers after dialysis in water using a dialysis tube with MWCO of 25000 g/mol (Scheme 11). A part of the polymer was also subjected to anion exchange from trifluoroacetate to chloride. Therefore, the polymer was dissolved in 1 M HCl and dialyzed again.



Unfortunately, the deprotected polymers could not be analyzed by GPC, since they were not detectable by UV and RI. The polymers do not contain a chromophore, which absorbs in the region >230 nm, rendering a UV-detection in DMF solutions impossible. The refraction index of the polymer is probably very close to that of DMF, also rendering detection by RI impossible. MALDI-TOF was not possible, since the PDI of the sample was too large for reliable analysis. Proton NMR was used to confirm total cleavage of the Boc group. Integration and broad shape of the proton signals agreed well with the polymeric structures (Figure 5).

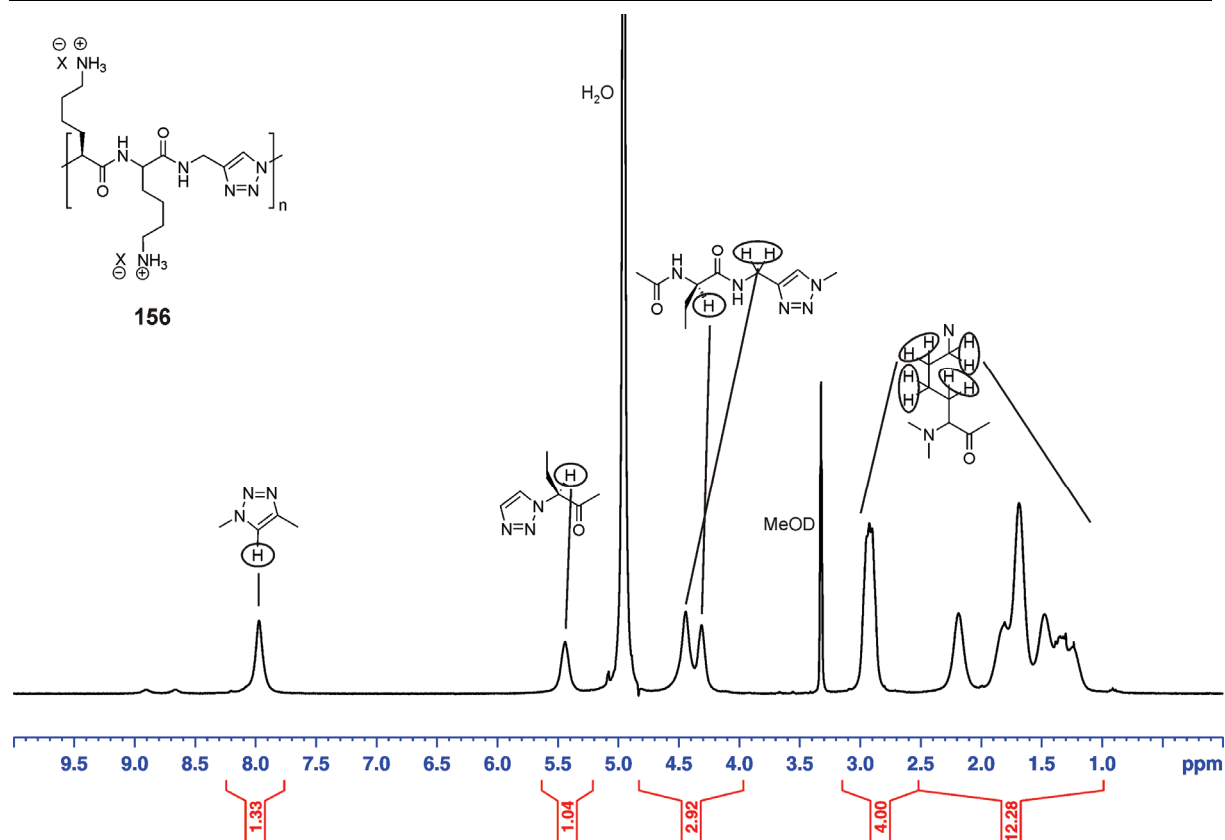


Figure 5: ^1H NMR of deprotected polypseudopeptide **156** ($\text{MeOH-}d_4$, 25°C).

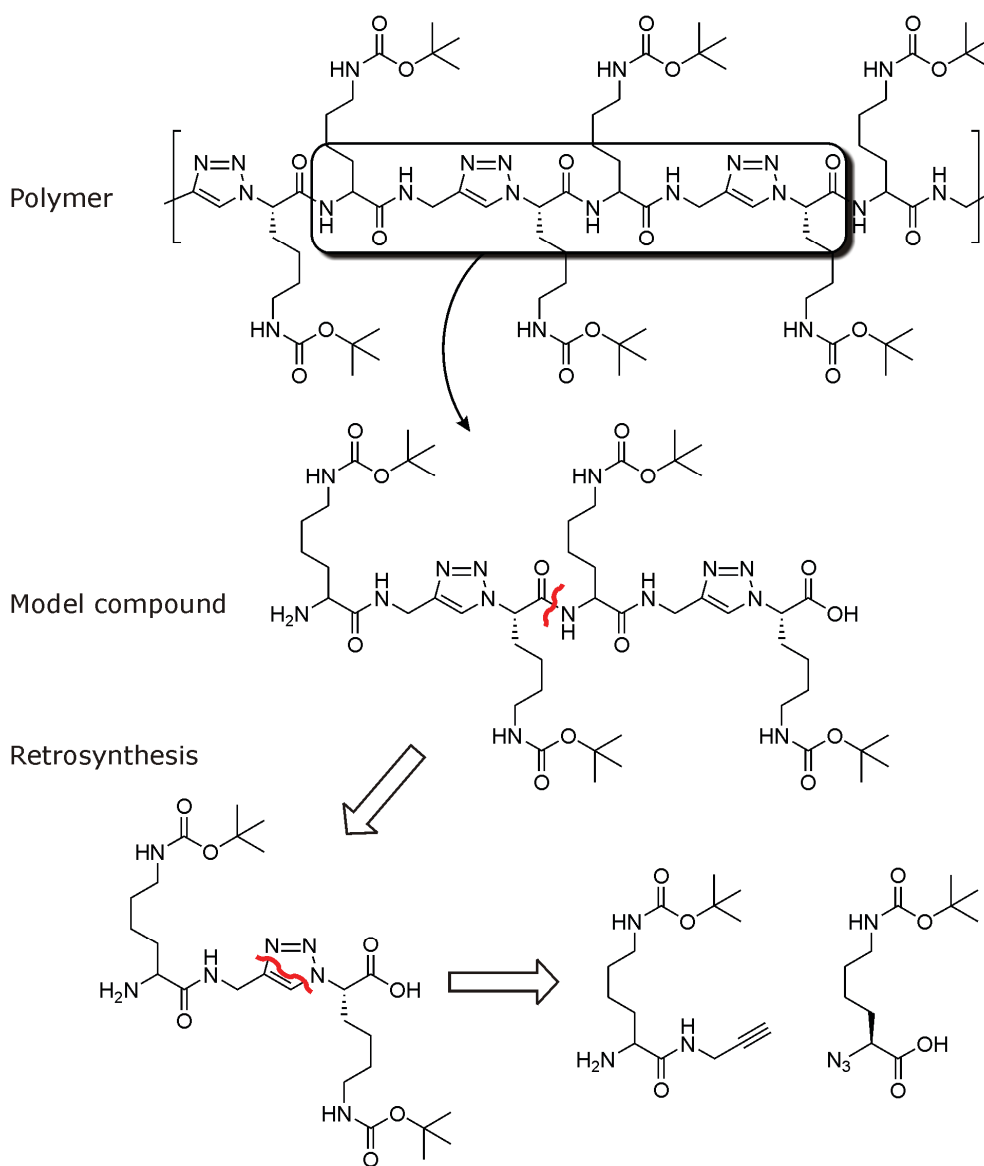
5.2 Model Compounds

5.2.1 General And Synthetic Considerations

The analysis and structural investigation of a new polymer class oftentimes suffers from the fact that signals (i.e. NMR, CD) can not be assigned to atoms or structural motifs. For a deeper understanding, the comparison of polymer signals with those of a model compound can be helpful. Sometimes, the monomer can serve as a good model for the polymer. NMR signals of the monomer for example can be extrapolated to the polymer, remarkably simplifying the assignment of the polymer signals. In this special case, the monomer was no sophisticated model for the polymer, since the triazole unit as major component of the polymer backbone was formed within the polymerization and was not present in the monomer yet. For a better assignment of NMR signals and in order to obtain reference signals for CD, model compounds with the key structural features of the polymer were

5 Linear Triazole Containing Polypseudopeptides

synthesized. A retrosynthetic approach to the model compound synthesis is shown in Scheme 12.

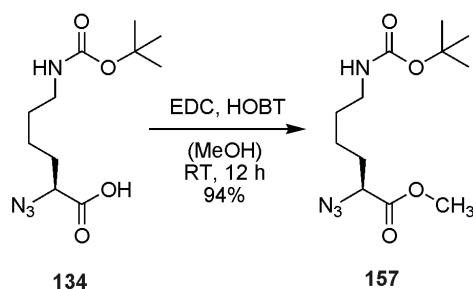


Scheme 12: Retrosynthetic approach of a model compound, mimicking the key structural features of the polymer.

A sophisticated model of the polymer has to consist of the dipeptide and at least one triazole unit. The model compound shown in Scheme 12 mimics the key structural features of the polymer. Retrosynthetically, the compound consists of two identical segments, connected by an amide bond. Cutting the molecule at this bond, one obtains the “Click” product of lysine propargylamide and azido lysine.

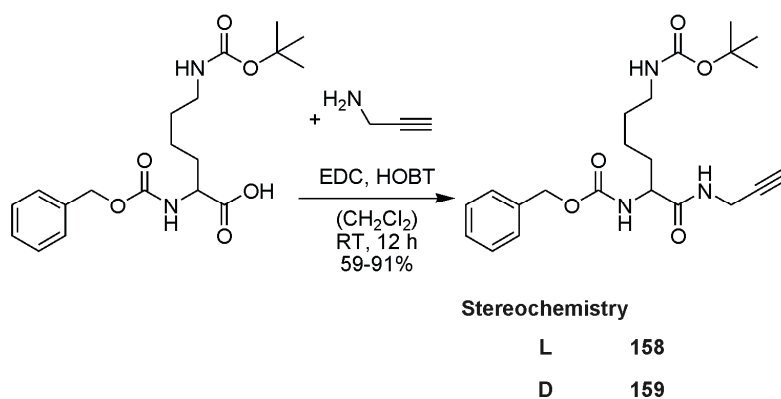
5.2.2 Synthesis Of The Modelcompounds

With the appropriate protecting group strategy, the synthesis started as depicted in Scheme 13 with the esterification of azido-L-Lys(Boc) to the methyl ester **157**. This reaction proceeded smoothly and gave the desired product in high yield after aqueous work-up. No further purification was necessary.



Scheme 13: Protection of azido-L-Lys(Boc) as methyl ester.

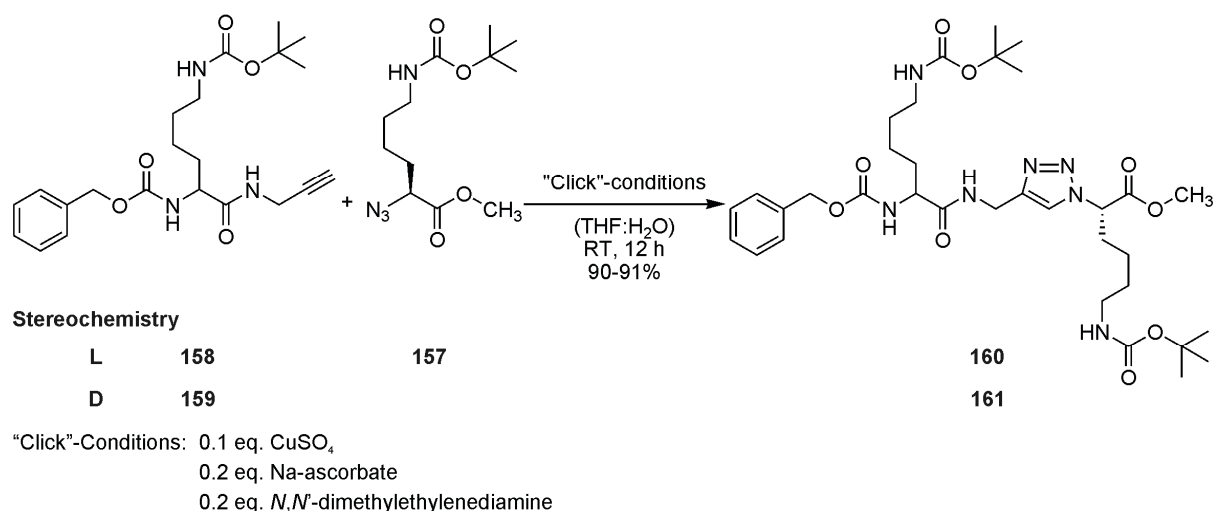
The second fragment of the prospective “Click”-product was obtained by coupling propargylamine with Z-Lys(Boc) (Scheme 14). This reaction usually gave the products **158** or **159** in high yields. The low yield of 59% was due to mistakes in the work-up procedure. Purification of the product was achieved via column chromatography on silica.



Scheme 14: Propargylamide formation of Z-Lys(Boc).

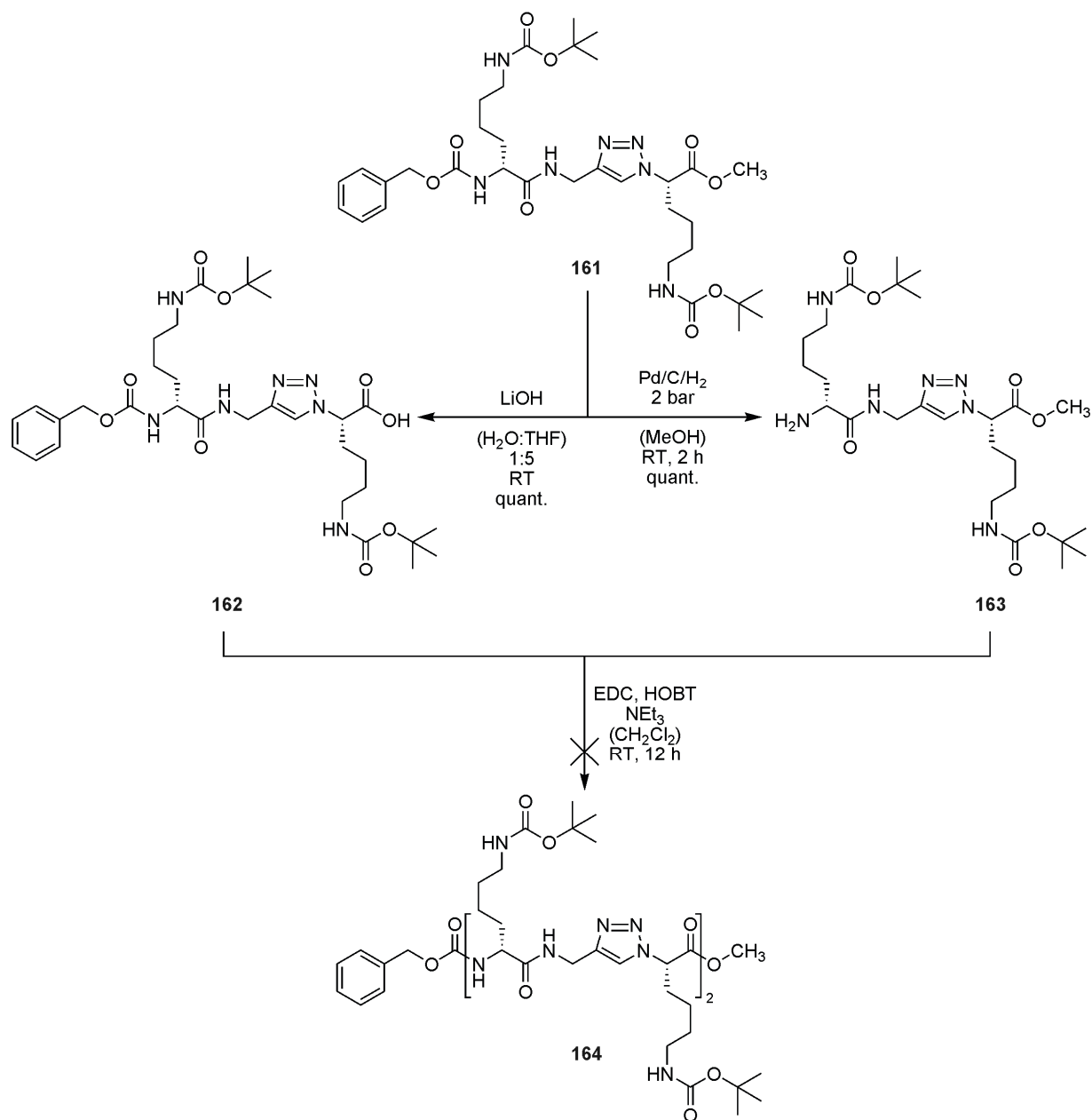
In the next step of the sequence, azido-L-Lys(Boc)-Me (**157**) was coupled with Z-L-Lys(Boc)-propargylamide (**158**) or Z-D-Lys(Boc)-propargylamide (**159**) (Scheme 15). The efficient reaction proceeded smoothly under optimized “Click”-conditions, using 0.1 equivalents CuSO₄, 0.2 equivalents sodium ascorbate and 0.2 equivalents ligand and gave the desired products in high yields after column chromatography.

5 Linear Triazole Containing Polypseudopeptides



Scheme 15: "Click"-reaction of Z-Lys(Boc) propargylamide and azido-L-Lys(Boc).

Further steps in the synthesis were first tried with one isomer. Compound **161** was subjected to a divergent/convergent synthesis protocol (Scheme 16). Both deprotections proceeded smoothly and gave the desired deprotected coupling fragments **162** and **163** in quantitative yields. The subsequent coupling to the desired protected model compound afforded a complex mixture of products that could not be separated. Precipitation of the desired compound failed and the R_F -values of the components were too similar for separation via column chromatography. The mixture was pre-purified via column chromatography in order to remove a major part of the impurities that could have prevented precipitation of the product. Unfortunately, the product did not precipitate even from the pre-purified mixture, so that despite all efforts, an isolation and purification of the desired model compound was not possible.



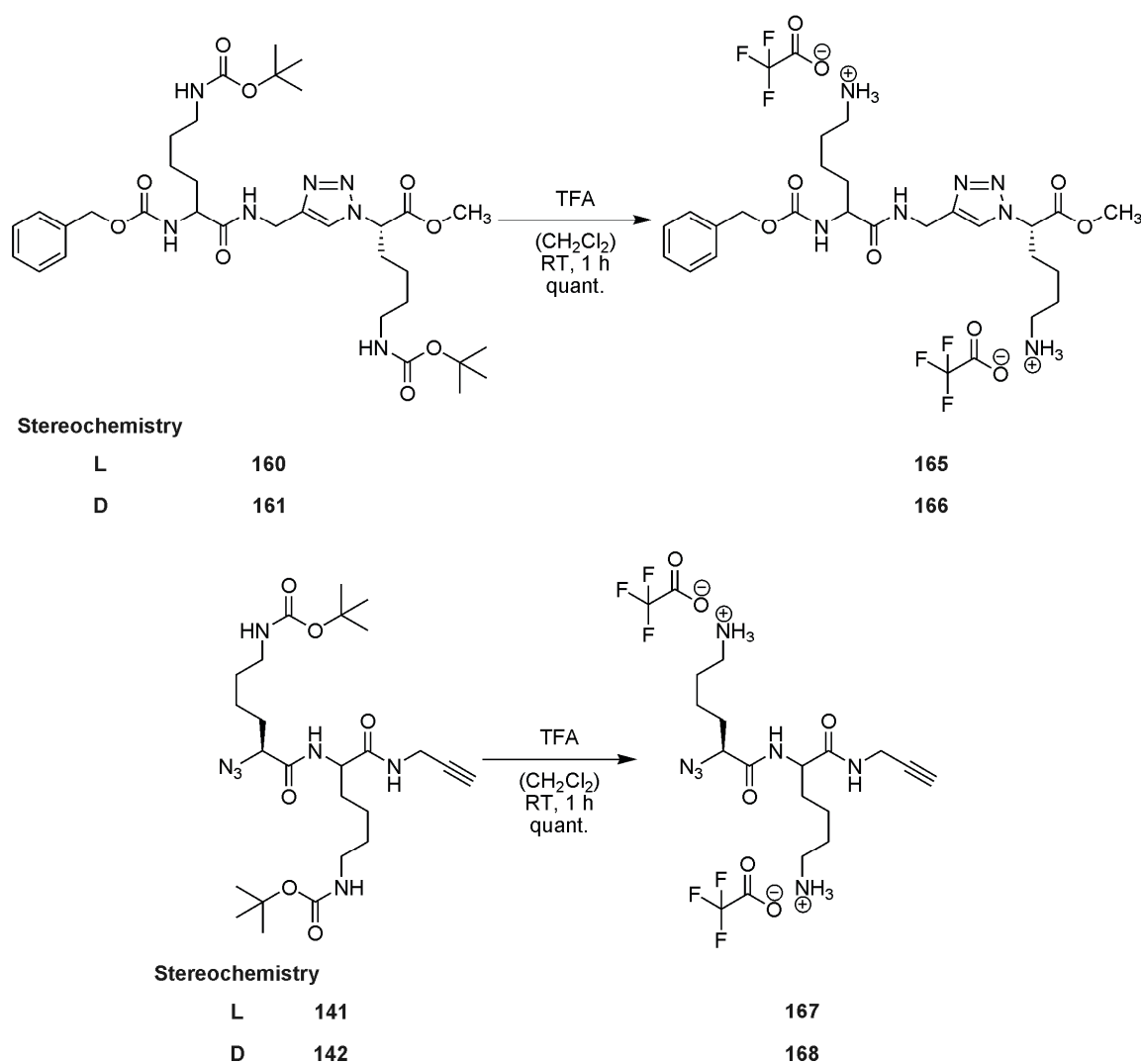
Scheme 16: Divergent/convergent synthesis approach to the model compound **164**.

The synthesis to the highly sophisticated model compound **164** failed, but the smaller protected fragments **160** and **161** turned out to be valuable models for the polymer structure as well. The smaller fragment consists of the triazole unit which was incorporated into an amino acid framework. The difference to the polymer backbone and the model compound **164** was the lacking dipeptide unit, spaced between the triazoles. Especially for CD experiments this could turn into a benefit, since one could clearly distinguish between the signals resulting from the triazole unit, which is incorporated into a chiral framework and the

5 Linear Triazole Containing Polypseudopeptides

contribution of the amides in the dipeptide unit to the polymer CD signal. So the small models **160** and **161** in combination with the monomers **141** and **142**, consisting of the dipeptide, lacking the triazole, represent a useful model system for the polypseudopeptide.

The final step in the synthesis of the model compound system was the Boc deprotection of the small models **160** and **161** and the monomers **141** and **142**.



Scheme 17: Boc deprotection of the model compounds **160** and **161** and of the monomers **141** and **142** to a model system for the polypseudopeptides.

5.2.3 Circular Dichroism Studies

Circular dichroism studies were performed with the Boc deprotected polymers **154** and **156**, with the monomers **167** and **168** and with the model

compounds **165** and **166**. CD spectra were recorded in water in a 1 mm cuvette at 25 °C over the wavelength region between 180 to 250 nm. Due to the low transmission of the sample at shorter wavelengths, results were only reliable at wavelengths above 200 nm. The polymers were measured at concentrations around 1×10^{-3} mol/L (as referred to monomeric repeat unit). Concentration and temperature scans were performed at acidic and basic pH. The samples were also measured in water:TFE mixtures. Untreated polymer solutions were at acidic pH (pH=4). The first experiment was a concentration screen (dilution series) at acidic and basic pH, in order to exclude aggregation effects in the spectra. Results are shown in Figure 6 and Figure 7.

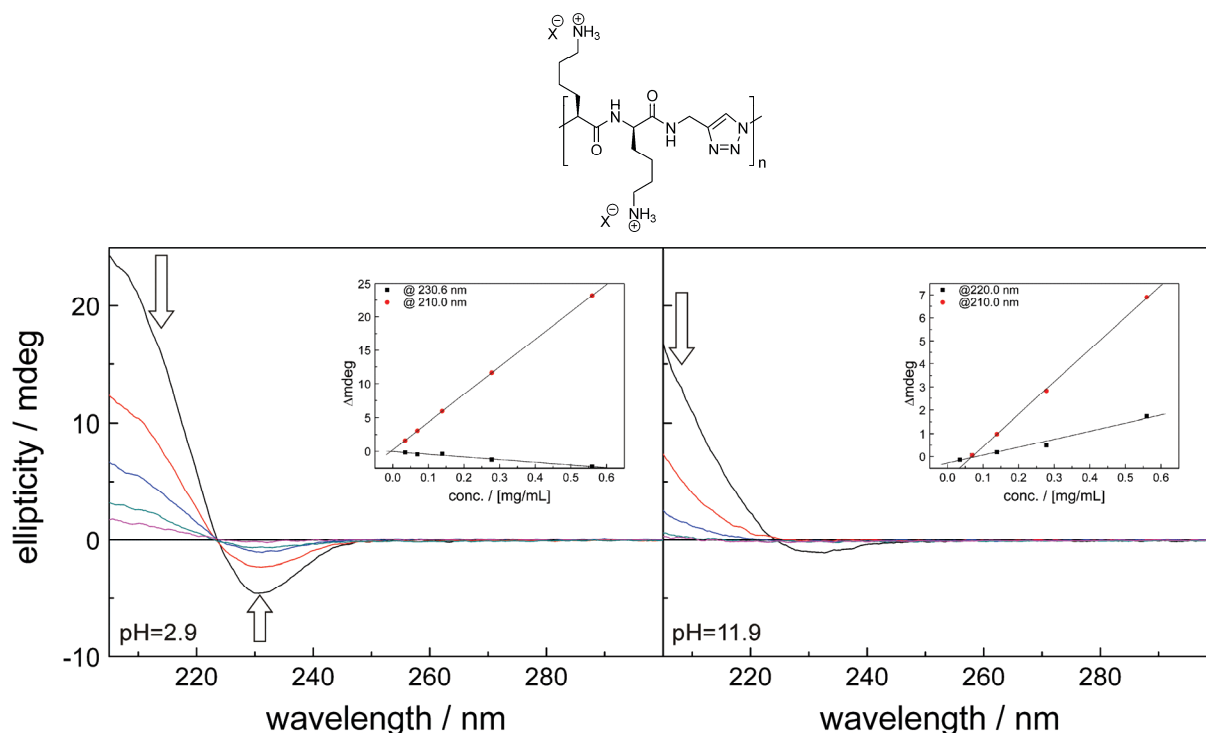


Figure 6: CD spectra of concentration screen of polymer **156** at acidic (left) and basic (right) pH. The linear plots of $\Delta mdeg$ against concentration are shown in the top right corners. Starting concentration of 9.84×10^{-4} mol/L (as referred to monomeric repeat unit) was decreased by a factor 2 in each step.

The CD spectra of polymer **156** (Figure 6) at acidic pH shows a minimum at 231 nm and passed through zero at the isodichroic point at 223 nm. The intensity of the CD signal decreased linearly with concentration. When the ellipticity difference ($\Delta mdeg$) at a specific wavelength are plotted against the

5 Linear Triazole Containing Polypseudopeptides

concentration, the resulting points could be fitted linearly. This is important to exclude aggregation effects in the spectrum. The spectra of the same polymer at basic pH changed notably. The negative band almost disappeared and was only visible at the highest concentration with a minimum at 232 nm. In lower concentrations, no negative signal could be detected. The plot of ellipticity difference against concentration could be fitted linearly, excluding aggregation effects. The CD signal of polymer **156** could not be switched reversibly from acidic to basic, once the sample had been exposed to basic pH. Decreasing the pH of the basic sample to acidic pH did not change the CD spectrum, whereas increasing the pH of the acidic sample changed the CD spectrum to the basic one.

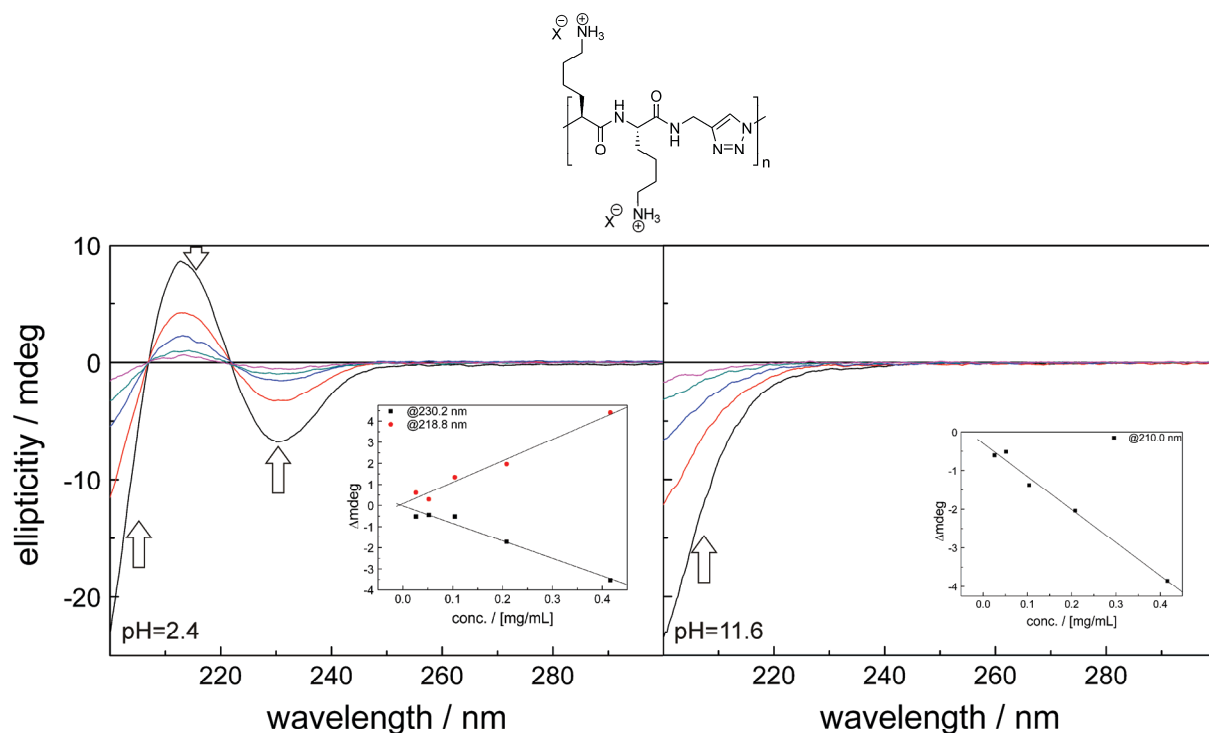


Figure 7: CD spectra of concentration screen of polymer **154** at acidic (left) and basic (right) pH. The linear plots of Δ mdeg against concentration are shown in the bottom right corners. Starting concentration of 9.76×10^{-4} mol/L (as referred to monomeric repeat unit) was decreased by a factor 2 in each step.

The CD spectra of polymer **154** (Figure 7) at acidic pH shows a negative band with a minimum at 230 nm, passing through zero in the isodichroic point at 222 nm, give a positive band with a maximum at 213 nm and pass again

through zero in the second isodichroic point at 207 nm. The CD signal decreased with concentration. The linear fit was not as precise as for polymer **154** but sufficient to exclude aggregation in the spectra. The CD spectra of the same polymer at basic pH had only a negative signal. The signal also decreased with concentration. The fit was almost linear, excluding aggregation. Increasing the pH of the acidic sample changed the signal to the basic one. Decreasing the pH of the basic sample did not change the spectrum. As in the case of polymer **156** (see above), the CD signal of polymer **154** could not be switched reversibly, once the sample had been exposed to basic pH.

Both polymers were subjected to a temperature experiment (Figure 8). The samples at unmodified pH (5 to 7) were equilibrated at 5 °C and measured. The samples were heated in 10 K steps up to 95 °C, equilibrated at each temperature for 15 minutes and measured. Under identical conditions, the samples were then cooled to 45 °C. Polymer **156** was measured at a concentration of $9.84 \cdot 10^{-4}$ mol/L (as referred to monomeric repeat unit), polymer **154** at a concentration of $4.88 \cdot 10^{-4}$ mol/L (as referred to monomeric repeat unit). Both spectra were normalized to a concentration of $1 \cdot 10^{-3}$ mol/L. The CD signal of polymer **156** decreased with rising temperature. The negative band totally disappeared, the positive signal also decreased to give in the end a weaker positive CD signal. This process was only reversible up to a temperature of 45 °C, where only very weak changes in the CD signal were obtained. Further heating and successive cooling led to more intense changes in the signal and an irreversible structural change (or degradation) of the polymer. Measurements of the heated polymer sample after several days did not show notable differences. Comparable results were obtained for polymer **154**. Temperature experiments were only reversible up to a temperature of 45 °C, where only weak changes in the CD signal were obtained. The signal intensities of all bands decreased with rising temperature and finally remained constant, even when cooling.

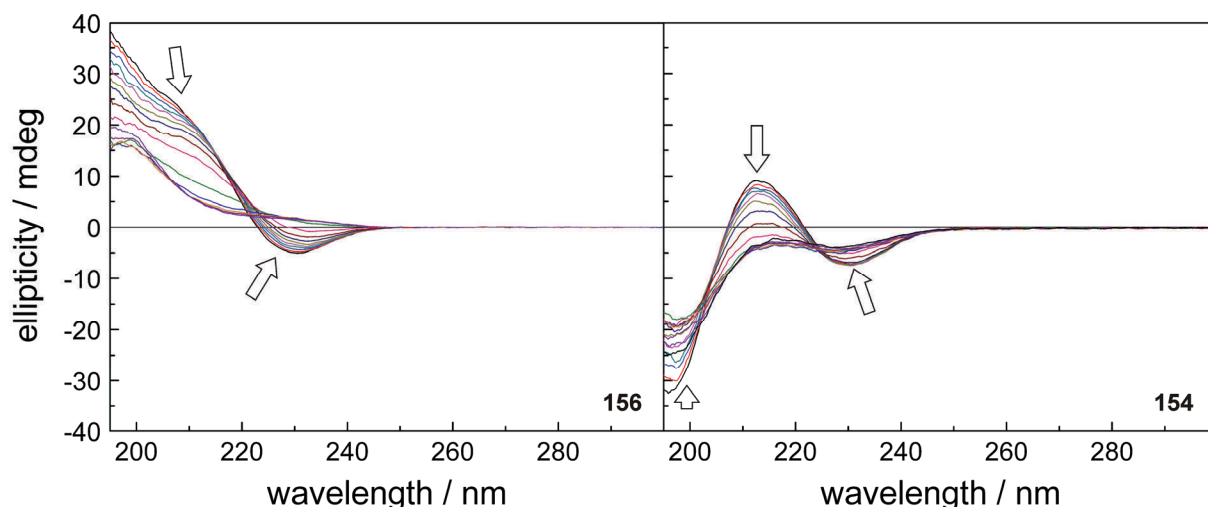


Figure 8: Variable temperature CD spectra of polymers **156** (left) and **154** (right). Polymer **156** was measured at a concentration of 9.84×10^{-4} mol/L (as referred to monomeric repeat unit), polymer **154** was measured at a concentration of 4.88×10^{-4} mol/L (as referred to monomeric repeat unit). Both spectra were normalized to a concentration of 1×10^{-3} mol/L. Samples were measured from 5 °C to 95 °C back to 45 °C in increments of 10 K.

The addition of a folding promoting solvent such as TFE did not change the spectra (data not shown). An overlay of acidic and basic spectra of polymers **154** and **153** in comparison to polylysine (MW = 66700 g/mol, DP = 319) is shown in Figure 9. The acidic spectra of **154** and **156** showed a similar shape in the wavelength region above 215 nm. At shorter wavelengths, the signals behaved to a certain extent as mirror images. The signal of the L,L-polypseudopeptide **154** showed a notable similarity to the polylysine spectrum at wavelengths shorter than 210 nm, different to L,D-polypseudopeptide **156**. At basic pH, the CD signals of polymers **154** and **156** behaved as mirror images and differed notably from the α -helical CD signal of polylysine. The signal intensities of all polymers in the spectra were comparable.

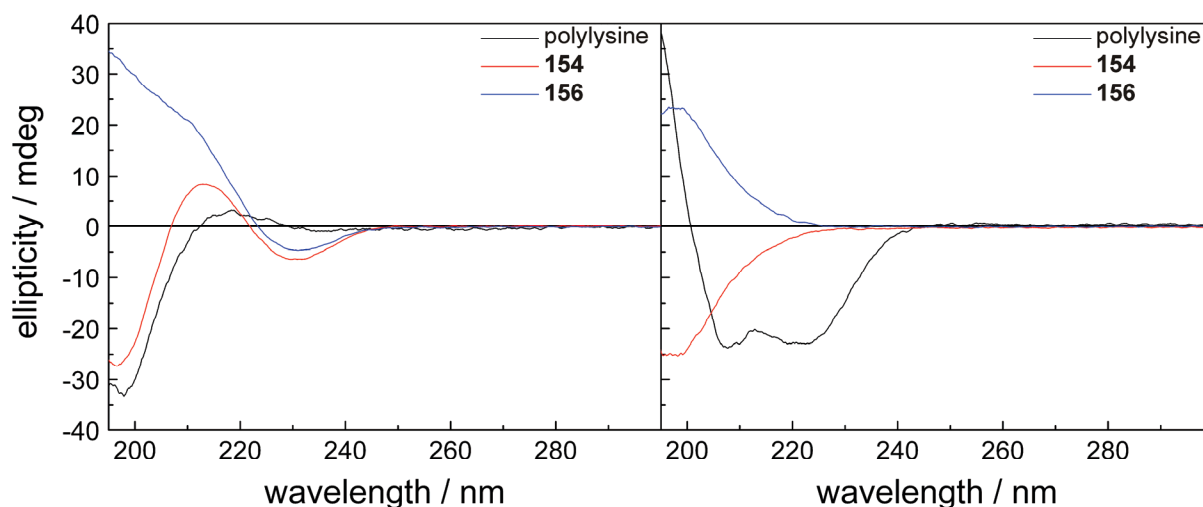


Figure 9: CD spectra of polymers **154** and **156** in comparison to polylysine (MW = 66700 g/mol, DP = 319) under acidic (left) and basic (right) conditions. Polymer **154** was measured at a concentration of $4.88 \cdot 10^{-4}$ mol/L, polymer **156** at a concentration of $4.95 \cdot 10^{-4}$ mol/L and polylysine at a concentration of $2.77 \cdot 10^{-4}$ mol/L (as referred to monomeric repeat unit). All spectra were normalized to a concentration of $1 \cdot 10^{-3}$ mol/L.

The monomers **167** (L,L) and **168** (L,D) and the model compounds **165** (L,L) and **166** (L,D) were measured under comparable conditions. The results are summarized in Figure 10. Monomer **167** showed the CD signature of a coiled *all*-L-peptide, what was expected for this compound. The CD signal of **168** did not pass zero, was positive and differed notably from the signal of **167**. This signature may have been that of a random coil structure of L-(*a/t*)-D-peptides, especially since aggregation was excluded by dilution experiments. This result did not fit well into the argumentation of the lacking CD signature of oligo-D-(*a/t*)-L-peptides (see special part chapter 1), but had not necessarily to be in contradiction to that. The model compounds **165** and **166** displayed similar CD signatures. **165** had a negative band with a minimum at ca. 230 nm, which passed through zero at 221 nm. **166** only had a positive band with a maximum at ca. 212 nm. These signals could most probably be attributed to the triazole units, which were neighbored by chiral amino acids, whereas the signals of **167** and **168** had to be the result of the amide chromophore.

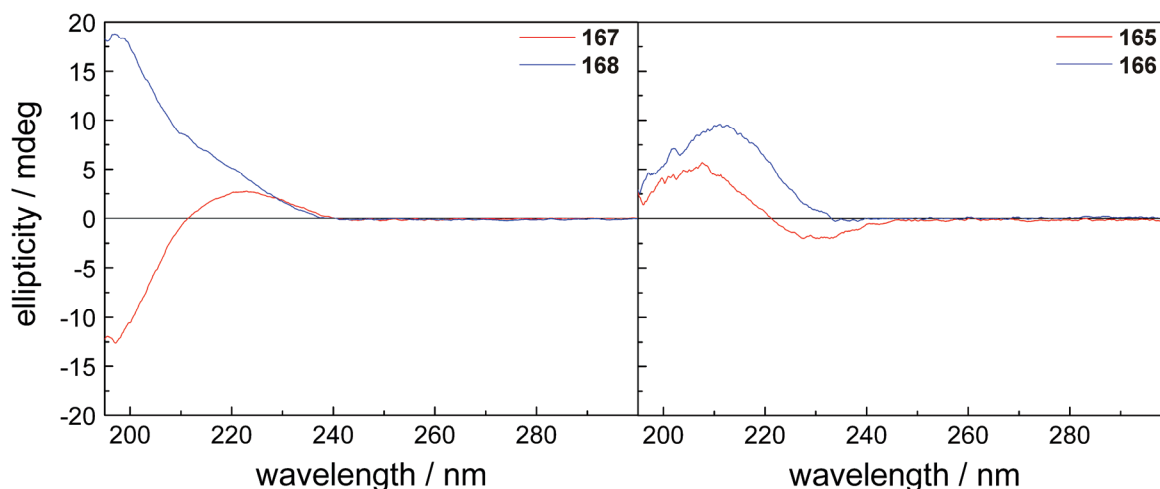


Figure 10: CD spectra of monomers **167** (L,L) and **168** (L,D) and model compounds **165** (L,L) and **166** (L,D). All spectra were measured under acidic conditions (pH 2 to 4) and at following concentrations: **167** ($7.52 \cdot 10^{-4}$ mol/L), **168** ($7.27 \cdot 10^{-4}$ mol/L), **165** ($8.71 \cdot 10^{-4}$ mol/L), and **166** ($8.57 \cdot 10^{-4}$ mol/L) (as referred to monomeric repeat unit). All spectra were normalized to a concentration of $1 \cdot 10^{-3}$ mol/L.

The polymer spectrum could in theory be separated into signals coming from amide chromophores and triazole signals. In analogy to the pH dependent structures of polylysine, polymers **154** and **156** were expected to adopt a random coil structure in acidic environment due to the Coulomb repulsion of the charged side chains. The CD spectra of monomers **167** and **168** and model compounds **165** and **166** were concentration independent. All four compounds were expected to be too small for secondary structure formation and their CD spectra may hence have represented a model for a random coil. The addition of the CD spectra of monomer and model compound (**165+167** and **166+168**) in a 1:1 ratio and overlay with the corresponding polymer spectra is shown in Figure 11. The shape of the CD curve of polymer **154** was relatively similar to that of the addition of model compound **165** and monomer **167**. The same was valid for polymer **156** and model compound **166** and monomer **168**. The fit was not perfect, but with this very simple model system, the expected random coil structure of the protonated polymers **154** and **156** could be rationalized.

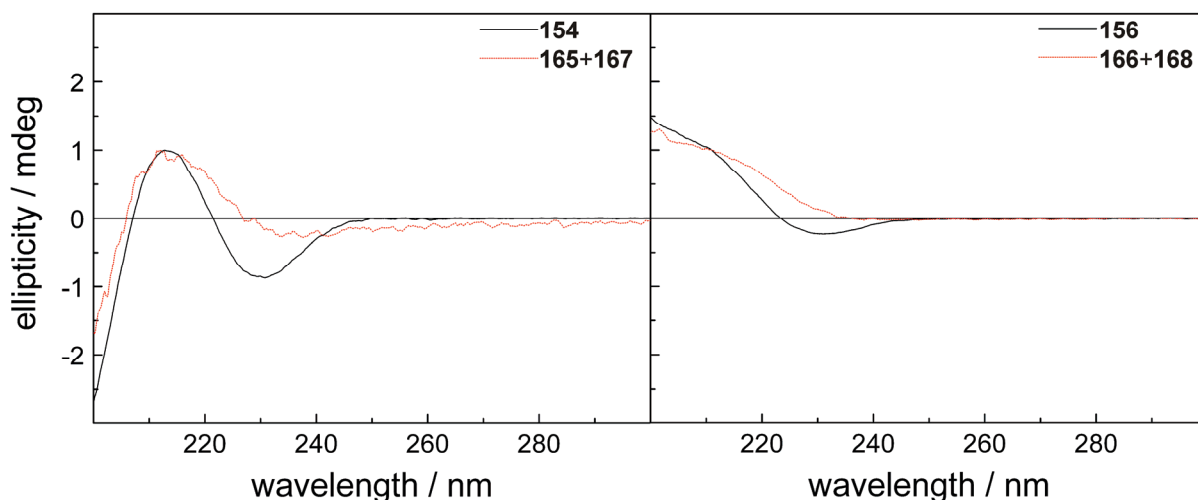


Figure 11: CD spectra of polymers **154** and **156** (black) and addition of monomer and model compound spectra **165+167** and **166+168**, respectively, (1:1) (red, dotted) under acidic conditions (pH=2-4). Spectra are normalized.

In basic environment, the side chains were deprotonated and the polymer may be able to adopt a secondary structure. The basic spectra of the polymers though may represent the CD signature of a (yet unknown) secondary structure of this unique type of polymers. Since the CD spectra of the basic samples remained unchanged, even when lowering the pH, the corresponding secondary structure is supposedly rather stable.

The deprotected polymers **154** and **156** displayed two different CD spectra each, depending on the pH of the solution. The acidic spectra could be transformed into the basic ones by increasing the pH. This process was not reversible. The random coil structure was expected for the protonated polymer. This theory could be supported by comparison of the polymer spectra with the spectra resulting from an addition of the corresponding model compounds and monomers. The transition of the random coil into another secondary structure was irreversible, rendering this structure very stable.

5.3 Side Chain Labeling

5.3.1 General Considerations

Polymers with side chain functionalities such as polylysines, polyglutamates or polymers **154** to **156** can be postfunctionalized with UV-active or fluorescent dyes, in order to attach labels to the polymer side chains. Pyrene is a very potent fluorescent dye. The photophysics of pyrene have intensively been studied and its possible application as side chain label in polymers has been reported.^[10] The way of pyrene attachment to the polymer is dependent on the side chain functionality. Polymers with nucleophilic side chain functionalities such as amines readily react with pyrenebutyric acid to give the resulting pyrenebutyric acid amides. The butyl spacer between the aromatic core and the acid assures the electronic independence of the pyrene unit from the polymer, notably simplifying the analysis of the optical spectra. Monomeric pyrene shows a very specific fluorescence spectrum (Figure 12 top left). When two pyrene units come in spatial proximity, they can form excimers, leading to a quenched monomer fluorescence and a red shifted, structure-less excimer band in the fluorescence spectrum (Figure 12 top right). The broad, featureless excimer emission is centered at ca. 480-500 nm and easily to recognize in the fluorescence spectrum.

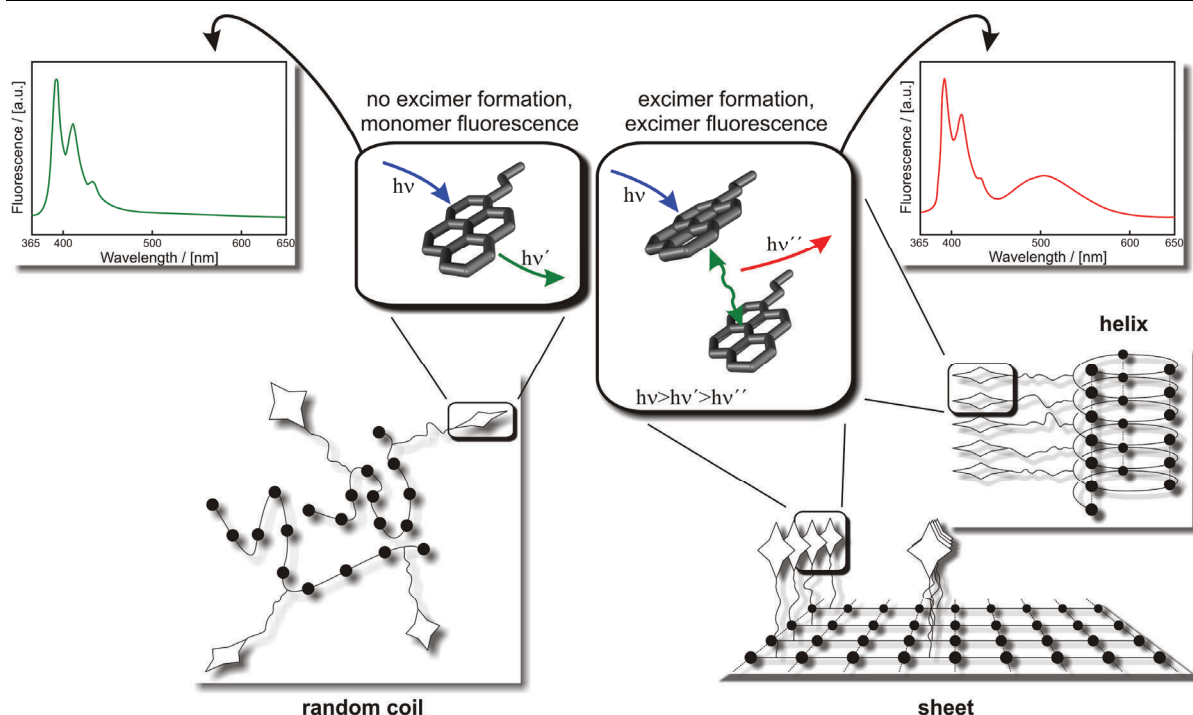


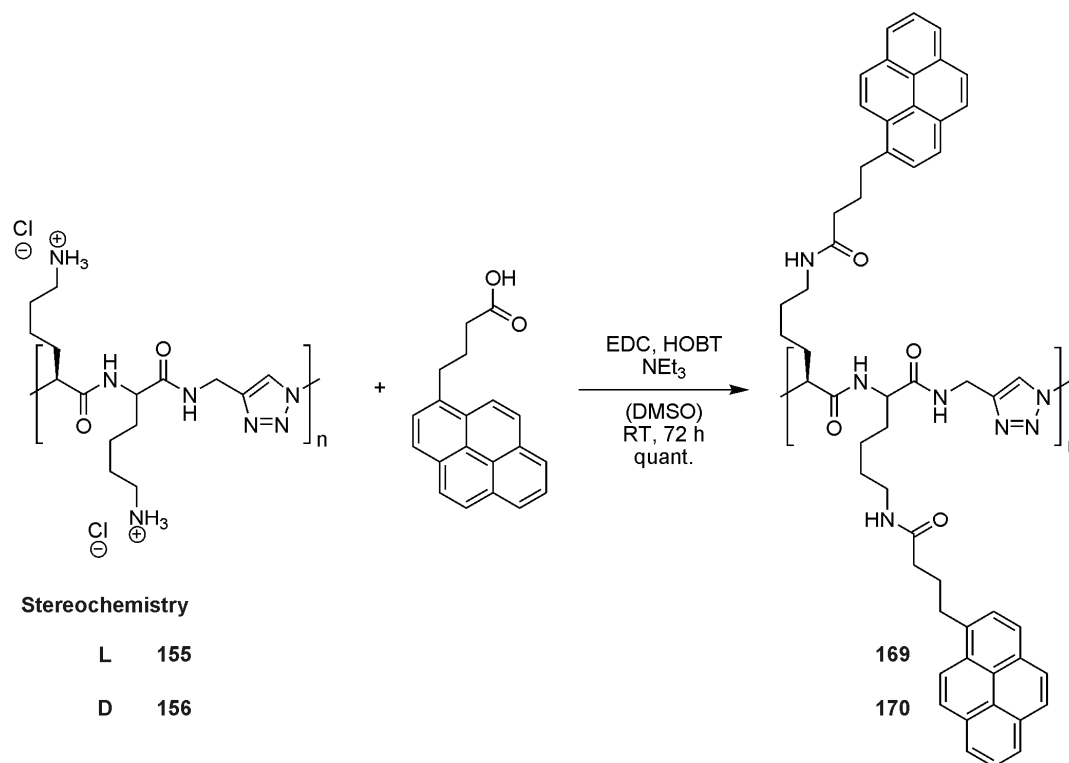
Figure 12: Fluorescence spectroscopy of a polymer with pyrene side chain labels. Possible spatial distances of pyrene units in unordered structures can lead to monomeric pyrene fluorescence (left). Ordered structures such as sheet or helix can bring pyrene units in close proximity to each other leading to excimer formation (right).

An (dynamic) excimer is defined by Birks as a dimer, which is associated in the excited state and dissociative in the ground state. The formation of a pyrene excimer requires encounter of an electronically excited pyrene with a second one in the ground electronic state. Hence, two pyrenes have to be in a certain spatial distance and orientation to each other in order to meet the requirements for excimer formation. The preferred orientation of the pyrenes in the excimer is the sandwich structure, since it yields the smallest distance between the molecular centers. The excimer then decays under excimer fluorescence to the dissociative electronic ground state dimer. The observed fluorescence is red shifted due to the radiationless dynamic excimer formation and structureless due to the dissociative electronic ground state of the dimer. It is also possible that two ground-state pyrene molecules form a dimer (preassociation), which can be excited to an excited dimer. This excited dimer decays under fluorescence. By standard fluorescence measurements, the distinction between excimer and excited dimer fluorescence is hardly possible.

In pyrene labeled polymers, the secondary structure of the polymer can have a tremendous effect on the ability of two pyrenes to form an excimer. If the requirements for excimer formation (spatial distance and orientation) can be met, strongly depends on the backbone structure of the polymer (Figure 12). The side chain residues in a random coil structure, have no preferred orientation, so that the probability that two pyrene units meet the requirements for excimer formation is much lower than in highly ordered structures such as sheet or helix, where the side chain residues are ordered and in close proximity. For statistical reasons, the probability of excimer formation also increases with a higher degree of labeling, so that excimer formation may occur in random coil structures as well. The labeling of polymer side chains with pyrene can give additional information on the structure of the polymer. Strong excimer formation is usually indicative for a highly ordered structure.

5.3.2 Synthesis

The side chain labeling was performed on the polymers **155** and **156** after anion exchange. The coupling was achieved in DMSO, using EDC and HOBT as coupling reagents. The use of triethylamine was necessary in order to deprotonate the amines (Scheme 18). In a first attempt, the coupling was done in DMF, but the polymer did not dissolve properly. Only after addition of water, the coupling took place. The result was comparable to the coupling in DMSO.



Scheme 18: Side chain labeling of polymers **155** and **156** with pyrenebutyric acid.

The reaction mixture was directly dialyzed in CH₂Cl₂:MeOH 1:1 with a dialysis tube with MWCO of 25000 g/mol. Aqueous work-up or precipitation procedures failed, since DMSO prevented phase separation and precipitation. Dialysis gave the desired polymer as a fawn solid in quantitative yield. GPC-traces of the pyrene labeled polymers **169** and **170** are shown in Figure 13. In comparison to the Boc protected polymers **149** and **153**, the peaks of the pyrene labeled polymers were slightly shifted to lower molecular weights. As the pyrene labeled polymers are derived from the parent polymers in a postfunctionalization reaction, the chain length should be unaffected and hence the shifts to lower molecular weights in the GPC most likely indicate more compact structures when comparing their hydrodynamic volume.

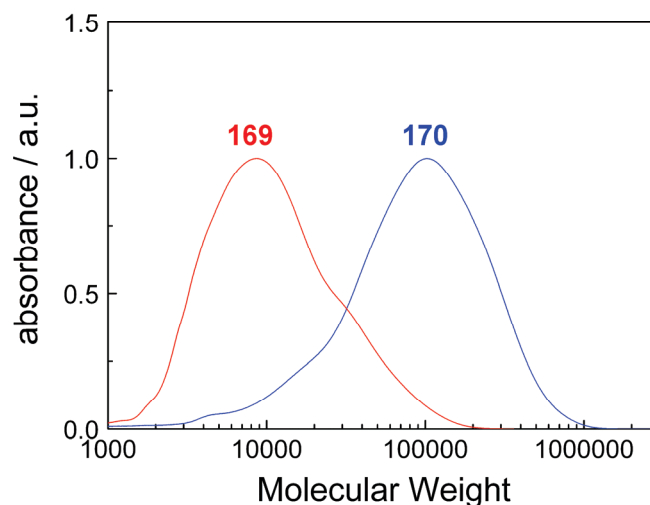


Figure 13: GPC-traces of pyrene labeled polypseudopeptides **169** and **170** after purification (GPC in DMF at 70 °C, calibrated with polystyrene standards, detection via UV).

For further analysis, the pyrene labeled polymer could only be dissolved in CH_2Cl_2 when adding minimal amounts of TFA to give dark brown solutions. The fawn product could be recovered from solution. In CDCl_3 -TFA mixtures, the polymer was insoluble. After solvent removal, the polymer had changed color from fawn to green-brown and was insoluble in all conventional solvents. Hence, for spectroscopic experiments and NMR, the polymer was dissolved in CH_2Cl_2 -TFA mixtures and CD_2Cl_2 -TFA mixtures, respectively. A proton NMR spectrum of polypseudopeptide **170** in a CD_2Cl_2 -TFA mixture is shown in Figure 14. Integration of the signals in the spectrum indicates practically quantitative side chain labeling.

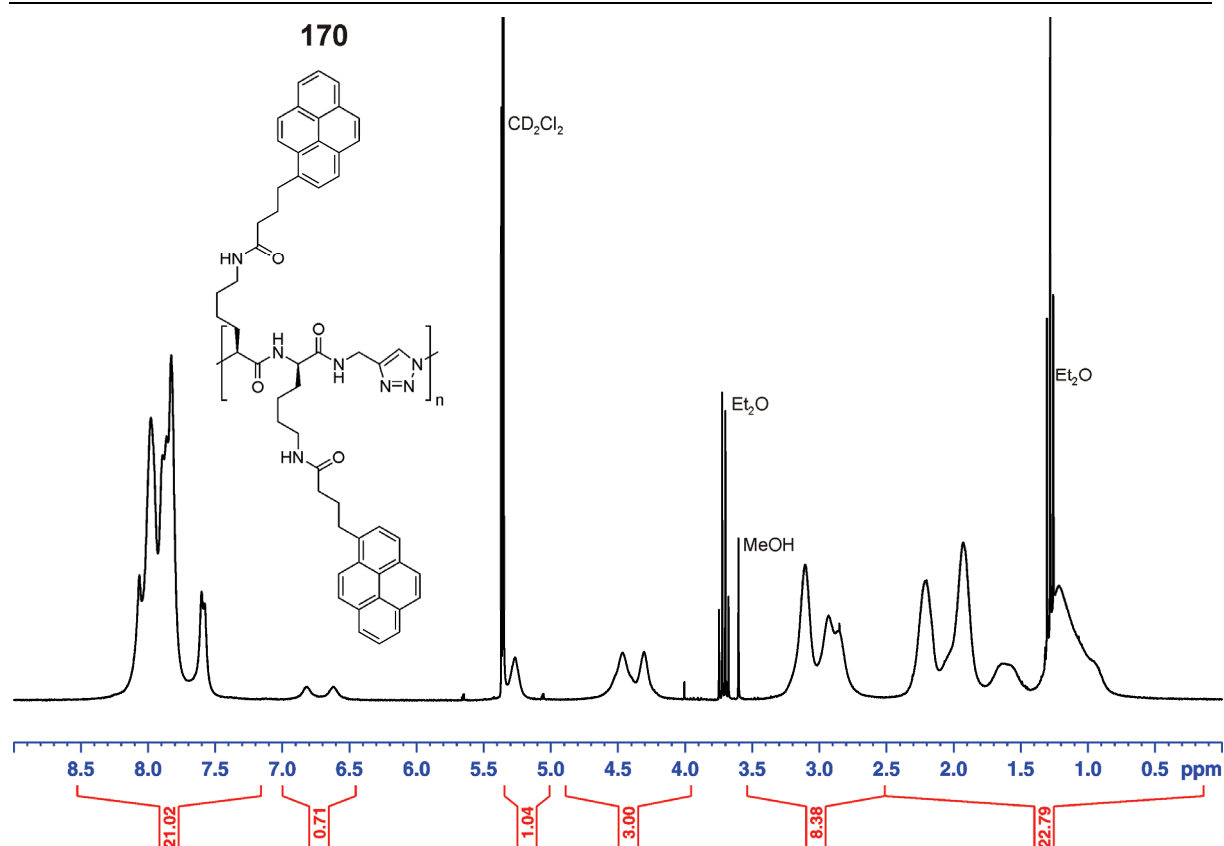


Figure 14: ^1H NMR of pyrene labeled polypseudopeptide **170** in CD_2Cl_2 under addition of TFA- d_1 (25 °C).

5.3.3 Spectroscopic Studies

The poor solubility of polymers **169** and **170** was one of the major obstacles for spectroscopic studies. It turned out that the polymers were only soluble in methylene chloride when adding small amounts of TFA. Therefore, the stock solution was prepared by suspending 1.00 mg (1.10×10^{-6} mol, as referred to monomeric repeat unit) of polymer in 50 μL methylene chloride and dissolving it by the addition of 2 μL TFA. The resulting solution was then diluted to a volume of 5 mL to give a stock solution with a concentration of 2.2×10^{-4} mol/L. UV and CD was measured in tenfold lower, fluorescence in 300- to 400-fold lower concentration. This reduced the amount of TFA in a sample to 0.004% for UV and CD and to less than 0.0001% for fluorescence measurements. For this reason, the amount of TFA in the sample solution could be neglected. For the solvation process of the polymer as such, the addition of 2 μL TFA (2.7×10^{-5} mol) played an important role. The ratio of monomer unit to TFA was

approximately 1:25. In the case that the TFA was to a certain degree included into the polymer, the local TFA concentration was much higher. Hence, it could not be eliminated that the TFA determined the polymer structure, even when its bulk concentration was negligibly small. In a first attempt to set up the stock solution, TFE instead of TFA was added to the polymer prior to the addition of methylene chloride. It turned out that small amounts of TFE were not able to dissolve the polymer completely. Polymer **170** was not dissolved at all. However, TFE was a much better additive than all other solvents used in this study.

5.3.3.1 UV

UV spectra of pyrene labeled polymers can give useful information on pyrene preassociation. One clear indication of pyrene preassociation is the broadening of the absorption bands compared to model systems. This decreased resolution can be quantified by measuring the ratio P_A of the absorption intensity of the most intense band to the adjacent minimum at shorter wavelength (Figure 15, left). In the absence of preassociation, this value is usually >3.0 for the 1L_a band. The broadening of the absorption bands is oftentimes accompanied by a small red shift and an decrease of the extinction coefficients.

UV spectra were recorded in a cuvette with 1 cm path length, using different solvent systems in a wavelength region between 250 to 400 nm. The solvents and solvent mixtures were CH_2Cl_2 , CH_2Cl_2 :ACN 1:1, CH_2Cl_2 :ACN 3:27, CH_2Cl_2 : CHCl_3 3:27, CH_2Cl_2 :MeOH 3:27, CH_2Cl_2 :THF 3:27, CH_2Cl_2 :TFE 1:1 and CH_2Cl_2 :cyclohexane 3:27. The polymer was soluble in all solvent systems except CH_2Cl_2 :cyclohexane, where it precipitated, when the concentrated stock solution was added to cyclohexane. The spectra of both polymers in CH_2Cl_2 , CH_2Cl_2 :MeOH 3:27, and CH_2Cl_2 :TFE 1:1 are shown in Figure 15.

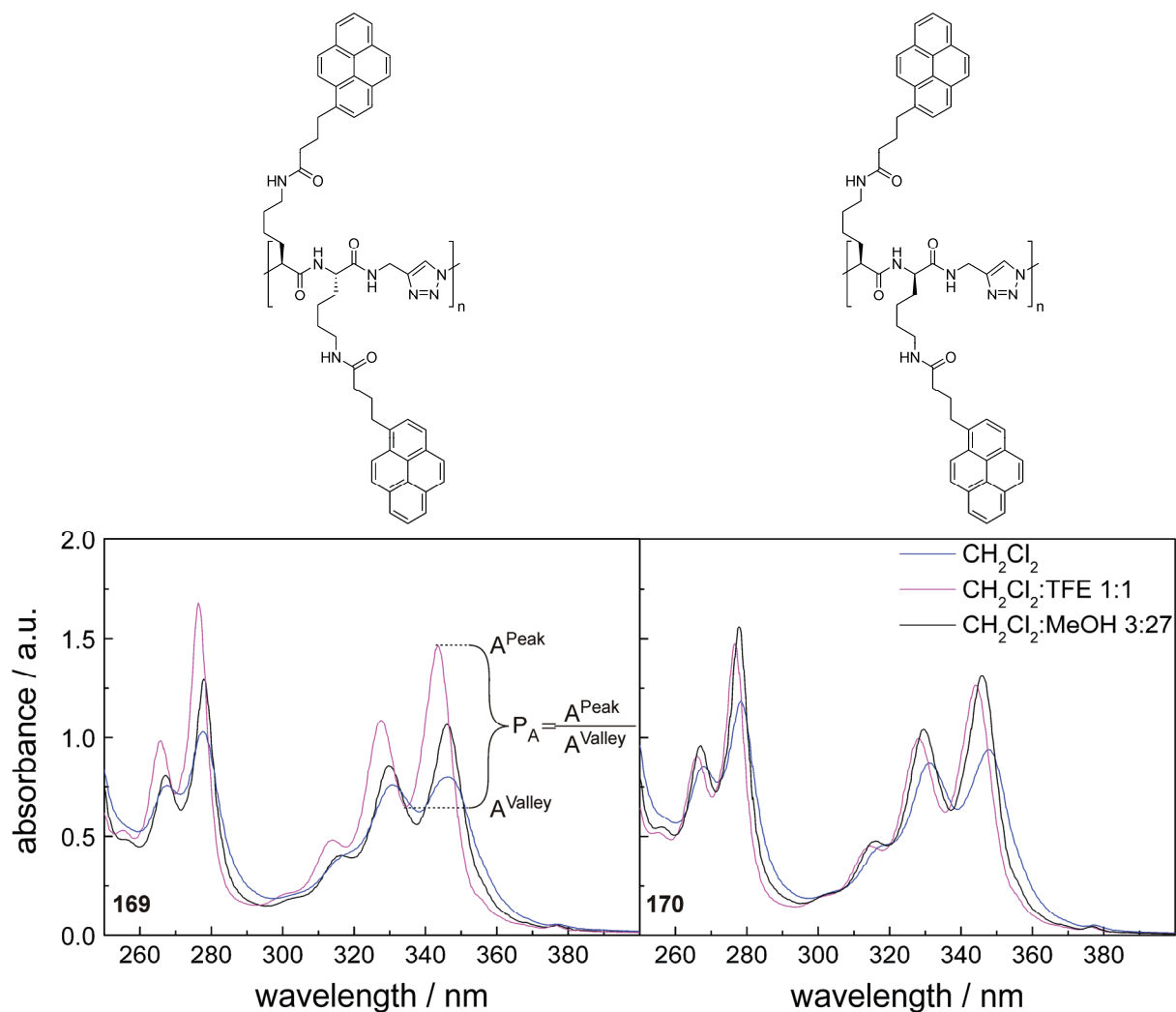


Figure 15: Overlay of UV spectra of polymers **169** and **170** in different solvents. Spectra were measured at polymer concentration of 2.2×10^{-5} mol/L. Quantification of spectrum resolution is shown on the left.

The absorption spectra of both polymers strongly depend on the solvent system. The spectrum of **169** in CH_2Cl_2 :TFE 1:1 displays very sharp and intense signals ($P_A=2.24$). The absorption maximum of this band is located at 343.8 nm. The spectrum of **170** in this solvent system displays a lower resolution ($P_A=2.02$). The absorption maximum of this band is located at 344.0 nm. The spectrum of **169** in pure CH_2Cl_2 displays a lower resolution and hypochromism ($P_A=1.91$). The absorption maximum of this band is red-shifted by 2.2 nm to 346.0 nm. The absorption spectrum of **170** in pure methylene chloride displays a comparable resolution than the spectrum in CH_2Cl_2 :TFE 1:1 ($P_A=2.07$) and no

hypochromism as seen for **169**. The absorption maximum of this band is also red-shifted by 2.0 nm to 346.0 nm. The spectrum of **169** in CH₂Cl₂:MeOH 3:27 displays no notable hypochromism, but a much lower resolution ($P_A=1.28$). The spectrum is red-shifted by further 0.3 nm to locate the absorption maximum at 346.3 nm. The spectrum of the L,D-polymer **170** in the same solvent system displays a higher resolution ($P_A=1.47$), no notable hypochromism and a red-shift by 1.8 nm to locate the absorption maximum at 347.8 nm.

According to the UV spectra, polymer **169** shows a strong solvent dependence. It displays the highest resolution in CH₂Cl₂:TFE 1:1, meaning a low degree of pyrene preassociation. The resolution decreases when the spectrum is recorded in pure methylene chloride and further drops in CH₂Cl₂:MeOH 3:27. This trend is also observable for the red-shift of the spectrum, correlating well with the solubility of the polymer, which is best in methylene chloride when adding TFE. The polymer is probably best solvated in this solvent system and present in a less ordered structure. This may lead to a bigger spatial distance between the pyrenes, resulting in a lower degree of preassociation. In pure methylene chloride, the polymer is probably less solvated and forced into a tighter structure, leading to smaller pyrene distances and a higher degree of preassociation. This effect is even stronger in methanol mixtures. Polymer **170** does not display such a strong solvent dependence. **170** has a higher molecular mass than **169** and its solubility is even poorer. This could lead to a lower solvation of the polymer in CH₂Cl₂:TFE 1:1 and a higher structural order, resulting in a higher degree of pyrene preassociation. This could explain the low resolution in this solvent system. The comparable and even higher resolutions of polymer **170** in the other solvent systems (compared to polymer **169**) could only be explained by a slightly different solubility of the polymers. According to the red-shift of the spectra, the trend of increasing preassociation is comparable for both polymers.

5.3.3.2 Fluorescence

The measurement of steady-state emission spectra provides two parameters. The ratio of excimer and monomer fluorescence intensities (I_E/I_M) and the wavelength corresponding to the maximum of the excimer emission (λ_E). The

steady-state emission spectrum can not give any further information on pyrene preassociation.

Fluorescence spectra were recorded in a 1 cm cuvette in the same solvent systems as compared to the UV spectra, but in much higher dilution (6.8×10^{-7} mol/L for **169** and 5.7×10^{-7} mol/L for **170**, as referred to monomeric repeat unit). The samples were excited at the respective absorption maxima of the 1L_a band. For one example, the fluorescence was measured at a concentration of 2.3×10^{-7} mol/L. At this concentration, a UV spectrum was hardly detectable. The ratio of excimer to monomer fluorescence intensities remained unchanged. For this reason, aggregation was excluded for the polymer samples. A selection of fluorescence spectra of both polymers is shown in Figure 16. The samples were excited at wavelengths between 328 nm and 331 nm (depending on the respective absorption maxima of the samples). Spectra collected at excitation wavelengths around 315 nm and 345 nm only differed in intensity, but not in I_E/I_M or λ_E .

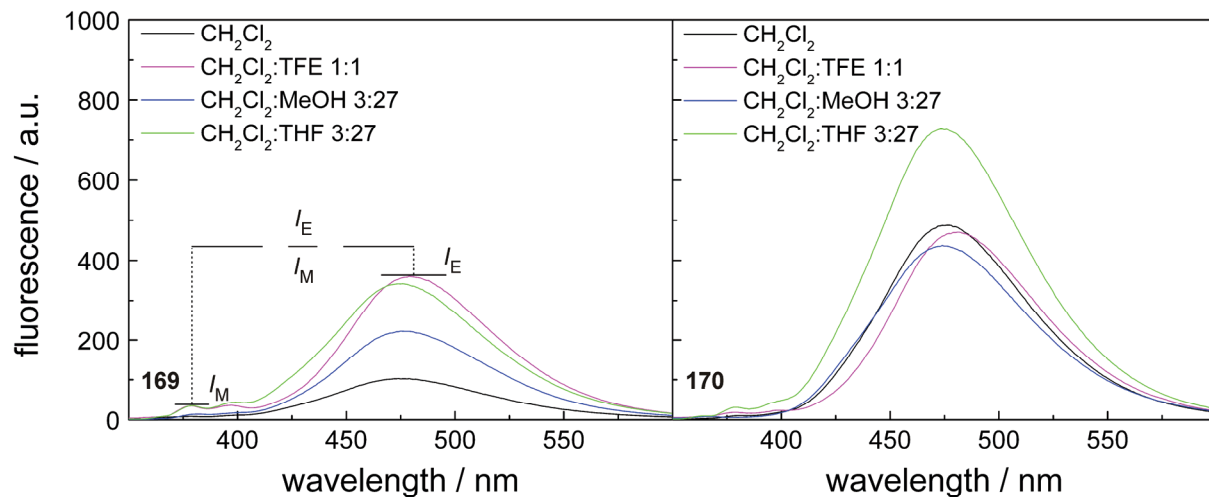


Figure 16: Overlay of fluorescence spectra of polymers **169** and **170** in different solvents. Spectra were measured at polymer concentration of 6.8×10^{-7} mol/L for **169** and 5.7×10^{-7} mol/L for **170** at excitation wavelengths between 328 nm and 331 nm (depending on the respective UV absorption maximum of the sample). Spectra of **169** were normalized to a concentration of 5.7×10^{-7} mol/L.

Polymers **169** and **170** display a very intense, structureless excimer fluorescence. The excimer fluorescence is so intense that a monomer fluorescence band is hardly detectable. A quantification of I_E/I_M is very inexact, since the monomer band can not be located precisely. Polymer **169** displays the most intense fluorescence in CH₂Cl₂:TFE 1:1 with a maximum at 479.0 nm. The ratio of I_E/I_M is calculated to be 10.2. The second intense band is recorded in CH₂Cl₂:THF 3:27 with a shift of the fluorescence maximum to shorter wavelengths by 2.9 nm to 476.1 nm ($I_E/I_M=9.8$). The polymer sample in CH₂Cl₂ displays a weaker fluorescence intensity. The maximum is shifted by 4.0 nm (in comparison to the sample in CH₂Cl₂:TFE 1:1) to 475.0 nm ($I_E/I_M=15.8$). The sample in CH₂Cl₂:MeOH 3:27 displays the weakest fluorescence intensity in this selection. The maximum is shifted to shorter wavelengths by 5.1 nm to 473.9 nm ($I_E/I_M=12.1$).

The fluorescence signals of polymer **170** are all significantly more intense than those of **169**. The most intense fluorescence signal by far is obtained in CH₂Cl₂:THF 3:27. The maximum is located at 473.9 nm and the ratio of I_E/I_M is calculated to be 22.4. The second intense signal is obtained in pure methylene chloride, resulting in an I_E/I_M of 47.4. The maximum is located at 477.0 nm. The sample in CH₂Cl₂:TFE 1:1 displays the next intense signal ($I_E/I_M=25.3$), located at 481.0 nm. The least intense signal is recorded in CH₂Cl₂:MeOH 3:27 ($I_E/I_M=70.5$), located at 473.9 nm. In comparison to the signal of **170** in CH₂Cl₂:TFE 1:1, the maxima of the other samples are blue-shifted (7.1 nm for CH₂Cl₂:THF 3:27, 4.0 nm for CH₂Cl₂, and 7.1 nm for CH₂Cl₂:MeOH 3:27).

The fluorescence spectra were measured in such low concentrations that intermolecular pyrene interaction could be eliminated. The quantitative degree of polymer labeling was probably the reason for the very intense excimer bands in the fluorescence spectra, rendering the calculations of I_E/I_M very tentative and inexact and the results not very reliable. Whether the intense excimer band was the result of excimer formation or excited dimer fluorescence, could not be revealed by static fluorescence studies.

5.3.3.3 Circular Dichroism

The CD experiments were performed in the wavelength region of pyrene absorbance. The pyrene labels are electronically independent from the polymer backbone and due to the long spacer spatially separated from chiral centers. A CD signal in the absorbance region of the pyrene labels can hence only occur, when the polymer adopts an ordered structure, where the pyrene units i.e. their transition dipole moments, are arranged in a chiral environment.

Circular dichroism spectra were recorded in the same solvent systems as compared to the UV and fluorescence spectra. The CD spectra in the different solvent systems looked similar. Three representative spectra are plotted in Figure 17.

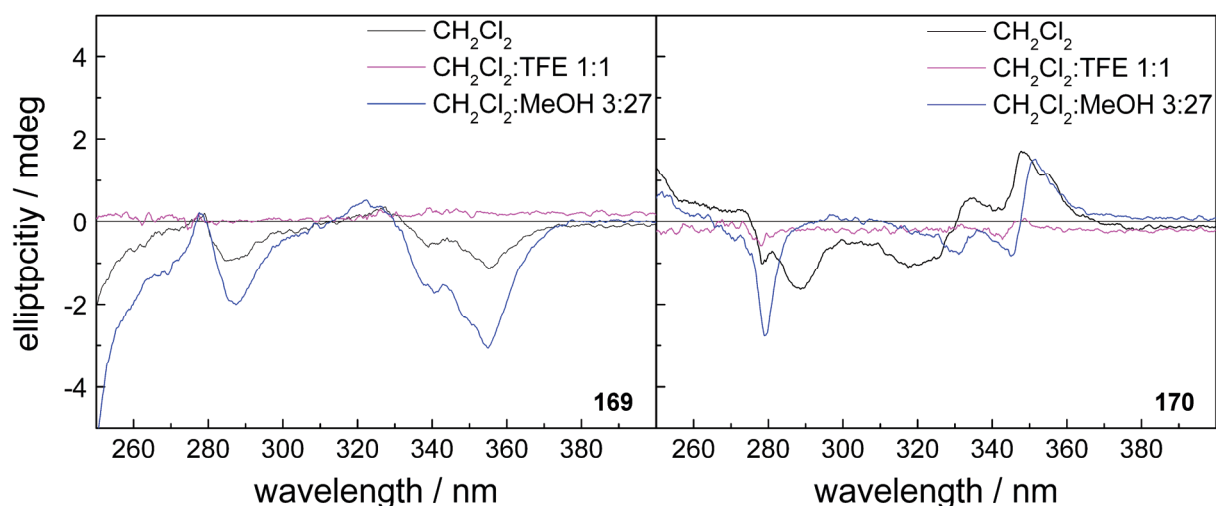


Figure 17: CD spectra of labeled polymers **169** and **170** in different solvent systems. Spectra were recorded in a 1 cm cuvette at 25 °C. Both polymers were measured at a concentration of $2.2 \cdot 10^{-5}$ mol/L.

The obtained CD signals are not very intense. Polymer **169** shows only negative signals. The spectrum in $\text{CH}_2\text{Cl}_2:\text{MeOH}$ 3:27 is much more intense than the spectrum in CH_2Cl_2 . In contrast, the CD signals of polymer **170** in $\text{CH}_2\text{Cl}_2:\text{MeOH}$ 3:27 and in CH_2Cl_2 have comparable intensities, but differ slightly in shape. The CD signals of **170** consist of negative and positive bands. In the wavelength regions of 250 nm to 270 nm and 310 nm to 380 nm, the CD spectra of both

polymers behave to a certain extent as mirror images (Figure 18). In the region between 270 nm and 310 nm, the shape of the CD signal is dependent on the solvent. In CH_2Cl_2 :MeOH, both polymer spectra behave to a certain extent as mirror images, whereas the spectra in CH_2Cl_2 and CH_2Cl_2 :ACN have almost identical shapes. Interestingly, the CD signals of both polymers vanished with the addition of TFE to the dissolved polymer (Figure 17). The poor solvation of the polymer in the solvent may force it to adopt an ordered structure, which displays these weak CD signals. The vanishing CD signal in TFE may be attributed to an improved solvation of the polymer, decreasing the driving force to adopt ordered structures.

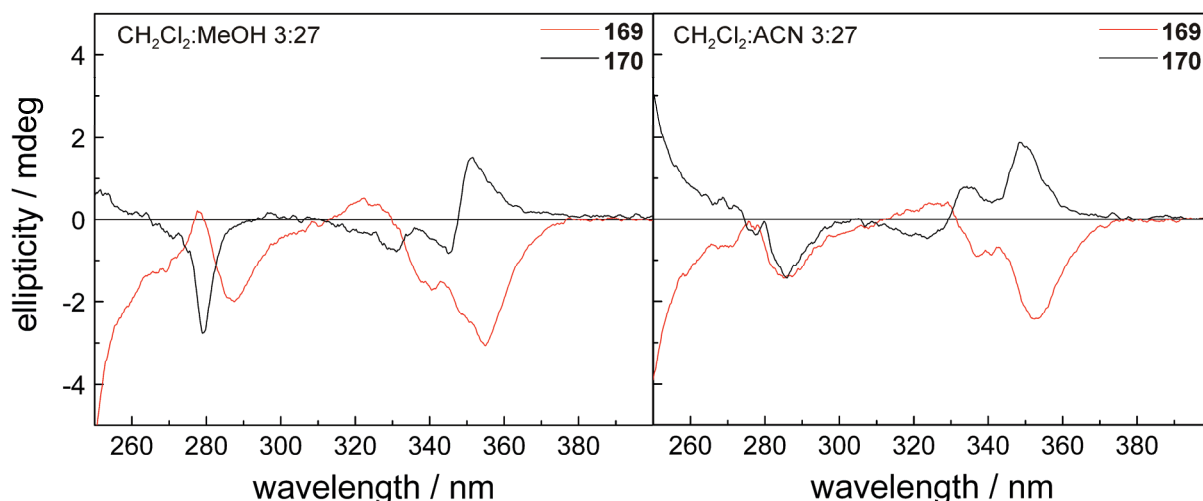


Figure 18: Overlay of CD spectra of polymers **169** and **170** in CH_2Cl_2 :MeOH 3:27 and CH_2Cl_2 :ACN 3:27.

The results of the spectroscopic studies on polymers **169** and **170** are summarized in Figure 19. The solubility experiments already revealed that CH_2Cl_2 :TFE-mixtures were much better solvents than all other solvent systems. This property was also visible in the spectroscopic measurements. In CH_2Cl_2 :TFE 1:1, the polymer displayed a UV spectrum with sharp signals. This high resolution was an indication for a good solvation and a low degree of pyrene preassociation. The well solvated polymer adopted a loosely coiled structure, in which the pyrenes were not fixed in a defined, chiral environment. This could be visualized by the absence of a CD signal. In poorer solvents, the polymer

displayed a UV spectrum with broad signals. This low resolution was indicative for a high degree of pyrene preassociation. Due to its poor solvation, the polymer was forced into a structure with a certain degree of order. In those tighter organized structures, the pyrene labels were highly preassociated in a chiral environment. This could be visualized by the existing CD signal. In good and in poor solvents, the polymer displayed a similar fluorescence spectrum dominated by a very intense excimer band. In fluorescence spectra, the distinction between excimer- and excited dimer fluorescence could not be made. For this reason, fluorescence spectra in good and poor solvents looked similar. In the case of a good solvent, the excimer band most probably resulted from dynamic excimer formation, whereas in poor solvents, the high degree of preassociation led to excited dimer fluorescence.

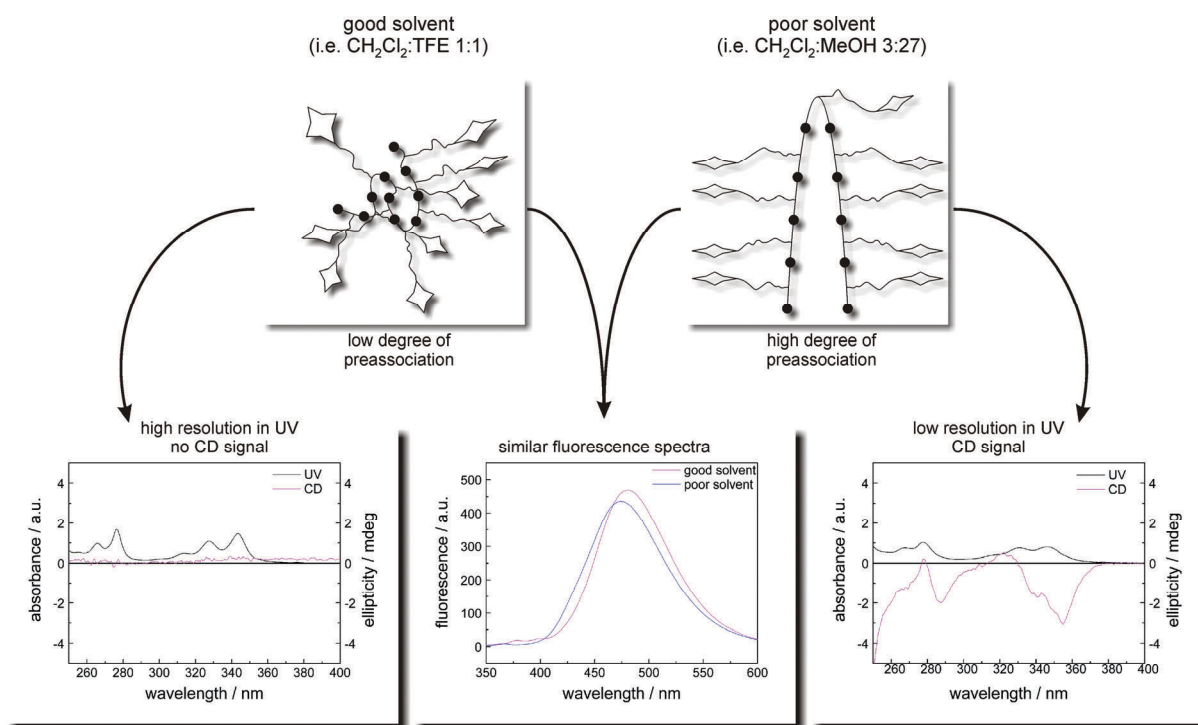


Figure 19: Influence of solvent on pyrene preassociation and polymer structure, as monitored by UV, fluorescence and CD.

5.4 Experimental Part

5.4.1 General

General Methods: Starting materials were commercial and used as received. All solvents used at FU Berlin and HU Berlin were distilled once prior to usage, all solvents used at MPI were used without further purification. THF was in all cases stored over KOH and freshly distilled prior to usage. Dry solvents were kindly provided by the respective facility of the MPI. Dry DMF was purchased from Acros. If mentioned, solvents were degassed by freeze drying or by purging with argon. Column chromatography was carried out with 130 – 140 mesh silica gel. Dialysis of the compounds was achieved using regenerated cellulose dialysis tubes Spectra/Por Dialysis Membrane MWCO:1000 or MWCO:25000. Slow compound addition was achieved using a Harvard Apparatus 11Plus syringe pump. Compound lyophilization was performed using Christ Alpha 2-4 LDC-1m apparatus. Microwave assisted reactions were performed in a CEM-Discover monomode microwave reactor having a continuous microwave power delivery system from 0 to 300 W. The reactions were carried out in 10 mL sealed glass vials. The temperature was monitored by an IR sensor on the outer surface of the reaction vessel. All the reactions were performed with max. power and super-cooling.

Analytic Methods:

NMR (^1H and ^{13}C , respectively) were recorded on Bruker DPX 300 (300.1 and 75 MHz for ^1H and ^{13}C , respectively), Bruker AV400 (400.1 and 100.6 MHz for ^1H and ^{13}C , respectively) spectrometers at 23 \pm 2 $^\circ\text{C}$ using residual protonated solvent signals as internal standard (^1H : $\delta(\text{CHCl}_3)$ = 7.26 ppm, $\delta(\text{DMSO})$ = 2.50 ppm, $\delta(\text{CH}_3\text{OH})$ = 3.31 ppm, $\delta(\text{H}_2\text{O})$ = 4.79 ppm, $\delta(\text{CH}_3\text{CN})$ = 4.79 ppm, $\delta(\text{CH}_2\text{Cl}_2)$ = 5.32 ppm, and ^{13}C : $\delta(\text{CHCl}_3)$ = 77.16 ppm, $\delta(\text{DMSO})$ = 39.52 ppm, $\delta(\text{CH}_3\text{OH})$ = 49.00 ppm, $\delta(\text{CH}_3\text{CN})$ = 1.32 ppm and 118.26 ppm, $\delta(\text{CH}_2\text{Cl}_2)$ = 53.80 ppm).

Mass spectrometry was performed on a Bruker APEX III Fourier Transform Ion Cyclotron Resonance Mass Spectrometer (FTICR-MS) or on a Waters LCT Premier XE.

TLC was performed on Merck Silica Gel 60 F254 TLC plates with a fluorescent indicator with a 254 nm excitation wavelength. Compounds were visualized under UV light at 254 nm and developed with ninhydrin solution.

HPLC/UPLC was performed with a Waters UPLC Acquity equipped with a Waters LCT Premier XE Mass detector for UPLC-HR-MS, with Waters Alliance systems (consisting of a Waters Separations Module 2695, a Waters Diode Array detector 996 and a Waters Mass Detector ZQ 2000) equipped with the columns described with the corresponding substances, with Shimadzu LC-10A systems equipped with a photodiode array detector (PAD or DAD).

GPC measurements in DMF as the mobile phase were performed on PSS columns in a WGE Dr.Bures TAU 2010 column oven at 70 °C, using a WGE Dr.Bures Q-2010 HPLC pump and a Knauer Smartline 3800 autosampler. Detection was achieved using a WGE ETA-2020 RI-visco-detector and a Knauer Smartline 2500 UV-detector. Flow-rate was 1.0 mL/min. Columns were calibrated using a Polystyrene Calibration Kit S-L-10 LOT 79, using 2,4-Di-*tert*-butyl-4-methoxy-phenol as internal standard.

Optical spectroscopy: UV/visible absorption and emission spectra were recorded in spectroscopic grade solvents, using Hellma quartz cuvettes of 1 cm for absorption and emission and 1 mm path length for absorption on a Cary 50 Spectrophotometer and a Cary Eclipse Fluorescence Spectrophotometer, respectively, both equipped with a Peltier thermostated cell holder ($T = 25 \pm 0.05$ °C). The fluorescence samples were excited at their respective absorbance maxima, slit was set to 5 nm bandpass for excitation and to 10 nm bandpass for emission. Circular dichroism spectra were recorded on a JASCO 710 Spectropolarimeter equipped with a JASCO PTC-423S/15 Peltier thermostated cell holder in spectroscopic grade solvents using Hellma quartz cuvettes of 1 cm and 1 mm path length. Prior to first use, the cuvettes were cleaned with 1:1 mixture of conc. H_2SO_4 / 30% H_2O_2 , washed with water and acetonitrile, and a 10 vol-% solution of *silyl-501* (BSTFA: N,O-Bis(trimethylsilyl)acetamide, 1%TMSCl) in acetonitrile added, stirred for 10 min at RT and 20 min at 50 °C, washed twice with acetonitrile and chloroform. After silylation, cuvettes were cleaned with aqueous Hellmanex II cuvette cleaning solutions. IR spectra were

recorded on a Biorad Excalibur FTS30MX equipped with a Golden Gate ATR Specac.

5.4.2 General Procedures

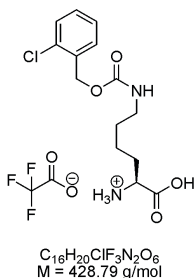
General procedure for the deprotection of the Boc group: Peptide was dissolved in CH_2Cl_2 or in $\text{CH}_2\text{Cl}_2:\text{CH}_3\text{OH}$ 9:1 (depending on solubility) and cooled to 0 °C. TFA (same amount as the solvent) was added and the solution allowed to warm up to room temperature. After stirring at room temperature until starting material was consumed (TLC monitoring), the solution was concentrated i.vac. When the uncharged, neutralized peptide was the desired product, the solution was extracted with water, saturated aqueous NaHCO_3 -solution (in case of longer peptides (starting from octamer), CH_3OH was added to assure solubility of the peptide), water, and brine. The combined organic layers were dried over MgSO_4 , filtered, and evaporated i.vac. to yield the crude product in quantitative yield. In case of remaining protected peptide, procedure was repeated. When the amine salt was the desired product, the reaction mixture was evaporated i.vac. and wrapped several times with CH_2Cl_2 to give the product in quantitative yield.

General procedure for the deprotection of the methyl ester: To a solution of methyl ester protected peptide in water:THF 1:5, a 1 M aqueous solution of LiOH (water:LiOH:THF 1:1:5) was added and the reaction mixture stirred at room temperature until starting material was consumed (TLC monitoring). Acetic acid was added to give pH=5, and the product subsequently extracted with CH_2Cl_2 . The united organic layers were dried over MgSO_4 and the solvent evaporated i.vac. to give the product in quantitative yield.

General procedure for the deprotection of the Z group or benzyl ester: To a solution of Z- or benzyl protected peptide in $\text{EE}:\text{CH}_3\text{OH}$ (ratio depending on solubility), Pd/C was added and the solution stirred under hydrogen atmosphere at room temperature. The reaction mixture was filtered and evaporated i.vac. to give the product.

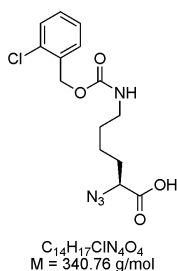
5.4.3 Synthetic Procedures

L-Lys(2Cl-Z) (**121**):



Boc-L-Lys(2Cl-Z) was reacted following the general procedure for the deprotection of the Boc group. The product was obtained in quantitative yield and was used without further purification and characterization.

Azido-L-Lys(2Cl-Z) (**122**):



NaN_3 (3.12 g, 48.0 mmol) was dissolved in water (13.0 mL) with CH_2Cl_2 (15.0 mL) and cooled to 0 °C. Triflyl anhydride (1.20 mL, 7.2 mmol) was added slowly within 5 minutes with stirring continued for 2 h. The emulsion formed 2 transparent layers after 30 minutes. The mixture was placed in a separation funnel and the CH_2Cl_2 layer was removed. The aqueous layer was extracted with CH_2Cl_2 (2x10 mL). The united organic layers were extracted once with saturated aqueous Na_2CO_3 -solution and used without further purification. **121** (1.03 g, 2.40 mmol) was combined with K_2CO_3 (0.50 g, 3.60 mmol) and CuSO_4 (solution of 0.01 g in 0.3 mL water) (0.34 mL, 0.024 mmol), water (10 mL) and MeOH (20 mL). A white emulsion was formed. The triflyl azide in CH_2Cl_2 was added and the mixture stirred at room temperature for 12 h. TLC showed low product content, so more triflyl azide was synthesized (1.1 mL triflyl anhydride dissolved in dry CH_2Cl_2 (10 mL) and added within 15 minutes to NaN_3 (3.1 g) in 10 mL

5 Linear Triazole Containing Polypseudopeptides

H₂O. The solution was then stirred for 2 h at room temperature.) and added to the reaction mixture, which was then stirred at room temperature for 12 h. The organic solvents were removed i.vac. and the aqueous slurry was diluted with water. This was acidified to pH = 6 with conc. HCl. Phosphate buffer (pH = 6.2) was added and the solution extracted with EE (4x20 mL). The combined organic layers were dried over MgSO₄ and evaporated i.vac. The crude product was purified via column chromatography on silica (eluent: EE (+0.1% HOAc) to EE:MeOH (95:5) (+ 0.1% HOAc)) to give 0.70 g (yield: 85%) of the desired product.

HSE-HB-054: HPLC (250 Nucleodur 100-5-C18 ec, 4 mm, Methanol/0.1% TFA = 55:45, 0.8 mL/min, 9.9 MPa, 308 K): 16.07 min (>99.9% peak area, **122**).

HPLC (250 Chiracel OJ, 4.6 mm, *n*-Heptan/2-Propanol/TFA = 80:20:0.1, 0.5 mL/min, 2.3 MPa, 298 K): 24.63 min (>99.9% peak area, **122**).

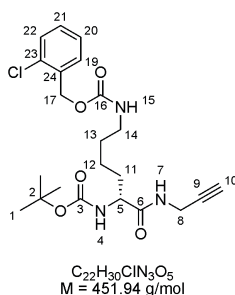
HPLC (250 Chiracel OD-H, 4.6 mm, *n*-Heptan/2-Propanol/TFA = 90:10:0.1, 0.5 mL/min, 2.8 MPa, 298 K): 36.33 min (>99.9% peak area, **122**).

HPLC (250 Chiralpak AD, 4.6 mm, *n*-Heptan/2-Propanol/TFA = 90:10:0.1, 0.5 mL/min, 1.5 MPa, 298 K): 37.01 min (>99.9% peak area, **122**).

R_F = 0.36 (CH₂Cl₂:MeOH 9:1 + 0.1% HOAc)

¹H NMR, ¹³C NMR, EI and ESI (M = 362 g/mol) showed impurities that could not be assigned and that were not visible in TLC and HPLC. Since ESI and EI found Mol peak, product was used without further characterization.

Boc-D-Lys(2Cl-Z)-propargylamide (**123**):



Boc-D-Lys(2Cl-Z) (0.21 g, 0.50 mmol), propargylamine (0.038 mL, 0.60 mmol) and HOBT (0.10 g, 0.75 mmol) were dissolved in CH₂Cl₂ (15 mL) and cooled to

0 °C. To the cold solution, a concentrated solution of EDC CH_2Cl_2 (0.19 g, 1.00 mmol) was added and the solution allowed to warm up to room temperature. After 1 h (TLC monitoring), the solution was extracted with water (1x200 mL). The organic layer was dried over MgSO_4 , filtered and evaporated i.vac. The crude product was purified via column chromatography on silica (eluent: CH_2Cl_2 :MeOH 9:1) to give the desired product in quantitative yield as pale yellow oil.

Alternatively with different work-up procedure: Water was added to the reaction mixture and biphasic system stirred for 10 minutes. After phase separation, the organic layer was extracted with water (1x200 mL), 1 M aqueous citric acid solution (1x200 mL), water (1x200 mL), saturated aqueous NaHCO_3 -solution (1x200 mL), water (1x200 mL), and brine (1x200 mL). The organic layer was dried over MgSO_4 , filtered and evaporated i.vac. to give the product in quantitative yield as pale yellow oil.

HSE-HB-070: HPLC (250 Nucleodur 100-5-C18 ec, 4 mm, Methanol/Water = 55:45, 0.8 mL/min, 9.8 MPa, 308 K): 26.96 min (>99.9% peak area, **(123)**).

R_F = 0.6 (CH_2Cl_2 :MeOH 9:1)

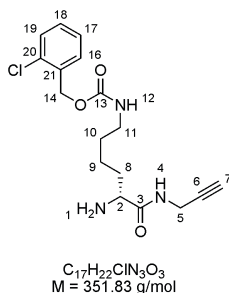
^1H NMR (400 MHz, CDCl_3 , 20 °C): δ 7.43 - 7.20 (m, 4 H, C^{19-22}H), 6.85 - 6.74 (br s, 1 H, N^7H), 5.31 (d, $^3J(\text{H,H}) = 7.7$ Hz, 1 H, N^4H), 5.19 (s, 2 H, C^{17}H_2), 5.10 - 5.06 (m, 1 H, N^{15}H), 4.17 - 4.04 (m, 1 H, C^5H), 4.04 - 3.93 (m, 2 H, C^8H_2), 3.20 - 3.15 (m, 2 H, C^{14}H_2), 2.20 (t, $^4J(\text{H,H}) = 2.4$ Hz, 1 H, C^{10}H), 1.87 - 1.74 (m, 1 H, 1 C^{11}H_2), 1.69 - 1.29 (m, 14 H, 3 C^1H_3 , $\text{C}^{11-13}\text{H}_2$).

^{13}C NMR (CDCl_3): δ 172.10, 156.51, 156.02, 134.40, 133.62, 129.84, 129.58, 129.44, 126.96, 80.29, 79.48, 71.10, 64.01, 54.22, 40.59, 32.00, 29.53, 29.18, 28.45, 22.58.

High-resolution ESI-MS: m/z = 474.176467 (calcd 476.176620 for $\text{C}_{22}\text{H}_{30}\text{ClN}_3\text{O}_5 + \text{Na}^+$).

5 Linear Triazole Containing Polypseudopeptides

D-Lys(2Cl-Z)-propargylamide (**124**):



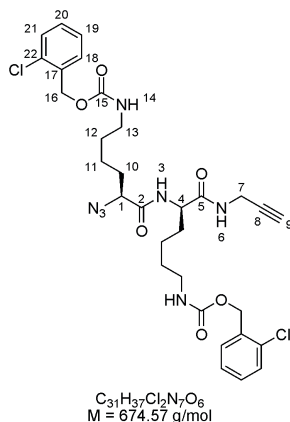
123 was reacted following the general procedure for the deprotection of the Boc group. The product was obtained in quantitative yield.

HPLC (250 Nucleodur 100-5-C18 ec, 4 mm, Methanol/10 mmol TEAA pH7.0 = 45:55, 0.8 mL/min, 9.7 MPa, 308 K): 15.16 min (>99.9% peak area, (**124**)).

$R_F = 0.16$ (CH_2Cl_2 :MeOH 9:1)

High-resolution ESI-MS: $m/z = 352.142596$ (calcd 352.142245 for $C_{17}H_{22}ClN_3O_3 + H^+$).

Azido-L-Lys(2Cl-Z)-D-Lys(2Cl-Z)-propargylamide (**125**):



122 (0.70 g, 2.06 mmol), **124** (1.02 g, 2.88 mmol) and HOBt (0.42 g, 3.09 mmol) were dissolved in CH_2Cl_2 :DMF 10:1 (110 mL) and the solution was cooled to 0 °C. To the cold solution, a concentrated solution of EDC in CH_2Cl_2 (1.19 g, 6.18 mmol) was added. The solution was allowed to warm up to room temperature and stirred for 1 h. After TLC monitoring, the solution was extracted with water (1x200 mL), 1 M aqueous citric acid solution (1x200 mL), water (1x200 mL), saturated aqueous $NaHCO_3$ -solution (1x200 mL), water (1x200 mL), and brine (1x200 mL). The organic layer was dried over $MgSO_4$,

filtered and evaporated i.vac. The crude product was suspended in Et₂O:pentane and filtered to remove remaining DMF. The yellow solid was purified via column chromatography on silica (eluent: CH₂Cl₂:MeOH 95:5) to give 0.98 g (yield: 70%) of the desired product as a white solid.

HPLC (250 Nucleodur 100-5-C18 ec, 4 mm, Methanol/Water = 65:35, 0.8 mL/min, 9.6 MPa, 308 K): 16.28 min (98.32% peak area, (**125**).

R_F = 0.4 (CH₂Cl₂:MeOH 9:1)

¹H NMR (400 MHz, DMSO-d₆, 20 °C): δ 8.50 (t, ³J(H,H) = 5.5 Hz, 1 H, N⁶H), 8.35 (d, ³J(H,H) = 8.3 Hz, 1 H, N³H), 7.49 - 7.32 (m, 10 H, N¹⁴H, 2 C¹⁸⁻²¹H₂), 5.07 (s, 4 H, 2 N¹⁶H₂), 4.28 - 4.21 (m, 1 H, C⁴H), 3.86 (dd, ⁴J(H,H) = 2.5 Hz, ³J(H,H) = 5.5 Hz, 2 H, C⁷H₂), 3.77 (m, 1 H, C¹H), 3.11 (t, ⁴J(H,H) = 2.5 Hz, 1 H, C⁹H), 3.05 - 2.92 (m, 4 H, 2 C¹³H₂) 1.12 - 1.77 (m, 12 H, 2 C¹⁰⁻¹²H₂).

¹³C NMR (DMSO-d₆): δ 171.02, 169.59, 155.81, 155.75, 134.62, 132.30, 129.67, 129.27, 127.29, 80.92, 73.11, 60.81, 52.19, 40.77, 40.59, 31.80, 30.78, 28.93, 28.84, 27.92, 22.70, 22.56.

ESI-MS: m/z = 674 (calcd 674 for C₃₁H₃₇Cl₂N₇O₆ + H⁺), 696 (calcd 696 for C₃₁H₃₇Cl₂N₇O₆ + Na⁺).

High-resolution ESI-MS: m/z = 696.207223 (calcd 696.207460 for C₃₁H₃₇Cl₂N₇O₆ + Na⁺).

Attempted polymerization of **125**:

125 (0.034 g, 0.050 mmol), sodium ascorbate (0.001 g, 0.005 mmol) and TBTA (0.001 g, 0.003 mmol) were dissolved in DMF:H₂O 2:1 (3.0 mL). CuSO₄ was added as aqueous solution (10 mg CuSO₄·5 H₂O in 0.3 mL, 0.03 mL). The solution was degased (4x at room temperature, 1x freeze degase) and stirred at room temperature under argon atmosphere. After 20 h, a white precipitate was visible. After 48 h, the reaction mixture was treated with Et₂O:pentane and EE:hexane to precipitate all product. The precipitate was filtered, washed and dried i.vac. to give 0.024 g of a green-white solid. To remove remaining copper, the solid was suspended in water and sonicated. The in water insoluble solid was filtered and dried i.vac. again. ESI-MS showed signals of mass that corresponded to dimer. Maldi-TOF also showed all higher oligomers up to

5 Linear Triazole Containing Polypseudopeptides

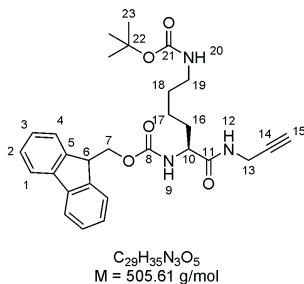
nonamer (signals of higher oligomers were very weak). TLC did not help, GPC found 2 peaks with masses that corresponded to dimer and trimer. ^1H NMR did not show acetylene-H-signals. This could be a sign for a very high number of n or for cyclic products.

Polymerization with minimum amount of water to increase solubility of product: **125** (0.034 g, 0.050 mmol), sodium ascorbate (0.001 g, 0.005 mmol) and TBTA (0.001 g, 0.003 mmol) were dissolved in DMF (3.0 mL). CuSO_4 was added as aqueous solution (10 mg $\text{CuSO}_4 \cdot 5 \text{H}_2\text{O}$ in 0.3 mL, 0.03 mL). The solution was degased (4x at room temperature, 1x freeze degase) and stirred at room temperature under argon atmosphere. After 48 h, TLC showed low degree of conversion, so sodium ascorbate (0.001 g) and degased water (0.3 mL) were added. 72 h later, degased water (0.7 mL) was added and a white solid precipitated from solution. After 2 days, the reaction mixture was diluted with H_2O and poured into aqueous EDTA-solution. The precipitate was filtered and washed with water to give 0.030 g of a white solid. Purification via preparative HPLC failed, because the solid did not dissolve completely. Solid was suspended in $\text{CH}_2\text{Cl}_2:\text{MeOH}$ 1:1 and filtered. The remaining solid was dissolved in DMSO. MALDI-TOF did not show peaks of higher oligomers.

Procedure as described above, but reaction was done in $\text{THF}:\text{H}_2\text{O}$ 3:1 instead of DMF. Work-up after 48 h at room temperature.

Procedure as described above, but reaction was done in DMSO. After 2 days, reaction mixture was heated to 50 °C and stirred at this temperature for 6 h. Work-up after further 13 days at room temperature.

Procedure as described above, but reaction was done in $\text{DMSO}:\text{H}_2\text{O}$ 2:1. Work-up after 14 days at room temperature.

Fmoc-L-Lys(Boc)-propargylamide (**131**):

Fmoc-L-Lys(Boc) (0.09 g, 0.20 mmol), propargylamine (0.02 mL, 0.24 mmol) and HOBT (0.04 g, 0.30 mmol) were dissolved in CH₂Cl₂ (5 mL) and the solution was cooled to 0 °C. To the cold solution EDC (0.08 g, 0.40 mmol) was added. The solution was allowed to warm up to room temperature and stirred under TLC monitoring. After completion of the reaction, the solution was extracted with water (1x50 mL), 1 M aqueous citric acid solution (1x50 mL), water (1x50 mL), saturated aqueous NaHCO₃-solution (1x50 mL), water (1x50 mL), and brine (1x50 mL). The organic layer was dried over MgSO₄, filtered and evaporated i.vac. The crude product was purified via column chromatography on silica (eluent: CH₂Cl₂ until more unpolar impurity was removed, then addition of MeOH to recover product) to give the desired product in quantitative yield.

HPLC-MS ((2x150 mm Luna Phenyl-Hexyl 3μm, acetonitrile:water Grad 5 95A): 20.60 min (>99.9% peak area, ESI(+): 406.24 (**131** – Boc) + 1 H⁺), 506.23 (**131** + 1 H⁺), 406.24 (**131** + 1 Na⁺)).

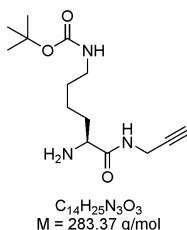
R_F = 0.5 (CH₂Cl₂:EE 1:1)

¹H NMR (300 MHz, CDCl₃, 20 °C): δ 7.75 (d, ³J(H,H) = 7.4 Hz, 2 H, 2 C¹H), 7.57 (d, ³J(H,H) = 7.4 Hz, 2 H, 2 C⁴H), 7.42 - 7.28 (m, 4 H, 2 C²H, 2 C³H), 6.63 - 6.61 (m, 1 H, N¹²H), 5.69 - 5.65 (m, 1 H, N⁹H), 4.66 - 4.63 (m, 1 H, N²⁰H), 4.43 - 4.28 (m, 2 H, C⁷H), 4.22 - 4.17 (m, 2 H, C⁶H, C¹⁰H), 4.03 - 3.99 (m, 2 H, C¹³H₂), 3.12 - 3.08 (m, 2 H, C¹⁹H₂), 2.16 (t, ⁴J(H,H) = 2.5 Hz, 1 H, C¹⁵H), 1.96 - 1.21 (m, 15 H, 2 C¹⁵⁻¹⁸H₂, 3 C²³H₃).

¹³C NMR (DMSO-d₆): δ 171.57, 156.39, 143.86, 143.82, 141.43, 127.89, 127.19, 125.19, 120.14, 79.29, 71.92, 67.22, 54.79, 47.35, 32.10, 29.72, 29.32, 28.56, 22.55.

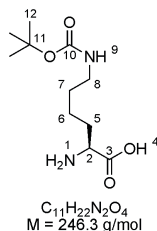
5 Linear Triazole Containing Polypseudopeptides

L-Lys(Boc)-propargylamide (**132**):



Fmoc-L-Lys(Boc)-propargylamide (0.06 g, 0.12 mmol) was dissolved in CH_2Cl_2 (8 mL). Piperidin (2 mL) was added and the solution stirred for 10 minutes (TLC monitoring). Isolation of the desired product by aqueous work-up as well as by directly evaporating the solvents was not possible. As compound was too polar for column chromatography, isolation and purification was not possible.

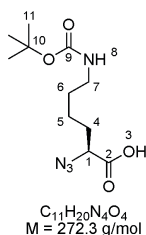
L-Lys(Boc) (**133**):



Z-L-Lys(Boc) (2.37 g, 6.00 mmol) was reacted following the general procedure for the deprotection of the Z group or benzyl ester. MeOH (50 mL), Pd/C (237 mg), reaction time: 1 h, hydrogen pressure: 6 bar. The product was used without further purification and analysis.

$R_F = 0.39$ (CH_2Cl_2 :MeOH 8:2)

Azido-L-Lys(Boc) (**134**):



NaN₃ (4.21 g, 64.80 mmol) was dissolved in water (10.5 mL) with CH₂Cl₂ (17.0 mL) and cooled to 0 °C. Triflyl anhydride (2.15 mL, 12.96 mmol) was added slowly within 5 minutes with stirring continued for 2 h. The emulsion formed 2 transparent layers after 30 minutes. The mixture was placed in a separation funnel and the CH₂Cl₂ layer was removed. The aqueous layer was extracted with CH₂Cl₂ (2x20 mL). The united organic layers were extracted once with saturated aqueous Na₂CO₃-solution and used without further purification.

133 (1.76 g, 6.48 mmol) was combined with K₂CO₃ (1.34 g, 9.72 mmol) and CuSO₄ (solution of 0.01 g in 0.3 mL water) (0.48 mL, 0.065 mmol), water (12 mL) and MeOH (24 mL). A white emulsion was formed. The triflyl azide in CH₂Cl₂ was added and the mixture stirred at room temperature for 12 h. TLC showed low product content, so more triflyl azide was synthesized (1.20 mL triflyl anhydride dissolved in dry CH₂Cl₂ (10 mL) and added within 15 minutes to NaN₃ (2.11 g) in 5.4 mL H₂O. The solution was then stirred for 2 h at room temperature.) and added to the reaction mixture, which was then stirred at room temperature for 12 h. The organic solvents were removed i.vac. and the aqueous slurry was diluted with water. This was acidified to pH = 6 with conc. HCl and extracted with EE (4x20 mL), in order to remove sulfonamide byproduct. The aqueous layer was acidified until it became turbid and extracted with EE (3x50 mL). These organic layers were dried over MgSO₄ and evaporated i.vac. The crude product was purified via column chromatography on silica (eluent: EE:MeOH (9:1) (+ 0.1% HOAc)) to give the desired product in quantitative yield.

HPLC-MS ((2x150 mm Luna Phenyl-Hexyl 3µm, acetonitrile:water Grad 5 95A): 16.39 min (>99.9% peak area, ESI(-): 271.10 (**134** – 1 H⁺)).

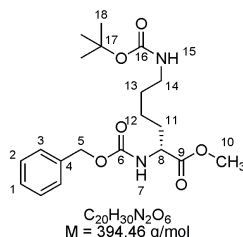
*R*_F = 0.40 (PE:EE 1:1)

¹H NMR (300 MHz, CDCl₃, 20 °C): δ 11.90 (br s, 1 H, O³H), 4.76 (br s, 1 H, N⁸H), 3.88 - 3.85 (m, 1 H, C¹H), 3.10 - 3.05 (m, 2 H, C⁷H₂), 1.83 - 1.79 (m, 2 H, C⁴H₂), 1.43 - 1.39 (m, 13 H, C⁵⁻⁶H₂, 3 C¹¹H₃).

¹³C NMR (DMSO-d₆): δ 173.97, 156.51, 79.86, 63.19, 41.03, 32.16, 30.41, 28.78, 24.07.

5 Linear Triazole Containing Polypseudopeptides

Z-D-Lys(Boc)-Me (**135**):



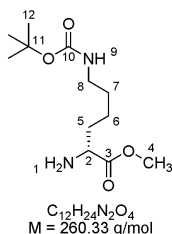
Z-D-Lys(Boc) (1.83 g, 4.80 mmol) and HOBT (0.65 g, 4.80 mmol) were dissolved in MeOH (30 mL) and cooled to 0 °C. To the cold solution, EDC (1.9 g, 9.6 mmol) was added. The solution was allowed to warm up to room temperature and stirred under TLC monitoring. After completion of the reaction, the solution was evaporated i.vac. The yellow oil was dissolved in CH_2Cl_2 and purified via column chromatography on silica (eluent: PE:EE 1:1) to give the desired product in quantitative yield.

$R_F = 0.40$ (PE:EE 1:1)

1H NMR (300 MHz, $CDCl_3$, 20 °C): δ 7.27 - 7.20 (m, 5 H, C^1H , 2 C^2H , 2 C^3H), 5.44(d, $^3J(H,H) = 8.1 \text{ Hz}$, 1 H, N^7H), 5.02 (s, 2 H, C^5H_2), 4.58 (br s, 1 H, $N^{15}H$), 4.29 - 4.14 (m, 1 H, C^8H), 3.64 (s, 3 H, $C^{10}H_3$), 3.15 - 2.95 (m, 2 H, $C^{14}H_2$), 1.82 - 1.50 (m, 2 H, $C^{11}H_2$), 1.40 - 1.18 (m, 13 H, $C^{12}H_2$).

^{13}C NMR ($CDCl_3$): δ 173.04, 156.17, 156.07, 136.31, 128.54, 128.20, 128.16, 79.20, 67.00, 53.77, 52.38, 40.09, 32.13, 29.60, 28.45, 22.39.

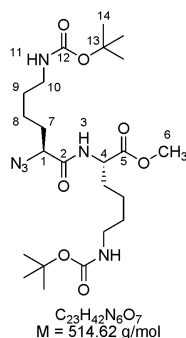
D-Lys(Boc)-Me (**136**)



Z-D-Lys(Boc)-Me (1.89 g, 4.80 mmol) was reacted following the general procedure for the deprotection of the Z group or benzyl ester. EE:MeOH (1:1) (40 mL), Pd/C (11 mg), reaction time: 2 h, hydrogen pressure: 5 bar. The product was filtered through a short silica plug to remove impurities.

$R_F = 0.32$ ($\text{CH}_2\text{Cl}_2:\text{MeOH}$ 9:1)

Azido-L-Lys(Boc)-L-Lys(Boc)-Me (**137**)



128 (0.33 g, 1.20 mmol), **18** (0.34 mL, 1.32 mmol), and HOBT (0.16 g, 1.20 mmol) were dissolved in CH_2Cl_2 (10 mL) and the solution was cooled to 0 °C. To the cold solution, EDC (0.46 g, 2.40 mmol) was added. The solution was allowed to warm up to room temperature and stirred under TLC monitoring. After completion of the reaction, the solution was evaporated i.vac. and the residue dissolved in EE. Water was added to the mixture and the biphasic system stirred for 10 minutes. After phase separation, the organic layer was extracted with water (1x20 mL), 1 M aqueous citric acid solution (1x20 mL), water (1x20 mL), saturated aqueous NaHCO_3 -solution (1x20 mL), water (1x20 mL), and brine (1x20 mL). The organic layer was dried over MgSO_4 , filtered and evaporated i.vac. The crude product was purified via column chromatography on silica (eluent: $\text{CH}_2\text{Cl}_2:\text{EE}$ 1:1) to give the desired product in quantitative yield.

HPLC-MS ((2x150 mm Luna Phenyl-Hexyl 3 μm , acetonitrile:water Grad 5 95A): 19.66 min (>99.9% peak area, ESI(+): 415.27 (**137** – Boc) + 1 H^+), 515.29 (**137** + 1 H^+), 537.29 (**137** + 1 Na^+)).

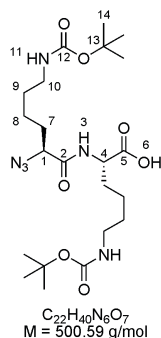
$R_F = 0.40$ ($\text{CH}_2\text{Cl}_2:\text{EE}$ 1:1)

^1H NMR (300 MHz, CDCl_3 , 20 °C): δ 6.93 (d, $^3J(\text{H},\text{H}) = 8.0$ Hz, 1 H, N^3H), 4.80 (br s, 2 H, 2 N^{12}H), 4.49 (dt, $^3J(\text{H},\text{H}) = 8.0$ Hz, $^3J(\text{H},\text{H}) = 4.9$ Hz, 1 H, C^4H), 3.90 (t, $^3J(\text{H},\text{H}) = 6.1$ Hz, 1 H, C^1H), 3.68 (s, 3 H, C^6H_3), 3.09 - 3.02 (m, 4 H, 2 C^9H_2), 1.91 - 1.23 (m, 30 H, 2 C^{7-9}H_2 , 6 C^{14}H_3).

5 Linear Triazole Containing Polypseudopeptides

^{13}C NMR (CDCl_3): δ 172.39, 171.14, 169.30, 156.15, 156.08, 79.03, 63.65, 52.48, 52.00, 40.15, 40.08, 31.75, 31.63, 29.62, 29.57, 28.40, 22.48.

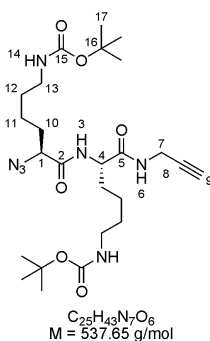
Azido-L-Lys(Boc)-L-Lys(Boc) (**139**)



137 was reacted following the general procedure for the deprotection of the methyl ester.

$R_F = 0.10$ (CH_2Cl_2 :MeOH 9:1)

Azido-L-Lys(Boc)-L-Lys(Boc)-propargylamide (**141**)



139 (0.13 g, 0.26 mmol), propargylamine (0.02 mL, 0.31 mmol), and HOBT (0.04 g, 0.26 mmol) were dissolved in CH_2Cl_2 (10 mL) and the solution cooled to 0 °C. To the cold solution EDC (0.10 g, 0.52 mmol) was added. The solution was allowed to warm up to room temperature and stirred under TLC monitoring. After completion of the reaction, the solution was extracted with water (1x20 mL), 1 M aqueous citric acid solution (1x20 mL), water (1x20 mL), saturated aqueous NaHCO_3 -solution (1x20 mL), water (1x20 mL), and brine (1x20 mL). The organic layer was dried over MgSO_4 , filtered and evaporated i.vac. The crude product was dissolved in EE and precipitated in PE. The residue

was purified via column chromatography on silica (eluent: CH₂Cl₂:EE 2:1 to CH₂Cl₂:EE 1:1) to give the desired product in 90% yield.

HPLC-MS ((2x150 mm Luna Phenyl-Hexyl 3 μ m, acetonitrile:water Grad 40 95A): 10.85 min (>99.9% peak area, ESI(+): 338.27 (**141** – 2 Boc) + 1 H⁺), 382.25 (**141** – 1 Boc – propargylamine) + 1 H⁺), 438.27 (**141** – 1 Boc) + 1 H⁺), 538.30 (**141** + 1 H⁺), ESI(-): 536.17 (**141** – 1 H⁺)).

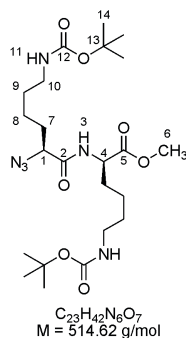
R_F = 0.24 (CH₂Cl₂:EE 1:1)

¹H NMR (300 MHz, CDCl₃, 20 °C): δ 7.06 (d, ³ J (H,H) = 8.3 Hz, 1 H, N³H), 6.94 (t, ³ J (H,H) = 5.1 Hz, 1 H, N⁶H), 4.80 (br s, 2 H, 2 N¹⁴H), 4.45 (dt, ³ J (H,H) = 7.9 Hz, ³ J (H,H) = 5.9 Hz, 1 H, C⁴H), 4.04 – 4.01 (m, 2 H, C⁷H₂), 3.90 (t, ³ J (H,H) = 6.0 Hz, 1 H, C¹H), 3.20 – 2.98 (m, 4 H, 2 C¹³H₂), 2.24 (t, 1 H, ³ J (H,H) = 2.5 Hz, C⁹H), 1.99 – 1.19 (m, 30 H, 2 C¹⁰⁻¹²H₂, 6 C¹⁷H₃).

¹³C NMR (CDCl₃): δ 171.01, 169.74, 156.35, 156.21, 79.39, 79.27, 71.90, 63.81, 52.87, 32.13, 31.81, 29.77, 29.66, 29.31, 28.56, 22.67, 22.60.

High-resolution ESI-MS: m/z = 538.3348 (calcd 538.3348 for C₂₅H₄₃N₇O₆ + H⁺), 560.3163 (calcd 560.3167 for C₂₅H₄₃N₇O₆ + Na⁺).

Azido-L-Lys(Boc)-D-Lys(Boc)-Me (**138**):



128 (1.27 g, 4.65 mmol), **136** (1.25 mL, 4.80 mmol), and HOBT (0.63 g, 4.65 mmol) were dissolved in CH₂Cl₂ (30 mL) and the solution was cooled to 0 °C. To the cold solution, EDC (1.96 g, 10.23 mmol) was added. The solution was allowed to warm up to room temperature and stirred under TLC monitoring. After completion of the reaction, the solution was evaporated i.vac. and the residue dissolved in EE. Water was added to the mixture and the biphasic system stirred for 10 minutes. After phase separation, the organic layer was extracted with water (1x20 mL), 1 M aqueous citric acid solution (1x20 mL),

5 Linear Triazole Containing Polypseudopeptides

water (1x20 mL), saturated aqueous NaHCO_3 -solution (1x20 mL), water (1x20 mL), and brine (1x20 mL). The organic layer was dried over MgSO_4 , filtered and evaporated i.vac. The crude product was purified via column chromatography on silica (eluent: CH_2Cl_2 :EE 1:1) to give 2.27 g (yield: 95%) of the desired product.

HPLC-MS ((2x150 mm Luna Phenyl-Hexyl 3 μm , acetonitrile:water Grad 40 95A): 11.80 min (>99.9% peak area, ESI(-): 513.17 (**138** + 1 H^+)).

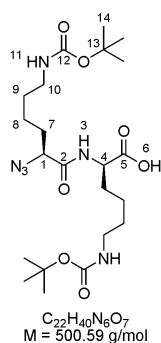
R_F = 0.40 (CH_2Cl_2 :EE 1:1)

^1H NMR (300 MHz, CDCl_3 , 20 °C): δ 6.93 (d, $^3J(\text{H,H})$ = 8.0 Hz, 1 H, N^3H), 4.80 (br s, 2 H, 2 N^{12}H), 4.49 (dt, $^3J(\text{H,H})$ = 7.9 Hz, $^3J(\text{H,H})$ = 5.3 Hz, 1 H, C^4H), 3.90 (t, $^3J(\text{H,H})$ = 6.0 Hz, 1 H, C^1H), 3.64 (s, 3 H, C^6H_3), 3.03 - 2.98 (m, 4 H, 2 C^9H_2), 1.89 - 1.08 (m, 30 H, 2 C^{7-9}H_2 , 6 C^{14}H_3).

^{13}C NMR (CDCl_3): δ 172.26, 169.35, 156.02, 155.97, 78.87, 63.48, 52.35, 51.91, 40.05, 31.53, 31.46, 29.49, 29.44, 28.30, 22.47, 22.33.

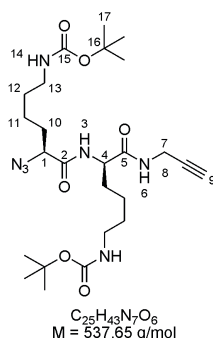
High-resolution ESI-MS: m/z = 515.3187 (calcd 538.3348 for $\text{C}_{23}\text{H}_{42}\text{N}_6\text{O}_7 + \text{H}^+$), 537.3005 (calcd 537.3007 for $\text{C}_{23}\text{H}_{42}\text{N}_6\text{O}_7 + \text{Na}^+$), 1051.6117 (calcd 1051.6122 for $(\text{C}_{23}\text{H}_{42}\text{N}_6\text{O}_7)_2 + \text{H}^+$).

Azido-L-Lys(Boc)-D-Lys(Boc) (**140**):



138 was reacted following the general procedure for the deprotection of the methyl ester.

R_F = 0.10 (CH_2Cl_2 :MeOH 9:1)

Azido-L-Lys(Boc)-D-Lys(Boc)-propargylamide (**142**):

140 (2.21 g, 4.41 mmol), propargylamine (0.34 mL, 5.29 mmol), and HOBT (0.60 g, 4.41 mmol) were dissolved in CH_2Cl_2 (50 mL) and the solution cooled to 0 °C. To the cold solution EDC (1.69 g, 8.82 mmol) was added. The solution was allowed to warm up to room temperature and stirred under TLC monitoring. After completion of the reaction, the solution was extracted with water (1x20 mL), 1 M aqueous citric acid solution (1x20 mL), water (1x20 mL), saturated aqueous NaHCO_3 -solution (1x20 mL), water (1x20 mL), and brine (1x20 mL). The organic layer was dried over MgSO_4 , filtered and evaporated i.vac. The crude product was purified via column chromatography on silica (eluent: CH_2Cl_2 :EE 2:1 to CH_2Cl_2 :EE 1:1) to give the desired product in 93% yield.

HPLC-MS ((2x150 mm Luna Phenyl-Hexyl 3 μm , acetonitrile:water Grad 40 95A): 10.77 min (78.8% peak area, ESI(+): 338.28 ((**142** – 2 Boc) + 1 H^+), 382.25 ((**142** – 1 Boc – propargylamine) + 1 H^+), 438.27 ((**142** – 1 Boc) + 1 H^+), 538.31 (**142** + 1 H^+), ESI(-): 536.17 (**142** – 1 H^+)).

$R_f = 0.24$ (CH_2Cl_2 :EE 1:1)

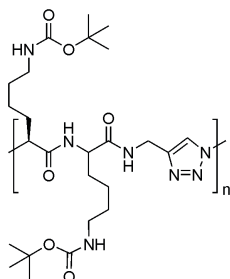
^1H NMR (300 MHz, CDCl_3 , 20 °C): δ 7.55 – 7.45 (m, 1 H, N^3H), 7.44 – 7.41 (m, 1 H, N^6H), 4.92 (br s, 2 H, 2 N^{14}H), 4.53 – 4.46 (m, 1 H, C^4H), 3.98 – 3.85 (m, 3 H, C^1H , C^7H_2), 3.10 – 2.98 (m, 4 H, 2 C^{13}H_2), 2.22 (t, $^3J(\text{H,H}) = 2.5 \text{ Hz}$, 1 H, C^9H), 1.93 – 1.09 (m, 30 H, 2 $\text{C}^{10-12}\text{H}_2$, 6 C^{17}H_3).

^{13}C NMR (CDCl_3): δ 171.31, 170.09, 156.18, 79.31, 79.08, 71.61, 63.22, 52.77, 40.21, 32.11, 31.62, 29.59, 29.53, 29.08, 28.43, 22.69, 22.64.

High-resolution ESI-MS: $m/z = 538.3340$ (calcd 538.3348 for $\text{C}_{25}\text{H}_{43}\text{N}_7\text{O}_6 + \text{H}^+$), 560.3156 (calcd 560.3167 for $\text{C}_{25}\text{H}_{43}\text{N}_7\text{O}_6 + \text{Na}^+$).

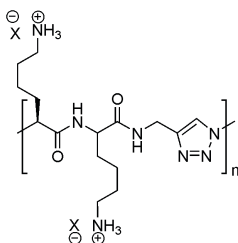
5 Linear Triazole Containing Polypseudopeptides

Polymerization reactions of: Azido-L-Lys(Boc)-L-Lys(Boc)-propargylamide (**141**) and Azido-L-Lys(Boc)-D-Lys(Boc)-propargylamide (**142**):



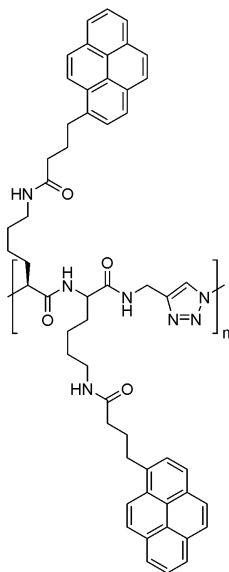
In a typical procedure, the AB-monomer was dissolved in the respective solvent. Copper wire was added and the solution degased by bubbling argon through it. Concentrated aqueous solutions of CuSO_4 and sodium ascorbate or tetrakis(acetonitrile)copper(I) hexafluorophosphate (depending on the protocol) and *N,N'*-dimethylethylenediamine were added and the solution was stirred. All details see Special Part Chapter 3, table 2.

Boc-cleavage of polymers **144**, **149**, **153** to **154**, **155**, **156**:



Polymers were dissolved in neat TFA and stirred for 2 h. TFA was removed i.vac. and product dialyzed in water (MWCO 25000 g/mol). Lyophilization gave the desired peptides. In case of anion exchange, the peptide was dissolved in aqueous 1 M HCl and dialyzed.

Pyrene labeling of the polymer side-chains to polymers **169**, **170**:



Aqueous conditions:

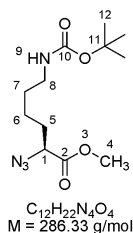
Pyrenebutyric acid (6 eq.), HOBT (10 eq.) and EDC (11 eq.) were dissolved in DMF. Polymer dissolved in DMF:H₂O (minimum amount of H₂O to dissolve polymer) was added and the reaction mixture stirred for 18 h. Within this time, EDC (44 eq.) was added in portions in order to compensate the amount of water. The reaction mixture was precipitated in basic water and centrifuged. The precipitate was dissolved in CH₂Cl₂ and dialyzed in CH₂Cl₂ and CH₂Cl₂:MeOH (1:1) (MWCO 25000 g/mol), to give the desired polymer in quantitative yield.

Water-free conditions:

Polymer, pyrenebutyric acid (6 eq.), and HOBT (10 eq) were dissolved in DMSO. EDC (11 eq.) and NEt₃ (6 eq.) were added and the solution stirred for 3 days. Within these 3 days, EDC (11 eq.) was added to the solution. The solution was subsequently dialyzed CH₂Cl₂:MeOH (1:1) (MWCO 25000 g/mol) to give the desired polymer in quantitative yield.

5 Linear Triazole Containing Polypseudopeptides

Azido-L-Lys(Boc)-Me (**157**):



134 (0.44 g, 1.60 mmol) and HOBt (0.11 g, 0.80 mmol) were dissolved in MeOH (30 mL) and the solution was cooled to 0 °C. To the cold solution, EDC (0.37 g, 1.92 mmol) was added. The solution was allowed to warm up to room temperature and stirred under TLC monitoring. After completion of the reaction, the solution was evaporated i.vac. and the residue dissolved in EE. The organic layer was extracted with water (1x200 mL), 1 M aqueous citric acid solution (1x200 mL), water (1x200 mL), saturated aqueous NaHCO_3 -solution (1x200 mL), water (1x200 mL), and brine (1x200 mL). The organic layer was dried over MgSO_4 , filtered and evaporated i.vac. to give 0.45 g (yield: 94%) of the desired product as colorless oil.

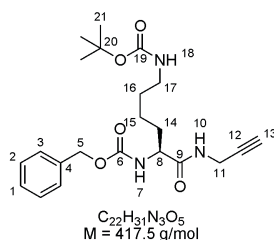
UPLC-MS ((2.1x100 mm HSS T3 1.8 μm , acetonitrile:water Grad 40 95A): 2.21 min (90.1% peak area, ESI(+): 309.18 (**157** + 1 Na^+)).

$R_f = 0.61$ (CH_2Cl_2 :MeOH 9:1)

^1H NMR (300 MHz, CDCl_3 , 20 °C): δ 4.55 (br s, 1 H, N^9H), 3.84 (dd, $^3J(\text{H},\text{H}) = 5.4 \text{ Hz}$, $^3J(\text{H},\text{H}) = 8.3 \text{ Hz}$, 1 H, C^1H), 3.78 (s, 3 H, C^4H_3), 3.17 - 3.04 (m, 4 H, 2 C^8H_2), 1.92 - 1.33 (m, 15 H, C^{5-7}H_2 , 3 C^{12}H_3).

^{13}C NMR (CDCl_3): δ 171.08, 156.10, 79.41, 61.98, 52.75, 40.46, 31.12, 29.68, 28.51, 23.08.

High-resolution ESI-MS: $m/z = 287.1749$ (calcd 287.1719 for $\text{C}_{12}\text{H}_{22}\text{N}_4\text{O}_4 + \text{H}^+$), 309.1760 (calcd 309.1539 for $\text{C}_{12}\text{H}_{22}\text{N}_4\text{O}_4 + \text{Na}^+$).

Z-L-Lys(Boc)-propargylamide (**158**):

Z-L-Lys(Boc) (2.47 g, 6.48 mmol), propargylamine (0.50 mL, 7.81 mmol), and HOBt (1.31 g, 9.72 mmol) were dissolved in CH_2Cl_2 (150 mL) and the solution was cooled to 0 °C. To the cold solution, a concentrated solution of EDC in CH_2Cl_2 (2.49 g, 12.97 mmol) was added. The solution was allowed to warm up to room temperature and stirred under TLC monitoring. After completion of the reaction, the solution was extracted with water (1x200 mL), 1 M aqueous citric acid solution (1x200 mL), water (1x200 mL), saturated aqueous NaHCO_3 -solution (1x200 mL), water (1x200 mL), and brine (1x200 mL). The organic layer was dried over MgSO_4 , filtered and evaporated i.vac. The crude product was dissolved in CH_2Cl_2 and precipitated in PE to give 2.66 g (yield: 91%) of the desired product.

HPLC-MS ((2x150 mm Luna Phenyl-Hexyl 3 μm , acetonitrile:water Grad 5 95A): 18.22 min (>99.9% peak area, ESI(+): 318.23 ((**158** – 1 Boc) + 1 H^+), 418.24 (**158** + 1 H^+)).

$R_F = 0.40$ (EE:PE 1:1)

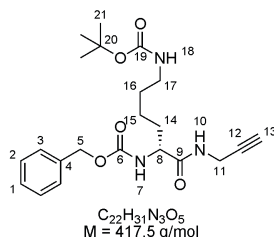
^1H NMR (300 MHz, CDCl_3 , 20 °C): δ 7.40 – 7.27 (m, 5 H, C^{1-3}H), 6.79 – 6.64 (m, 1 H, N^{10}H), 5.62 (d, $^3J(\text{H,H}) = 7.5 \text{ Hz}$, 1 H, N^7H), 5.09 (s, 2 H, C^5H_2), 4.66 – 4.65 (m, 1 H, N^{18}H), 4.19 – 4.13 (m, 1 H, C^8H), 4.03 – 3.99 (m, 2 H, C^{11}H_2), 3.08 – 3.06 (m, 2 H, C^{17}H_2), 2.21 (t, $^3J(\text{H,H}) = 2.5 \text{ Hz}$, 1 H, C^{13}H), 1.92 – 1.24 (m, 15 H, $\text{C}^{14-16}\text{H}_2$, 3 C^{21}H_3).

^{13}C NMR (CDCl_3): δ 171.68, 156.38, 136.20, 128.67, 128.36, 128.22, 79.44, 71.85, 67.28, 54.82, 32.07, 29.71, 29.29, 28.54, 22.51.

High-resolution ESI-MS: $m/z = 418.2332$ (calcd 418.2336 for $\text{C}_{22}\text{H}_{31}\text{N}_3\text{O}_5 + \text{H}^+$), 440.2152 (calcd 440.2156 for $\text{C}_{22}\text{H}_{31}\text{N}_3\text{O}_5 + \text{Na}^+$).

5 Linear Triazole Containing Polypseudopeptides

Z-D-Lys(Boc)-propargylamide (**159**):



Z-D-Lys(Boc) (1.07 g, 2.82 mmol), propargylamine (0.22 mL, 3.39 mmol), and HOBt (0.57 g, 4.24 mmol) were dissolved in CH_2Cl_2 (70 mL) and the solution was cooled to 0 °C. To the cold solution, a concentrated solution of EDC in CH_2Cl_2 (1.08 g, 5.64 mmol) was added. The solution was allowed to warm up to room temperature and stirred under TLC monitoring. After completion of the reaction, the solution was extracted with water (1x200 mL), 1 M aqueous citric acid solution (1x200 mL), water (1x200 mL), saturated aqueous NaHCO_3 -solution (1x200 mL), water (1x200 mL), and brine (1x200 mL). The organic layer was dried over MgSO_4 , filtered and evaporated i.vac. The crude product was dissolved in CH_2Cl_2 and precipitated in PE to give 0.75 g (yield: 59%) of the desired product.

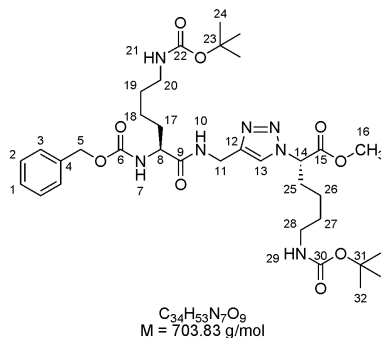
HPLC-MS ((2x150 mm Luna Phenyl-Hexyl 3 μm , acetonitrile:water Grad 5 95A): 18.22 min (>99.9% peak area, ESI(+): 318.23 ((**159** – 1 Boc) + 1 H^+), 418.24 (**159** + 1 H^+)).

$R_F = 0.59$ (CH_2Cl_2 :MeOH 9:1)

^1H NMR (300 MHz, CDCl_3 , 20 °C): δ 7.37 – 7.29 (m, 5 H, C^{1-3}H), 6.70 – 6.65 (m, 1 H, N^{10}H), 5.59 (d, $^3J(\text{H,H}) = 7.1 \text{ Hz}$, 1 H, N^7H), 5.10 (s, 2 H, C^5H_2), 4.68 – 4.62 (m, 1 H, N^{18}H), 4.23 – 4.10 (m, 1 H, C^8H), 4.07 – 3.95 (m, 2 H, C^{11}H_2), 3.10 – 3.05 (m, 2 H, C^{17}H_2), 2.21 (t, $^3J(\text{H,H}) = 2.5 \text{ Hz}$, 1 H, C^{13}H), 1.92 – 1.26 (m, 15 H, $\text{C}^{14-16}\text{H}_2$, 3 C^{21}H_3).

^{13}C NMR (CDCl_3): δ 171.64, 156.37, 136.18, 128.66, 128.35, 128.21, 79.33, 71.85, 67.28, 54.80, 32.02, 29.70, 29.28, 28.52, 22.48.

High-resolution ESI-MS: $m/z = 418.2332$ (calcd 418.2336 for $\text{C}_{22}\text{H}_{31}\text{N}_3\text{O}_5 + \text{H}^+$), 440.2151 (calcd 440.2156 for $\text{C}_{22}\text{H}_{31}\text{N}_3\text{O}_5 + \text{Na}^+$).

Z-L-Lys(Boc)-triazolo-L-Lys(Boc)-Me (**160**):

158 (200 mg, 0.48 mmol), **157** (137 mg, 0.48 mmol) were dissolved in THF (15 mL) and cooled to 0 °C. The solution was degased by bubbling argon through it. Sodium ascorbate (19 mg, 0.096 mmol), dissolved in H₂O (0.20 mL), CuSO₄ (0.012 g, 0.048 mmol) dissolved in H₂O (0.20 mL), and *N,N'*-dimethylethylenediamine (0.010 mL, 0.096 mmol) were added under stirring. TLC monitoring displayed no conversion of the starting material. A purple precipitate was formed, which could be dissolved by the addition of H₂O (5 mL). After 1 minute, the purple solution became colorless. After 12 h, THF was removed i.vac. and replaced by EE. The organic layer was extracted with aqueous EDTA-solution (1x20 mL) and water (1x20 mL). The organic layer was evaporated i.vac. to give the crude product, which was purified via column chromatography on silica (eluent: EE:PE 4:1) to give 303 mg (yield: 90%) of the desired product as a white solid.

UPLC-MS ((2.1x100 mm HSS T3 1.8um, acetonitrile:water Grad 5 95A): 3.96 min (>99.9% peak area, ESI(+): 704.40 (**160** + 1 H⁺)).

*R*_F = 0.36 (EE:PE 4:1)

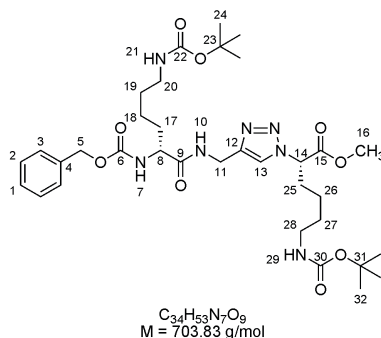
¹H NMR (400 MHz, CDCl₃, 20 °C): δ 7.75 (s, 1 H, C¹³H), 7.36 – 7.18 (m, 6 H, C¹⁻₃H, N¹⁰H), 5.77 (br s, 1 H, N⁷H), 5.36 – 5.21 (m, 1 H, C¹⁴H), 5.04 (s, 2 H, C⁵H₂), 4.89 – 4.38 (m, 4 H, C¹¹H₂, 2 N²¹H), 4.23 – 4.11 (m, 1 H, C⁸H), 3.75 (s, 3 H, C¹⁶H₃), 3.10 – 2.96 (m, 4 H, C²⁰H₂, C²⁸H₂), 2.28 – 2.05 (m, 2 H, C²⁵H₂), 1.88 – 1.57 (m, 2 H, C¹⁷H₂), 1.53 – 1.05 (m, 26 H, C¹⁸⁻¹⁹H₂, C²⁶⁻²⁷H₂, 3 C²⁴H₃, 3 C³²H₃).

¹³C NMR (CDCl₃): δ 172.25, 169.17, 156.48, 156.37, 156.19, 144.82, 136.31, 128.64, 128.27, 128.16, 122.27, 79.34, 67.13, 62.88, 55.05, 53.23, 40.10, 35.00, 32.09, 29.68, 29.24, 22.91, 22.52.

5 Linear Triazole Containing Polypseudopeptides

High-resolution ESI-MS: $m/z = 704.4011$ (calcd 704.3983 for $C_{34}H_{53}N_7O_9 + H^+$).

Z-D-Lys(Boc)-triazolo-L-Lys(Boc)-Me (**161**):



159 (200 mg, 0.48 mmol), **157** (137 mg, 0.48 mmol) were dissolved in THF (15 mL) and cooled to 0 °C. The solution was degassed by bubbling argon through it. Sodium ascorbate (19 mg, 0.096 mmol), dissolved in H₂O (0.20 mL), CuSO₄ (0.012 g, 0.048 mmol) dissolved in H₂O (0.20 mL), and *N,N'*-dimethylethylenediamine (0.010 mL, 0.096 mmol) were added under stirring. TLC monitoring displayed no conversion of the starting material. A purple precipitate was formed, which could be dissolved by the addition of H₂O (5 mL). After 1 minute, the purple solution became colorless. After 12 h, THF was removed i.vac. and replaced by EE. The organic layer was extracted with aqueous EDTA-solution (1x20 mL) and water (1x20 mL). The organic layer was evaporated i.vac. to give the crude product, which was purified via column chromatography on silica (eluent: EE:PE 4:1) to give 308 mg (yield: 91%) of the desired product as a white solid.

UPLC-MS ((2.1x100 mm HSS T3 1.8um, acetonitrile:water Grad 5 95A): 4.01 min (>99.9% peak area, ESI(+): 704.40 (**161** + 1 H⁺)).

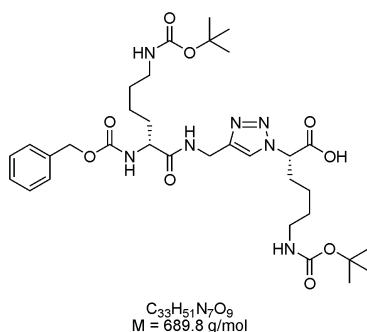
$R_f = 0.36$ (EE:PE 4:1)

¹H NMR (400 MHz, CDCl₃, 20 °C): δ 7.84 (s, 1 H, C¹³H), 7.39 – 7.27 (m, 6 H, C¹⁻3H, N¹⁰H), 5.75 (br s, 1 H, N⁷H), 5.34 – 5.31 (m, 1 H, C¹⁴H), 5.08 (s, 2 H, C⁵H₂), 4.79 – 4.39 (m, 4 H, C¹¹H₂, 2 N²¹H), 4.22 – 4.09 (m, 1 H, C⁸H), 3.77 (s, 3 H, C¹⁶H₃), 3.11 – 2.95 (m, 4 H, C²⁰H₂, C²⁸H₂), 2.29 – 2.03 (m, 2 H, C²⁵H₂), 1.90 – 1.61 (m, 2 H, C¹⁷H₂), 1.54 – 0.97 (m, 26 H, C¹⁸⁻¹⁹H₂, C²⁶⁻²⁷H₂, 3 C²⁴H₃, 3 C³²H₃).

^{13}C NMR (CDCl_3): δ 172.26, 169.20, 136.30, 128.64, 128.18, 128.18, 122.16, 79.34, 67.15, 62.93, 55.03, 53.22, 40.07, 34.99, 32.12, 29.67, 28.52, 22.55.

High-resolution ESI-MS: m/z = 704.4000 (calcd 704.3983 for $\text{C}_{34}\text{H}_{53}\text{N}_7\text{O}_9 + \text{H}^+$), 726.3820 (calcd 726.3802 for $\text{C}_{34}\text{H}_{53}\text{N}_7\text{O}_9 + \text{Na}^+$).

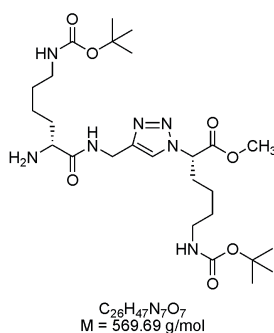
Z-D-Lys(Boc)-triazolo-L-Lys(Boc) (**162**):



161 was reacted following the general procedure for the deprotection of the methyl ester.

R_F = 0.16 (PE:EE 1:4)

D-Lys(Boc)-triazolo-L-Lys(Boc)-Me (**163**)

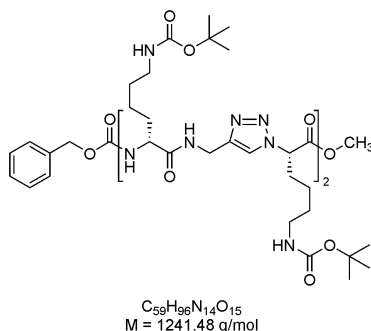


161 (0.10 g, 0.14 mmol) was reacted following the general procedure for the deprotection of the Z group or benzyl ester. MeOH (20 mL) (reaction did not take place in EE), Pd/C (11 mg), reaction time: 2 h, hydrogen pressure: 5 bar.

R_F = 0.1 (Et_2O)

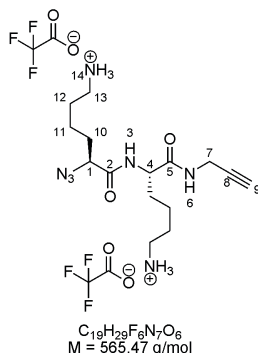
5 Linear Triazole Containing Polypseudopeptides

Z-(D-Lys(Boc)-triazolo-L-Lys(Boc))₂-Me (**164**):



163 (0.08 g, 0.14 mmol), **162** (0.09 g, 0.14 mmol), and HOBT (0.02 g, 0.14 mmol) were dissolved in CH_2Cl_2 (10 mL) and cooled to 0 °C. To the cold solution EDC (0.03 g, 0.16 mmol) was added. The solution was allowed to warm up to room temperature and NEt_3 (0.01 mL, 0.07 mmol) was added. Solution was turbid. After 12 h, CH_2Cl_2 was evaporated i.vac. and replaced by DMF. After 12 h, DMF was evaporated i.vac. and replaced by CH_2Cl_2 . The solution was extracted with water (1x200 mL), 1 M aqueous citric acid solution (1x200 mL), water (1x200 mL), saturated aqueous $NaHCO_3$ -solution (1x200 mL), water (1x200 mL), and brine (1x200 mL). The organic layer was dried over $MgSO_4$, filtered and evaporated i.vac. According to TLC, isolation of the product via column chromatography was hardly possible. The product could not be purified by precipitation in Et_2O or PE. Dialysis in MeOH (MWCO 1000g/mol) did not remove any impurity. Column chromatography on silica (eluent: CH_2Cl_2 :MeOH 9:1) removed part of the impurities. Purification of the pre-purified crude product by precipitation was not achieved. Isolation of the desired compound was not possible.

R_F = 0.60 (CH_2Cl_2 :MeOH 9:1)

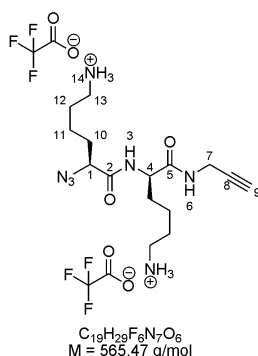
Azido-L-Lys-L-Lys-propargylamide (**167**):

141 was reacted following the general procedure for the deprotection of the Boc group. The product was obtained in quantitative yield.

UPLC was not possible.

^1H NMR (300 MHz, CDCl_3 , 20 °C): δ 7.55 – 7.45 (m, 1 H, N^3H), 7.44 – 7.41 (m, 1 H, N^8H), 4.92 (br s, 2 H, 2 N^{16}H), 4.53 – 4.46 (m, 1 H, C^4H), 3.98 – 3.85 (m, 3 H, C^1H , C^9H_2), 3.10 - 2.98 (m, 4 H, 2 C^{15}H_2), 2.22 (t, 1 H, $^3J(\text{H},\text{H}) = 2.5 \text{ Hz}$, C^{11}H), 1.93 - 1.09 (m, 30 H, 2 $\text{C}^{12-14}\text{H}_2$, 6 C^{19}H_3).

High-resolution ESI-MS: $m/z = 336.2138$ (calcd 336.2148 for $\text{C}_{15}\text{H}_{27}\text{N}_7\text{O}_2 - \text{H}^+$).

Azido-L-Lys-D-Lys-propargylamide (**168**):

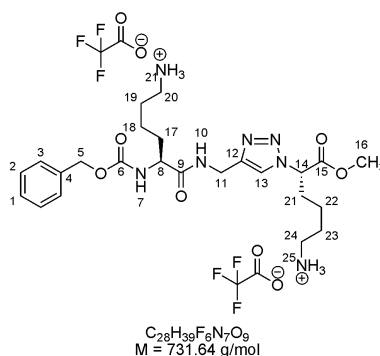
142 was reacted following the general procedure for the deprotection of the Boc group. The product was obtained in quantitative yield.

HPLC-MS ((2x150 mm Luna Phenyl-Hexyl 3 μm , acetonitrile:water Grad 5 95A): 2.60 min (90.7% peak area, ESI(+): 338.30 (**142** + 1 H^+)). HPLC was hardly possible due to very polar, salt character of the molecule.

5 Linear Triazole Containing Polypseudopeptides

^1H NMR (300 MHz, $\text{CD}_3\text{OD}:\text{D}_2\text{O}$, 20 °C): δ 3.96 (t, $^3J(\text{H,H}) = 7.1$ Hz, 1 H, CH), 3.82 (t, $^3J(\text{H,H}) = 6.5$ Hz, 1 H, CH), 3.68 – 3.66 (m, 2 H, C^7H_2), 2.73 – 2.67 (m, 4 H, 2 C^{13}H_2), 2.30 (t, $^3J(\text{H,H}) = 2.4$ Hz, 1 H, C^{11}H), 1.61 – 1.01 (m, 12 H, 2 $\text{C}^{10-12}\text{H}_2$).

Z-L-Lys-triazolo-L-Lys-Me (**165**):

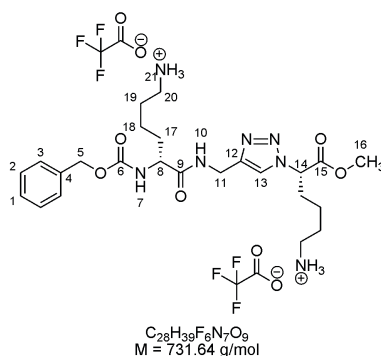


160 was reacted following the general procedure for the deprotection of the Boc group. The product was obtained in quantitative yield.

^1H NMR (300 MHz, CD_3OD , 20 °C): δ 7.99 (s, 1 H, C^{13}H), 7.38 – 7.25 (m, 6 H, C^{1-3}H , N^{10}H), 5.44 (dd, $^3J(\text{H,H}) = 5.2$ Hz, $^3J(\text{H,H}) = 9.9$ Hz, 1 H, C^{14}H), 5.09 (s, 2 H, C^5H_2), 4.48 (s, 2 H, C^{11}H_2), 4.08 (dd, $^3J(\text{H,H}) = 5.4$ Hz, $^3J(\text{H,H}) = 8.5$ Hz, 1 H, C^8H), 3.75 (s, 3 H, C^{16}H_3), 2.93 – 2.83 (m, 4 H, C^{20}H_2 , C^{28}H_2), 2.40 – 2.14 (m, 2 H, C^{21}H_2), 1.90 – 1.10 (m, 8 H, $\text{C}^{18-19}\text{H}_2$, $\text{C}^{22-23}\text{H}_2$).

^{13}C NMR (CDCl_3): δ 174.97, 170.43, 158.52, 146.51, 138.09, 129.51, 129.08, 128.81, 124.40, 67.74, 63.74, 56.44, 53.55, 40.42, 40.26, 35.74, 32.49, 32.21, 28.07, 27.70, 23.80, 23.69.

High-resolution ESI-MS: $m/z = 504.2896$ (calcd 504.2934 for $\text{C}_{24}\text{H}_{37}\text{N}_7\text{O}_9 + \text{H}^+$).

Z-D-Lys-triazolo-L-Lys-Me (**166**):

142 was reacted following the general procedure for the deprotection of the Boc group. The product was obtained in quantitative yield.

^1H NMR (300 MHz, CD_3OD , 20 °C): δ 7.99 (s, 1 H, C^{13}H), 7.39 – 7.26 (m, 6 H, C^{1-3}H , N^{10}H), 5.45 (dd, $^3J(\text{H,H}) = 5.1 \text{ Hz}$, $^3J(\text{H,H}) = 10.0 \text{ Hz}$, 1 H, C^{14}H), 5.10 (s, 2 H, C^5H_2), 4.48 (s, 2 H, C^{11}H_2), 4.08 (dd, $^3J(\text{H,H}) = 5.3 \text{ Hz}$, $^3J(\text{H,H}) = 8.6 \text{ Hz}$, 1 H, C^8H), 3.75 (s, 3 H, C^{16}H_3), 2.94 – 2.83 (m, 4 H, C^{20}H_2 , C^{28}H_2), 2.39 – 2.14 (m, 2 H, C^{21}H_2), 1.89 – 1.12 (m, 8 H, $\text{C}^{18-19}\text{H}_2$, $\text{C}^{22-23}\text{H}_2$).

^{13}C NMR (CDCl_3): δ 175.02, 170.46, 158.56, 146.61, 138.08, 129.51, 129.08, 128.82, 124.30, 67.78, 63.76, 56.52, 53.55, 40.42, 40.25, 35.77, 32.48, 32.23, 28.07, 27.71, 23.81, 23.71.

High-resolution ESI-MS: $m/z = 504.2894$ (calcd 504.2934 for $\text{C}_{24}\text{H}_{37}\text{N}_7\text{O}_9 + \text{H}^+$).

5.5 Literature

- [1] J. H. van Maarseveen, W. S. Horne, M. R. Ghadiri, *Org. Lett.* **2005**, 7, 4503.
- [2] W. S. Horne, C. D. Stout, M. R. Ghadiri, *J. Am. Chem. Soc.* **2003**, 125, 9372.
- [3] N. G. Angelo, P. S. Arora, *J. Am. Chem. Soc.* **2005**, 127, 17134.
- [4] E. Benedetti, B. Di Blasio, C. Pedone, G. P. Lorenzi, L. Tomasic, V. Gramlich, *Nature* **1979**, 282, 630.
- [5] B. A. Wallace, K. Ravikumar, *Science* **1988**, 241, 182.
- [6] D. A. Langs, *Science* **1988**, 241, 188.
- [7] B. Lotz, F. Heitz, G. Spach, *C. R. Acad. Sci., C, Sci. Chim.* **1973**, 276, 1715.
- [8] A. Caille, F. Heitz, G. Spach, *J. Chem. Soc., Perkin Trans. 1* **1974**, 1621.
- [9] P. B. Alper, S.-C. Hung, C.-H. Wong, *Tetrahedron Lett.* **1996**, 37, 6029.
- [10] F. M. Winnik, *Chem. Rev.* **1993**, 93, 587.

6 Glutamate Dendrimers

6.1 Discrete Glutamate Dendrimers With Variable Stereochemistry

6.1.1 General Considerations

Dendrimers are well defined, perfectly branched macromolecules and interesting target structures for biomedical applications such as drug delivery. The dendrimers reported by Denkewalter,^[1] Kraatz,^[2, 3] and Vinogradov^[4] are based on amino acids, fully chiral and biocompatible. The key building block in these dendrimers are single amino acids such as glutamic acid or lysine, allowing a fast growth of the molecule, using readily available starting materials. Nevertheless, following this strategy, it is impossible to create dendrimers with alternating stereochemistry. The smallest possible building block for the generation of a macromolecule or a polymer with alternating stereochemistry is a dipeptide. In dendrimers, the steric demand of the side chains increases notably with every generation, resulting in a spherical shape of the molecule. Hence, the influence of the stereochemistry on the shape of the dendrimer is a very interesting subject. Here, the unprecedented, straightforward, high yielding, and fast growing synthesis of fully chiral glutamate dendrimers with *all*-L- and D-(*alt*)-L-stereochemistry and addressable periphery with variable charge density is described.

6.1.2 Synthetic Considerations

The incorporation of a D,L-alternating stereochemical information into a macromolecule requires the use of at least a dimeric building block as repeat unit. For a fast growth of the molecule, the divergent/convergent synthesis strategy is the strategy of choice.^[5] Since the molecule is extended at the side chain functionalities and not along the backbone, the protecting group strategy has to be adapted (Figure 1). In the divergent/convergent synthesis of a linear peptide, the protecting groups of the main chain (PG₁ and PG₃) are temporary protecting groups, whereas the side chain protecting groups (PG₂) are permanent. In our synthesis approach to a glutamate dendrimer with alternating stereochemistry, PG₂ become temporary protecting groups and PG₃ becomes a permanent protecting group.

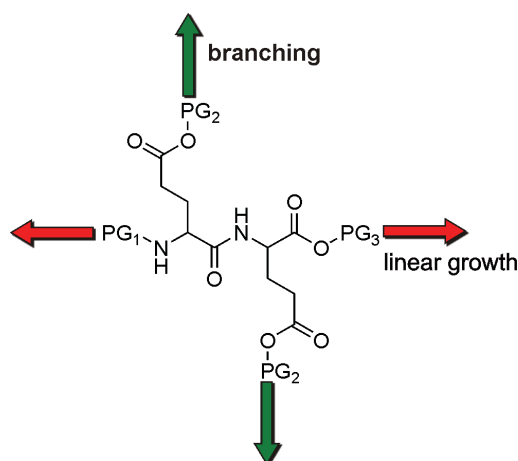
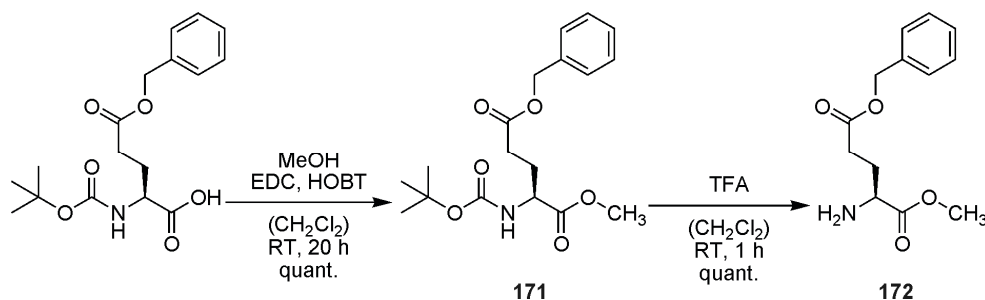


Figure 1: Smallest building block for the incorporation of D,L-alternating stereochemistry. Comparison of branching (green arrows) and linear growth (red arrows) of the building block.

A protecting group strategy, which meets these requirements uses the Boc group as protecting group of the amine (PG_1), the benzyl ester as side chain protecting group (PG_2), and the methyl ester for the protection of the C-terminus (PG_3). The Boc group can easily be cleaved with TFA without touching both esters and the benzyl ester can be cleaved under hydrogenolysis without touching the methyl ester and the Boc group. This protecting group strategy allows a differentiation of the carboxylic acids and the cleavage of either all acid protecting groups by saponification or only the benzyl protected ones by hydrogenolysis and thereby a variation of the charge density in the dendrimer. The targeted building block is Boc-Glu(Z)-Glu(Z)-Me. For the investigation of the influence of the stereochemistry on the shape of the dendrimer, *all*-L- and D- (*alt*)-L-dendrimers have been synthesized.

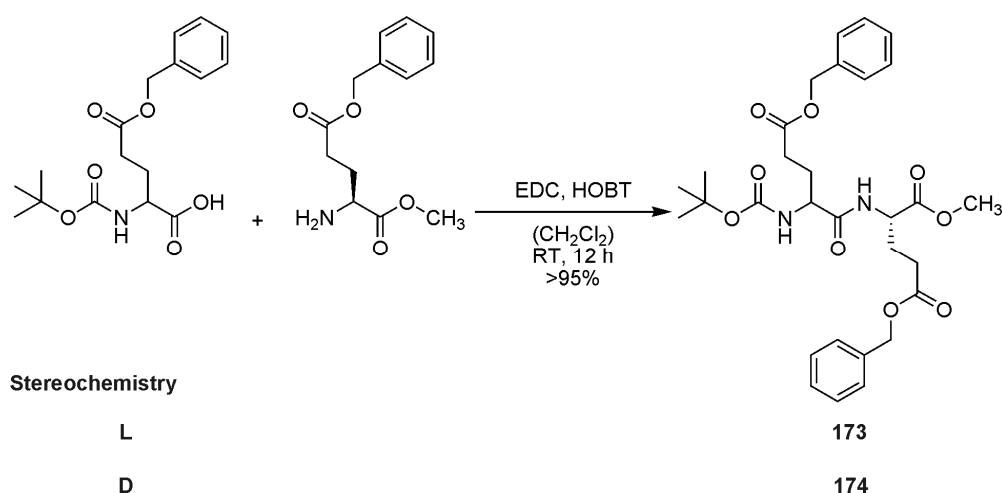
6.1.3 Dendrimer Synthesis

The synthesis of the dipeptide building block started with the esterification of Boc-L-Glu(Z) to the methyl ester Boc-L-Glu(Z)-Me (**171**) and the subsequent Boc cleavage to L-Glu(Z)-Me (**172**) (Scheme 1). The esterification afforded the product in quantitative yield after column chromatography. The Boc deprotection afforded the product in quantitative yield after aqueous work-up.



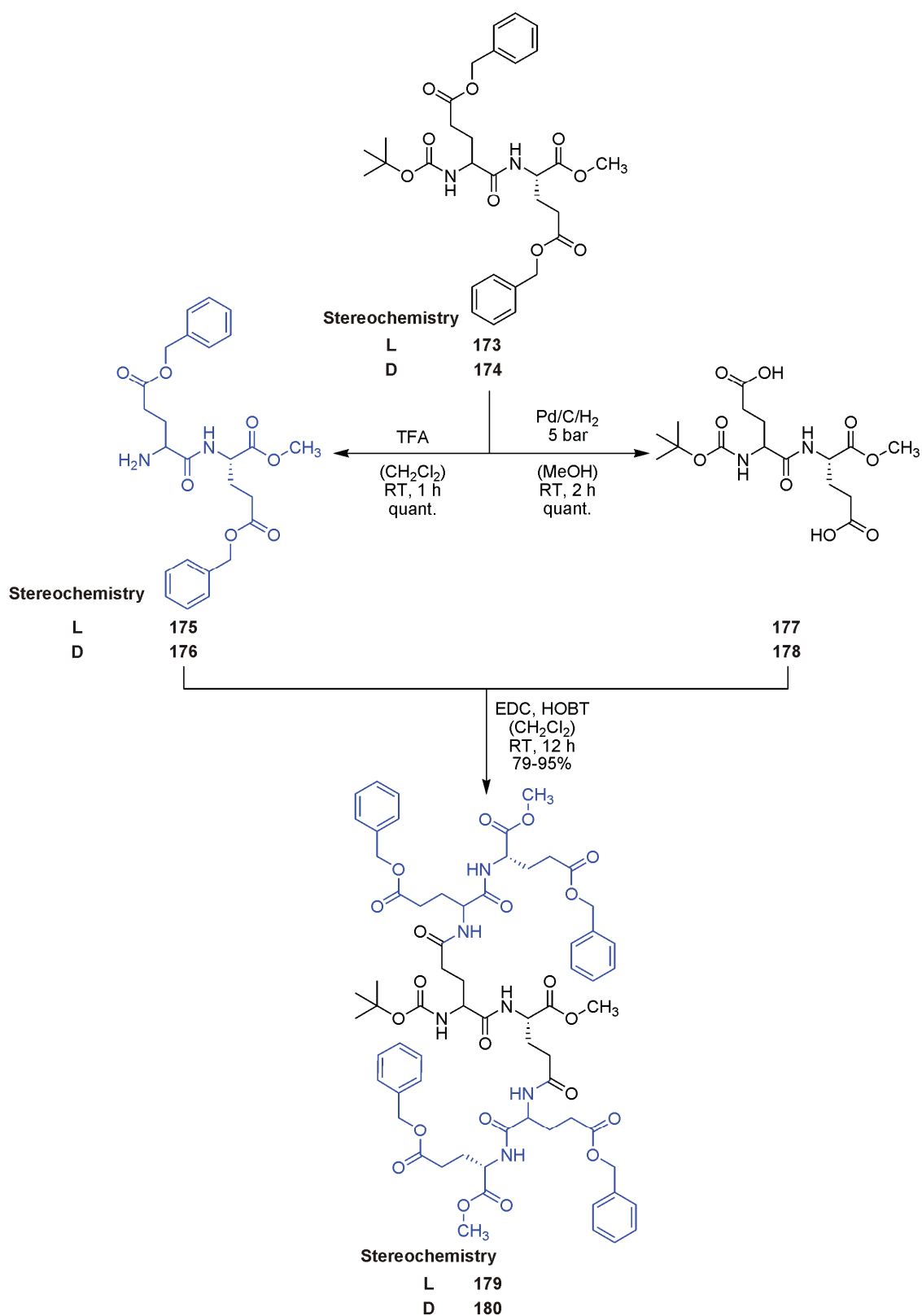
Scheme 1: Synthesis of L-Glu(Z)-Me (**172**) from Boc-L-Glu(Z).

The subsequent coupling to the dipeptide building blocks proceeded smoothly and gave the desired dipeptides Boc-L-Glu(Z)-L-Glu(Z)-Me (**173**) and Boc-D-Glu(Z)-L-Glu(Z)-Me (**174**) in very good yields (Scheme 2). The purification of the dipeptides was achieved by repetitive column chromatography on silica (minimum of two columns).



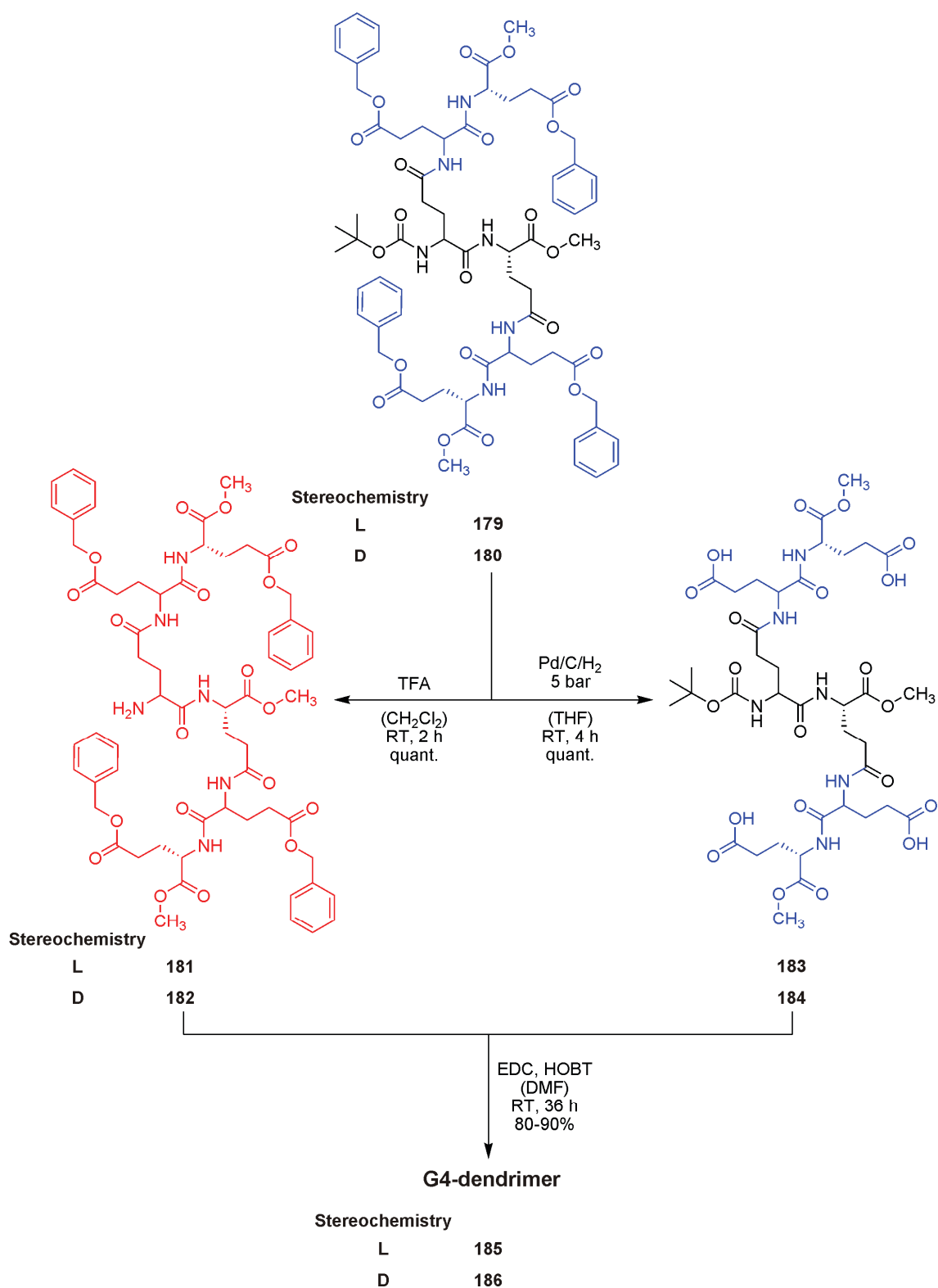
Scheme 2: Coupling to the dipeptide building blocks Boc-L-Glu(Z)-L-Glu(Z)-Me (**173**) and Boc-D-Glu(Z)-L-Glu(Z)-Me (**174**).

The dipeptides **173** and **174** were subjected to the divergent/convergent synthesis protocol to give the G2-dendrimers **179** and **180** (Scheme 3). The sequence started with the Boc and Z deprotection reactions of **173** and **174** to give the *N*- and *C*_γ-deprotected dipeptides **175**, **176** and **177**, **178**. Both reactions proceeded smoothly and gave the prospective coupling fragments in quantitative yields. Both fragments were used without further purification. The subsequent coupling to the G2-dendramer afforded the desired products **179** and **180** in good to very good yields. The purification of the G2-dendrimers was achieved by column chromatography and repetitive precipitation in diethylether.

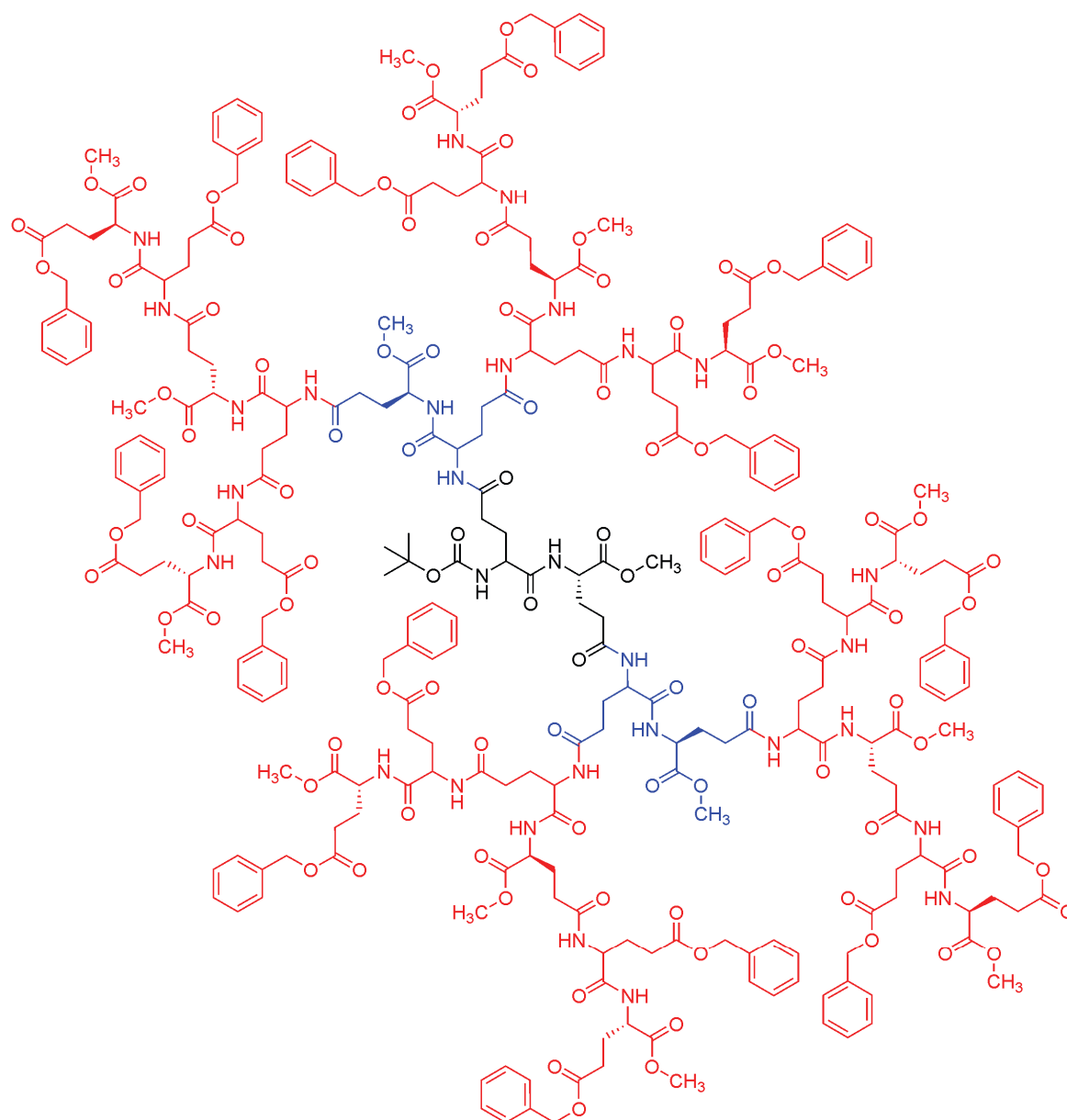


Scheme 3: Divergent/convergent synthesis to the G2-Dendrimers **179** and **180**. Fragments of the G2-dendrimer are colored for clarity.

The G2-dendrimers **179** and **180** were then Boc and Z deprotected to give the *N*- and *C γ* -deprotected G2-dendrimers **181**, **182** and **183**, **184** (Scheme 4). Both reactions gave the prospective coupling fragments in quantitative yields. The Z deprotection was performed in THF, since hydrogenation in MeOH led to partial esterification of the acid functionalities. Both fragments were used without further purification. The subsequent coupling to the G4-dendrimer gave the desired products **185** and **186** in good to very good yields. The purification of the G4-dendrimers was achieved by precipitation in diethylether and extensive washing of the residue with diethylether and MeOH yielding a white powder of high purity. The structure of the G4-dendrimer is shown in Figure 2.



Scheme 4: Divergent/convergent synthesis to the G4-dendrimers **185** and **186**. Fragments of the G4-dendrimer are colored for clarity.



G4-dendrimer

Stereochemistry

L	185
D	186

Figure 2: Structure of the G4-Dendrimers **185** and **186**. Fragments of the G4-dendrimer are colored for clarity.

The GPC-trace of each generation is shown in an overlay in Figure 3. The molecular masses determined by GPC fit quite well the real molecular masses of the molecules. On top of Figure 3 are shown the molecular models of each generation. Due to the increasing steric pressure in the periphery of the

dendrimer, the molecule becomes more and more spherical with each generation. The ^1H NMR spectrum of the *all*-L-G4-dendrimer **185** is shown in Figure 4. The integral values fit very well the structure of the desired compound.

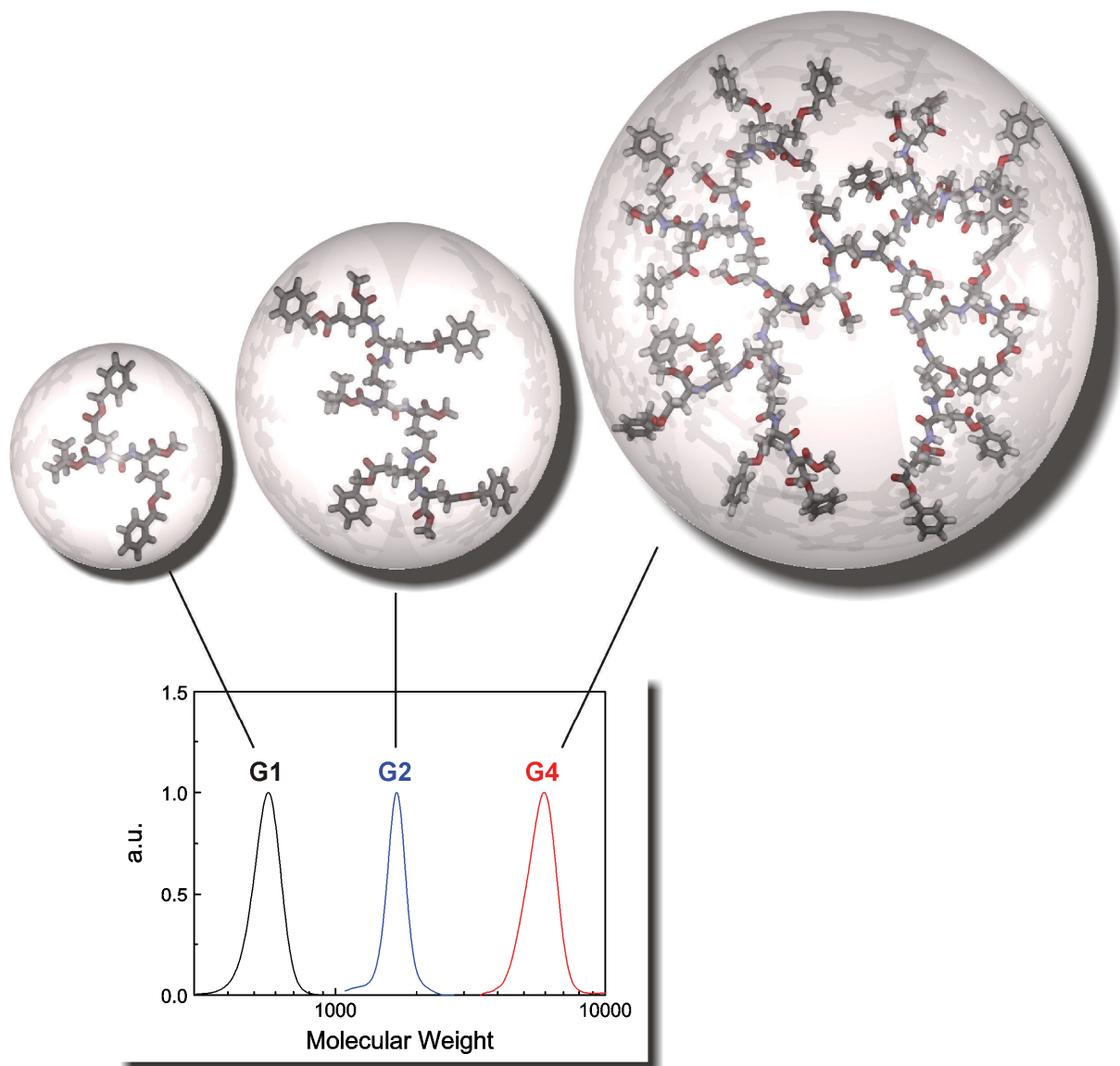


Figure 3: Overlay of the GPC-traces of G1-, G2- and G4-dendrimers with schematic representation of the spherical shape of the generations (GPC in DMF at 70 °C, calibrated with polystyrene standards, detection via RI).

Further growth to the G8-dendrimer by another divergent/convergent cycle failed. The Boc deprotection proceeded smoothly and gave the free amine after precipitation in very good yield (Scheme 5, left). The Z deprotection yielded the desired product after optimization of the reaction conditions. Due to the poor solubility of the G4-dendrimers, the hydrogenation could not be performed in

MeOH or other alcohols, in water, THF or EE, but could be realized in DMF (Scheme 5, right). The subsequent coupling to G8-dendrimer only yielded starting material. The free amine in the core of the G4-dendrimer was probably too shielded and not accessible for the activated acids. Further growth than to the stage of G4 was not possible similar to the observation made by Moore in his exponential dendrimer synthesis.^[5]

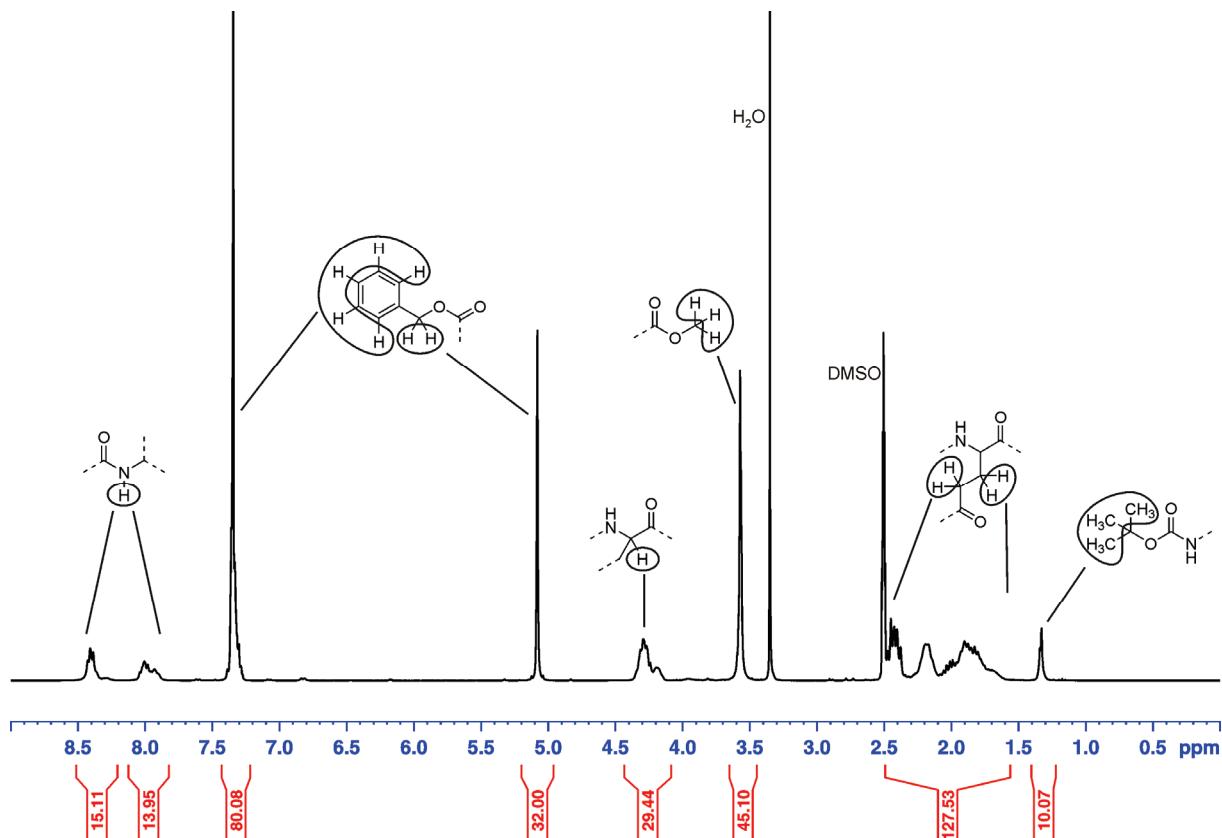
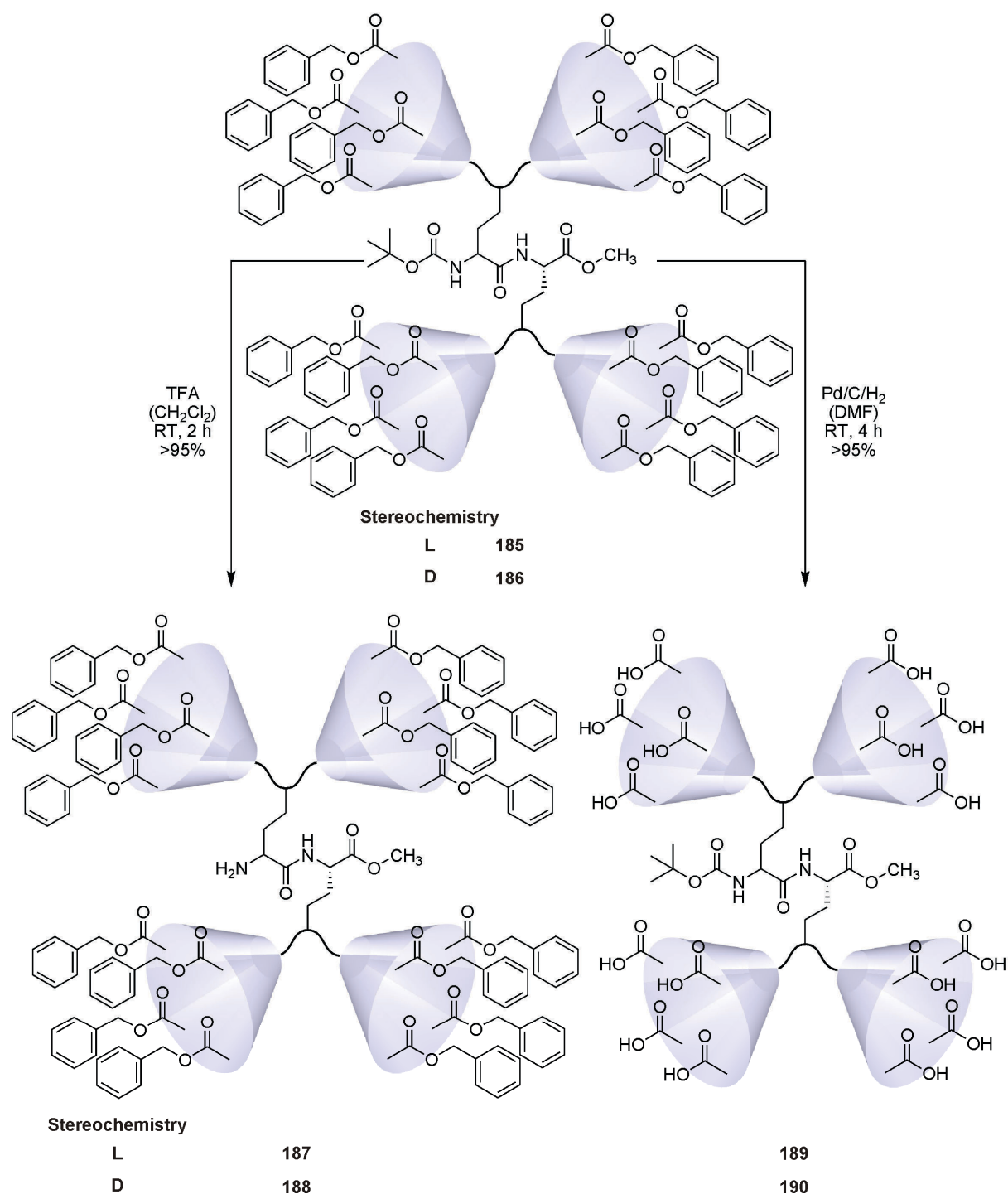


Figure 4: ^1H NMR spectrum of *all*-L-G4-dendrimer **185** ($\text{DMSO-}d_6$, 25 °C).

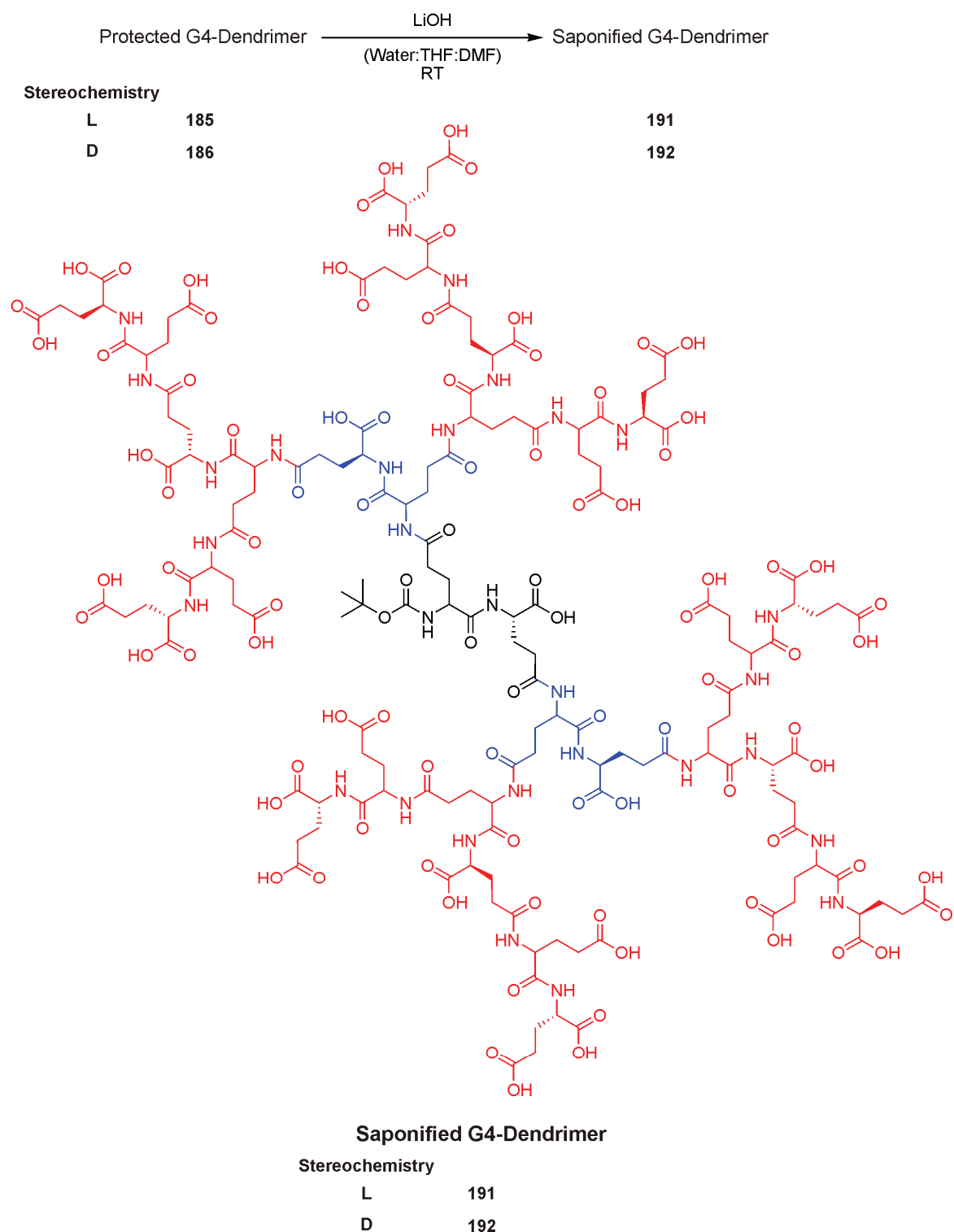


Scheme 5: Boc deprotection of G4-dendrimers **185** and **186** to the free amines **187** and **188** (core deprotection) (left). Z deprotection of the G4-dendrimers **185** and **186** to the free acids **189** and **190** (periphery deprotection) (right). (Schematic representation of each dendron with cones).

In further studies, such as CD and complexation experiments, the influence of stereochemistry and charge density on the shape of the dendrimers and

complexes is being investigated. Dendrimers **189** and **190** possess 16 free carboxylic acid functionalities after cleavage of the Z groups. With the protecting group strategy chosen, it was also possible to create a G4-dendrimer with altogether 31 free carboxylic acid functionalities from the same precursors **185** and **186**. Under saponification conditions, the Z groups and the methyl esters were cleaved to yield the desired G4-dendrimers **191** and **192** (Scheme 6).

6 Glutamate Dendrimers



Scheme 6: Saponification of the G4-dendrimers **185** and **186** to the 31 carboxylic acid containing G4-dendrimers **191** and **192**.

The saponified G4-dendrimers **191** and **192** were purified via dialysis in water with a dialysis tube with MWCO of 1000 g/mol in order to remove inorganic salts

and benzyl alcohol. This dialysis decreased the yield of the quantitative reaction remarkably to 50-60%. Prior to further experiments, the Z deprotected G4-dendrimers **189** and **190** were also subjected to dialysis under identical conditions.

6.1.4 Circular Dichroism Studies

The deprotected dendrimers are formerly oligopeptides and potentially able to adopt secondary structures, stabilized by intramolecular hydrogen bonds.^[6,7] Since they are oligocarboxylates, their potential secondary structure may be sensitive to pH variation. In basic environment, the periphery of the dendrimer is expected to be negatively charged and the resulting Coulomb repulsion should lead to a spherical deformation of the molecule. In acidic media, the carboxylic acids are protonated, potentially leading to an intramolecular hydrogen bonding network, reflected in a higher ordered secondary structure. This switching behavior could be monitored by CD experiments.

Circular dichroism studies were performed with the dendrimers Boc-G4-*all*-L-Glu-Me **189**, Boc-G4-*all*-L-Glu **191**, Boc-G4-D-(*a/t*)-L-Glu-Me **190**, and Boc-G4-D-(*a/t*)-L-Glu **192**. CD spectra were recorded in water, water:ACN 1:1 and water:TFE in a 1 mm cuvette at 25 °C in a wavelength region between 190 and 270 nm. The dendrimers were measured at concentrations around 2×10^{-5} mol/L. All spectra were normalized to a concentration of 2×10^{-5} mol/L. The totally deprotected dendrimers **191** and **192** were measured at unmodified, acidic (~ 2.8), and basic (~ 10.5) pH. The pH was adjusted using 1 N aqueous HCl- and NaOH-solutions. The Z deprotected dendrimers **189** and **190** were measured at unmodified pH, since acidic or basic pH could potentially lead to partial cleavage of the methyl ester. Representative spectra are displayed in Figure 5.

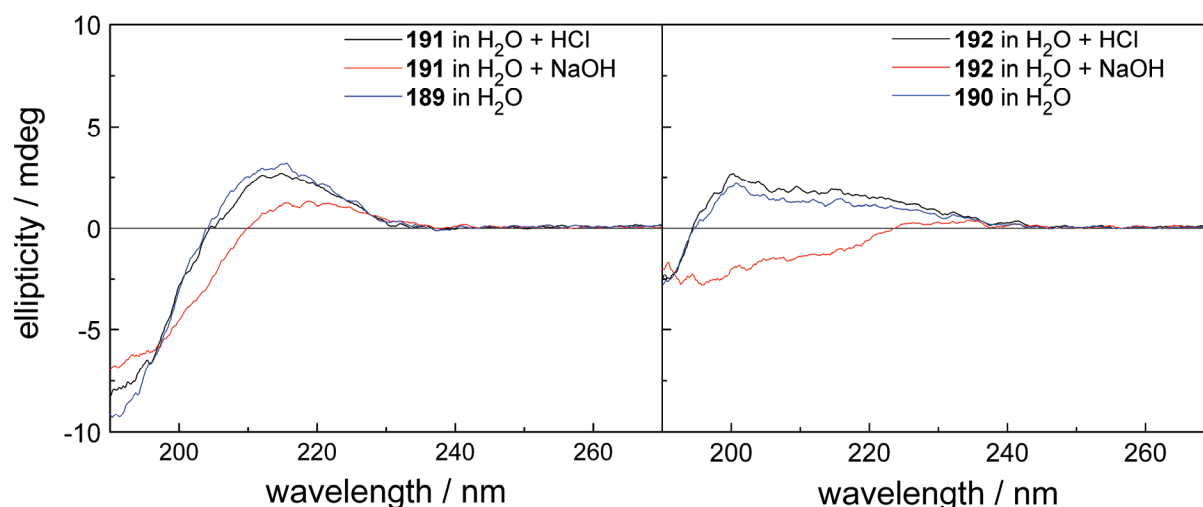


Figure 5: CD spectra of Boc-G4-*all*-L-Glu-Me **189**, Boc-G4-*all*-L-Glu **191**, Boc-G4-D-*(alt)*-L-Glu-Me **190**, and Boc-G4-D-*(alt)*-L-Glu-Me **192** in water. Spectra of **189** and **190** were recorded at unmodified pH, **191** and **192** at acidic (~ 2.8) and basic (~ 10.5) pH. Spectra were recorded at the following concentrations: **189** ($1.88 \cdot 10^{-5}$ mol/L), **190** ($1.83 \cdot 10^{-5}$ mol/L), **191** ($1.87 \cdot 10^{-5}$ mol/L), **192** ($1.92 \cdot 10^{-5}$ mol/L). All spectra were normalized to a concentration of $2.00 \cdot 10^{-5}$ mol/L.

The spectra in Figure 5 were recorded in pure water. The respective spectra in water:ACN 1:1 and water:TFE 1:1 are comparable in shape and hence are not displayed. The CD spectra of **189** and of **191** in acidic solution are identical, showing the spectrum of a random coil peptide. The spectra of **191** in basic solution is similar in shape, but less intense. **190** and **192** in acidic solution display identical spectra. The CD signal is positive between 240 and 195 nm. Between 195 and 190 nm, the signal is negative. **192** in basic solution displays a different CD signal, which is positive between 246 and 224 nm and negative between 224 and 190 nm.

In summary, the *all*-L-dendrimers **189** and **191** show a random coil signal in all solvent systems applied and at different pH, indicating the absence of a higher ordered secondary structure, even in the protonated state. The random coil signal is expected to result from the dendrimer L,L-dipeptide subunits. The shape of the CD signals of **190** and **192** can not be attributed to a structural motif. The dendrimer is expected to display a random coil signal in basic

environment. The negative signal may hence be attributed to a coiled D-(*alt*)-L-dendrimer. The different shape in acidic solution is most likely the result of a significant structural reorganization of the dendrimer. For the *all*-L- and D-(*alt*)-L-dendrimer, the influence of the methyl ester on the dendrimer structure was negligible, leading to identical CD signals for **189** and **192** and for **190** and **192** in acidic environment.

6.1.5 Dendrimer Complexation Experiments

The deprotected dendrimers **189**, **190**, **191**, and **192** are oligoelectrolytes with different charge density on the dendrimer surface, due to different numbers of negative charges (16 for **189** and **190**, 31 for **191** and **192**) and varying stereochemistry. The salt formation of the dendrimer oligoanion with surfactant molecules, such as alkyl amines, is expected to lead to complexes adopting interesting structures, depending on the charge density of the dendrimer. The spatial organization of these structures can be monitored with small angle X-ray scattering (SAXS).

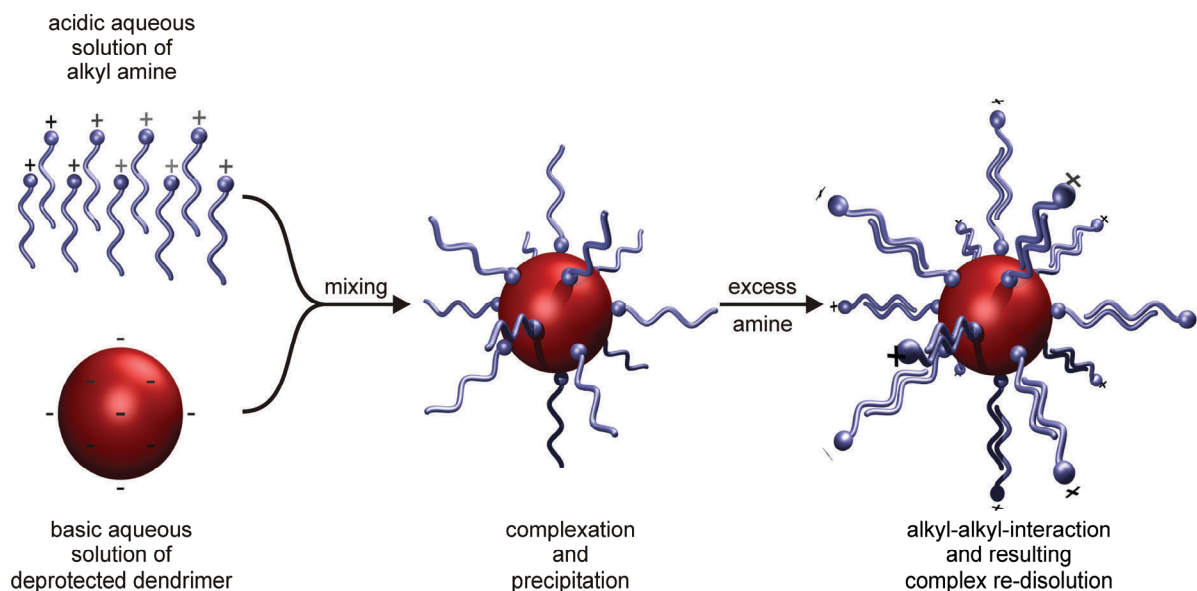


Figure 6: Complexation of anionic deprotected dendrimers with cationic surfactants.

The complexation experiments were performed with the dendrimers **189**, **190**, **191**, and **192** and primary linear alkyl amines. The experimental set-up is in principle displayed in Figure 6. An aqueous solution of the dendrimer was

brought to pH~9 to assure quantitative deprotonation of the periphery, using aqueous NaOH-solutions. An aqueous solution of the alkyl amine was slightly acidified to pH~5 to assure protonation of the amine, using aqueous HCl-solution. Both solutions were mixed and the resulting precipitate centrifuged and washed with water at pH~5 and pH~8. The carboxylate:ammonium ratio was 1:1, with a negligible excess of surfactant to assure quantitative complexation of the dendrimers. The use of bigger amounts of amphiphile was expected to increase the solubility of the complex as displayed in Figure 6 and was hence avoided. The experiment was attempted using decyl-, tetradecyl-, and octadecylamine. The preparation of the aqueous solution of octadecylamine could not be achieved. The amine could not be quantitatively dissolved even under heating, acidifying the solution and the addition of small amounts *n*-propanol, rendering the experiments impossible. In contrast, decylamine was readily soluble in water. Mixing the acidic surfactant solution with the basic dendrimer solution led to no precipitate. The C₁₀-chains of the amine were most probably too short and hence sufficiently solubilized the complex in water to prevent precipitation. Tetradecylamine was expected to display intermediate properties. The preparation of an aqueous solution was achieved under heating and under adjusting the pH to slightly acidic. The clear hot solution formed a white emulsion/suspension when cooling down to room temperature. This fact determined the way of mixing dendrimer and amine. In order to avoid potential precipitation of pure amine, when the clear warm solution was added to cold dendrimer solution, the dendrimer solution was added to warm amine solution. The resulting precipitate was hence expected to be pure complex. The formation of the complexes was monitored by IR (Figure 7). The appearance of the two sharp signals at 2918 and 2851 cm⁻¹, originating from RNH₃⁺, the vanishing signal at 1720 cm⁻¹ and the decreasing signal at 1638 cm⁻¹ of uncomplexed COOH confirmed the formation of the desired complexes.

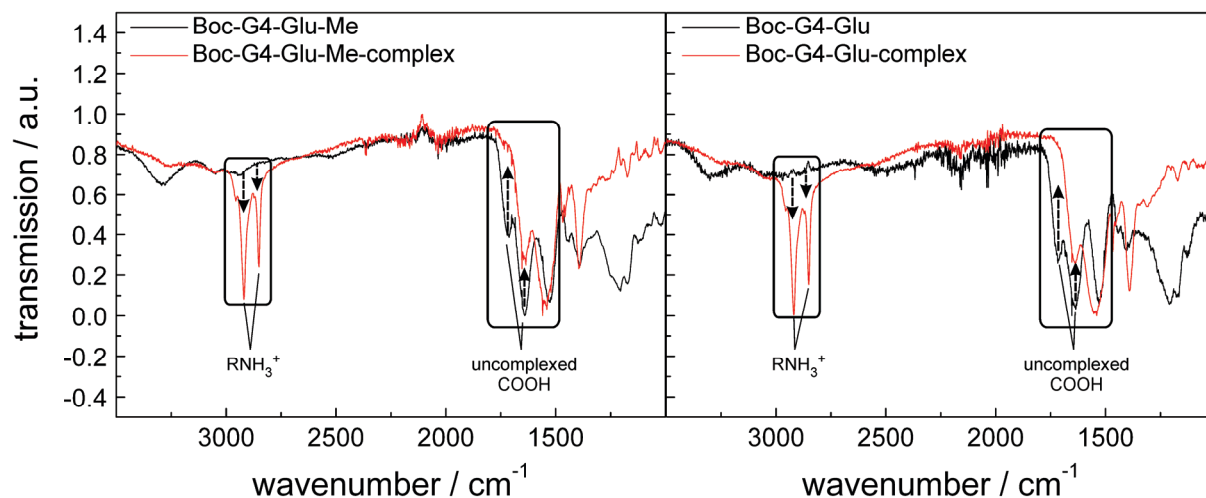


Figure 7: IR (ATR) of the dendrimers Boc-G4-Glu-Me and Boc-G4-Glu and their respective complexes. Regions of interest in the spectra are highlighted.

All four dendrimers formed white precipitates with tetradecylamine. The precipitates were centrifuged, washed with water at slightly basic and acidic pH and dried under lyophilization to afford white powders, which are currently being studied by SAXS.^b

6.1.6 Core Functionalization With Dyes

The deprotected dendrimers are oligoelectrolytes with 16 or 31 carboxylates, depending on the degree of deprotection and are best soluble in water. By the attachment to the dendrimers, water insoluble dyes are expected to become water soluble via encapsulation and can be transferred into physiological environment (Figure 8). The dyes could then be read out by spectroscopy to give information about dendrimer aggregation, cation complexation or incorporation into physiological processes.

^b In collaboration with Prof. Raffaele Mezzenga and Nadia Canilho, University of Fribourg, Switzerland.

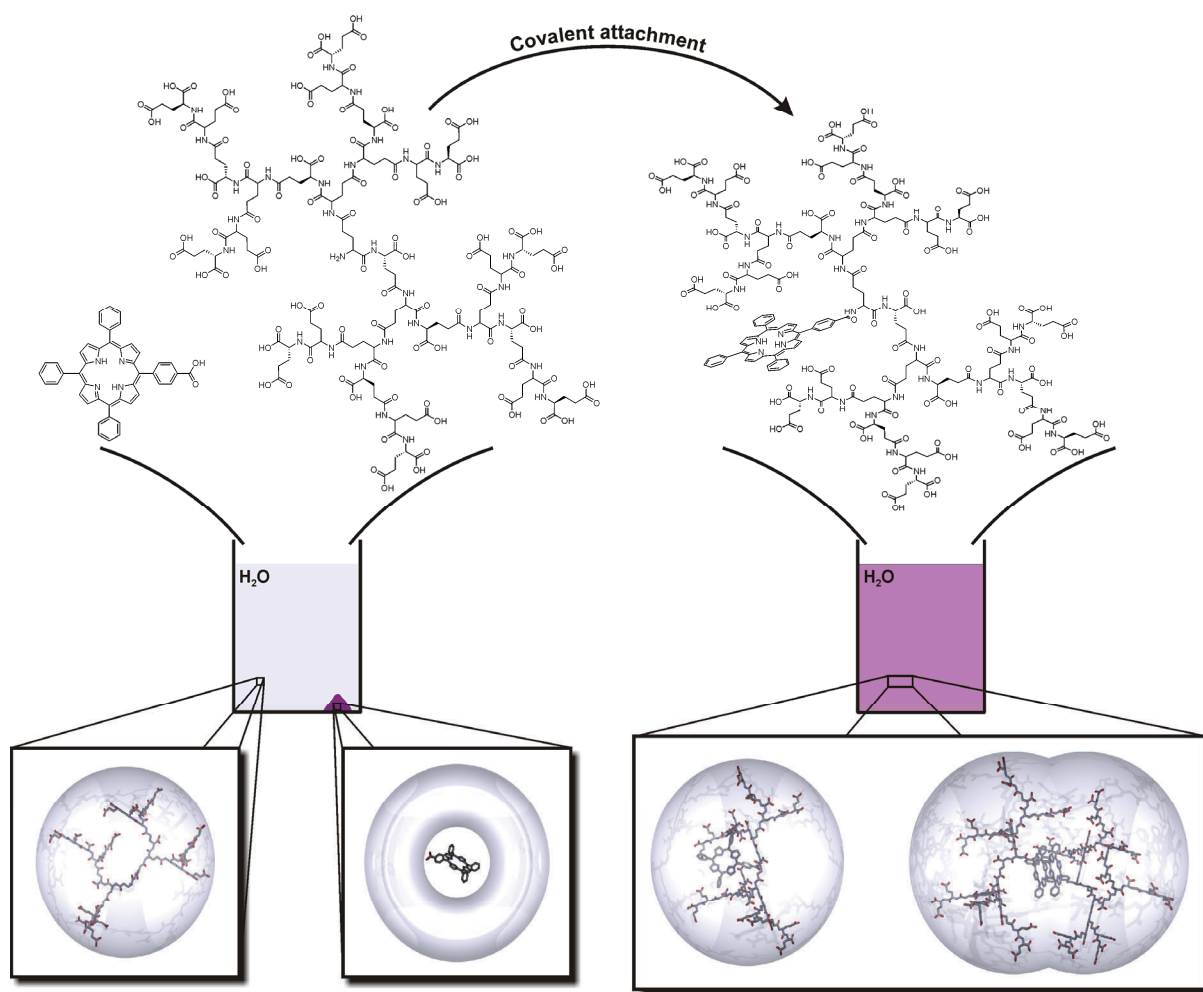
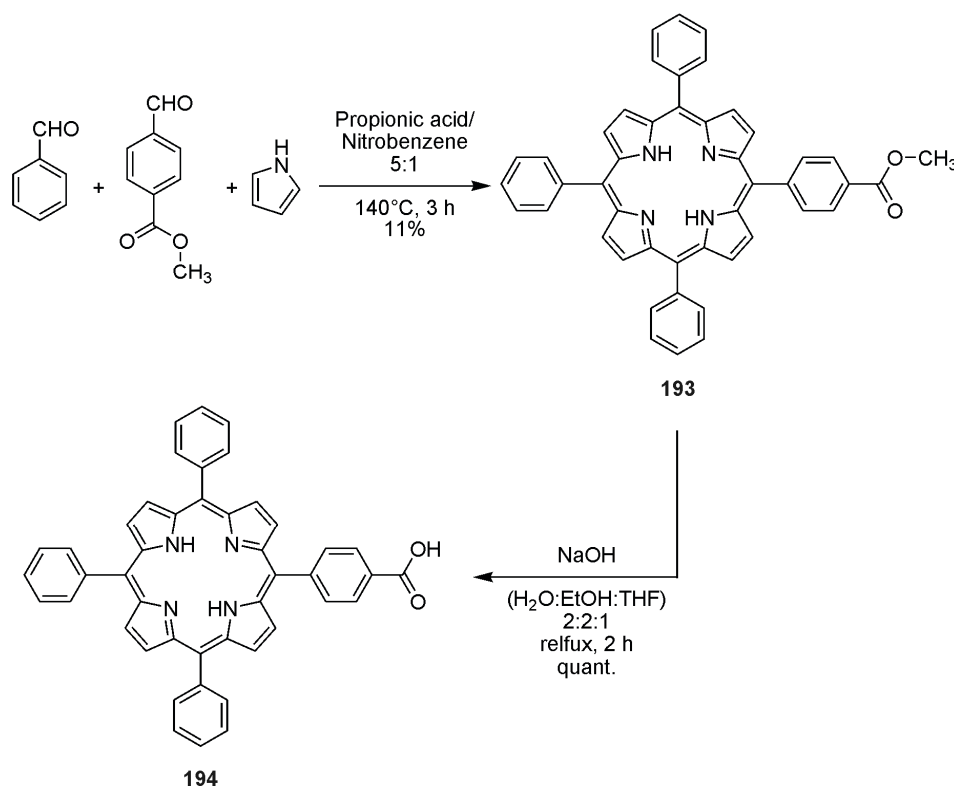


Figure 8: Effect of covalent attachment of a water insoluble dye to the deprotected glutamate dendrimers at the example of porphyrine. The water insoluble dye (left) becomes soluble by covalent linkage to the dendrimer (right).

A very potent class of dyes with special spectroscopic features is the class of porphyrins (as shown in the example in Figure 8), of which tetraphenylporphyrin (TPP) is a very basic representative. Due to lacking functional groups in the molecule, TPP can not be covalently linked to the dendrimer. The amine in the dendrimer core can readily react with carboxylic acids, rendering 5-(4'-carboxyphenyl)-10,15,20-triphenylporphyrin the target dye structure. The synthesis is described in Scheme 7. 5-(4'-Carboxymethylphenyl)-10,15,20-triphenylporphyrin (**193**) was prepared following the Adler-Longo-procedure^[8] and was saponified using NaOH in a H₂O:EtOH:THF-mixture under reflux conditions. The overall yield of the synthesis was determined to be 11%. The

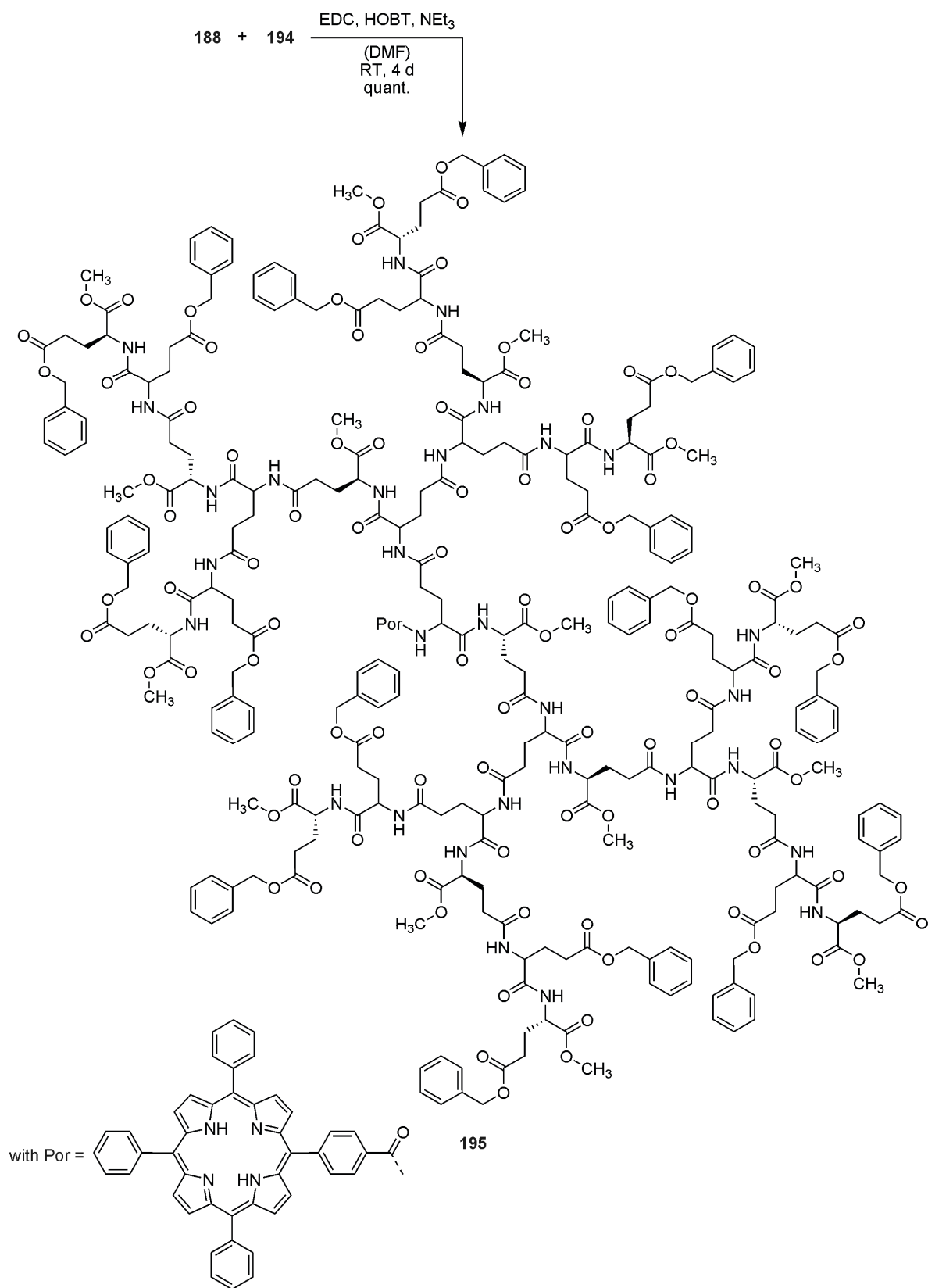
purification of **193** was very tedious and achieved via repetitive column chromatography.



Scheme 7: Synthesis of 5-(4'-carboxyphenyl)-10,15,20-triphenylporphyrin following the Adler-Longo-procedure.

In the next step, the porphyrin **194** was coupled to the D,L-dendrimer **188**, using EDC and HOBT as coupling reagents. After 4 days, the solvents were evaporated and the remaining solid washed with water and acetone. This simple procedure removed all impurities and gave the desired labeled dendrimer in quantitative yield.

6 Glutamate Dendrimers



Scheme 8: Porphyrin-labeling of D,L-dendrimer **188**.

The GPC-trace of porphyrin labeled D,L-dendrimer **195** is shown in Figure 9. The product was detected using a UV-detector at 277 nm and at 420 nm and a RI-detector. The GPC-traces were normalized to the RI-signal. UV-detection at 277 nm led to a very weak signal compared to RI-detection. Due to the high extinction coefficient of the porphyrin label, the detection at the absorption maximum of the porphyrin at 420 nm led to a 15-fold more intense UV-signal.

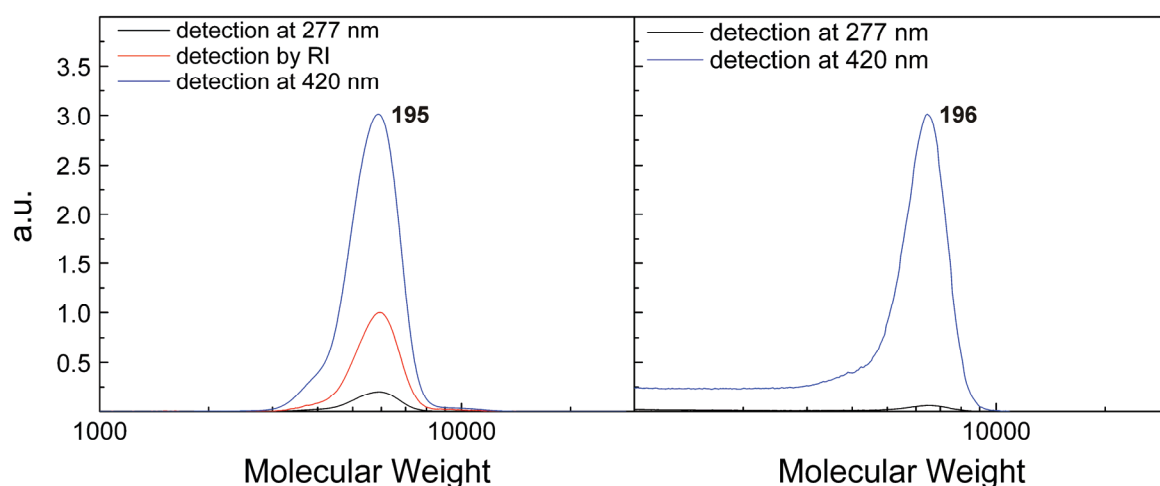


Figure 9: GPC-trace of protected porphyrin labeled D,L-dendrimer **195** and of saponified porphyrin labeled D,L-dendrimer **196** (GPC in DMF at 70 °C, calibrated with polystyrene standards, relative intensities of UV signals at different wavelengths are normalized to the corresponding RI signal; in the case of **196**, the respective RI signal is not detectable, hence the relative intensities of UV signals at different wavelengths are normalized to RI signal of added standard; absolute intensities of **195** and **196** are normalized to the detection at 420 nm).

The proton NMR spectrum of **195** is shown in Figure 10. The spectrum was recorded in DMSO-*d*₆. The relative values of the integrals fit well with a quantitative core labeling of the dendrimer.

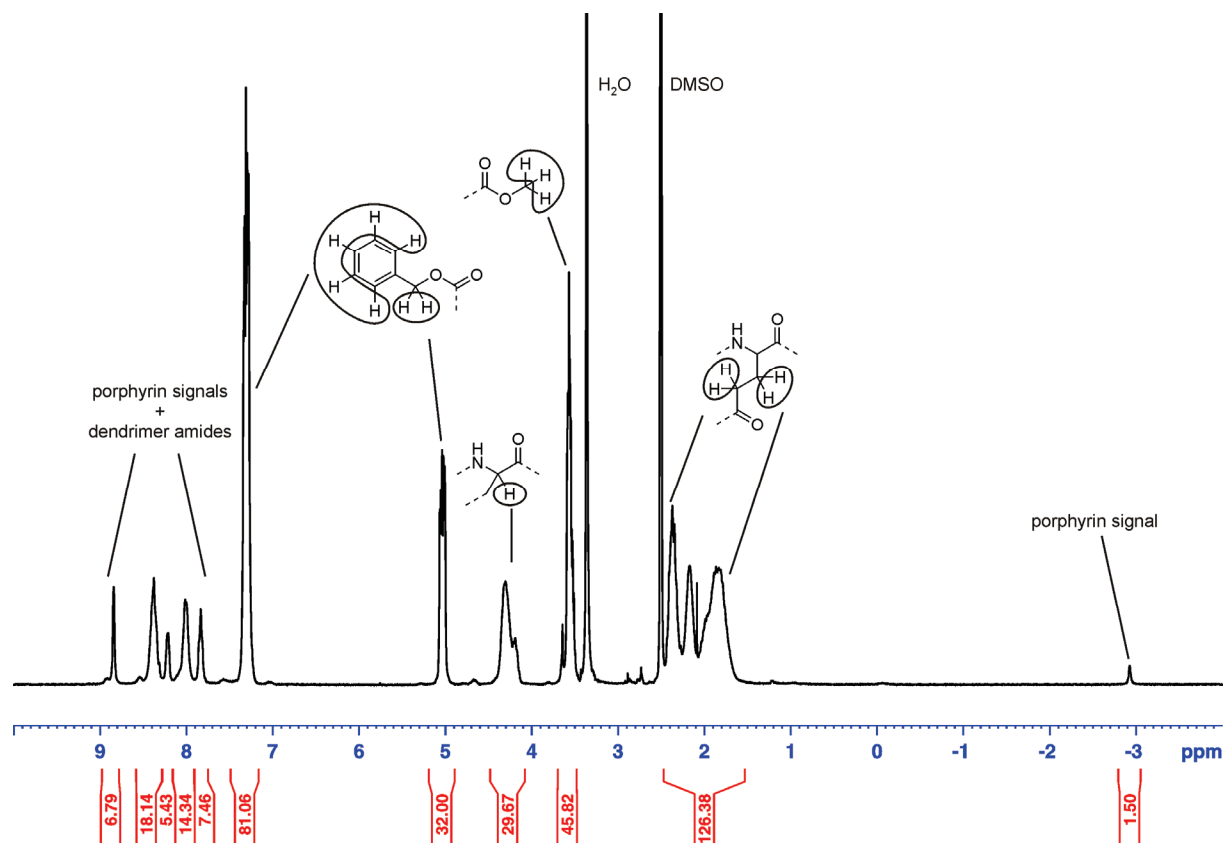
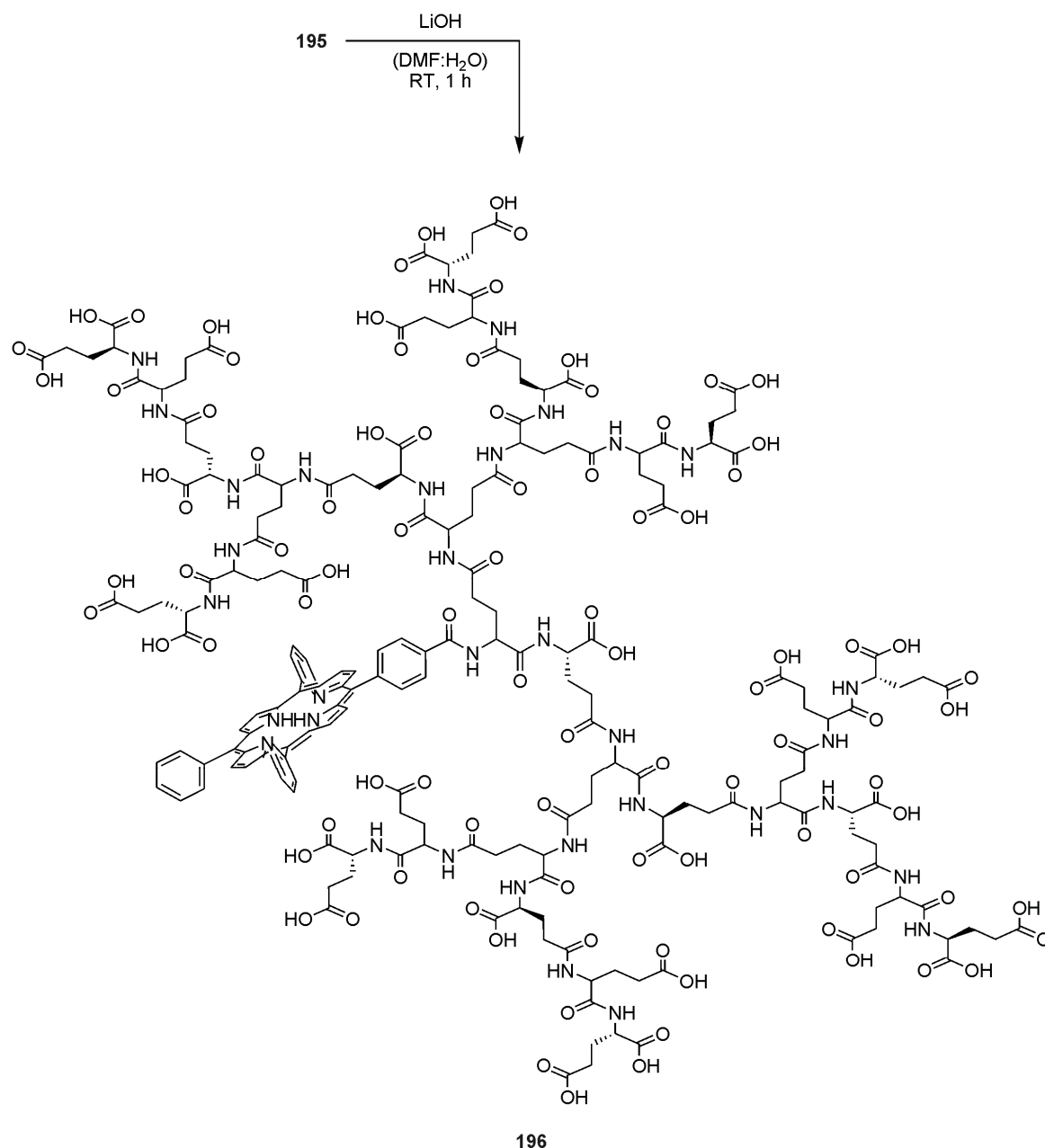


Figure 10: ^1H NMR spectrum of porphyrin labeled D,L-dendrimer **195** (DMSO- d_6 , 25 °C).

195 was subjected to saponification using LiOH. In a first attempt, the NMR sample in DMSO was used and treated with aqueous LiOH. After 1 h, the solution was acidified and dialysed, using a dialysis tube with MWCO of 1000 g/mol. These conditions led to total decomposition of the compound. In ^1H NMR, the porphyrin colored solution showed no porphyrin and dendrimer signals and GPC detected no molecular masses higher than 500 g/mol. In a second approach, a DMF solution of **195** was treated with an aqueous LiOH solution. Although ^1H NMR did not give valuable information on the result of the reaction, GPC with detection at 420 nm showed a peak with a molecular mass of ca. 6500 g/mol, fitting well with the expected GPC-trace, thereby confirming product formation (Figure 9). The peak detected at 420 nm is 50-fold more intense than the peak detected at 277 nm, confirming cleavage of the Z group. The RI signal of the compound is probably very close to that of DMF, rendering a detection by RI impossible.



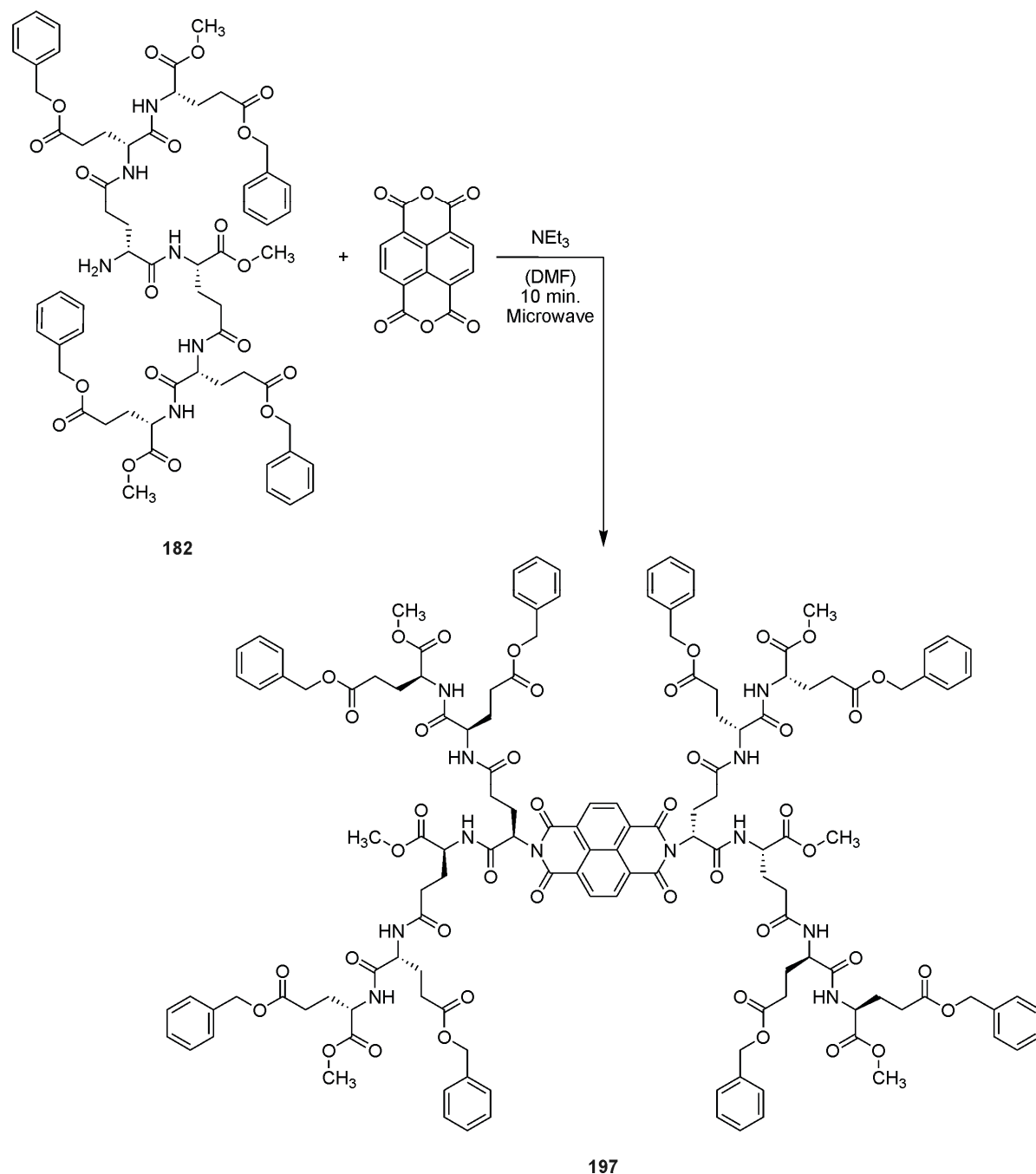
Scheme 9: Saponification of porphyrine-labeled dendrimer **195** (porphyrin and side chains are 3D-rotated for clarity).

6.1.6.1 Bifunctional Core

Besides the labeling of the dendrimer core with a monofunctional dye, such as porphyrin **194**, the junction of two dendrimers via a bifunctional, symmetrical dye was attempted. 1,4,5,8-Naphthalenetetracarboxylic dianhydride is known to undergo microwave assisted coupling with amino acids and small peptide segments.^[9] In a first attempt, the D,L-G2-dendrimer **182** was coupled to

6 Glutamate Dendrimers

1,4,5,8-naphthalenetetracarboxylic anhydride. The reaction under elaborated conditions afforded the desired product in 40% yield and high purity after column chromatography on silica and precipitation in Et₂O. The proton NMR spectrum is shown in Figure 11.



Scheme 10: Microwave assisted labeling of G2-dendrimer **182** with bifunctional 1,4,5,8-naphthalenetetracarboxylic dianhydride

The integrals are in accordance with the expected structure of the molecule. The subsequent benzyl deprotection of **197** was achieved using Pd/C/H₂ in a MeOH:EE mixture and gave the desired product in 53% yield after dialysis (Scheme 11). Despite all purification efforts, compound **198** could not be isolated in higher purity than 78%. Due to the very poor yields and the low purity of the debenzylated product, the synthesis was not extended to the *all*-L-G2-dendrimer and to G4-dendrimers.

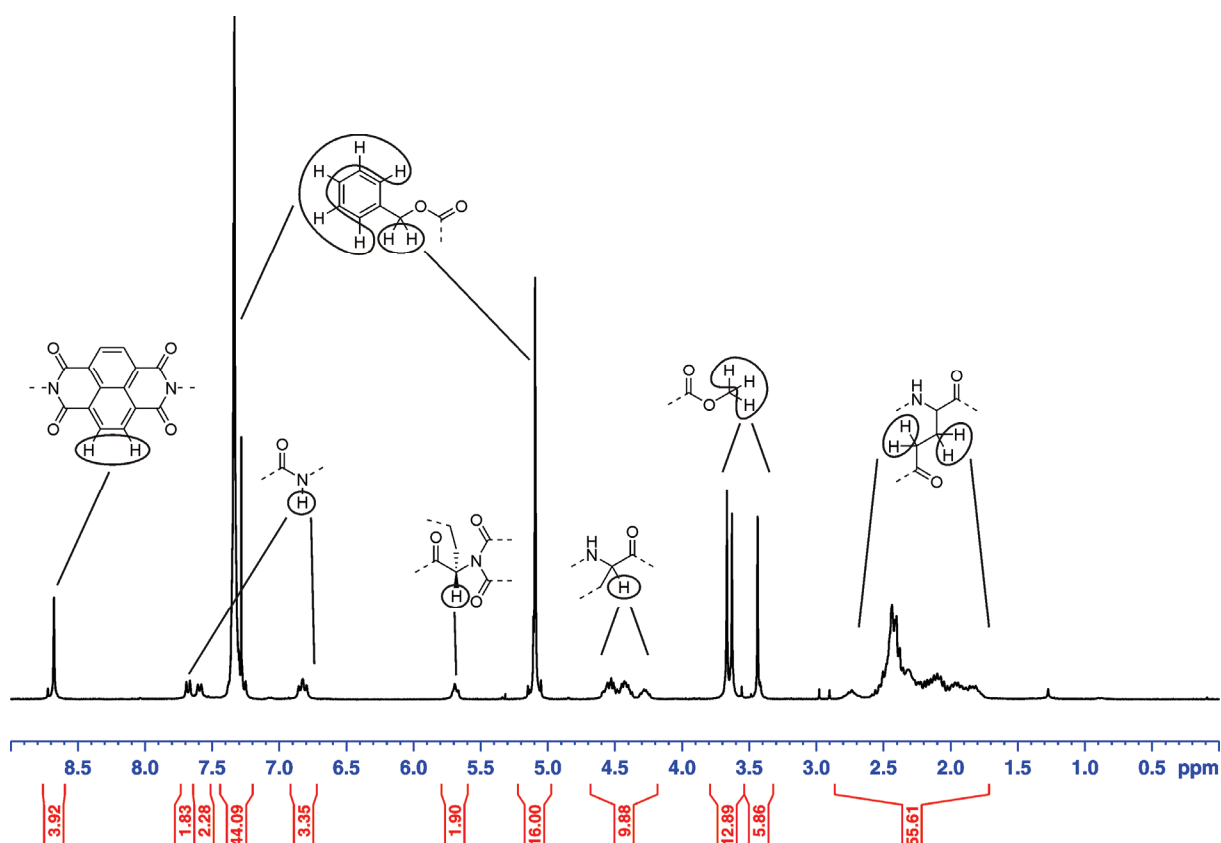
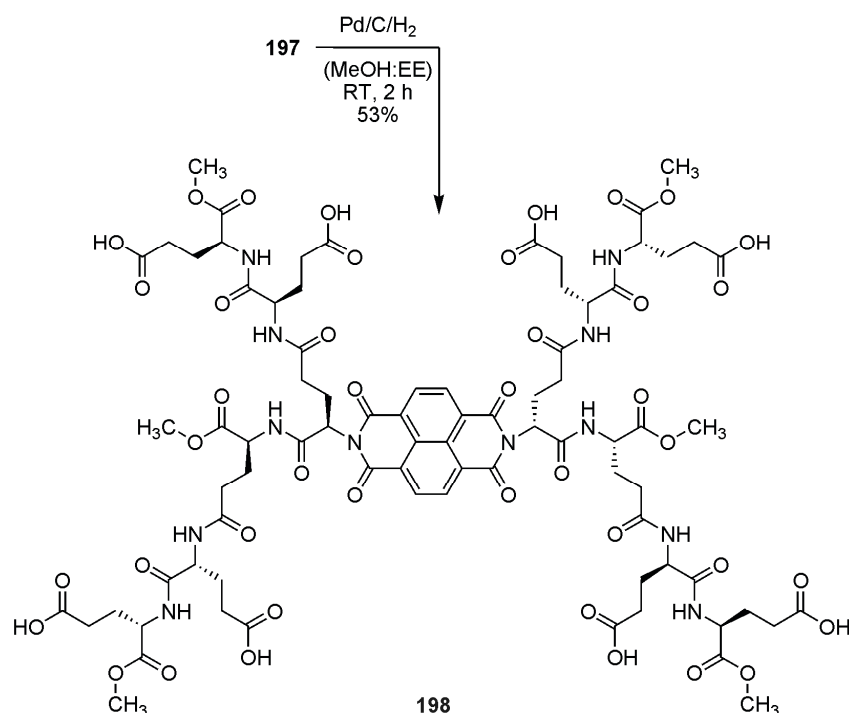


Figure 11: ¹H NMR spectrum of **197** (CDCl₃, 25 °C).



Scheme 11: Benzyl deprotection of **197** using palladium on charcoal with H_2 .

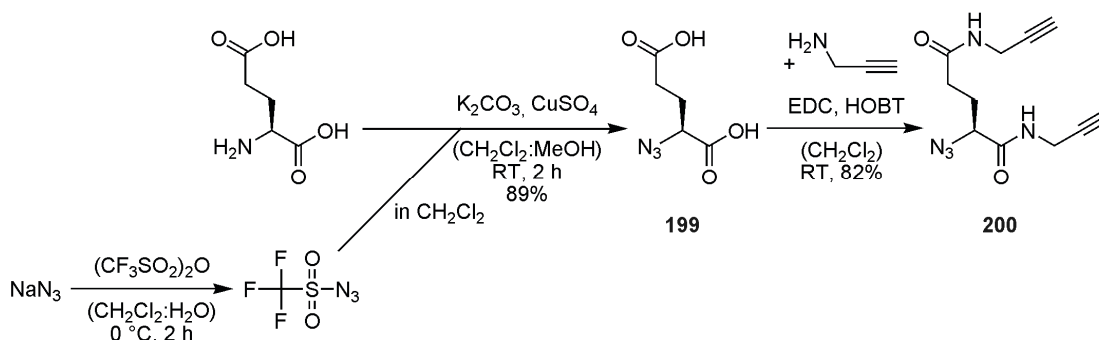
6.2 Hyperbranched Polyglutamate Based Polymers

The synthesis of chiral, glutamate based dendrimers turned out to be very efficient and afforded interesting and unique structures, potentially opening the door to various biochemical applications. As demonstrated in the polymerization of the AB-monomer to linear polypseudopeptides, the “Click”-reaction was a highly efficient reaction for the synthesis of long polymers. Consequently, the combination of the “Click”-polymerization with the glutamate based dendrimer synthesis should give easy access to chiral, high molecular, hyperbranched materials. The use of the trifunctional glutamate enables the synthesis of an AB_2 -monomer. As in the synthesis of the AB-monomer, the *N*-terminus is transformed to the azide and the carboxylic acids are coupled with propargylamine to the corresponding propargylic amides. The straightforward, high yielding synthesis of this AB_2 -monomer is described in the following section.

6.2.1 Monomer Synthesis

The diazo transfer on glutamate has already been described by Roberts and proceeded in yields of 23%.^[10] The reaction was performed under the

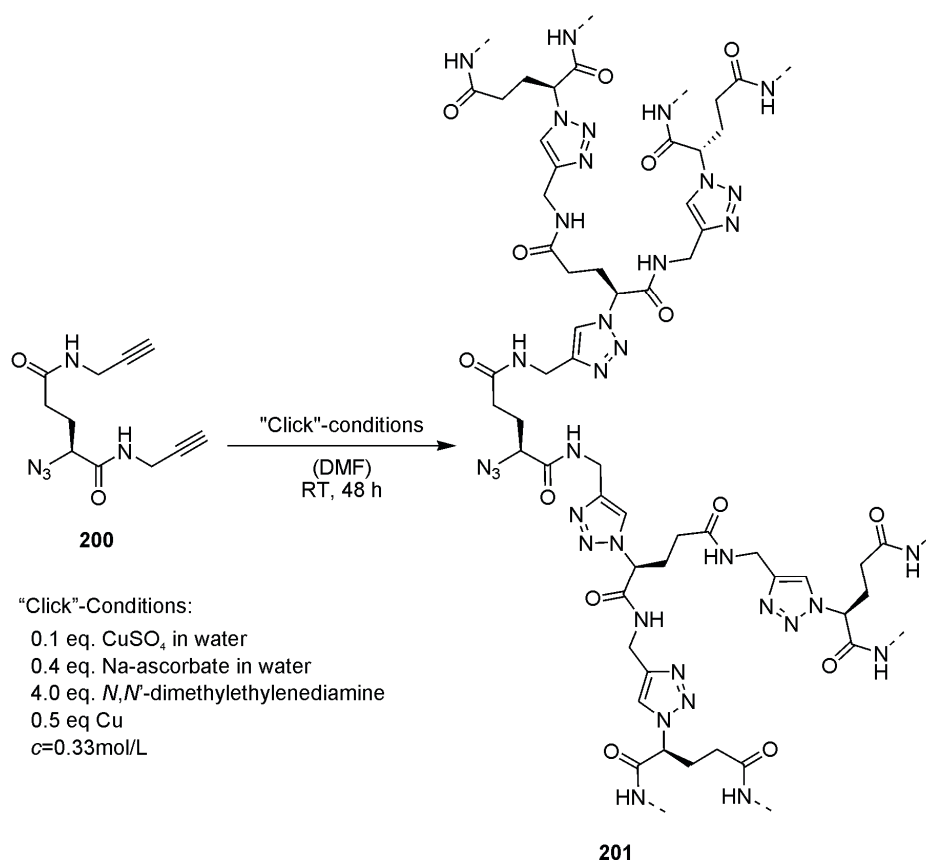
elaborated conditions for the AB-monomer synthesis and gave the desired product in 89% yield (Scheme 12). This high yield has not been reported so far. Subsequent coupling of the azido glutamate with 2.1 eq. propargylamine gave the desired monomer in 82% yield after column chromatography and precipitation. The desired AB₂-“Click”-monomer could hence be synthesized in a very efficient 2-step synthesis with an overall yield of 73%.



Scheme 12: Highly efficient, 2-step AB₂-“Click”-monomer synthesis.

6.2.2 Polymerizations

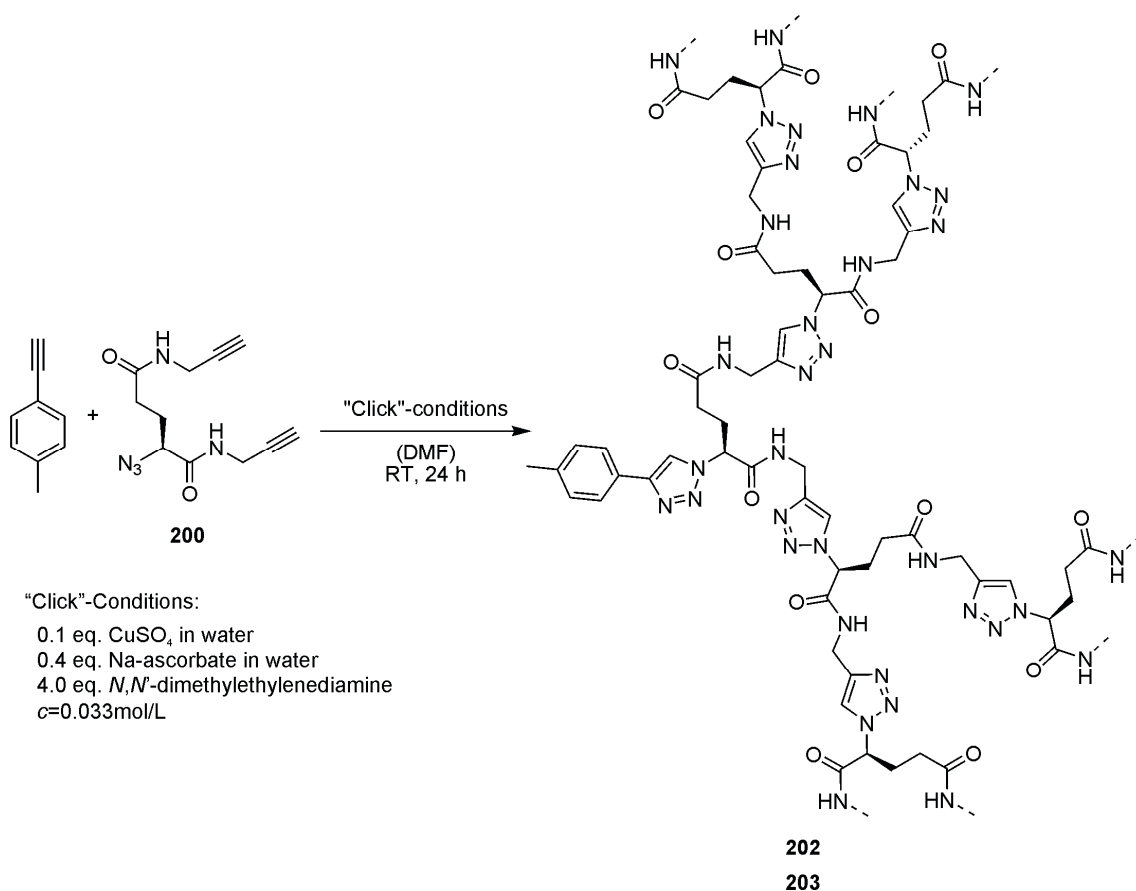
In a first attempt, monomer **200** was polymerized under elaborated conditions, using CuSO_4 , sodium ascorbate, copper wire, and *N,N'*-dimethylethylenediamine in DMF (0.5 mL) with 0.04 mL water (Scheme 13). The highly viscous solution was stirred for 48 h and subsequently precipitated in aqueous EDTA-solution, resulting in a yellow-brown gel, which was stable in shape and could not be dissolved in THF, Et_2O , CH_2Cl_2 , MeOH, DMF, DMSO, NMP, H_2O , TFA, conc. H_2SO_4 and mixtures of these solvents. Several solvents led to a reversible swelling of the solid, but not even partial dissolution was observed, preventing analysis of the polymer **201**.



Scheme 13: Polymerization of AB₂-monomer **200** to the hyperbranched polymer **201**.

The insolubility of **201** was most probably a result of the high molecular weight of the hyperbranched polymer. In order to synthesize polymers with lower molecular weight, a stopper could be added to the reaction mixture, inhibiting further propagation of the polymerization. This stopper could be an acetylene or an azide, terminating the propagation. The length of the resulting polymer should depend significantly on the monomer:stopper ratio. It seemed more attractive to add an acetylene to the mixture and hence stop the reaction at the core of the hyperbranched polymer, since this was expected to afford more symmetrical polymers. Two different stoppers in different monomer:stopper ratios were added to the polymerization reaction. In a first attempt, 0.06 eq. 4-tolylacetylene was added to the reaction mixture (Scheme 13). The reaction was achieved using standard conditions without the addition of copper wire in a tenfold lower concentration of 0.033 mol/L. The lower concentration was expected to afford lower molecular weight material. Both polymerizations were

performed under identical conditions. Precipitation of the mixture in aqueous EDTA-solution afforded the polymers **202** and **203**, which were soluble in DMF.



Scheme 14: Co-polymerization of AB₂-monomer **200** with 4-tolylacetylene to the hyperbranched polymer **202** and **203**.

The GPC-traces of both polymers are shown in Figure 12. Polymer **202** displayed a molecular weight of 32000 g/mol, **203** of 14000 g/mol according to GPC. **202** displayed a shoulder in the GPC-trace, possibly resulting of aggregation effects of the polymer. Assuming a comparable molecular weight of both polymers of around 15000 g/mol would determine the number of repeat units to be around 60.

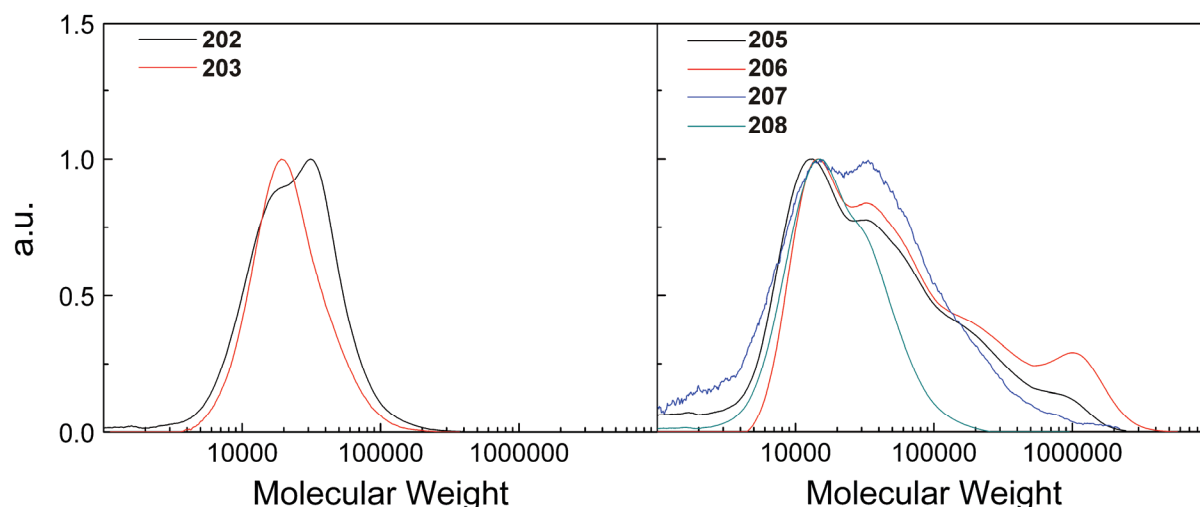
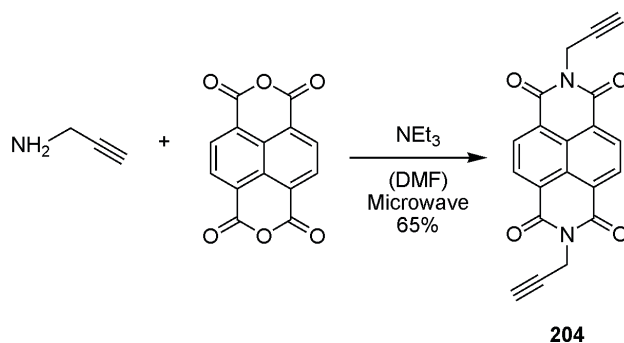


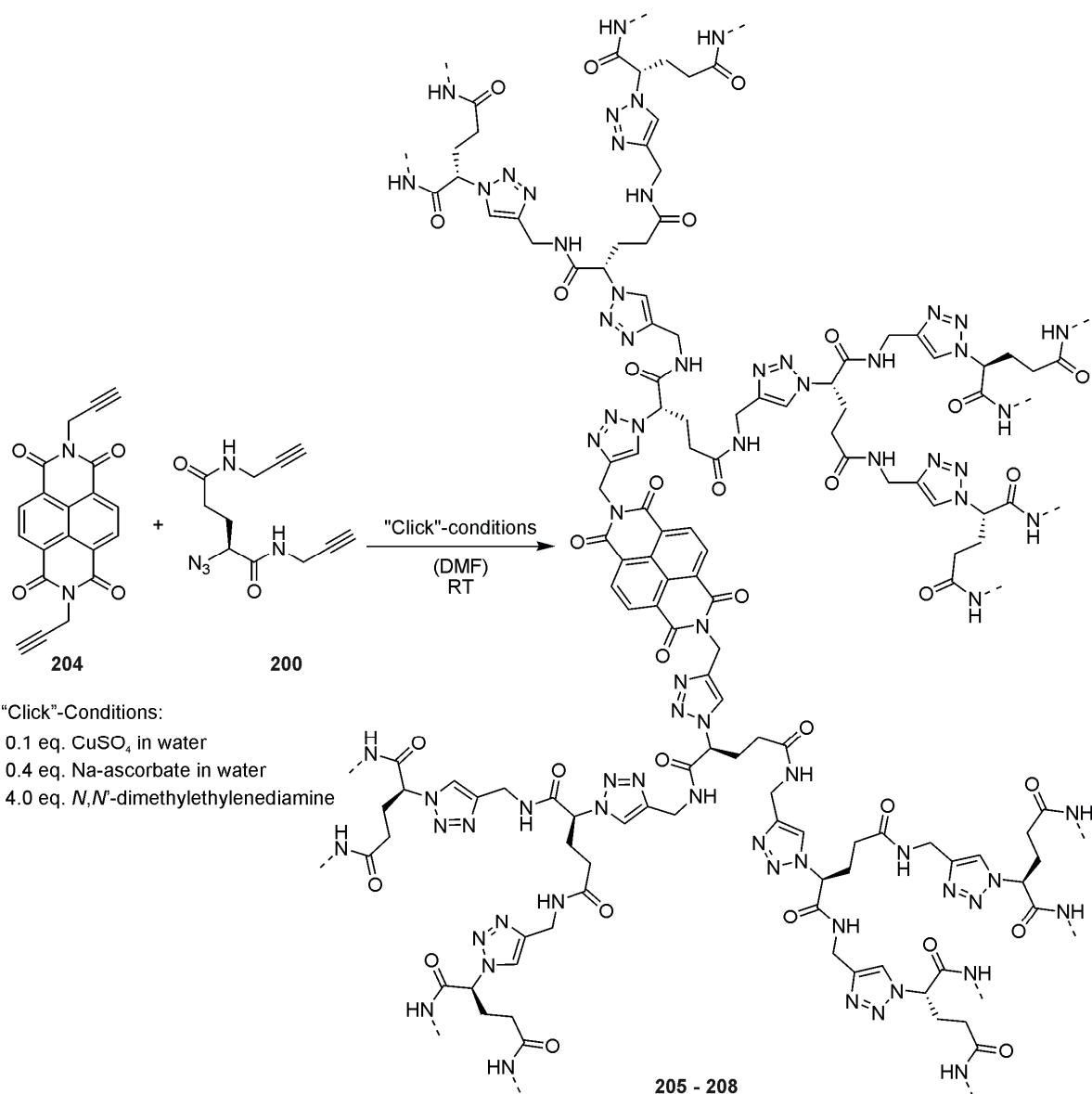
Figure 12: GPC-traces of hyperbranched polymers. **202** and **203** are the products of a copolymerizations of AB₂-monomer **200** with monofunctional 4-tolylacetylene. **205**, **206**, **207**, and **208** are the products of a copolymerization of **200** with bifunctional **204** (GPC in DMF at 70 °C, calibrated with polystyrene standards).

In analogy to the attachment of the G2-dendrimer to the bifunctional naphthalene core, it seemed more sophisticated to use a bifunctional stopper instead of the monofunctional 4-tolylacetylene. Two hyperbranched polymers could hence be connected via a bifunctional core. Since 1,4,5,8-naphthalenetetracarboxylic dianhydride was known to undergo microwave assisted coupling with amino acids and small peptide segments, it was subjected to coupling with propargylamine to give the desired bis-acetylene, which could be used as bifunctional stopper (Scheme 15). The synthesis was achieved in DMF under microwave assistance. During the reaction, the product precipitated from hot DMF. The precipitate was filtered and washed with DMF. It was only soluble in hot DMSO and precipitated in water to give the desired product as a gray powder in 65% yield.



Scheme 15: Microwave assisted synthesis of the bis-acetylene **204**.

The bisacetylene **204** was subsequently co-polymerized with the AB₂-monomer **200** in different monomer:stopper ratios. Since **204** was only soluble in DMSO, a stock solution of **204** in DMSO was diluted with DMF to a total volume of 1 mL. This defined volume was added to the polymerization in order to keep the concentration in the different polymerization reactions constant. The polymerization mixtures hence contained different amounts of DMSO. The polymerization results are summarized in Table 1. The GPC-traces of the soluble parts of the polymer samples **205** – **208** are shown in Figure 12. With the exception of **207**, all polymers displayed a peak maximum in the GPC-trace at around 15000 g/mol. This peak was the second intense peak in the GPC-trace of polymer **207**. This value was comparable to polymers **202** and **203**. The number of shoulders at higher molecular weights in the GPC-traces of **205** – **208** decreased with increasing monomer:stopper ratio. These shoulders were also expected to be the result of aggregation effects on the column. These findings support a solubility-limited growth of the polymer to a maximum of 15000 g/mol.

Table 1: Co-polymerization of AB₂-monomer **200** with the bisacetylene **204** to the hyperbranched polymers **205** - **208**.

Entry	Product	Ratio (monomer:stopper)	Mn [g/mol] ³	Mw [g/mol] ³	PDI	Mp [g/mol] ³
1 ¹	205	40:1	12700	100000	8.1	13000
2 ¹	206	100:1	27000	200000	7.4	15000
3 ¹	207	200:1	8800	70000	8.0	36000
4 ²	208	167:1	8600	35000	4.5	13000

¹ Concentration of the reaction mixture: 0.033 mol/L, reaction time: 48 h; ² concentration of the reaction mixture: 0.067 mol/L, reaction time: 24 h; ³ GPC-analysis (in DMF at 70 °C, calibrated with polystyrene standards, detection by RI).

In future, the issue of size limitation could be circumvented by increasing the solubility of the polymer. The AB₂-monomer as such offers no possibility to introduce solubilizing groups into the polymer. The only approach could hence be the co-polymerization of **200** with solubilizing monomers. This could easily be achieved by the co-polymerization of **200** with azido-L-Glu (**199**), introducing a C-terminal stopper in the same step. This could lead to hyperbranched, water soluble L-Glu-polymers. The size of the polymer could be varied by the monomer:stopper ratio, leading to chiral, potentially spherical oligoelectrolytes with predictable sizes. This step is the scope of this project.

6.3 Experimental Part

6.3.1 General

General Methods: Starting materials were commercial and used as received. All solvents used at FU Berlin and HU Berlin were distilled once prior to usage, all solvents used at MPI were used without further purification. THF was in all cases stored over KOH and freshly distilled prior to usage. Dry solvents were kindly provided by the respective facility of the MPI. Dry DMF was purchased from Acros. If mentioned, solvents were degased by freeze drying or by purging with argon. Column chromatography was carried out with 130 – 140 mesh silica gel. Dialysis of the compounds was achieved using regenerated cellulose dialysis tubes Spectra/Por Dialysis Membrane MWCO:1000 or MWCO:25000. Slow compound addition was achieved using a Harvard Apparatus 11Plus syringe pump. Compound lyophilization was performed using Christ Alpha 2-4 LDC-1m apparatus. Microwave assisted reactions were performed in a CEM-Discover monomode microwave reactor having a continuous microwave power delivery system from 0 to 300 W. The reactions were carried out in 10 mL sealed glass vials. The temperature was monitored by an IR sensor on the outer surface of the reaction vessel. All the reactions were performed with max. power and super-cooling.

Analytic Methods:

NMR (^1H and ^{13}C , respectively) were recorded on Bruker DPX 300 (300.1 and 75 MHz for ^1H and ^{13}C , respectively), Bruker AV400 (400.1 and 100.6 MHz for ^1H and ^{13}C , respectively) spectrometers at 23 \pm 2 $^\circ\text{C}$ using residual protonated solvent signals as internal standard (^1H : $\delta(\text{CHCl}_3)$ = 7.26 ppm, $\delta(\text{DMSO})$ = 2.50 ppm, $\delta(\text{CH}_3\text{OH})$ = 3.31 ppm, $\delta(\text{H}_2\text{O})$ = 4.79 ppm, $\delta(\text{CH}_3\text{CN})$ = 4.79 ppm, $\delta(\text{CH}_2\text{Cl}_2)$ = 5.32 ppm, and ^{13}C : $\delta(\text{CHCl}_3)$ = 77.16 ppm, $\delta(\text{DMSO})$ = 39.52 ppm, $\delta(\text{CH}_3\text{OH})$ = 49.00 ppm, $\delta(\text{CH}_3\text{CN})$ = 1.32 ppm and 118.26 ppm, $\delta(\text{CH}_2\text{Cl}_2)$ = 53.80 ppm).

Mass spectrometry was performed on a Bruker APEX III Fourier Transform Ion Cyclotron Resonance Mass Spectrometer (FTICR-MS) or on a Waters LCT Premier XE.

TLC was performed on Merck Silica Gel 60 F254 TLC plates with a fluorescent indicator with a 254 nm excitation wavelength. Compounds were visualized under UV light at 254 nm and developed with ninhydrin solution.

HPLC/UPLC was performed with a Waters UPLC Acquity equipped with a Waters LCT Premier XE Mass detector for UPLC-HR-MS, with Waters Alliance systems (consisting of a Waters Separations Module 2695, a Waters Diode Array detector 996 and a Waters Mass Detector ZQ 2000) equipped with the columns described with the corresponding substances, with Shimadzu LC-10A systems equipped with a photodiode array detector (PAD or DAD).

GPC measurements in DMF as the mobile phase were performed on PSS columns in a WGE Dr.Bures TAU 2010 column oven at 70 °C, using a WGE Dr.Bures Q-2010 HPLC pump and a Knauer Smartline 3800 autosampler. Detection was achieved using a WGE ETA-2020 RI-visco-detector and a Knauer Smartline 2500 UV-detector. Flow-rate was 1.0 mL/min. Columns were calibrated using a Polystyrene Calibration Kit S-L-10 LOT 79, using 2,4-Di-*tert*-butyl-4-methoxy-phenol as internal standard.

Optical spectroscopy: UV/visible absorption and emission spectra were recorded in spectroscopic grade solvents, using Hellma quartz cuvettes of 1 cm for absorption and emission and 1 mm path length for absorption on a Cary 50 Spectrophotometer and a Cary Eclipse Fluorescence Spectrophotometer, respectively, both equipped with a Peltier thermostated cell holder ($T = 25 \pm 0.05$ °C). The fluorescence samples were excited at their respective absorbance maxima, slit was set to 5 nm bandpass for excitation and to 10 nm bandpass for emission. Circular dichroism spectra were recorded on a JASCO 710 Spectropolarimeter equipped with a JASCO PTC-423S/15 Peltier thermostated cell holder in spectroscopic grade solvents using Hellma quartz cuvettes of 1 cm and 1 mm path length. Prior to first use, the cuvettes were cleaned with 1:1 mixture of conc. H_2SO_4 / 30% H_2O_2 , washed with water and acetonitrile, and a 10 vol-% solution of *silyl-501* (BSTFA: N,O-Bis(trimethylsilyl)acetamide, 1%TMSCl) in acetonitrile added, stirred for 10 min at RT and 20 min at 50 °C, washed twice with acetonitrile and chloroform. After silylation, cuvettes were cleaned with aqueous Hellmanex II cuvette cleaning solutions. IR spectra were

recorded on a Biorad Excalibur FTS30MX equipped with a Golden Gate ATR Specac.

6.3.2 General Procedures

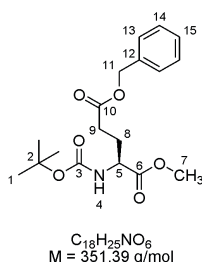
General procedure for the deprotection of the Boc group: Peptide was dissolved in CH_2Cl_2 or in $\text{CH}_2\text{Cl}_2:\text{CH}_3\text{OH}$ 9:1 (depending on solubility) and cooled to 0 °C. TFA (same amount as the solvent) was added and the solution allowed to warm up to room temperature. After stirring at room temperature until starting material was consumed (TLC monitoring), the solution was concentrated i.vac. When the uncharged, neutralized peptide was the desired product, the solution was extracted with water, saturated aqueous NaHCO_3 -solution (in case of longer peptides (starting from octamer), CH_3OH was added to assure solubility of the peptide), water, and brine. The combined organic layers were dried over MgSO_4 , filtered, and evaporated i.vac. to yield the crude product in quantitative yield. In case of remaining protected peptide, procedure was repeated. When the amine salt was the desired product, the reaction mixture was evaporated i.vac. and wrapped several times with CH_2Cl_2 to give the product in quantitative yield.

General procedure for the deprotection of the methyl ester: To a solution of methyl ester protected peptide in water:THF 1:5, a 1 M aqueous solution of LiOH (water:LiOH:THF 1:1:5) was added and the reaction mixture stirred at room temperature until starting material was consumed (TLC monitoring). Acetic acid was added to give pH=5, and the product subsequently extracted with CH_2Cl_2 . The united organic layers were dried over MgSO_4 and the solvent evaporated i.vac. to give the product in quantitative yield.

General procedure for the deprotection of the Z group or benzyl ester: To a solution of Z- or benzyl protected peptide in EE: CH_3OH (ratio depending on solubility), Pd/C was added and the solution stirred under hydrogen atmosphere at room temperature. The reaction mixture was filtered and evaporated i.vac. to give the product.

6.3.3 Synthetic Procedures

Boc-L-Glu(Z)-Me (**171**):



Boc-L-Glu(Z) (1.69 g, 5.00 mmol) and HOBT (0.74 g, 5.50 mmol) were dissolved in CH_2Cl_2 :MeOH 1:1 (20 mL) and cooled to 0 °C. To the cold solution, EDC (1.25 g, 6.50 mmol) was added. The solution was allowed to warm up to room temperature and stirred for 18 h. Water was added to the reaction mixture and the biphasic system stirred for 20 min. After phase separation, the organic layer was extracted with aqueous 1 M citric acid solution (1x50 mL), water (1x50 mL), saturated aqueous $NaHCO_3$ -solution (1x50 mL) and water (1x50 mL). The organic layer was dried over $MgSO_4$, filtered and evaporated i.vac. to give the crude product which was purified via column chromatography on silica (eluent: CH_2Cl_2 :MeOH 98:2) to give 1.74 g (yield: 98%) of the desired product **171** as a pale yellow oil.

HPLC (125 mm Nucleodur 100-5 C-18, 4.0 mm, Methanol:Water = 70:30, 0.8 mL/min, 9.3 MPa, 308 K): 4.15 min (96.5% peak area, **171**).

HPLC (250 mm Chiracel OJ, 4.6 mm, *n*-Heptan:2-propanol = 80:20, 0.5 mL/min, 1.9 MPa, 298 K): 18.02 min (91.7% peak area, **171**).

$R_F = 0.80$ (CH_2Cl_2 :MeOH 9:1)

1H NMR (400 MHz, DMSO- d_6 , 20 °C): δ 7.39 - 7.28 (m, 5 H, 2 $C^{13}H$, 2 $C^{14}H$, $C^{15}H$), 5.09 (s, 2 H, $C^{11}H_2$), 4.02 - 3.90 (m, 1 H, C^5H), 3.62 (s, 3 H, C^7H_3), 2.47 - 2.42 (m, 2 H, C^9H_2), 2.02 - 1.94 (m, 1 H, C^8H), 1.86 - 1.76 (m, 1 H, C^8H), 1.37 (s, 9 H, 3 C^1H_3).

^{13}C NMR (DMSO- d_6): δ 172.66, 172.05, 155.52, 136.15, 128.42, 127.99, 127.87, 78.31, 65.49, 52.61, 51.82, 29.91, 28.14, 25.90.

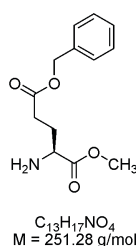
EI-MS: $m/z = 57$ (calcd 57 for $C(CH_3)_3$), 91 (calcd 91 for CH_2Ph), 108 (calcd 108 for OCH_2Ph), 144 (calcd 144 for $C_6H_{10}NO_3$), 160 (calcd 160 for $C_6H_9NO_4$),

6 Glutamate Dendrimers

192 (calcd 192 for $C_{11}H_{14}NO_2$), 251 (calcd 251 for **171** - Boc), 292 (calcd 292 for **171** - (H_3COCO)), 295 (calcd 295 for **171** - $(C(CH_3)_3)$).

High-resolution ESI-MS: $m/z = 374.157298$ (calcd 374.157405 for $C_{18}H_{25}N_1O_6 + 1 Na^+$).

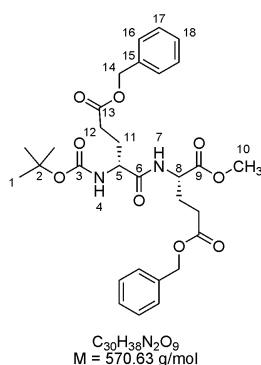
L-Glu(Z)-Me (**172**):



171 (2.11 g, 6.00 mmol) was reacted following the general procedure for the deprotection of the Boc group. TFA (20 mL), CH_2Cl_2 (80 mL). The product was used without further purification and analysis to avoid diketopiperazine-formation.

$R_F = 0.50$ (CH_2Cl_2 :MeOH 9:1)

Boc-D-Glu(Z)-L-Glu(Z)-Me (**174**):



Boc-D-Glu(Z) (2.13 g, 6.30 mmol), HOBT (0.89 g, 6.60 mmol) and **172** (1.51 g, 6.00 mmol) were dissolved in CH_2Cl_2 (20 mL) and cooled to 0 °C. A concentrated solution of EDC (1.50 g, 7.80 mmol) in CH_2Cl_2 (20 mL) was added drop wise. The solution was allowed to warm up to room temperature and stirred for 14 h. Water was added to the solution and the resulting biphasic system stirred for 10 min. After phase separation, the organic layer was dried

over MgSO_4 , filtered and evaporated i.vac. The crude product was purified via column chromatography on silica (eluent: CH_2Cl_2 :MeOH 95:5) to give 3.38 g (yield: 99%) of **174** as a yellow oil. Extraction of this oil with PE removed yellow color.

HPLC: (125 mm Nucleodur 100-5 C-18, 2.0 mm, Methanol:Water = 70:30, 0.2 mL/min, 11.9 MPa, 308 K): 9.99 min (96.6% peak area, **174**).

GPC (DMF): $M_n = 546$ g/mol, $M_w = 556$ g/mol, $M_p = 562$ g/mol, PDI = 1.02.

$R_F = 0.80$ (CH_2Cl_2 :MeOH 9:1)

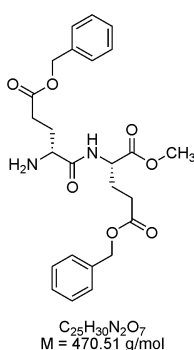
^1H NMR (400 MHz, DMSO-d_6 , 20 °C): δ 8.23 (d, $^3J(\text{H,H}) = 6.9$ Hz, 1 H, N^7H), 7.39 - 7.31 (m, 10 H, 4 C^{16}H , 4 C^{17}H , 2 C^{18}H), 6.91 (d, $^3J(\text{H,H}) = 7.9$ Hz, 1 H, N^4H), 5.08 (s, 4 H, 2 C^{14}H_2), 4.31 - 4.25 (m, 1 H, C^8H), 4.00 - 3.86 (m, 1 H, C^5H), 3.60 (s, 3 H, C^{10}H_3), 2.43 - 2.37 (m, 4 H, 2 C^{12}H_2), 2.06 - 1.75 (m, 4 H, 2 C^{11}H_2), 1.36 (s, 9 H, 3 C^1H_3).

^{13}C NMR (DMSO-d_6): δ 172.18, 171.99, 171, 86, 171.78, 155.21, 136.18, 136.08, 128.39, 127.97, 127.94, 127.88, 127.81, 78.20, 65.49, 65.41, 53.55, 51.89, 51.01, 29.94, 29.69, 28.09, 27.09, 25.91.

EI-MS: $m/z = 57$ (calcd 57 for $\text{C}(\text{CH}_3)_3$), 91 (calcd 91 for CH_2Ph), 108 (calcd 108 for OCH_2Ph), 192 (calcd 191 for $\text{C}_{11}\text{H}_{13}\text{NO}_2$), 236 (calcd 236 for $\text{C}_{12}\text{H}_{14}\text{NO}_4$), 292 (calcd 292 for $\text{C}_{16}\text{H}_{22}\text{NO}_4$), 362 (calcd 362 for $\text{C}_{18}\text{H}_{22}\text{N}_2\text{O}_6$), 514 (calcd 513 for **174** - $\text{C}(\text{CH}_3)_3$), 570 (calcd 570 for **174**).

High-resolution ESI-MS: $m/z = 593.246646$ (calcd 593.246951 for $\text{C}_{30}\text{H}_{38}\text{N}_2\text{O}_9 + 1 \text{ Na}^+$).

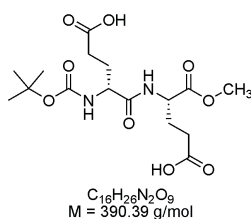
D-Glu(Z)-L-Glu(Z)-Me (**176**):



174 (2.40 g, 4.20 mmol) was reacted following the general procedure for the deprotection of the Boc group. TFA (50 mL), CH₂Cl₂ (50 mL). The product was used without further purification and analysis to avoid diketopiperazine-formation.

$R_F = 0.50$ (CH₂Cl₂:MeOH 9:1)

Boc-D-Glu-L-Glu-Me (**178**):

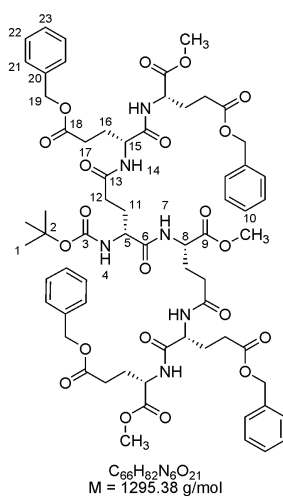


174 (0.80 g, 0.14 mmol) was reacted following the general procedure for the deprotection of the Z group or benzyl ester. MeOH (20 mL), Pd/C (80 mg), reaction time: 2.5 h, hydrogen pressure: 5 bar. The product was obtained in quantitative yield and was used without further purification.

UPLC was not reliable due to missing UV-labels.

High-resolution ESI-MS: $m/z = 389.1517$ (calcd 389.1560 for C₁₆H₂₄N₂O₉ - 1 H⁺).

Boc-G2-D-(*alt*)-L-Glu(Z)-Me (**180**):



178 (0.55 g, 1.40 mmol), **176** (1.37 g, 2.90 mmol) and HOBT (0.19 g, 1.40 mmol) were dissolved in CH₂Cl₂ (40 mL) and cooled to 0 °C. To the cold solution, EDC (0.81 g, 4.20 mmol) was added. The solution was allowed to warm up to room temperature and stirred under TLC monitoring. After completion of the reaction, water was added and the biphasic system stirred for 10 minutes. After phase separation, the organic layer was extracted with aqueous 1 M citric acid solution (1x20 mL), water (1x20 mL), saturated aqueous NaHCO₃-solution (1x20 mL) and water (1x20 mL). The organic layer was dried over MgSO₄, filtered and evaporated i.vac., to give the crude product, which was dissolved in CH₂Cl₂ and precipitated in Et₂O. The purified crude product was further purified via column chromatography on silica (eluent: CH₂Cl₂:MeOH 9:1) to give 1.72 g (yield:95%) of the desired product as white powder.

UPLC-HRMS ((2.1x100 mm BEH Phenyl 1.7um, acetonitrile:water Grad 40 95A): 5.08 min (>99.9% peak area, ESI(+): 1317.55 (**180** + 1 Na⁺)).

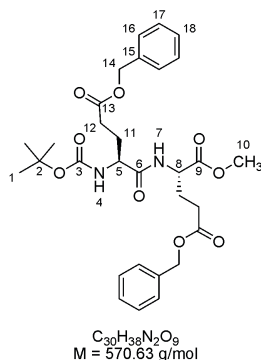
GPC (DMF): Mn = 1655 g/mol, Mw = 1677 g/mol, Mp = 1690 g/mol, PDI = 1.01.

R_F = 0.60 (CH₂Cl₂:MeOH 9:1)

¹H NMR (300 MHz, CDCl₃, 20 °C): δ 7.63 (d, ³J(H,H) = 7.9 Hz, 1 H, NH), 7.44 (d, ³J(H,H) = 7.9 Hz, 1 H, NH), 7.39 - 7.14 (m, 23 H, 4 C²¹⁻²³H, 3 NH), 5.72 - 5.70 (m, 1 H, NH), 5.10 - 5.07 (m, 8 H, 4 C¹⁹H₂), 4.67 - 4.43 (m, 5 H, 3 C⁸H, 2 C¹⁵H), 4.21 - 4.10 (m, 1 H, C⁵H), 3.68 - 3.66 (3xs, 9 H, 3 C¹⁰H₃), 2.61 - 1.73 (m, 24 H, 2 C¹¹⁻¹²H₂, 1.39 (s, 9 H, 3 C¹H₃).

¹³C NMR (CDCl₃): δ 172.41, 171.33, 172.17, 172.14, 172.02, 172.03, 135.91, 135.86, 135.77, 128.65, 128.62, 128.39, 128.35, 128.31, 128.28, 128.24, 80.22, 66.65, 66.54, 66.46, 52.66, 52.58, 52.51, 51.84, 51.74, 51.62, 30.64, 30.54, 30.47, 30.39, 28.36, 26.77.

High-resolution ESI-MS: m/z = 1295.5606 (calcd 1295.5606 for C₆₆H₈₂N₆O₂₁ + 1 H⁺).

Boc-L-Glu(Z)-L-Glu(Z)-Me (**173**):

Boc-L-Glu(Z) (7.42 g, 22.00 mmol), HOBT (2.70 g, 20.00 mmol) and **172** (5.03 g, 20.00 mmol) were dissolved in CH₂Cl₂ (100 mL) and cooled to 0 °C. A concentrated solution of EDC (4.99 g, 26.00 mmol) was added. The solution was allowed to warm up to room temperature and stirred for 48 h. The reaction mixture was extracted with aqueous 1 M citric acid solution (1x20 mL), water (1x20 mL), saturated aqueous NaHCO₃-solution (1x20 mL) and water (1x20 mL). The organic layer was dried over MgSO₄, filtered and evaporated i.vac. dried over MgSO₄, filtered and evaporated i.vac. The crude product was purified via column chromatography on silica (eluent: PE:EE 2:1) to give 11.20 g (yield: 98%) of the desired product as a colorless oil.

UPLC-HRMS ((2.1x100 mm HSS T3 1.8um, acetonitrile:water Grad 40 95A): 4.69 min (>99.9% peak area, ESI(+): 571.27 (**173** + 1 H⁺)).

GPC (DMF): Mn = 546 g/mol, Mw = 556 g/mol, Mp = 562 g/mol, PDI = 1.02.

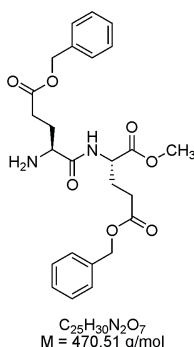
R_F = 0.80 (CH₂Cl₂:MeOH 9:1)

¹H NMR (300 MHz, CDCl₃, 20 °C): δ 7.37 - 7.30 (m, 10 H, 4 C¹⁶H, 4 C¹⁷H, 2 C¹⁸H), 6.87 (d, ³J(H,H) = 7.4 Hz, 1 H, N⁷H), 5.22 (d, ³J(H,H) = 7.4 Hz, 1 H, N⁴H), 5.13 (s, 2 H, C¹⁴H₂), 5.11 (s, 2 H, C¹⁴H₂), 4.60 (dt, ³J(H,H) = 8.0 Hz, ³J(H,H) = 5.0 Hz, 1 H, C⁸H), 4.25 - 4.14 (m, 1 H, C⁵H), 3.71 (s, 3 H, C¹⁰H₃), 2.62 - 2.35 (m, 4 H, 2 C¹²H₂), 2.34 - 1.85 (m, 4 H, 2 C¹¹H₂), 1.42 (s, 9 H, 3 C¹H₃).

¹³C NMR (CDCl₃): δ 173.28, 172.58, 171.97, 171, 60, 155.21, 135.78, 128.71, 128.45, 128.41, 66.60, 52.55, 51.63, 30.39, 30.15, 28.26, 27.85, 27.12.

High-resolution ESI-MS: $m/z = 571.2650$ (calcd 571.2656 for $C_{30}H_{38}N_2O_9 + 1 Na^+$).

L-Glu(Z)-L-Glu(Z)-Me (**175**):



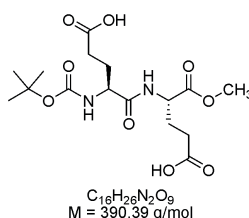
173 (6.59 g, 11.55 mmol) was reacted following the general procedure for the deprotection of the Boc group. TFA (17 mL), CH_2Cl_2 (17 mL). The product was used without further purification and analysis to avoid diketopiperazine-formation.

$R_F = 0.50$ (CH_2Cl_2 :MeOH 9:1)

1H NMR (300 MHz, $CDCl_3$, 20 °C): δ 7.71 (d, $^3J(H,H) = 8.2$ Hz, 1 H, NH), 7.37 - 7.30 (m, 10 H, Ar-H), 5.10 (s, 4 H, CH_2), 4.60 (dt, $^3J(H,H) = 8.1$ Hz, $^3J(H,H) = 5.5$ Hz, 1 H, CH), 3.71 (s, 3 H, CH_3), 3.49 - 3.40 (m, 1 H, CH), 2.52 - 1.75 (m, 8 H, CH_2).

^{13}C NMR ($CDCl_3$): δ 173.19, 172.45, 172.19, 135.79, 135.73, 128.59, 128.31, 128.27, 66.56, 66.46, 54.41, 52.48, 51.33, 30.72, 30.37, 30.10, 27.23.

Boc-L-Glu-L-Glu-Me (**177**):



173 (3.14 g, 5.50 mmol) was reacted following the general procedure for the deprotection of the Z group or benzyl ester. EE (20 mL), Pd/C (260 mg),

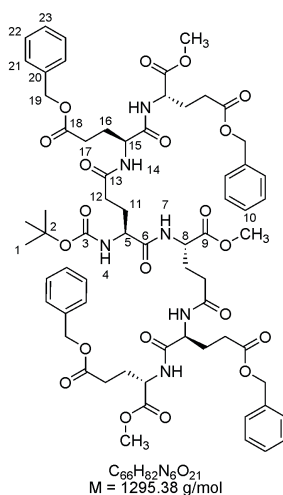
6 Glutamate Dendrimers

reaction time: 2.5 h, hydrogen pressure: 5 bar. The product was obtained in quantitative yield and was used without further purification.

^1H NMR (300 MHz, CDCl_3 , 20 °C): δ 7.54 - 7.53 (m, 1 H, NH), 5.64 - 5.62 (m, 1 H, NH), 4.65 - 4.63 (m, 1 H, CH), 4.40 - 4.38 (m, 1 H, CH), 3.75 (s, 3 H, CH_3), 2.52 - 1.90 (m, 8 H, CH_2), 1.44 (s, 9 H, CH_3).

High-resolution ESI-MS: m/z = 391.1530 (calcd 391.1717 for $\text{C}_{16}\text{H}_{26}\text{N}_2\text{O}_9$ + 1 H^+).

Boc-G2-*all*-L-Glu(Z)-Me (**179**):



177 (2.15 g, 5.50 mmol), **175** (5.44 g, 11.55 mmol), and HOBT (0.74 g, 5.50 mmol) were dissolved in CH_2Cl_2 (100 mL) and cooled to 0 °C. To the cold solution EDC (3.16 g, 16.50 mmol) was added. The solution was allowed to warm up to room temperature and stirred under TLC monitoring. After completion of the reaction, water was added and the biphasic system stirred for 10 minutes. After phase separation, the organic layer was extracted with aqueous 1 M citric acid solution (1x20 mL), water (1x20 mL), saturated aqueous NaHCO_3 -solution (1x20 mL) and water (1x20 mL). The organic layer was dried over MgSO_4 , filtered and evaporated i.vac., to give the crude product, which was dissolved in CH_2Cl_2 and precipitated in Et_2O . The purified crude product was further purified via column chromatography on silica (eluent: CH_2Cl_2 :MeOH 95:5). The white solid was dissolved in CH_2Cl_2 :MeOH and precipitated in ice-cold Et_2O , to give 6.57 g (92%) of the desired product as a white powder.

UPLC-HRMS ((2.1x100 mm HSS T3 1.8um, acetonitrile:water Grad 60 95A): 3.54 min (>99.9% peak area, ESI(+): 1317.42 (**179** + 1 Na⁺)).

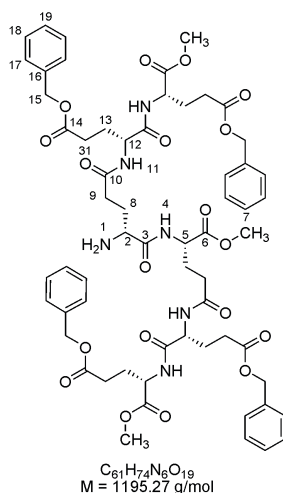
GPC (DMF): Mn = 1684 g/mol, Mw = 1709 g/mol, Mp = 1717 g/mol, PDI = 1.01.

R_F = 0.60 (CH₂Cl₂:MeOH 9:1)

¹H NMR (300 MHz, CDCl₃, 20 °C): δ 8.29 (d, ³J(H,H) = 8.3 Hz, 1 H, NH), 7.57 (d, ³J(H,H) = 7.2 Hz, 1 H, NH), 7.30 - 7.17 (m, 20 H, Ar-H), 6.99 (d, ³J(H,H) = 6.6 Hz, 2 H, NH), 6.79 (d, ³J(H,H) = 6.8 Hz, 1 H, NH), 5.17 - 5.08 (m, 8 H, CH₂), 5.02 - 4.97 (m, 1 H, NH), 4.59 - 4.28 (m, 5 H, CH), 3.79 - 3.69 (m, 1 H, CH), 3.58 - 3.55 (3xs, 9 H, CH₃), 2.49 - 1.61 (m, 24 H, CH₂), 1.27 (s, 9 H, CH₃).

High-resolution ESI-MS: m/z = 1317.4174 (calcd 1317.5431 for C₆₆H₈₂N₆O₂₁ + 1 Na⁺).

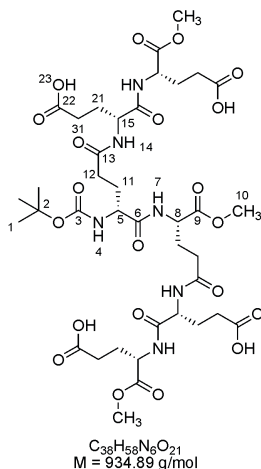
G2-D-(*alt*)-L-Glu(Z)-Me (**182**):



180 (0.32 g, 0.25 mmol) was reacted following the general procedure for the deprotection of the Boc group. TFA (2.0 mL), CH₂Cl₂ (4.0 mL). The crude product was dissolved in CH₂Cl₂ and precipitated in Et₂O to give the pure product.

R_F = 0.22 (CH₂Cl₂:MeOH 9:1)

Boc-G2-D-(*alt*)-L-Glu-Me (**184**):



180 (0.10 g, 0.08 mmol) was reacted following the general procedure for the deprotection of the Z group or benzyl ester. THF (MeOH led to partial transesterification) (60 mL), Pd/C (25 mg), reaction time: 6 h, hydrogen pressure: 5 bar. The product was obtained in quantitative yield and was used without further purification.

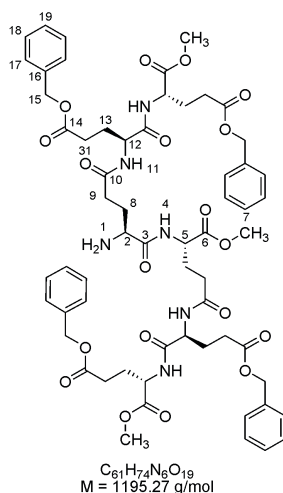
UPLC-HRMS ((2.1x100 mm BEH Phenyl 1.7um, acetonitrile:water Grad 20 50A): 2.75 min (>99.9% peak area, ESI(+): 934.42 (**184** + 1 H⁺)).

$R_F = 0.10$ (CH₂Cl₂:MeOH 9:1)

¹H NMR (300 MHz, CD₃OD, 20 °C): δ 4.50 – 4.32 (m, 5 H, CH), 4.10 – 4.05 (m, 1 H, CH), 3.72 (s, 9 H, CH₃), 2.61 – 1.74 (m, 24 H, CH₂), 1.45 (s, 9 H, CH₃).

High-resolution ESI-MS: $m/z = 933.3750$ (calcd 933.3577 for C₃₈H₅₈N₆O₂₁ - 1 H⁺).

G2-*all*-L-Glu(Z)-Me (**181**):



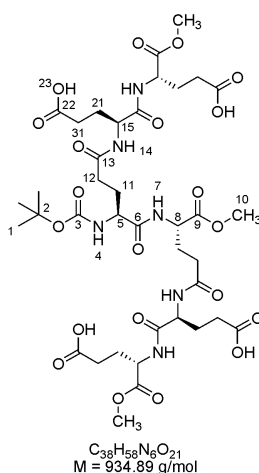
179 (0.33 g, 0.25 mmol) was reacted following the general procedure for the deprotection of the Boc group. TFA (3.0 mL), CH_2Cl_2 (6.0 mL). The product was used without further purification.

UPLC-HRMS ((2.1x100 mm BEH Phenyl 1.7um, acetonitrile:water Grad 40 95A): 5.48 min (>99.9% peak area, ESI(+): 1195.51 (**181** + 1 H^+)).

$R_F = 0.22$ (CH_2Cl_2 :MeOH 9:1)

High-resolution ESI-MS: $m/z = 1195.5051$ (calcd 1195.5087 for $C_{61}H_{74}N_6O_{19} + 1 H^+$).

Boc-G2-*all*-L-Glu-Me (**183**):



179 (0.26 g, 0.20 mmol) was reacted following the general procedure for the deprotection of the Z group or benzyl ester. THF (MeOH led to partial

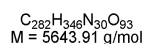
6 Glutamate Dendrimers

transesterification) (60 mL), Pd/C (25 mg), reaction time: 6 h, hydrogen pressure: 5 bar. The product was obtained in quantitative yield and was used without further purification.

$R_F = 0.10$ (CH_2Cl_2 :MeOH 9:1)

High-resolution ESI-MS: $m/z = 935.3724$ (calcd 935.3733 for $\text{C}_{38}\text{H}_{58}\text{N}_6\text{O}_{21} + 1 \text{ H}^+$).

Boc-G4-D-(*alt*)-L-Glu(Z)-Me (**186**):

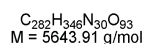


182 (0.19 g, 0.20 mmol), **184** (1.02 g, 0.85 mmol) and HOBT (0.05 g, 0.40 mmol) were dissolved in DMF (15 mL) and cooled to 0 °C. To the cold solution EDC (0.23 g, 1.20 mmol) was added. The solution was allowed to warm up to room temperature and stirred for 3 days. The reaction was monitored by GPC. The solution was precipitated in Et_2O . The precipitate was extensively washed with Et_2O and MeOH (TLC monitoring). The remaining white powder was extracted with EE, until GPC displayed pure product. This procedure afforded 1.03 g (yield: 91%) of the desired product as a white powder.

GPC (DMF): $M_n = 5706 \text{ g/mol}$, $M_w = 5827 \text{ g/mol}$, $M_p = 5939 \text{ g/mol}$, PDI = 1.02.

^1H NMR (300 MHz, DMSO-d_6 , 20 °C): δ 8.47 – 7.88 (m, 30 H, NH), 7.40 – 7.25 (m, 80 H, Ar-H), 5.06 (s, 32 H, CH_2), 4.40 – 4.13 (m, 29 H, CH), 3.90 – 3.89 (m, 1 H, CH), 3.65 – 3.51 (m, 45 H, CH_3), 2.46 – 1.63 (m, 120 H, CH_2), 1.35 (s, 9 H, CH_3).

Boc-G4-*all*-L-Glu(Z)-Me (**185**):



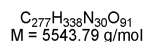
181 (0.19 g, 0.20 mmol), **183** (1.02 g, 0.85 mmol) and HOBT (0.05 g, 0.40 mmol) were dissolved in DMF (15 mL) and cooled to 0 °C. To the cold solution EDC (0.23 g, 1.20 mmol) was added. The solution was allowed to warm up to room temperature and stirred for 3 days. The reaction was monitored by GPC. The solution was precipitated in Et_2O . The precipitate was extensively

washed with Et₂O and MeOH (TLC monitoring). The remaining white powder was extracted with EE, until GPC displayed pure product. This procedure afforded 0.95 g (yield: 84%) of the desired product as a white powder.

GPC (DMF): Mn = 5552 g/mol, Mw = 5744 g/mol, Mp = 6009 g/mol, PDI = 1.04.

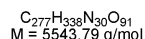
¹H NMR (300 MHz, DMSO-d₆, 20 °C): δ 8.49 – 7.85 (m, 30 H, NH), 7.41 – 7.25 (m, 80 H, Ar-H), 5.08 (s, 32 H, CH₂), 4.37 – 4.12 (m, 29 H, CH), 3.90 – 3.89 (m, 1 H, CH), 3.62 – 3.51 (m, 45 H, CH₃), 2.48 – 1.59 (m, 120 H, CH₂), 1.33 (s, 9 H, CH₃).

G4-D-(*alt*)-L-Glu(Z)-Me (**188**):

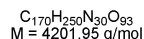


186 (0.10 g, 0.02 mmol) was reacted following the general procedure for the deprotection of the Boc group. TFA (3.0 mL), CH₂Cl₂ (3.0 mL). The crude product was dissolved in C₂Cl₂ and precipitated in Et₂O to give the pure product. In case of anion exchange, the product was dissolved in DMF, NEt₃ (0.075 mL, 30 eq) was added and the solution precipitated in Et₂O. The solid was washed with Et₂O to give the product in quantitative yield.

G4-*all*-L-Glu(Z)-Me (**187**):



185 (0.10 g, 0.02 mmol) was reacted following the general procedure for the deprotection of the Boc group. TFA (3.0 mL), CH₂Cl₂ (3.0 mL). The crude product was dissolved in C₂Cl₂ and precipitated in Et₂O to give the pure product in quantitative yield.

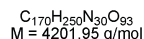
Boc-G4-D-(*alt*)-L-Glu-Me (**190**):

186 (0.11 g, 0.02 mmol) was reacted following the general procedure for the deprotection of the Z group or benzyl ester. DMF (10 mL), Pd/C (12 mg), reaction time: 3 h, hydrogen pressure: 2 bar. The crude product was dissolved in H₂O and filtered. Dialysis of the filtrate (MWCO 1000 g/mol) and subsequent lyophilization afforded 69 mg (yield: 82%) of the desired product as white solid.

¹H NMR (300 MHz, D₂O, 20 °C): δ 4.45 – 4.23 (m, 29 H, CH), 4.06 – 3.96 (m, 1 H, CH), 2.53 – 1.83 (m, 120 H, CH₂), 1.37 (s, 9 H, CH₃).

MALDI-TOF (sinapinic acid matrix): 4099.94 ((**190** – Boc) + 1 H⁺).

ESI-MS: 4200.57 (**190** + 1 H⁺).

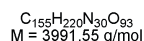
Boc-G4-*all*-L-Glu-Me (**189**):

185 (0.11 g, 0.02 mmol) was reacted following the general procedure for the deprotection of the Z group or benzyl ester. DMF (10 mL), Pd/C (12 mg), reaction time: 3 h, hydrogen pressure: 2 bar. The crude product was dissolved in H₂O and filtered. Dialysis of the filtrate (MWCO 1000 g/mol) and subsequent lyophilization afforded 77 mg (yield: 92%) of the desired product as white solid.

¹H NMR (300 MHz, D₂O, 20 °C): δ 4.42 – 4.14 (m, 29 H, CH), 4.04 – 3.91 (m, 1 H, CH), 2.57 – 1.85 (m, 120 H, CH₂), 1.36 (s, 9 H, CH₃).

MALDI-TOF (sinapinic acid matrix): 4100.27 (**189** + 1 H⁺).

ESI-MS: 4200.58 (**189** + 1 H⁺).

Boc-G4-D-(*alt*)-L-Glu (**192**):

186 (0.20 g, 0.04 mmol) was reacted following the general procedure for the deprotection of the methyl ester. Starting material did not dissolve completely in solvent mixture. Evaporation of THF, addition of DMF instead. After 5 h, acetic

acid was added and the reaction mixture concentrated i.vac. The reaction mixture was dialyzed twice in water (MWCO 1000 g/mol) to afford 79 mg (yield: 57%) of the desired product as a white solid.

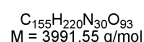
UPLC-MS ((2.1x100 mm BEH C18 1.7um, acetonitrile:water Grad 5 15A): 3.98 (24.1% peak area, ESI(+): 3890.27 ((**192** – Boc) + 1 H⁺), 5.30 min (72.1% peak area, ESI(+): 3990.34 (**192** + 1 H⁺)).

¹H NMR (300 MHz, D₂O, 20 °C): δ 4.48 – 4.25 (m, 29 H, CH), 4.05 – 3.95 (m, 1 H, CH), 3.78 – 3.67 (m, 45 H, CH₃), 2.52 – 1.87 (m, 120 H, CH₂), 1.38 (s, 9 H, CH₃).

MALDI-TOF (sinapinic acid matrix): 3888.97 ((**192** – Boc) + 1 H⁺).

ESI-MS: 3990.34 (**192** + 1 H⁺).

Boc-G4-*all*-L-Glu (**191**):



185 (0.20 g, 0.04 mmol) was reacted following the general procedure for the deprotection of the methyl ester. Reaction was accomplished, using DMF (3 mL), aqueous 1 M LiOH solution (1.75 mL, 1.75 mmol) and H₂O (1.5 mL). The reaction mixture was dialyzed twice in water (MWCO 1000 g/mol) to afford 104 mg (yield: 74%) of the desired product as a white solid.

UPLC-MS ((2.1x100 mm BEH C18 1.7um, acetonitrile:water Grad 5 15A): 4.96 (>90% peak area).

¹H NMR (300 MHz, D₂O, 20 °C): δ 4.47 – 4.15 (m, 29 H, CH), 4.03 – 3.91 (m, 1 H, CH), 3.76 – 3.62 (m, 45 H, CH₃), 2.49 – 1.79 (m, 120 H, CH₂), 1.33 (s, 9 H, CH₃).

No ESI-MS and MALDI-TOF possible.

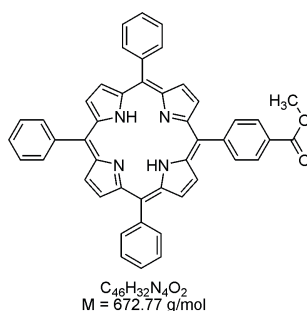
Dendrimer complexation experiments:

An aqueous solution of the dendrimer (0.0027 mmol in 5 mL H₂O) was brought to pH~9 to assure quantitative deprotonation of the periphery, using aqueous NaOH-solutions and added to a warm aqueous solution of the alkyl amine (16.1

6 Glutamate Dendrimers

or 32.1 eq. in 15 mL H₂O), which was slightly acidified to pH~5 to assure protonation of the amine, using aqueous HCl-solution. The resulting precipitate was centrifuged and washed with water at pH~5 and pH~8. The remaining white solid was dried i.vac. to give a white powder. The complex formation was monitored via IR. For further details, see Special Part.

5-(4'-Carboxymethylphenyl)-10,15,20-triphenylporphyrin (**193**):



Benzaldehyde (4.6 mL, 45.0 mmol) and methyl 4-formylbenzoate (2.5 g, 15.0 mmol) were dissolved in propionic acid:nitrobenzene 5:1 (400 mL) and heated to 140 °C. Pyrrole (4.2 mL, 60.0 mmol) was added dropwise and the solution was stirred for 3 h. After standing over night, the solvent was removed i.vac. The dark purple solid was dissolved in CH₂Cl₂ and stirred with saturated aqueous NaHCO₃-solution, to neutralize remaining propionic acid. The resulting emulsion was filtered through an alox plug. The solution was evaporated i.vac. Purification was achieved via repetitive column chromatography on silica and afforded 1.14 g (yield: 11%) of the desired product as a dark purple solid.

$R_F = 0.60$ (EE:PE 7:3 + 0.1 vol-% NEt₃)

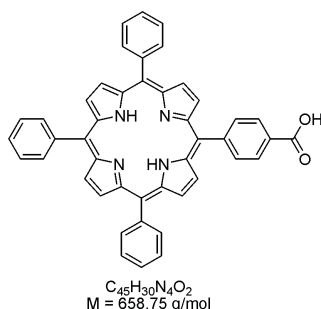
¹H NMR (300 MHz, CDCl₃, 20 °C): δ 8.91 – 8.87 (m, 6 H, Ar-*H*), 8.83 (d, ³*J*(H,H) = 4.8 Hz, 2 H, Ar-*H*), 8.50 – 8.45 (m, 2 H, Ar-*H*), 8.36 – 8.32 (m, 2 H, Ar-*H*), 8.27 – 8.22 (m, 6 H, Ar-*H*), 7.81 – 7.74 (m, 9 H, Ar-*H*), 4.13 (s, 3 H, CH₃), -2.73 (2 H, NH).

¹³C NMR (DMSO-*d*₆): δ 167.49, 147.20, 142.21, 142.18, 134.73, 134.70, 129.70, 128.07, 127.93, 126.87, 120.73, 120.53, 118.68, 52.58.

ESI-MS: $m/z = 673.28$ (**193** + 1 H⁺).

High-resolution ESI-MS: $m/z = 673.2480$ (calcd 673.2604 for $C_{46}H_{32}N_4O_2 + 1 H^+$).

5-(4'-Carboxyphenyl)-10,15,20-triphenylporphyrin (**194**):



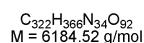
193 (1.04 g, 1.55 mmol) was refluxed in aqueous 2 M NaOH:EtOH:THF 2:2:1 (200 mL) for 2 h. The organic solvents were removed i.vac. and the basic aqueous suspension acidified with acetic acid. The aqueous layer was extracted with CH_2Cl_2 . The united organic layers were evaporated i.vac and the remaining purple solid was dried under vacuum at 150 °C, to give the desired product in quantitative yield.

UPLC-MS ((2.1x100 mm BEH HILIC 1.7um, acetonitrile:water Grad 5 15A): 10.95 min (>99.9% peak area, ESI(+): 660.00 (**194** + 1 H^+).

$R_F = 0.40$ (CH_2Cl_2 :MeOH 95:5 + 0.1 vol-% HOAc)

1H NMR (300 MHz, $CDCl_3$, 20 °C): δ 8.79 (br s, 8 H, Ar-*H*), 8.38 (d, $^3J(H,H) = 8.3$ Hz, 2 H, Ar-*H*), 8.24 (d, $^3J(H,H) = 8.3$ Hz, 2 H, Ar-*H*), 8.16 – 8.13 (m, 6 H, Ar-*H*), 7.72 – 7.66 (m, 9 H, Ar-*H*).

Porphyrin-G4-D-(*a/t*)-L-Glu(Z)-Me (**195**):



194 (0.006 g, 0.008 mmol) and HOBT (0.004 g, 0.032 mmol), dissolved in a small amount of DMF (1 mL) were cooled to 0 °C and EDC (0.003 g, 0.016 mmol) was added. The solution was stirred at room temperature for 10 minutes. **188** (0.022 g, 0.004 mmol), dissolved in 0.2 mL DMF and NEt_3 (0.002 mL) were added to the solution. After stirring for 4 days, the solvents

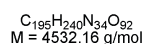
6 Glutamate Dendrimers

were removed i.vac. Washing of the remaining purple solid with H₂O and acetone (3x) afforded 0.021 g (yield: 91%) of the desired product as dark red solid.

GPC (DMF): Mn = 4989 g/mol, Mw = 5689 g/mol, Mp = 5961 g/mol, PDI = 1.14.

¹H NMR (300 MHz, DMSO-d₆, 20 °C): δ 8.95 – 8.80 (m, 7 H, Ar-H), 8.60 – 7.78 (m, 50 H, Ar-H, NH), 7.40 – 7.19 (m, 80 H, Ar-H), 5.08 – 5.00 (m, 32 H, CH₂), 4.42 – 4.12 (m, 30 H, CH), 3.62 – 3.46 (m, 45 H, CH₃), 2.45 – 1.60 (m, 120 H, CH₂).

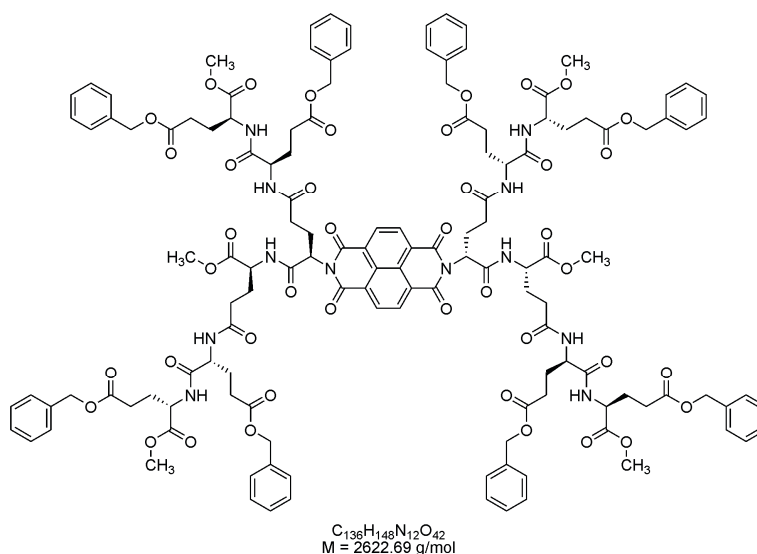
Porphyrin-G4-D-(*a/t*)-L-Glu (**196**):



195 (0.015 g, 0.003 mmol) was reacted following the general procedure for the deprotection of the methyl ester. Reaction was achieved in DMF. After 1 h, the reaction mixture was concentrated i.vac. The reaction mixture was dialyzed in water (MWCO 1000 g/mol) to afford the desired product as a dark red solid.

GPC (DMF): Mn = 5692 g/mol, Mw = 6028 g/mol, Mp = 6484 g/mol, PDI = 1.06.

No interpretable ¹H NMR.

Naphthalene-(G2-D-(*alt*)-L-Glu(Z)-Me)₂ (**197**):

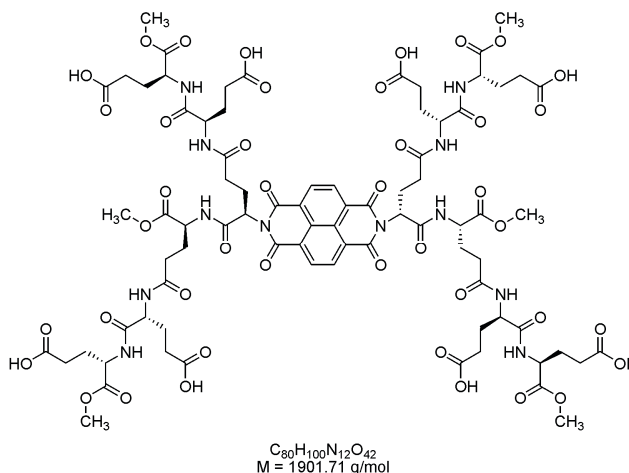
182 (0.20 g, 0.17 mmol) and 1,4,5,8-Naphthalenetetra-carboxylic dianhydride (0.023 g, 0.085 mmol) with NEt₃ (0.23 mL) were dissolved in DMF (6 mL). The solution was heated in the microwave (full power, super cooling, ramp: 1:00 minute, hold: 9:00 minutes). Second run under identical conditions to ensure conversion of all starting material. The solution was concentrated i.vac. and precipitated in cold Et₂O. The residue was purified via column chromatography on silica (eluent: CH₂Cl₂:MeOH 95:5). The most pure fractions were evaporated i.vac., dissolved in CH₂Cl₂ and precipitated in Et₂O, to give 94 mg (yield: 42%) of the desired product.

UPLC-MS ((2.1x100 mm HSS T3 1.8um, acetonitrile:water Grad 40 95A): 7.95 min (86.4% peak area, ESI(+): 2623.98 (**197** + 1 H⁺).

R_F = 0.40 (CH₂Cl₂:MeOH 95:5)

¹H NMR (300 MHz, CDCl₃, 20 °C): δ 8.66 (s, 4 H, Ar-H), 7.65 (d, ³J(H,H) = 8.0 Hz, 2 H, NH), 7.57 (d, ³J(H,H) = 7.6 Hz, 2 H, NH), 7.38 – 7.21 (m, 42 H, Ar-H, NH), 6.80 (t, ³J(H,H) = 8.7 Hz, 4 H, NH), 5.68 – 5.63 (m, 2 H, CH), 5.15 – 5.02 (m, 16 H, CH₂), 4.60 – 4.20 (m, 10 H, CH), 3.64 (s, 6 H, CH₃), 3.61 (s, 6 H, CH₃), 3.42 (s, 6 H, CH₃), 2.80 – 1.70 (m, 48 H, CH).

High-resolution ESI-MS: Could not be determined due to double charged molecule.

Naphthalene-(G2-D-(*alt*)-L-Glu-Me)₂ (**198**):

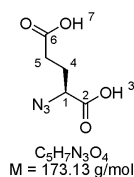
197 (0.03 g, 0.01 mmol) was reacted following the general procedure for the deprotection of the Z group or benzyl ester. EE:MeOH (1:1) (10 mL), Pd/C (5 mg), reaction time: 2 h, hydrogen pressure: 2 bar. Crude product was purified via precipitation in Et₂O and subsequent dialysis in MeOH (MWCO 1000 g/mol), to give 10 mg (yield: 53%) of the desired product as a yellow solid.

UPLC-MS ((2.1x100 mm HSS T3 1.8um, acetonitrile:water Grad 5 95A): 2.98 min (77.9% peak area, ESI(+): 951.17 (**198** + 2 H⁺), 1902.4103 (**198** + 1 H⁺).

R_F = 0.00 (CH₂Cl₂:MeOH 9:1)

¹H NMR (300 MHz, CD₃OD, 20 °C): δ 8.81 (s, 4 H, Ar-*H*), 5.81 – 5.69 (m, 2 H, CH), 4.55 – 4.29 (m, 8 H, CH), 4.20 – 4.09 (m, 2 H, CH), 3.69 (s, 6 H, CH₃), 3.65 (s, 6 H, CH₃), 3.61 (s, 6 H, CH₃), 2.84 – 1.75 (m, 48 H, CH).

High-resolution ESI-MS: m/z = 1901.3411 (calcd 1901.6136 for C₃₈H₅₈N₆O₂₁ + 1 H⁺). Deviation due to calculation from double charged molecule.

Azido-L-Glu (**199**):

NaN₃ (4.22 g, 64.80 mmol) was dissolved in water (10.5 mL) with CH₂Cl₂ (17.0 mL) and cooled to 0 °C. Triflyl anhydride (2.20 mL, 13.26 mmol) was added slowly within 5 minutes with stirring continued for 2 h. The emulsion formed 2 transparent layers after 30 minutes. The mixture was placed in a separation funnel and the CH₂Cl₂ layer was removed. The aqueous layer was extracted with CH₂Cl₂ (2x20 mL). The united organic layers were extracted once with saturated aqueous Na₂CO₃-solution and used without further purification. L-Glu (0.95 g, 6.48 mmol) was combined with K₂CO₃ (1.34 g, 9.72 mmol) and CuSO₄ (16.4 mg, 0.066 mmol), water (12 mL) and MeOH (24 mL). A white emulsion was formed. The triflyl azide in CH₂Cl₂ was added and the mixture stirred at room temperature. After 12 h more triflyl azide was synthesized (1.20 mL triflyl anhydride dissolved in dry CH₂Cl₂ (8.8 mL) and added within 15 minutes to NaN₃ (2.11 g) in 5.4 mL H₂O. The solution was then stirred for 2 h at room temperature.) and added to the reaction mixture, which was then stirred at room temperature for 12 h. The organic solvents were removed i.vac. and the aqueous slurry was diluted with water. This was acidified to pH = 6 with conc. HCl and extracted with EE (4x20 mL), in order to remove sulfonamide byproduct. The aqueous layer was acidified until it became turbid and extracted with EE (3x50 mL). These organic layers were dried over MgSO₄ and evaporated i.vac. to give 997 mg (yield: 89%) of the desired product as a colorless oil.

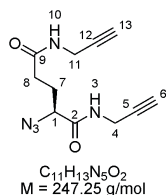
UPLC-MS ((2.1x100 mm HSS T3 1.8um, acetonitrile:water Grad 5 95A): 1.48 min (>99.9% peak area, ESI(+): 174.05 (**199** + 1 H⁺).

R_F = 0.05 (CH₂Cl₂:MeOH 9:1)

¹H NMR (300 MHz, CDCl₃, 20 °C): δ 11.30 (s, 2 H, 2 O⁷H), 4.12 (dd, ³J(H,H) = 5.3 Hz, ³J(H,H) = 8.4 Hz, 1 H, C¹H), 2.58 (t, ³J(H,H) = 7.2 Hz, 2 H, C⁵H), 2.29 – 2.01 (m, 2 H, C⁴H₂).

¹³C NMR (CDCl₃): δ 179.15, 176.26, 60.72, 29.83, 26.10.

High-resolution ESI-MS: m/z = 174.0534 (calcd 174.0515 for C₅H₇N₃O₄ + 1 H⁺).

Azido-L-Glu(propargylamide)-propargylamide (**200**):

199 (0.18 g, 1.02 mmol) and HOBt (0.14 g, 1.02 mmol) were dissolved in CH_2Cl_2 (20 mL). EDC (0.43 g, 2.24 mmol) was added. The solution was stirred under TLC monitoring. After preactivation, propargylamine (0.14 mL, 2.14 mmol), dissolved in CH_2Cl_2 (4 mL) was added slowly. After stirring for 14 h, TLC monitoring displayed no further changes in the reaction, hence water was added and the biphasic system was stirred for 10 minutes. All solvents (inc. H_2O) were removed i.vac. The crude product was purified via column chromatography on silica (eluent: CH_2Cl_2 :MeOH 95:5). A second column (eluent: CH_2Cl_2 :MeOH 92:8 to 95:5) gave the product in quantitative yield.

UPLC-MS ((2.1x100 mm HSS T3 1.8um, acetonitrile:water Grad 5 95A): 2.21 min (>99.9% peak area, ESI(+): 270.10 (**200** + 1 Na^+).

$R_f = 0.05$ (CH_2Cl_2 :MeOH 9:1)

^1H NMR (300 MHz, CDCl_3 , 20 °C): δ 6.89 – 6.80 (m, 1 H, N^3H), 6.29 – 6.22 (m, 1 H, N^{10}H), 4.12 – 4.03 (m, 5 H, C^1H , C^4H_2 , C^{11}H_2), 2.43 – 2.37 (m, 2 H, C^8H_2), 2.30 – 2.17 (m, C^7H_2 , C^6H , C^{13}H).

^{13}C NMR (CDCl_3): δ 171.42, 169.09, 79.50, 78.96, 72.19, 71.82, 62.59, 31.73, 29.37, 29.33, 28.15.

High-resolution ESI-MS: $m/z = 270.0951$ (calcd 270.0967 for $\text{C}_{11}\text{H}_{13}\text{N}_5\text{O}_2 + 1 \text{Na}^+$).

Polymerization of **200** to **201**:

200 (49 mg, 0.20 mmol) was dissolved in DMF (0.5 mL), cooled to 0 °C and degased by purging with Ar. Copper wire (6 mg, 0.1 mmol), sodium ascorbate (16 mg, 0.08 mmol) (dissolved in 0.02 mL water), CuSO_4 (0.010 g, 0.04 mmol) (dissolved in 0.02 mL water), and *N,N'*-dimethylethylenediamine (0.043 mL, 0.40 mmol) were added under stirring. After stirring for 48 h and addition of

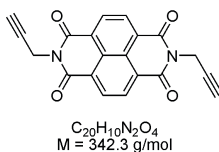
N,N'-dimethylethylenediamine (0.01 mL), the mixture was precipitated in aqueous EDTA-solution at pH~8. The resulting yellow-brown gel was stable in shape and could not be dissolved in THF, Et₂O, CH₂Cl₂, MeOH, DMF, DMSO, NMP, H₂O, TFA, conc. H₂SO₄ and mixtures of these solvents.

Co-polymerization of **200** and 4-tolylacetylene to **202** and **203**:

A solution of 4-tolylacetylene (1 mg, 0.012 mmol) in DMF (1.0 mL) was cooled to 0 °C and degased by purging with Ar. Sodium ascorbate (16 mg, 0.08 mmol) (dissolved in 0.1 mL water), CuSO₄ (0.010 g, 0.04 mmol) (dissolved in 0.1 mL water), and *N,N'*-dimethylethylenediamine (0.043 mL, 0.40 mmol) were added under stirring. **200** (49 mg, 0.20 mmol), dissolved in DMF (5.0 mL) was added a dropwise. After stirring for 24 h, the mixture was precipitated in aqueous EDTA-solution at pH~8 to give the polymer sample.

Co-polymerization of **200** and **204** to **205**, **206**, **207**, and **208**:

Different amounts of a stock solution of **204** (5mg/mL solution in DMSO) were dissolved in DMF to give a total amount of 1 mL and was cooled to 0 °C. The solution was degased by purging with Ar. Sodium ascorbate (16 mg, 0.08 mmol) (dissolved in 0.1 mL water), CuSO₄ (0.010 g, 0.04 mmol) (dissolved in 0.1 mL water), and *N,N'*-dimethylethylenediamine (0.043 mL, 0.40 mmol) were added under stirring. **200** (49 mg, 0.20 mmol), dissolved in DMF (5.0 mL) was added dropwise. After stirring for 44 h and further addition of sodium ascorbate (5 mg), the mixture was precipitated in aqueous EDTA-solution at pH~8 to give the polymer samples.

1,4,5,8-Naphthalenetetracarboxylic dipropargylamide (**204**):

Propargylamine (0.13 mL, 2.00 mmol), 1,4,5,8-naphthalenetetracarboxylic dianhydride (0.27 g, 1.00 mmol), and NEt_3 (0.20 mL) were dissolved in DMF (5 mL). The solution was heated in the microwave (full power, super cooling, ramp: 1:00 minute, hold 9:00 minutes). Needles were precipitating of the hot solution. These brown needles were filtered, washed with DMF, dissolved in hot DMSO (80 mL), and precipitated in H_2O . The grey solid was filtered and washed with H_2O and MeOH, to give 224 mg (yield: 65%) of the desired product as a grey solid.

^1H NMR (300 MHz, DMSO-d_6 , 20 °C): δ 8.73 (s, 4 H, Ar-H), 4.81 (d, $^3J(\text{H,H}) = 2.5 \text{ Hz}$, 4 H, 2 CH_2), 3.22 (t, $^3J(\text{H,H}) = 2.5 \text{ Hz}$, 2 H, 2 CH).

^{13}C NMR (CDCl_3): δ 161.95, 130.81, 126.33, 78.89, 73.56, 29.55.

6.4 Literature

- [1] R. G. Denkwalter, J. F. Kolc, W. J. Lukasavage, (Allied Corp., USA). *Us*, **1983**, pp. 9 pp. Cont.
- [2] F. E. Appoh, D. S. Thomas, H. B. Kraatz, *Macromolecules* **2005**, *38*, 7562.
- [3] F. E. Appoh, D. S. Thomas, H. B. Kraatz, *Macromolecules* **2006**, *39*, 5629.
- [4] S. A. Vinogradov, L. W. Lo, D. F. Wilson, *Chem.-Eur. J.* **1999**, *5*, 1338.
- [5] T. Kawaguchi, K. L. Walker, C. L. Wilkins, J. S. Moore, *J. Am. Chem. Soc.* **1995**, *117*, 2159.
- [6] B. H. Huang, M. A. Prantil, T. L. Gustafson, J. R. Parquette, *J. Am. Chem. Soc.* **2003**, *125*, 14518.
- [7] J. R. Parquette, *C. R. Chim.* **2003**, *6*, 779.
- [8] J. B. Kim, A. D. Adler, F. R. Longo, *Porphyrins* **1978**, *1*, 85.
- [9] P. Pengo, G. D. Pantos, S. Otto, J. K. M. Sanders, *J. Org. Chem.* **2006**, *71*, 7063.
- [10] J. Zaloom, D. C. Roberts, *J. Org. Chem.* **1981**, *46*, 5173.

7 Summary and Outlook

The inspiration for the work in this thesis arose from the antibiotics of the Gramicidin family and their D-(*alt*)-L amino acid sequence, enabling these oligopeptides to adopt fascinating β -helical secondary structures. Hence, the main focus throughout all projects was set on the stereochemical variation from regular *all*-L sequences to alternating, i.e. D-(*alt*)-L, sequences and its influence on the compounds' structures and properties.

7.1 Linear Oligo- and Poly-D-(*alt*)-L-peptides

The aim of the work on this project was the generation of a D-(*alt*)-L-peptide, which is able to adopt a β -helical secondary structure. In contrast to existing works on synthetic D-(*alt*)-L-peptides, hydrophilic amino acids with chargeable side chains were used, in order to generate a water-soluble and pH-sensitive β -helix. A series of oligo-D-(*alt*)-L-lysines up to a total length of 16 residues was synthesized by divergent/convergent peptide synthesis in solution. The deprotected peptides displayed no signal in circular dichroism studies in water at acidic and basic pH, pointing to a random coil structure. The idea to synthesize poly-D-(*alt*)-L-lysine was inspired by the established ring opening polymerization chemistry of α -amino acid *N*-carboxy anhydrides. The D-(*alt*)-L stereochemical information should be incorporated into the monomer unit by synthesizing a macrocyclic NCA by ring closing a tetra-D-(*alt*)-L-lysine. Attempts to this synthesis were not successful. Future work on this project should benefit from solid phase peptide synthesis, in order to synthesize larger peptides, which may be long enough to exceed the critical length for the adoption of a β -helical secondary structure.

7.2 Linear Oligo- and Poly(ester-[*alt*]-urea)s With Variable Stereochemistry

This project focused on the influence of stereochemistry and hydrogen bonding pattern on aggregation behavior, which was studied by the synthesis of leucine peptides and the stepwise replacement of backbone amide bonds by ester-(*alt*)-urea moieties. For these studies, oligoleucines and oligopseudoleucines with 50% and 0% amide content, respectively, with *all*-L and D-(*alt*)-L sequence were synthesized by divergent/convergent synthesis in solution. The straightforward

and rapid synthesis of oligoleucines was achieved up to the stage of tetrapeptides. The generation of the *all*-L and D-(*alt*)-L-pseudopeptides based on one key building block each, which was transferred into the respective pseudopeptides by straightforward and versatile synthesis. By this, hexadecamers of the pseudopeptides with 50% amide content were readily accessible. The synthesis of pseudopeptides with 0% amide content in economic yields was feasible to the stage of tetramers, but could be extended to the stage of octamers for the proof of concept. To the best of our knowledge, these novel oligopseudoleucine motifs have not been reported so far. The aggregation process of the six different tetramers was studied by concentration dependent proton shift NMR experiments. The generation of polymers with these unique structural motifs was targeted with the design and attempted synthesis of suitable cyclic monomers. The synthesis of these monomers was attempted by two different pathways. It turned out that the required high-dilution reaction conditions were not feasible for the synthesis of the required monomer amounts. In one cyclization experiment, the formation of the desired macrocycle was indicated by the analytical data of the reaction mixture. Future work on this project should focus on a more detailed elucidation of the tetramer aggregation process, involving further NMR experiments, such as solvent titration and temperature experiments, circular dichroism, IR, dynamic light scattering (DLS), molecular modeling, and SAXS, in order to determine exact aggregate structures. Furthermore, the aggregation and folding process of the pseudopeptides with 50% amide content could be studied in dependence on oligomer length.

7.3 Linear Triazole Containing Polypseudopeptides With Variable Stereochemistry

This project targeted the generation of nanosize water soluble and pH-sensitive polycations, benefiting of the highly efficient "Click"-reaction to polymerize appropriately designed monomers to triazole containing polypseudopeptides. Therefore, a versatile, straightforward and high yielding synthesis to dipeptide based AB-"Click"-monomers was developed, affording azide and acetylene terminated *all*-L and D-(*alt*)-L-lysines. Polymerization of the second generation

monomers yielded high molecular weight polymers, which were subjected to circular dichroism studies, revealing different secondary structures in basic and acidic aqueous environment. STM studies on the orientation of the cationic polymers on oriented alkyl carboxylic acid monolayers are currently being interpreted. Quantitative side chain labeling of the polypseudopeptides was achieved using pyrene butyric acid. Spectroscopic studies of the labeled *all*-L and D-(*alt*)-L-polymers in different solvent systems displayed strong excimer formation, pointing to close spatial proximity of the pyrene units, caused by a rather compact polymer solution structure. Further efforts on this field could be invested in the optimization of the polymerization reaction but also in diverse biochemical studies, such as DNA transfection experiments. Moreover, the triazole:amino acid ratio could be varied by synthesizing AB-monomers based on larger peptide units, i.e. tetrapeptides, opening the door to diverse heteropeptide structures.

7.4 Glutamate Dendrimers With Variable Stereochemistry

The aim of this project was the introduction of branching into glutamate peptides, affording fully chiral dendrimers with addressable focal and peripheral functionalities and variable charge density via an exponential growth approach. The straightforward and high yielding synthesis afforded 4th generation *all*-L-Glu and D-(*alt*)-L-Glu-dendrimers, which, after selective peripheral deprotection, contained 16 or 31 carboxylic acid functionalities. These deprotected G4-dendrimers were subjected to complexation experiments with surfactant molecules, such as alkyl amines. The influence of charge density and stereochemistry on the spatial organization of the obtained complexes with tetradecylamine in the solid state are currently being investigated by SAXS. Furthermore, the focal point of the G4-dendrimer could be attached to a porphyrin dye, in order to transfer the water insoluble dye into physiological environment. Similarly, microwave assisted coupling of the G2-dendrimer to the bifunctional 1,4,5,8-naphthalenetetracarboxylic anhydride and subsequent peripheral deprotection could be achieved. Moreover, the high yielding and straightforward synthesis of a glutamate based AB₂-“Click”-monomer and its polymerization to related chiral hyperbranched polypseudopeptides was achieved. Future work in this field should involve biochemical investigations of

the oligoelectrolyte dendrimers. Therefore, the labeling of the focal point with different dyes is very interesting to give information about dendrimer aggregation, cation complexation or incorporation into physiological processes. Additionally, the polymerization reaction of the AB_2 -“Click”-monomer can be further explored, increasing the solubility of the hyperbranched polymer by copolymerization with solubilizing monomers, leading to chiral, potentially spherical oligoelectrolytes with predictable sizes.

8 Appendix

8.1 Abbreviations

2Cl-Z	2-chlorobenzyloxycarbonyl
ACN	acetonitrile
ADP	adenosine diphosphate
ATP	adenosine triphosphate
Boc	<i>tert</i> -butoxycarbonyl
Bzl	Benzyl
CD	circular dichroism
CDI	1,1'-carbonyldiimidazole
CEC	capillary electro-chromatography
COSY	correlation spectroscopy
DCC	N,N'-dicyclohexylcarbodiimide
DIAD	diisopropyl azodicarboxylate
DIPEA	N,N'-diisopropylethylamine
DMAP	4-dimethylaminopyridine
DMF	N,N'-dimethylformamide
DMSO	dimethyl sulfoxide
DPTS	4-(dimethylamino) pyridinium-4-toulenesulfonate
EDC	1-(3-dimethylaminopropyl)-3-ethylcarbodiimide hydrochloride
EDT	1,2-ethanedithiol
EDTA	ethylenediaminetetraacetic acid
ee-value	enantiomeric excess value
EI	electron ionization
ESI	electrospray ionization
Et ₂ O	diethylether
EtOH	ethanol
Fmoc	fluorenylmethyloxycarbonyl
GC	gas chromatography
GPC	gel permeation chromatography

8 Appendix

HPLC	high performance liquid chromatography
HOBt	1-hydroxybenzotriazole
IR	infrared
LAH	lithium aluminium hydride
MALDI	matrix assisted laser desorption ionization
MeOH	methanol
MPEG	monomethylethyleneglycol
MS	mass spectrometry
MWCO	mol weight cut off
NCA	<i>N</i> -carboxy anhydride
NEt ₃	triethylamine
NMR	nuclear magnetic resonance
- br s	broad singlet
- d	doublet
- dd	doublet of a doublet
- m	multiplet
- s	singlet
NOESY	nuclear overhauser enhancement spectroscopy
PAM	polyacrylamide
PDI	polydispersity index
PE	petrol ether
PM3	parameterized model number 3
<i>R_F</i>	retardation factor
RI	refractive index
RT	room temperature
SAXS	small angle X-ray scattering
TBDMSCl	<i>tert</i> -butyldimethylsilyl chloride
TBDPSCI	<i>tert</i> -butyldiphenylsilyl chloride
TBTA	tris[(1-benzyl-1H-1,2,3-triazol-4-yl)methyl] amine
TBTU	<i>O</i> -(benzotriazol-1-yl)- <i>N,N,N',N'</i> -

	tetramethyluronium tetrafluoroborate
TEAA	triethylammonium acetate
TFA	trifluoroacetic acid
TFE	2,2,2-trifluoroethanol
TFMSA	trifluoromethanesulfonic acid
THF	tetrahydrofuran
TIPSCI	triisopropylsilyl chloride
TLC	thin layer chromatography
TOF	time of flight
TPP	tetraphenylporphyrin
UPLC	ultra performance liquid chromatography
UV	ultraviolet-visible
Z	benzyloxycarbonyl